UNIVERSITY OF LONDON THESIS

Degree PhD Year 2005 Name of Author MORLEY, D.W.

Reconstructing Past Climate Variability in Continental Eurasia

Thesis submitted for the degree
of Doctor of Philosophy in the
University of London
by

David William Morley

Department of Geography
University College London

January 2005

ProQuest LLC
789 East Eisenhower Parkway
P.O. Box 1346
Ann Arbor, MI 48106-1346

Abstract

The aim of this thesis was to reconstruct high-resolution climatic variability from continental Eurasia over the Late Glacial and Holocene as recorded in the sediments of Lake Baikal, Siberia. The palaeoclimatic records obtained in this study were used to assess teleconnection mechanisms between Central Asia and the North Atlantic and the extent to which climatic events are synchronous, or whether a lead or lag is shown. Lake Baikal is a key site for such palaeoclimatic research due to its extreme continental location and its remoteness from the direct climatic influence of oceanic circulation and Asian monsoonal systems. The study of climatic teleconnections is vital to improving our knowledge of how different aspects of the global climate system interact.

Two main techniques were used as palaeoclimatic proxies, namely diatom analysis and stable isotope analysis of bulk organic carbon and diatom silica oxygen. As Lake Baikal is both ecologically and limnologically unique, the dynamics of these proxies were investigated in the modern environment to aid interpretation of the palaeo record. Seasonal phytoplankton variability in the Lake was monitored and related to measured environmental variables. In addition, remote sensing was used to map spatial changes in lake ice cover. These data was used to further develop an existing diatom transfer function to model past ice cover characteristics.

Climatic reconstruction showed that events over the Late Glacial are semi-synchronous with those recorded in the North Atlantic (GS-1, GI-1 events). Inferred Holocene climate events also correlate well to other northern hemisphere records. The synchroneity of climatic events between Lake Baikal and the North Atlantic implies a teleconnection mechanism between the two areas. This is most likely to be the advection of North Atlantic climate change via Westerly airflow affecting the strength of the Siberian High pressure system.

Acknowledgements

I would like to thank my principal supervisor, Anson Mackay for his excellent advice, ideas and guidance throughout the course of this research. I would also like to my secondary supervisor, Melanie Leng for her invaluable knowledge of stable isotopes. Special thanks are also due to Patrick Rioual for helping in many different ways, mostly with diatom identification, providing entertainment on fieldwork in Russia, but also with the innovative techniques of inverse core sampling and random bag labelling.

I am grateful to Hedi Oberhänsli and other members of the CONTINENT project for discussions and supplying data, in particular Xavier Boës, Florence Hauregard, Birgit Heim, Georg Heumann, Dieter Demske, Natalia Piotrowska, François Demory, Jens Klump, Susanne Fietz and Mike Sturm.

David Jewson helped considerably with the interpretation of the phytoplankton data and Nick Granin collected the phytoplankton samples and environmental data. The assistance of John Birks, Dave Ryves and Gavin Simpson with statistical analysis is much appreciated, while Annette Witt carried out the wavelet analyses that is presented at the end of this study. Particular thanks go to Tula Cloke, Ian Patmore and Janet Hope for assistance in the lab at UCL, while I am also indebted Carol Arrowsmith and Hilary Sloane at NIGL. Elizabeth Mackie at the University of Durham helped with the SPT methodology. I am also grateful to my old landlord Mike Hughes for assistance with remote sensing, GIS and UNIX computing. Sarah 'you need more commas' Grove is acknowledge for her very thorough proof reading services. Peter R. Evans provided free colour printing. Rick Battarbee, Roger Flower, Don Monteith, Viv Jones and Neil Rose contributed to the discussions that led to the development of a method to clean samples for isotope analysis.

Finally, I would like to thank my friends at UCL for entertainment, in particular; Jon Tyler, Tom Davidson, Andy Henderson, Gina Clarke, Andrew 'lanterne rouge' McGovern, Patrick Austin, Jo Thorpe, Adam Young, George Swann, Ben Goldsmith, James Shilland, Eliza Cook, Ewan Shilland, Sophie Theophile, Helene Coleman, Ellie Liptrot, Dan Hoare and Carl Sayer.

This work was funded by a NERC Ph.D. studentship (number NER/S/A/2001/06430), a CASE studentship with NIGL, the CONTINENT project and the Royal Society UKBICER programme.

Contents

Title Page 1
Abstract 2
Acknowledgements 3
Contents 4
List of figures 8
List of tables 12

Chapter one: Introduction

1.1 The CONTINENT project 14
1.2 Climate variability in Central Asia 15
1.3 Holocene climate variability in the North Atlantic 15
1.3.1 Late Glacial climatic event stratigraphy 16
1.3.2 Late Glacial climatic events 18
1.3.3 Holocene climatic events 18
1.4 Possible causes of Late Glacial-Holocene global climate variability 19
1.4.1 External forcing 20
1.4.2 Internal forcing 22
1.5 Teleconnections between the North Atlantic and Central Asia 26
1.5.1 Chinese loess records of monsoon variability 26
1.5.2 Lake Baikal region and Siberia 28
1.5.3 Teleconnection mechanisms 29
1.5.3.1 Westerlies, Siberian High and Summer and Winter Monsoons 29
1.5.3.2 North Atlantic Oscillation (NAO) and snow extent 30
1.5.4 Summary 33
1.6 Aims and objectives 33
1.7 Thesis outline 34

Chapter two: Study site and general methodology

2.1 Introduction 35
2.2 Lake Baikal 35
2.2.1 Physical characteristics 35
2.2.2 Modern limnology 40
2.2.2.1 Ice cover and water budget 40
2.2.2.2 Thermal stratification 40
2.2.2.3 Mechanisms of deep water ventilation 41
2.2.3 Modern regional climate 42
2.3 Sediment material 45
2.3.1 Site selection 45
2.3.2 Coring 46
2.3.3 Correlation of cores 54
2.4 Chronology 56
2.4.1 Problems of dating Lake Baikal sediments 56
2.4.2 Sample preparation and analysis 56
2.4.3 Age models 57
2.5 Statistical methods (ordination) 60
2.6 Diatoms as palaeoclimatic indicators 61
2.7 Stable isotopes as palaeoclimatic indicators 63
2.7.1 Controls on $\delta^{13}C$ in bulk organic matter 63

2.7.2 Controls on $\delta^{18}O$ in precipitation ($\delta^{18}O_{PPT}$) 68
2.7.3 Controls on $\delta^{18}O$ in lake water ($\delta^{18}O_{LW}$) 70
2.7.4 Controls on $\delta^{18}O$ in diatom silica ($\delta^{18}O_{DIAT}$) 71
2.7.5 Summary 72

Chapter three: Modern environment I: Stable isotope dynamics

3.1 Controls on the modern oxygen isotope content of Lake Baikal 74
3.1.1 Lake water 74
3.1.2 Precipitation input 77
3.1.3 Fluvial input 83
3.1.4 Mass balance 81
3.1.4.1 Inputs 81
3.1.4.2 Outputs 81
3.1.4.3 Status of Lake Baikal water budget 84
3.2 Controls on the modern carbon isotope content of Lake Baikal 84
3.3 Summary 92

Chapter four: Modern environment II: Phytoplankton monitoring

4.1 Phytoplankton monitoring 93
4.2 General controls on phytoplankton dynamics 94
4.3 Seasonal and interannual dynamics of Lake Baikal phytoplankton 96
4.4 Methodology 103
4.4.1 Sampling methodology 103
4.4.2 Sample preparation 105
4.4.3 Counting methodology 105
4.4.4 Taxonomy 105
4.4.5 Data analysis 109
4.5 Surface waters 109
4.5.1 Results 109
4.5.2 Discussion 121
4.6 Depth profiles 123
4.6.1 Results 123
4.6.1.1 Listvyanka-Tankhoy 123
4.6.1.2 4 km Ivanovsky 133
4.6.2 Discussion 142
4.7 Conclusion 145

Chapter five: Modern environment III: Environmental controls on diatom species distribution and transfer function development

5.1 Introduction 147
5.2 Ice cover on Lake Baikal 149
5.3 Effects of ice cover on diatom populations 150
5.4 Diatom based inference models for Lake Baikal 151
5.5 Satellite remote sensing 156
5.5.1 Introduction 156
5.5.2 Remote sensing of snow and ice cover 156
5.6 Remote sensing methodology 158

5.6.1 The Advanced High Resolution Radiometer (AVHRR) 158
5.6.2 Image selection 158
5.6.3 Image processing 160
5.6.4 Creation of new environmental variables 168
5.7 Transfer function development 171
5.7.1 Species data 171
5.7.2 Environmental data 172
5.7.3 Variance partitioning of environmental data 175
5.7.4 Explanatory power of environmental variables 176
5.7.5 Inference models 181
5.7.5.1 Statistical methods 181
5.7.5.2 Weighted averaging method selection 182
5.7.5.3 Outlier detection 183
5.7.5.4 Final model performance 184
5.8 Diatom autecological information 193
5.8.1 Culturing studies 193
5.8.2 Training set species response to ice cover variables 196
5.8.3 Spatial distribution of training set species 207
5.8.4 Diatom species autecological summary 211

Chapter six: Diatom based palaeoclimatic reconstruction

6.1 Diatom records from Lake Baikal 218
6.2 Methodology 221
6.2.1 Diatom slide preparation and counting 221
6.2.2 Calculation of diatom concentration, flux and biovolume 223
6.2.3 Numerical and graphical methods 225
6.2.4 Diatom taxonomy 225
6.3 Results 233
6.3.1 Diatom percentage abundance, fluxes and biovolumes 233
6.3.2 Ordination of diatom data 243
6.3.3 Transfer function reconstructions 245
6.4 Discussion 251
6.4.1 Late Glacial climatic events 251
6.4.2 Holocene climatic events 259
6.4.3 Taphonomic considerations and core representivity 263
6.5 Conclusion 265

Chapter seven: Biogenic silica oxygen isotope climate reconstruction

7.1 Oxygen isotope records from Lake Baikal 267
7.2 Applications to palaoeclimatic research 267
7.3 Methodology 269
7.3.1 Development of the $\delta^{18}O_{DIAT}$ technique 269
7.3.2 Method used at NERC Isotope Geosciences Laboratory (NIGL) 269
7.3.3 Possible limitations of the technique 270
7.3.4 Summary of published cleaning techniques 273
7.4 Cleaning experiment design 274
7.4.1 Introduction 274
7.4.2 Site selection 275
7.4.3 Development of a cleaning method 277

7.4.4 Protocol for obtaining clean diatom samples 277
7.4.5 Results 281
7.4.5.1 Diatom content and $\delta^{18}O$ 281
7.4.5.2 Diatom species assemblage change 287
7.4.6 Discussion 291
7.4.7 Conclusions 292
7.5 Application of $\delta^{18}O_{DIAT}$ analysis to Lake Baikal sediments 292
7.5.1 Methodology 292
7.5.2 Results 293
7.5.3 Discussion 295
7.5.4 Conclusions 299

Chapter eight: Palaeoclimatic reconstruction from organic material

8.1 Previous work on the possible controls on $\delta^{13}C_{ORG}$ and C/N in Lake Baikal 301
8.1.1 Catchment vegetation changes 303
8.1.2 Algal species composition and productivity 304
8.1.3 Palaeo-*p*-CO_2 levels 305
8.1.4 Gas hydrate release 306
8.1.5 Summary of previous work 309
8.2 Methodology 310
8.3 Results 312
8.4 Discussion 315
8.4.1 Catchment vegetation changes 315
8.4.2 Algal species composition and productivity 317
8.4.3 Palaeo-*p*-CO_2 levels 318
8.4.4 Gas hydrate release 321
8.5 Conclusion 323

Chapter nine: Summary, conclusions and future research

9.1 Introduction 325
9.2 Late Glacial climate change 327
9.3 Holocene climate changes 328
9.4 Teleconnection mechanisms 329
9.5 Future work 330

References 332

List of figures

Chapter one

1.1: GRIP ice core $\delta^{18}O$ ‰ vs. SMOW between 11.0 and 23.0 kGRIPaBP 17
1.2: The global thermohaline circulation 24
1.3: Schematic diagram of main atmospheric characteristics over Asia during the winter and summer 27
1.4: a) Schematic surface pressure distribution during the positive phase of the NAO. b) Schematic surface pressure distribution during the negative NAO phase 32

Chapter two

2.1: Map of Lake Baikal and principal features 37
2.2: Photopgraphs of Lake Baikal 38
2.3: Map of Lake Baikal catchment and tributaries 39
2.4: General mean sea level pressure (hPa) over Russia in January 44
2.5: General mean sea level pressure (hPa) over Russia in July 44
2.6: Sonogram of the Vydrino Shoulder area 46
2.7: The R/V Vereshchagin at Listvyanka (photograph) 49
2.8: The piston corer being prepared (photograph) 49
2.9: Weights for the box and trigger corers (photograph) 49
2.10: Weight for the piston corer (photograph) 50
2.11: Retrieval of the kasten corer (photograph) 50
2.12: Box core casing crumpled during core retrieval (photograph) 51
2.13: Piston core casing damaged by gas hydrate release during core retrieval (photograph) 51
2.14: a) Lithological description of cores CON01-605-3 and 3a, b) Key 52
2.15: Correlation of the Vydrino cores 55
2.16: Age-depth model and error for the trigger/piston core 59
2.17: Age-depth model and error for the box/piston core 59
2.18: Carbon isotope values for the major sources of carbon into lakes 65
2.19: Discrimination of algae, C_3 and C_4 plants using $\delta^{13}C$ and C/N measurements 67

Chapter three

3.1: a) $\delta^{18}O$ and δD of Lake Baikal's fluvial inputs, lake water, precipitation in the catchment and the nearby rivers with relation to the GMWL, b) Simplified version 76
3.2: $\delta^{18}O$ and δD in precipitation, monthly precipitation and average air temperatures measured at Irkutsk during 1990 78
3.3: $\delta^{18}O$ and δD in precipitation, monthly precipitation and average air temperatures measured at Ulan Bator during 1998-2001 79
3.4: Weighted annual $\delta^{18}O$ in precipitation over Asia 80
3.5 Summary of Lake Baikal's hydrological cycle 83
3.6: C/N ratio and $\delta^{13}C$ for sediments in Lake Baikal tributaries, core-tops (surface sediments) and soils 86
3.7: C/N ratio and $\delta^{13}C$ for Lake Baikal core-top (surface sediment) material; Central Basin, Southern Basin, Northern Basin, Selenga Delta area and Academician Ridge. 86
3.8: Map of sampling locations for $\delta^{13}C$ of Selenga River tributary material 89
3.9: Generalised $\delta^{13}C$ and C/N limits for C_3 , C_4 plants; catchment soil, core-tops, plankton and tributaries 91

Chapter four

4.1: Sampling locations for phytoplankton in 2001 – 2002 on Lake Baikal 104
4.2: Common planktonic diatoms species found in Lake Baikal 107
4.3: Distribution of *A. baicalensis* live and dead cells in Lake Baikal surface waters, February 2001 – June 2002 112
4.4: Distribution of *A. skvortzowii* live and dead cells in Lake Baikal surface waters, February 2001 – June 2002 113
4.5: Distribution of *A. skvortzowii* resting spore live and dead cells in Lake Baikal surface waters, February 2001 – June 2002 114
4.6: Distribution of *C. minuta* complex live and dead cells in Lake Baikal surface waters, February 2001 – June 2002 115
4.7: Distribution of *S. acus* v. *radians* live and dead cells in Lake Baikal surface waters, February 2001 – June 2002 116
4.8: Distribution of *S. acus* v. *pusilla* live and dead cells in Lake Baikal surface waters, February 2001 – June 2002 117
4.9: Distribution of *S. meyerii* live and dead cells in Lake Baikal surface waters, February 2001 – June 2002 118
4.10: Distribution of *N. acicularis* live and dead cells in Lake Baikal surface waters, February 2001 – June 2002 119
4.11: Distribution of *A. formosa* live and dead cells in Lake Baikal surface waters, February 2001 – June 2002 120
4.12: Bubble plots showing abundance of the main diatom species (live and dead) throughout the water column at Listvyanka-Tankhoy, 2001-2002 126
4.13: RDA of Listvyanka-Tankhoy depth profiles and environmental data, a) March, b) June, c) July, d) September/October 129
4.14: Bubble plots showing abundance of the main diatom species (live and dead) throughout the water column at 4 km Ivanowsky, 2001-2002 135
4.15: RDA of 4 km Ivanowsky depth profiles and environmental data, a) March, b) June, c) July, d) September/October 138

Chapter five

5.1: Location of 93 core top surface sediment training sites from Mackay *et al.* (2003) 152
5.2: An example of a full AVHRR image before processing 162
5.3: AVHRR image subset of the Lake Baikal region 163
5.4: Georeferenced vector coverage of the Lake Baikal boundary 163
5.5: Geocorrected AVHRR image 163
5.6: Corrected image subset to the Lake Baikal boundary 163
5.7: Thematic maps showing the snow, ice and water classes for the 1996-1997 ice covered period on Lake Baikal defined from AVHRR images 164
5.8: PCA biplot of the 33 explanatory variables and 92 sampling locations 173
5.9: Scatterplots of observed against predicted snow depth (left) and observed against residual snow depth (right) for all three training sets 187
5.10: Scatterplots of observed against predicted clear ice duration (left) and observed against residual clear ice duration (right) for all three training sets 188
5.11: Scatterplots of observed against predicted white ice/snow duration (left) and observed against residual white ice/snow duration (right) for all three training sets 189
5.12: Scatterplots of observed against predicted snow depth (left) and observed against residual snow depth (right) for all three training sets, after outlier deletion 190
5.13: Scatterplots of observed against predicted clear ice duration (left) and observed against residual clear ice duration (right) for all three training sets, after outlier deletion 191
5.14: Scatterplots of observed against predicted white ice/snow duration (left) and observed against residual white ice/snow duration (right) for all three training sets, after outlier deletion 192
5.15: The effect of temperature on some cultured Lake Baikal diatoms 195
5.16: The effect of quantum irradiance on some cultured Lake Baikal diatoms 196
5.17: HOF responses for *C. minuta* to snow depth, clear ice and white ice/snow duration in the full training set 199

5.18: HOF responses for *A. baicalensis* to snow depth, clear ice and white ice/snow duration in the full training set 200
5.19: HOF responses for *A. skvortzowii* to snow depth, clear ice and white ice/snow duration in the full training set 201
5.20: HOF responses for *C. inconspicua* to snow depth, clear ice and white ice/snow duration in the full training set 202
5.21: HOF responses for *S. meyerii* to snow depth, clear ice and white ice/snow duration in the full training set 203
5.22: HOF responses for *S. acus* v. *radians* to snow depth, clear ice and white ice/snow duration in the full training set 204
5.23: HOF responses for *C. baicalensis* to snow depth, clear ice and white ice/snow duration in the full training set 205
5.24: HOF responses for *S. acus* v. *pusilla* to snow depth, clear ice and white ice/snow duration in the full training set 206
5.25: Spatial distribution in the full training set of percentage abundance of, a) *C. baicalensis,* b) *C. inconspicua,* c) *A. baicalensis,* d) *A. skvortzowii* 209
5.26: Spatial distribution in the full training set of percentage abundance of, a) *C. minuta,* b) *S. acuc* v. *pusilla* c) *S. acus* v. *radians,*d) *S. meyerii* 210

Chapter six

6.1: Examples of dissolution stage 1 to 3 for *A. baicalensis* and *C. minuta* 222
6.2: Water content, dry bulk density, accumulation rates and diatom and chrysophyte cyst calculations per gram wet weight and per gram dry weight for the Vydrino Shoulder 224
6.3: Photographs of common diatom species found at the Vydrino Shoulder, Lake Baikal 229
6.4: SEM photographs of common diatom species found at the Vydrino Shoulder, Lake Baikal 231
6.5: Percentage diatom abundance against depth for the Vydrino Shoulder 239
6.6: Percentage diatom abundance against age for the Vydrino Shoulder 240
6.7: Flux of diatom species against age for the Vydrino Shoulder 241
6.8: Biovolume of diatom species against age for the Vydrino Shoulder 242
6.9: PCA biplot for the 534 core samples and 23 diatom species at abundance >5% 244
6.10: Reconstructed snow depth, clear ice cover and white ice/snow cover for the 5 corrected species training set 248
6.11: Reconstructed snow depth, clear ice cover and white ice/snow cover for the full training set 249
6.12: Reconstructed snow depth, clear ice cover and white ice/snow cover for the planktonic species training set 250
6.13: Summary diagram of diatom reconstructions for the Late Glacial and GRIP $\delta^{18}O$ 258

Chapter seven

7.1: Diatom concentration and bulk $\delta^{18}O$ for a core representing the Eemian to Early Holocene from the Academician Ridge, Lake Baikal. 272
7.2: Flow diagram showing the four stage cleaning method for concentrating diatom for oxygen isotope analysis from lake sediments 280
7.3: Graphs of samples 1-7 showing percentage diatom and contaminant content 283
7.4: Graphs of $\delta^{18}O_{DIAT}$ for Samples 1-7 after the four cleaning stages and the residue left after Stages 3 283
7.5: Photographs of the cleaning stages for the sample 3 284
7.6: Photographs of the cleaning stages for the sample 1 285
7.7: Photographs of the cleaning stages for the sample 6 286
7.8: Changing species assemblages through the cleaning process (Sample 3) 288
7.9: Changing species assemblages through the cleaning process (Sample 5) 289
7.10: Changing species assemblages through the cleaning process (Sample 4) 290
7.11: $\delta^{18}O_{DIAT}$ bulk and mass balanced, sample % diatom content and sediment diatom concentration for the Vydrino Shoulder against age 294

Chapter eight

8.1: General trends in $\delta^{13}C_{ORG}$ and C/N in found in Lake Baikal over the Late Glacial and Holocene 302

8.2: The correlation of the Lake Baikal $\delta^{13}C_{ORG}$ record of Prokopenko and Williams (2004) with the SPECMAP template, Vostock ice core methane and carbon dioxide content 306

8.3: Locations of mapped areas of gas hydrate layers in Lake Baikal 307

8.4: $\delta^{13}C_{ORG}$, C/N, %TOC and %TN for the Vydrino Shoulder, Lake Baikal plotted against age 313

8.5: Biplot of $\delta^{13}C_{ORG}$ and C/N of core samples from the Vydrino Shoulder as well as general ranges for materials as shown in figure 3.9 314

8.6: The palaeo-*p*-CO_2 LGIT record from GISP2 after Smith *et al.* (1997) 320

Chapter nine

9.1: Summary diagram of palaeoclimatic reconstructions from the Vydrino Shoulder against age 326

List of tables

Chapter one

1.1: Event stratigraphy for the Late Glacial based on the GRIP ice core 17

Chapter two

2.1: Morphological characteristics of Lake Baikal 36
2.2: An example of core naming protocol as used by the CONTINENT project 48
2.3: Cores collected by the CONTINENT project from the Vydrino Shoulder, Lake Baikal used in this study 48
2.4: Radiocarbon ages, calibrated ages and errors for dated sections of the Vydrino Shoulder piston and box cores 58

Chapter three

3.1: Mean North, Central and South Basin lake water, river input and hot spring water $\delta^{18}O$ and δD 75
3.2: Average $\delta^{18}O$ values and percentage of total fluvial input for the three largest tributary rivers to Lake Baikal. 81
3.3: ^{13}C and C/N of Selenga River channel material with sample site names and distance from the water line. 90

Chapter four

4.1: RDA summary for the Listvyanka-Tankhoy depth profiles 128
4.2: RDA summary for the 4 km Ivanowsky depth profiles 137

Chapter five

5.1: Comparison of light transmission through different ice and snow types 150
5.2: Average diatom fluxes observed from the water column for dominant species between 1994-1998 and for sediment core BAIK38 (valves sq cm^{-1}) and correction multiplication factors to adjust core data to expected values 154
5.3: Training set and core data used in the inference models of Mackay *et al.* (in press) 155
5.4: Results for models 1-4 using weighted averaging (Mackay *et al.* in press) 155
5.5: Spectral channels and ranges for the AVHRR 158
5.6: AVHRR image temporal coverage for the 1996-1997 ice covered period on Lake Baikal 159
5.7: Summary statistics for the temporal distribution of AVHRR images for the 1996-1997 ice covered period on Lake Baikal 160
5.8: Classified cover type for the surface sediment locations 169
5.9: Environmental variables used by Mackay *et al.* (2003) and new variables as potential explanatory variables for distribution of diatoms in the surface sediments 170
5.10: Results of DCA for the floristic data of the three calibration set formulated in this study 171
5.11: Correlation matrix for the 33 explanatory variables 174
5.12: Summary of variance partitioning of the four main groups of environmental variables 175
5.13: DCCA of full training set with each explanatory variable the sole predictor in turn 177
5.14: DCCA of 5 corrected species training set with each explanatory variable the sole predictor in turn 178
5.15: DCCA of planktonic training set with each explanatory variable the sole predictor in turn 179
5.16: Variables with $\lambda 1/\lambda 2$ ratio ≥ 0.50 in the three training sets (in rank order) 180

5.17: Comparative performance (r^2_{boot} and RMSEP) for the five WA methods for each reconstructed variable 183
5.18: Summary of WA model performance for reconstructed variables for the full, planktonic and 5 dissolution corrected species training sets. 186
5.19: Summary of the diatom culturing experiments of Jewson *et al.* (unpublished) 194

Chapter six

6.1 Calculation of diatom fluxes and concentrations 223
6.2 Estimated biovolumes of the common diatom taxa in Lake Baikal 225
6.3 Summary results from the DCA of percentage diatom abundances (species occurring >5% in any one sample) 243
6.4 Summary results from the PCA of percentage diatom abundances (species occurring >5% in any one sample) 243
6.5 The boundaries of the Blytt-Sernander division of the Holocene 259

Chapter seven

7.1: Details of samples 1-7 used in the cleaning experiment 276

Chapter eight

8.1: Processes and their effects on Total organic carbon (TOC), nitrogen (TN), C/N and $\delta^{13}C_{ORG}$ in Lake Baikal sediments 310

Chapter One

Introduction

1.1 The CONTINENT project

This work forms part of the larger EU funded CONTINENT project with the primary aim of reconstructing high-resolution palaeoclimatic records from Lake Baikal during the Holocene and Eemian to investigate teleconnections between the North Atlantic and Central Asia. In particular it was hoped that time transgressive offsets of large hemispheric scale climatic events could be investigated. A main aim of the project was to fully understand the meaning of climatic proxies by assessing the contemporary environment. This included assessment of mechanisms of sediment supply and formation and also biological responses to climate through monitoring. This was achieved mainly with the use of sediment traps to quantify the flux of particles through the water column, but also with remote sensing of spatial and temporal trends in aquatic productivity. To understand diatom autecologies, an existing systematic phytoplankton sampling program was utilised.

Coring sites were first investigated using sonar profiling methods to confirm sediments were undisturbed. The CONTINENT project also attempted to establish an accurate chronology for Lake Baikal sediments using a combined approach of radiometric techniques for the Holocene and OSL dating (although unsuccessful) and palaeomagnetics over the last 150000 years.

Reconstruction of climatic signals used a multi-proxy approach using biological indicators (diatoms, pollen, stable isotopes and biomarkers) and also minerogenic proxies (bulk and clay mineralogy, geochemistry, grain size and lithological analyses). Full details of the CONTINENT project can be found at: http://Continent.gfz-potsdam.de.

The first section of this introduction will outline climatic events that have been reconstructed from proxy data predominantly in the North Atlantic region and possible causes for this variability. Potential teleconnections and mechanisms linking the North Atlantic climate variability to Central Asia are then discussed. Finally, issues that need further study concerning the indentification of related climatic events in Central Asia and the North Atlantic and teleconnections are discussed as an underpinning for the present study.

1.2 Climate variability in Central Asia

Throughout this study calender years before present (aBP) or thousand years before present (kaBP) will be used unless otherwise stated (for example in the case of radiocarbon years (^{14}CaBP) or ice core years (e.g. GRIPaBP, ss08aBP). Most palaeoclimatic reconstructions over the Late Glacial (15 – 11.5 kaBP (thousand years before present, i.e. 1950 AD)) and Holocene (11.5 kaBP to present) have been centred on the North Atlantic and bordering areas, with a recognised series of well defined climatic events appearing to be synchronous over the region, albeit with some local variations. Fewer Holocene palaeoclimatic studies have been applied to Central Asia. Changes in the North Atlantic region related to ice-sheet dynamics are thought to control global climate change (Imbrie *et al.* 1992) and these are transmitted to remote regions by teleconnection mechanisms. A teleconnection can be defined as a weather pattern in one region that can influence those in a distant region. They are driven by large scale features of the global climatic system such as atmospheric waves and jet streams which in turn can be altered by changing boundary conditions forced by solar insolation variability, as well as internal feedbacks of the climate system such as oceanic and ice sheet changes (Adams *et al.* 1999). Further work is needed to investigate the magnitude and timing in terms of leads, lags or synchronicity of climatic events in areas removed from the direct influence of the North Atlantic such as Central Asia. This will aid in understanding the role of teleconnection patterns in determining past and possibly future climate variability. Lake Baikal is an ecosystem far removed from oceanic influence that provides an ideal study site to investigate the remote influence of ocean circulation during periods of climate instability. Palaeoclimatic studies in this area will be useful to identify modifications to atmospheric systems and how this relates to past climate variability on a hemispheric to global scale. The degree to which these climatic shifts are synchronous or diachronous are pivotal to our understanding of global climate mechanisms (Lowe 2001).

1.3 Holocene climate variability in the North Atlantic

Changes in the North Atlantic are considered to drive global climate due to ice-sheet-ocean circulation changes in the region (Broecker and Denton 1990, Imbrie *et al.* 1992, Broecker 1994, Alley and Clark 1999). Modifications of the atmospheric systems and circulation patterns may relate these changes to Central Asia. These teleconnections will be discussed after general climatic events occurring in the North Atlantic have been outlined. Over the Northern Hemisphere, changes can be mostly synchronous but when transferred to the

Southern Hemisphere, a lagged response may be shown. This is termed the 'bipolar seesaw' and is related to the slow response of ocean circulation (Broecker 1998).

1.3.1 Late Glacial climatic event stratigraphy

The subdivision of the North Atlantic Late Glacial – Interglacial transition (LGIT) was formally described by Mangerud *et al.* (1974); chronozones defined by radiocarbon dating identify two warmer episodes (Bølling and Allerød) separated by two colder periods (Older and Younger Dryas) (table 1.1). This scheme was intended to be used in a strict chronostratigraphic sense, however due to the temporal and spatial variability of climate change there are limitations to this application (Björck *et al.* 1998, Lowe 2001). The described chronozones have been used interchangeably as biozones and correlation problems have arisen due to the limitations of radiocarbon dating, lagged responses of some proxies and asynchronous regional signatures.

As a solution to these problems, Björck *et al.* (1998) propose a stratotype for the North Atlantic region based on the GRIP Greenland ice core. This scheme uses an independent chronology based on annual ice layer counts and adopts a new terminology for event names (fig 1.1, table 1.1). The intended use of this sequence is as an event stratigraphy and not in a chronographic sense, and as a result regional time transgression of events can be accommodated (Björck *et al.* 1998, Lowe 2001). When making correlations to the GRIP record, local climatic zones should be independently defined and dated, before comparing to the GRIP sequence (Lowe 2001, Lowe *et al.* 2001, Walker 2001, Renssen *et al.* 2001). In this study, the GRIP terminology will be used except when citing studies which have used the old Mangerud-style classification.

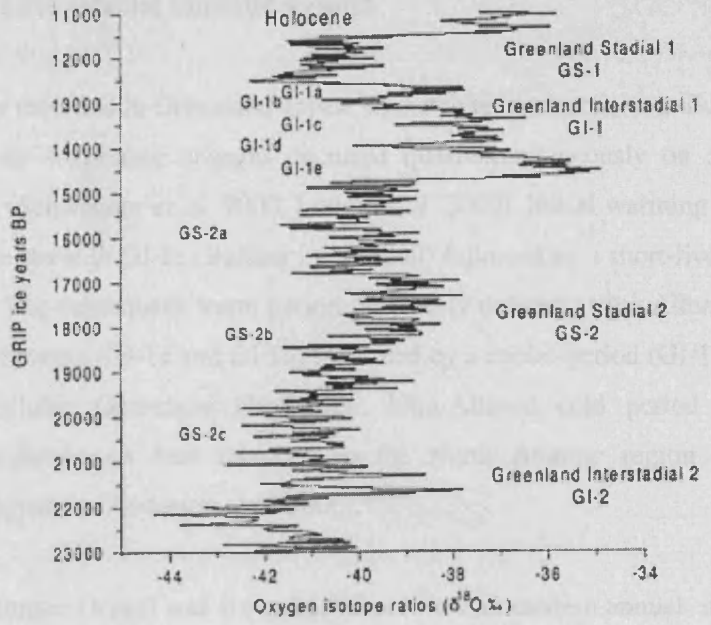

Figure 1.1: GRIP ice core $\delta^{18}O$ ‰ vs. SMOW (Standard Mean Ocean Water) (Johnson *et al.* 1992, Dansgaard *et al.* 1993) between 11.0 and 23.0 kGRIPaBP and division into interstadials and sub-interstadials and stadials and sub-stadials (Björck *et al.* 1998).

Events	Episodes	Ice core age for onset (yrs)	Equivalent in Mangerud scheme	^{14}C age for onset in Mangerud scheme (yrs)
Holocene epoch		11500		
GS-1		12650	Younger Dryas	11000
	GI-1a	12900	Allerød	11800
	GI-1b	13150	Allerød	
	GI-1c	13900	Allerød	
	GI-1d	14050	Older Dryas	12000
GI-1	GI-1e	14700	Bølling	13000
	GS-2a	16900		
	GS-2b	19500		
GS-2	GS-2c	21200		
GI-2		21800		

Table 1.1: Event stratigraphy for the Late Glacial based on the GRIP ice core (Björck *et al.* 1998) (ss08c chronology) and equivalents in the Mangerud *et al.* (1974) scheme.

1.3.2 Late Glacial climatic events

Climate events recorded in Greenland appear to match reconstructions in European and North Atlantic records suggesting changes occurred quasi-simultaneously on at least an extra-regional scale (Schwander *et al.* 2000, Lotter *et al.* 2000). Initial warming at the start of the Late Glacial began with GI-1e (Bølling interstadial) followed by a short-lived cooling (GI-1d, Older Dryas). The subsequent warm period previously defined as the Allerød is now divided into two warm events (GI-1c and GI-1a) separated by a cooler period (GI-1b). Episode GI-1b (synonyms include: Gerzensee Oscillation, Intra-Allerød cold period (IACP) and the Killarney Oscillation) is best recorded in the North Atlantic region but may have a hemispheric signature (Andresen *et al.* 2000).

The GS-1 (Younger Dryas) was around 15°C colder than modern annual mean temperatures (Alley 2000), the event lasted about 1000 years and ended abruptly with the start of the Holocene (Taylor *et al.* 1993). Over continental Eurasia the average temperature of this event may have been similar to that in the North Atlantic although seasonal temperature difference was much greater (Velichko *et al.* 2002). While the GS-1 is well recorded in the Northern Hemisphere, the extent of its signature in the Southern Hemisphere is more contentious (Peteet 1995). However, there is evidence of a global scale GS-1 event (Stager and Mayewski 1997, Andres *et al.* 2003). Overall, an apparent synchronicity of events has been noted on a global scale (Lowe 2001).

1.3.3 Holocene climatic events

Since the start of the Holocene, the most significant climatic cooling in the North Atlantic region has been the 8.2 kaBP cooling event. Based on ice-core data, a 6±2°C cooling can be inferred for the event which lasted *c.*400 years (Alley *et al.* 1997). Holocene climate change since this point has been reconstructed by numerous studies utilising many different proxies and geographic regions, as a result, a synthesis of Holocene climate variability is not valid due to local climate variability and possible lagged response of different proxies. However, some larger climatic shifts of note include a climate deterioration (7-5 kaBP) bringing the end of the mid-Holocene climatic optimum - this cooling appears to have been on a global scale (Steig 1999). A cold event at 4.2 kaBP is thought to coincide with the collapse of many early civilisations and for example, in Asia this coincides with the decline of the Hongshan culture (de Menocal 2001). The period from *c.* 3 kaBP to the present is known as the neoglaciation, representing overall cooler conditions since the climatic optimum up to the modern period,

covering approximately the last 3000 years (Porter and Denton 1967). A well documented warming known as the Medieval Warm Period (MWP) (Broecker 2001), occurred at *c.* 1050-650 aBP while a return to cooler conditions (450-150 aBP) is described as the Little Ice Age (LIA) (Grove 1988).

Bond *et al.* (1997) identify a periodicity of 1470±500 years in the occurrence of North Atlantic ice-rafted debris (IRD) with peaks at 1400, 2800, 4200, 5900, 8100, 9400, 10300 and 11100 aBP representing cooling events. IRD is simply material carried by floating ice that eventually melts and is deposited on the ocean floor. During periods associated with maximum IRD, floating ice and water of low sea surface temperature (SST) advected further south (2-4°C cooler (Maslin *et al.* 2003)), while higher SSTs would have occurred through periods of minimum IRD deposition. Some of these peaks in IRD match with recognised shifts in palaeoclimatic records, for example the GS-1, GI-1b, the 8.2 kaBP cooling and the LIA and it is likely climate change over the Holocene has been periodic at ~1500 years (Bond *et al.* 2001, Viau *et al.* 2002). However, evidence of these periodicities in the Greenland ice $\delta^{18}O$ records is less forthcoming (Bond *et al.* 1997), although O'Brien *et al.* (1995) identify a quasi-2600 year cycle in the Greenland Summit glaciochemical sequences which may be linked to global climatic changes for example, as shown by Holocene glacier advances (Denton and Karlen 1973). In addition, the Holocene millennial cycle (~1500 years) has been found by spectral analysis of GISP2 chemical composites (Witt and Schuman in prep.). Millennial scale climate variability was much more significant during the last glacial period manifest as Dansgaard-Oeschger events (Dansgaard *et al.* 1993) possibly due to the amplifying effect of large ice sheets (Schultz 2002a, b) via the mechanisms explained below. The weaker Holocene millennial cycle is either considered to be analogous in (unknown) cause to these Dansgaard-Oeschger events (Bond *et al.* 1997, 2001) or to be independent and solely caused by cyclic solar variability (Timmermann *et al.* 2003).

1.4 Possible causes of Late Glacial-Holocene global climate variability

The possible causes of climate variability in the Late Glacial-Holocene involve both external mechanisms relating to climate forcing from a source, such as variations in insolation input (e.g. orbital variation, solar activity), but also due to internal amplification of these external mechanisms by often non-linear positive and negative feedbacks manifest in the complex global atmospheric-ocean-biosphere system (ocean circulation, albedo change, atmospheric gas compositions). Most of these causes focus on changes in the North Atlantic, in particular

the dynamics of high latitude ice sheets. How these mechanisms related to climate change in Central Asia is explained subsequently and related to teleconnection mechanisms.

1.4.1 External forcing

Orbital variations: Cyclic variations in the Earth's orbit have been shown to cause the major shifts in climate, such as glacial/interglacial cycles over the Quaternary (Hays *et al.* 1976). These periodicities (also known as Milankovitch cycles) include the eccentricity cycle (100 ka), obliquity cycle (41 ka) and the precessional cycles (19 ka, 21 ka). Only the eccentricity cycle influences the amount of insolation received by the Earth while obliquity and precession influences the seasonal and latitudinal distribution of energy of the Earth's surface. In the northern hemisphere, Early Holocene summer insolation was higher than at present and has actually been decreasing over the last 12 ka (Bradley 2003). Translation of these changes in energy distribution to Holocene climate change is difficult as the effects are modulated by internal feedbacks (described below) and reorganisations of atmospheric circulation. Declining insolation is thought to have initiated the current neoglaciation period (Kutzbach 1981) but Bond *et al.* (1997) and Stuiver (1997) state harmonics of orbital periodicities are too long to explain millennial scale periodicities.

Solar variations: There are many known cycles in solar activity, including the 11 year Schwabe, 22 year Hale, 88 year Geisberg, 211 year Suess and ~2200 year Hallstattzet cycles as well as a possible 500 year and a millennial cycle. Over the past few millennia solar activity has been linked to known climate changes such as the Maunder Minimum (AD 1645-1715) causing the LIA and the Medieval Solar Maximum leading to the MWP. Solar activity has also been linked to an extreme climatic cooling at 2700 aBP in Chile (van Geel *et al.* 2000), Aaby (1976) related periodicities in reconstructed peat bog surface wetness to solar cycles, while a record from a Chinese peat bog associated 16 periodicities over the last 6000 a to solar cycles (Hong *et al.* 2000). The modern increase in temperature associated with the greenhouse effect may also be due to increased solar activity (Friis-Christensen and Lassen 1991, Khilyuk and Chilingar 2003). Model simulations have shown that the effects of solar variability over continental regions can be much greater due to the removed dampening influence of the oceans, it was shown that winter cooling over continental areas can be up to five times as great (Shindell *et al.* 2001).

As solar variations are relatively small, feedback mechanisms are required for the climate to be influenced. Van Geel *et al.* (1999) summarise two that can either act alone or in concert.

Firstly, increased UV radiation leads to stratospheric heating as ozone absorbs more sunlight. This strengthens stratospheric winds and tropospheric subtropical jetstreams are displaced polewards. Subsequently, the descending limbs of the Hadley Cells are also shifted polewards causing high latitude warming. Secondly, increased cosmic ray flux during lowered solar activity can alter the optical properties and radiation balance of the atmosphere. Ozone layer density can change, as well as the development of an aerosol layer and increased cloudiness. The level of cloudiness is important as this can effect albedo and result in increased precipitation (Chambers *et al.* 1999).

Although Bond *et al.* (1997) and Stuiver *et al.* (1997) initially state a solar forcing of the 1470±500 cycle is doubtful, van Geel *et al.* (1999) present evidence that a millennial periodicity is evident in cosmogenic nuclides (^{10}Be and ^{14}C) records from GISP2 and tree rings. Bond *et al.* (2001) subsequently examined North Atlantic Holocene IRD in relation to solar flux and concluded that millennial scale increases in drift ice are linked to periods of reduced solar output. Linked to this, spectral analysis of the δ^{14}C residual series (a proxy for solar variability) of Stuiver and Braziunas (1993) by Mayewski *et al.* (1997) revealed strong cycles of length 1450 years and 2300 years as well as at 512 years. These cycles can be linked to the ~1470 cycle in the North Atlantic but also an apparent ~2500 cycle of Holocene cooling as demonstrated by Denton and Karlen (1973). However, such correlations do not necessarily imply a solar-climate link (Mayewski *et al.* 1997).

Volcanic activity: Explosive volcanic eruptions can cause a reduction in global temperatures over a few years and during periods of frequent eruptions decadal or multi-decadal impacts are possible, especially if enhanced by a positive feedback mechanism such as increased albedo from more extensive snow or sea-ice cover (Bradley 2003). Sulphate levels in the GISP2 ice core show periods of increased volcanic activity, especially around the Early Holocene (Zielinski *et al.* 1994, Stuiver *et al.* 1995). The effects of volcanic activity are most noticeable when simultaneous with reduced solar activity, for example as occurred during the LIA (Bradley 2003).

Tidal forcing: Well defined tidal cycles exist, defined by the gravitational pulls of the moon and the sun; Keeling and Whorf (1997) noted that periodicities in global temperature over the period of instrumental recordings do not correlate well to solar cycles. Instead they suggest tidal cycles can explain these periodicities. Extreme ocean tides can increase depth and vertical mixing of water and lower sea-surface temperature (SST), this will be amplified by

positive feedbacks of increased cloudiness and snow or ice cover (Keeling and Whorf 1997). This mechanism has also been used to explain the millennial cycle noted by Bond *et al.* (1997) with the discovery of a 1800 year tidal cycle (Keeling and Whorf 2000). However, Munk *et al.* (2002) consider the tidal forcing to be weak and unlikely to able to cause millennial scale climate variability.

1.4.2 Internal forcing

Ocean circulation – ice sheet interaction: Thermohaline Circulation (THC) in the North Atlantic Ocean can have a considerable influence on global climates. THC is a system of ocean currents that transfers heat. For example, warm, low salinity water is carried polewards from the tropics. In the North Atlantic the water cools, increases in salinity and density and sinks to form North Atlantic Deep Water (NADW). This process gives off large amounts of heat (Broeker and Denton 1990). The NADW then travels southwards before upwelling in the Pacific (Figure 1.2).

This 'ocean conveyor belt' is unstable and weakens even if small amounts of fresh water are inputted, thereby causing cooling in the North Atlantic (Tzipermann 1997) and subsequent global cooling via teleconnections to weather systems. It is not known whether THC shuts down under extreme freshwater forcing or simply shifts to another weaker state of operation (Rahmstorf 1994). Freshwater input can result from the calving of ice shelves. Such a mechanism has been used as a possible explanation to the Heinrich Event cycles. Heinrich Events occurred during the last glacial period at least since 80 kaBP (Bond *et al.* 1993). A gradual cooling episode leads to a Heinrich Event every 7-10 ka (ice sheet collapse marked by increased IRD in ocean sediments). Succeeding this there is a period of climatic warming. During the cooling leading to a Heinrich Event, there are periodic climatic oscillations operating on a 2000-3000 year cycle (Bond and Lotti 1995). These are known as Dansgaard-Oeschger cycles and are considered analogous to the 1470±500 cycle (Bond *et al.* 1997).

It can be seen that increased ice-rafting and subsequent freshwater input to the North Atlantic causes at the very least a regional cooling, but the cause of these periodic increases in ice-rafting is unknown. One theory involves internal ice-sheet dynamics (MacAyeal 1993). The binge/purge model states an ice sheet can collapse when continuous gradual build up creates instability and eventually surging, hence only an indirect climatic cause. However, since it appears surges in the North Atlantic are synchronous with glacial advances worldwide (Leuschner and Sirocko 2000) a direct climatic cause would have to be the origin of the surging. The fact that the cycle appears 'pervasive' over glacial and interglacial periods with

limited ice sheets, implies a climatic mechanism rather than an internal ice sheet dynamics theory (Bond *et al.* 1997). A cause related to solar activity has been identified as a possible reason of the 1470±500 cycle. If changes in solar activity led to increased periods of ice-rafting in the North Atlantic, it is possible that the subsequent impact on THC will amplify any climate change and aid in global transmission (Bond *et al.* 2001).

Changes in THC may also have caused the Younger Dryas and the 8.2 kaBP cold events. The Younger Dryas could have been caused by changes in atmospheric CO_2, solar variation or volcanic dust input (Berger 1990, Renssen *et al.* 2000). It is also synchronous with Heinrich Event (H-0) and part of the 1470±500 cycle. However, the hypothesis of a perturbation of THC due to massive freshwater input to the North Atlantic from the melting of the Laurentide Ice Sheet is the most widely accepted explanation for this cooling (Broecker *et al.* 1989).

The 8.2 kaBP cooling event has been interpreted as an amplification of a cooling associated with the 1470±500 cycle with a similar cause to the Younger Dryas (Bond *et al.* 1997, Ramrath *et al.* 2000). THC could have been altered by an influx of fresh water from the final break-up of the Laurentide Ice Sheet. There has been some disagreement as to the nature of this discharge event. Rahmstorf (1995) estimated from modelling experiments that only a small freshwater input is required to switch THC mode. As a result, Alley *et al.* (1997) suggest a weak forcing mechanism and the 8.2 kaBP event was caused by the drainage of small glacial lakes as they found no evidence for a catastrophic discharge. Weak forcing mechanisms are supported by Klitgaard-Kristensen *et al.* (1998), however, they acknowledge evidence of a large outburst due to the collapse of the Hudson ice-dome 600 years before the 8.2 kaBP event but expect THC would respond instantaneously to such a large modification.

A strong forcing associated with a catastrophic outburst is favoured by von Grafenstein *et al.* (1998). They question why a large freshwater input 600 years before the 8.2 kaBP event did not cause a cooling event and put this lag between the two events down to poor chronological control. Barber *et al.* (1999) also support this theory and provide improved chronology for the catastrophic drainage of glacial lakes Agassiz and Ojibway.

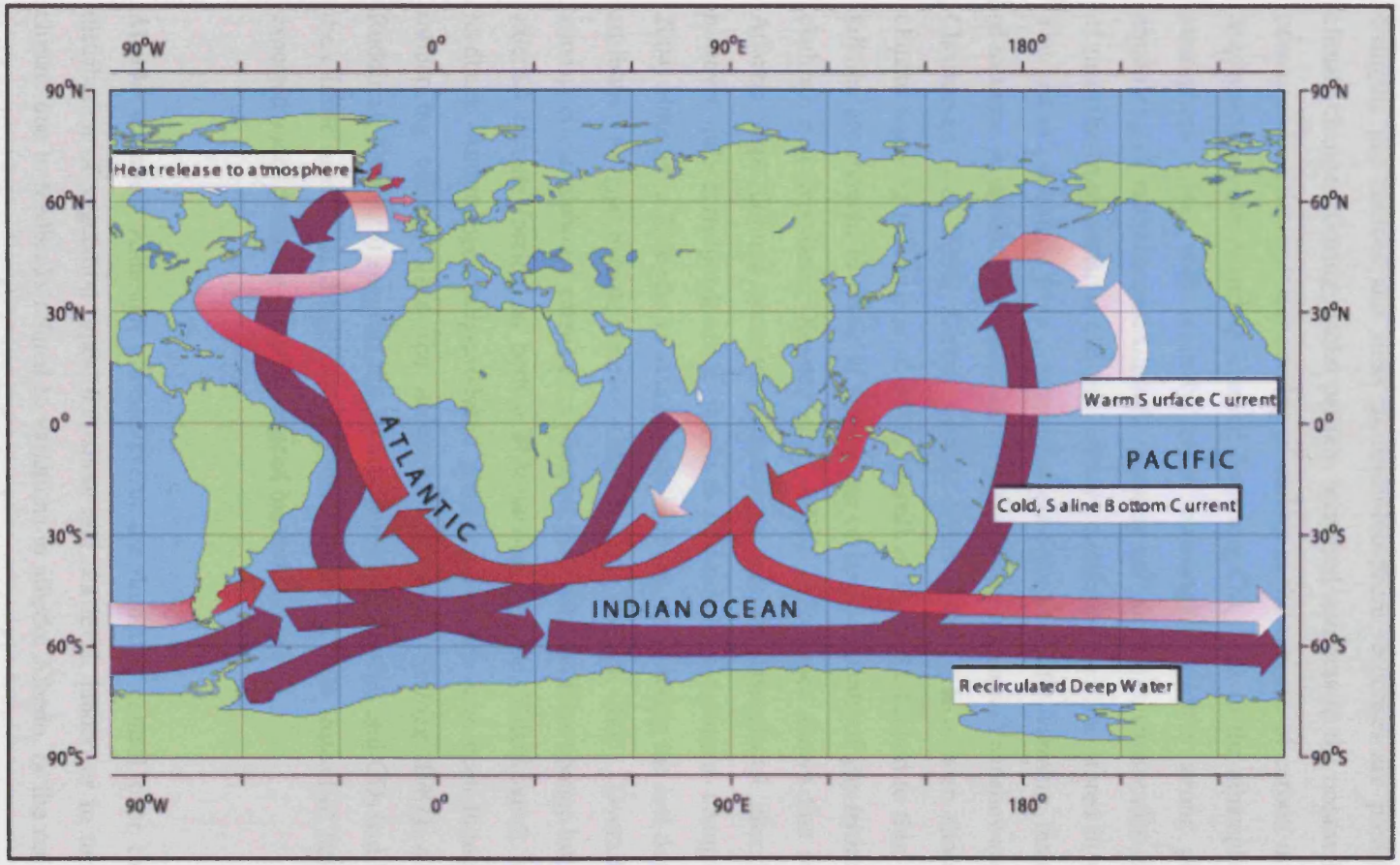

Figure 1.2: The global thermohaline circulation. Darker arrows represent deep water currents, while lighter arrows represent surface currents. Arrows indicate the direction of water movement. Areas of heat relaease to the atmosphere are shown (North Atlantic) and areas where deep currents return to the surface (Indian Ocean and North Pacific) (http://www.clivar.org/publications/other_pubs/clivar_transp/d3_transp.htm, accessed August 2004).

Atmospheric gases: During the last glacial period, lower atmospheric content of greenhouse gasses (CH_4, CO_2, N_2O) are recorded in Greenland ice-cores (Raynaud *et al.* 1993, Severinghaus and Brook 1999). Increased atmospheric content of these gases can cause rises in global temperature by absorbing outgoing reflected solar radiation. This variation is due to changing gas sources and sinks as ocean-biosphere responses are predominantly due to climate changes. During glacial periods, increased nutrients in the oceans lead to enhanced ocean productivity and sequestering of carbon at the expense of carbon in the atmosphere. Subsequent climate warming allowed degassing CO_2 back to the atmosphere. Increases of atmospheric gases with orbitally forced warming provides a strong positive feedback amplifying climate changes. Climatic warming and moisture increase also allows the release of methane from wetlands and gas hydrates containing methane stored in ocean sediments. The loss of permafrost from northern Eurasia due to climatic warming, results in the release of methane in significant amounts to influence global climates (Yakushev and Chuvilin 2000, Christensen *et al.* 2004). Global methane levels however, have been shown to lag behind climate warming (Sirocko *et al.* 1996, Morrill *et al.* 2003). Linked to this, submarine slope failures are thought to result in the release of large amounts of gas hydrate, the so-called clathrate gun hypothesis (Kennett *et al.* 2003). It has been shown that a series of North Atlantic slope failures correlate to warming over the last glacial interglacial transition, however little correspondence is shown to millennial scale climate changes (Maslin *et al.* 2004) although a 30% rise in atmospheric methane since during the last deglaciation can be attributed to gas hydrate release (Maslin and Thomas 2003). Overall, the levels of atmospheric greenhouse gasses are a complex response to climate change but serve to amplify external climate forcing on both a Milankovitch and sub-Milankovitch scale by positive feedback. Anthropogenically-produced greenhouse gasses have been thought to have been influencing climate since the industrial revolution (Kellogg 1987) although recently Ruddiman (2003a, b) suggests that human generation of CH_4 and CO_2 had been influencing the climate as early as 8 kaBP as the level of gases increase instead of falling as would be expected under declining orbitally induced insolation receipt.

Albedo changes: Although climate exerts the dominant control over the global spatial distribution of vegetation types, ice, snow and sea level, landcover in turn can affect the climate due to feedbacks related to variations in albedo. Albedo, or the ratio of reflected to incident light from a surface, can influence how much of incoming solar energy is absorbed or reflected back into space. Snow has a high albedo, absorbing only 15% of incident radiation, while the oceans have low albedo absorbing 90% (Barry and Chorley 2003). Deserts, tundra and steppe also have high albedo compared to boreal forests. Climate modelling experiments

simulate a reduction in climate induced by positive feedback associated with increasing albedo related to both expanding snow cover and sea-ice and declining forest cover (Foley *et al.* 1994, Ganopolski *et al.* 1998, Brovkin 2002). The extent of Eurasian snow cover can also have a feedback to Asian Monsoon strength by altering temperature gradients over the region: this mechanism is explained fully in section 7.5.3. The extent of permafrost, which is common over large parts of mid – high latitude Eurasia can have a climatic feedback. The presence of permafrost provides a heat sink in summer and reduces heat flux to the atmosphere and so a loss of this permafrost would amplify any subsequent climatic warming (Eugster *et al.* 2000). Linked to this, the succession of permafrost or tundra regions to boreal forests will lower albedo and lead to positive feedbacks resulting in climatic warming over Eurasia (Renssen and Lautenschlager 2000, MacDonald *et al.* 2000). As discussed in the solar variations section, the distribution of clouds (high albedo) can also influence the level of radiation received at the Earth's surface.

1.5 Teleconnections between the North Atlantic and Central Asia

1.5.1 Chinese loess records of monsoon variability

The most extensive palaeoclimatic studies carried out in Central Asia have used the wind-blown deposits of the Chinese Loess Plateau to elucidate the history of glacial cycles and monsoon variability in the region, in particular the East Asian Monsoon. The East Asian Monsoon is a sub-system of the Asian Monsoon circulation and is driven by land-to-ocean pressure gradient created by differential heating between the Pacific Ocean and Asia (Zhou *et al.* 1996). Currently, it directly influences the climate to the east of the Bay of Bengal and the Tibetan Plateau and reaches the China-Mongolia border in the north (An 2000). The East Asian Monsoon is linked to cold air associated with the Siberian High and also the Pacific subtropical high and warm pool (figure 1.3).

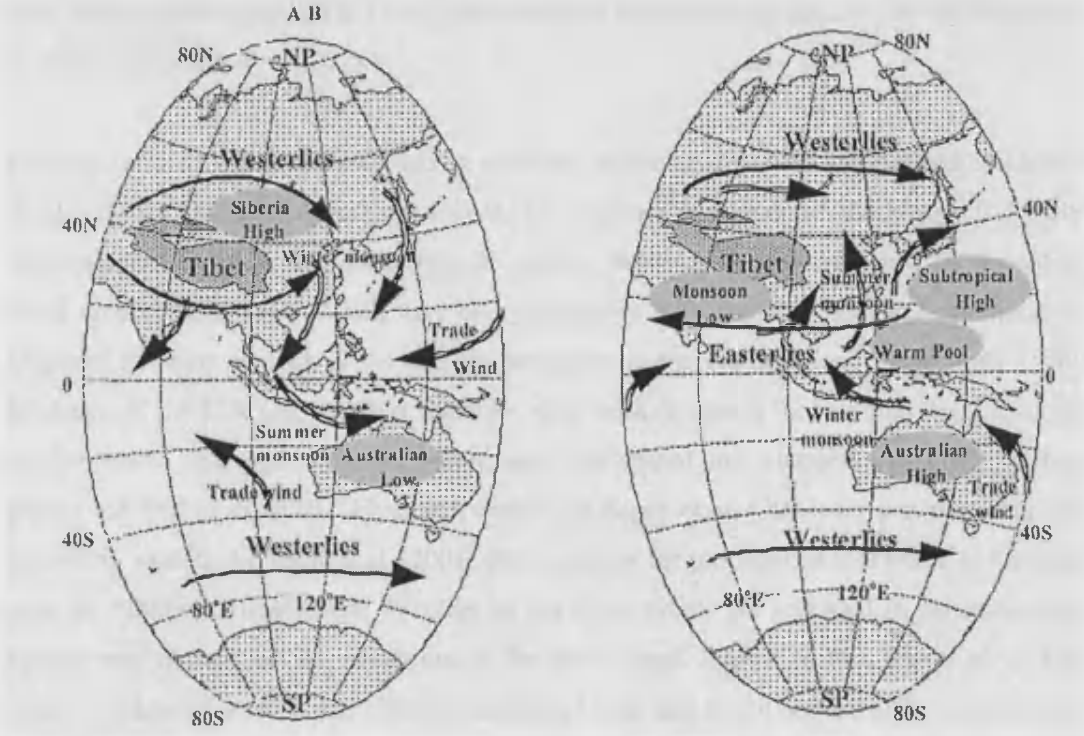

Figure 1.3: Schematic diagram of main atmospheric characteristics over Asia during the winter (left) and summer (right). The East Asian Summer Monsoon is marked as 'Monsoon Low' to the south-west of Tibet on the summer diagram. (An 2000).

Loess layers are defined by unweathered, fine wind-blown silt deposited under cool, arid climates while layers of palaeosoils indicate a warmer, humid climate (Bloemendal *et al.* 1995). The basal age of the loess deposits are thought to coincide with the initiation of the Quaternary. Alternations between loess and palaeosol layers are highly correlated to the marine oxygen-isotope record implying that variations in monsoon strength are in phase with global ice volume changes and Milankovitch orbital variations (Bloemendal *et al.* 1995, Ding *et al.* 1995, An 2000, Porter 2001, Zhao *et al.* 2003).

On a sub-Milankovitch scale, teleconnections have also been identified, in particular the propagation of ice discharge events in the North Atlantic to the Monsoon region. During the Last Glacial Maximum, episodes of iceberg calving related to Heinrich Events led to reduced temperatures over the North Atlantic. Heinrich Events have been reported in the Chinese loess by Porter and An (1995), Sirocko *et al.* (1996), An and Porter (1997) and Chen *et al.* (1997). In terms of millennial-scale changes, the equivalent North Atlantic Late Glacial sequence (GI-1 to GS-1) has been reported from Chinese loess sequences (An *et al.* 1993, Zhou *et al.* 1999, Y. J. Wang *et al.* 2001, Zhao *et al.* 2003). Periodicities of 2 ka and 1.5 ka have been found for the Holocene (Porter 2001) and may be linked to the millennial periodicity, while other cycles

have been tentatively linked to Dansgaard-Oeschger Events during the last glacial (Sirocko *et al.* 1996, Anderson *et al.* 2002).

Holocene climate change as recorded by monsoon variability has been synthesised by Morrill *et al.* (2003). During the Early Holocene, no evidence is found for the abrupt 8.2 kaBP cooling event found in the North Atlantic region. However there is evidence for a cooling event around 4.5-5 kaBP which may be synonymous with the mid-Holocene deterioration observed in many regions worldwide, in particular in the North Atlantic millennial cycle. Evidence of the LIA and MWP is however very weak, a reason for this may be due to the relative lower magnitude of these events, and high spatial and temporal variability of their impact (Morrill *et al.* 2003). However, studies by Esper *et al.* (2002) on tree ring data and modelling work by Shindell *et al.* (2001) give evidence for pronounced MWP and LIA events over the Northern Hemisphere. Whether or not these events are recorded in palaeoclimatic studies may depend on the resolution of the proxy used. Linked to this, He *et al.* (2004) review evidence for Holocene climate change in China and found considerable variability in the timing and magnitude of the Holocene temperature optimum. Due to local variations in topography and monsoon influence, the optimum began later and terminated earlier in eastern than in western China.

1.5.2 Lake Baikal region and Siberia

Much less palaeoclimatic work has been carried out in the Lake Baikal region in comparison to the extensive studies on Chinese loess, however, Bush (2004) state that records from these areas show great similarity, suggesting that the two regions are interlinked and respond to the same forcing mechanisms. For example, like the loess records, biogenic silica content in Lake Baikal gives a record of Quaternary glaciation (Qui *et al.* 1993, Shimaraev *et al.* 1994, Colman *et al.* 1995, BDP-Members 1997, Williams *et al.* 1997, Karabanov *et al.* 2000, Antipin *et al.* 2001, Khursevich *et al.* 2001). Siberian loess records also display glacial cycles (Chlachula 2003). North Atlantic Heinrich Events are also suggested to be present in the South Basin of Lake Baikal marked by increased terrigenous carbon input resulting from increased river discharge into the lake caused by greater moisture transport from the North Atlantic during Heinrich Events (Prokopenko *et al.* 2001). In comparison, Swann *et al.* (in press) link declines in diatom abundance to climatic cooling and increased ice cover to Heinrich Events in the North Basin. Evans *et al.* (2003) also reported Heinrich Events to be present in the Siberian loess, while Goldberg *et al.* (2001) claim that Dansgaard-Oeschger cycles are detectable during OI stage 3 in Lake Baikal. Evidence for teleconnections over the last interglacial – glacial period will be investigated fully in chapter 6.

1.5.3 Teleconnection mechanisms

1.5.3.1 Westerlies, Siberian High and Summer and Winter Monsoons

The climate of Central Asia is dominated by the position of the Siberian High, the jet streams and summer and winter monsoons (Dodson and Lui 1995) (figure 1.3). The synchronicity of events between the North Atlantic and Central Asia suggests a direct atmospheric forcing rather than a slower paced ocean-atmospheric mechanism (An and Porter 1997). Porter and An (1995) suggest the two regions are linked via the Westerlies and that cold North Atlantic SSTs can have a large effect on climate downstream. Modelling studies by Kutzbach *et al.* (1993) confirm this and indicate the presence of a westerly storm track carrying cold North Atlantic air across Eurasia during the Last Glacial Maximum (LGM). These Westerlies are ultimately caused by the more intense heating in equatorial regions than at the poles to due to differing angles of incidence of radiation. In the Northern Hemisphere this creates a north-south temperature gradient and a northward flow of air that is deflected to the east by the Coriolis effect. During periods of North Atlantic ice discharge, THC disruption and colder SSTs led to increased westerly inflow of cold air to continental Eurasia, strengthening and prolonging the Siberian High creating a very cold and arid climate. This in turn leads to a strengthened winter monsoon driven by intense cold outflow southwards from the Siberian High, meaning the Chinese loess region will be governed by a cold, arid windy climate due to the enhanced temperature and pressure gradients between the regions (Ding *et al.* 1995, Zhou *et al.* 1999, Alley 2000, figure 1.3). Concurrent with this, the Summer Monsoon weakens due to a reduced Pacific Ocean-land thermal gradient and lower western Pacific SSTs resulting in lower moisture availability (Zhao *et al.* 2003). During warmer periods characterised by increased NADW production and warmer North Atlantic SSTs, the above situation will be reversed with a weakening of the Siberian High and accordingly a decline in winter monsoon but an increase in summer monsoon strength. This has been described by Overpeck *et al.* (1996) who suggest increased NADW formation and the advection of warm anomalies over Eurasia via the Westerlies would enhance the Summer Monsoon. A subsequent decrease in snow cover would increase spring land temperatures and enhance the land-sea temperature gradient that drives the Summer Monsoon.

The East Asian Monsoon dominates precipitation patterns to the south of Lake Baikal and variations of monsoon strength are recorded in Chinese loess sequences (for example, Bloemendal *et al.* 1995, An 2000, An *et al.* 1993, Zhou *et al.* 1996, Porter 2001). However, it is unlikely that the East Asian Summer Monsoon has ever reached Lake Baikal's catchment.

The current northerly limit of the monsoon rains lies at the China-Mongolia border (Xiao *et al.* 1995, Black 2002, Chen *et al.* 2003, An *et al.* 1993). An (2000) also states the monsoon front has not reached further north than the north-western Chinese Loess Plateau over the Last Glacial Maximum or last interglacial as indicated by loess records. Consequently, the important source of moisture to the Lake Baikal catchment is via the Westerlies from the North Atlantic. During the Late Glacial an anticyclone existed over the Fennoscandian Ice Sheet which reduced the direct transport of Westerlies to Eurasia (Khotinsky 1984). As the ice sheet ablated with the onset of deglaciation, the anticyclone weakened and Westerlies penetrated further inland. The strengthening of THC and the Gulf Stream related to the melting of Arctic sea ice in the North Atlantic also aid the transfer of warm moist air to continental Eurasia (Driscoll and Haug 1998, Karabanov *et al.* 1998).

1.5.3.2 North Atlantic Oscillation (NAO) and snow extent

While the above teleconnection mechanisms may be most important in explaining climate changes relating to large scale events in the North Atlantic, it is not really known how well these mechanisms fully explain Holocene climate variability in Central Asia (Zhou *et al.* 1999). Another teleconnection mechanism is the North Atlantic Oscillation (NAO) and its related phenomena the Arctic Oscillation (AO). Variation in these has been shown to have a strong influence on climate in Siberia (Hurrell 1995, 1996). The NAO is a north-south oscillation of pressure field between the Icelandic low (65°N) and the Azores High (40°N). The positive (high index) NAO mode has a well developed Icelandic low and Azores High resulting in stronger Westerlies (figure 1.4a), the negative NAO mode occurs when these two systems are weak leading to reduced Westerlies (figure 1.4b). Complete reversals of these pressure systems are rare (Wanner *et al.* 2001). High NAO indices (strong Westerlies) can lead to higher temperatures over Lake Baikal and this connection has been used to explain documented earlier ice break-up dates in southern Lake Baikal (Livingstone 1999). Lake Baikal ice cover duration also has a strong link to the AO and to other modes of Northern Hemisphere circulation, most notably the Scandinavian Oscillation but also the NAO (Todd and Mackay 2003). A positive phase of the AO will result in advection of warm temperatures over Eurasia and subsequently a decrease in ice cover on Lake Baikal (Todd and Mackay 2003). It is also possible that the Asian monsoons will be influenced indirectly via the NAO driven Westerlies altering the Siberian High.

The NAO/AO and Westerly transport of warm air have been shown to determine snow depth over Eurasia, a positive mode results in warmer temperatures and increased precipitation and snow depth (Clark *et al.* 1999, Ye 2001a, b, Aizen *et al.* 2001). This relationship is not

thought to hold for areas under the influence of the Siberian High due to the extreme cold temperatures to which the NAO driven temperature changes will have little influence (Clark *et al.* 1999). The importance of the NAO/AO index in Northern Hemisphere climate has been modelled, e.g. a low NOA/AO index existed during the Maunder Minimum-LIA period that propagated cooling 'downstream' to continental areas via the Westerlies. This mechanism allowed the amplification of the cooling caused by a decrease in solar activity (Shindell *et al.* 2001).

The extent of Eurasian snow cover in turn has a teleconnection to Asian summer monsoon strength. High Eurasian snow cover can delay the build up of monsoon circulation through reducing solar radiation absorption due to snow's high albedo and consumation of solar energy via snow melt and evaporation (Ye and Bao 2001). Modelling studies have shown this to be the case (Barnett *et al.* 1988, 1989, Overpeck *et al.* 1996), while Liu and Yanai (2002) identify the area in northern Mongolia (Lake Baikal's catchment) to have a strong correlation between high Eurasian snow cover and a reduction in summer rainfall.

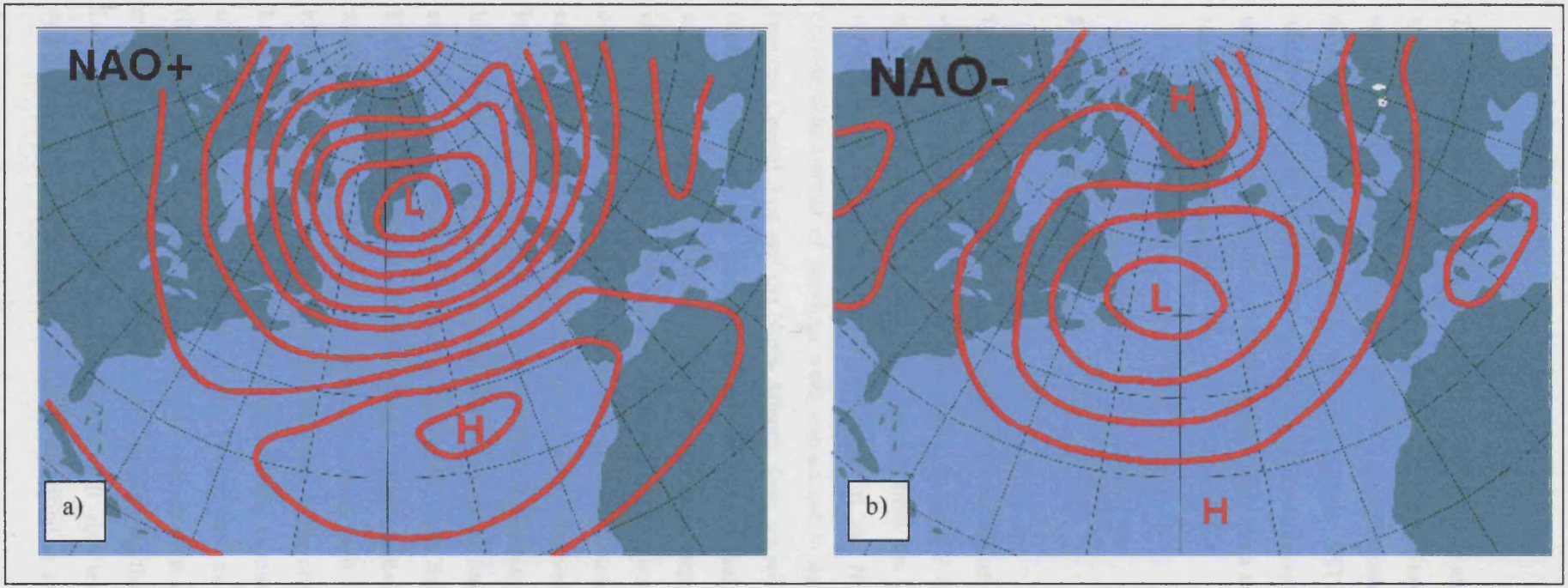

Figure 1.4: a) Schematic surface pressure distribution during the positive phase of the NAO with a strong Islandic Low and Azores High leading to stronger Westerly transport. b) Schematic surface pressure distribution during the negative NAO phase with a weak Islandic Low and weak Azores High leading to reduced Westerly transport (adapted from http://www.defra.gov.uk/environment/marine/quality/03.htm).

1.5.4 Summary

Teleconnections are present between the North Atlantic and Central Asia as shown by similar climatic events recorded in these regions. Air temperature change in the North Atlantic can reorganise atmospheric circulation on a hemispheric scale mainly via heat/moisture transfer through the Westerlies. Changes in North Atlantic SSTs can influence the Siberian High, which in turn can affect the strength of the Asian monsoons. Snow cover extent over Eurasia, which can be driven from the North Atlantic, also has a significant impact on the subsequent summer monsoon strength.

1.6 Aims and objectives

The aim of this thesis is to reconstruct to a high resolution, Holocene and Late Glacial climate variability from the sediments of Lake Baikal in order to aid understanding of climate change in continental Eurasia, an area far removed from the influence of ocean-driven climate variability, and how this relates to change in the North Atlantic region. Despite the considerable amount of previous work carried out to describe and explain teleconnections between Central Asia and the North Atlantic there are still some problematic areas that need further investigation, in particular around the Lake Baikal region which is removed from the direct influence of the Asian Monsoons. Although large glacial/interglacial shifts can be identified, and substantial research on biogenic silica content as a climate proxy has been carried out at a resolution adequate for this purpose (Colman *et al.* 1995), it is still not known conclusively if the millennial scale periodicities observed in the North Atlantic during the Holocene (Bond *et al.* 1997) are present in Central Asian records mainly due to the lack of high resolution records. The Late Glacial sequence as found in the Greenland ice cores has also only been analysed at coarse resolution from Baikal (e.g. Bradbury *et al.* 1994, Karabanov *et al.* 2000) and this needs further investigation to elucidate comparative magnitude and timing of events. Holocene events such as the 8.2 ka event have not been irrefutably identified in the region possibly due to the coarse resolution of some studies. In Lake Baikal, the favoured proxy for palaeoclimatic reconstructions has been either biogenic silica content or diatom valve abundance. Factors such as diatom dissolution in Lake Baikal (Ryves *et al.* 2003) have been given little consideration and may mean that some climatic events are not recorded by this proxy thus highlighting the need for a multi-proxy approach. Local variability and site specific factors will also mean climatic events may not be synchronous, this asynchroneity has been identified in monsoonal China (He *et al.* 2004)

Comparisons to the Lake Baikal region in the north should further substantiate the nature of local climate variability. Overall, previous studies of Lake Baikal as a Holocene palaeoclimatic archive have been at a relatively coarse resolution (centinnial to millennial) and often only based on diatom reconstructions.

In this study, a high resolution palaeoclimatic record from Lake Baikal is obtained using diatoms and oxygen and carbon isotopes as complimentary proxies. Combined with better dating of records, this will help identify further teleconnections or discrepancies between the presence/absence and timing and magnitude of climatic events. Specific aims and objectives relating to the application of these techniques to Lake Baikal sediments will be outlined in the following chapters. However, a main objective is to gain understanding of modern diatom autecology by using a transfer function approach and investigating contemporary phytoplankton and also an assessment of stable isotope dynamics in relation to current climate and limnology as a guide to interpret the palaeo record.

1.7 Thesis outline

This thesis has begun with an assessment of the possible causes of Holocene climate variability. Teleconnections between the North Atlantic and Central Asia have also been discussed and areas that need additional research have been identified. The two applied palaeoclimatic proxies of stable isotopes and diatom analysis are introduced in chapter 2 along with a general description of the study site Lake Baikal and the methodologies of coring and radiocarbon dating. The following three chapters attempt to understand the modern lake; in terms of isotope dynamics (chapter 3), modern diatom distributions in relation to environmental variables with a monitoring approach (chapter 4) and a transfer function approach along with autecological summaries for the main diatom species found (chapter 5). With this understanding of the modern lake, the Holocene palaeoclimatic record is interpreted with specific reference to North Atlantic teleconnections. Diatom reconstructions are presented in chapter 6, oxygen isotopes in chapter 7 and carbon isotopes in chapter 8. Results are synthesised and concluding remarks given in chapter 9.

Chapter Two

Study site and general methodology

2.1 Introduction

This chapter deals with a description of the study site and the methods that are applicable to the project as a whole such as coring and statistical techniques as well as a introduction to diatoms and stable isotopes as palaeoclimatic indicators. Specific methodologies such as sample preparation and analysis will be dealt with in detail in the following chapters.

2.2 Lake Baikal

2.2.1 Physical characteristics

Lake Baikal (N56°50' E104°24') (figure 2.1, 2.2), formed in a rift zone estimated to be over 30 million years old (Belova *et al.* 1983), as a result the lake is the oldest in the world. The Baikal rift zone is the deepest continental depression on the planet, consequently Lake Baikal is the world's deepest lake although only 7th in terms of surface area. Details of morphological characteristics are given in table 2.1. Tectonic activity still has an influence on lake morphology with the expansion of the rift zone, but earthquakes can also lead to the submerging of shallow bays. In 1861, a large earthquake caused an area of the Proval Bay (figure 2.1) in the south of the lake to subside (Kozhova and Izmest'eva 1998). Although tectonic activity may locally disturb basal sediments, these have never been modified by glaciation. This means there is approximately 7.5 km of possibly undisturbed sediment in some areas, making Lake Baikal a promising site for palaeoclimatic work. The lake is situated in a mountainous region with principal ranges including the Hamar-Daban Range, the Primorsky Range and the Eastern Sayan Massif in the south, while in the north the Baikalsky range and the Bargusinsky Range border the lake (figure 2.1). These mountains give rise to 365 tributaries to the lake, the principal one being the Selenga River (1480 km long), which forms the world's largest inland delta on the south-east shore of the lake. Lake Baikal's catchment is predominantly to the south of the lake and covers a large area of the northern Mongolian highlands (figure 2.3). Further details of fluvial input are outlined below but the other main tributaries are the Upper Angara River and Barguzin River at 640km and 370km

in length respectively. Lake Baikal's outflow is the Lower Angara River in the south (figure 2.1). The geology of Lake Baikal's catchment is heterogeneous, although very similar in most regions. Mountain ranges to the south of the lake consist of Archean crystalline rocks (micas, marble, gneisses) with areas of younger granites (Kozhova and Izmest'eva 1998). Tertiary basalts top the crests of the mountains, while Quaternary basalts lie within the rift valleys. The area around the central basin is dominated by Quaternary and Tertiary lacustrine and glacial deposits. Mountains in the north of the catchment consist of Archean and Proterozoic rocks

Characteristic	Value
Altitude	455.6 m asl
Length	636 km
Mean width	49.3 km
Total area	315000 km^2
Maximum depth	1642 m
Mean depth	738 m
Volume	23015 km^3
Catchment area	540000 km^2

Table 2.1: Morphological characteristics of Lake Baikal (Mackay *et al.* 2002 after Kolokoltseva 1968).

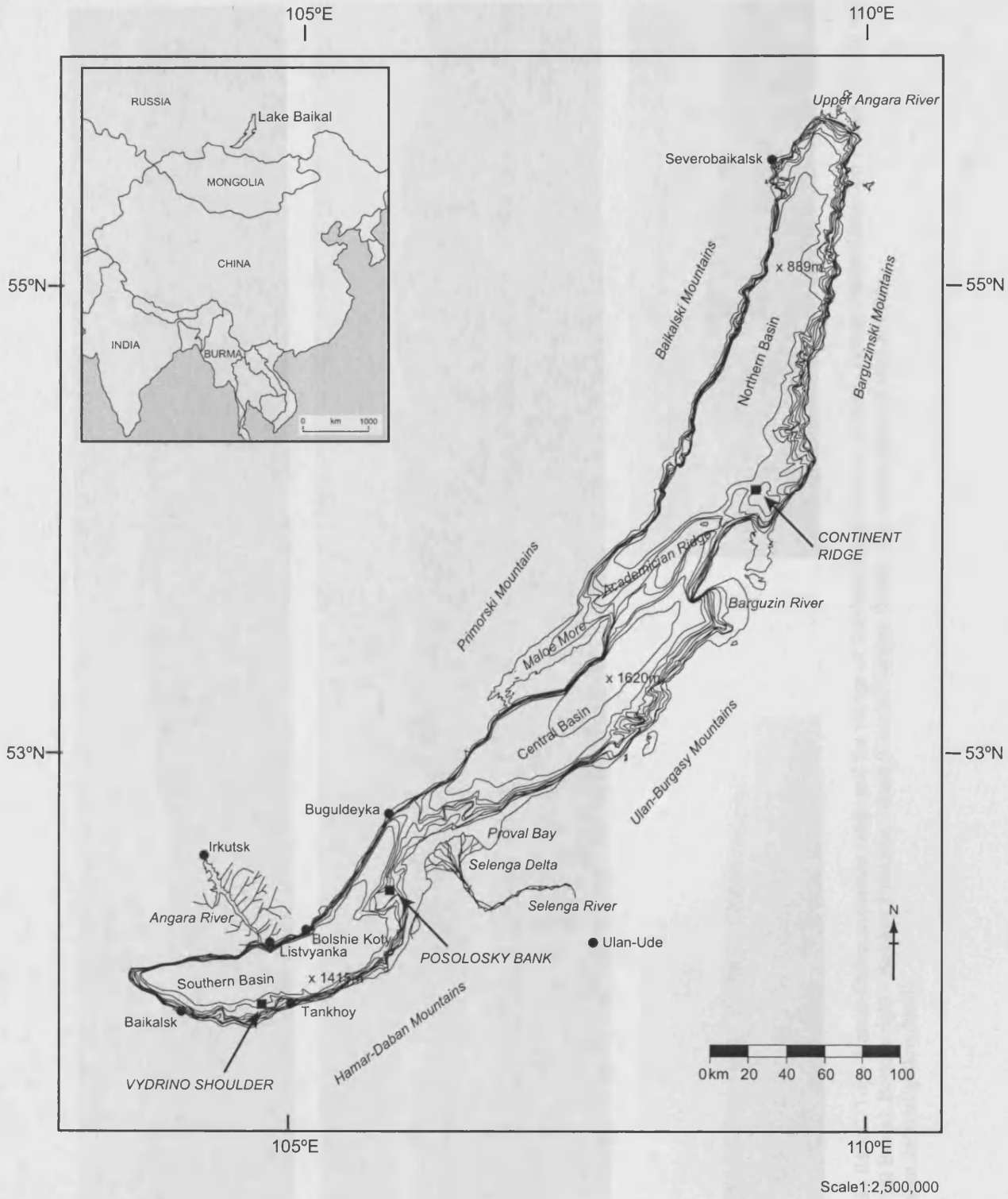

Figure 2.1: Map of Lake Baikal showing CONTINENT coring locations (capital letters), principal settlements, rivers, mountain ranges and batyhmetric features. The three basins of the lake are shown with the maximum depth of each. Bathymetric contours are every 100 m.

Figure 2.2: Photographs of Lake Baikal. Top - Hamar-Daban mountain range and the village of Taikhan (South Basin). Middle - Hamar-Daban Mountain Range. Bottom left - Svyatoy Nos Peninsula (Central Basin). Bottom right - Bolshoy Ushkaniy Island (Central/Northen Basin). All photographs by Jens Klump. (http://CONTINENT.gfz-potsdam.de/html/gallery.html).

Figure 2.3: Map of Lake Baikal catchment and tributaries (Prokopenko *et al.* 2001).

The lake itself consists of three basins (North, Central and South) separated by underwater highs (figure 2.1). The South and Central basins, maximum depths 1415 m and 1620 m respectively, are separated by a ridge opposite the Selenga Delta. The Central and North Basin (maximum depth of 889 m) are separated by the Academician Ridge. According to long term records before 1956, Lake Baikal's water surface stood at an average of 455.6 m above sea-level with variability of up to ±2 m (Kozhova and Izmest'eva 1998). In 1956, the first of a series of dams were built on the Lower Angara River which raised the lake level by about 2m. Lake levels are now a direct result of hydro-power plant activity.

Pollution from anthropogenic activity in the area may also be having a detrimental impact on the lake. Industrialisation, in particular from two paper and pulp mills built in the 1960s and 1970s in the shore of the South Basin, extensive logging in the catchment and overfishing were thought to be linked to a decline of Lake Baikal's endemic taxa (Mackay *et al.* 2002). However, several studies have shown that the lake's diatom community is not being affected

by pollution but is responding to natural environmental or climate change (Flower *et al.* 1995, Mackay *et al.* 1998).

2.2.2 Modern limnology

2.2.2.1 Ice cover and water budget

Lake Baikal is typically ice covered 4-6 months a year, with ice formation occurring earlier and persisting longer in the North Basin. Freezing usually begins in the north in late October, and early December in the south (Shimaraev *et al.* 1994) - full consideration of the lake's ice cover is given in chapter five. The most up-to-date estimation of Lake Baikal's water budget is given by Shimaraev *et al.* (1994). Modern lake water is made up of 83% river input and 17% direct from precipitation. Of the major tributaries, the Selenga River supplies 47%, the Upper Angara River, 13% and the Barguzin River, 6%. Water loss from the lake is mainly by outflow from the Lower Angara River (81%) and evaporation (19%). Superimposed on these general figures are minimal losses and gains from seepage and groundwater flow respectively (Seal and Shanks 1998). Average lake water residence time is estimated at 377-400 years (Gronskaya and Litova 1991). This figure varies in the lake's three basins, being highest in the North Basin at 580 years compared to 105 years in the South Basin (Hohmann *et al.* 1997).

2.2.2.2 Thermal stratification

The relationship between water temperature (T) and density is important for the convective turnover and stratification of water bodies. At atmospheric pressure, fresh water is at maximum density at 4°C (T_{md}), above and below this temperature the density of surface water decreases. However, with increased depth, water is at maximum density at slightly lower temperature due to increased pressure. Lakes in temperate regions are often dimictic in that they circulate freely twice a year in spring and autumn (Wetzel 2001). Solar radiation during the summer heats the surface water faster than the heat can be distributed by mixing, this causes development of direct stratification with a layer of warm water (epilimnion) overlying cooler waters (hypolimnion) with a boundary zone between the two called the metalimnion. During autumn there is net heat loss causing the epilimnion to cool and become denser, sinking water causes the metalimnion to deepen until the whole water column circulates beginning the autumn turnover and temperature loss continues until $T \leq 4$°C. Winter ice begins to form and an inverse stratification occurs with cold, less dense water overlying

warmer denser water at around 4°C. During spring ice-out the lake overturns and becomes isothermal again allowing direct summer stratification to begin.

Due to Lake Baikal's great depth the above processes only occur in the upper part of the water column as convection currents and wind stress can only mix to a depth of 200-300 m (Shimaraev *et al.* 1994). As a result the water column can be divided into two layers; an upper zone to a depth of 250 m where free convection occurs and a lower zone from 250 m to the bottom sediments of permanently stratified deep water (Shimaraev 1977, Shimaraev and Granin 1991, Ravens *et al.* 2000). The boundary between these layers is known as the mesothermal temperature maximum (MTM) where $T = T_{md}$. T_{md} decreases with depth due to increasing pressure at a rate of 0.021°C bar^{-1} (Chen and Millero 1986, Eklund 1965). Consequently the MTM in Baikal is ~3.5°C (Shimaraev *et al.* 1994).

Due to the MTM, free convection cannot occur between the two layers as water at the MTM is at maximum density. As a result it may be expected that deep water in the lower layer is poorly ventilated and will have a low oxygen content as is the case for other deep lakes such as Lake Malawi (Martin *et al.* 1993). However, the high oxygen content of Baikal's deep waters (Weiss *et al.* 1991) must mean ventilation is occurring (Shimaraev *et al.* 1993). Water ages of these deep waters are shown to be no greater than 16 years using CFC tracers (Weiss *et al.* 1991).

2.2.2.3 Mechanisms of deep water ventilation

Weiss *et al.* (1991) suggest a mechanism for deep water ventilation based on thermobaric instability which involves the interdependence of temperature and pressure. They recognise a stable inversely stratified lake during spring, with surface waters at 4°C over colder water near T_{md}. If the interface between the two layers is deepened (e.g. by wind stress or salinity change), the overlying water becomes nearer to T_{md} than the deeper water resulting in a plume of colder water sinking to displace deep water. However, Hohmann *et al.* (1997) noted a problem with this mechanism in that the deepest waters can be as cold as 3.1°C meaning the corresponding depth of the MTM would have to be pushed down to an unrealistic ~350 m to allow water at 3.1°C to sink.

Shimaraev *et al.* (1993, 1994) considered deepwater ventilation to be localised at thermal bars. Littoral/coastal waters warm and stratify in spring while the main water body remains cold and isothermal. The transition between these two zones is the thermal bar. The mechanism of ventilation that occurs is called cabbeling and is based on the fact that mixing

water of two different temperatures results in a mean increase in density (Hohmann *et al.* 1997). Mixing of the warm littoral waters and colder open waters results in a denser water mass which sinks along the bottom slope of the lake to great depths allowing ventilation of deep water. However, Hohmann *et al.* (1997) state that it is still unclear how the sinking cold water can cross the MTM and it may be the thermal bar only accounts for mixing in the top 200-300 m.

In order for descending water to pass through the MTM, Hohmann *et al.* (1997) propose that small changes in salinity are enough to induce thermobaric instability where a plume of denser water descends and causes deep water convection. This occurs in areas where water masses of differing temperatures and salinity meet horizontally. For example, such a situation occurs where relatively saline water in the Central Basin (due to the influence of the Selenga River) meets the colder and fresher water of the North Basin at the Academician Ridge.

2.2.3 Modern regional climate

The climate of Eastern Siberia is marked by the highest level of continentality on Earth (Lydolph 1977). The climate is dominated by the position of the Siberian High, jet stream, Summer and Winter East Asian Monsoons (figure 1.3). The Lake Baikal region is currently dominated by the Siberian High pressure cell in winter as cold arctic air settles in western Mongolia and is trapped by surrounding mountains. This deflects moist Westerlies and cyclonic storms away from the Baikal catchment and leads to extremely cold and arid winters (Lydolph 1977) (figure 2.4). A moist 'cyclonic corridor' exists to the north through which storms forming on the Asiatic Arctic Front pass from the Kara Sea, over the continent and out to the Pacific via the Sea of Okhotsk (Lydolph 1977). Precipitation through this corridor is much greater than in the high-pressure regions either side. During summer, westerly transport is reduced and the catchment is usually engulfed in a low-pressure system and cyclonic storms form along the Asiatic Polar Front to the south of Lake Baikal (figure 2.5). As a result precipitation over the whole catchment is much higher and air is kept moist by thawing of the ground and convection due to higher temperatures (Lydolph 1977). Between 70 – 90% of annual precipitation falls during the summer months (Shimareav *et al.* 1994).

During summer, precipitation is highest over the Khamar-Daban mountains at up to 1400 mm yr^{-1}. Over the lake surface precipitation ranges from 200 – 500 mm yr^{-1}, the lowest being over the Central Basin. Minimum precipitation of 1 – 3% of the annual total is usually recorded in February. (Shimaraev *et al.* 1994). Total cloudiness has two annual maxima: July – August and November – December; and two minima, February and September – October (Kozhova

and Izmest'eva 1998). During winter, temperature can reach an absolute minimum of -40 to -50°C but usually range from -17 to 25°C. During summer, the average temperature of the warmest month (July) can be 13 to 14°C but reaching up to 30°C on hot and calm days. Winter temperatures in the areas nearby to Lake Baikal, for example Ulan-Ude (figure 1.1) tend to be colder by up to 10°C while summer temperatures on Lake Baikal are warmer (Kozhova and Izmest'eva 1998). This is due to the waters of Lake Baikal modifying the local climate via its immense thermic capacity (Lydolph 1977). Cool lake waters during summer cool the air masses above the lake, while during winter the lake surface is relatively warm in comparison to the surrounding catchment. The winds during cold seasons blow from land over the lake and during warm seasons this is from lake to land. During colder periods, the average velocity for all winds increase, the greatest being the lake's 'lengthwise' winds, the Verkhovik and Kultuk reaching 9 to 10 m s^{-1} (Kozhova and Izmest'eva 1998).

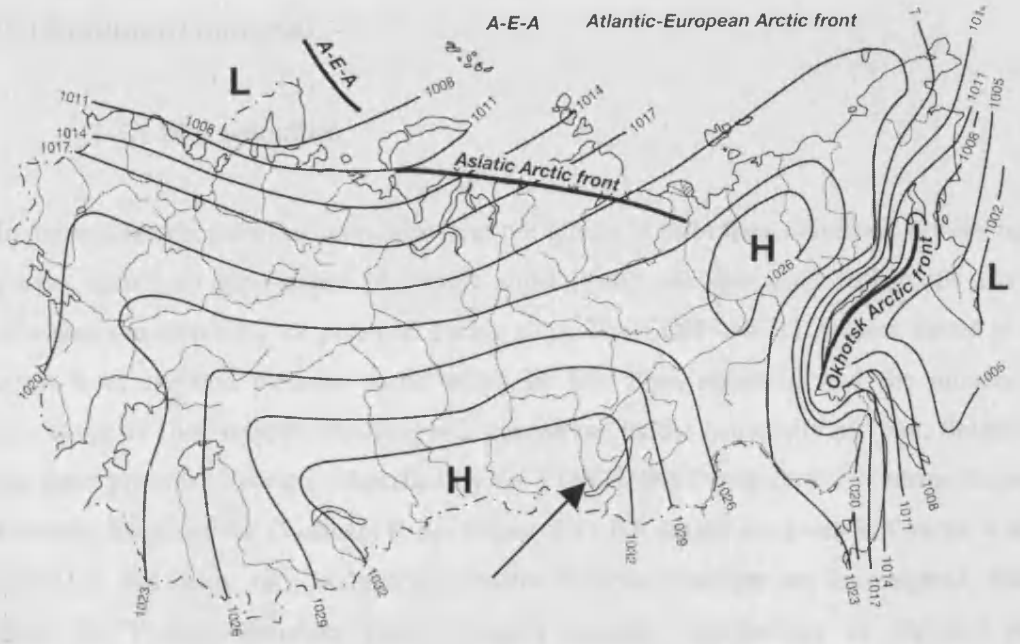

Figure 2.4: General mean sea level pressure (hPa) over Russia in January (Shahgedova 2002). Lake Baikal is highlighted by an arrow.

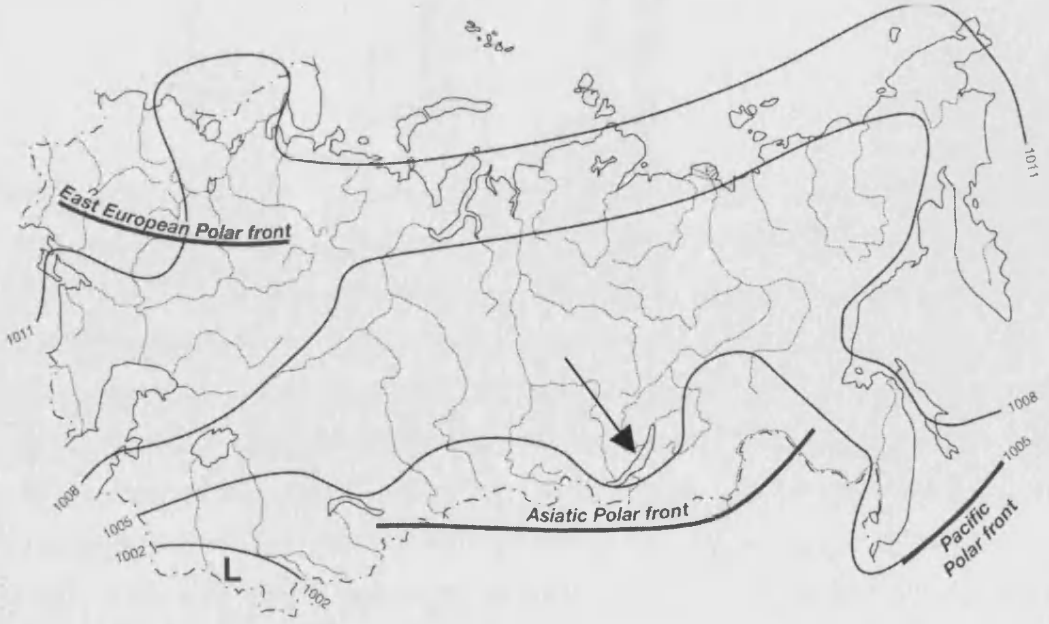

Figure 2.5: General mean sea level pressure (hPa) over Russia in July (Shahgedova 2002). Lake Baikal is highlighted by an arrow.

2.3 Sediment material

2.3.1 Site selection

In order to obtain sediment cores free from the effects of turbidites, slumping, reworking and seismic activity, a combination of seismic profiling and side-scan sonar techniques was used to assess the suitability of potential coring sites. The CONTINENT project aimed to take cores from elevated plateaus suspected to be free from turbidites and the influence of reworking by river inflows. Profiling was carried out by the University of Gent, Belgium on the three potential locations identified by the CONTINENT project: the Vydrino Shoulder, Posolsky Bank and the Continent Ridge (figure 2.1), full details are given in Charlet *et al.* (in press). In this study, only sediments from the Vydrino Shoulder are investigated. Profiles from the Vydrino Shoulder show a highly complex morphology of elevated ridges perpendicular to the coast separated by deep incised channels (figure 2.6). These channel fills are flat and contain coarse sandy sediments. A coring location was selected on an elevated plateau which offered a calm sedimentary environment with little potential for reworking. At least the upper 100 m of sediment appear to be undisturbed by tectonic activity and reworking.

Figure 2.6: Sonogram of the Vydrino Shoulder area showing the high-relief levee and channel environment. The coring site is not shown here, but was located on top of a flat, high-relief plateau (Marc de Batist, unpublished).

2.3.2 Coring

Long coring was carried out during summer 2001 from the R/V Vereshchagin (figure 2.7) using a piston corer and a shorter box (kasten) corer both of which rely on weights to drive the core tube into the sediment. Piston cores were 11.7 m in length (two 6 m sections bolted together) and 12 cm diameter, driven by a 1.5 tonne weight (figure 2.8, 2.9). A trigger core of 2.1 m length and 9 cm diameter with a 150 kg weight (figure 2.10) was used with the main piston corer to capture the surface-water interface undisturbed. The piston core and the trigger core (suspended a short distance below) were winched to the lake bed and as the trigger core collected the surface interface, the loss of tension on the cable attaching it to the main corer causes a latch to be released and allows the piston corer to free-fall several metres and drive into the sediment. During retrieval, material was retained in the corer by a copper lamellae 'core catcher' fitted at the end of the tube. Cores were opened longitudinally by sawing through the tubes. The box corer was driven by a 1 tonne weight (figure 2.10), measured 15 cm by 15 cm and was 6 m long (figure 2.11). Cores were taken by winching the corer down through the water column and allowing the weight to drive the core tube into the sediment.

Material was retained by a self-closing mechanism fitted to the end of the tubing. Cores were opened by unscrewing the core casing. Additional short gravity cores have been taken throughout the duration of the project in particular during the ice-covered period in the South Basin. The gravity corer used had a much narrower diameter than the other corers used (6 cm) and shorter (1 m), it collects sediment by being released and driven vertically into the sediment. This method of coring nearly always captures the surface-water interface intact unlike piston coring. Gravity cores were sealed and opened longitudinally at the GFZ where they were checked for turbidites and sub-sampled by slicing with copper discs. sub-samples were stored in plastic sample bags and refrigerated.

Several problems were encountered during the summer coring campaign included the lack of reliability of the power supply for the winch on board the R/V Vereshchagin. A box core casing was crumpled during core retrieval meaning only a shorter core could be retrieved at one site (figure 2.12) and a release of gas hydrates at a core from the Posolosky Bank disturbed sediments in one of the piston cores causing several of the bolts joining the two sections of the core to be sheared off while also warping the metal joining clamp (figure 2.13). None of these problems affected the profiles analysed here.

On opening at the GFZ, cores were split into a working half and an archive half and both sections were kept refrigerated at 4°C. Working sections were then photographed, described visually and analysed using a GEOTEK Multi-Sensor Core Logger for X-ray radiography and colour line scans while gamma-ray density, p-wave velocity, magnetic susceptibility and water content were also measured. All results are archived on the CONTINENT website.

During the long coring campaign, multiple cores were taken at each of the three coring sites, consisting of one box core from each site and three piston cores. A standard nomenclature was used for all sampling and coring carried out during the CONTINENT project, an example for core CON01-605-5 is explained by table 2.2.

The details of the Vydrino cores used in this study are given in table 2.3. The lithology of cores CON01-605-3 and 3a have been described (figure 2.14), this shows that at least for the Holocene, cores appear to be undisturbed by tectonic activity, turbidites slumping or reworking. However, it is not possible to correlate the trigger and piston cores on the basis of this log.

Description	Code	Explanation
Project code	CON	CONTINENT Project
Campaign	01-6	Year 2001 – 6th Campaign
Station	05-	Station (i.e. 5th of 01-6)
Activity	1	First activity at station 05

Table 2.2: An example of core naming protocol as used by the CONTINENT project. Activities included coring, water sampling (for phytoplankton, water chemistry, isotopic analysis), seismic surveys and surface sediments sampling amongst others.

Core code	Type	Latitude	Longitude	Date	Water depth	Core length
CON01-605-3	Piston	51.5849	104.8548	31/07/01	675m	10.45m
CON01-605-3a	Trigger	51.5849	104.8548	31/07/01	675m	1.73m
CON01-605-5	Box	51.5835	104.8518	01/08/01	665m	2.50m
CON01-105-6	Gravity	51.6000	104.9000	13/03/01	Unknown	Unknown

Table 2.3: Cores collected by the CONTINENT project from the Vydrino Shoulder, Lake Baikal used in this study.

Figure 2.7: The R/V Vereshchagin at Listvyanka, southern Lake Baikal

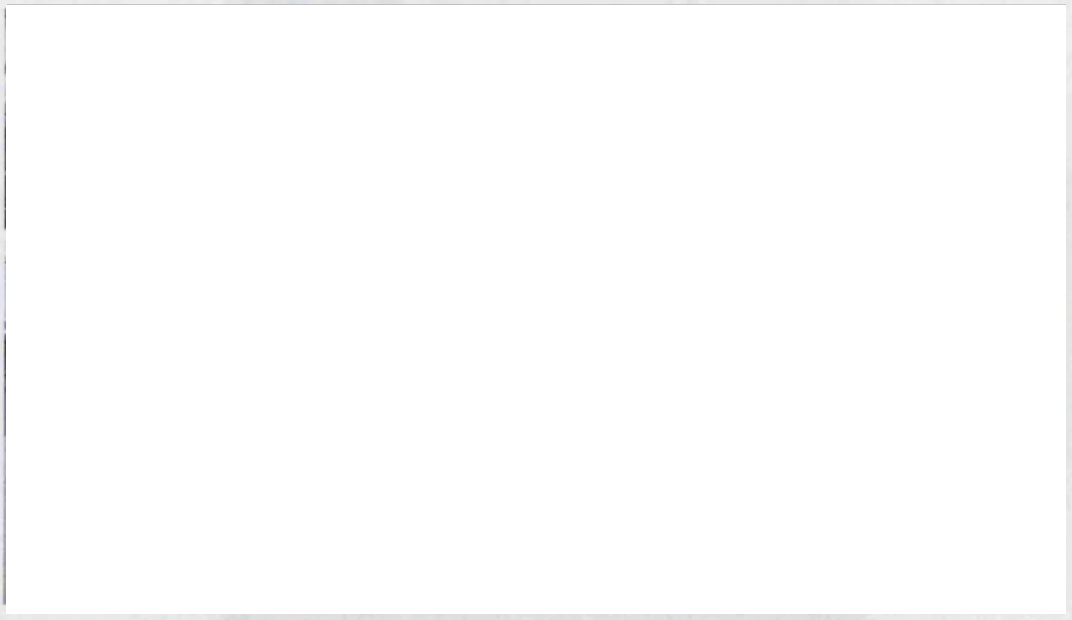

Figure 2.8: The piston corer being prepared

Figure 2.9: Weights for the box corer (left) and trigger corer (right).

Figure 2.10: Weight for the piston corer

Figure 2.11: Retrieval of the kasten corer

Pictures taken by Jens Klump (http://CONTINENT.gfz-potsdam.de/html/gallery.html).

Figure 2.12: Box core casing crumpled during core retrieval. The core retrived (at the Posolsky site) was shortened as material below the crumpled section had to be disgarded. Photo by Jens Klump.

Figure 2.13: Piston core casing damaged by gas hydrate release during core retrieval. Photo by Anson Mackay

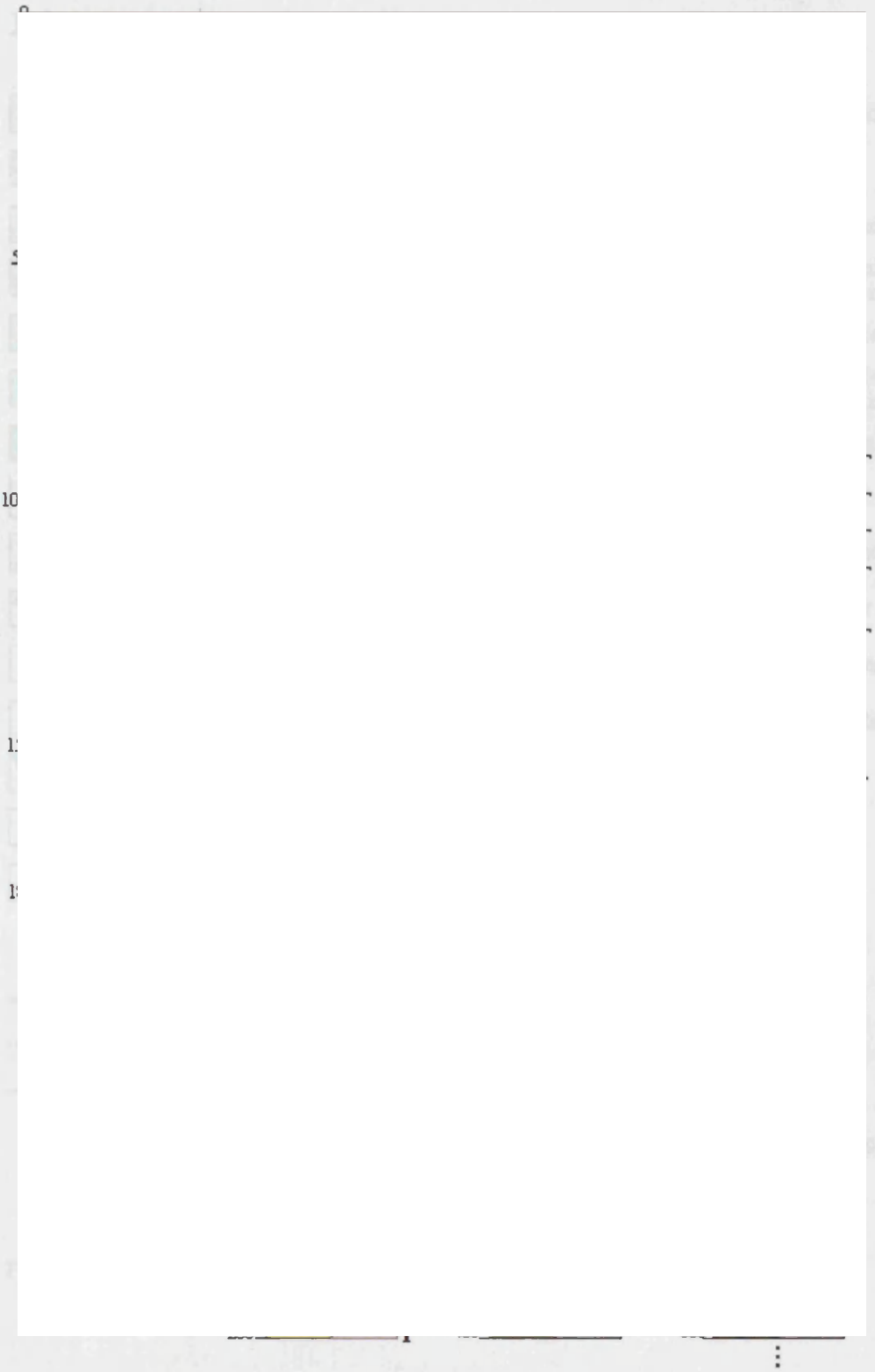

Figure 2.14a: Lithological description of cores CON01-605-3 and 3a from the Vydrino Shoulder, all units are in cm (Florence Hauregard, unpublished). For key see figure 2.14b (overleaf).

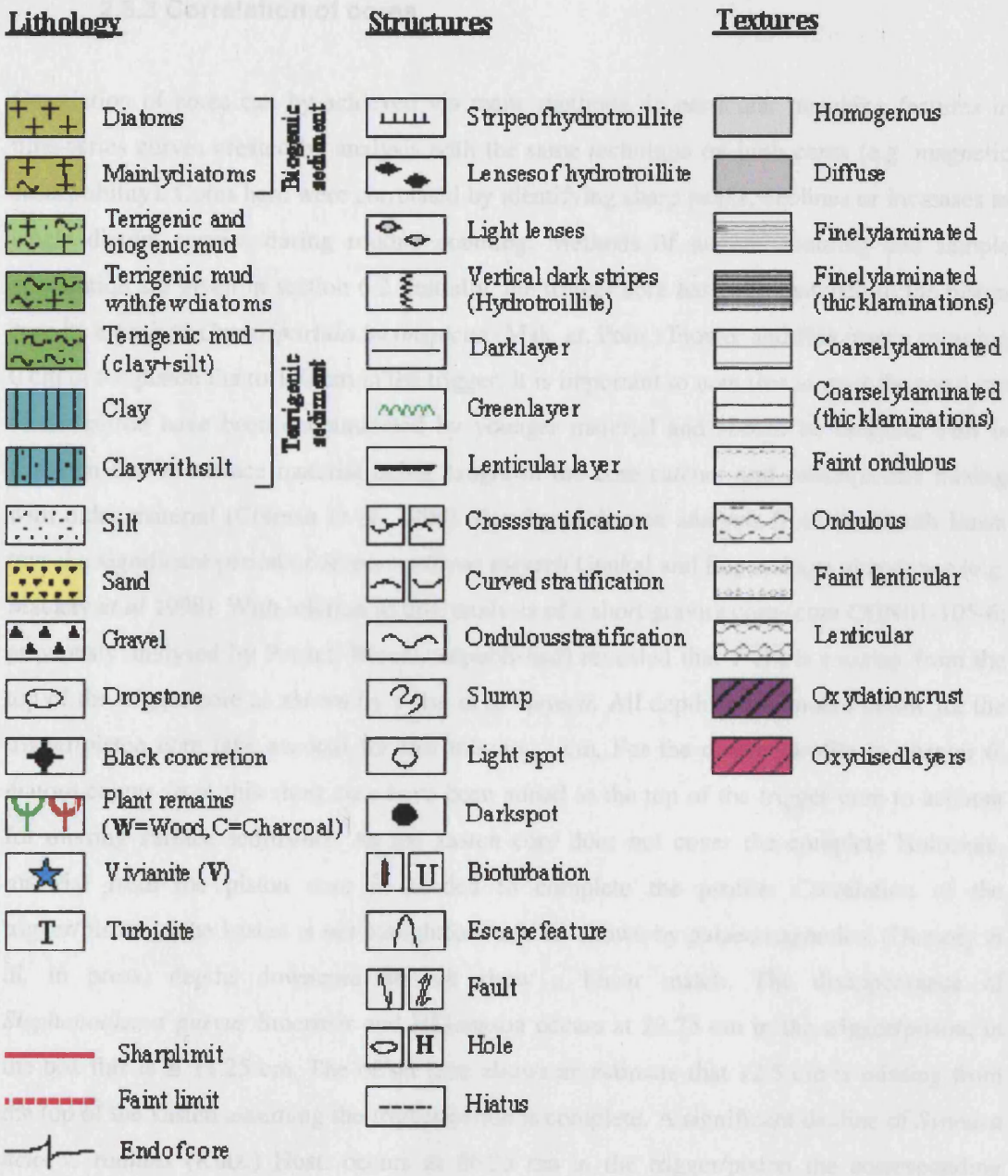

Figure 2.14b: Key to the lithological description.

2.3.3 Correlation of cores

Correlation of cores can by achieved via many methods, in particular matching features in time-series curves created by analysis with the same technique on both cores (e.g. magnetic susceptibility). Cores here were correlated by identifying sharp peaks, declines or increases in single diatom species during routine counting. Methods of diatom counting and sample preparation are given in section 6.2. Initially, the trigger core has been matched to the piston core by a peak of *Crateriportula inconspicua* (Mak. *et.* Pom.) Flower and Håkansson meaning 0 cm in the piston fits to 130 cm in the trigger. It is important to note that at least the top 4 cm of the piston have been contaminated by younger material and should be omitted. This is common due to surface material being caught in the core catcher and subsequently mixing with older material (Colman *et al.* 1996). Results of diatom analysis from the South Basin reveal a significant period of *Stephanodiscus meyerii* Genkal and Popovskaya abundance (e.g. Mackay *et al* 1998). With relation to this, analysis of a short gravity core (core CON01-105-6; previously analysed by Patrick Rioual, unpublished) revealed that 7 cm is missing from the top of the trigger core as shown by a rise in *S. meyerii*. All depths now quoted below for the trigger/piston core take account for this missing 7 cm. For the diatom profile in chapter 6, diatom counts from this short core have been added to the top of the trigger core to account for missing surface sediments. As the kasten core does not cover the complete Holocene, material from the piston core is needed to complete the profile. Correlation of the trigger/piston to the kasten is not straightforward. As shown by palaeomagnetics, (Demory *et al.* in press) depths downcore do not show a linear match. The disappearance of *Stephanodiscus parvus* Stoermer and Håkansson occurs at 23.75 cm in the trigger/piston, in the box this is at 11.25 cm. The offset here allows an estimate that 12.5 cm is missing from the top of the kasten assuming the trigger/piston is complete. A significant decline of *Synedra acus v. radians* (Kutz.) Hust. occurs at 86.25 cm in the trigger/piston the corresponding decline in the box is at 86.75 cm or 99.25 cm adjusting for the missing surface. A unique peak of *Hannaea arcus* (Ehrenb.) Patr. in Patr. and Reimer is present at 158.75 cm in the trigger/piston and 160.75 cm in the box (173.25 cm adjusted for missing surface), this gives an offset of 14.5 cm between the two cores at this point. Using these diatom horizons it has been possible to create two complete Holocene-Glacial profiles: firstly, the piston core, trigger core and short gravity core then secondly the box core with material from the piston core to extend the profile to the Late Glacial. These correlations are summarised in figure 2.15. It is hoped that as the cores correlated here were taken from the same locations within a few hundred metres at most (assessed by GPS), the correlations described here are viable and are not distorted by possible spatial variability of diatom abundance.

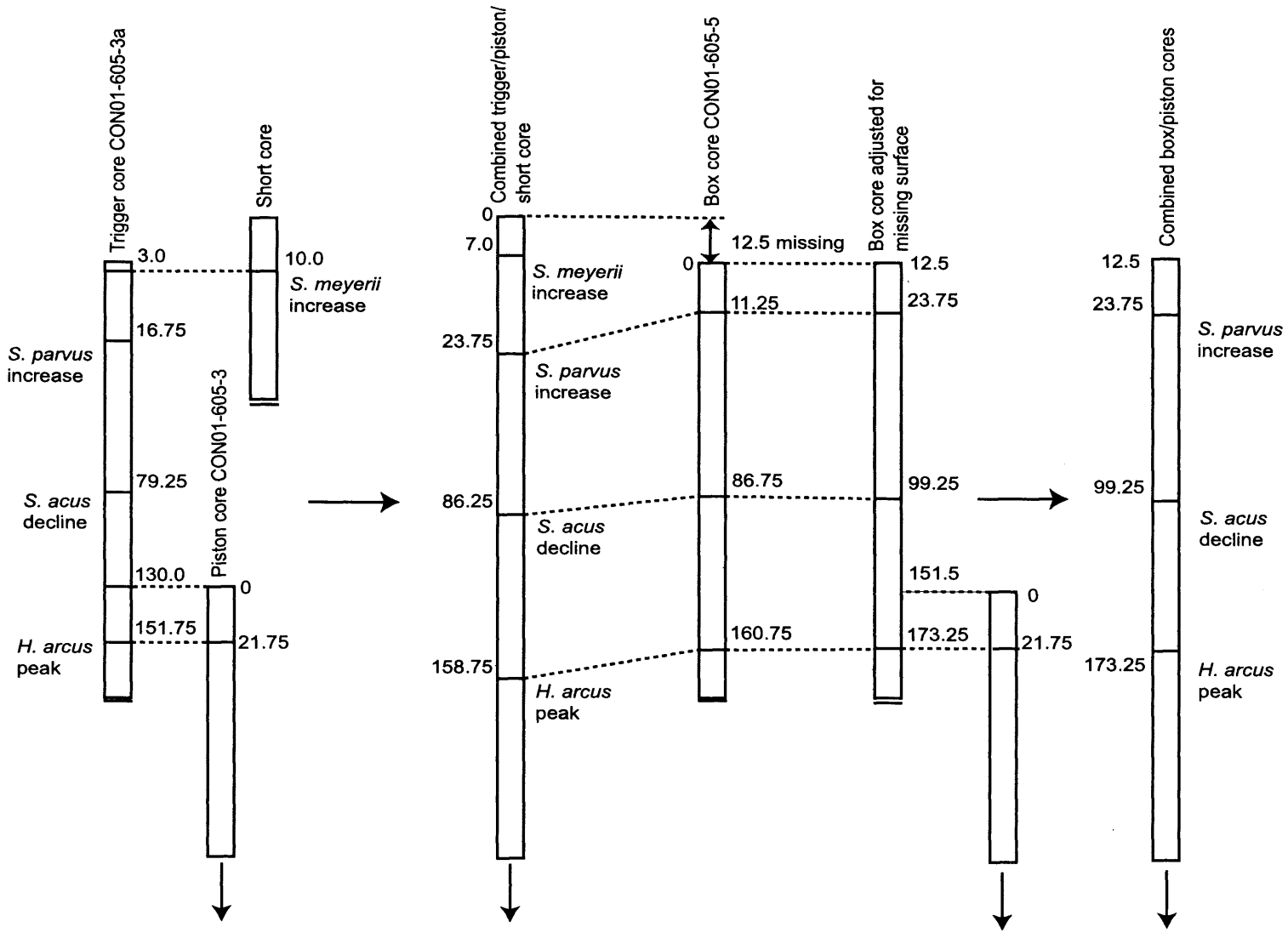

Figure 2.15: Correlation of the Vydrino Shoulder cores (box, piston, trigger and short cores) to make two profiles for the Late Glacial - Holocene Firstly a combined short core - trigger core - piston core and secondly, a combined box and piston core. All units are cm.

2.4 Chronology

2.4.1 Problems of dating Lake Baikal sediments

Dating methods applied by the CONTINENT project include ^{210}Pb, ^{14}C AMS, OSL (optically stimulated luminescence) and palaeomagnetics. For the timescale considered in this study an age model will be based on ^{14}C AMS dating. Radiocarbon dating of bulk TOC from Lake Baikal is problematic mainly due to the low organic carbon content of the lake with surface sediments containing 2-4% carbon and glacial sediments containing as little as 0.2±0.1% (Williams *et al.* 1997). The dating of glacial age sediments are especially problematic as they are susceptible to contamination even from very small amounts of younger carbon. Also, due to the deposition of old carbon material with contemporary organic matter and reworking of material, surface ages are usually older by 1000±500 years (Colman *et al.* 1996). Colman *et al.* (1996) suggest subtracting this apparent surface age from dates obtained downcore. However, it has to be assumed that this contribution from redeposited carbon has remained constant through time. Poor chronological control may have led to the conflicting conclusions of several studies, for example, Qui *et al.* (1993), Bradbury *et al.* (1994), Karabanov *et al.* (2000). Some of the problems posed by dating bulk carbon, in particular, the apparent older surface age, can be reduced with the application of ^{14}C AMS dating of pollen extracts. The analysis of pure pollen samples should remove the problem of organic matter that is not contemporary with pollen. However resuspension of grains and delayed transport from the catchment (due to fluvial erosion of grains buried in soil) can still introduce error. AMS dating has the specific advantage over conventional radiocarbon dating as it counts the actual amount of ^{14}C atoms rather than their decay products (ß emissions) and the ability to measure small samples.

2.4.2 Sample preparation and analysis

Methods to obtain pure pollen samples have been published based mainly on existing palynological methods (Brown *et al.* 1989, 1992, Richardson and Hall 1994, Zhou *et al.* 1997). Samples were cleaned for the CONTINENT project by Dieter Demske (Berlin University) based on a modified standard palynological approach. Sediment was treated with potassium hydroxide (to remove humic matter), sieved at 250 µm, given further chemical treatments of Hydrochloric acid and hydrofluoric acid (silicate removal) before sieving again at 7 µm. A heavy liquid separation stage followed with further treatment with sulphuric acid, bleaching and a final sieve at 10 µm.

AMS dating was carried out at the Marie Curie-Skłodowska University, Lublin, Poland by Natalia Piotrowska and Andrzej Bluszcz. Methods used are given in detail by Goslar and Czernik (2000) and Czernik and Goslar (2001). 1 mg of carbon (pollen) was baked in a quartz tube with copper oxide and silver wool, the tube was then sealed and combusted at 800°C for 4 hours. The CO_2 created by this process is captured and water vapour removed with dry ice. The CO_2 is then reduced to graphite by reaction with hydrogen at 630°C for 3 hours with iron as a catalyst. The obtained iron-graphite powder is pressed into a tablet and stored in an argon atmosphere until measurement with a mass spectrometer against standards of oxalic acid and coal.

2.4.3 Age models

Sediment from the box core (CON01-605-5) and the piston core (CON01-605-3) were dated, the dates have been calibrated using OxCal v. 3.5 (Bronk-Ramsey 2001) by Piotrowska *et al.* (2004). These depths, CO_2 ages and calibrated ages are shown in table 2.4. Corresponding depths in the trigger core to those dated in the box core were estimated by interpolating between the fixed points of diatom species marker horizons (figure 2.15). An age model for the trigger/piston profile and the box/piston profile was formulated by fitting a second order polynomial through the dated points. 0 cm in both cores was taken as the present day (-50 aBP) and no reservoir effect was considered as the dated pollen should not be contaminated with older carbon. Due to different core overlaps, not all 17 ages were used to make each age model. Disregarded ages are shown by 'N/A' in the final two columns of table 2.4. Figure 2.16 and 2.17 show the age models for the trigger/piston profile and box/piston core respectively. 14 of the dated levels were used to formulate the trigger/piston age model while 16 were used for the box/piston age model (table 2.4). These are plotted with error bars indicating ±2 SD on figures 2.16 and 2.17. Disregarded (i.e overlapping) ages are plotted passively on these graphs to support the core correlations given in section 2.3.3.

Sample name	Core	Thickness of sample (cm)	Depth in box core (midpoint) (cm) (adjusted)	Depth in piston core (midpoint) (cm)	Radiocarbon age aBP	Calibrated age aBP (95.4% probability)	Corresponding depth in trigger/piston profile (cm)	Corresponding depth in box/piston profile (cm)
LBB-AMS-1	Box	4	14.5	N/A	1950±35	1905±85	14.5	14.5
LBB-AMS-2	Box	4	34.5	N/A	2375±25	2400±70	32.6	34.5
LBB-AMS-3	Box	3	46.0	N/A	2945±30	3105±115	42.2	46.0
LBB-AMS-4	Box	3	70.0	N/A	4530±40	5180±140	62.0	70.0
LBB-AMS-5	Box	3	91.0	N/A	5455±35	6240±70	79.4	91.0
LBB-AMS-6	Box	3	103.0	N/A	6170±40	7085±145	89.9	103.0
LBB-AMS-7	Box	3	115.0	N/A	6700±40	7575±95	101.7	115.0
LBB-AMS-8	Box	3	135.0	N/A	7760±40	8510±90	121.3	135.0
LBB-AMS-9	Box	3	152.0	N/A	8620±40	9615±95	137.9	152.0
LBB-AMS-10	Box	3	159.0	N/A	8750±50	9750±200	(144.8)	159.0
LBB-AMS-11	Box	4	173.5	N/A	9470±50	10825±275	(159.0)	173.5
LBB-AMS-12	Box	4	186.0	N/A	10030±50	11500±250	(171.5)	186.0
LBF-AMS-11	Piston	6	N/A	15.0	8810±50	9900±300	152.0	(166.5)
LBF-AMS-12	Piston	8	N/A	52.0	10340±60	12300±550	189.0	203.5
LBF-AMS-13	Piston	8	N/A	69.0	10730±60	12700±300	206.0	220.5
LBF-AMS-14	Piston	8	N/A	94.0	11820±70	14350±900	231.0	245.5
LBF-AMS-15	Piston	8	N/A	120.0	13340±130	15850±800	257.0	271.5

Table 2.4: Radiocarbon ages, calibrated ages and errors for dated sections of the Vydrino Shoulder piston and box cores together with depths and ages used to construct age models for the trigger/piston profile and the box/piston profile. Depths in brackets are those on core overlaps and are disregarded from the age model.

58

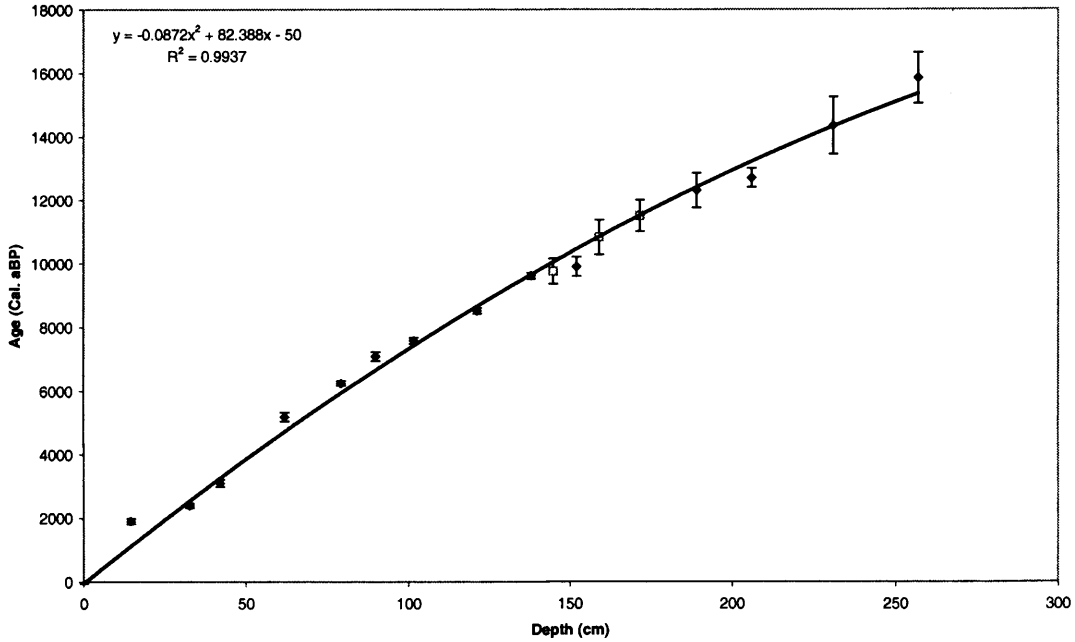

Figure 2.16: Age-depth model and error for the trigger/piston core. Calibrated ages and error, points are fitted with a second order polynomial. Open squares indicate dates on overlapping sections and are plotted passively.

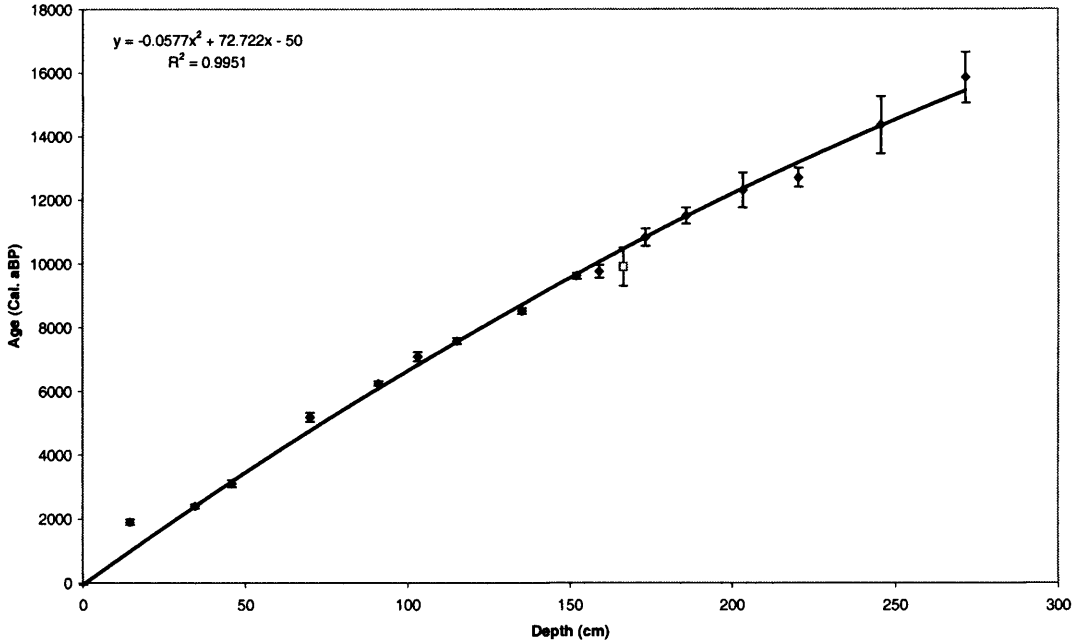

Figure 2.17: Age-depth model and error for the box/piston core. Calibrated ages and error, points are fitted with a second order polynomial. The open squares indicate dates on overlapping sections and are plotted passively.

2.5 Statistical methods (ordination)

Palaeoecological data are usually multidimensional with many species and samples thus ordination is a useful technique to reduce dimensionality and to aid visualisation of the main trends in a dataset (Kovach 1995). The aim of ordination is to arrange sample sites (or core samples) along axes based in species composition. Commonly the end result of ordination is a two dimensional scatterplot with similar species, samples or environmental variables plotted closely while dissimilar variables are plotted further apart. Most ordination methods are based on a process of eigenanalysis which performs linear transformations on multivariate data to extract new axes that summarise as much of the data as possible. Axes are described by an eigenvalue that indicates the relative total amount of variance explained by the dataset, the higher the value, the more important the axis (Kovach 1995).

There are four basic types of ordination based on the underlying species response model (unimodal or linear) and whether the ordination is constrained or unconstrained (Lepš and Šmilauer 2003). A unimodal model assumes the majority of species are distributed along an environmental variable with a well defined optima and tolerance similar to a Gaussian curve. This response is the most ecologically viable. A linear model assumes that as the value of an environmental variable increases, species abundance also increases. This may be observed if only a small part of the environmental gradient has been sampled and the species optimum habitat is not represented. The axes of indirect (unconstrained) methods are interpreted by assuming result is the response to an underlying latent environmental variable which is defined using *a priori* ecological knowledge. Direct (constrained, canonical) methods can only be applied if environmental data are collected with species data. Here, ordination can be used to show species responses to an environmental variable or combination of variables of interest (ter Braak 1995).

The choice of whether to use linear or unimodal methods usually depends on the length of the gradients of the first axis. This can be more complex however, when applying transfer functions (see section 5.7). A species can be seen to appear, rise to its mode and disappear over 4 SD units. This is a complete species turnover (Kent and Coker 1992). Over shorter gradient lengths complete species turnover is not possible and the data appear linear. The exact gradient length to determine whether to use unimodal or linear methods is difficult to define. Kent and Coker (1992) suggest linear methods should be used if axis one gradient is less than 1.5 SD units while ter Braak (1995) considers this value to be 2 SD units. Lepš and Šmilauer (2003) state that unimodal methods are appropriate for gradients over 4.0 SD and

linear for gradients shorter than 3.0 SD linear methods should be used while between 3.0 – 4.0 SD both methods can be used.

Unconstrained unimodal methods include correspondence analysis (CA) and detrended correspondence analysis (DCA) which corrects the faults in CA of an arch effect over the first two axes and a compression of points at the axis ends, both of which are artifacts created during data reduction (Hill and Gauch 1980). Rare species were downweighted in DCA so as to reduce their influence on the final result (ter Braak and Prentice 1989). Constrained unimodal approaches are canonical correspondence analysis (CCA) and a detrended form (DCCA). Unconstrained linear ordination techniques include principal components analysis (PCA) and its constrained form, redundancy analysis (RDA). These techniques were applied using the software package CANOCO v. 4.5 (ter Braak and Šmilauer 2002) and diagrams plotted with CanoDraw v.4.0 (Šmilauer 2002). In ordination diagrams samples are plotted as points. Species are represented as vectors indicating direction of increasing species abundance in linear methods and as points indicating optima (maximum abundance) in unimodal methods. In constrained ordinations, environmental variables are displayed as vectors.

The statistical significance of ordination axes and species-environment relationships can be tested by Monte Carlo permutation tests in CANOCO. To test if the species response is independent of environmental variables (a random response), new permuted datasets are created by assigning environmental variables randomly to species. These are compared to the initial ordination output to calculate a test statistic (Lepš and Šmilauer 2003). For axes to be significant, the variation calculated by the real data should be greater than that of the randomised data.

2.6 Diatoms as palaeoclimatic indicators

Diatoms are unicellular algae of the class *Bacillariophyceae* and consist of an external cell wall composed of silica. A diatom frustule is made up from two valves held together by siliceous belts called girdle bands. Diatoms have been recognised as environmental indicators due to their narrow ecological tolerances and well-defined optima (reviewed in Battarbee 1986, Battarbee *et al.* 2001) and have been applied to palaeoclimatic work to reconstruct two main climatic variables; effective moisture (precipitation minus evaporation) and temperature (Battarbee 2000). This is achieved via two approaches. Firstly, the indirect approach investigates a change in a variable such as pH which can be altered by climate change. Secondly, the direct approach aims to link temperature directly to diatom distribution.

Recently, quantitative reconstructions have been attempted using the transfer function approach (a full consideration of this will be given in chapter 5).

Indirect climate reconstructions have used salinity changes in semi-arid regions (Cumming *et al.* 1995 Fritz *et al.* 1991, 1999 *et al.* Laird *et al.* 1996a, b, 1998a, b), water level change as shown by the ratio of planktonic to littoral diatoms (Gasse *et al.* 1989, Barker *et al.* 1994a, Brugham *et al.* 1998), lake stratification linked to species successions (Reynolds 1973, Bradbury and Dietrich-Rurup 1993), ice cover linked to habitat availability (Smol 1983, 1988, Wolfe 1994, Douglas and Smol 1999) (through-ice light penetration is also important for Lake Baikal and is discussed fully in chapter 3), nutrients (Kilham *et al.* 1996) and pH or alkalinity (Psenner and Schmidt 1992, Sommaruga-Wögrath *et al.* 1997, Koinig *et al.* 1998, Laing *et al.* 1999).

Direct climate reconstructions rely on the assumption that temperature drives the growth and distribution of individual diatom species. Although little is known about the effects of temperature on individual diatom species (Smol 1991), several studies attempt to link diatom distribution to a direct temperature control. Early work such as Hustedt (1956), Foged (1964) and Hasle (1976) describe diatom distributions relative to temperature, and quantitatively divide species into cold, warm and cosmopolitan groups. Other similar studies include Rodhe (1948), Hutchinson (1967), Patrick and Reimer (1966) Patrick *et al.* 1969 and Patrick (1974). The roles of nutrients along with temperature (Goldman and Carpenter 1974, Goldman 1977), and light (Sommer 1994) have been considered. Temperature controls the rate of metabolic processes and photosynthesis. It has been shown that van't Hoff's Q_{10} rule (a 10°C rise in temperature doubles biological processes) holds for diatoms (Goldman and Carpenter 1974). Lotter *et al.* (1995) show that diatoms respond well to large climatic changes such as the Younger Dryas.

Diatom species are the most species-rich class of algae in Lake Baikal consisting of 60% of the entire number of species. In excess of 700 species are thought to exist and of these species about one third are thought to be endemic (Kozhov 1963, Kozhova and Izmest'eva 1998). This high level of endemism is true for many flora and fauna of Lake Baikal. As the lake is extremely old it has provided a relatively stable environment for millions of years giving the opportunity for *in situ* evolution of species (Kozhova and Izmest'eva 1998). The majority of diatom species are epiphytic and are found live up to depths of 60-70 m but are commonly transported into pelagic regions after being detatched from their substrates (Kozhova and Izmest'eva 1998). These benthic communities are extremely diverse although there appears to be no relationship between communities in Lake Baikal's three basins (Flower *et al.* 2004).

Planktonic communities are however dominated by a few endemic species of *Aulacoseira, Stephanodiscus* and *Cyclotella* although non-endemic *Synedra, Asterionella* and *Nitzschia* species are also present in abundance.

Skvortzow (1937) divided Lake Baikal diatom species into groups defined by their possible origin including: Siberian and subalpine, Tertiary freshwater or tropical remnants, marine remnants, brackish species and those of uncertain origin. The habitats of diatoms (whether planktonic or littoral) have been listed in a synthesis of many data sources in Kozhova and Izmest'eva (1998) while little work has been carried out on diatom autecology. Interpretation of diatom species as climatic indicators have been based on limited observations of their seasonal abundances in the phytoplankton (chapter 4) and comparisons to generic analogues (Bradbury *et al.*1994).

Laboratory culture studies are also important in defining optimum temperature tolerances as well as optimum light and nutrient levels. For example, Jewson (1992) and Jewson *et al.* (unpublished) describe the life cycle of *Aulacoseira subarctica* (O. Mull.) Haworth and *Aulacoseira baicalensis* (Meyer) Sim. respectively. However such culture experiments are non-representational of natural conditions and results may not be transferable to natural environments (Anderson 2000).

Diatom palaeoclimatic records can be tempered by differential dissolution of diatom species biasing the record. When using diatoms as environmental indicators it is important to consider the role of dissolution (Barker *et al.* 1990, Fritz *et al.* 1991, Barker 1992, Ryves 1994, Reed 1994). Dissolution has been shown to be an important taphonomic process in Lake Baikal, as only 1% of the planktonic crop is thought to be finally preserved in the sediments (Ryves *et al.* 2003), this is similar to marine systems. Following on from these results, correction factors for differential dissolution have been calculated for five of the main planktonic diatoms in Lake Baikal (Battarbee *et al.* in press) to help aid palaeoclimatic reconstructions (Mackay *et al.* in press) (see section 5.4).

2.7 Stable isotopes as palaeoclimatic indicators

An isotope of an element has the same number of protons and chemical properties as the original element but a different number of neutrons. Isotopes are measured by mass spectrometry and results given as relative difference from a standard (delta, δ) in units of per

mil (‰) and as a ratio of a heavier to a lighter isotope. Delta values are given in relation to the heavier isotope, for example $\delta^{18}O$ represents the ratio of ^{18}O to lighter ^{16}O in terms of deviation from a standard. Two standards are in common use V-SMOW (Vienna – Standard Mean Ocean Water) and V-PDB (Vienna – PeeDee Belemnite), by definition both have δ values of 0‰. Positive delta values are refered to as isotopically higher in relation to the standard, while negative delta values are refered to as isotopically lower in relation to the standard.

The isotopes of interest in this study are the ratios of $^{13}C/^{12}C$ (referred to as $\delta^{13}C$) and $^{18}O/^{16}O$ (referred to as $\delta^{18}O$) and these ratios can be preserved in sedimentary lake material. The only materials in Lake Baikal that are suitable for routine stable isotope analysis are diatom silica and bulk organic matter. Other materials that can be used include ostracods, mollusc shells and authigenic carbonates although these are not present or do not preserve in Lake Baikal. These ratios ($\delta^{13}C$, $\delta^{18}O$) are changed by a process of fractionation which occurs due to differences in rates of reaction for different molecular species leaving a disproportional concentration of one isotope over another on either side of the reaction (Leng 2003). Controls on fractionation can be by environmental processes such as temperature or metabolic effects indirectly linked to climate (Clark and Fritz 1997). As a result δ values can be used for palaeoclimatic reconstructions. Mollusc shells have been used by Fritz *et al.* (1975), von Grafenstein *et al.* (1996, 2000), Leng *et al.* (1998, 1999) and Abell and Hoelzmann (2000). Ostracod carbonate has been studied by von Grafenstein *et al.* (1994, 1999), Schwalb *et al.* (1995), Holmes (1996), Xia *et al.* (1997a, b, c) and Lamb *et al.* (1999) while studies using authigenic carbonate include Stuiver (1970), Eicher and Siegenthaler (1976), Gasse *et al.* (1991), Whittington *et al.* (1996), Lamb *et al.* (2000) and Schwander *et al.* (2000). Finally, diatom silica has been used by Shemesh *et al.* (1992), Barker *et al.* (2001) and Leng *et al.* (2001) (this is discussed fully in section 7.2). However, only diatom silica and bulk organic matter can be used in this study.

2.7.1 Controls on $\delta^{13}C$ in bulk organic matter

The value of $\delta^{13}C$ in bulk organic matter ($\delta^{13}C_{ORG}$) can vary due to many factors. These include the $\delta^{13}C$ values of lake water TDIC (total dissolved inorganic carbon) ($\delta^{13}C_{TDIC}$) which is influenced by the $\delta^{13}C$ of the water feeding the lake from the catchment, exchange of lake water carbon with atmospheric CO_2, biological productivity and lake residence time.

Input of terrestrial carbon from the catchment will also be recorded in analysis of bulk organic material (figure 2.18).

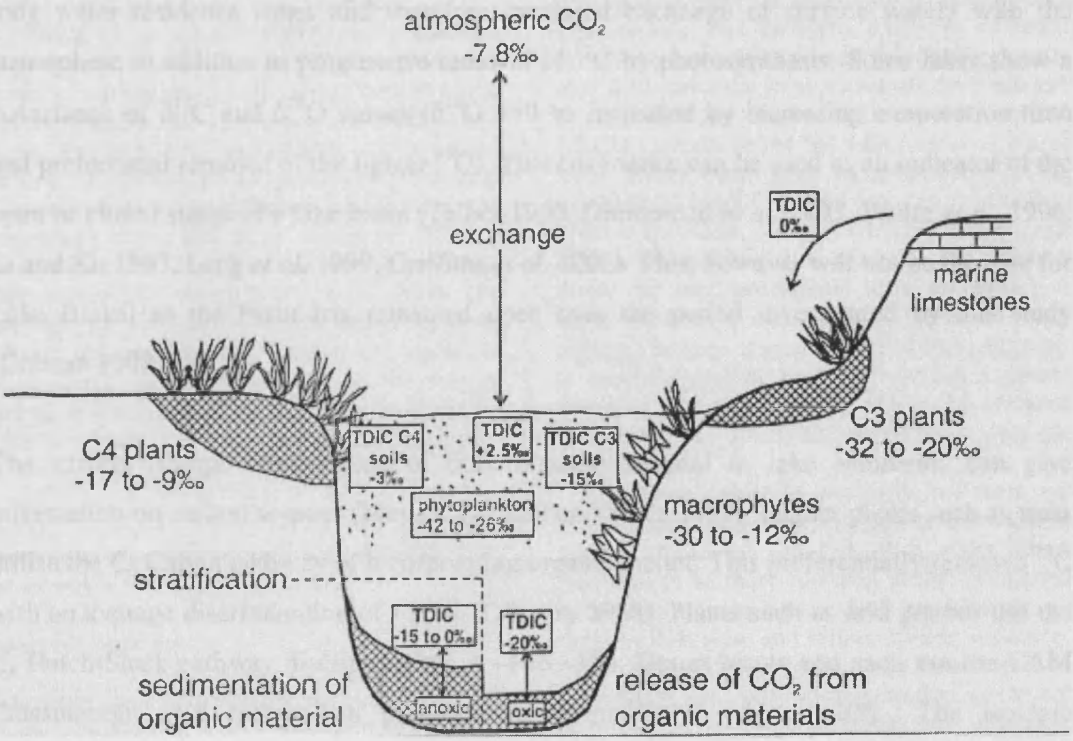

Figure 2.18: Carbon isotope values for the major sources of carbon into lakes and examples of $\delta^{13}C_{TDIC}$ (Leng and Marshall 2004).

$\delta^{13}C$ of lake water TDIC pool will also be influenced by inflow of groundwaters that can have isotopically lower $\delta^{13}C$ values through interactions with rocks, especially in limestone areas. Lake surface waters can exchange with atmospheric CO_2. As a result, changes in atmospheric CO_2 concentration are driven by marine sequestering and release of carbon and other changes to the carbon cycle such as expansion of the terrestrial biomass and fossil fuel burning (Maslin *et al.* 1995). During glacial periods atmospheric CO_2 content is low and subsequent $\delta^{13}C_{TDIC}$ values are isotopically higher relative to interglacial times when CO_2 levels are higher and $\delta^{13}C_{DIC}$ lower. This is due to greater availability of CO_2 during interglacials and a greater discrimination of the heavier ^{13}C isotope during photosynthesis (Prokopenko *et al.* 1999, Yan *et al.* 1999).

Aquatic productivity will alter $\delta^{13}C_{TDIC}$ as photosynthesis preferentially removes ^{12}C leaving a higher $\delta^{13}C_{TDIC}$ during periods of increased productivity. This organic material is then incorporated into the lake sediments, although this can be reworked releasing isotopically

lower carbon back into the water column. Positive shifts in $\delta^{13}C$ values related to increased productivity have been found by Mackenzie (1985), Meyers and Ishiwateri (1993), Wolfe *et al.* (1999) and Prokopenko *et al.* (1999) and also due to eutrophication (Schleske and Hodell 1991, 1995). Linked to this, water residence time can affect $\delta^{13}C_{TDIC}$. Closed lake basins have long water residence times and therefore increased exchange of surface waters with the atmosphere in addition to progressive removal of ^{12}C by photosynthesis. Some lakes show a covariance of $\delta^{13}C$ and $\delta^{18}O$ values ($\delta^{18}O$ will be increased by increasing evaporation time and preferential removal of the lighter ^{16}O). This covariance can be used as an indicator of the open or closed status of a lake basin (Talbot 1990, Drummond *et al.* 1995, Wolfe *et al.* 1996, Li and Ku 1997, Leng *et al.* 1999, Griffiths *et al.* 2002). This, however will not be the case for Lake Baikal as the basin has remained open over the period investigated by this study (Colman 1998).

The carbon isotope composition of bulk organic material in lake sediments can give information on carbon sources (Meyers and Lallier-Vergès 1999). Higher plants such as trees utilise the C_3 Calvin pathway of incorporating organic matter. This preferentially removes ^{12}C with an average discrimination of –20‰ (O'Leary 1988). Plants such as arid grasses use the C_4 Hatch-Slack pathway discriminating at –4 to –6‰. Desert plants and cacti use the CAM Crassulacean acid metabolism pathway discriminating at –4 to –20‰. The isotopic composition of bulk organic matter ($\delta^{13}C_{ORG}$) can sometimes be used to determine the source of organic material (Lamb *et al.* 2004). However, lacustrine algae have a similar range of $\delta^{13}C$ values to most C_3 terrestrial plants (figure 2.19), but it is possible to separate these by using the C/N ratio calculated by dividing percentage organic carbon (TOC) by percentage organic nitrogen (TN). Algae are low in carbon as they are protein rich and relatively high in nitrogen and will generate a low C/N ratio while lignin and cellulose-rich higher plants (e.g. trees) will generate high C/N ratios (Meyers 1994) (figure 2.19).

TOC can vary due to dilution by addition of clastic material in a sample and concentration due to dissolution of carbonates (Meyers and Teranes 2001). As the size of clastic material increases, TOC generally decreases. Sedimentation rate is important in controlling this process, therefore it is often useful to consider the accumulation rate of organic material rather than simple percentage content as, when combined with $\delta^{13}C_{ORG}$, accumulation rates can give an estimates of allochthonous versus autochthonous carbon input. Degradation in oxic conditions of sedimented carbon can also lead to lower values of TOC, this may be an issue in Lake Baikal as the sediment-water interface is oxygen rich (Weiss *et al.* 1991).

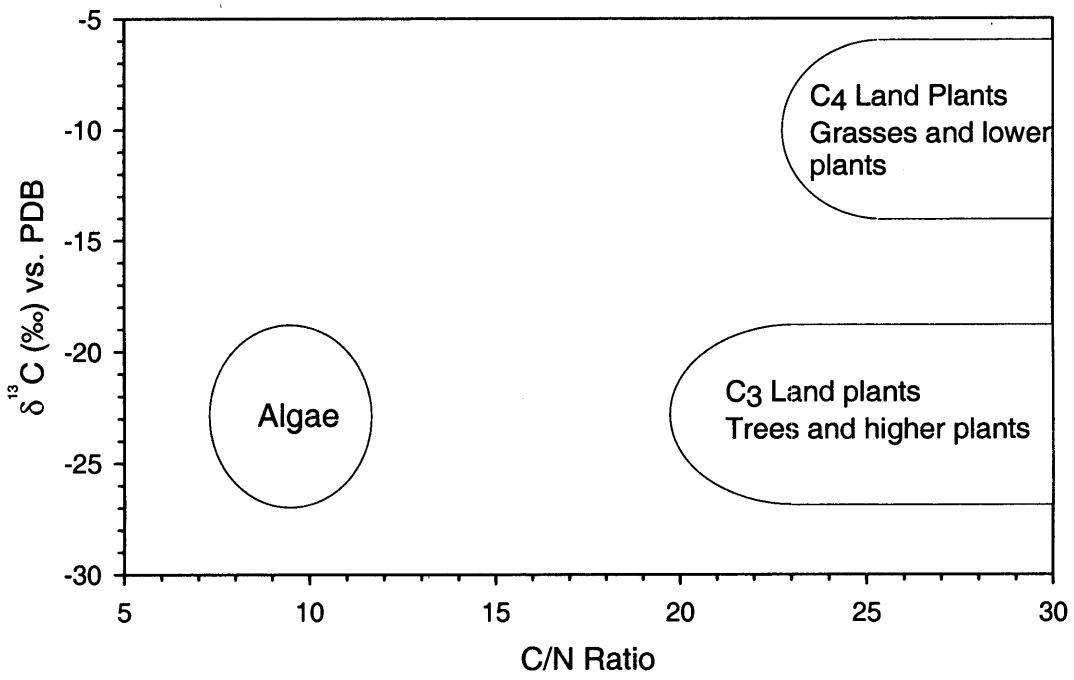

Figure 2.19: Discrimination of algae, C_3 plants and C_4 plants using comparative $\delta^{13}C$ and C/N measurements (Meyers and Lallier-Vergès 1999).

There are problems of using $\delta^{13}C$ values of lacustrine material such as microbial reworking that can alter the isotopic content, as bulk matter is a mixture of isotopically distinct compounds that can be selectively reworked (Meyers and Lallier-Vergès 1999). However, this tends to occur in the upper layers of sediment. Secondly, as the carbon cycle is complex, bulk organic matter represents a mixture of carbon from many and varying sources. It may be difficult to establish any firm conclusions although analysis of $\delta^{13}C$ from individual biomarkers may help (Rossell-Melé 2003). This is currently being carried out on Lake Baikal sediments (Russell and Rossell-Melé, in press).

Factors other than primary productivity may alter the signal, such as atmospheric CO_2 level, pH, temperature and N-limitation (Laws *et al.* 1995). However, these are all directly or indirectly linked to climate. Fractionation from dissolved CO_2 to organic material can depend on CO_2 concentration and temperature, e.g. low $\delta^{13}C$ can be caused by elevated CO_2 concentrations (Wolfe *et al.* 1999). In addition, dissolved CO_2 for photosynthesis can become scarce so algae begin to use HCO_3^- as their carbon source. This can bias $\delta^{13}C$ signals as HCO_3^- can elevate $\delta^{13}C$ values towards those of C_4 plants (Meyers and Lallier-Vergès 1999). The presence of large reservoirs of gas hydrates has been recently detected in Lake Baikal's sediments (Klerkx *et al.* 2003). As these are a source of isotopically low methane gas, they

are a potential source of low $\delta^{13}C$ to the TDIC pool. The dynamics of Lake Baikal gas hydrates are discussed fully in chapter 8.

The climatic importance of $\delta^{13}C$ is linked to changing vegetation and productivity creating shifts in $\delta^{13}C$ values. It is possible to record climatically caused vegetation changes (Yan *et al.* 1999), and changes in the carbon cycle. Overall, it is important to know the source of organic matter before interpreting $\delta^{13}C$ values (Wolfe *et al.* 1999).

2.7.2 Controls on $\delta^{18}O$ in precipitation ($\delta^{18}O_{PPT}$)

This study will consider $\delta^{18}O$ in diatom silica as a palaeoenvironmental indicator, however it is necessary first to understand the variability of $\delta^{18}O$ in both precipitation ($\delta^{18}O_{PPT}$) and lake water ($\delta^{18}O_{LW}$) before the oxygen is incorporated into biogenic silica. Water has two isotope ratios: $^{18}O/^{16}O$ and $^{2}H/^{1}H$ (often referred to as D/H). Dansgaard (1964) noted for mid to high latitude regions, higher surface temperatures correspond to isotopically higher $\delta^{18}O_{PPT}$. Ideally, this relationship would be with cloud base temperature but this data is often not available. This relationship also holds for δD in precipitation (Edwards *et al.* 1996) and the concept applied here is the Rayleigh model. With continuing formation of precipitation from an air mass, remaining vapour is progressively lowered in ^{18}O and D because heavier $D_2{}^{18}O$ condenses preferably to lighter $^{1}H_2{}^{16}O$. This is because the vapour pressure of $D_2{}^{18}O$ is lower than $^{1}H_2{}^{16}O$ and poleward movement causes cooling, therefore depletion of the heavier isotopes. During adiabatic cooling, low temperatures favour the removal of heavy isotopes and create isotopically lower precipitation (Dansgaard 1964, Siegenthaler and Oeschger 1980, Rozanski *et al.* 1992, Fricke and O'Neil 1999).

Dansgaard (1964) noted a change of $0.69‰°C^{-1}$ in $\delta^{18}O_{PPT}$, although for quantitative reconstructions of temperature from $\delta^{18}O_{PPT}$, the starting $\delta^{18}O$ value of the airmass needs to be known (Jouzel *et al.* 2000), otherwise only relative temperature changes can be obtained. This temperature relationship appears to be the overriding control on $\delta^{18}O_{PPT}$, but variations exist as fractionation does not follow a simple Rayleigh model (Dansgaard 1964). Other geographical factors are important, e.g. continental stations are generally isotopically lower in $\delta^{18}O$ than according to the temperature relationship, due to the rainout history of an airmass (Sonntag *et al.* 1978), a decrease of $0.0002‰km^{-1}$ over land has been noted. An increase in altitude will also cause a progressive depletion of $\delta^{18}O_{PPT}$, approximately 2‰ every vertical kilometre. For tropical stations, $\delta^{18}O_{PPT}$ is governed by the amount effect: $\delta^{18}O_{PPT}$ is isotopically lower in rainy months and isotopically higher in drier months (Dansgaard 1964).

This is because convective rain is dominant, air masses move in a vertical direction and condensate can form at any altitude. This falls, exchanging with other water droplets and ambient water vapour. As a result there is a preferential loss of ^{18}O, hence depletion of precipitation in rainy months. Linked to this, falling rain can become isotopically higher due to evaporation (Siegenthaler and Oeschger 1980).

Changes in the vapour source will also alter $\delta^{18}O_{PPT}$. The initial $\delta^{18}O$ of an air mass can vary before fractionation by rainout and temperature effects. Changes of $\delta^{18}O$ of the moisture source can be caused by variations of ocean water composition during glacial/interglacial cycles – oceans being isotopically higher during glacials. Large shifts in $\delta^{18}O_{PPT}$ can be caused by changing atmospheric circulation and moisture source area which can be isotopically diverse (Plummer 1993, Edwards *et al.* 1996, Amundson *et al.* 1996, Yu *et al.* 1997, Yu and Eicher 1998, Smith and Hollander 1999).

Globally, D and ^{18}O in precipitation are linearly related and plot on the Global Meteoric Water Line (Craig 1961). (GMWL: $\delta D = \delta^{18}O + 10‰$). An excess of D over ^{18}O is possible in precipitation (Craig *et al.* 1963, Merlivat and Jouzel 1979). Changes in D-excess are due to secondary moisture flux to the atmosphere caused by evapotranspiration (Gat *et al.* 1994). This fractionates moisture and returns isotopically lower vapour to the atmosphere, thus depletion is greater for ^{18}O than D so returned moisture has relatively more D than ^{18}O. This D-excess can show admixture from secondary sources and is an indicator of relative humidity (Merlivat and Jouzel 1979). Large lakes especially are an important source of secondary moisture (Machavaram and Krishnamurthy 1995). Lake Baikal is known to have a profound influence on climate in its immediate vicinity. Evaporation from the lake is highest in November and December and this is likely to be an important source for (secondary) precipitation (Lydolph 1977).

The $\delta^{18}O_{PPT}$-temperature relationship varies temporally as well as spatially. A good $\delta^{18}O_{PPT}$-temperature relationship may be shown by modern data, but to use this relationship as a palaeothermometer, it is necessary to understand how the association between $\delta^{18}O_{PPT}$ and temperature can vary with changing climatic mode (Fricke and O'Neil 1999). Different climatic modes such as glacial/interglacial shifts or even just different seasons have offset $\delta^{18}O_{PPT}$-temperature relationships. Using only the slope of modern data, a reduced amount of climate change can be represented. This underestimation is because the temporal relationship is shallower than the spatial (Delaygne *et al.* 2000). Jouzel *et al.* (2000) state the spatial relationship must hold during climate change for $\delta^{18}O_{PPT}$ to be used as a temperature proxy.

Wolfe *et al.* (2000) used the modern spatial relationship as a surrogate for the temporal to infer climate in north-central Russia. However, the problems of shifting moisture sources and atmospheric circulation causing deviation from the spatial relationship are acknowledged (Edwards *et al.* 1996, Wolfe *et al.* 2000).

2.7.3 Controls on $\delta^{18}O$ in lake water ($\delta^{18}O_{LW}$)

A relationship exists between annual lake surface temperatures and annual weighted $\delta^{18}O$ in precipitation. Hydrology at the study site has to be understood as $\delta^{18}O_{PPT}$ does not always transfer directly to $\delta^{18}O$ of lake water. $\delta^{18}O_{PPT}$ does not always equal $\delta^{18}O_{LW}$ because lake water is modified by local hydrology and water balance of the lake (Anderson *et al.* 2001). Lake water is controlled by the combined isotopic composition of input waters from the catchment, including precipitation falling onto the catchment. $\delta^{18}O_{PPT}$ values vary seasonally (heavier values being correlated to higher summer temperatures, snow having very light values) and as a result $\delta^{18}O_{LW}$ may also vary seasonally. Some lakes have large catchments and many inlets which contribute water of differing $\delta^{18}O$. Lake water will therefore represent a weighted average of inputs. Groundwaters and spring inflow can introduce waters that fell as precipitation under different climatic regimes or have exchanged with local rocks and are not consistent with modern $\delta^{18}O_{PPT}$-temperature relationships. Hot springs supply water to some areas of Lake Baikal although their contribution to the total lake water is thought to be minimal (Seal and Shanks 1998). The melting of snow and glaciers can release a pulse of isotopically lower water to a lake. Lake Baikal is surrounded by several mountain ranges (see figure 2.1) which are predominantly snow covered during winter. Throughout the Quaternary, these ranges have been periodically covered by glaciers whose ablation may have led to sudden inputs of iosotopically low water. In addition, lake mixing and stratification can cause anomalies in $\delta^{18}O_{LW}$ spatially over the same lake. Also, lakes with long residence times may have water that is non-representative of current temperatures (Benson 1994, Schleser *et al.* 1999). Lake Baikal has a well-defined seasonal cycle of stratification, which is outlined in section 2.2.2, while issues of Lake Baikal's long water residence time are discussed in section 3.1.

These inputs are modified by outputs of evaporation and outflow. Varying importance of these two factors will mean different climatic signals will be captured by $\delta^{18}O_{LW}$ (Leng 2002). For closed basin lakes evaporation dominates over precipitation, so $\delta^{18}O_{LW}$ will be a proxy for precipitation minus evaporation (effective moisture). For open basin lakes with a short residence time and minimal evaporation, $\delta^{18}O_{LW}$ should be a temperature proxy. Open

lakes with a large catchment relative to surface area have low evaporation to input values so $\delta^{18}O_{LW}$ should compare to $\delta^{18}O_{PPT}$. For open lakes with small catchments relative to surface area, there will be a higher evaporation to input ratio. These lakes may be more of a proxy for effective moisture (Anderson *et al.* 2001).

$\delta^{18}O$ of evaporated lake waters will fall on local evaporation lines (LEL) off the GMWL. During evaporation, kinetic fractionation of ^{18}O exceeds that of D meaning evaporating lake waters become progressively isotopically higher in D. The LEL will have a lower slope than the GMWL depending on the relative humidity (Gat 1971).

2.7.4 Controls on $\delta^{18}O$ in diatom silica ($\delta^{18}O_{DIAT}$)

The value of $\delta^{18}O_{LW}$ is further modified by fractionation when incorporated into mineral precipitates lake sediments. This discrimination is dependent on metabolic factors as well as temperature. Another problem for quantitative palaeoclimatic interpretation is the value of $\delta^{18}O_{LW}$, as the starting point for fractionation is often unknown (Stuiver 1970, Schleser *et al.* 1999). $\delta^{18}O$ from biogenic silica ($SiO_2.H_2O$ in diatoms, chrysophytes, sponges) may be a useful proxy, especially as diatoms are present in most lakes even if carbonates are not. As diatoms have a short generation time and bloom at a specific time of year, they will give a seasonal $\delta^{18}O$ signal (Raubitschek *et al.* 1999) and will be complementary to other seasonal records of $\delta^{18}O$ (Leng *et al.* 2001).

The incorporation of $\delta^{18}O_{LW}$ into diatom silica follows a temperature dependant fractionation. This is also the case for authigenic carbonates, studies of carbonate formation under varying temperature led to $\delta^{18}O$-carbonate palaeotemperature scales (Epstein *et al.* 1953) involving three variables: 1) temperature at formation; 2) $\delta^{18}O$ of lake water at formation, which can be estimated by studying the modern lake (von Grafenstein 1999, 2000, Teranes and Mckenzie 2001); 3) $\delta^{18}O$ of carbonate, which is measured. The signal of any reconstruction is also dampened by the negative fractionation coefficients in these relationships (Eicher and Siegenthaler 1976, Siegenthaler *et al.* 1984, Schleser *et al.* 1999). While the $\delta^{18}O_{PPT}$-temperature relationship has a positive coefficient (increasing temperature relates to isotopically higher precipitation), the $\delta^{18}O_{LW}$-carbonate relationship is negative (increasing temperature, isotopically lower carbonate $\delta^{18}O$).

Attempts have been made to develop a similar temperature scale for $\delta^{18}O_{DIAT}$. As for carbonates, several fractionation relationships have been published. The most widely used

being the curve of Leclerc and Labeyrie (1987) based on a study of the Southern Ocean. Again, the coefficient is negative reducing the bandwidth of the signal (Schleser *et al.* 1999). Published estimates of temperature fractionation in ocean water range from ~-0.3 to -0.5‰°C^{-1} although the lower end of the range is more likely for lake water (Brandriss *et al.* 1998). Overall, fractionation relationships vary greatly from study to study (Matheney and Knauth 1989) mainly due to limited investigations and poor analytical techniques.

Schmidt *et al.* (1997) analysed culture grown diatoms from water of known $\delta^{18}O$ and found no correlation between oxygen fractionation and temperature. However, it was shown by Brandriss *et al.* (1998) that live diatoms contain an anomalously unstable silica layer, which has to be removed by HF (hydrofluoric acid) prior to analysis. It was also suggested in this study that vital effects and species dependent fractionation could bias the $\delta^{18}O$ signal. Such effects were not observed by Shemesh *et al.* (1995) though. Calculated fractionation relationships assume a linear relationship between increasing temperature and depletion of $\delta^{18}O_{DIAT}$. Schleser *et al.* (1999) suggest nutrient availability and extreme weather conditions may cause a non-linear relationship. Another major problem, is that a diatom sample containing clay and silt will give anomalous results as the method used to liberate oxygen from diatom silica will also liberate oxygen from any other material (section 7.3.3). Juillet-Leclerc (1986), Shemesh *et al.* (1998) and Barker *et al.* (2001) claim to have obtained pure diatom samples using differential settling, sieving and chemical cleaning. Heavy liquids such as sodium polytungstate (SPT) can be used to float out diatoms in a density separation (Battarbee *et al.* 2001, Shemesh *et al.* 2001b).

2.7.5 Summary

Stable isotopes can be used as climatic proxies because the fractionation of isotopes often has a climatic cause, either directly in the case of oxygen, or indirectly in the case of carbon isotopes through biological changes, such as productivity and biological activity. Carbon isotopes and C/N ratios of organic matter may be able to show differing sources of organic matter, lake residence time, productivity changes, and atmospheric CO_2 levels as Lake Baikal is relatively non-evaporative (section 3.1). It may be possible to obtain a quantitative reconstruction of temperature from oxygen isotopes. However, a relationship between $\delta^{18}O_{PPT}$ and temperature has to be assumed and the $\delta^{18}O$ signal is modified through incorporation in lake water and lake sediments respectively, and clean samples must be obtained. It is important to understand how the measured isotopic signal has been modified. The best way to

approach this is to fully understand the modern lake system as in studies of the Pyramid Lake basin, USA, by Benson (1994), Hoestler and Benson (1994) and Benson and White (1994). To an extent, the modern isotope dynamics of Lake Baikal will be investigated in chapter 3.

Chapter three

Modern environment I: Stable isotope dynamics

3.1 Controls on the modern oxygen isotope content of Lake Baikal

3.1.1 Lake water

The most extensive study of Lake Baikal oxygen and hydrogen isotopic dynamics has been carried out by Seal and Shanks (1998). $\delta^{18}O$ and δD from Lake Baikal fluvial inputs and drainage, precipitation, hot springs and the Lena and Aldan Rivers (900 km northeast of Lake Baikal) were measured to understand the modern lake water isotopic composition (figure 3.1). The most remarkable feature of the modern lake water is the consistent isotopic values both spatially over the lake and also with depth ($\delta^{18}O$ = -15.8±0.2‰ (2σ), δD = -123±2‰ (2σ)) (figure 3.1). The measurements taken by Seal and Shanks (1998) were constrained to June and July but additional data collected in this study shows the values above to be constant on a temporal basis as well (table 3.1). On the other hand, values for river waters and precipitation are much more variable, this is mostly due to seasonal variability in $\delta^{18}O$. This stability in isotopic values in lake water indicates that the lake is very well mixed (*c.f.* Weiss *et al.* 1991, Faulkner *et al.* 1997). However, Seal and Shanks (1998) find evidence of surface evaporation with isotopically higher surface waters at one station in July 1992. Linked to this, values for Baikal lake water plot to the slightly to right of the GMWL (figure 3.1). This leads Seal and Shanks (1998) to suggest significant evaporation is taking place. Alternatively this deviation is very small, for example values for river waters and precipitation have a similar scatter around the GMWL, and it may be lake water is representative of its inputs.

Site	Date	n	$\delta^{18}O$	δD
North Basin	June 1992	6	-15.8 ± 0.1	-124 ± 1
Central Basin	June 1992	8	-15.9 ± 0.1	-123 ± 2
Central Basin	July 1992	12	-15.8 ± 0.9	-123 ± 3
South Basin	June 1992	6	-15.8 ± 0.1	-123 ± 2
South Basin*	April 2000	7	-15.9 ± 0.1	-123 ± 2
South Basin*	July 2000	5	-15.7 ± 0.1	-122 ± 1
South Basin*	March 2001	3	-15.8 ± 0.1	-125 ± 1
North Basin Rivers	1991-1992	12	-20.4 ± 2.2	-151 ± 13
Central Basin Rivers	1991-1992	9	-17.6 ± 3.7	-132 ± 21
South Basin Rivers	1991-1992	13	-15.9 ± 4.9	-120 ± 31
Hot Springs	June-July 1991	6	-21.1 ± 1.5	-159 ± 6

Table 3.1: Mean North, Central and South Basin lake water, river input and hot spring water $\delta^{18}O$ and $\delta D \pm 2\sigma$ (‰ vs. SMOW) and number of samples taken (n), from Seal and Shanks (1998) and this study (*). Precision for $\delta^{18}O$ and δD analysis is ±0.1‰ and ±2‰ respectively.

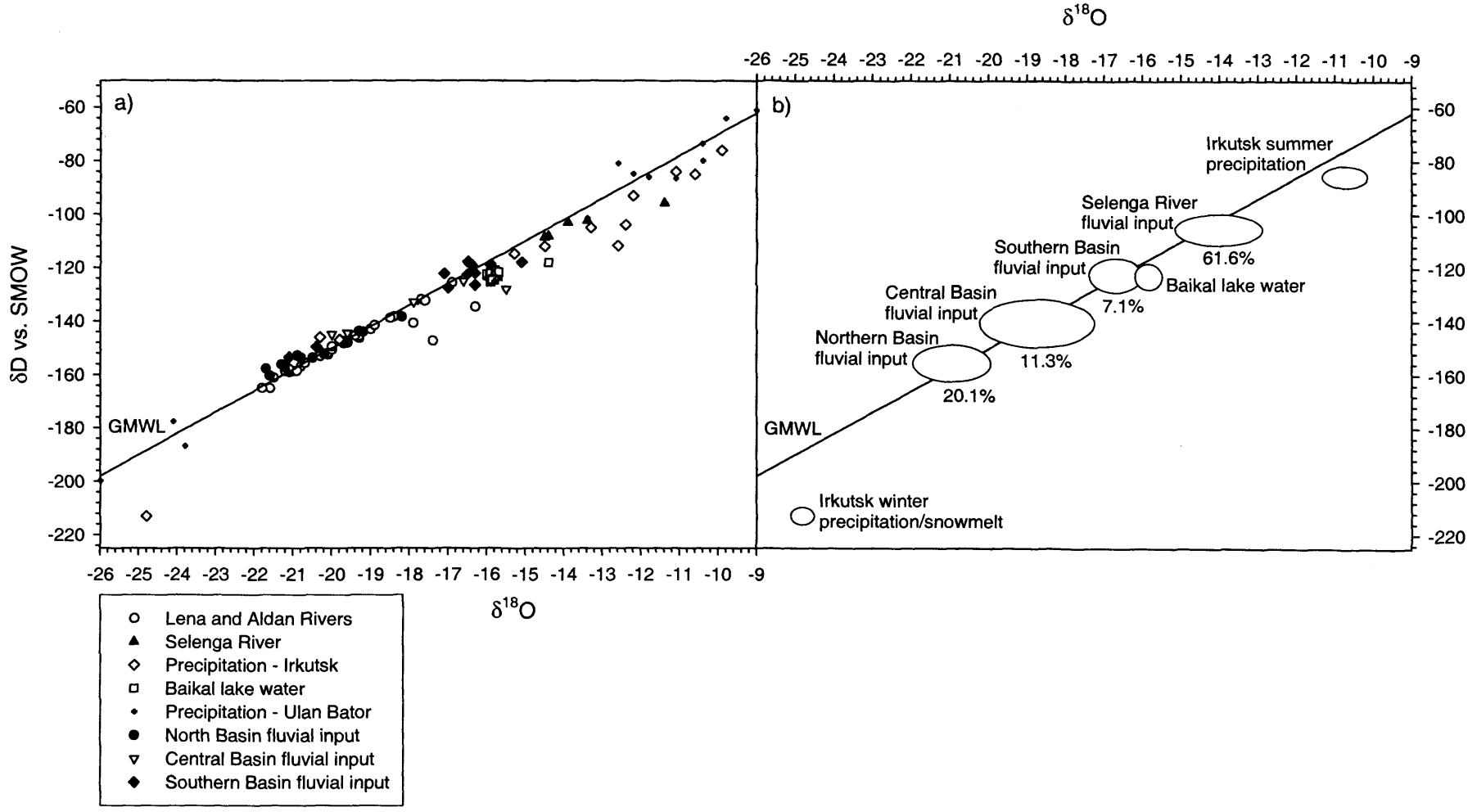

Figure 3.1: a) Oxygen and hydrogen isotope composition of Lake Baikal's fluvial inputs, lake water, precipitation in the catchment and the nearby Lena and Aldan Rivers with relation to the GMWL. b) Simplified version showing general isotopic values for fluvial inputs from the North, Central and South Basins and their respective percentage of total fluvial input. Irkutsk summer and winter precipitation and Lake Baikal lake water also shown. Data from Seal and Shanks (1998) and IAEA GNIP.

3.1.2 Precipitation input

The International Atomic Energy Agency (IAEA) Global Network of Isotopes in Precipitation (GNIP) has monthly $\delta^{18}O$, δD, precipitation amount and air temperature for Irkutsk (figure 3.2) and Ulan Bator in the lake's catchment (figure 3.3), for the years 1990 and 1998-2000 respectively. $\delta^{18}O$ in precipitation at Irkutsk ranges from –24.8‰ in January to –9.9‰ in May with higher temperatures corresponding to isotopically higher values. Most precipitation falls in the summer months (163 mm in July 1990) while the cold, arid winters mean winter precipitation is very low (3 mm with –19.9°C air temperature in January 1990). Consequently the isotopic input from precipitation will be weighted towards the summer months (July: -10.6‰) with values isotopically higher in comparison to the winter. These values for precipitation generally adhere to the GMWL (figure 3.1) and Seal and Shanks (1998) calculated the $\delta^{18}O$ - temperature dependence (Dansgaard relationship) of 0.361‰ $°C^{-1}$ for Irkutsk precipitation based on the 1990 GNIP data ($r^2 = 0.768$, $\sigma = 2.6$, $n = 14$).

The GNIP data from Ulan Bator, Mongolia (figure 3.3) covers two and a half years and displays similar trends to the Irkutsk data. Values do conform to the GMWL and again summer $\delta^{18}O$ shows the most isotopically high values varying between –8.5‰ to –12.2‰ while winter $\delta^{18}O$ reaches as low as -30.1‰ in February 2000. Isotopic input is again weighted towards summer precipitation with values of up to 138 mm in August 2000 compared to winter precipitation of less than 5 mm.

Figure 3.4 shows globally weighted $\delta^{18}O$ in precipitation over Asia. There is a lack of measuring stations in the Lake Baikal area although the catchment to the south over Mongolia appears to have an annual $\delta^{18}O$ of between –10‰ to -6‰. The Dansgaard effect can be noted in this map with equatorial areas recording higher $\delta^{18}O$ in comparison to the colder mid to high latitudes.

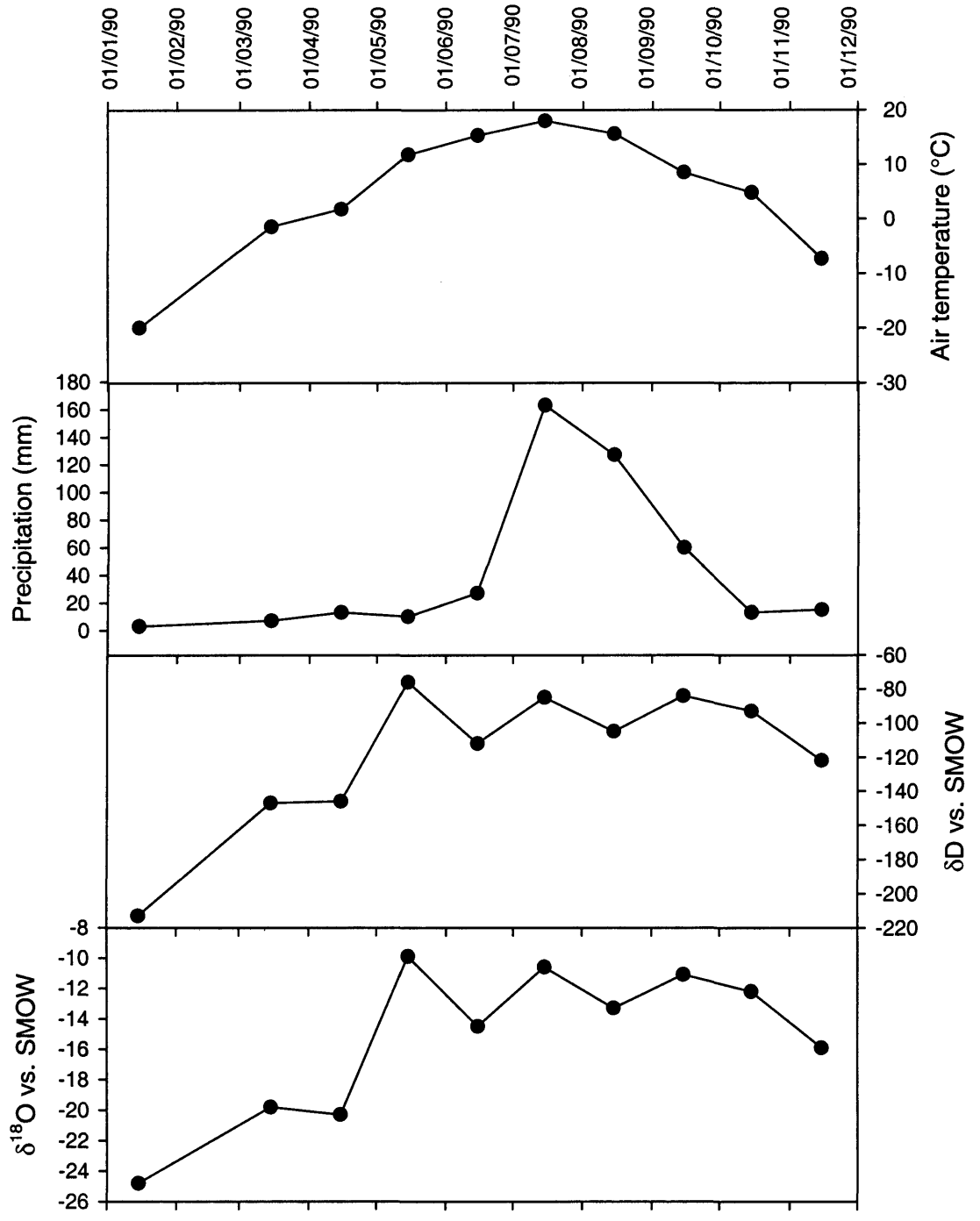

Figure 3.2: $\delta^{18}O$ and δD in precipitation, monthly precipitation and average air temperatures measured at Irkutsk during 1990 (GNIP IAEA).

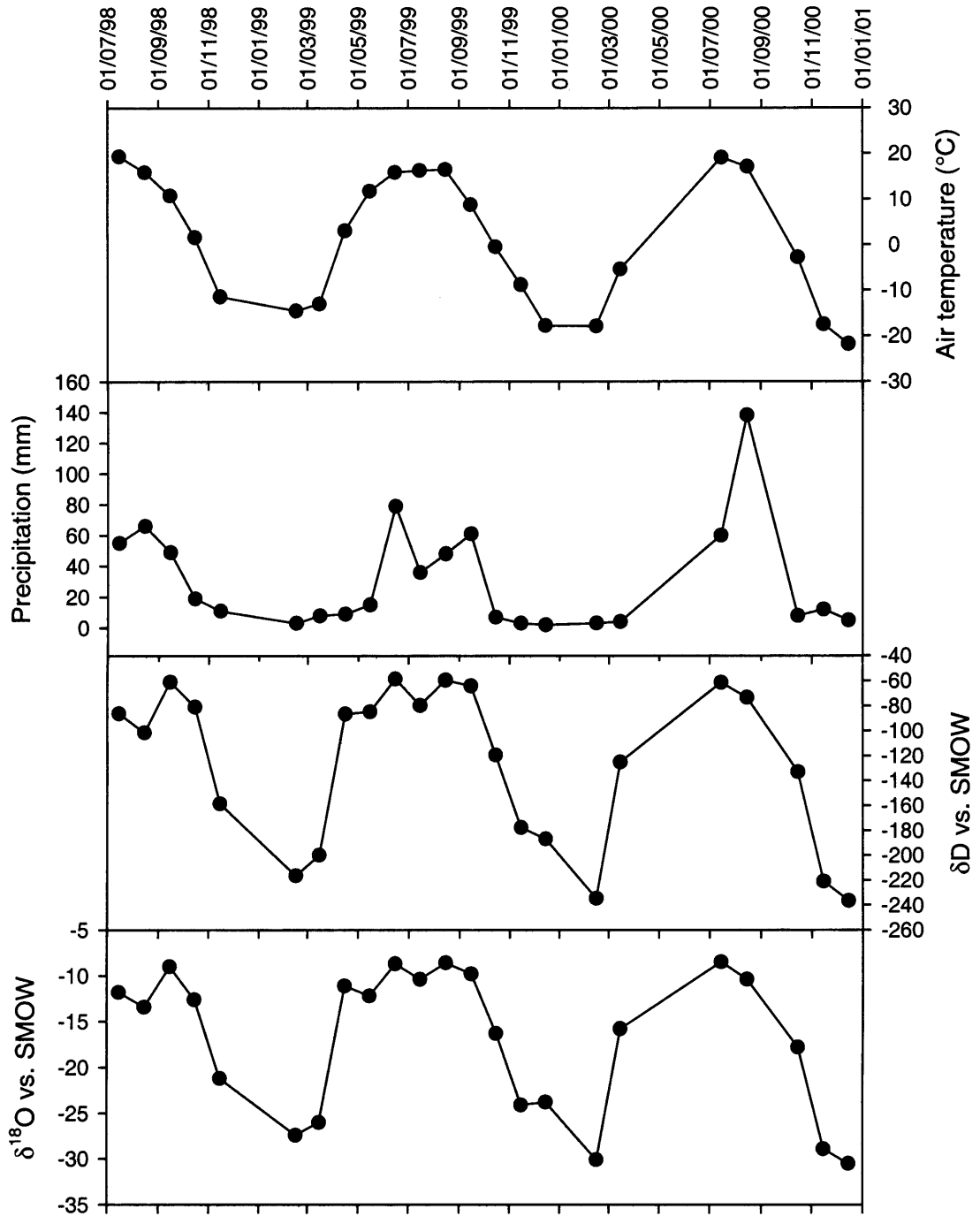

Figure 3.3: $\delta^{18}O$ and δD in precipitation, monthly precipitation and average air temperatures measured at Ulan Bator during 1998-2001 (GNIP IAEA).

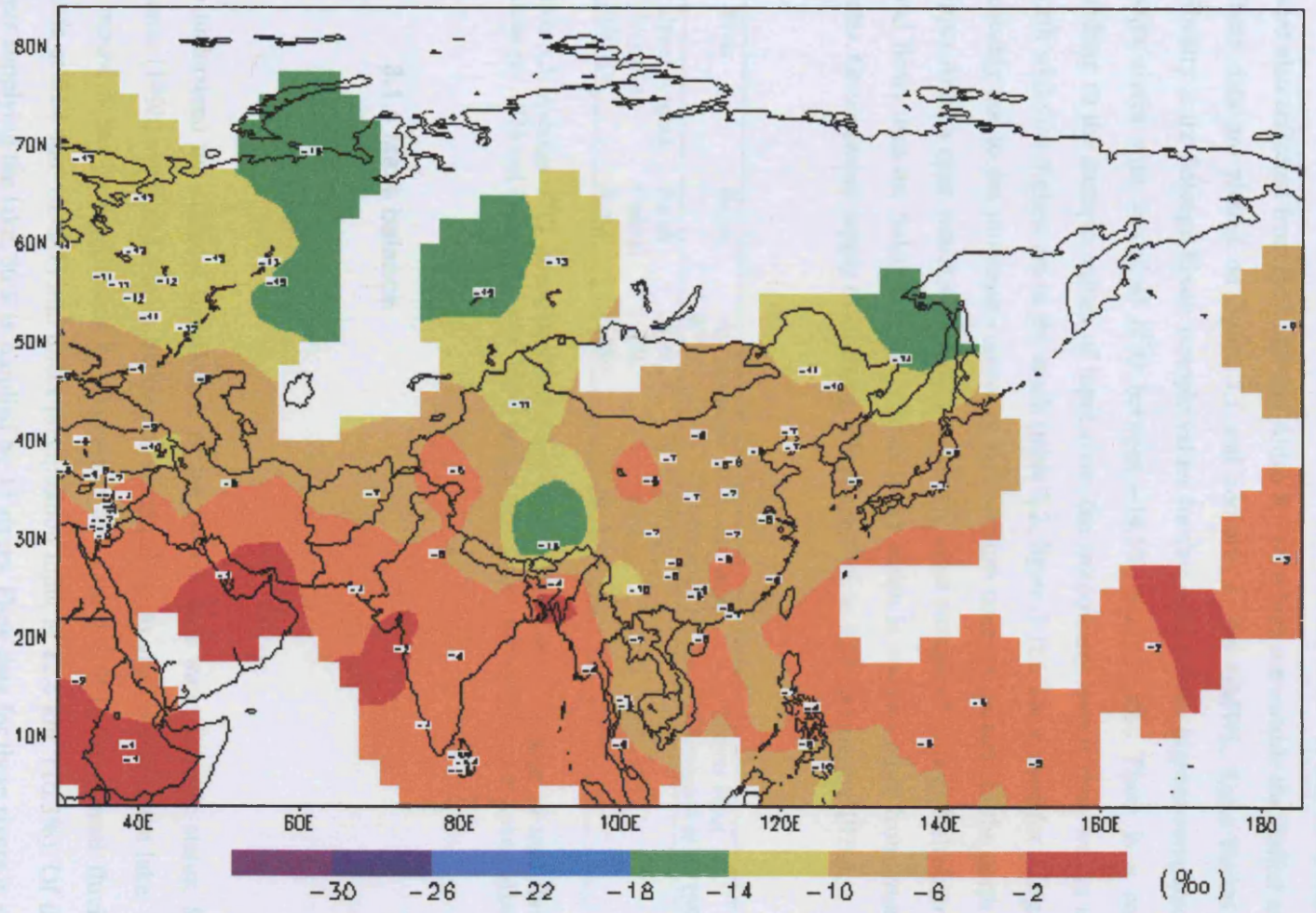

Figure 3.4: Weighted annual $\delta^{18}O$ in precipitation over Asia, small white rectangles mark the location of measuring stations (GNIP IAEA).

3.1.3 Fluvial input

Seal and Shanks (1998) collected samples from 18 of the largest rivers draining into Lake Baikal. $\delta^{18}O$ values range from –21.7‰ to –11.4‰ and δD from –158‰ to –96‰. Samples were also collected from the Lena and Aldan Rivers which are outside the Baikal catchment. These data are plotted on figure 3.1 and conform to the GMWL. Lake Baikal's largest tributary is the Selenga River; isotopic values for this river are the highest compared to other major rivers with values of $\delta^{18}O$ between –14.5‰ and –11.4‰. There is a north-south gradient to the isotopic values of input river, the isotopically lowest river waters are in the north while the highest are in the south (table 3.2, figure 3.1b). The reason for this gradient is probably due to the snowmelt content of rivers. Snow cover is greatest in the north meaning Upper Angara river waters will contain relatively more isotopically lower meltwater (32% of total flow) than the Selenga (15% of total flow) which is sourced more from summer rain water. Groundwater supply to all rivers is between 44% to 52% (Afanasjev 1976).

River	Basin	Approximate $\delta^{18}O$	% total input (Afanasjev 1976)	% total input (Shimaraev *et al.* 1994)
Upper Angara	North	-20‰	17.1%	13%
Barguzin	Central	-16‰	8.1%	6%
Selenga	South	-14‰	61.6%	47%

Table 3.2: Average $\delta^{18}O$ values (from Seal and Shanks 1998) and percentage of total fluvial input (Afanasjev 1976 and Shimaraev *et al.* 1994) for the three largest tributary rivers to Lake Baikal.

3.1.4 Mass balance

3.1.4.1 Inputs

To understand the climatic significance of the current lake water isotopic status, Seal and Shanks (1998) attempted a mass balance of weighted inputs and outputs to the lake. In terms of inputs, it has been estimated by Gronskaya and Litova (1991) that annual fluvial input stands at 61.1 km^3 (83.2%) and direct precipitation input at 12.4 km^3 (16.3%). Of the 300+ rivers supplying the lake, 80% is supplied by 15 rivers. Flow data for these rivers is available from Afanasjev (1976) and Leibovich-Granina (1987) who ascribe 61.6% of input to the Selenga and 17.1% to the Upper Angara in the far north of the lake. All other rivers account for less than 10% of total input.

Between 75-85% of river discharge occurs in the months May to September (Afanasjev 1976) hence river water samples measured in this period were thought to represent bulk river input. However, problems associated with inputs of isotopically lower snowmelt and groundwater are addressed by Seal and Shanks (1998), groundwater is considered to be a minor source supplying <4.5% of lake water. As a result bulk annual riverine input was estimated to have isotopic values $\delta^{18}O$ of –15.5‰ and δD –117‰. Weighted averaging of monthly precipitation gave $\delta^{18}O$ of –13.3‰ and δD of –103‰. As a result, modern annual input to the lake from precipitation and rivers is estimated at –15.2‰ $\delta^{18}O$ and –116‰ δD. These figures are higher than the current lake water values ($\delta^{18}O$ = -15.8±0.2‰ (2σ), δD = -123±2‰ (2σ)). The river discharge estimates used by Seal and Shanks (1998) of Afanasjev (1976) are possibly not the most accurate available though (see section 2.2.2.1). Alternate estimates by Shimareav *et al.* (1994) are given in table 3.2.

3.1.4.2 Outputs

Outflow from the Lower Angara accounts for 81% of lake water output and isotopic values of this river are identical to lake water. Evaporation explains the remaining 19% (Gronskaya and Litova 1991) although estimates of this figure can vary. Outputs from seepage are thought to be minimal (Seal and Shanks 1998). The modern bulk estimated input ($\delta^{18}O$ of –15.2‰) is isotopically higher in comparison to the measured modern lake value ($\delta^{18}O$ of –15.8‰). This is the opposite situation expected if the lake water is evaporating, as evaporation should leave current lake water isotopically higher relative to input water. Inputs from groundwater would be unrealistically high to explain the isotopically lower modern waters. The long water residence time of the lake (377 – 400 years, Gronskaya and Litova 1991) may mean isotopic values of the lake are not at a steady state in relation to modern climate and are still partly representative of a past climate. Figure 3.5 summarises the main outputs and inputs of Lake Baikal.

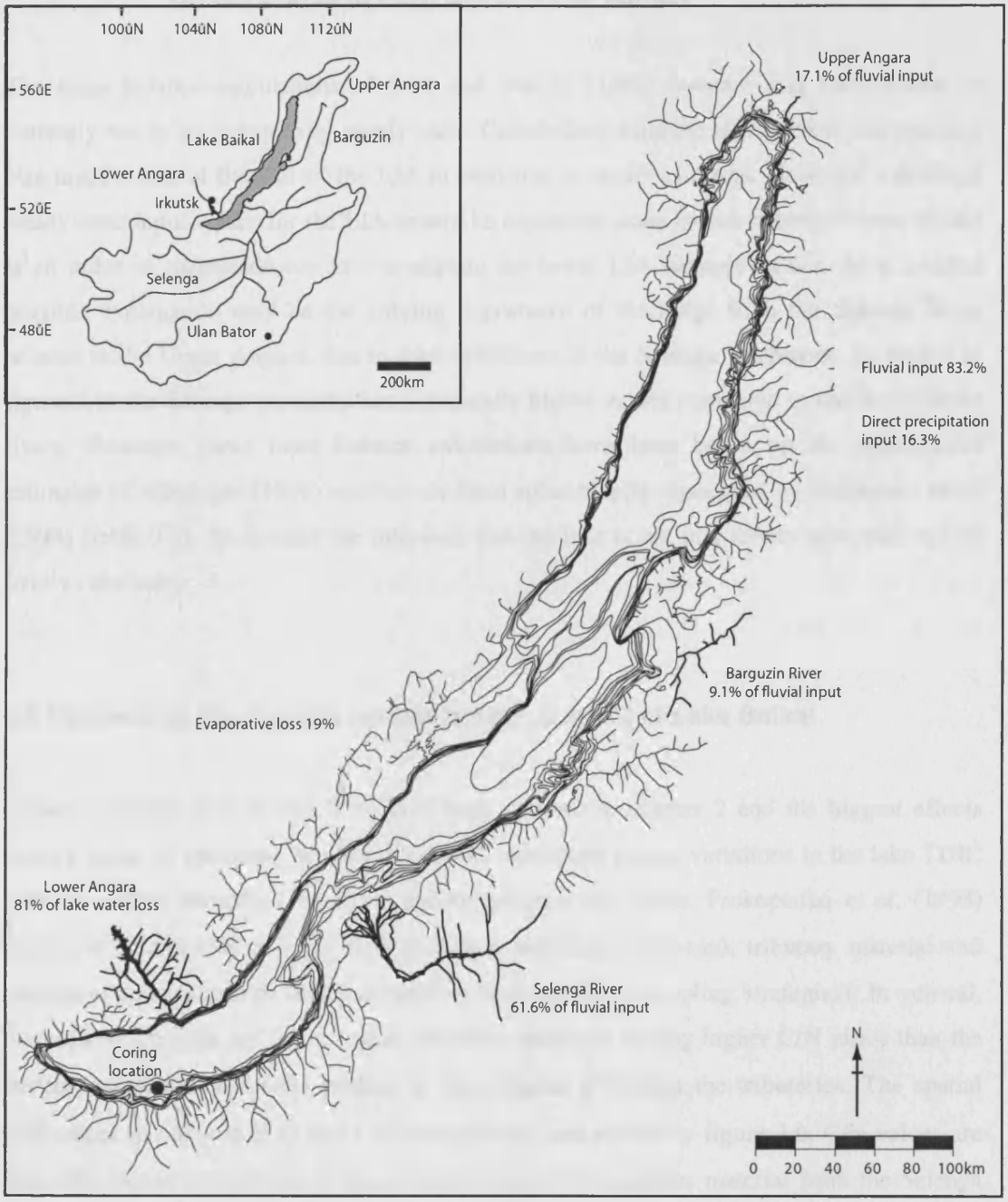

Figure 3.5: Summary of the main inputs to Lake Baikal including main river inflows and direct precipitation. Outputs include evaporation and drainage from the Lower Angara River

3.1.4.3 Status of Lake Baikal water budget

The mass balance calculations of Seal and Shanks (1998) indicate that Lake Baikal is currently not in an isotopically steady state. Calculations estimate that isotopic composition was much lower at the end of the LIA in response to cooler climates. However, calculated steady-state input values for the LIA cannot be explained alone by lower temperatures as this is an order of magnitude too low to explain the lower LIA isotopic values. As a result a possible explanation may be the varying importance of discharge from the Selenga River relative to the Upper Angara, due to drier conditions in the Selenga catchment. As shown in figure 3.1b the Selenga generally has isotopically higher values compared to the North Basin rivers. However, these mass balance calculations have been based on the input/output estimates of Afanasjev (1976) which have been subsequently reassessed by Shimaraev *et al.* (1994) (table 3.2). As a result the inference that the lake is not in a steady state may not be totally conclusive.

3.2 Controls on the modern carbon isotope content of Lake Baikal

General controls on C/N and $\delta^{13}C$ have been outlined in chapter 2 and the biggest effects usually relate to variations between C_3 and C_4 catchment plants, variations in the lake TDIC pool as well as terrestrial input vs. aquatic productivity levels. Prokopenko *et al.* (1993) studied $\delta^{13}C$ and C/N in Lake Baikal surface sediments (core-top), tributary material and catchment soils (although little information is given about sampling strategies). In general, three distinct groups are formed with tributaries and soils having higher C/N ratios than the surface sediments, and soils tending to have higher $\delta^{13}C$ than the tributaries. The spatial differences in core-top $\delta^{13}C$ and C/N over the lake are shown by figure 3.6, C/N values are generally higher in the Central Basin due to input of terrigenous material from the Selenga while lower C/N is recorded at the Academician Ridge isolated from river sourced carbon inputs. These spatial differences may also be influenced by differences in the productivity of phytoplankton over the lake, as indicated by phytoplankton monitoring campaigns (Grachev and Likhosway 1996, Popovskaya 2000, see also chapter 4) and also by analysis of pigments by Fietz *et al.* (in press) who show lower phytoplankton productivity in the North Basin compared to the South Basin, and to areas influenced by river inputs. The alternating dominance of different types of phytoplankton can influence the value of $\delta^{13}C_{ORG}$. Watanabe *et al.* (2004) speculate that higher cyanobacteria abundance during cold periods influences the $\delta^{13}C_{ORG}$ record as it has a lower $\delta^{13}C$ compared to diatoms. A study of lipid biomarkers in the

modern water column (Russell and Rosell-Melé, in press) also found differences in the input and preservation of autogenic and allogenic organic matter between the lake's basins. There are higher levels of organic material, in particular greater algal material in the South Basin compared to the North, although algal remains are the dominant organic constituent in both basins. This difference is put down to a longer productive season in the south due to a longer ice free period. This study also showed that more littoral areas received greater terrestrial plant input, possibly meaning a greater C/N ratio for littoral areas compared to pelagic regions.

Prokopenko *et al.* (1993) empirically consider a C/N value of 12 to be the cut-off point for a purely terrestrial source of carbon as neither tributary or soil C/N drops below this value. Although tributary material and soils ultimately have the same source, soil material has a higher $\delta^{13}C$ due to 'enrichment via oxidation' (Prokopenko *et al.* 1993). A shift of +2‰ and a shift to lower C/N is observed for material in the surface sediments and tributaries relative to soil material because of oxidation. This can be seen in figure 3.7, as the dashed line represents the oxidisation trend of tributaries/soils to core-tops. As is the case for soil, Prokopenko *et al.* (1993) also state that oxygenation of this non-altered plant material and subsequent enrichment continues in the lake surface sediments and is unaffected by deposition (burial) rates.

However, enrichment by what is termed oxidation by Prokopenko *et al.* (1993) may actually be more accurately described as degradation. As sediment organic matter consists of a mixture of different compounds which have different $\delta^{13}C$ signatures, it is possible that during degradation only the more volatile compounds are removed, thereby altering the $\delta^{13}C$ signal (Meyers and Teranes 2001). Therefore, degradation of the organic matter in the surface sediments of Prokopenko *et al.* (1993) possibly caused the observed +2‰ shift in $\delta^{13}C$ relative to soils. This is supported by reduced carbon material in the surface sediments shown by the shift to lower C/N ratios.

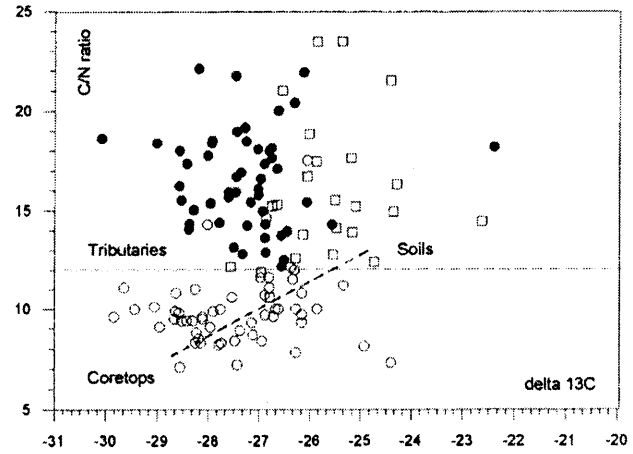

Figure 3.6: C/N ratio and $\delta^{13}C$ for sediments in Lake Baikal tributaries (•), core-tops (surface sediments) (○) and soils (□) (Prokopenko *et al.* 1993). The dotted line indicates the C/N boundary between aquatic and terrestrial sources. The dashed line represents the trend of values from soils to core tops due to 'oxidisation'/degradation.

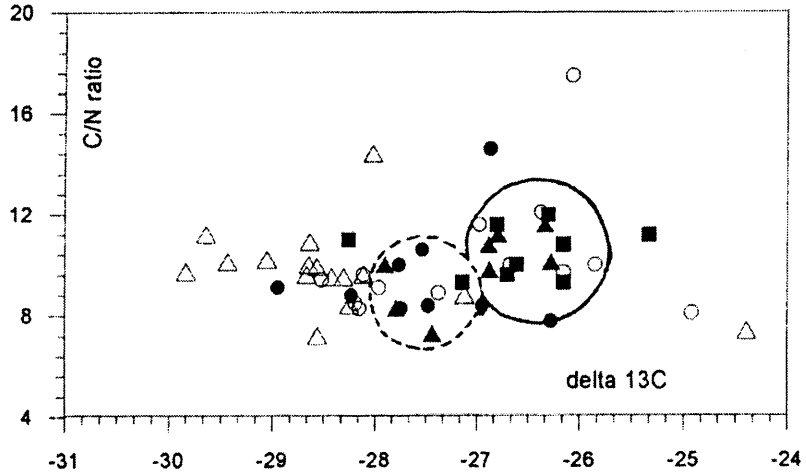

Figure 3.7: C/N ratio and $\delta^{13}C$ for Lake Baikal core-top (surface sediment) material; Central Basin (■), Southern Basin (○), Northern Basin (△), Selenga Delta area (▲) and Academician Ridge (•). Dashed circled group defines the Central Basin – Selenga Delta area, solid circled group defines Academician Ridge (Prokopenko *et al.* 1993).

The core-top material of Prokopenko *et al.* (1993) shows a much lower C/N than soils due to the contribution of algal material, while the $\delta^{13}C$ values still cover a wide range (-24‰ to -30‰). This is also due to core-tops being a mixture of soil, tributary and autogenic algae. Variations in $\delta^{13}C$ occur between benthic algae (-5‰ to -12‰) and phytoplankton (-29‰ to -30‰) in Lake Baikal (Prokopenko *et al.* 1993) meaning that littoral areas will be isotopically higher in terms of algal content compared to pelagic regions. The role of catchment inwash related to increased precipitation has been shown by remote sensing of organic material in the

modern surface waters (Heim *et al.* in press). After storms in the catchment, it was found that allogenic organic carbon persisted in the surface waters for several weeks as a result of a brief increase in river discharge and erosion. This is most pronounced in the area around the Selenga Delta. The contribution of individual plant species can be investigated by compound specific $\delta^{13}C$ and lipid biomarker analysis. A compound specific study by Brincat *et al.* (2000) of a core from the North Basin of Lake Baikal found that the sediment record consisted entirely of C_3 plant remains. These results in the context of the palaeo record are discussed fully in chapter 8.

Overall, organic matter is sourced from two major components of oxidised aquatic and oxidised terrestrial matter but with a complicating addition of non-altered (by oxidisation) phytoplankton and terrestrial material (Prokopenko *et al.* 1993). However, in the modern lake, the dominance of diatom productivity is shown by Muller *et al.* (in press) who find a predominance of biogenic silica in trap samples, with very little carbon from sources other than algae.

Additional data for $\delta^{13}C$ and C/N relating to the Selenga River sediments have been collected in this study. Samples were collected by F. Hauregard (University of Liège) as part of the CONTINENT project and stored in plastic vials prior to preparation for isotope analysis. Samples were prepared and analysed in accordance to the methods outlined in section 8.2. Sampling locations along the Selenga are shown in figure 3.8. Specific sample locations (plus distance from the water line, i.e. measured up the bank at a right-angle from the river) and $\delta^{13}C$ and C/N values are given in table 3.3 and subsequently plotted in figure 3.9 along with generalised limits for C_3 plants and algae, C_4 plants and core-top, tributary and soil limits defined by Prokopenko *et al.* (1993).

The most notable feature about these new measurements from the Selenga River is that the C/N ratio for all but one of the samples is lower than 12 which, by the limits set by Prokopenko *et al.* (1993), suggest this tributary material is different to that measured in their study. $\delta^{13}C$ values are also around +2‰ higher for this Selenga River material than that measured by Prokopenko *et al.* (1993). Possible reasons for this could be due to a higher algal content of the samples collected in this study, perhaps due to different sampling times or strategies. Samples here may be a mixture of both aquatic and terrestrial material, while those collected by Prokopenko *et al.* (1993) may contain much more terrestrial material. It is difficult to reconcile this as details of the sampling methods or exact locations of Prokopenko *et al.* (1993) are not known. However, a lower C/N value could be obtained due to a greater

level of decomposition in this material in the present study (Rundgren *et al.* 2003). Decomposition may have occurred as samples were not refrigerated before analysis. $\delta^{13}C$ values for the Selenga material does plot in the range for tributaries and soils defined by Prokopenko *et al.* (1993) and although C/N values are similar to general C_3 algae, $\delta^{13}C$ values are higher compared to core-top values. Diagenesis aside, this may suggest Selenga values are a mixture between mainly algal sources and catchment soils.

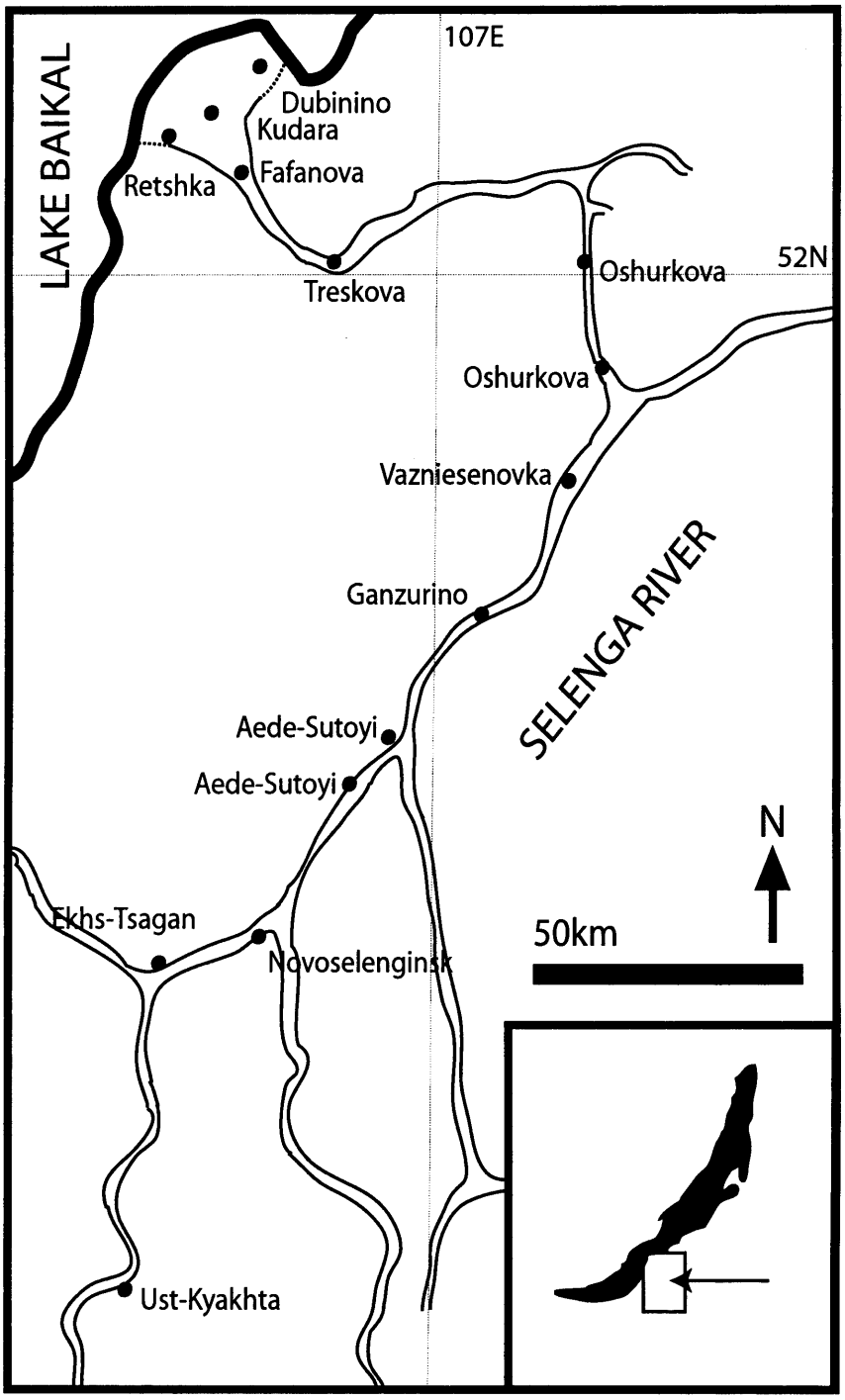

Figure 3.8: Map of the main channels of the Selenga River and the sampling locations for $d^{13}C$ and C/N analysis of Selenga Channel material. Note that some sites have the same name as these refer to a small region rather than a point location.

Location	Distance from the water line	$\delta^{13}C$	C/N
Ust-Kyakhta	no data	-25.0	10.5
Novoselenginsk	40 cm	-25.5	10.1
Novoselenginsk	0 cm	-25.6	10.2
Ekha-Tsagan	0 cm	-25.7	11.8
Ekha-Tsagan	10 cm	-25.8	11.3
Aede-Sutoyi	10 cm	-25.6	10.1
Aede-Sutoyi	0 cm	-24.0	10.5
Aede-Sutoyi	no data	-25.6	10.0
Aede-Sutoyi	no data	-23.3	9.9
Ganzurino	0 cm	-25.6	10.2
Ganzurino	20 cm	-25.2	9.6
Vazniesenovka	0 cm	-25.5	9.9
Vazniesenovka	60 cm	-25.3	9.7
Oshurkova	0 cm	-25.4	10.1
Oshurkova	30 cm	-25.5	10.0
Oshurkova	0 cm	-25.7	10.2
Oshurkova	20 cm	-25.6	10.0
Oshurkova	23 cm	-25.9	10.0
Oshurkova	25 cm	-25.9	10.0
Oshurkova	40 cm	-26.0	10.0
Treskova	0 cm	-23.6	8.5
Treskova	20 cm	-26.1	11.6
Treskova	no data	-25.3	11.1
Treskova	no data	-23.9	8.5
Treskova	no data	-25.0	10.5
Retshka	0 cm	-26.3	12.9
Dubinino	no data	-25.5	10.6
Kudara	0 cm	no data	5.5
Kudara	25 cm	-25.7	10.5
Fafanova	0 cm	no data	6.0

Table 3.3: $\delta^{13}C$ and C/N of Selenga River channel material with sample site names and distance from the water line.

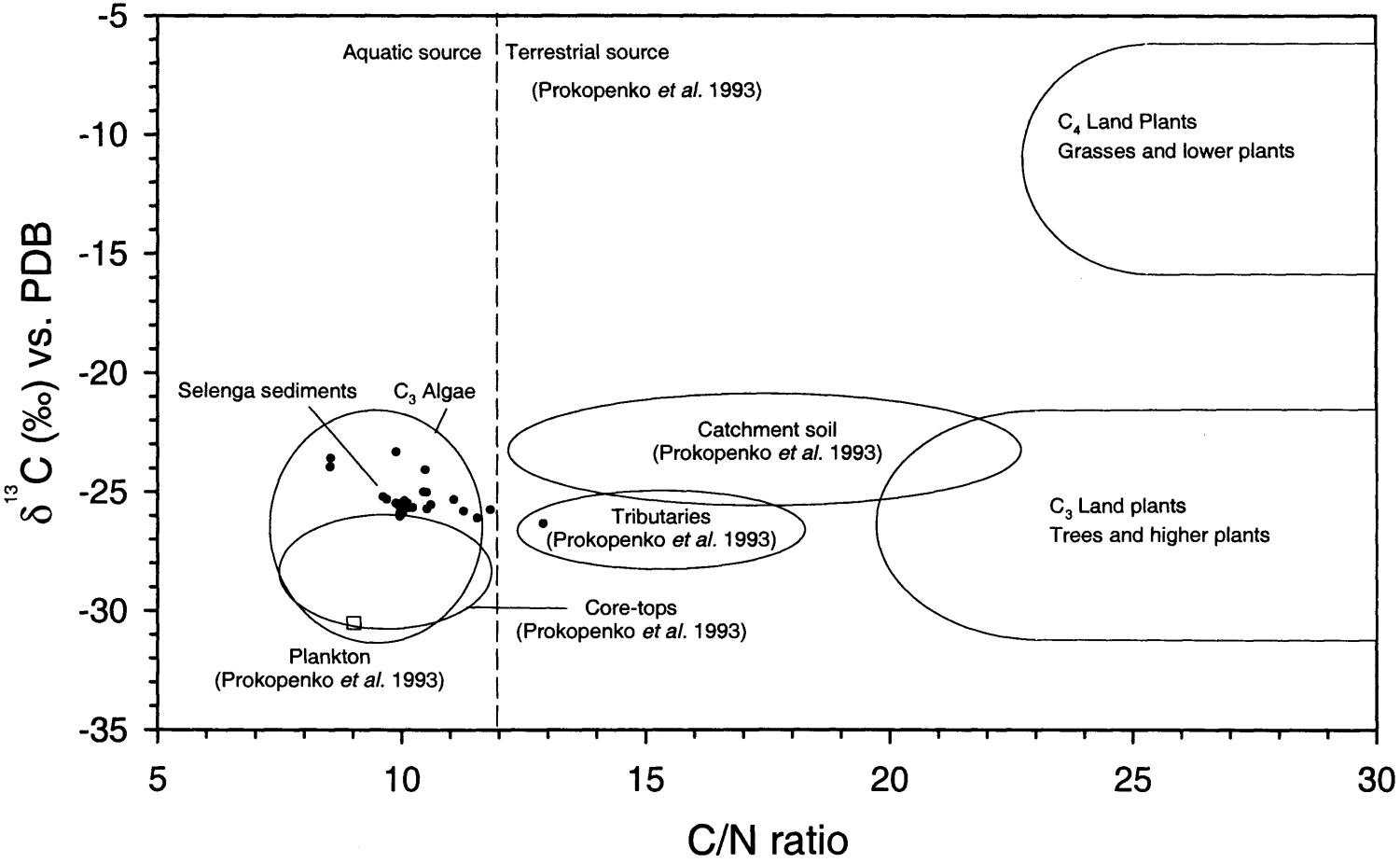

Figure 3.9: Generalised $\delta^{13}C$ and C/N limits for C_3 plants and algae, C_4 plants (Meyers and Lallier-Vergès 1999); catchment soil core-tops, plankton and tributaries (Prokopenko *et al.* 1993) and new data from the Selenga River sediment.

3.3 Summary

Modern $\delta^{18}O_{PPT}$ in the Lake Baikal region appears to conform to the Dansgaard relationship, while lake water is a mixture of direct precipitation input and river input. Tributaries to Lake Baikal show a northward trend to enrichment. $\delta^{18}O_{LW}$ can be raised by evaporation, but the proximity of measured lake water values to the GMWL suggests that evaporation is minimal at present. The consistent $\delta^{18}O$ value measured for lake water suggests the lake is very well mixed and seasonal variations in $\delta^{18}O$ will not be a concern in this study. Interpretation of the palaeo record may therefore be centred on the varying importance of the discharge of the main tributaries to Lake Baikal linked to variations in summer precipitation versus snowmelt input. Other complicating factors include the input of isotopically lower water from melting glaciers, particularly in the Early Holocene and the assumption that these modern relationships can be extrapolated over the Holocene.

Records of $\delta^{13}C$ and C/N in Lake Baikal are driven by changes in the source of carbon; this may be the alternation between C_3 and C_4 plants and aquatic versus terrestrial productivity. It can be shown that modern catchment material and lake algae have distinctly different $\delta^{13}C$ and C/N values. As a result palaeo data may record a mixture of changing importance of these carbon sources driven by large-scale climate changes. Studies of phytoplankton, biomarkers and remote sensing of surface waters indicate that there is great spatial variability in algal productivity and terrigenous input over the lake on a predominant north – south gradient and also in relation to areas under the influence of fluvial input. This means that palaeo records from different locations in the lake will differ. Superimposed onto this will be alterations to the signature due to diagenesis, oxidisation and changes in productivity, lake TDIC pool and atmospheric CO_2 content. Gas hydrate release in the past may have also had an influence on lake TDIC, this is explored fully in chapter 8.

Chapter four

Modern Environment II: Phytoplankton monitoring

4.1 Phytoplankton monitoring

Although long term phytoplankton monitoring has been carried out on Lake Baikal, these studies have tended not to be systematic (Popovskaya 2000). This chapter attempts to define both the temporal and spatial dynamics of phytoplankton over 2001-2002, however, this provides only a snapshot in time and a more complete knowledge of Lake Baikal's phytoplankton dynamics will only be achieved with continued long term monitoring and synthesis with past studies. The variability in productivity and composition of Lake Baikal's phytoplankton is well documented but the causes of this variability are poorly understood although most likely linked to climatic factors (Kohzov 1963). Knowledge of the mechanisms driving variations in the productivity of diatom species in the modern lake will be of considerable use when interpreting down-core records of diatom abundance. This should give a sound ecological base for interpretation and should be complementary to the more ecologically detached, empirical approach of transfer function models (*c.f.* Sayer 2001).

Some of the earliest studies of phytoplankton dynamics linked to environmental conditions were carried out on Lake Windermere and Blelham Tarn in the English Lake District investigating the dynamics of *Asterionella formosa* (Hassall) and *Melosira* species in particular (Lund 1949, 1950, 1954, Lund *et al.* 1963). The seasonal dynamics of these species were related to lake trophic status, silica availability, light levels, thermal stratification and the ability of species to form resting stages when under stress. Continued long term phytoplankton monitoring on Lake Windermere has considerably increased the autecological understanding of diatom species (Haworth 1980). Other long term phytoplankton monitoring programs developed to understand phytoplankton seasonal changes include a study on Lake Geneva (Anneville *et al.* 2002). The autecology of individual species has also been investigated: Bradshaw and Anderson (2003) use monitoring data to describe the distribution of *Cyclostephanos dubius* (Frike) Round in Danish lakes in relation to water chemistry. The autecology of *A. subarctica* has been also described with reference to its modern distributions at two sites in the UK (Gibson *et al.* 2003). This chapter will attempt to describe the seasonal

distribution of Lake Baikal's phytoplankton at two depth profiles in the South Basin linked to measured environmental data and define spatial patterns over the lake's surface waters.

The importance of such neolimnological studies combining phytoplankton analysis and environmental monitoring has been expressed by Anderson (1995) and is highlighted in a study of Elk Lake, Minnesota (Bradbury *et al.* 2002). Seasonal successions of species were associated with changing stratification and nutrient conditions, and this information was used to interpret down-core species shifts. The analysis of modern phytoplankton has been used to assess the representivity of the sedimentary record to that of diatoms present in the water column (Cameron 1995, Ryves *et al.* 2003) and to monitor the response to acidification and liming in Swedish lakes (Anderson *et al.* 1997).

4.2 General controls on phytoplankton dynamics

Variations in phytoplankton assemblage over an annual cycle generally tend to replicate the following year although considerable variability can be observed (Wetzel 2001). Dissimilarities may be caused due to changes in individual species performances related to shifts in environmental conditions (Reynolds 1984). The specific causes of interannual differences are not precisely known but are related to interaction and variability in the physical, chemical and biotic factors which may trigger different responses among different species or groups of algae (Reynolds 1984, 1990, 1997). Even though this study is principally concerned with diatom population dynamics, it is also important to consider the role of other algal types such as picoplankton within the lake ecosystem, as reduced diatom productivity (often inferred from palaeo studies) does not necessarily mean reduced algal productivity. This will be discussed later in terms of Lake Baikal's picoplankton (section 8.4.2).

In temperate dimictic lakes, the first diatom blooms of a seasonal cycle occur in spring under ice as light penetration creates turbulence and allows the suspension of diatoms within the photic zone (explained below), although motile algae such as Cryptophyceans and Dinoflagellates as well as diatoms in low abundance, can be present under midwinter ice (Wetzel 2001). In spring, stronger turbulence possibly driven by more intense solar input will allow heavier diatoms to be suspended, thereby influencing the composition of the spring bloom. Suspension is also aided with the development of chitin fibrils from surface processes that have the effect of increasing cell surface area. This mechanism is used by the large *Cyclotella* species, for example, *Cyclotella baicalensis* Skv. has over fifty central processes (Ryves and Flower 1998). During years of reduced turbulence it may only be possible for

smaller centric diatoms to remain in the upper water column (Reynolds 1984). Increases in temperature and irradiance also promote photosynthesis, as diatom species can have well defined optima and tolerances for light and temperature. Changes in climate may have a direct control in determining optimum condition for certain species (section 2.6).

The size and composition of the spring bloom can be limited by nutrient availability. Different species have different nutrient requirements, and abundances may be determined by competition for resources along nutrient gradients. This is demonstrated by the Tilman-Kilham resource based competition theory (Tilman and Kilham 1976). The most important nutrients for diatom growth are P, N and Si amongst others (C, O, H, S, K, Mg, Ca, Na, Cl and other metals at trace levels). As one or more of these nutrients become limiting, one or more diatom species will become more competitive dependant on the ability to prosper without the limiting nutrient. This is assuming that other limiting factors such as light and temperature remain constant. Changes to the ratio of P:Si:N can have a leading role in influencing competition and dominance among phytoplankton assemblages (Kilham and Kilham 1980). For example, Tilman and Kilham (1976) showed that under limiting P, *A. formosa* would dominate over *Cyclotella meneghiniana* (Kutz.) but when Si became limiting the *C. meneghiniana* became more abundant. Under a balanced Si:P ratio or non-limiting conditions both species could coexist.

Nutrient concentrations and ratios through a lake's water column are constantly changing due to biotic uptake but also due to stratification and circulation changes linked to climate variability (Wetzel 2001). Persistent stratification will mean that productivity will leave the epilimnion depleted in nutrients relative to the hypolimnion until being replenished by convective overturn. Climate change can also alter the nutrient supply to a lake through vegetation changes in the catchment, erosion and inflow changes and also modifications to the levels of nutrient cycling. Independent of, or indirectly linked to climate, are biological factors that can control diatom growth. Most importantly is the size of the innoculum or the starting population from which a diatom bloom develops. A larger innoculum of a certain taxon will mean that this species has a good chance of becoming dominant and out-competing other diatoms. The size of the innoculum is a function of the size of the last seasons crop, sinking rates, the ability to form resting stages or overwintering stocks, and zooplankton grazing pressure (Lund 1954). Species with a large innoculum and fast growth rates will be able to establish quickly and dominate a niche at the expense of other diatoms even if environmental conditions change to favour other species. For example, *Nitzschia acicularis* (W. Smith) can reproduce very quickly and fill a niche even at conditions that are not optimal for its growth (Bonderenko 1999).

The development of the summer stratified period sees a decline of diatoms and the dominance of other algal groups (e.g. picoplankton). This can be sometimes due to Si (not needed to such an extent by other algal groups) becoming limiting and increased competition by other algae for nutrients. High light levels and temperature can often be lethal for diatoms during periods of silica limitation, and they sink from the photic layer, aided by a lack of turbulent mixing to form the innoculum for the next bloom (Reynolds 1984). Species-specific grazing and parasitic attacks may also help bias the species composition (Reynolds 1984). The breakdown of summer stratification in autumn and increased convection can lead to an autumn diatom bloom as the innocula are entrained from depth. Again, competition between species (growth rates, nutrient availability, innocula sizes) will determine the biomass and composition of the bloom.

Phytoplankton dynamics are also indirectly controlled by climate which influences stratification, ice cover and nutrient cycling as well as light and heat for photosynthesis (Wetzel 2001). Biological factors are also important in the form of inter-species competition, relative growth rates, the speed of expansion to fill a niche, grazing pressures and innocula sizes. The next section details the documented spatial and temporal dynamics of Lake Baikal's phytoplankton and identifies possible causes for variability while identifying areas where further study is needed.

4.3 Seasonal and interannual dynamics of Lake Baikal phytoplankton

The first studies of Lake Baikal phytoplankton began in the late 19th Century and were based mainly in the South Basin and on a mostly unorganised point sampling methodology. Systematic surveys were started in 1916-29 mostly near the Bolshie Koty biological station in the South Basin by Prof. K.I. Meyer and from the 1960s onwards, lakewide sampling programs began (Popovskaya 2000).

The dynamics of Lake Baikal phytoplankton has been linked to the influence of the timing of ice out and the local influence of rivers and wind in effecting patterns of thermal stratification stabilisation of the water column (Goldman *et al.* 1996). In terms of the general annual productivity of diatoms, the first blooms are under clear ice in the spring where IR light penetrates to the upper water layer and increases its density by bringing the temperature to around 4°C. The subsequent turbulent mixing reduces sinking losses and allows cell numbers to increase in a thin photic zone below the ice. The most rapid period of cell division is in

spring just after ice break-up with intensive turbulence and mixing to around 100 m (Popovskaya 2000). With the development of summer stratification in May-June and increased water temperatures, most diatoms begin to sink from the photic zone often to a depth of around 200-300 m, e.g. in the case of *A. baicalensis* (Kozhova and Izmest'eva 1998) to avoid these higher temperatures. Sinking rates of 60 – 100 m d^{-1} have been reported (Ryves *et al.* 2003). Diatoms are mostly replaced in the upper water column in summer by blue-green algae, cyanobacteria such as *Synechocystis limnetica* Popovsk., *Anabaena lemmermanii* P.G. Richter, chyrosphytes and other algal species adapted to warm, calm, stratified water and high irradiances, while the diatoms present in the summer period are mainly crops of small centric species (Popovskaya 2000). A second peak of diatoms occurs in autumn as summer stratification breaks down and deep wind driven convection of up to 250 m allows the cells of diatoms, such as *A. baicalensis* (Sturm, unpublished) but predominantly *Cyclotella minuta* (Skv.) Antipova, that sank from the photic zone in summer, to return to the upper water column. As *C. minuta* sinks to a much shallower depth than *A. baicalensis* during summer stratification (30 – 50 m), due to its large surface area, it can subsequently be drawn back up to the photic zone faster and in larger numbers to establish a dominant population (Jewson pers. comm). However, this peak is smaller than the spring bloom, as the deep convection limits diatom growth by keeping cells out of the photic zone for long periods. Lake productivity can vary from 9-70 gm^{-3} in low productivity years and from 80-500 gm^{-3} in highly productive years (Popovskaya 2000). In years of low diatom productivity the phytoplankton can be dominated by the picoplankton *S. limnetica* whose abundance is inversely proportional to the level of biomass. During the summer stratified period, picoplankton may account for 60-100% of primary production (Nagata *et al.* 1994). Hence, when considering productivity in Lake Baikal it is important not to just base interpretations on diatom productivity but consider other algal groups too. Although no algal types other than diatoms leave recognisable microfossils in the sediment record, their presence can be detected by the analysis of photosynthetic pigments. A recent study of pigments in the modern lake by Fietz and Nicklisch (2004) estimated the contribution of each dominant phytoplankton group, although not individual species, to total chlorophyll *a* (Chl *a*). As Chl *a* occurs in most algal groups, it is often a better indicator of biomass than biogenic silica content. Fietz and Nicklisch (2004) note a considerable latitudinal difference in surface algal communities, in particular the presence of a 'summer community' in the south during July 2001, but a delayed 'spring community' in the north at the same time, possibly due to the different durations of ice cover. Overall, a decrease in autotrophic picoplankton abundance was found from south to north. However, due to diagenesis through the water column, full reconstuctions of palaeo-phytoplankton crops may not be possible but the relative contributions of algal groups to Chl *a* is possible (Fietz *et al.* in press). Contemporary Chl *a* concentrations in Lake Baikal have

been mapped using remote sensing data. Again results show a latitudinal gradient with lower concentrations in the north compared to the south, while areas influenced by river input also show higher levels (Heim *et al.* in press).

Productivity and distribution of species are not uniform over the lake (Popovskaya 2000), possibly due to climatic gradients, as shown in chapter 5 (in particular the timing of ice formation and melting), interacting with hydrophysical factors, but also lake morphology with different habitats provided by shallow and abyssal regions as well as mountains surrounding the lake providing shelter from wind and precipitation. Bonderenko *et al.* (1996) showed that in May - June 1991, areas of higher biomass were associated with shallow eutrophic waters and areas influenced by river inputs, and there was a pronounced difference in species composition between the North and South Basins. In particular, smaller forms of algae were present in the south while larger cells (*Aulacoseira*) were present in the north. Kozhova and Kobanov (2001) also note a spatial variability of species composition with an abundance of *A. baicalensis* in the South Basin during May 2000, while *S. meyerii* dominated in the Central Basin. A spatial variability of species is also present across the thermal bars. On the shore-side of a bar, marked by high water temperatures and nutrients, high amounts of *A. formosa, N. acicularis, Aulacoseira skvortzowii* Edlund Stoermer and Taylor, and river diatoms were found by Likhoshway *et al.* (1996), while beyond the thermal bar pelagic *Cyclotella* species and *A. baicalensis* dominated in the colder oligotrophic waters. The thermal bar can be seen as a barrier dividing two very different habitats during the early summer period (Holland and Kay 2003) while they also play an important role in bringing nutrient rich deep water up to the photic zone via cabbeling (see section 2.2.2.3) (Botte and Kay 2000). Investigation of individual species abundances at a single location has revealed large interannual variability. This was assigned to the fact that innoculum sizes will differ between years (Grachev and Likhoshway 1996). Total phytoplankton biomass through the water column has been studied (Atlas Baikalia 1993, Bondarenko *et al.* 1996, Popovskaya 2000). It is often found that maximum productivity is found several metres below the water surface due to light inhibition at the lake's surface (Straskrabova *et al.* in press). Biomass then declines from this maximum with increasing water depth. Although the spatial distribution of total phytoplankton biomass has been investigated extensively (Popovskaya 2000), less published work exists on the quantification of the lake-wide spatial distribution and abundance of individual diatom species during the year. For example, Grachev and Likhoshway (1996) summarise existing data, although the authors state existing records are problematic and patchy. Grachev and Likhoshway (1996) also present lake-wide abundances of the main diatom species but, for only a May – June average for water depth 0 – 50 m for 1991 - 1993. There are however detailed records of species' annual and seasonal abundances from the monitoring station at

Bolshie Koty (Grachev and Likhoshway 1996). A study by Fietz *et al.* (in prep.) indicates variability over the lake of phytoplankton types shown by pigment analysis. An assessment of the contributions of microplankton and picoplankton revealed again a north–south gradient in species composition which can be related to climatic differences between the lake's three basins. Additional more detailed studies of Lake Baikal's phytoplankton are needed, particularly over seasonal cycles. This information would be useful when linked to measured climatic, limnological and chemical variables to aid in understanding of planktonic diatom ecologies.

Moving beyond the seasonal succession and spatial distribution of species, Lake Baikal's phytoplankton also shows a distinct interannual variability and possible periodicity in species assemblage composition. The main variation is due to the occurrence of *Melosira* years dominated by *A. baicalensis* (formerly known as *Melosira baicalensis* (Meyer) Wisl.) (Kozhov 1963). Biomass can be greater by 10 times during these years than in non-*Melosira* years. Analysis of monitoring data by Rychkov *et al.* (1989) showed a quasi-periodicity between *Melosira* years, pre-*Melosira* years defined by *C. minuta* and post-*Melosira* years often marked by *Synedra* species. *Melosira* years commonly occur ever 2-4 years but rarely in successive years. Rychkov *et al.* (1989) noted an 11 year cycle in this trend between 1950-71 although weakening in the 1970s. The true causes of this interannual variability are not known but are possibly linked to variations in ice-cover duration and subsequent mixing regimes, variations in ice snow depth, nutrient availability, temperature/climate change and grazing activity. Timing and impact of these factors alone or in combination determine the seasonal abundance and composition of diatom crops (Flower *et al.* 1998).

As diatoms need light for photosynthesis, longer ice cover duration especially with deep snow cover or an opaque snow-ice amalgam will reduce light penetration and suppress the spring diatom bloom. Light generated turbulence is also vital to keep the heavy *A. baicalensis* cells suspended in the water column. At this point in their life cycle cells become longer with an increased surface area to overcome sinking (Skabichevskyii 1977). Another mechanism by which turbulence is generated is via changes in water density, linked to varying salinity and temperature below the ice (Granin *et al.* 2000). The importance of light intensity on *A. baicalensis* crop size linked to snow cover has been shown by Granin *et al.* (2000), they observe smaller crops during a year with deeper snow cover. However, the importance of the starting innoculum size is also noted. As a result the strength of the spring *A. baicalensis* bloom may fluctuate interannually due to variations in light transmission through the ice, and *A. baicalensis* should be dominant following winters of minimal snow cover (Kelley 1997) as light will not penetrate snow >10 cm thick (Jewson and Granin 2000). Snow cover will be

influenced by changes in winter precipitation amount, wind speed and direction and temperature (Bush 2004). Reduction in ice cover duration and an earlier of ice-off date can cause an earlier and longer summer stratification (Jewson and Granin 2000). This in turn will mean that *A. baicalensis* cells that sank to avoid the warmer waters will continue sinking and are less likely to be resuspened as the innoculum for the next bloom. Therefore another species may fill the niche left behind. The *Aulacoseira* species form resting spores at the termination of the vegetative period to preserve overwintering stocks. In the case of *A. skvortzowii* these spores can be entrained from shallow littoral sediments at the start of spring overturn in the photic zone to initiate sexual reproduction (Kobanova 2000).

The most important limiting nutrients for diatom growth are N, P and Si as shown above. N and P have been considered not to be limiting in Lake Baikal but during *Melosira* years NO_3-N in surface waters can become depleted while PO_4-P never becomes fully exhausted (Verkhozina *et al.* 2000a). This is mainly a result of rapid P recycling by picoplankton (Jewson pers. comm.). After ice break-up, nutrient concentrations are restored by the mixing of the nutrient rich deep waters. However, observed deficiencies in NO_3-N (Votintsev *et al.* 1975) in the trophogenic layer probably mean Lake Baikal is N-limited. Fluctuations in biomass are not proportional to these changes in N concentration, and Verkhozina *et al.* (2000b) state that changes in N may be of an order of magnitude too low to explain observed shifts in biomass. This means that other limiting factors are also involved. Verkhozina *et al.* (2000a) suggest lake hydrodynamics linked to nutrient supply are also limiting, that is the level of mixing of the deep nutrient rich waters that replenish the depleted surface waters. During spring and early summer, phytoplankton growth is not considered to be nutrient limited, as waters are well mixed (Goldman *et al.* 1996). During summer stratification, nutrients cannot be replenished from deeper waters and may become limiting. However, Genkai-Kato *et al.* (2002) analysed particulate carbon, nitrogen and phosphorus in lake water over one year (1999) and concluded that although Lake Baikal was nutrient poor, the ratios of nutrients were stable and phytoplankton is not exposed to limiting nutrients. This study was undertaken in a non-*Melosira* year of relatively low productivity meaning that nutrient supplies were possibly not overly stressed. However, it is important to consider the role of mixing in transferring these nutrients to the photic zone (*c.f.* Verkhozina *et al.* 2000a). Although Si is not often recognised as a limiting nutrient (Verkhozina *et al.* 2000b), the extensive growth of the heavily silicified *A. baicalensis* during *Melosira* years can leave the lake limited in Si (Jewson pers. comm.). As a result, subsequent diatom populations, for example the autumnal *Cyclotella* bloom or the next spring bloom will be Si limited until the reservoir is replenished. Si limitation (for *A. baicalensis*) also favours the development of lightly silicified diatoms such as *N. acicularis* (Bondarenko 1999). In these years of low

diatom productivity, the dominant producer is the picoplankton which does not require Si (Popovskaya 2000).

Laboratory culturing experiments have determined the temperature and light optima and ranges for several Lake Baikal diatom species (fully discussed in section 5.8.1) (Richardson *et al.* 2000, Jewson *et al.* unpublished). The cultured diatoms, five endemic and two non-endemic taxa showed clear responses in growth rate to varying light and temperature. Most notably, *A. baicalensis* was found to grow best at lower temperatures and light regimes. This indicates that at least some of Lake Baikal's endemic diatoms are adapted to thrive in cold waters under ice. Levels of irradiance can change with the amount of snow cover in winter-spring and the depth of mixing in summer-autumn. Deep circulation means diatoms will be removed from the photic zone for a longer time than during periods of shallower convection. However, optima derived in the laboratory cannot be used exclusively to understand diatoms in the real lake, due to the variability and competition in the natural environment compared to laboratory conditions (Anderson 2000, Jewson *et al.* unpublished). The occurrence of the temperature optimum of a certain species in Lake Baikal may not imply that the species will become dominant in the plankton. The size of the innoculum of the population and the speed at which a bloom develops are important. For example, *Synedra* species can establish quickly into a niche and dominate over a broad range of temperatures at the expense of other taxa which could be growing under optimal conditions (Jewson pers. comm.).

General levels of diatom phytoplankton biomass have been directly linked to climate variability. Kozhova and Izmest'eva (1998) note a correlation between higher summer temperatures and greater plankton biomass in deep water regions, while Verkhozina *et al.* (2000b) notice a correlation between spring phytoplankton biomass and potato harvests in the Irkutsk district that implies a common climatic control by empirical comparison only. Assuming that nutrients and light availability are not limiting, lacustrine productivity may be driven by climate in the same way terrestrial productivity is. However, this is a rather simplistic correlation that does not consider other limiting factors on phytoplankton. The role of climate in the form of solar cycles has also been considered as an important factor in determining the interannual variability of *A. baicalensis* and *A. skvortzowii* (Evstaf'ev and Bondarenko 2002) although this observation may be explained equally as well by the three year life cycle seen in these *Aulacoseira* species.

Grazing of diatoms by zooplankton also reduces the size of diatom populations. The endemic copepod *Epischura baicalensis* Sars. is the major grazing species in Lake Baikal and plays a vital role in the cycling of organic matter (Mazepova 1998). The other main zooplankton

species is *Cyclops kolensis* Lill. although production is only 4% that of *E. baicalensis* (Mazepova 1998). Other species from the *Cyclopodia* and *Harpacticoida* genera are present but their numbers are small. The impact of grazing has been considered to be insignificant through analysis of sediment trap and surface sediment data (Ryves *et al.* 2003). However, grazing under the ice may be important in determining the size of the innoculum for the following season. It is also possible that diatoms can be transferred to the sediment very quickly via faecal pellets, although chains of diatoms are likely to be broken and slightly digested by the grazing process (Ryves *et al.* 2003). Grazing may also be species specific to some extent, e.g. centric diatoms may be more palatable than the needle like form of the pennate *Synedra* diatoms. Numbers of *E. baicalensis* are insignificant during winter ice cover but numbers increase under the spring ice as nauplii begin to hatch in deeper water before rising to the surface (Kozhva and Izmest'eva 1998). As a result of fast reproduction, a second generation of *E. baicalensis* in the summer leads to the annual maximum zooplankton abundance. As autumn progresses, numbers decline and the adult *E. baicalensis* subsides through the water column (Kozhva and Izmest'eva 1998). Zooplankton is also able to 'follow' the vertical migrations of algae to maximise food-gathering potential (Reynolds 1984). During periods of deep mixing, *E. baicalensis* can follow diatom cells to such depths that the zooplankton may not be able to return to the photic zone (Jewson, pers. comm.).

In summary, spatial and temporal and seasonal and interannual changes in diatom bloom productivity and composition are driven by the complex linkages between climatic, limnological and biological factors. It may be that climate is the overriding factor by varying the physical and temporal characteristics of ice cover, which in turn can alter hydrophysical factors (Popovskaya 2000). This is demonstrated by the occurrence of diatom species over N-S environmental (climatic) gradients (chapter 3). However, certain aspects of phytoplankton dynamics need additional study, in particular quantitatively linking diatom abundances to measured environmental and chemical variables. Also, a higher resolution study of populations in the surface waters over the whole lake will help elucidate any N-S trends in phytoplankton species' compositions and productivity. Monitoring data analysed in this study can also be added to the 10 years of data collected by D.H. Jewson, N.G. Granin, P. Rioual and G.H. Clarke (unpublished) from the same sampling program.

4.4 Methodology

4.4.1 Sampling methodology

All samples analysed were taken as part of the long-term phytoplankton monitoring program co-ordinated by N.G. Granin (Limnological Institute, Irkutsk). Samples taken consist of surface waters taken from stations as shown in figure 4.1. At five stations depth profiles were also sampled. These were at 4 km Ivanovsky and Listvyanka-Tankhoy in the South Basin, Ukhan-Tonky in the Central Basin, Elokhin-Davsha and Baikalskoe-Turali in the North Basin (figure 4.1). Samples were taken at depths of 0, 5, 10, 15, 25, 50, 100, 150, 250, 500, 750, 1000, 1200, 1300 – 1400 m or until the sediment surface was reached. Samples analysed in this study are from the South Basin depth profiles (as the cores analysed are from the south) and South Basin surface waters collected during 13 campaigns between February 2001 and October 2002, although not all stations were sampled during each campaign and there was little sampling during the ice-cover period. To achieve a complete surface coverage of the lake with the samples available, surface waters for the North and Central Basins for this period counted by P. Rioual (unpublished) are combined with the data set of this study.

Initial water samples of 1.5 l were preserved with Lugol's iodine on site and then concentrated to 30 ml by a two stage process of settling and decanting over 10 days in the laboratory. Samples were sealed in sterilin tubes and kept refrigerated. Boxes of samples from each campaign were sent by post to UCL where they were catalogued and kept in refrigeration at 4°C until being counted.

At each sampling location of the depth profiles, water chemistry data were also collected, measured variables were N, NO_3, P, PO_4 and O_2. To aid interpretation, further environmental variables of water temperatures and secchi depth were added from secondary data (Shimaraev *et al.* 1994). These measurements are not contemporary with the samples taken, but as these measurements are averaged over a period of several years, interannual variations will be smoothed out and they can be considered representative of general environmental conditions. It is also known that the timing of water temperature variations over several years are very minor (Jewson, pers. comm.).

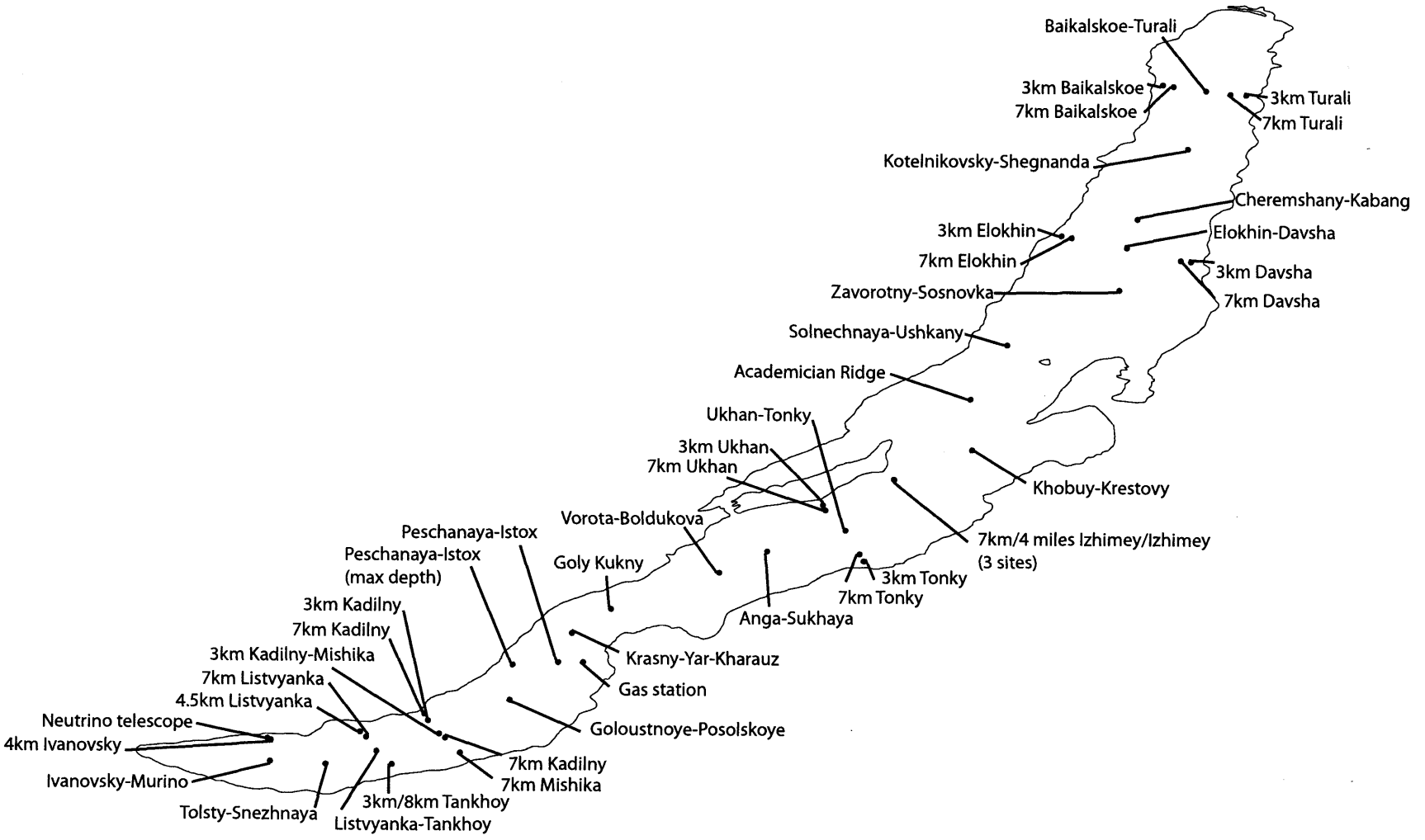

Figure 4.1: Sampling locations for phytoplankton in 2001 - 2002. Each location was not always sampled during every campaign.

4.4.2 Sample preparation

Before phytoplankton counting, samples were further concentrated. This was done quantitatively by settling the sample, removing a portion of the supernatant with a pipette and weighing the sample. The amount of liquid removed varied between samples and depended on a visual inspection of the amount of material settled at the bottom of the sterilin. Samples containing a lot of material often did not require any further concentration. Counting methodology was based on that outlined by Utermöhl (1958). Samples were allowed to acclimatise to room temperature to avoid the bubbles that form if the sample warms in the counting chamber. Samples were homogenised by gently rolling the sterilin tube to avoid breaking diatoms and the disintegration of colonies. 1 ml of sample was placed in a counting cell of volume 2 ml and diameter of 25 mm with a micro-pipette and topped up to 2 ml with distilled water to prevent drying out. It was not considered necessary to use settling towers as described by Utermöhl (1958), as the samples were concentrated enough for counting to allow the counting cell to be filled directly. Samples were allowed to settle for at least 2 hours before counting at x400 magnification on Leitz Diavert inverted microscope.

4.4.3 Counting methodology

Several published methods exist describing best practice for phytoplankton counting with an inverted microscope, including Acker (2003) and Flachseen-Forschung in Deutschland (2003). It was decided to count between 40-80 fields of view (FOV) per sample in this study. This figure was reached after preliminary analysis, when it was discovered that increasing the numbers of FOV did not greatly alter the species assemblage. FOVs were defined along transects moving the slide at 1 mm intervals. Using this method, FOV were located both at the centre of the cell but also around the edges. This helps remove the problem of biasing the counted assemblage, as certain sized species can settle out nearer the chamber walls rather than the centre.

4.4.4 Taxonomy

Although this study is primarily interested in diatom population dynamics, other algal groups were also enumerated but are not presented here. Diatom taxonomy is detailed in section 6.2.4, but identification under the inverted microscope was aided by Cox (1996). Figure 4.2 shows the main diatom species found in phytoplankton samples. It was also very difficult to identify some centric diatoms to species level. Where this was a particular problem, a light microscope slide was prepared to aid in identification. The endemic species *C. minuta, C.*

ornata and *C. baicalensis* were lumped together as *C. minuta* complex because of the difficulty of distinguishing between these species under the inverted microscope. A distinction between live diatom cells containing chloroplasts and completely empty (dead) cells was made. Dead diatom cells were often broken or separated so two frustules (or corresponding fragments of) were counted as one cell. Live cells that were broken, were also counted as half a live cell, as breakage most likely occurred during sampling, transit or sample preparation. Other algal groups were identified with the aid of general floras such as Belcher and Swale (1976), Canter-Lund and Lund (1995) and John *et al.* (2003) while floras specific to Lake Baikal included Timoshkin (1995), Khozova and Izmest'eva (1998) and the species lists of Bondarenko *et al.* (1996) and G. Kobanova (pers. comm.).

Cyclotella baicalensis

Cyclotella ornata/minuta

Synedra acus v. radians

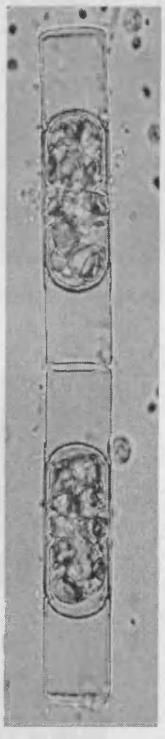

Aulacoseira skvortzowii
resting spore and dead vegetitive cell

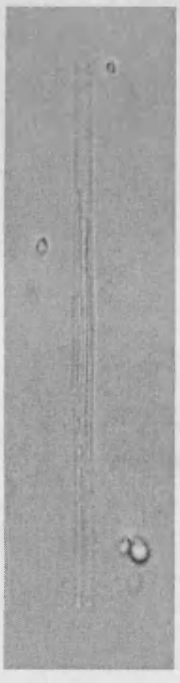

Synedra acus v. pusilla

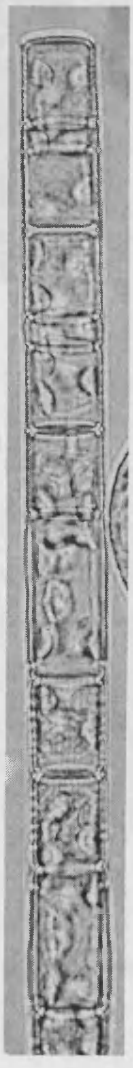

Aulacoseira baicalensis

20 microns

Figure 4.2: Common planktonic diatom species found in Lake Baikal in 2001-2002, all cells are live unless otherwise stated.

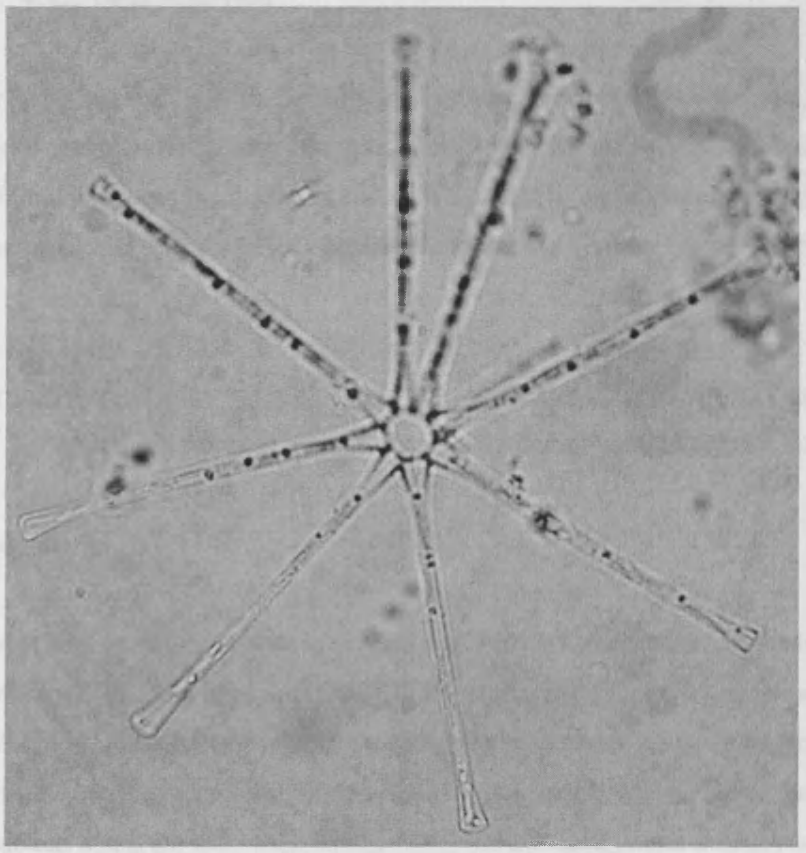

Asterionella formosa

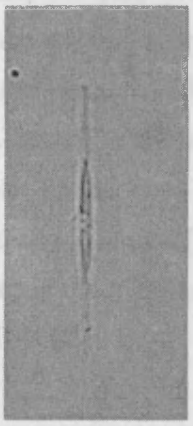

Nitzschia acicularis

Cyclotella minuta

20 microns

Stephanodiscus meyerii

Figure 4.2: Continued.

4.4.5 Data analysis

As the sampling and counting procedure is entirely quantitative it is possible to transform species counts into the number of a species cells per original litre of lake water (cells l^{-1}). The area of the FOVs counted is known and with the total area of the counting cell and the volume of material placed into the cell, it is possible to use the conversion of Acker (2002) (equation 4.1).

$$\text{Cells } l^{-1} = \frac{((\text{Area of counting cell}/\text{Area of FOV})*(\text{species cell count}/\#\text{FOV counted}))*1000}{(\text{Original sample volume}/\text{subsample volume})*\text{sample volume counted}}$$

Equation 4.1.

Counts of identified species were entered into Excel 97 and transformed into cells l^{-1} using equation 4.1. The data were subsequently transformed by log(x+1) to allow easier graphical representation, although numerical analysis was performed on untransformed cells l^{-1} data. The spatial distribution of diatom species over the lake for a particular sampling campaign were plotted using the GIS software ArcView v.3.2a while depth profiles were plotted using SigmaPlot v.8. Constrained ordination was used to aid with interpretation of the environmental data in comparison to the phytoplankton counts. The significance of the ordination axes was tested using a restricted Monte Carlo permutation test so as to confine randomisation only within each profile from a certain campaign and not between the whole dataset, as individual profiles are not directly comparable. As no environmental data are available to combine with the surface water biological data, these were interpreted qualitatively in terms of changing season and latitude. Ideally, remotely sensed ice cover data would be of use to compare to biological surface water data, but images could not be obtained for 2001-2002.

4.5 Surface waters

4.5.1 Results

The investigation of surface water productivity is useful in terms of diatom autecological information as these data are not complicated by differential dissolution as in the case of investigating species responses with surface sediments (Ryves *et al.* 2003). Figures 4.3 to 4.11 show the abundance and spatial lake-wide distribution of the main planktonic diatom

species on a log scale for seven campaigns between February 2001 and June 2002. For February and April, samples could only be taken in the South Basin but there is almost complete coverage for June, July and October. Live cells of *A. baicalensis* were mostly absent in February and April 2001 except for an isolated occurrence at Listvyanka-Tankhoy in February 2001 (figure 4.3). By June 2001, *A. baicalensis* was still absent from the South Basin but abundant in the North Basin (205900 cells l^{-1} at 3km Baikalskoe). Abundance was still high in the north in July but the bloom was beginning to die out with a greater occurrence of dead cells and an even more extreme northern distribution. By October live cells were almost totally absent from the whole lake surface. The next *A. baicalensis* bloom was recorded only in the South Basin during June 2002 where the species was apparently not present in 2001. *A. skvortzowii* was abundant in the south under ice in February 2001 (13200 cells l^{-1} at Listvyanka-Tankhoy) but did not establish outside the South Basin despite some scattered occurrences of live and dead cells in June 2001 (figure 4.4). The same pattern of distribution appeared to repeat in 2002. *A. skvortzowii* resting spores were produced in the areas of maximum bloom (mostly the South Basin) in June of both years as the crop died out (figure 4.5). According to the samples analysed, *C. minuta* complex was absent during winter and spring periods and became dominant lake-wide in June 2001 and 2002 (figure 4.6). Productivity was highest in the south with 4900 cells l^{-1} at Kadilny-Mishika compared to 350 cells l^{-1} at Baikalskoe-Turali in the North Basin (June 2001). In July 2001, numbers appeared to reduce, before increasing again in October. This may be due to summer stratification and sinking of cells to deeper waters. There was a greater abundance of dead *C. minuta* complex dead cells in October indicating a dying out of the crop. The bloom in 2002 occurred at a similar time however, and a small number of live cells were present in February 2002.

S. acus v. radians and *S. acus v. pusilla* had similar distributions (figures 4.7 and 4.8). Both were common under the spring ice in February and April 2001 and also in June over the South and Central Basins, but not in the North Basin. The bloom began to die during July with dead cells present in greater numbers. At this time, the most abundant *S. acus v. radians* was isolated to the Central Basin while *S. acus v. pusilla* receded southwards although being present in the North Basin at low numbers. By October 2001 both species (live and dead cells) were almost absent from the lake surface. The distribution in June 2002 was almost identical to 2001 with the South and Central Basins abundant in *Synedra* sp. only as far north as Ukhan-Tonky. As these *Synedra* species often bloom in near-shore eutrophic waters influenced by riverine input (Bradbury *et al.* 1994), their paucity in the North Basin may be due to a lack of habitat. The Selenga River in the south will promote a larger bloom with areas of warm waters and nutrients. *S. meyerii* first appeared in scattered occurrences at eight stations mostly, over the Central Basin during June 2001 (figure 4.9). This crop died out in

July 2001 and was all but absent in both live and dead forms by October 2001. The summer bloom in 2002 was confined to the South Basin and was not seen to spread to the Central Basin as in 2001. This bloom was very large reaching up to 740600 cells l^{-1} at Peschanaya-Istok in June 2002. *N. acicularis* occurred at relatively lower numbers for the whole of the monitoring period (figure 4.10). It was present under the ice in spring, and by June 2001 was most abundant in the north and south extremes of the lake. Abundance declined by October but it also appeared over the whole lake in June 2002. As found in the depth profiles, *A. formosa* was almost absent in 2001 although present by October mostly in the Central Basin. Low abundance was recorded over the South Basin in June 2001 (figure 4.11).

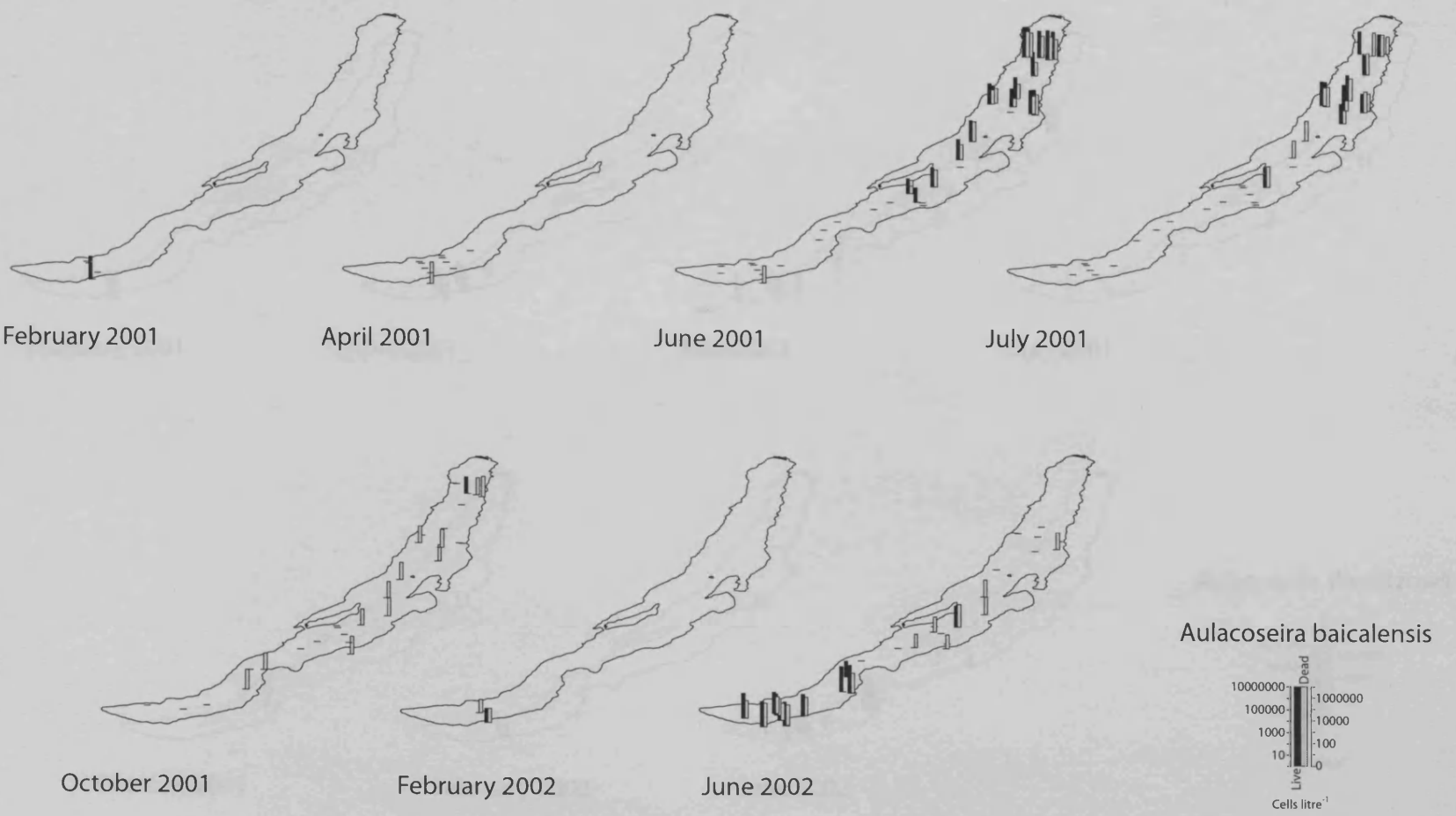

Figure 4.3: Distribution of *Aulacoseira baicalensis* live and dead cells in Lake Baikal surface waters February 2001 - June 2002.

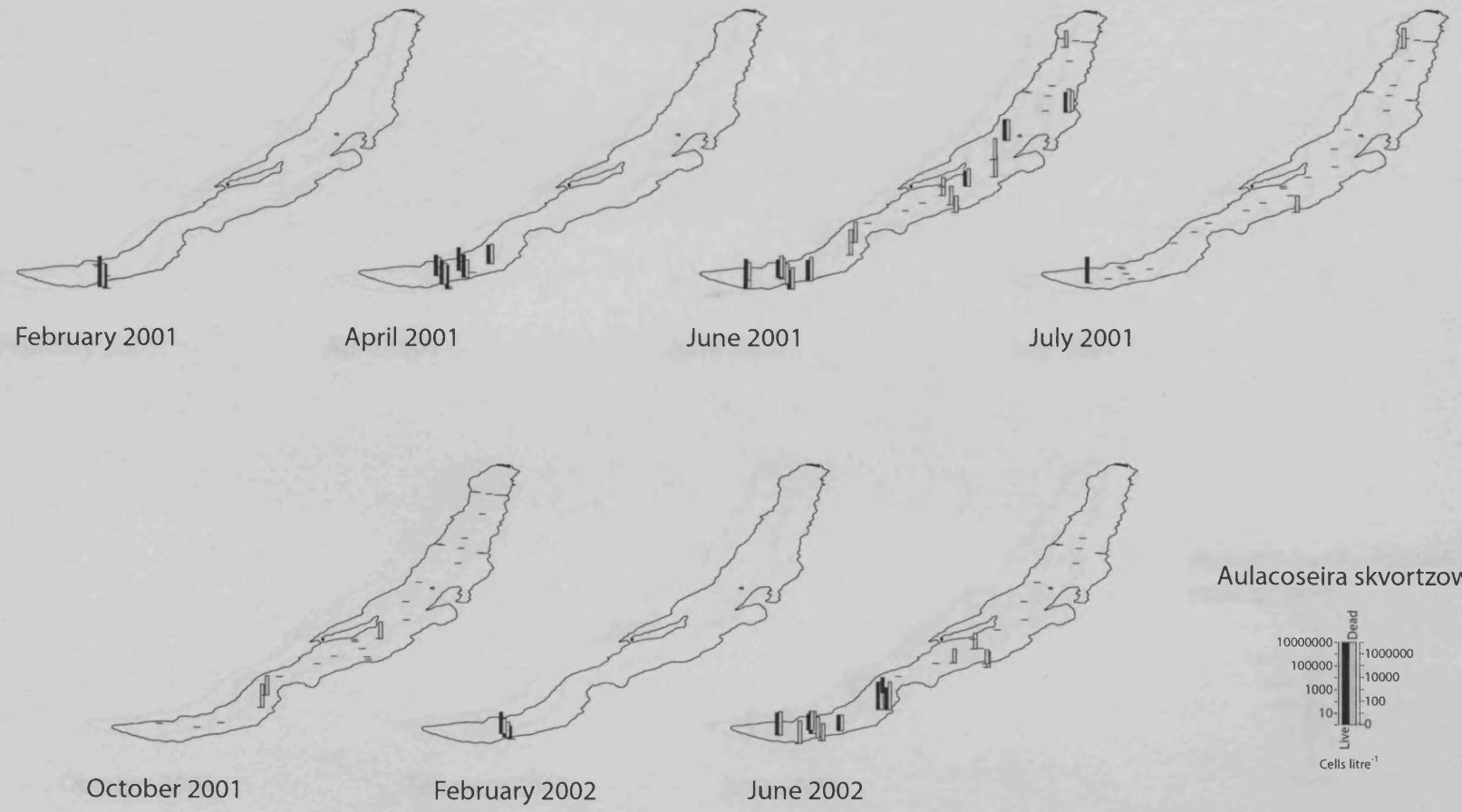

Figure 4.4: Distribution of *Aulacoseira skvortzowii* live and dead cells in Lake Baikal surface waters February 2001 - June 2002.

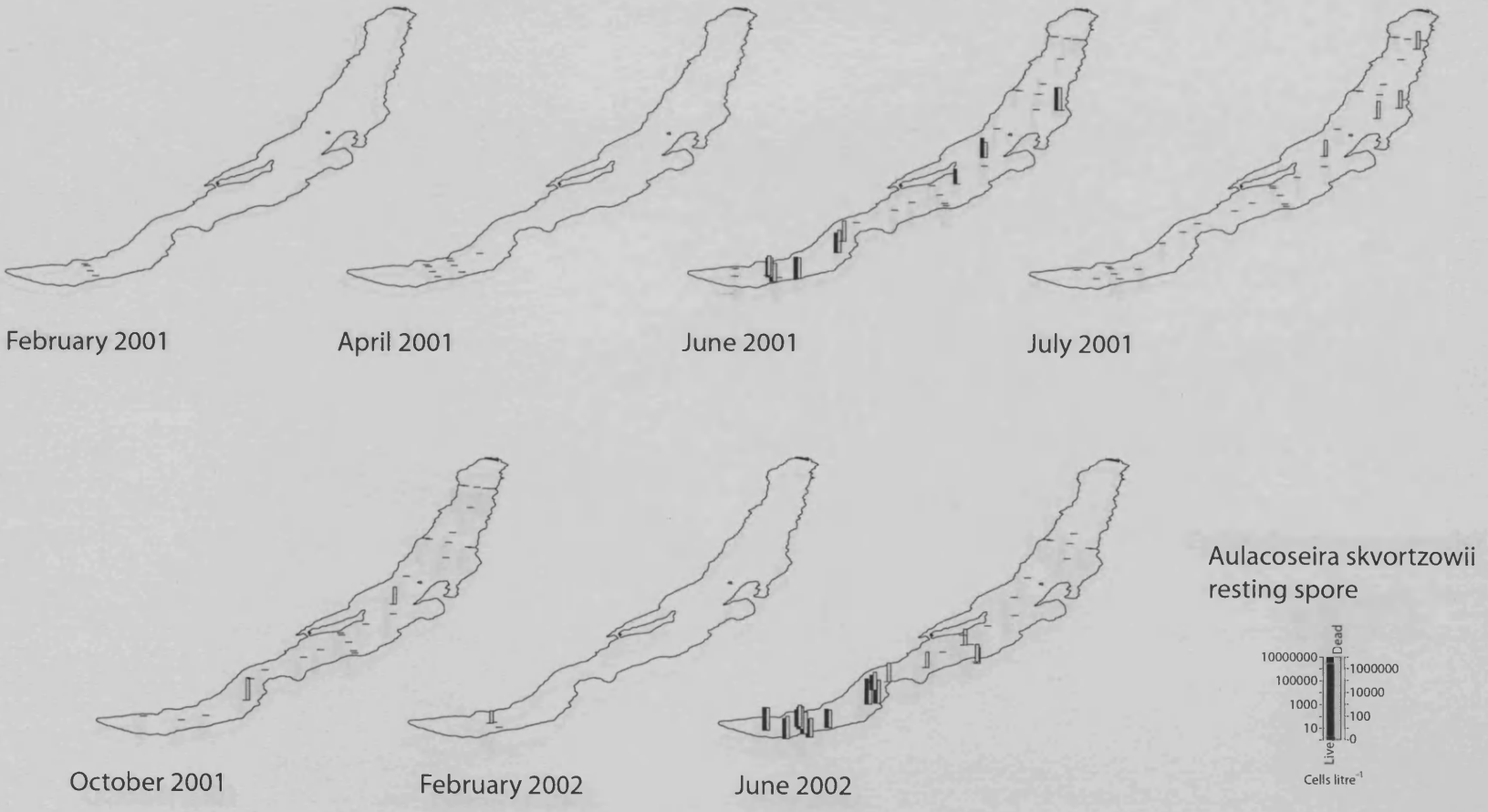

Figure 4.5: Distribution of *Aulacoseira skvortzowii* resting spore live and dead cells in Lake Baikal surface waters February 2001 - June 2002.

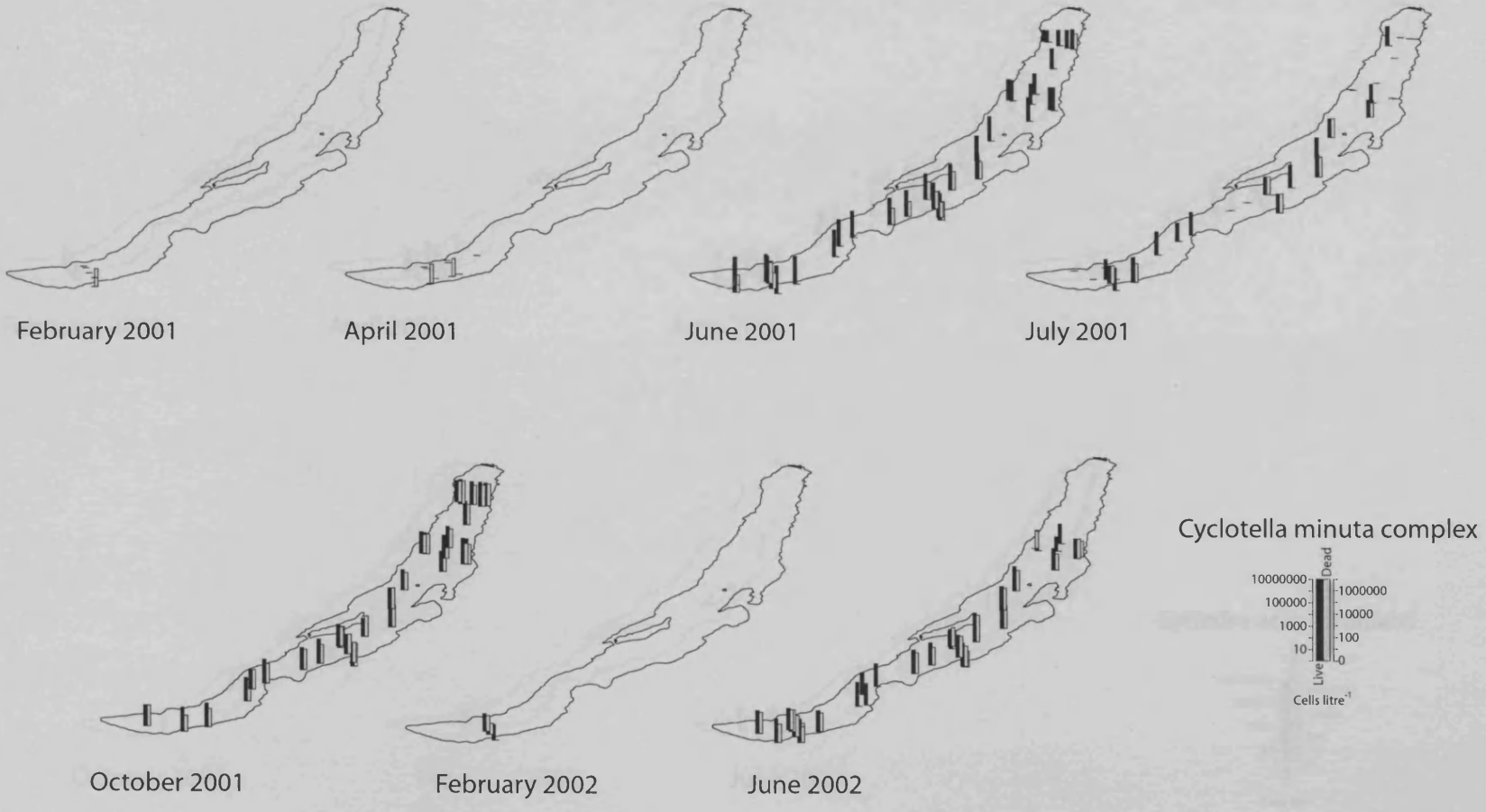

Figure 4.6: Distribution of *Cyclotella minuta* complex live and dead cells in Lake Baikal surface waters February 2001 - June 2002.

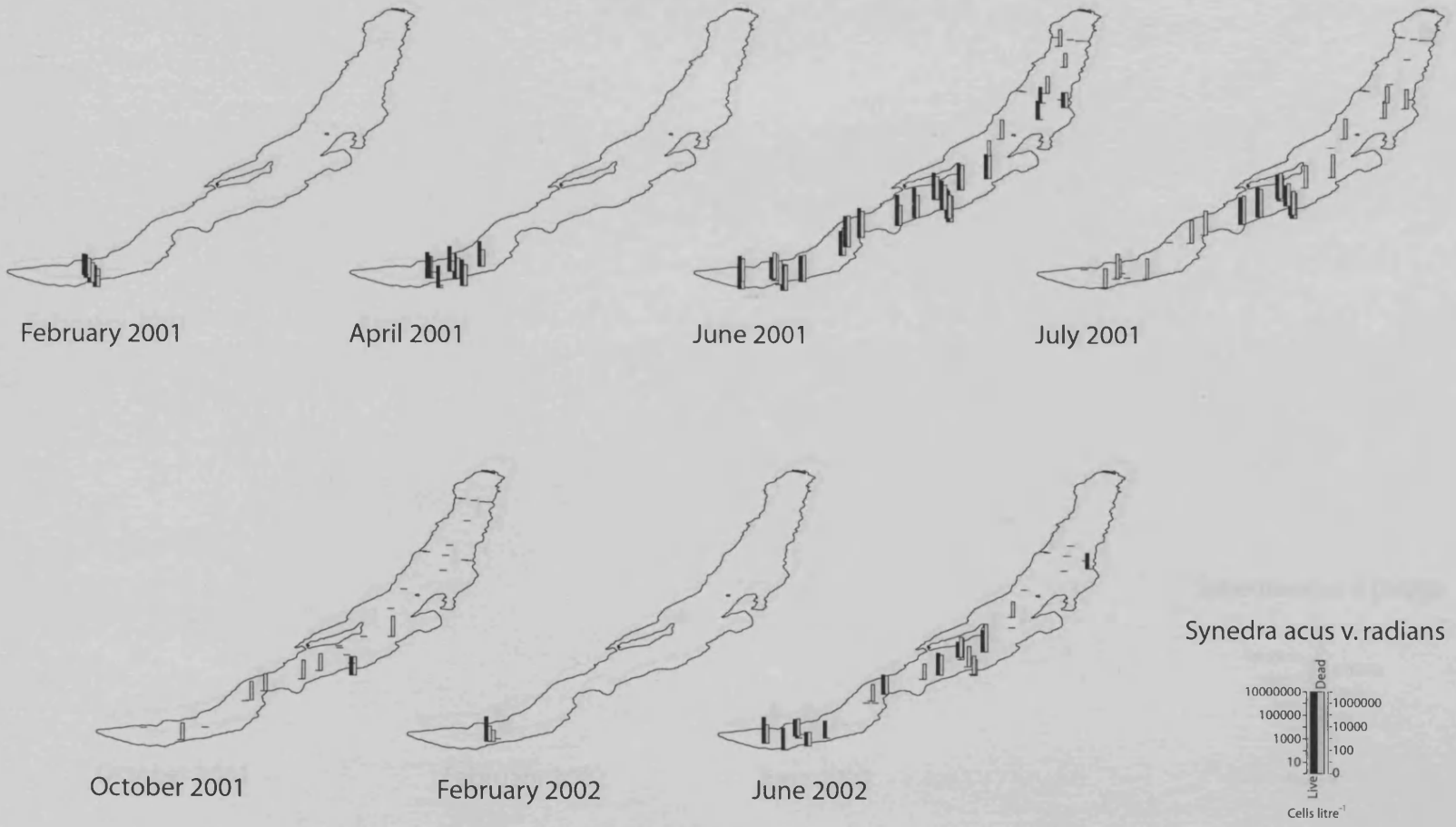

Figure 4.7: Distribution of *Synedra acus* v. *radians* live and dead cells in Lake Baikal surface waters February 2001 - June 2002.

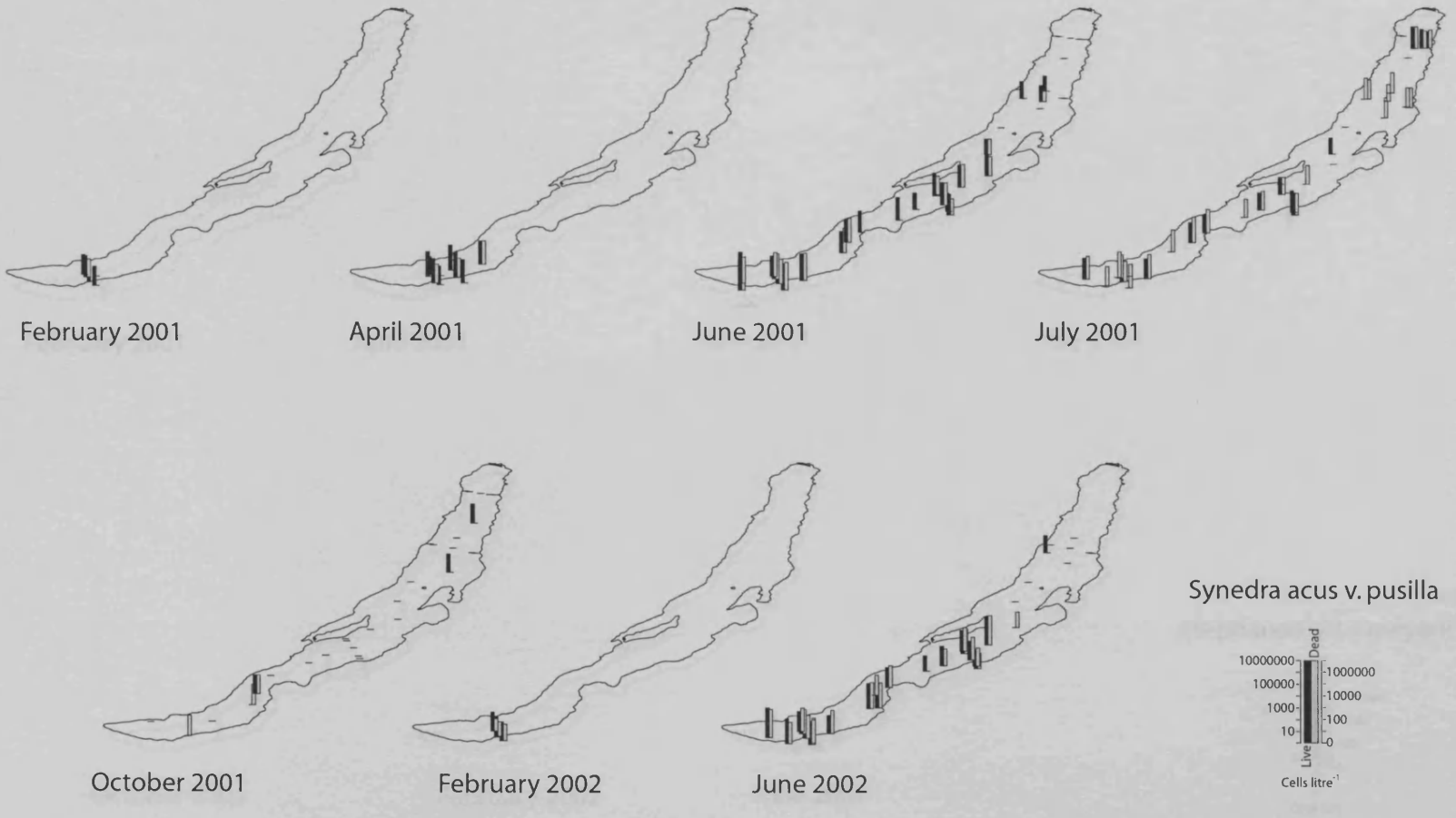

Figure 4.8: Distribution of *Synedra acus* v. *pusilla* live and dead cells in Lake Baikal surface waters February 2001 - June 2002.

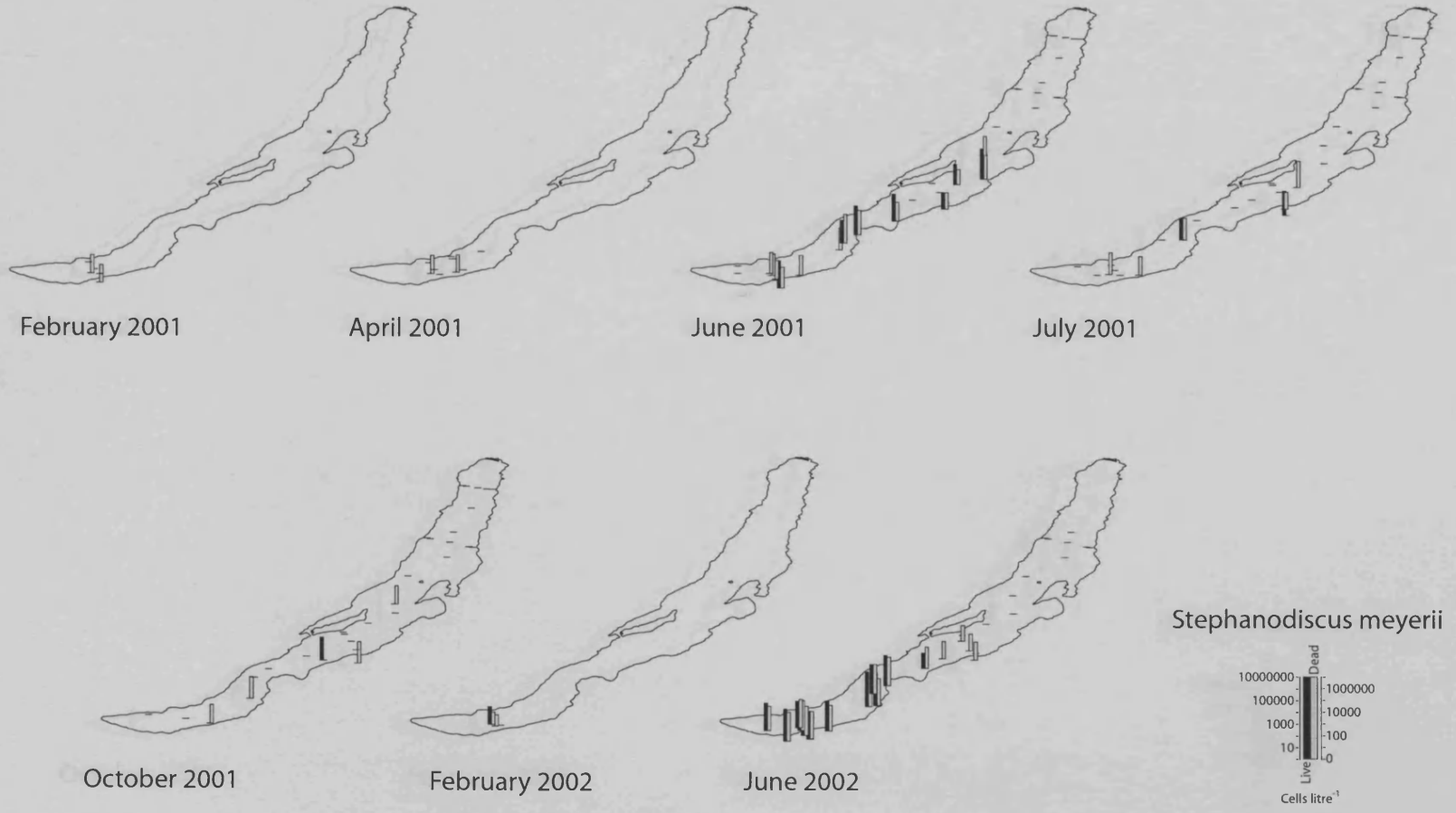

Figure 4.9: Distribution of *Stephanodiscus meyerii* live and dead cells in Lake Baikal surface waters February 2001 - June 2002.

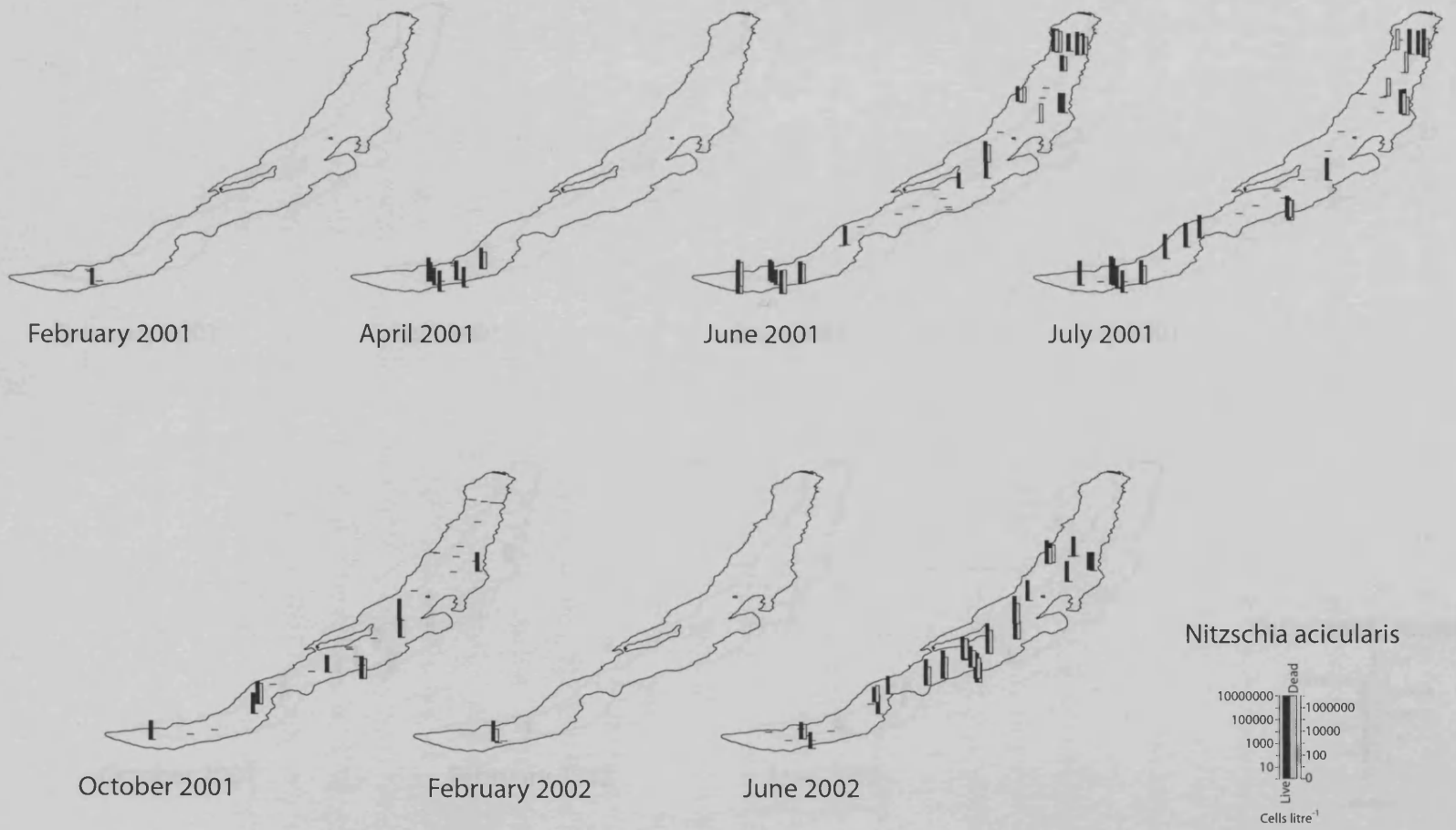

Figure 4.10: Distribution of *Nitzschia acicularis* live and dead cells in Lake Baikal surface waters February 2001 - June 2002.

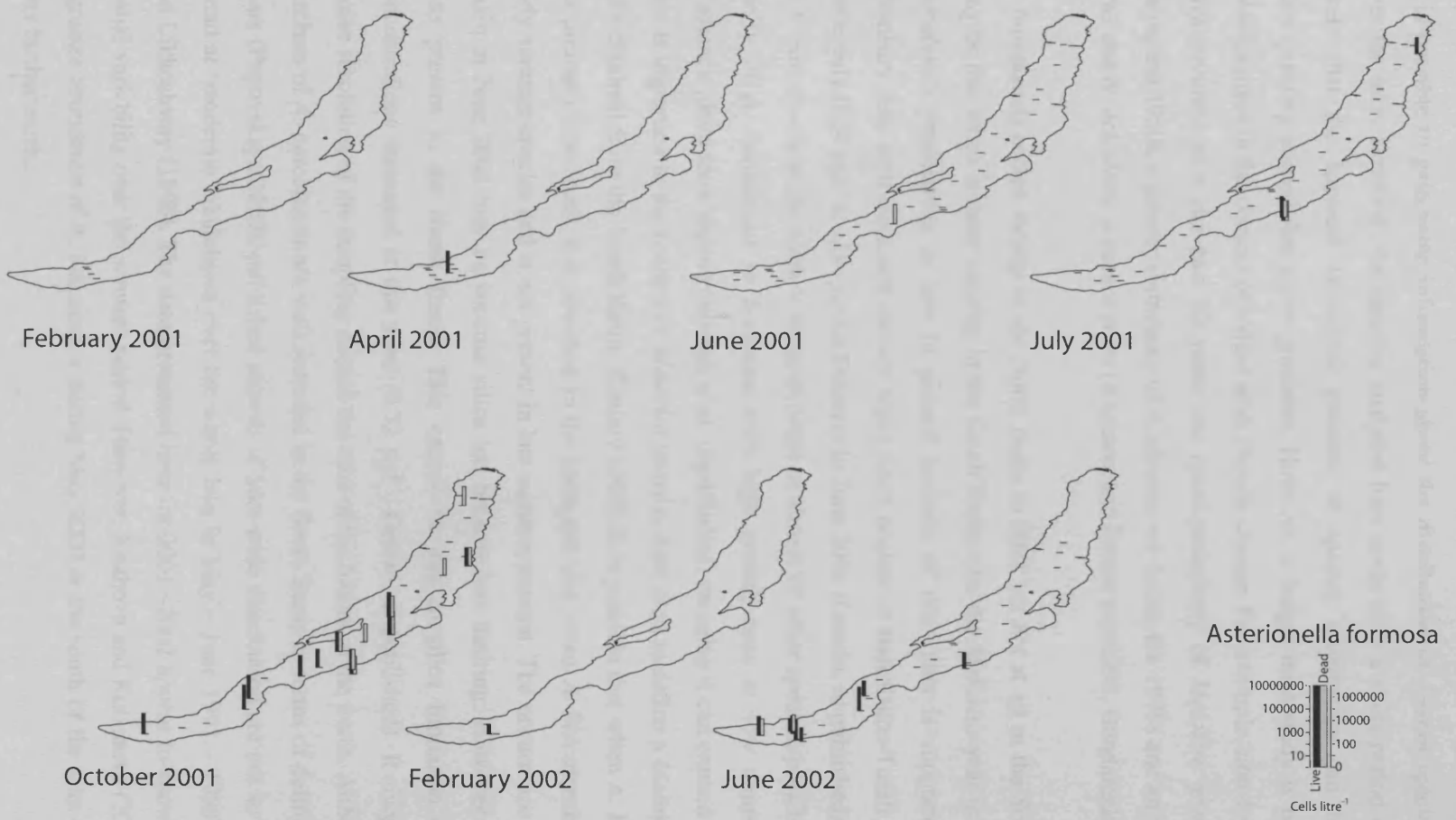

Figure 4.11: Distribution of *Asterionella formosa* live and dead cells in Lake Baikal surface waters February 2001 - June 2002.

4.5.2 Discussion

It is possible to gain some information about the distribution of diatom species seasonally over the lake. However, the samples analysed here cover only a short period of time. It is likely that the apparent latitudinal gradient of species distribution can be linked to corresponding climatic/ice cover gradients. However, a longer term study is needed to put these changes in the context of longer term climate change. For example, noted species shifts have occurred over the past 50 years; the quasi-periodicity of *Melosira* years especially during the 1950s, a greater abundance of *A. skvortzowii* during the 1970s and an increase in *S. acus* and *N. acicularis* in recent years (Kozhova and Izmest'eva 1998, Bondarenko 1999).

A. baicalensis occurs mostly in the North Basin in 2001 but not at all in the South Basin. It may be that silica is more limiting in the South Basin after the *Melosira* year in 2000 and *A. baicalensis* productivity is low in general because of this. This is supported by water chemistry data with measured surface water silica content at Baikalskoe-Turali at 0.71 μgl^{-1} while only 0.24 μgl^{-1} at Listvyanka-Tankhoy in June 2001 (Granin, unpublished). Abundance of *A. baicalensis* in the north is at the expense of almost all other species, possibly due to the ability of *A. baicalensis* to dominate with high growth rates at low temperatures and irradiance (deep snow cover) (Jewson *et al.* unpublished) meaning it can expand into a niche. This is important in the context of *Melosira* years as data used to define a *Melosira* year was only obtained from the South Basin (Kozhov 1963). It is possible that when *A. baicalensis* is not present in the south, it is abundant in the north and *vice versa. A. baicalensis* is a spring-early summer species and is not present in late summer-autumn. The occurrence in the South Basin in June 2002 may be because silica has become less limiting. However there are no cells present in the North Basin. This cannot be due to silica limitation due to high concentrations measured at this time (0.72 μgl^{-1}, Granin, unpublished). It may be that the coarse resolution of the sampling missed the start of the bloom in the north. Although, annual numbers of *A. baicalensis* are well recorded in the South Basin in terms of defining *Melosira* years (Popovskaya 2000), published records of lake-wide distribution are not so clear. It was found at 'moderate' abundance over the whole lake in May – June 1991 – 1993 by Grachev and Likhoshway (1996). The data presented here for 2001 –2002 appear to show much more spatial variability over the summer period. However, Kozhova and Kobanova (2001) did find a greater abundance of *A. baicalensis* during May 2000 in the south of the lake compared to sites further north.

The generally colder waters of the North Basin (Shimaraev *et al.* 1994) may be restrictive to some species combined with the competitive dominance of *A. baicalensis. Synedra* sp. occur

only in the South and Central Basins. This may be due to the competitive factors, but also because *Synedra* sp. may prefer earlier ice-out, greater through ice light transmission and warmer waters as found in the south. It is also possible that the North Basin does not provide enough shallow, littoral areas for the *Synedra* sp. to develop. As a result fully pelagic species can dominate. The greatest numbers of *Synedra* sp. are found in the South Basin, with Ivanovsky-Murino (the southernmost station) having maximum *Synedra* sp. abundance in June 2001. However, this clearly defined north-south distribution is not shown by the study of Grachev and Likhoshway (1996) where low abundances and a patchy distribution are shown for the May – June in 1991 – 1993. In contradiction, a presence/absence survey of May – June 1991 by Bondarenko *et al.* (1996) does indicate an absence of *S. acus* v. *radians* in the North Basin but also of *A. baicalensis* and *A. skvortzowii.*

S. meyerii is present in June 2001 mainly in the Central Basin, apparently associated with areas of clear ice, if the general patterns shown in figure 5.7 are constant on a yearly basis. The June 2002 bloom exclusively in the South Basin may also be related to increased light availability perhaps due to lower snow cover, early ice-out and also warmer waters. These conditions would not be present further north. The study of Kozhova and Kobanova (2001) also found dominant *S. meyerii* in the central basin during early summer while the distribution of this species was not defined by Grachev and Likhoshway (1996). As mass development of *S. meyerii* is expected in the Maloe More, linked to the presence of high winds and clear, snow free ice (Kozhova and Izmest'eva 1998). However the development of this species in the Maloe More may also be due to high phosphorus levels (Muller *et al.* in press).

A. skvortzowii only ever occurs in abundance in the South Basin over 2001-2002 according to available data. Maxima are associated with under ice blooms indicating that the species is tolerant of cold waters, but this species never significantly establishes outside the South Basin. This may be because an earlier ice-out date is preferred and survival could be limited by longer ice duration even though the species is cold tolerant. Summer abundance is low and warmer waters promote the production of resting spores in June 2001 and 2002. The presence of *A. skvortzowii* was also found to be confined to the South Basin by Kozhova and Kobanova (2001) but again not described by Grachev and Likhoshway (1996).

N. acicularis appears to have the most cosmopolitan distribution with no clear seasonal or spatial pattern. This species may be more opportunistic by colonising niches rapidly, due to a high growth rate (Bondarenko 1999). The distribution of *N. acicularis* found by Grachev and Likhoshway (1996) in summer 1991 is very similar to that found in 2001 with maximum abundance in the far north and far south. This may be expected as 1990 was a *Melosira* year

as was 2000. 1991 is defined as a *Nitzshia* year by Grachev and Likhoshway (1996) with 1992 and 1993 having a much lower *N. acicularis* abundance. Bondarenko (1999) maps the spatial distribution of *N. acicularis* in 1987, 1991 and 1995 and although overall abundance has been increasing since at least the 1960s, the species appears to have a lower abundance in deeper pelagic areas but is most common in shallower areas, linked to eutrophic river inputs and possibly anthropogenic pollution.

Unlike other species, *C. minuta* complex does not have a clear latitudinal distribution but blooms in autumn over the whole lake, thus appearing to be tolerant of warmer waters. Overall cell numbers are lower than for *Aulacoseira* and *Synedra* species. Lake-wide low abundance is shown by Grachev and Likhoshway (1996), although the sampling time of May-June probably missed the start of the autumnal *Cyclotella* bloom. It is not known why *A. formosa* was mostly absent in 2001 but with some occurrences in October 2001. Again, this species may be correlated with warm stratified summer and eutrophic waters, in particular the Selenga River inflow. No other records exist of the spatial distribution of this species in the phytoplankton. *C. inconspicua* was rare in the samples analysed. Identification was also difficult at x400 magnification. Plots for this species are not shown here but abundance is slightly higher in the North Basin.

4.6 Depth profiles

4.6.1 Results

4.6.1.1 Listvyanka-Tankhoy

Figures 4.12 shows the main planktonic diatom species in Lake Baikal's phytoplankton between 2001-2002 at the Listvyanka-Tankhoy station, plotted as live cells on the left graph and dead cells on the right graph against water depth (y) and date (x). *A. baicalensis* began to increase in abundance under ice in February 2001 with surface waters containing a maximum 10600 cells l^{-1} with low abundance by June 2001. In February 2002, little *A. baicalensis* was present in the water column but the June crop was much larger than in 2001 with 5000-10000 cells l^{-1} recorded for a longer period, and to greater depths of up to 250 m. Dead cells of *A. baicalensis* were generally present throughout the whole water column, even when abundance of the species was low. *A. skvortzowii* had a similar distribution to *A. baicalensis* but appeared in greater numbers during February 2001 (13200 cells l^{-1} at the surface) while during the next

years bloom concentrations reached up to 46700 cells l^{-1} in March 2001. *A. skvortzowii* does not appear to be able to survive in deeper waters as well as *A. baicalensis,* with live cells concentrated only in the upper 25 m in March 2001 when live *A. baicalensis* cells could be found to 250 m. Resting stages of *A. skvortzowii* formed after the main bloom of the species as expected, and were also found dead throughout the entire water column. *C. minuta* complex dominated the autumn assemblage in 2001 reaching a maximum at 18200 cells l^{-1} in October at the surface. Live cells were initially only in surface waters but appeared to inhabit deep waters as winter approaches. This pattern was repeated through 2002 but was not as clear due to gaps in the sampling. *S. meyerii* had a scattered occurrence through 2001 but became dominant in the summer with 415000 cells l^{-1} at 100 m depth during June, considerably more prolific than any other species recorded at any time. Live *S. meyerii* cells were absent by autumn (October/November) although dead cells were abundant. Initial blooms of *S. acus v. radians* seem to be concurrent with *A. baicalensis* but this species was confined only to March/April indicating extensive under ice blooming, but does not appear to survive into the ice-free period. However *S. acus v. pusilla* was much more abundant under the ice than *S. acus v. radians* and survived longer into the summer with 9000 cells l^{-1} in June 2001 at 5 m. Dead cells of *S. acus v. pusilla* occured at relatively high abundances throughout the water column. *N. acicularis* had a similar spatial and temporal distribution to *S. acus v. pusilla* but with lower abundances. Although dead cells of *S. acus* v. *pusilla* were abundant, dead *N. acicularis* were rare below 250 m indicating extensive dissolution. However this may also be caused by a slower sinking rate. A similar level of dissolution was shown by *A. formosa* at depth. *A. formosa* was present at low numbers in the surface 250 m during 2002 but almost absent during 2001.

A DCA of the Listvyanka-Tankhoy species data revealed an axis one gradient length of 1.624 SD units meaning a linear method of constrained ordination should be used (RDA). Figure 4.13 is a biplot of the RDA of diatom abundance (cells l^{-1}) constrained by chemical and environmental data. To aid interpretation of the diagram, samples from different months for 2001 and 2002 have been plotted on separate biplots although each of the plots is from the same ordination. The *p*-value of the axes tested by a restricted Monte Carlo permutation test was 0.2350. A summary of the RDA is given in table 4.1. Most of the variance in the data is captured in the first two RDA axes. Axis 1 displays a water depth-diatom abundance gradient with positive values relating to deeper water, which also generally correlates to higher nutrient contents, and negative scores to higher diatom occurrence. Abundance of live diatom species is inversely correlated with depth as expected, as growth is only possible in the shallow surface photic zone. Diatom abundance also has an inverse correlation with water nutrient content as nutrients in the photic zone become depleted by algal productivity. Oxygen

is positively correlated with diatom abundance as it is generated by photosynthesis. Diatom abundance also appears to be associated with greater secchi depths, possibly due to the fact that reduced transparency is a result of summer blue-green algae growth. That is, with increased relative diatom abundance, water transparency is greater. There is also a similarity between species scores from the same months from the two different years.

The biplot, figure 4.13a shows the subset of samples for March 2001 and 2002. The top left quadrant is associated with colder water, oxygen and spring blooming diatoms such as *A. skvortzowii, Synedra* sp., and *A. baicalensis* to a lesser extent. Samples with scores in this area are mostly all in the top 50 m of the water column. Below 50 m samples show an inverse association with diatom abundance indicating losses with dissolution and settling with depth. By June 2001 and 2002 (figure 4.13b) surface water samples shift to the bottom left quadrant of the ordination diagram. The assemblage now represents early summer species including *S. meyerii, C. minuta* complex, *A. baicalensis* and *A. skvortzowii* resting spore. Deeper samples still show low productivity and are correlated with higher water temperatures and nutrient concentrations than surface waters. In July 2001 and 2002 (figure 4.13c) surface waters are now warmer as shown by their axis 1 scores shifting to positive values. There is less overall diatom abundance but more nutrients are available. Samples correlated with diatom abundance are deeper at 25-500 m and represent an assemblage similar to that found in near surface waters in June, possibly indicating increased mixing. Finally, during the autumn period (figure 4.13d), water temperatures are higher and diatom productivity low. *S. meyerii, C. minuta* complex and *A. skvortzowii* resting spore dominate the assemblage. Surface waters are now correlated more with increased nutrients as overturn starts to replenish the trophic layer with nutrients from deeper water.

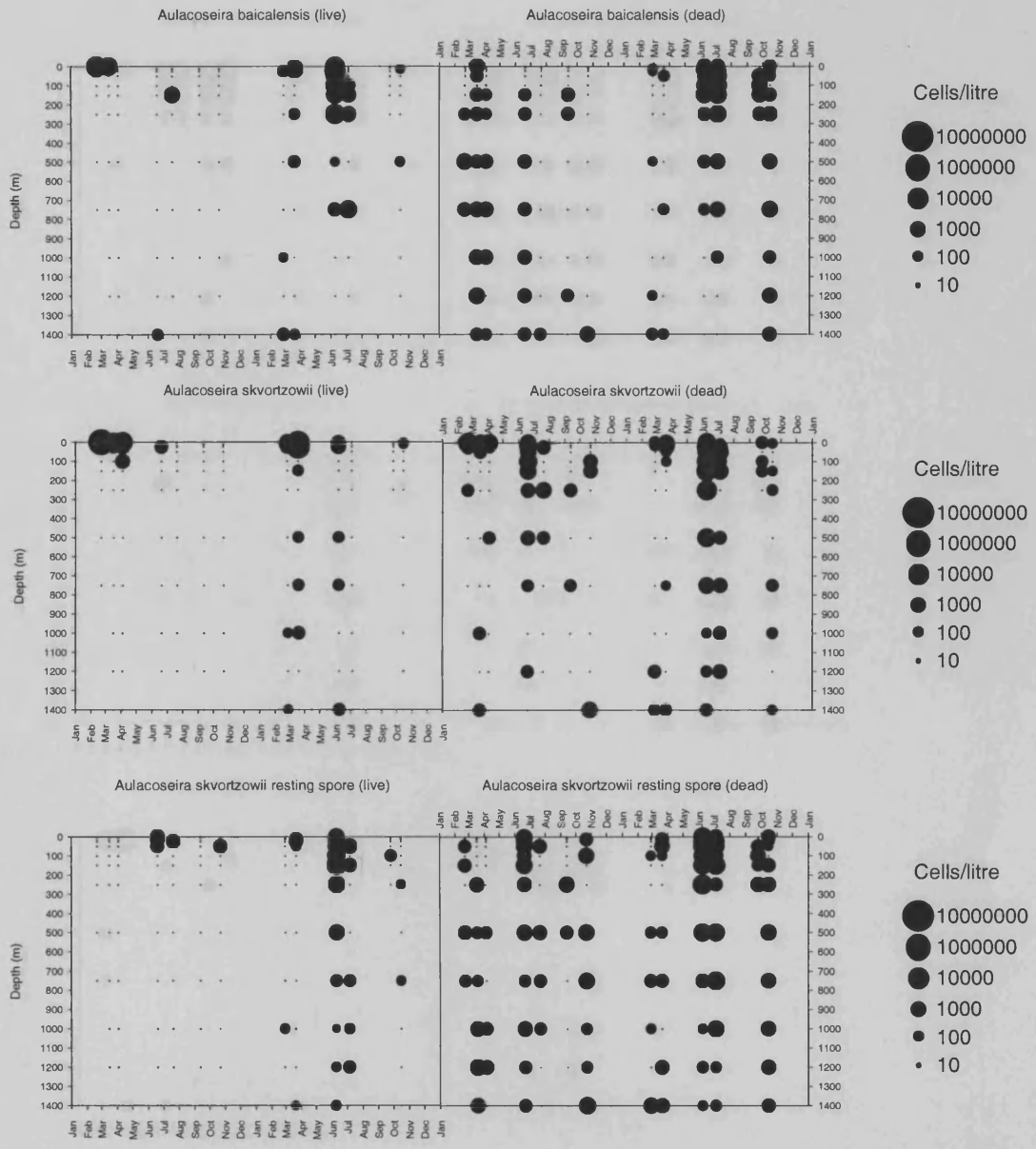

Figure 4.12: Bubble plots showing abundance of main diatom species throughout the water column at Listvyanka-Tankhoy during 2001-2002 on a logarithmic scale. Live cells are plotted on the left, dead cells plotted on the right. Small dots indicate a sampling location/time with zero abundance of the corresponding diatom species.

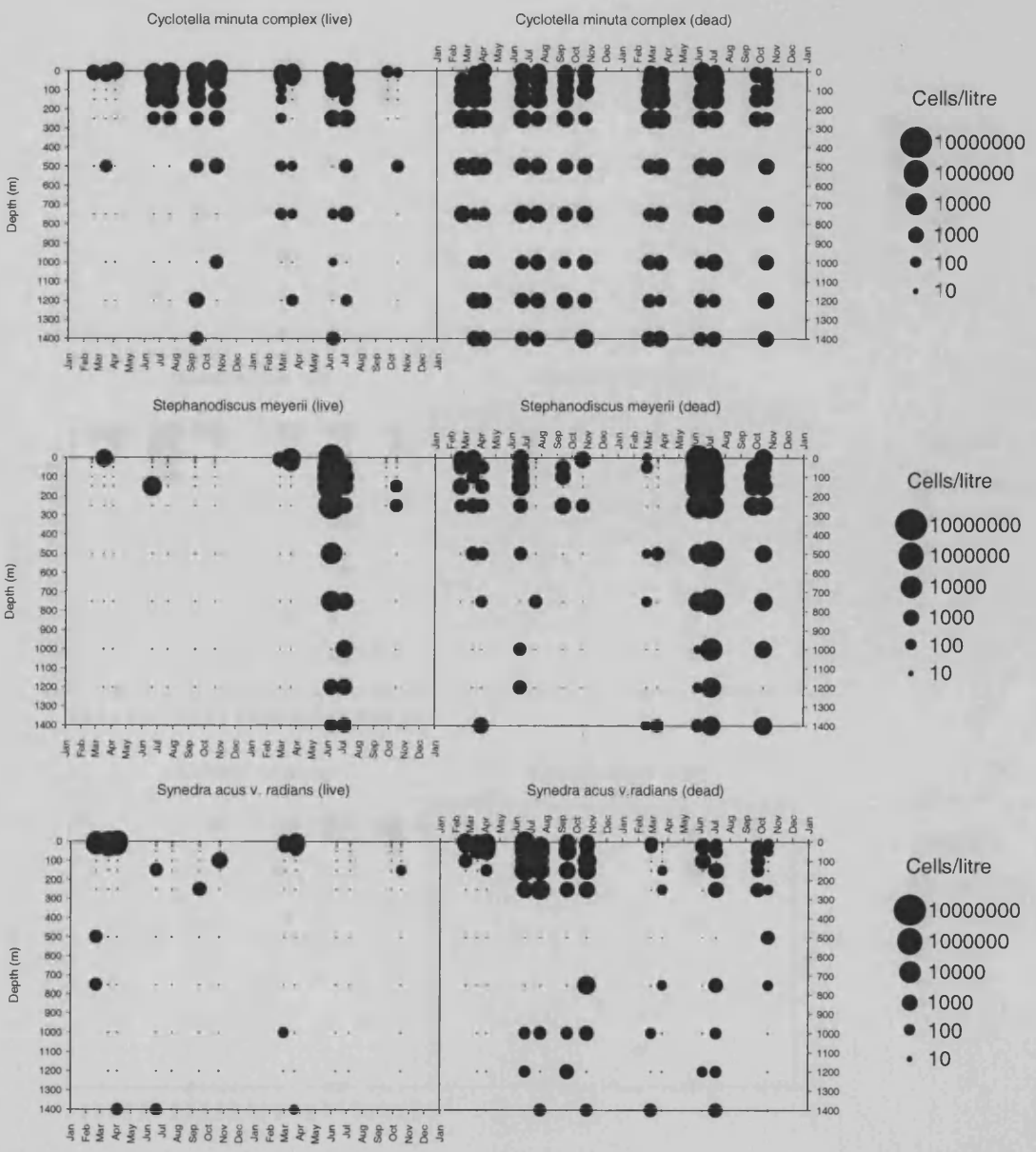

Figure 4.12: Continued.

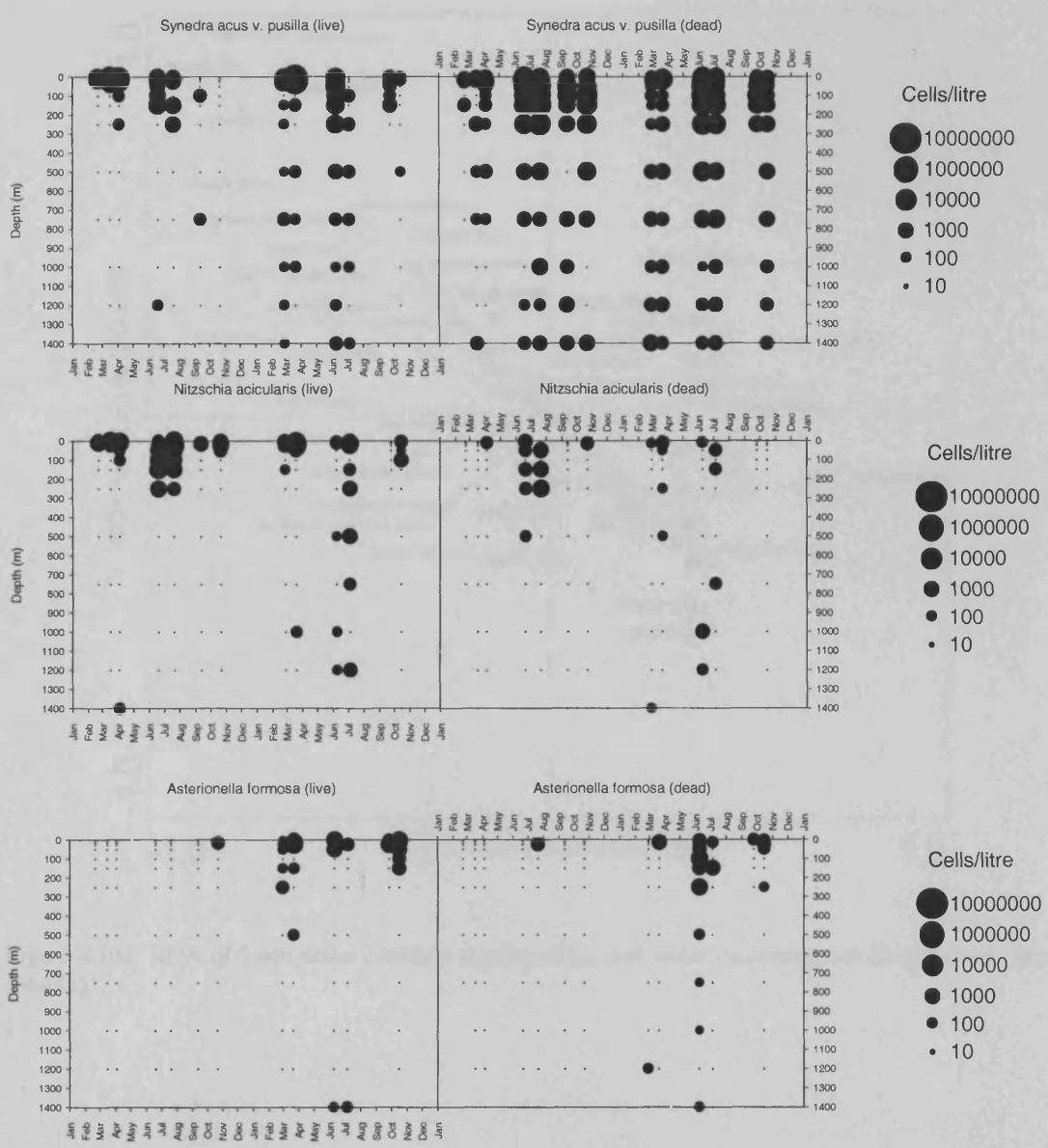

Figure 4.12: Continued.

Axes	1	2	3	4
Eigenvalue	0.187	0.041	0.001	0.000
Species-environment correlation	0.495	0.449	0.544	0.356
Cumulative percentage variance of species data	19.3	23.5	23.5	23.6
Cumulative percentage variance of species-env. relation	81.7	99.6	99.9	100.0
Sum of all eigenvalues 0.969				
Sum of all canonical eigenvalues 0.228				
Total variance 1.000				

Table 4.1: RDA summary for the Listvyanka-Tankhoy depth profiles

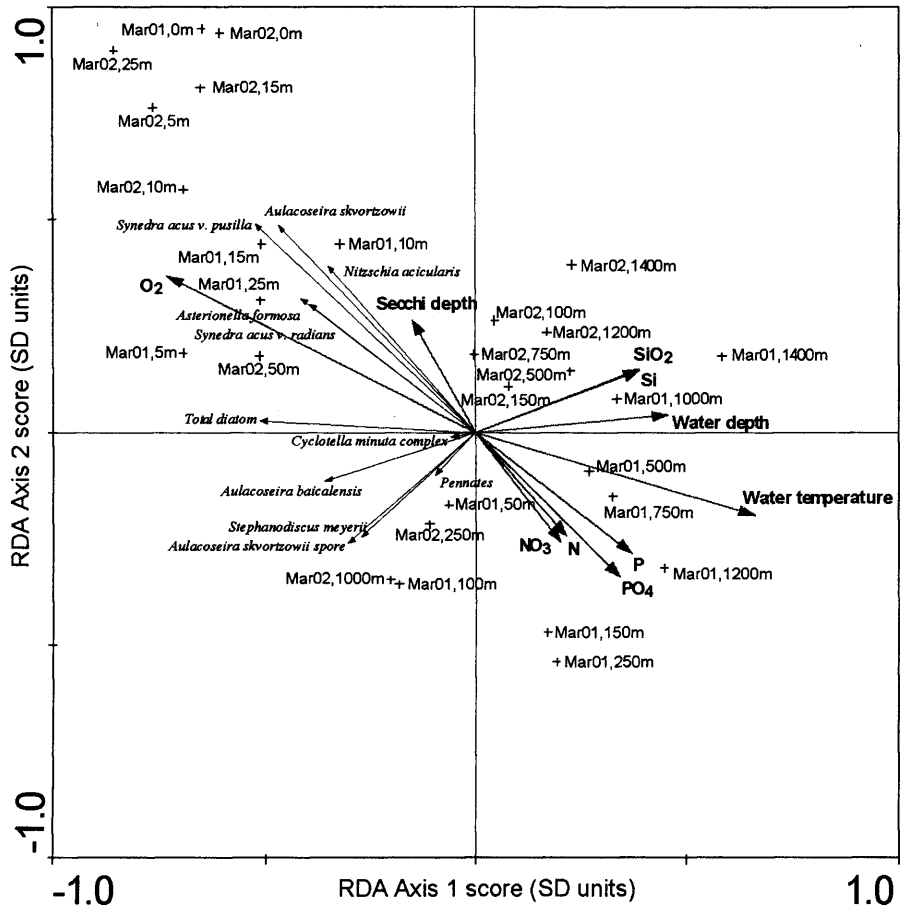

Figure 4.13a: RDA of Listvyanka-Tankhoy depth profiles and water chemistry and limnological data (March)

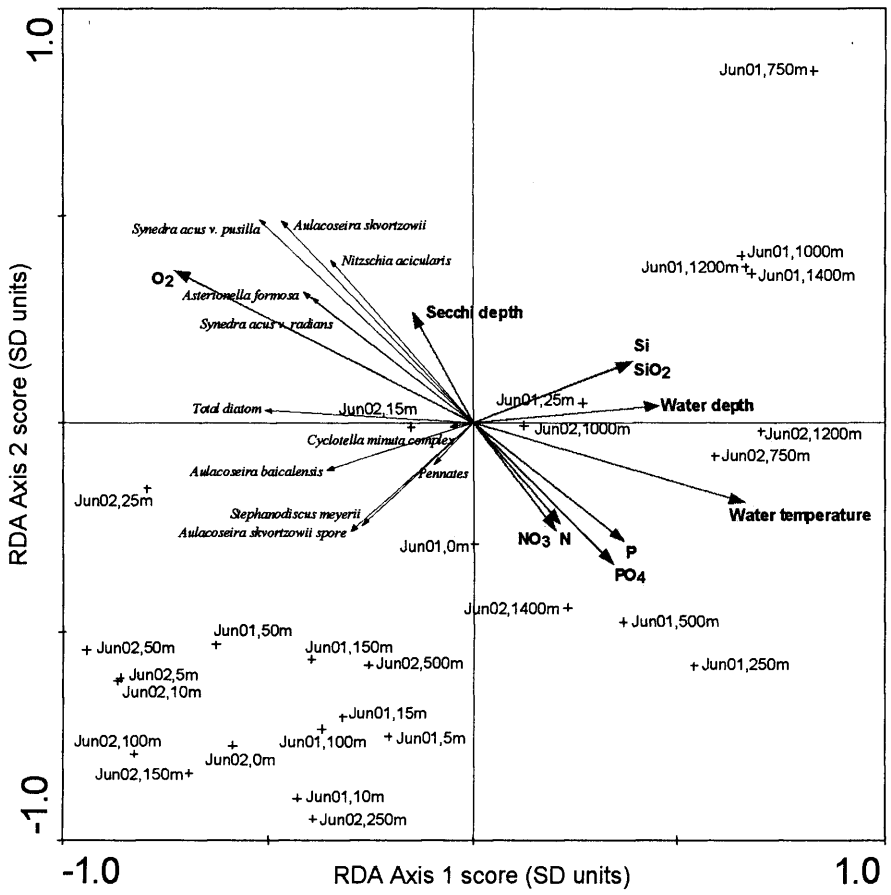

Figure 4.13b: RDA of Listvyanka-Tankhoy depth profiles and water chemistry and limnological data (June).

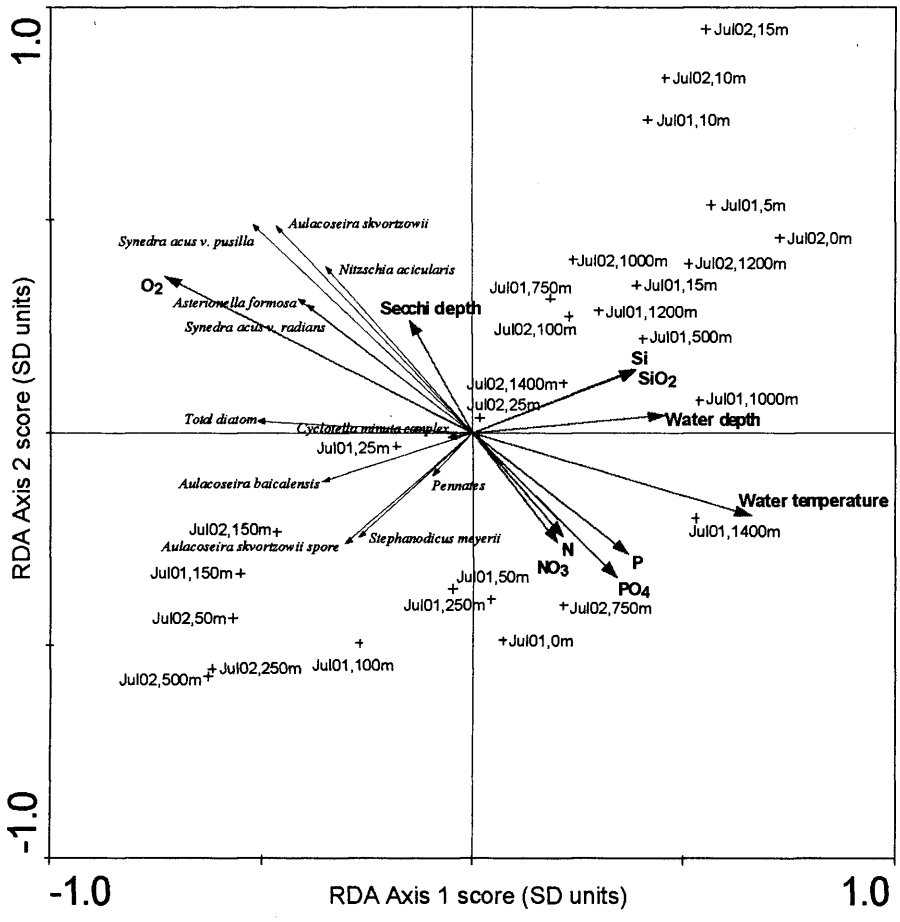

Figure 4.13c: RDA of Listvyanka-Tankhoy depth profiles and water chemistry and limnological data (July)

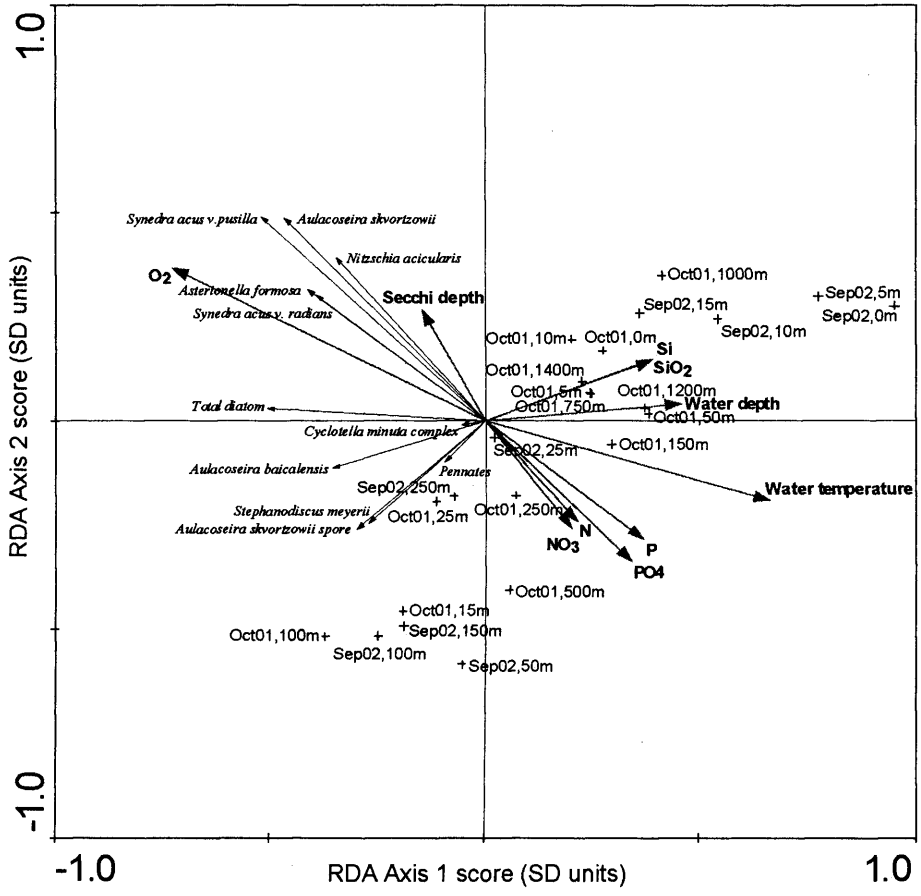

Figure 4.13d: RDA of Listvyanka-Tankhoy depth profiles and water chemistry and limnological data (September/October).

4.6.1.2 4 km Ivanovsky

Overall, the distribution of diatom species at 4 km Ivanovsky (figure 4.14) was very similar to that at Listvyanka-Tankhoy but with some minor differences. The main problem in comparing the two stations is that fewer samples have been taken at 4 km Ivanovsky, especially during spring and autumn 2001. *A. baicalensis* was not present in March 2001 and had a low maximum of 8200 cells l^{-1} in June 2001 at 25 m, but appeared earlier at Listvyanka-Tankhoy. The distribution of *A. baicalensis* in 2002 was similar to that at Listvyanka-Tankhoy, with a maximum of 36000 cells l^{-1} at 5 m in June 2002. This was the same timing and location in the water column as the Listvyanka-Tankhoy maximum (9200 cells l^{-1}). Like *A. baicalensis, A. skvortzowii* reached a maximum later in 2001 than at Listvyanka-Tankhoy but at a similar time in 2002. *A. skvortzowii* resting spores did not appear at all in 2001 possibly due to gaps in sampling but were probably present as dead cells appear in deeper waters in February 2002. During 2002, resting spores were abundant after the main *A. skvortzowii* bloom as for Listvyanka-Tankhoy. Again the main bloom of *C. minuta* complex was in autumn 2001 with 26000 cells l^{-1} at 5 m in October 2001, peak abundance was earlier in the year than at Listvyanka-Tankhoy. Dead cells were common throughout the water column indicating low dissolution. *S. meyerii* maxima occurred in summer 2002 (173600 cells l^{-1}, 25 m, June 2001) and to a lesser extent in 2001 as at Listvyanka-Tankhoy. *S. acus v. radians* started blooming under the ice in February with a maximum later in the year (19200 cells l^{-1}, 0 m, July 2001) than at Listvyanka-Tankhoy. This pattern reoccurred in 2002 albeit with a larger spring-summer bloom. *S. acus v. pusilla* also achieved maxima later in the year than at Listvyanka-Tankhoy but this was not as apparent as for *S. acus v. radians*. The size of the blooms of *S. acus v. pusilla* appeared to be similar between 2001-2002. The distribution of *N. acicularis* and *A. formosa* were almost identical at 4 km Ivanovsky and Listvyanka-Tankhoy, notably the lack of dead cells below 500 m and the absence of *A. formosa* in 2001.

The axis 1 gradient length (DCA) of the 4 km Ivanovsky species data is 2.038 SD units which is relatively short so constrained ordination was again carried out using RDA. The restricted Monte Carlo test showed a *p*-value of 0.2510. Table 4.2 gives a summary of the RDA, again the first two axes account for almost all the explainable variation in the data. As for the biplots displaying the Listvyanka-Tankhoy data, four separate plots showing individual months from 2001-2002 are presented to aid interpretation (figure 4.15a to d). Again, axis 1 shows a gradient of diatom abundance and water depth with positive scores indicating high diatom abundance and negative scores generally showing unproductive and usually deeper waters. Nutrient levels are also inversely correlated with diatom abundance, however unlike at Listvyanka-Tankhoy, water temperature is not correlated with depth but appears to be

represented as the main gradient on axis 2, which may be used to indicate temperature tolerance of individual diatom species. In March 2001-2002 water depths 0-15 m were colder and species present include *A. baicalensis, Synedra* sp., *S. meyerii* and *A. skvortzowii* resting spores (figure 4.15a). As at Listvyanka-Tankhoy, waters below this level were much more unproductive but contain an excess of nutrients compared to the epilimnion. By June 2001-2002 the surface 100 m were still associated with diatom productivity with a similar assemblage to March, with deeper nutrient rich waters being unproductive (figure 4.15b). A shift in the diatom assemblage occured in July 2001-2002 towards more autumnal species such as *C. minuta* complex, *N. acicularis* and *A. formosa* associated with warmer waters (figure 4.15c). By October-September 2001-2002 this shift was complete with an autumnal diatom assemblage in the top 100 m (figure 4.15d).

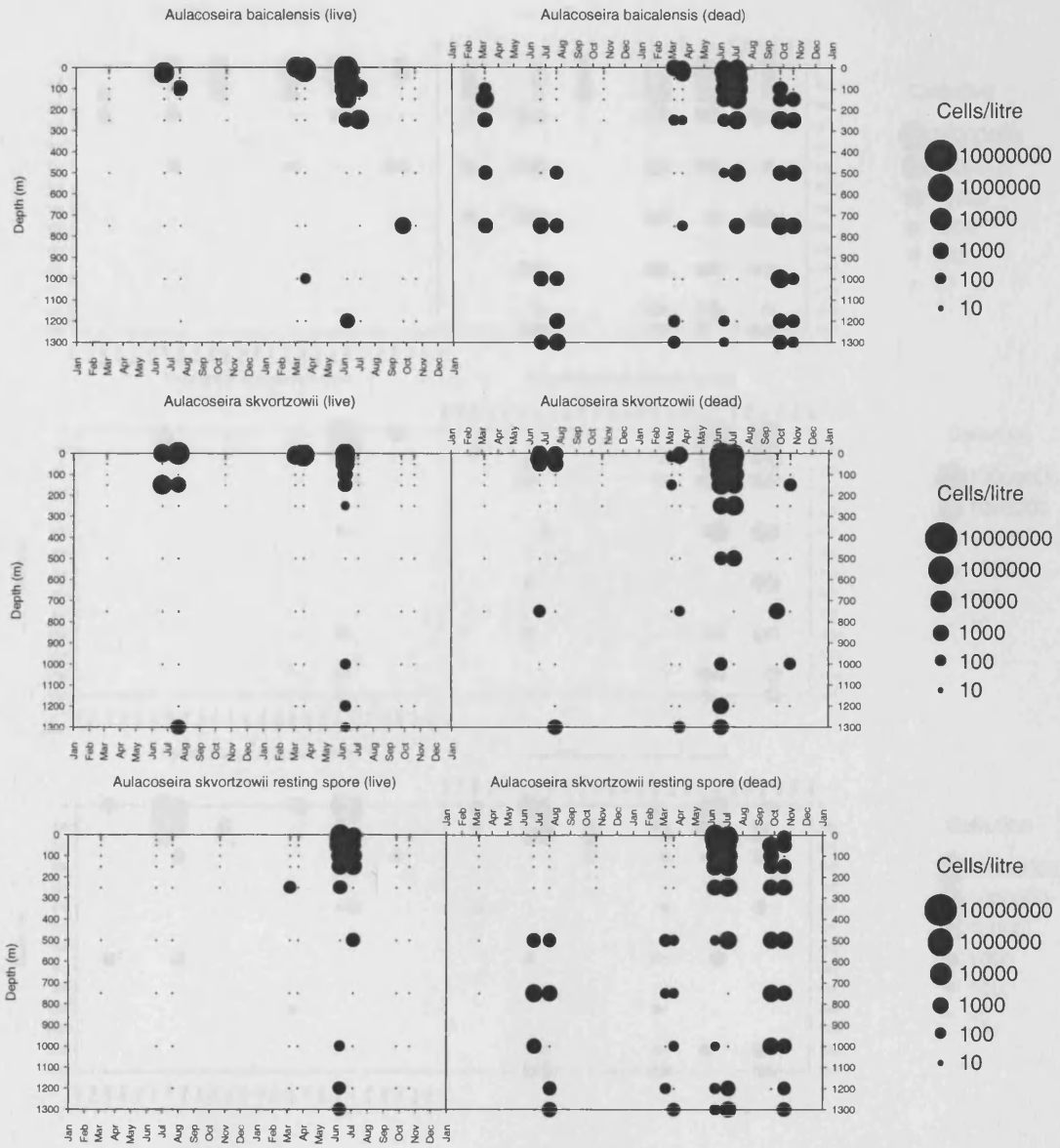

Figure 4.14: Bubble plots showing abundance of main diatom species throughout the water column at 4 km Ivanovsky during 2001-2002 on a logarithmic scale. Live cells are plotted on the left, dead cells plotted on the right. Dots indicate a sampling location/time with zero abundance of the corresponding diatom species.

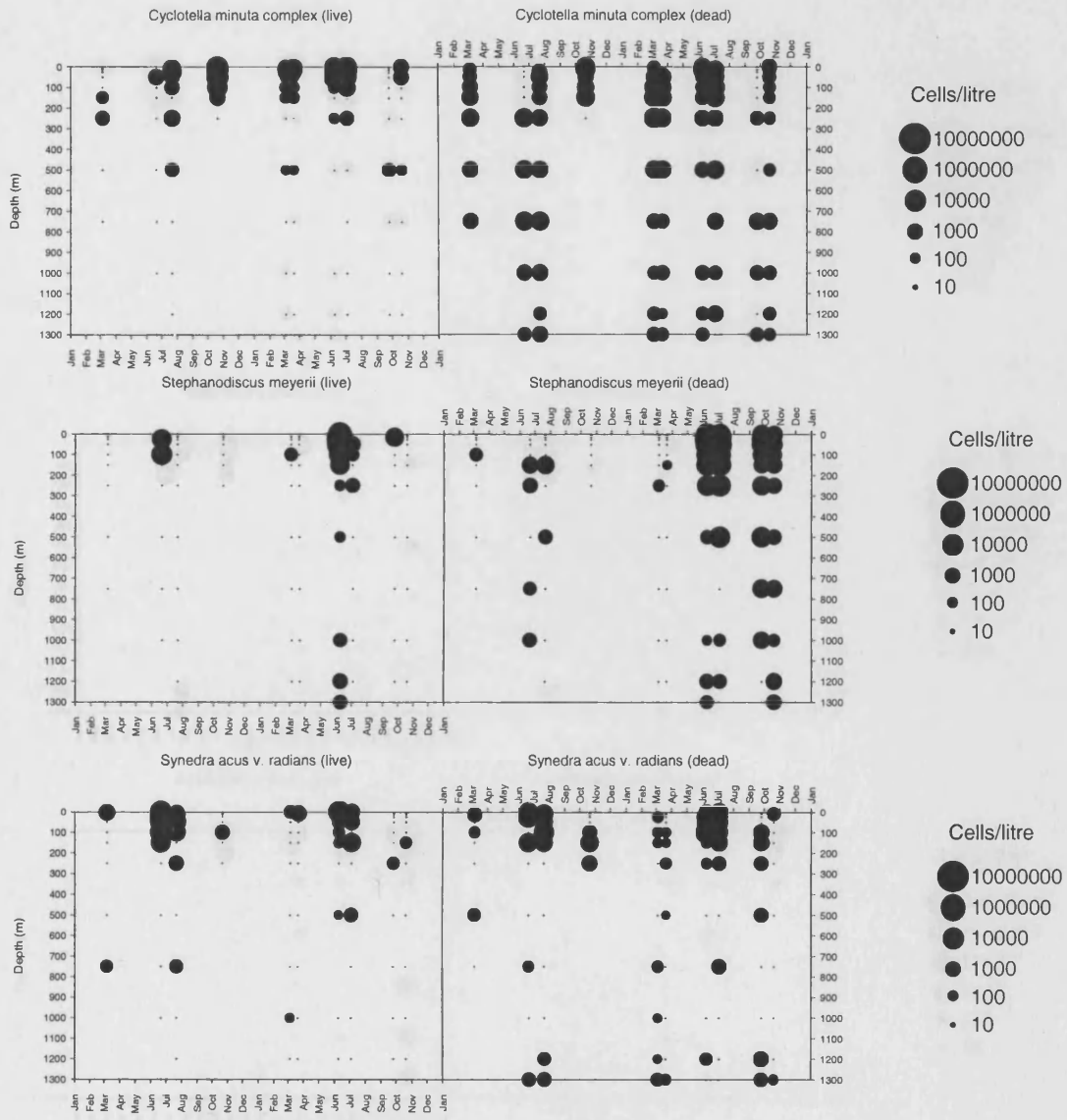

Figure 4.14: Continued

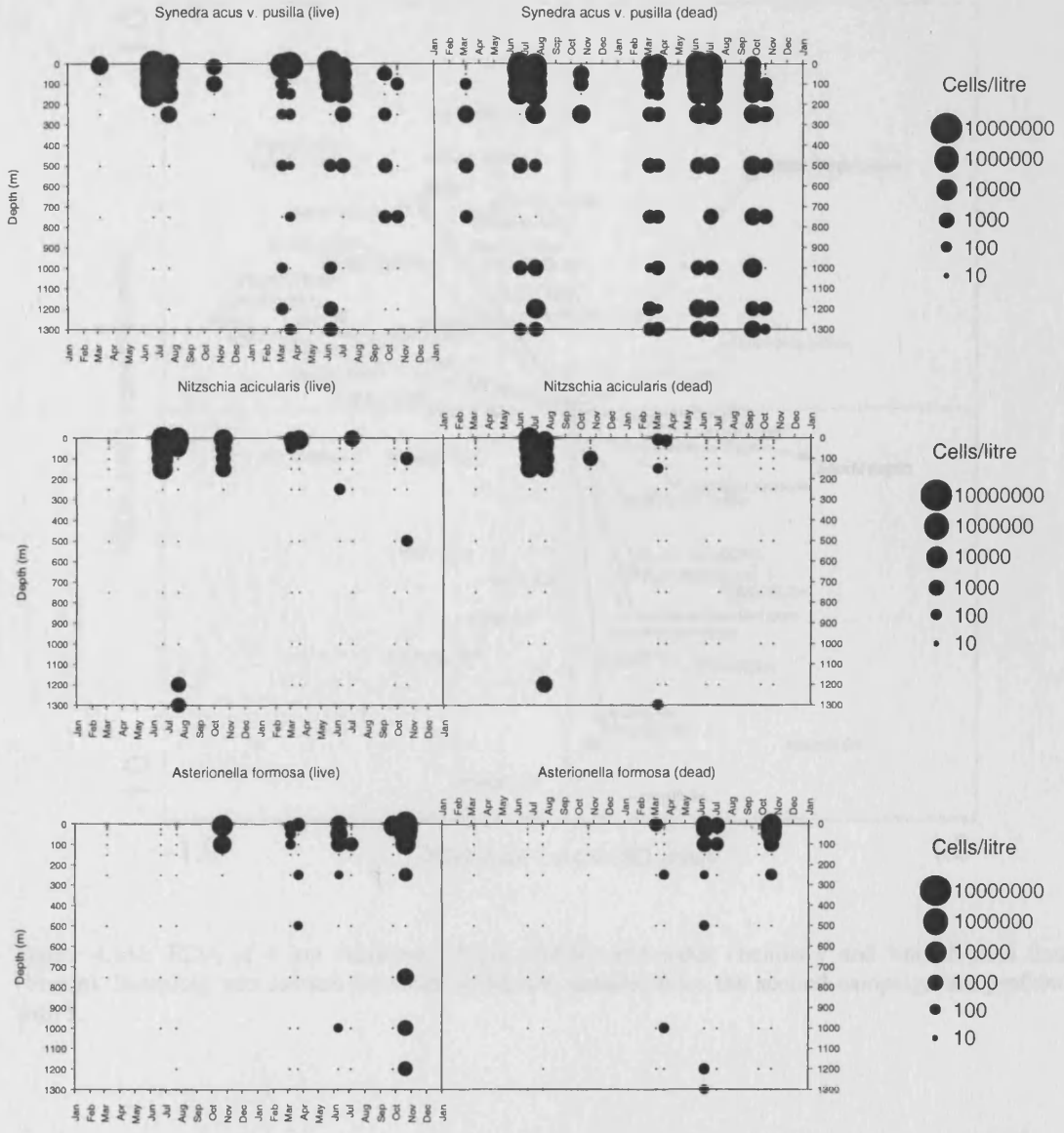

Figure 4.14: Continued.

Axes	1	2	3	4
Eigenvalue	0.095	0.009	0.001	0.000
Species-environment correlation	0.324	0.383	0.334	0.220
Cumulative percentage variance of species data	9.6	10.6	10.7	10.7
Cumulative percentage variance of species-env. relation	89.7	98.6	99.6	99.9
Sum of all eigenvalues 0.990				
Sum of all canonical eigenvalues 0.106				
Total variance 1.000				

Table 4.2: RDA summary of the 4 km Ivanovsky depth profiles.

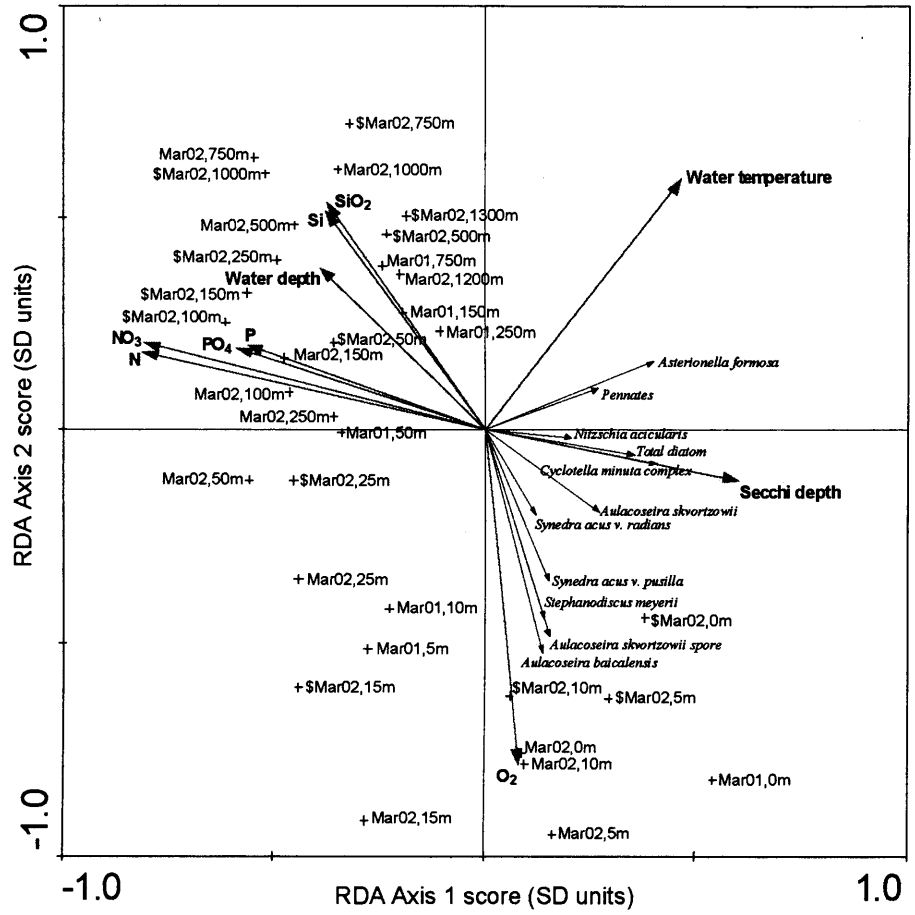

Figure 4.15a: RDA of 4 km Ivanovsky depth profiles and water chemistry and limnological data (March). Sampling was carried out twice in March, samples from the second campaign are prefixed with $.

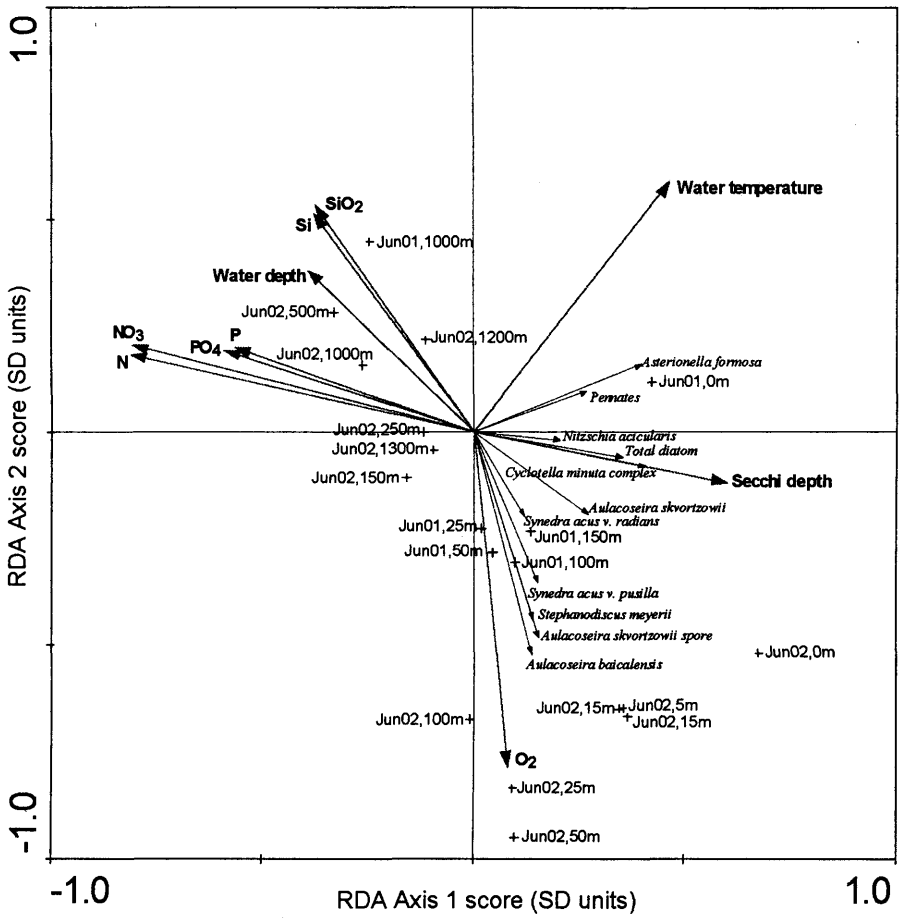

Figure 4.15b: RDA of 4 km Ivanovsky depth profiles and water chemistry and limnological data (June).

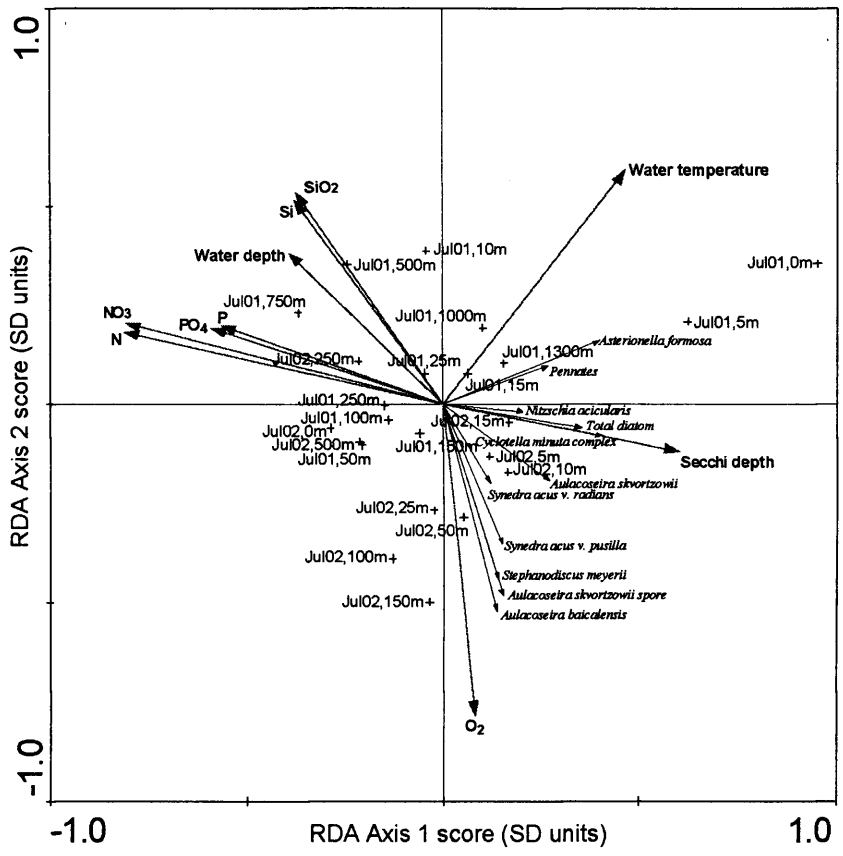

Figure 4.15c: RDA of 4 km Ivanovsky depth profiles and water chemistry and limnological data (July).

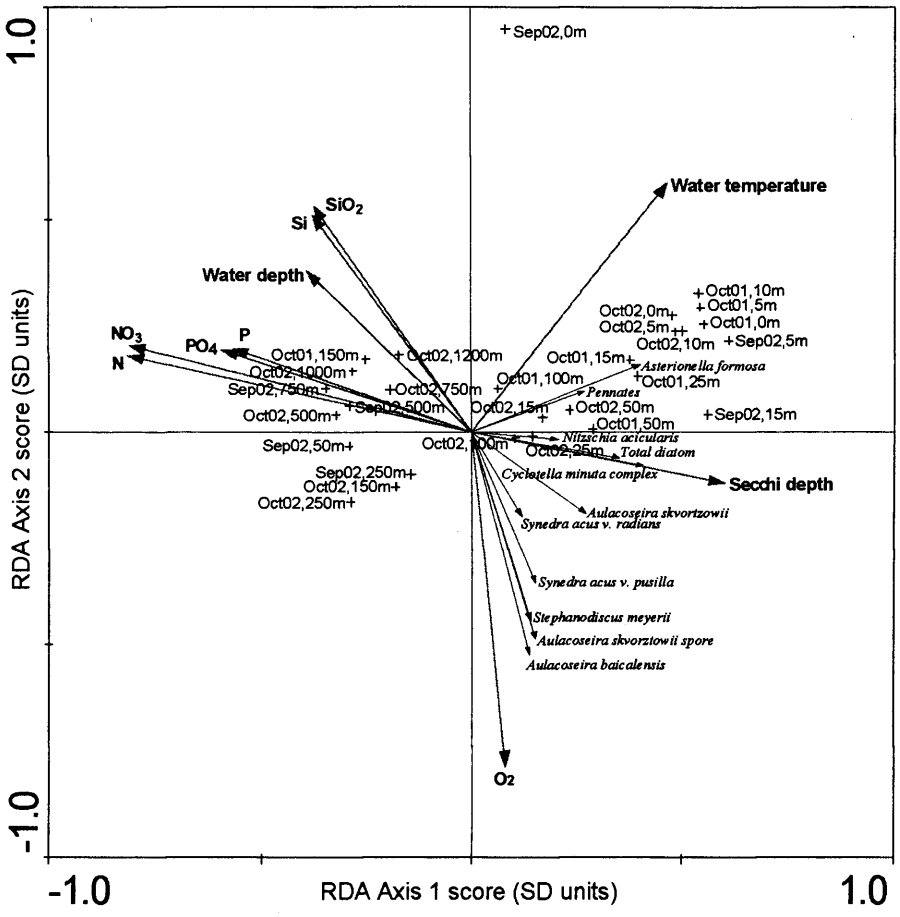

Figure 4.15d: RDA of 4 km Ivanovsky depth profiles and water chemistry and limnological data (September/October).

4.6.2 Discussion

Although the spatial and temporal distribution of diatom species through the depth profiles at Listvyanka-Tankhoy and 4 km Ivanovsky are similar, there are several differences, e.g. the later peak of cell abundance of some spring species at 4 km Ivanovsky. As it has been shown that snow cover and light transmission through ice has an important influence on the spring bloom, differences in snow cover at the two stations may be causing these differences. 4 km Ivanovsky is a sheltered littoral site (figure 4.1) meaning snow drifts can accumulate while at the more exposed Listvyanka-Tankhoy station, wind action may remove snow leaving relatively clear ice (Jewson, pers. comm). This earlier and longer period of light penetration at Listvyanka-Tankhoy (in the middle of the lake along a transect between Listvyanka and Tankhoy) may promote the earlier production of spring crops. The differences in thermal regimes (summer stratification duration and overturn) between the more littoral 4 km Ivanovsky site and the pelagic Listvyanka-Tankhoy site may be driven by gyre circulations and wind driven convection (Shimaraev *et al.* 1994). As wind speeds and gyre circulation are more active at Listvyanka-Tankhoy (Shimaraev *et al.* 1994), the influence of these factors on water column overturn and stratification may also influence specific diatom productivity. The apparent greater abundance of *Cyclotella minuta* complex at Listvyanka-Tankhoy may indicate an earlier breakdown of summer stratification and overturn, allowing a longer autumn growth period.

In terms of interannual species variability, the fact that the year before these results (2000) was a *Melosira* year may influence the diatom species present (Jewson, pers. comm). It is thought that *Melosira* years leave the photic zone depleted in silica and limiting for the next innoculum of heavily silicified *A. baicalensis*. This may explain the low occurrence of *A. baicalensis* at both stations in 2001, with a slight increase in 2002 as silica concentrations were gradually replenished. *S. meyerii* is common after *Melosira* years as it grows very quickly and competitively in littoral areas and is transported offshore in the absence of *A. baicalensis* (Bondarenko *et al.* 1996), which may explain the *S. meyerii* dominance in 2001-2002. Rychkov *et al.* (1989) also find *N. acicularis* and *Synedra* sp. after *Melosira* years. Bondarenko (1999) also finds *N. acicularis* to be especially abundant after a *Melosira* year. As these species are lightly silicified in comparison to *A. baicalensis*, they will be more competitive as silica limitation is less restrictive to growth. The presence of live species throughout the water column (well beyond the photic zone) can be partly explained by rapid sinking if colonies of diatoms clump together or are grazed by zooplankton and are deposited as faecal pellets.

There is a well defined progression of diatom species over the course of 2001 and 2002. Initially with species adapted to growth under the ice (*A. baicalensis, A. skvortzowii, Synedra* sp.), productivity will be mainly governed by snow and ice conditions but also by competitive biological factors such as growth rate and innoculum size. Species that appear dominant during summer are *S. meyerii* and *Synedra* sp. while later autumnal species include *N. acicularis, A. formosa* and *Cyclotella minuta* complex which develop after summer stratification breaks down in relatively warmer waters. The varying abundance of these seasonal species may be used to gauge season length in Lake Baikal and so help understand the impact of climate. However, other factors such as nutrient limitation, competition, innoculum size, grazing and dissolution will be important too.

The RDAs of diatom cells l^{-1} and environmental data from Listvyanka-Tankhoy and 4 km Ivanovsky indicate that diatom productivity can be related to season, water temperature and depth, where productivity occurs and nutrients become depleted. Overall, diatom production is in the shallow photic layer while deeper, nutrient rich but light limited waters are unproductive. Nutrients in the epilimnion are renewed during autumn turnover. RDA plots graphically show shifts in species assemblages during 2001-2002 from a spring assemblage often signified by a shallow productive layer and colder water temperatures. Species present include cold tolerant *A. baicalensis* but also *Synedra* sp. which can grow in cold as well as warmer waters. The summer assemblage is indicative of production in pelagic water while overall diatom abundance during this period is relatively lower than during the spring bloom. The *S. meyerii* and *Synedra* sp. present are tolerant of high temperatures (Jewson *et al.* unpublished). The autumnal assemblage tends to be tolerant of warmer waters (*C. minuta* complex) in comparison to colder spring species. This pattern of seasonal species dynamics related to water temperature is backed up by the culturing work of Jewson *et al.* (unpublished) and the gradient is shown best at the 4 km Ivanovsky site, with diatom species distributed over a water temperature gradient on axis 2. However, water temperature is not the only factor influencing diatom productivity as stated above, although climatic factors will have an influence on determining water column stratification and overturn.

Although some general autecological conclusions can be drawn, the results presented above are only for 2001 – 2002 and so their representivity on a longer timescale is doubtful. General seasonal distributions of individual species appear to correspond to those found by Grachev and Likhoshway (1996) but also Ryves *et al.* (2003). However there is huge interannual variability. For example, Ryves *et al.* (2003) found abundant *C. minuta* in South Basin sequencing traps (~550 m and 1280-1380 m depth) during 1996 although it was mostly absent during 1997. These results are not directly comparable to the results here, because no

distinction was made between live and dead cells, hence maximum *C. minuta* abundance in early spring 1996 was a response to sinking of the 1995 autumnal crop. Peaks of cells of other species found in the study of Ryves *et al.* (2003) also appear to lag those in this study, again due to the depth of the sequencing traps. However, as shown in the data presented here, considerable interannual variability is visible even over a study of just two years. Grachev and Likhoshway (1996) present monthly variability of phytoplankton at the Bolshie Koty station between 1973 and 1981. Again these graphs show a huge amount of species variability between years. However, when a species becomes abundant, this usually occurs during the same months of the year. Therefore, even though the full range of interannual variability has not been captured in the 2001 – 2002 data, the species bloom times should provide some autecological information.

Although not presented here, non-diatom algae were also enumerated. During periods of low diatom productivity it was found that other algal species were present, for example *Chlorophyta, Dinobryon, Gymnodium, Cloisteriposis, Monoraphidium* and coccoid green algae amongst others. These were mostly abundant during the summer months but not at depths outside the photic zone. Periods of low diatom abundance during the winter were also marked by low occurrence of other algal groups. As stated before, the importance of algal groups other than diatoms should be considered when investigating lake productivity. It has been described above how the role of non-diatom algae can be assessed with the analysis of pigments (section 4.3). However, there are problems of assessing pigments through the water column as they are subject to degradation (Fietz *et al.* in press). Similar to the diatom profiles above, Fietz *et al.* (in press) do note a decline in pigments (i.e. algal abundance) outside the wind mixed upper layers of Lake Baikal. Monthly abundances of non-diatom algae at Bolshie Koty between 1973 and 1981 (Grachev and Likhoshway 1996) show huge interannual variability, however seasonal shifts are consistent between years as is the case for diatoms. A depth profile in the South Basin has been investigated by Straskrabova *et al.* (in press) for Chl *a* and bacteria, the majority of production was found to be by diatoms while 9% of Chl *a* was produced by picocyanobacteria. Again, signs of aquatic productivity decreased with depth. The role of increased cyanobacteria during periods of low diatom productivity (cold) has been stressed by Watanabe *et al.* (2004) who indicate even though diatom productivity will be low, aquatic productivity may be higher than that indicated by the microfossil record.

4.7 Conclusion

The data on the seasonal and spatial distribution of diatom species over both the lake surface and with depth in the South Basin can be linked with climatic (water temperature, ice cover dynamics and snow depth on ice) and water chemistry data, both quantitatively and qualitatively. However, the data analysed only cover two years at coarse resolution. It is possible that some of the details of diatom population dynamics and exact bloom times have been lost due to the long periods between repeat sampling campaigns. Although beyond the scope of this study, more conclusive inferences about the ecology of Lake Baikal's diatom phytoplankton will be possible by extending this monitoring data beyond two years with existing data held by D.H. Jewson (a subset of which is presented in Battarbee *et al.* in press).

From the (albeit temporally restricted) phytoplankton monitoring presented here, it is possible to make some basic assumptions on diatom autecologies. This information will be further developed after an investigation of diatoms in modern surface sediments related to measured environmental variables, and a review of literature concerning Lake Baikal diatoms response to climate. Full autecological summaries for the main diatom species will be presented in chapter 5 to aid interpretation of the palaeo record in chapter 6. It is important to remember that biological factors and nutrient limitation may also influence diatom productivity as well as climate, but it has been possible to determine that *A. baicalensis* can tolerate cold waters, low light availability and a long ice covered period. The *Synedra* sp. are spring blooming and can also tolerate colder waters although perhaps not the extremes in the North Basin. They can also tolerate warmer temperatures too and appear during the early summer. *C. minuta* complex occurs lake-wide, is autumnal blooming and can tolerate warmer waters after the summer stratified period. *S. meyerii* is also tolerant of warm waters and maybe areas with higher through ice light transmission or earlier ice-out. *A. skvortzowii* is spring blooming in areas of early ice-out, it can tolerate cold waters but perhaps not to extremes. *N. acicularis* and *A. formosa* may be related to more eutrophic waters, for example, around the Selenga outflow. Although existing studies of spatial – temporal phytoplankton variability are limited, they generally support the conclusions on diatom distributions made here.

The two analysed depth profiles from the South Basin add further support to the interpretation of the abundance of diatoms in surface waters, in relation to climatic gradients in the context of the coring location. Indications of the levels of dissolution may be shown by the abundance of *C. minuta* complex at relatively high levels throughout the water column after a bloom, while species such as *N. acicularis* and *A. formosa* are often not found in deeper waters after blooming. The RDA ordinations help to summarise seasonal diatom species changes with

depth, in relation to environmental variables, the depth of the productive layer, the availability of nutrients available during diatom blooms and how these vary over the year. For example, it is shallower in spring with *Aulacoseira* and *Synedra* blooms and then deeper in the autumn. Tentative temperature tolerances can be made from the RDAs with warmer water summer species such as *N. acicularis* and *A. formosa* separated from colder water spring species such as *A. baicalensis.*

The phytoplankton monitoring study presented here has built on previously published literature documenting the temporal and spatial dynamics of diatom species. In particular, this study has examined variability on a high temporal resolution at two depth profiles and also with a representative survey of lake surface waters. Along with a comparison of measured environmental data this has led to improved knowledge of some of Lake Baikal's planktonic diatoms. The conclusions of this study will be further developed with an extension of the existing monitoring program and a synthesis with data collected over recent years.

Chapter five

Modern environment III: Environmental controls on diatom species distribution and transfer function development

5.1 Introduction

The aim of this chapter is to provide autecological information for the common diatom species found in Lake Baikal to aid the interpretation of the Holocene – Late Glacial record presented in the next chapter in terms of climate change. This is achieved through the further development of an existing snow depth transfer function for Lake Baikal which is described in the first part of this chapter. Following this, the inference models developed will be used to assess individual species responses and the spatial distribution of species in the training set related to environmental variables. Combined with the plankton monitoring data (chapter 4) and previously published information, autecological summaries are presented at the end of this chapter.

Quantitative reconstruction of environmental variables has been made possible by the transfer function approach first presented by Imbrie and Kipp (1971). The basic objective is to express an environmental variable as a function of biological (proxy) data. In order to do this, responses of modern taxa to measured environmental variables have to be modelled statistically with the creation of a training set. A training set should consist of over 100 surface sediment samples (although often fewer are used) combined with 10 - 20 measured environmental variables over a region showing significant spatial gradients. After the modern relationships between taxa and environmental variables have been modelled by regression techniques, the resultant transfer functions can be used to infer quantitative estimates of past environmental variables based on fossil assemblages (Birks 1995). Some basic assumptions of the transfer function approach are that the distributions of taxa are a function of environmental conditions and that this relationship has not changed with time. It also has to be assumed that the statistical techniques used adequately model biological responses to environmental variables of interest (Birks 1995). Despite the doubts over the diatom-temperature link, some transfer functions have been created. Vyverman and Sabbe (1995) show diatom distribution along an altitudinal gradient, therefore implying a temperature link. This led to a transfer function to infer surface water temperature in Papua New Guinea.

Pienitz *et al.* (1995) successfully modelled water temperature for Yukon and Northwest Territories, Canada (RMSEP 2.00°C). However, in both these studies it is still unknown whether the modelled signal is a direct temperature response or a related indirect variable such as nutrient status that has been altered climatically. Weckström *et al.* (1997a) created a training set of 30 Fennoscandian lakes and used this to reconstruct surface water temperatures (RMSEP 0.88°C) (Weckström *et al.* 1997b).

The transfer functions described above all aim to reconstruct surface water temperature. Air temperature is of more interest in palaeoclimatic work. Lake surface temperature does have a link to air temperature although this is dependent on individual lake characteristics (Hondzo and Stefan 1993). Both Lotter *et al.* (1997b) (RMSEP 1.62°C) and Rosén *et al.* (2000) (RMSEP 0.86°C) attempt to reconstruct air temperature. The main problem with this approach is acknowledged in most studies and described in detail by Anderson (2000). It is possible that the diatoms are not responding directly to temperature, but to other factors such as pH, nutrient levels or DOC which can be driven by temperature. With the exception of Lotter *et al.* (1997b), temperature is a very weak explanatory variable and other variables explain more variation in the dataset (Anderson 2000). Anderson (2000) also highlights the fact that, over long periods such as the Holocene, variables like pH or nutrient levels can change independently of temperature. As a result, diatom temperature inferences will be artefacts if indeed temperature only has a major influence on diatoms indirectly. In addition to these limitations, there are more general problems that need to be considered when attempting environmental reconstructions using diatoms. For example, dissolution and differential preservation (Ryves 1994, Barker *et al.* 1994b, Reed 1998, Ryves *et al.* 2001), resuspension and taphonomy (Gasse *et al.* 1997) and the limitations of the transfer function approach such, as the no-analogue problem (Hutson 1977, Sayer 2001). Subsequently, climatic reconstructions using diatoms may be improved with a greater ecological understanding by using an integrated approach of monitoring modern diatom populations, and their responses to measured environmental variables combined with an assessment of diatom flux through the water column to the sediment and levels of dissolution. This is of particular need in studies of Lake Baikal (Mackay *et al.* 2003).

It has already been shown that ice cover dynamics are important in controlling diatom spatial distributions in Lake Baikal (Mackay *et al.* 2003). Therefore, the first part of this chapter will describe the further development of ice and snow cover inference models for Lake Baikal based on remotely sensed data.

5.2 Ice cover on Lake Baikal

Ice formation typically begins in shallow bays in late autumn. By early December the major part of the North Basin is frozen and by late December to early January the far south is frozen (Shimaraev *et al.* 1994). Ice formation takes longest on the east coast due to high winds which can cause ice drifts and repeated break up of ice up to 30 cm thick (Verbolov *et al.* 1965). Conditions during formation such as wind, temperature and snow amount determine the structure of ice (Shimaraev *et al.* 1994). Regions of clear ice form in the central basin and off the west coast while the remainder of the lake is covered by semi-transparent white ice (Le Core 1998). Snow and ice cover are thickest in the North Basin due to the harsher climatic conditions. Thawing usually begins in March or April and is aided by strong winds (Shimaraev *et al.* 1994). In spring, further freezing stops even if air temperatures are below freezing due to increased incoming solar radiation and upwelling of warmer waters. Areas of transparent ice thaw faster than those with deep snow cover due to lower albedo of clear ice and the fact that the water column is being directly warmed (Verbolov *et al.* 1965). Ice sheet break-up is aided by the formation of frazil ice (needle ice or pipkrake) as air bubbles formed on the ice surface propagate downwards essentially creating a honeycomb. The ice subsequently turns to ice 'needles' which eventually disintegrate and turn to slush (Verbolov *et al.* 1965, Shimaraev *et al.* 1994, Le Core 1998, Semovski *et al.* 2000). Current monitoring of Lake Baikal ice cover is limited to observations of ice break-up and onset dates from Listvyanka and the Lower Angara River in the South Basin and these have been recorded since 1869 (Shimaraev *et al.* 1994, Magnuson *et al.* 2000). Ice thickness data have also been recorded since 1950 (Shimaraev *et al.* 1994). These data show considerable variability over short (2 – 8 years) to long (24 – 45 years) timescales while a tendency to a shorter frozen period has been observed over the last 20 – 30 years related to global climatic warming (Shimaraev *et al.* 1994, Magnuson *et al.* 2000). Magnuson *et al.* (2000) relate trends in observed ice cover dynamics at several sites (including the ice phenology records listed above) in the northern hemisphere to climatic change as similar patterns are shown between disparate locations. Furthermore, the observational data of Lake Baikal ice cover has been linked directly to climate variability in the form of the NAO/AO systems (Livingstone 1999, Todd and Mackay 2003). The application of remote sensing to ice cover monitoring will increase spatial and temporal knowledge of ice cover dynamics on Lake Baikal and hopefully how this links to diatom distributions and climate.

5.3 Effects of ice cover on diatom populations

Ice dynamics of any lake are obviously linked to climatic processes, as has been shown by Magnuson *et al.* (2000). Snow cover itself can have an important influence on climate by lowering albedo (section 1.4.2) and altering weather patterns on a regional scale (Liu and Xanai 2002, see also section 7.5.3) Changes in the duration and timing of lake ice cover can have a direct influence on within-lake temperature gradients, water column mixing and stratification, nutrient availability and productivity. This can be via reduced physical mixing by sealing the lake surface from the effect of wind or by reduced light transmission affecting both turbulence and productivity. Granin *et al.* (2000) show the importance of this turbulence related to light intensity for the suspension of *A. baicalensis* cells in Lake Baikal. The type of ice cover has a bearing on the amount of light transmitted: clear ice allows a high transmission of light, while white ice (containing air bubbles and formed due to thawing and re-freezing, especially after melt water has saturated lower snow layers (Wetzel 2001)) allows much less light through. Table 5.1 shows the amount of ice that can penetrate through different types of ice and snow cover. The effect of white versus clear ice on phytoplankton dynamics has been shown at Lake Bonney, Antarctica (Fritsen and Priscu 1999).

Ice-snow conditions	Thickness (cm)	% transmission of surface radiation
Clear ice	43	72
Clear ice	154	23.2
Clear ice with vestige snow	39	53
Clear ice with sediment floc	149	14.8
Milky ice with bubbles	29	54
Wet ice with bubbles	39	41
Translucent ice (snow ice)	25	11-18
Ice with irregular surface	29	58
Clear ice with 3cm snow	149 + 3	0.57
New snow	0.5	34
New snow	5	20
New snow	10	9
New snow	17-20	8.8-6.7
Compacted old snow	17-20	5-1

Table 5.1: Comparison of light transmission through different ice and snow types and thickness (from Wetzel (2001) based on data of Albrecht (1964) and Bolsenga *et al.* (1991)).

During periods of long non-transparent ice cover, little or no light is transmitted to the water body and lake productivity will decline as light is required for photosynthesis. Changes in ice formation and break-up dates related to climate can alter seasonal patterns of stratification and circulation and therefore also nutrient availability (Livingstone 1997). For example, longer ice cover duration leads to decreased turbulence and increased stability which in turn results in

less mixing and nutrient delivery from deep water (Bradbury and Dieterich-Rurup 1993). Changes in ice cover can also alter the availability of habitats for planktonic and benthic diatoms. A greater period of ice cover will reduce the productivity of planktonic species (Smol 1988).

Water column mixing is vital in determining the distribution of diatoms in the photic zone. Light penetration especially through clear ice or wind mixing in ice-free periods is needed to generate turbulence in the upper water column to suspend heavily silicified diatom species such as *Aulacoseira*. During periods of non-transparent ice cover, reduced stratification and turbulence the diatom assemblage can be dominated by other smaller, often centric diatoms (Padisak *et al.* 1998).

5.4 Diatom based inference models for Lake Baikal

Standard transfer function approaches of using a multi-lake calibration set cannot be used for Lake Baikal as the dominant diatom species are endemics. However, as Lake Baikal extends over 4° of latitude, this provides a large enough environmental gradient for the development of an internal calibration set (Mackay *et al.* 2003). It has to be assumed that horizontal water movements transporting diatoms from their exact location of growth are minimal. However well documented patterns of water circulation do exist (Shimaraev *et al.* 1994), although these are confined to localised areas and there is relatively less circulation and water exchange between basins. Mackay *et al.* (1998) indicated that diatom assemblages are responding to climate change rather than anthropogenic pollution and nutrient loading, meaning surface sediments can be used for a training set. Mackay *et al.* (2003) collected 93 surface sediment (core top) samples between 1992-1997 distributed throughout the lake surface to exploit the north-south environmental gradient (figure 5.1). These core-tops were chosen from a total of 120 cores taken; cores with visibly disturbed sediments such as turbidites in the upper layers, or those with the sediment water interface disturbed, were rejected. Sample preparation for diatom analysis followed the procedure as outlined in section 6.2.1 and 300 valves were counted for each sample. Taxonomy also followed that outlined in section 6.2.4.

Environmental data for each sampling location was assimilated from a secondary source summarising environmental observations of a number of limnological, chemical, biological and climatic variables collected during the Soviet era: the Atlas Baikala (1993) and from several observation and monitoring datasets (detailed in Mackay *et al.* 2003). In the Atlas, data are presented as contour maps, and linear interpolation was used between contour lines to

obtain specific values for core top locations; most commonly data were restricted to June to December (i.e. the ice free period). Although over 40 variables are mapped in the Atlas, only those showing a clear north – south gradient were selected, giving a total of 23 variables which are shown in table 5.9. There is a problem of temporal mis-match between the environmental data and core top sampling times, although Mackay *et al.* (1998) have shown diatom assemblages over the last 50 years to have remained, at least in pelagic regions, relatively unchanged. All environmental variables except total annual absorbed radiation were transformed using log(x+1) to remove observed positive skew. Statistics and additional information for these original 23 environmental variables are shown in the non-highlighted rows of table 5.9.

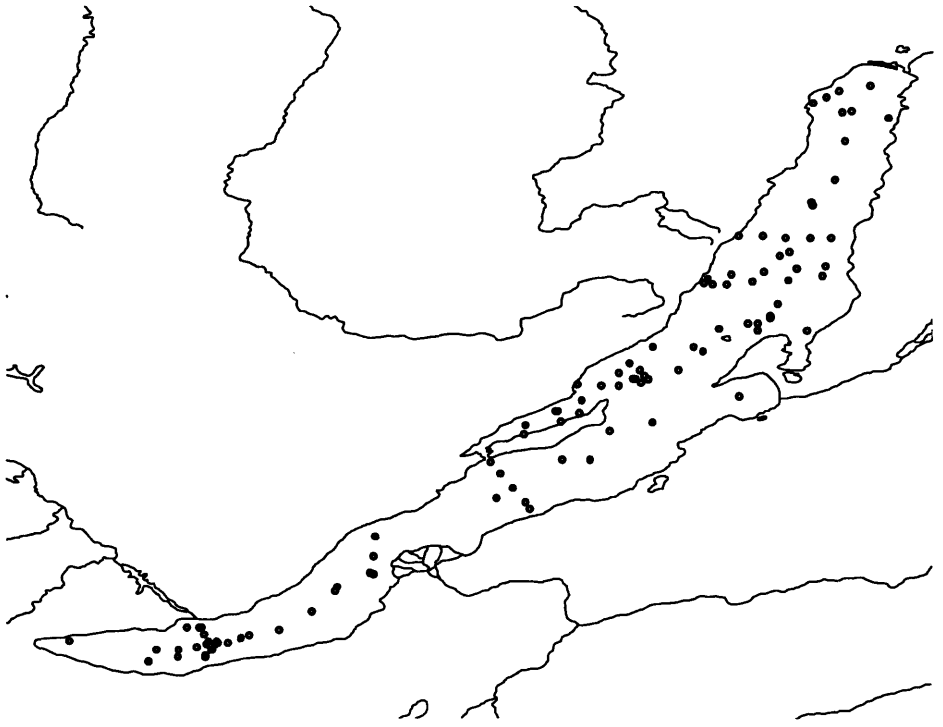

Figure 5.1: Location of 93 core top surface sediment training sites from Mackay *et al.* (2003).

The trends shown by the explanatory data were investigated using PCA. This revealed axis one was dominated by ice cover and snow thickness while axis two was driven by snow depth on the ice, phosphate and nitrate levels. The calibration training set was explored using DCA revealing a first axis score of 3.06 SD units, and as a result unimodal species responses were assumed by Mackay *et al.* (2003). Relationships between diatom distributions and explanatory variables were also explored using CCA with forward selection. This allowed ordination axes to be constrained as a linear combination of environmental variables selected

so as to include only those that explain significant amounts of variation in the species data. This allowed variables that were not significant to be removed from further analysis. Variables selected by CCA were: snow depth, water depth, suspended matter, temperature of the water surface and annual solar radiation, explaining together 26.7% of total variance.

Inference models should only be developed for variables with λ_1/λ_2 greater than 0.50 (Dixit *et al.* 1991). Only snow depth had a λ_1/λ_2 ratio of >0.50 meaning that this is the only environmental variable in the training set from which reliable inference models can be reconstructed. Subsequently, the model was developed using weighted averaging (WA), it was found $WA_{(tol)}$ down-weighting performed better than simple WA (r^2_{jack} = 0.607, RMSEP = 0.138 log cm).

Species dependant dissolution of diatoms has been shown to be an important taphonomic process in Lake Baikal with only 0.1 to 9% of valves (depending on species) produced in the water column becoming incorporated in the sediments (Ryves *et al.* 2003). As a result, such inference models as that described above can be biased due to over or under representation of certain species depending on their resistance to dissolution. However, inference models from dissolved assemblages can be still be useful (Pichon *et al.* 1992). A solution to this problem can be through the development of correction factors to adjust species abundances for differential dissolution. This gives a more accurate quantification of the sedimentary record. Correction factors for five of the common planktonic diatoms in Lake Baikal (*A. baicalensis, A. skvortzowii, C. minuta, S. meyerii* and *S. acus v. radians*) have been developed with reference to modern phytoplankton and sediment trapping samples taken in the water column and compared to the surface sediments (Battarbee *et al.* in press). By comparing the expected flux of diatoms to that observed in the sediment, it has been possible to calculate difference factors to correct for dissolution and these are shown in table 5.2. Presently, these correction factors can only be applied to the South Basin, but work is underway to develop correction factors for the North Basin too (Mackay, pers. comm.).

Diatom species	Average in water column 1994-1998	Average flux of valves from surface sediment	Difference factor
A. skvortzowii	1847868	12942	x 143
A. baicalensis	1375303	38038	x 36
C. minuta	385548	35562	x 11
S. meyerii	1157408	3264	x 355
S. acus v. radians	3745882	5514	x 680
N. acicularis	3481749	0	N/A

Table 5.2: Average diatom fluxes observed from the water column for dominant species between 1994-1998 and for sediment core BAIK38 (valves sq cm^{-1}) and correction multiplication factors to adjust core data to expected values (Battarbee *et al.* in press).

A further study by Mackay *et al.* (in press) adopts these correction factors to assess the importance of dissolution on model performance and snow depth reconstruction. However, as correction factors only exist for five species, datasets have to be limited to these five and recalculated so the five species sum to 100% in both the training set and core data. Mackay *et al.* (in press) compare four models; firstly the uncorrected model as used in Mackay *et al.* (2003) with a short core (BAIK38) containing all taxa found (model 1), a model with the five dominant taxa (uncorrected) in the core but a full training set containing all taxa (model 2), an uncorrected model consisting of the five dominant species in both the training set and the core (model 3) and a fully corrected model with the five species in the training set and the core (model 4). A summary of these four models is given in table 5.3, while their relative performances are given in table 5.4. Model 4 showed the lowest errors and best fits after testing using 1000 bootstrap cycles (table 5.4) and also appears to be most sensitive to reconstruct snow depth changes over the last 1000 years, in comparison to uncorrected models (Mackay *et al.* in press). This shows that at least for the last 1000 years diatom dissolution has the effect of dampening the reconstructed snow depth signal. However, beyond 1000 years there may be analogue problems of using a limited training set as different species occur in abundance in the Mid to Early Holocene that cannot have correction factors developed as they are either extinct or rare in the modern environment.

As snow depth on Lake Baikal's ice has been shown to be important in controlling diatom populations by altering the amount of light transmitted into the water column during the ice covered period, to develop this inference model further, additional data on lake ice and snow cover can be collected. As the data on snow depth from the Atlas Baikala (1993) are limited spatially and temporally, remotely sensed data will provide greater resolution. The next section attempts to improve the transfer functions of Mackay *et al.* (2003, in press) using remote sensing.

	Training set	Core data (BAIK38)
Model 1	Full, 87 taxa (as in Mackay *et al.* 2003)	Full, all 22 taxa
Model 2	Full, 87 taxa (as in Mackay *et al.* 2003)	5 dominant taxa (uncorrected) recalculated to sum to 100%
Model 3	5 dominant taxa (uncorrected) recalculated to sum to 100%	5 dominant taxa (uncorrected) recalculated to sum to 100%
Model 4	5 dominant taxa (corrected) recalculated to sum to 100%	5 dominant taxa (corrected) recalculated to sum to 100%

Table 5.3: Training set and core data used in the four inference models of Mackay *et al.* (in press).

	Number of samples	Number of outliers	number taxa after deletions	DCA axis 1	Model type	Apparent r^2	RMSE (log cm)	Boot r^2	RMSEP (log cm)
Model 1	89	4	83	2.217	$WA_{(Tol)}$-Inv	0.681	0.124	0.607	0.138
Model 2	89	4	73	2.323	WA-Inv	0.655	0.128	0.583	0.145
Model 3	87	6	5	2.152	$WA_{(Tol)}$-Inv	0.684	0.123	0.662	0.130
Model 4	87	6	5	2.173	$WA_{(Tol)}$-Inv	0.733	0.113	0.709	0.120

Table 5.4: Results for models 1-4 using weighted averaging (Mackay *et al.* in press). All models are based on untransformed % diatom data and assessed using 1000 bootstrap cycles.

5.5 Satellite remote sensing

5.5.1 Introduction

Remote sensing is a useful tool in the study of environmental processes at a high temporal and spatial resolution. Information about the Earth's land and water surfaces are obtained from an overhead perspective using electromagnetic radiation reflected from the Earth's surface in one or more regions of the electromagnetic spectrum (Campbell 1996). Remote sensing has the particular advantage over *in situ* ground-based measurement campaigns as images can cover a continuous geographical area whereas ground-based measurements may be based on a sparse point sampling strategy. Also, remote sensing has the advantage of being able to record observations in remote or inaccessible regions such as the north of Lake Baikal during winter, combined with a frequent revisit time of sensors to a region. There is a range of sensors in use with different specifications and the selection of an appropriate data set depends on the features being studied. Usually the optimal data set is chosen on the basis of the spatial and spectral resolution required, satellite revisit time, image size (cost of storage) and the cost of purchasing the images themselves.

5.5.1 Remote sensing of snow and ice cover

Remote sensing mapping of snow cover depth, extent and snow water equivalent (SWE) calculated as a function of snow depth and density, has received particular attention because of interest in flood forecasting and understanding the hydrological cycle (Deerskin and Redrew 2000). However remote sensing of snow thickness/depth is problematic. The best results are obtained from high spatial resolution synthetic aperture radar (SAR) data combined with an extensive network of actual measured snow depths over the scene to calibrate and/or validate any classified image. This calibration is needed as the radar response depends on snow conditions, in particular the wetness of the snow (Sokol *et al.* 2003). Srivastan and Singh (1991) have had some success using SAR and ground validation to map snow extent, type and depth.

Radar data are not as commonly available and as easy to handle as data in the optical spectrum. As a result optical data have been used mostly to map snow extents over large regions and there are many methods to do this, ranging from simple manual digitising to classification algorithms (Derksen and LeDrew 2000, Bitner *et al.* 2002). Although very problematic, snow depth and SWE have been mapped using AVHRR data in the visible and infrared range combined with ground observations. Only very broad depth classes of shallow,

medium or deep are often obtained (Xu *et al.* 1993), however Ranzi *et al.* (1999) claim to record continuous values for SWE using a similar method.

Because snow depth mapping is fraught with difficulties, in particular the need for ground truthing which is not possible in the present study, it is more appropriate to map the dynamics of snow, water and different ice type extent over Lake Baikal. It has been shown that different ice types have varying optical properties (table 5.1) which may be important for diatom distributions. Ice cover type distinction and mapping has been applied to the marine environment using a combination of optical and SAR remote sensing (Lythe *et al.* 1999), while ice cover mapping on Lake Baikal has been attempted by Bolgrien *et al.* (1995), Le Core (1998), Semovski *et al.* (2000) and Semovski and Mogilev (2003) using optical sensors.

The simplest method is to use images in the visual range to distinguish water, white ice, clear ice and snow due to the difference in surface reflection. Classes for each cover type are defined by locating peaks in histograms of reflectance values (Le Core 1998). This method is not the most accurate, as spectral signatures defined for each coverage class may overlap, leading to misclassification. An approach similar to this was used by Bolgrien *et al.* (1995) who used a thermal channel to define either ice or water covered regions. Another variation of this was applied by Semovski *et al.* (2000) and Semovski and Mogilev (2003) with the use of a PCA approach over several channels to identify the main signatures attributable to snow and ice types for the period 1994 - 1998 on Lake Baikal.

The most accurate approach available uses the normalised difference snow index (NDSI) (Riggs *et al.* 1994). The NDSI is the normalised difference between red and infrared bands and allows clouds, land and ice/snow to be distinguished from a scene. In order to break the snow/ice category into specific ice types, the brightness temperatures (BT) from a thermal channel must be compared. On the basis of this NDSI/BT approach, Le Core (1998) working on the 1996 - 1997 ice covered period in Lake Baikal identified: water, cloud, land, clear (fresh) ice, slush ice, frazil ice, fresh white ice, old white ice, white ice melt ponds, clear/white ice mix, ice/snow mix, snow melt ponds and snow. This level of detail is unnecessary for the present study, therefore the simple classification of coverage types using optical bands and thresholding of image histograms will be used here.

5.6 Remote sensing methodology

5.6.1 The Advanced High Resolution Radiometer (AVHRR)

The data used here for the classification of Lake Baikal ice cover were collected by the AVHRR meteorological satellite. The 1996-1997 period of ice coverage was chosen, as this corresponds to the final surface sediment samples taken by Mackay *et al.* (2003) and also corresponds to the study of Le Core (1998) which is of use when assigning actual cover types to the images processes in this study.

The AVHRR acquires data on a swath width of 2800 km providing a global coverage on a twice-daily basis. Resolution at nadir is 1.1 km meaning that each image pixel covers 1.1 km^2 on the ground. The sensor operates in five channels shown in table 5.5. These data are of particular use in this study because the spatial resolution is optimal for studying an area as large as Lake Baikal but most importantly the data can be obtained for no cost.

Channel	Spectral range	Region
1	0.58 – 0.68 μm	Visible (red)
2	0.72 – 1.10 μm	Near infrared
3	3.55 – 3.93 μm	Thermal infrared
4	10.30 – 11.30 μm	Thermal infrared
5	11.5 – 12.5 μm	Thermal infrared

Table 5.5: Spectral channels and ranges for the AVHRR.

5.6.2 Image selection

AVHRR images are obtainable free of cost for registered users via the National Oceanographic and Atmospheric Administration's (NOAA) Satellite Active Archive (SAA) – http://www.saa.noaa.gov. User defined queries regarding the dates and spatial coverage of required images return a list of all available images in the SAA database along with reduced thumbnails of the image in channels 2 and 4. This preview image allows the selection of only images that are free of cloud. After screening the entire database for cloud free images of Lake Baikal for 1996-1997, a total of 34 cloud-free images of ice cover were obtained between 10th December 1996 and 2nd June 1997 covering the entire period of ice coverage. These images were ordered from the SAA and downloaded via FTP. The temporal distribution of these images are shown in table 5.6, while summary statistics of the

distribution are shown in table 5.7. The average time between images is about 5 days although during May there are intervals of 10 and 15 days without cloud-free images.

1996 **Nov**	1996 **Dec**	1997 **Jan**	1997 **Feb**	1997 **Mar**	1997 **Apr**	1997 **May**	1997 **Jun**	1997 **Jul**
			970201		970401			
							970602	
		970103				970503		
			970204		970404			
				970306				
						970507		
			970208					
		970109						
	961210			970310	970410			
					970411			
	961213							
				970314	970414			
			970215					
		970116						
		970118		970318		970518		
					970420			
	961221		970221					
					970422			
		970123						
				970324				
	961226							
			970227					
		970128						
				970329				
	961231							

Table 5.6: AVHRR image temporal coverage for the 1996-1997 ice covered period on Lake Baikal, images are named by date in the format yymmdd. The grey shaded region indicates periods of complete open water, the white area indicates the period of ice cover.

Mean	5.18 days
Standard Deviation	2.73 days
Minimum	1 day
Maximum	15 days
Count	34 images

Table 5.7: Summary statistics for the temporal distribution of AVHRR images for the 1996-1997 ice covered period on Lake Baikal.

5.6.3 Image processing

Processing of AVHRR data was carried using the image processing software package Imagine 8.5 made by Erdas. For each of the 34 images the following stages were followed to obtain firstly a thematic map of lake coverage type and secondly a cover type for each training set location of Mackay *et al.* (2003).

1. The downloaded binary image file was imported into Imagine (figure 5.2) and subset to an area of just the lake and immediate area to reduce the file storage size (figure 5.3).

2. During acquisition, images become distorted due to pitch and roll of the satellite. This can be corrected by resampling the image with reference to a geometrically correct base image. Here, a georeferenced vector coverage of Lake Baikal's boundary was used (figure 5.4) (downloadable from Geocommunity: http://data.geocomm.com/catalog/RS/datalist.html). Corresponding geographical features in both images such as abrupt changes in coastline were identified. For each image 60-70 of these ground control points (GCPs) were marked. A new spatial (x, y) grid is created for the image by fitting 2nd order polynomials. Resampling of the image was done by bilinear interpolation, this calculates a new pixel values for image pixels using weighted averaging based on a nearest neighbour approach. Atmospheric correction was not considered necessary as atmospheric distortions would not influence the very clear differences between ice cover signatures, and no atmospheric corrections were used in the study of Baikal ice with AVHRR by Bolgrien *et al.* (1995).

3. The rectified image (figure 5.5) was then subset to just the region contained by the lake using the same vector coverage in stage 2 as a mask (figure 5.6).

4. The complete multispectral image was then classified using an unsupervised classification into groups of like pixels. Imagine 8.5 uses the ISODATA clustering algorithm which is a centroid based iterative approach. Once a thematic map has been produced, classes according to coverage type can be assigned based on comparisons to the work of Le Core (1998) and looking at the spectral signatures of certain classes, for example the relative higher reflectance of snow compared to white ice in the visible channel. Classes identified in this study are water, white ice, clear ice, snow and wet ice. The 34 thematic maps created are shown in figure 5.7.

5. In order to obtain an ice cover class for each training sample location the GIS software ARC version 7.2.1 was used. A coverage containing points relating to the training sites was created and then overlain on the thematic map in Imagine 8.5. Corresponding ice cover classes were then recorded for each location. The assigned cover types for the 93 training sites over the 34 thematic maps are shown in table 5.8.

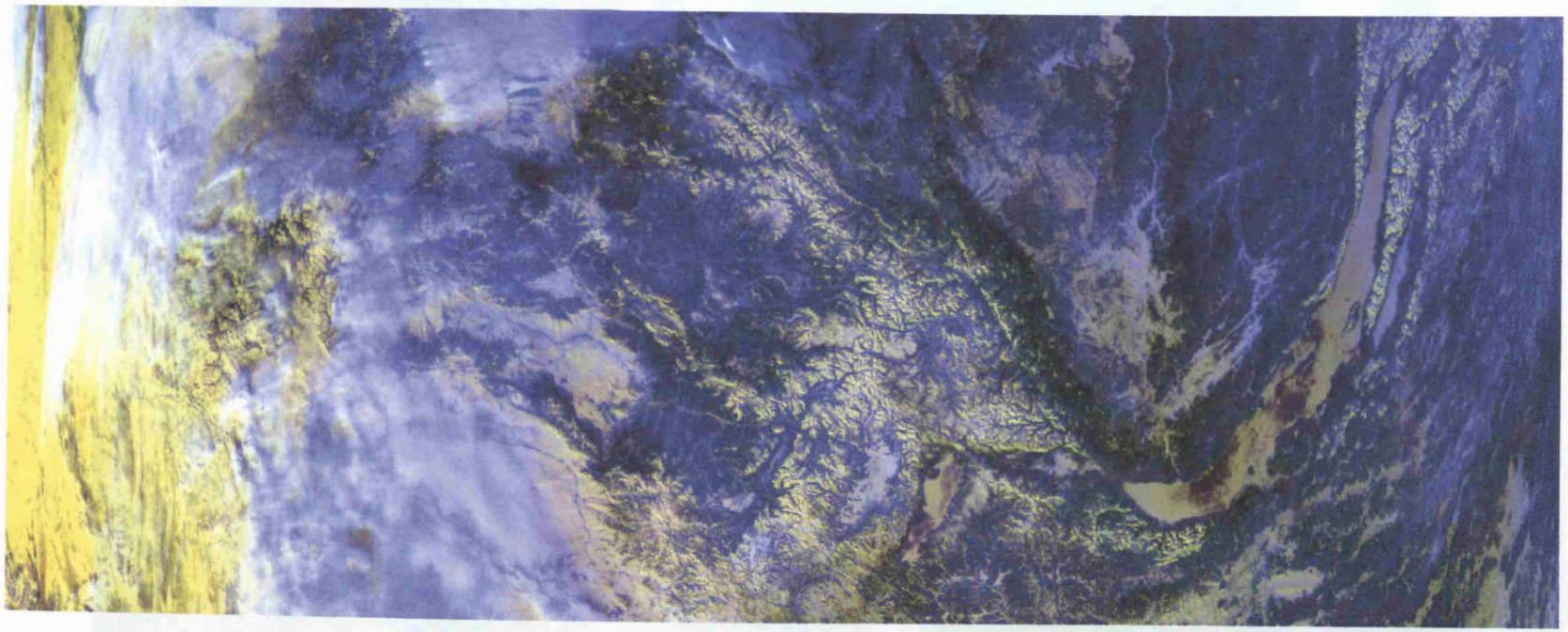

Figure 5.2: An example of a full AVHRR image of the Lake Baikal region before processing. Downloadable from the SAA.

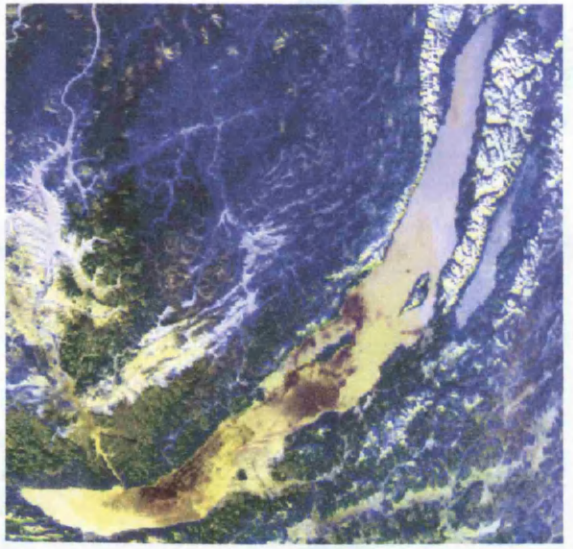

Figure 5.3: AVHRR image subset of the Lake Baikal region.

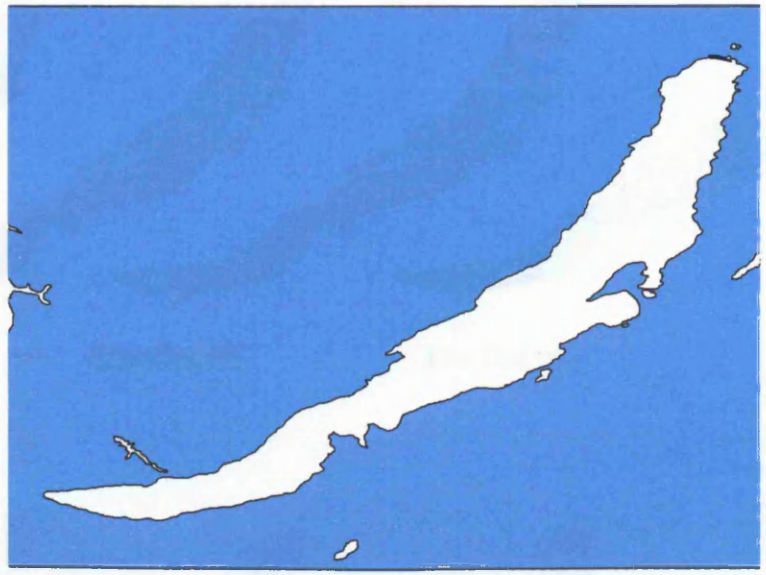

Figure 5.4: Georeferenced vector coverage of the Lake Baikal boundary.

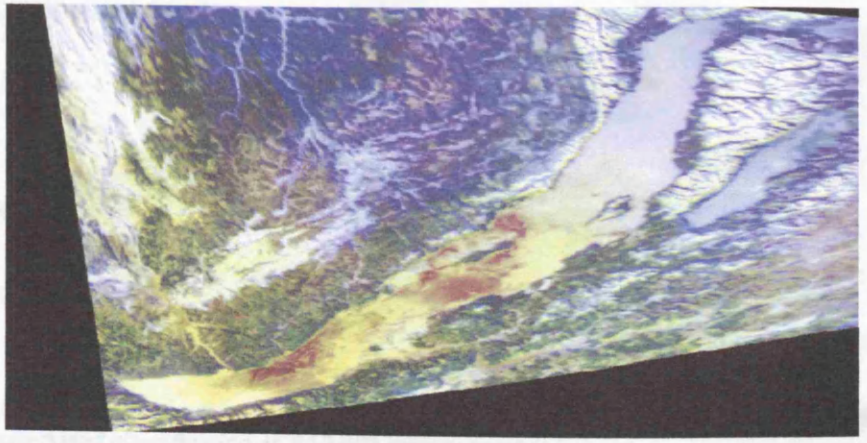

Figure 5.5: Geocorrected AVHRR image.

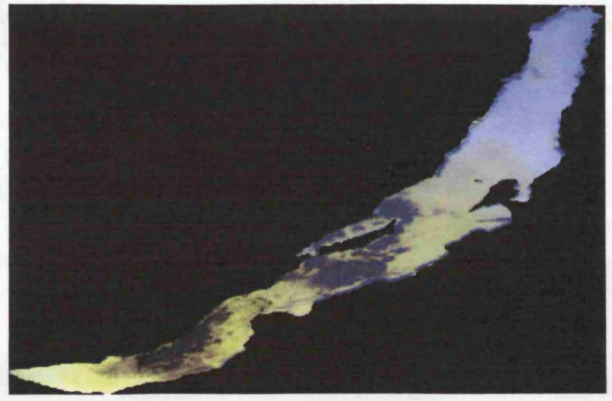

Figure 5.6: Corrected image subset to just the Lake Baikal water body

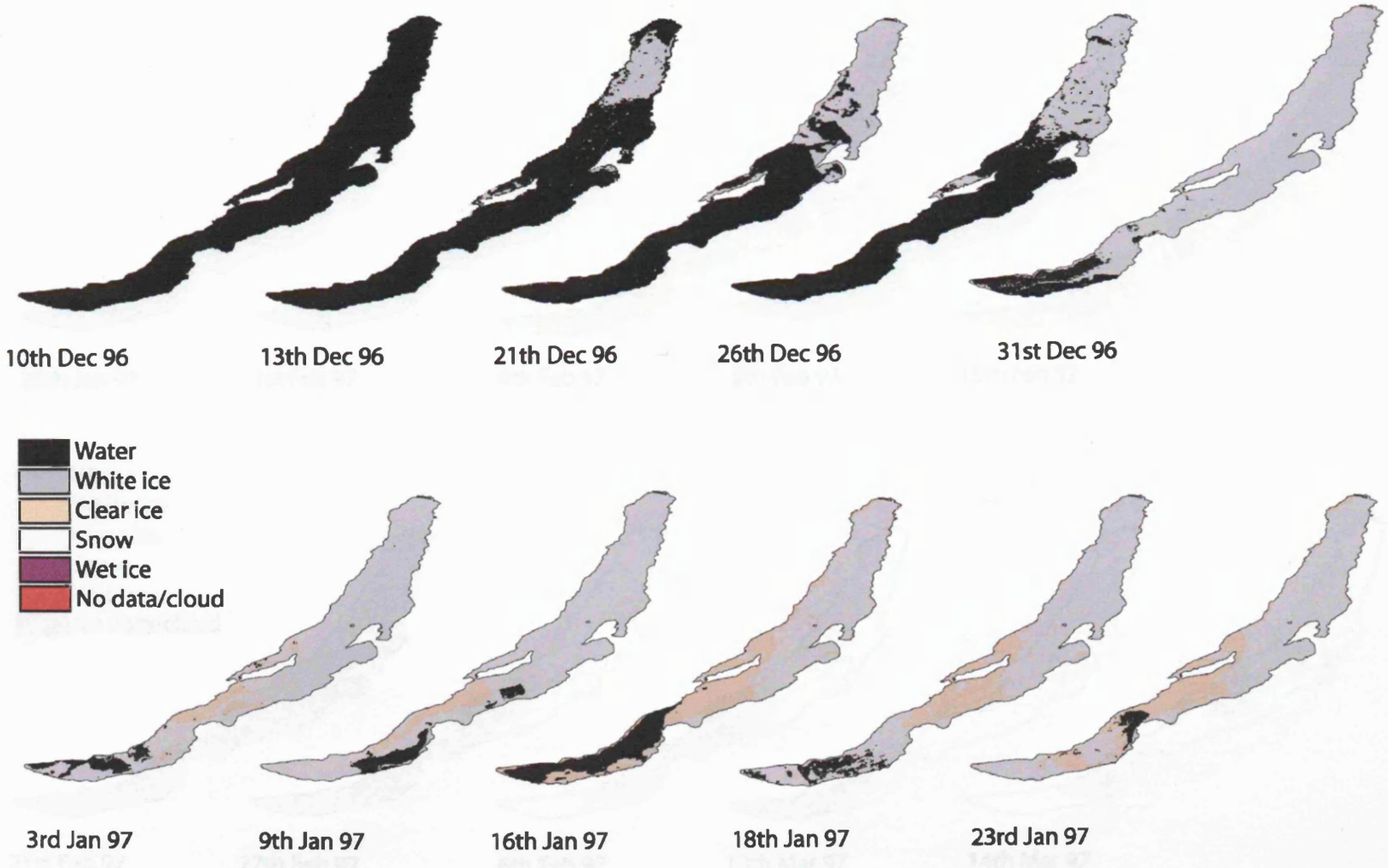

Figure 5.7: Thematic maps showing the snow, ice and water classes for the 1996-1997 ice covered period on Lake Baikal defined by an unsupervised classification of AVHRR remote sensing images.

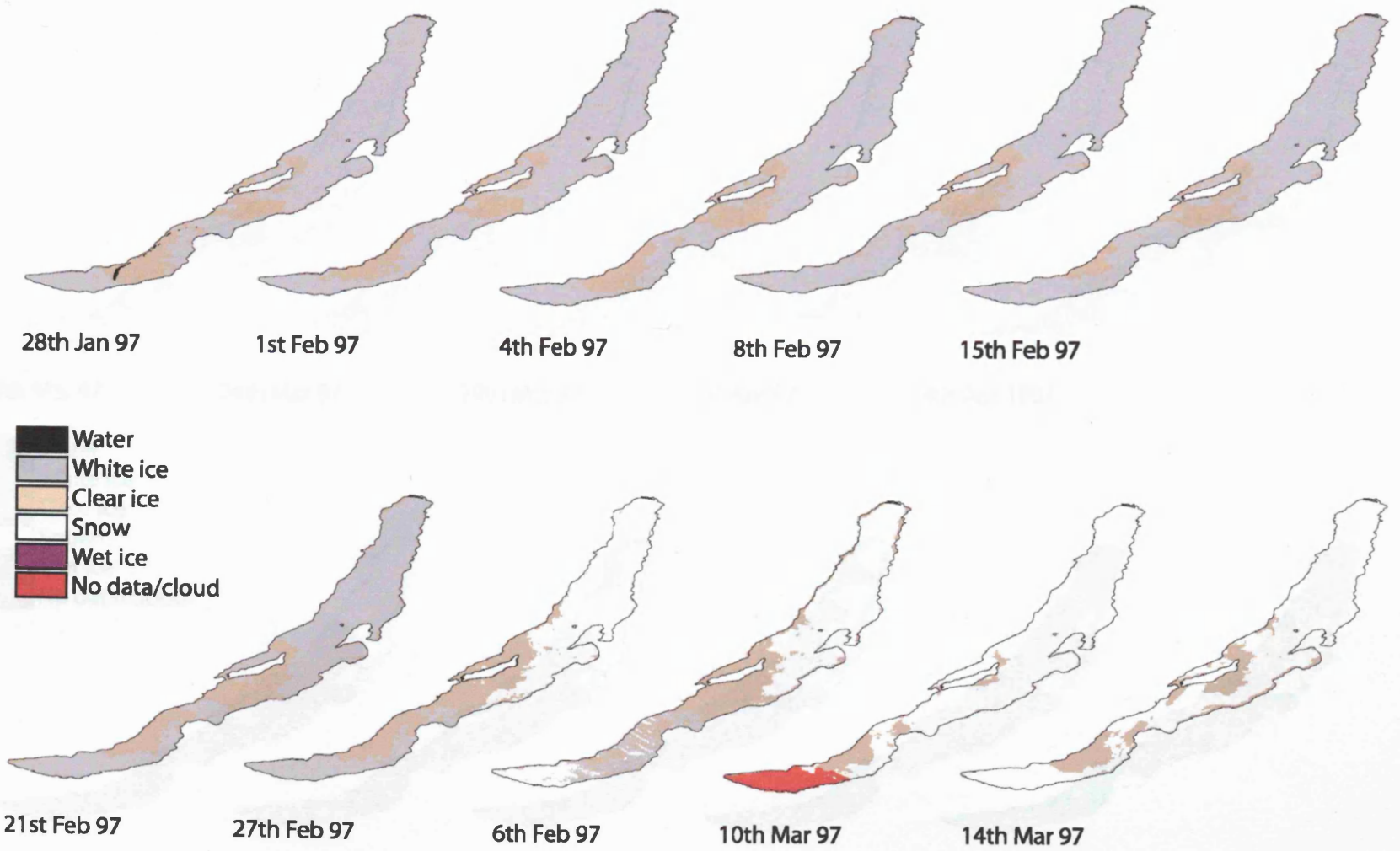

Figure 5.7: Continued

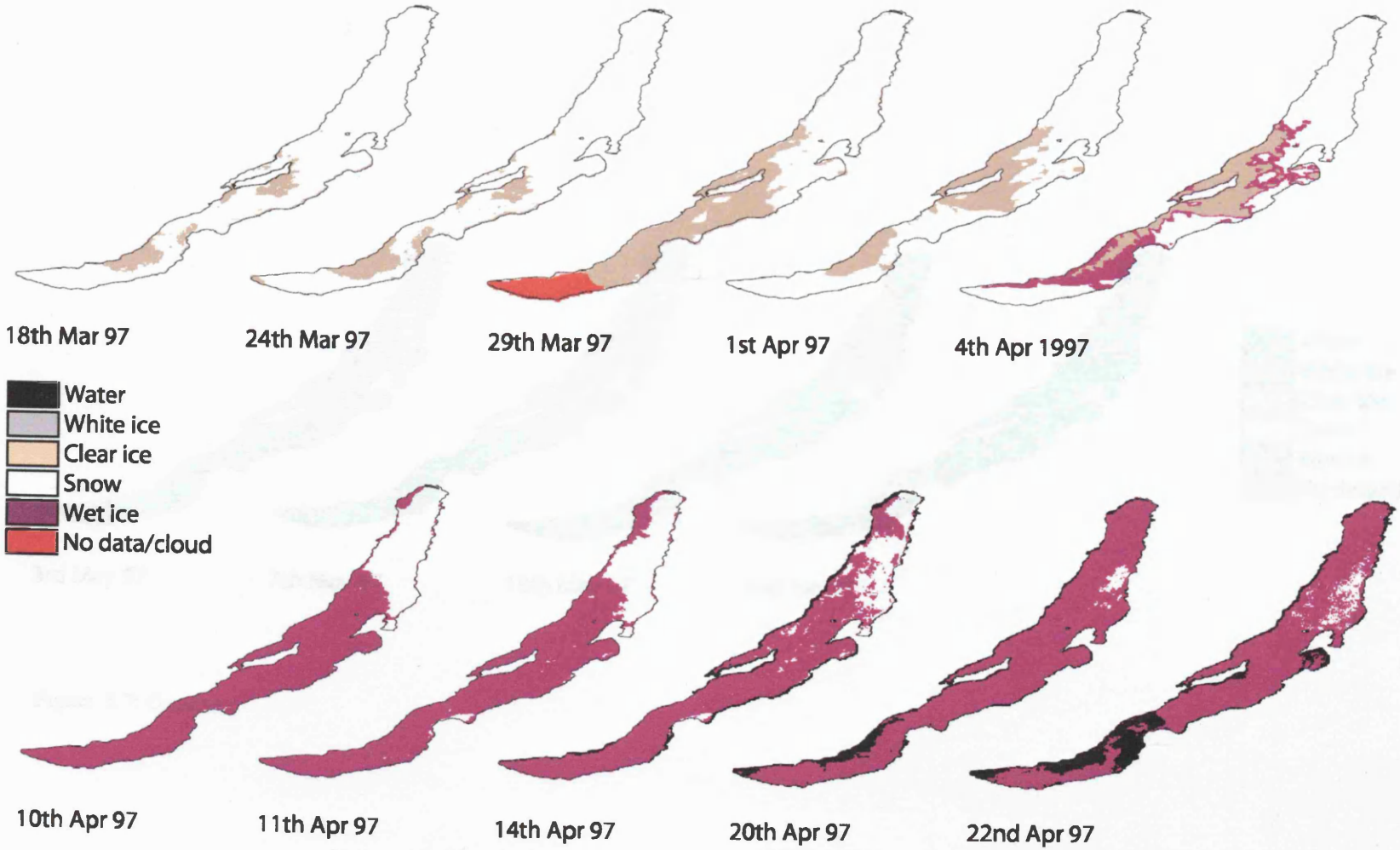

Figure 5.7: Continued

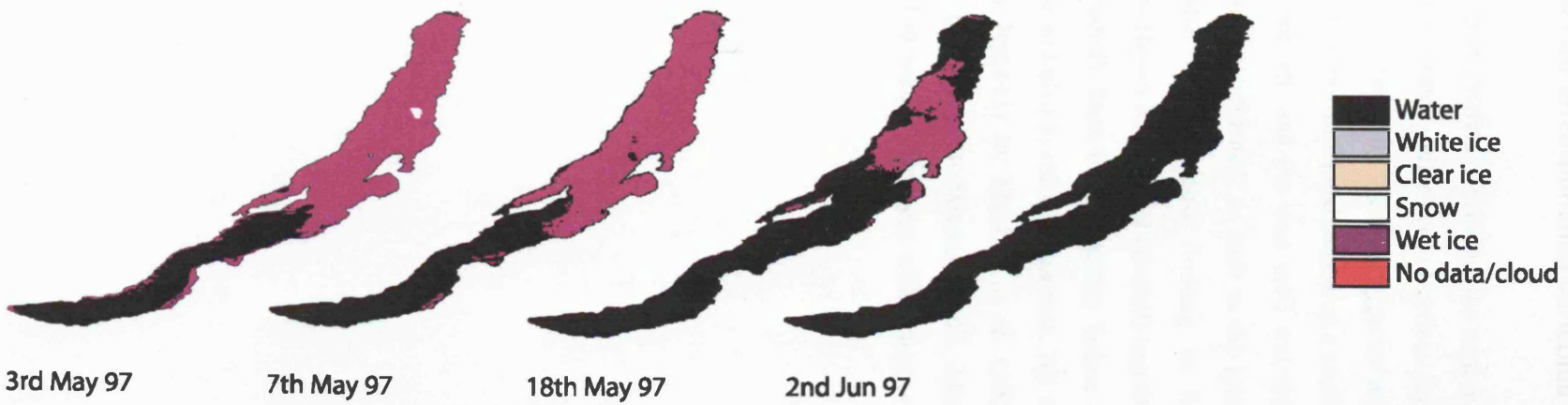

Figure 5.7: Continued

5.6.4 Creation of new environmental variables

Using the data in table 5.8, it is possible to estimate the total number of days of the year when the lake is covered by either water, white ice, clear ice, snow or wet ice. A training site location is considered to be covered by a certain type up until this coverage changes in a subsequent image. Other variables formulated (based on a starting point of 10th December) are the time until ice on and ice off, and the time until wet ice forms. The total time of ice duration for each site was also estimated, as well as the total time of white ice and snow coverage together as these will be most limiting to light penetration. These new environmental variables are shown in table 5.9 (shaded) together with the original Mackay *et al.* (2003) variables (unshaded). Data transformation before ordination is often needed to make variables comparable and also to reduce skewness. All environmental variables except one were transformed by log(x+1) by Mackay *et al.* (2003). Individual environmental variables were plotted as histograms in Minitab v. 13. After visual assessment of these histograms, it was decided to reduce skewness with a log(x+1) transformation for all new variables (table 5.9).

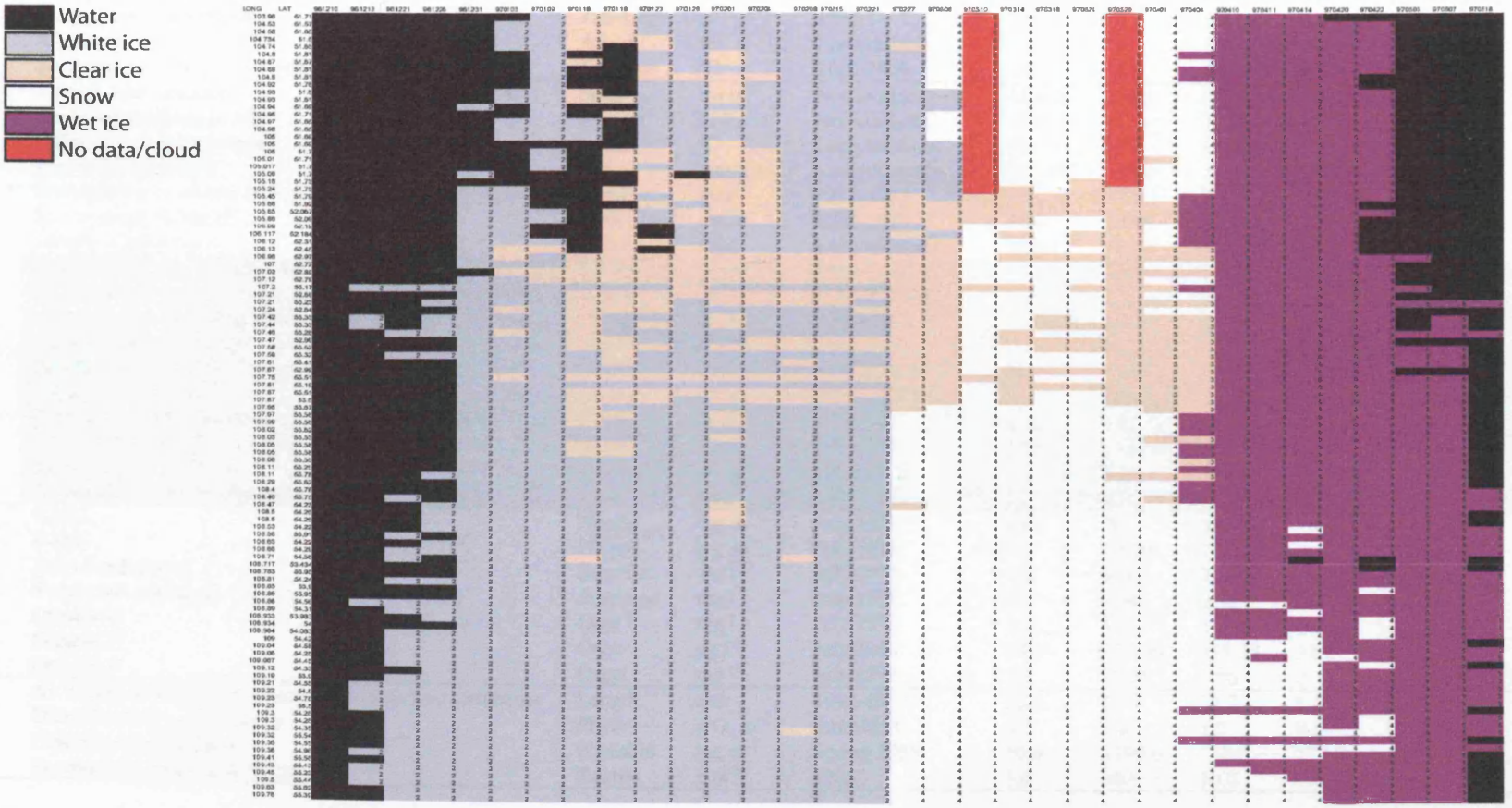

Table 5.8: Classified cover type for the 93 surface sediment locations ordered by decreasing latitude (rows) for the 34 images ordered by date (columns)

Type	Explanatory variable	Code	Units	Dates measured	Min	Max	Mean	STDS	Transformation
Limnology	Water depth	Depth	m	1992-1997	20.0	1678.0	809.6	480.3	log(x+1)
	Transparency in July	Transjul	m	1961	9.0	25.0	21.4	4.6	log(x+1)
	Transparency in September	Transsep	m	1961	2.0	11.0	6.0	2.0	log(x+1)
	Albedo in July	Albedo	%	Not available	5.0	7.0	5.1	0.4	log(x+1)
	Temperature of July water surface	Tempws	°C	1896-1959	1.0	13.0	5.9	2.3	log(x+1)
Climate	Annual solar radiation	Solar	mJ m^{-2}	Not available	4100.0	4700	4478.5	187.6	log(x+1)
	Absorbed radiation in July	Absorb	kcal cm^{-2}	Not available	13.0	15.0	14.2	1.0	None
	Mean July air temperature	Julair	°C	Long term obs.	9.0	15.0	14.2	1.7	log(x+1)
	Annual precipitation	Precip	mm	Long term obs.	175.0	550.0	12.2	67.7	log(x+1)
	Snow thickness on lake in March	Snow	mm	1972-1973	2.5	12.5	6.2	3.2	log(x+1)
	Ice thickness in March	Icedep	mm	1972-1973	65.0	100.0	82.9	7.2	log(x+1)
	Length of ice cover	Icecov	days	Long term obs.	126.0	168.0	145.3	10.7	log(x+1)
	Annual duration of water coverage	Twater	days	1996-1997	197	270	231.4	21.1	log(x+1)
	Annual duration of white ice coverage	Twhite	days	1996-1997	0	76	53.0	17.1	log(x+1)
	Annual duration of clear ice coverage	Tclear	days	1996-1997	0	85	16.2	22.6	log(x+1)
	Annual duration of snow coverage	Tsnow	days	1996-1997	0	63	32.4	15.7	log(x+1)
	Annual duration of wet ice coverage	Twet	days	1996-1997	10	57	32.0	11.0	log(x+1)
	Ice cover duration	Ice dura	days	1996-1997	83	168	131.0	24.7	log(x+1)
	Time until wet ice formation (from 10th December)	to wet	days	1996-1997	114	142	121.2	6.8	log(x+1)
	Time until ice off (from 10th December)	to ic of	days	1996-1997	130	171	153.8	12.9	log(x+1)
	Time until ice on (from 10th December)	to ic on	days	1996-1997	3	53	22.9	13.5	log(x+1)
	Annual duration of white ice and snow coverage	Tw+s	days	1996-1997	14	131	85.5	29.8	log(x+1)
Chemistry	$N\text{-}NO_3$	Nitrate	mg m^{-3}	July 1978	15.0	70	58.17	16.4	log(x+1)
	$P\text{-}PO_4$	Phosp	mg m^{-3}	July 1978	4.0	12.00	7.73	2.7	log(x+1)
	Suspended matter	Suspmat	mg l^{-1}	July 1978	0.8	4.00	2.32	0.6	log(x+1)
	Suspended organic C	Susporgc	mg l^{-1}	July 1978	0.3	1.50	0.38	0.2	log(x+1)
	Organic C	Orgc	mg l^{-1}	July 1978	1.1	1.70	1.33	0.2	log(x+1)
	Organic N	Orgn	µg l^{-1}	July 1978	70.0	175.00	118.38	24.2	log(x+1)
	Organic P	Orgp	mg l^{-1}	July 1978	7.0	16.50	9.96	2.1	log(x+1)
Biology	Av. length of 100 *A.baicalensis* cells in surface sediments	Length	mm	1992-1997	20.3	29.4	25.2	1.7	log(x+1)
	Diurnal primary productivity	Phyto	g O_2 m^{-2}	June 1991	0.3	2.8	1.0	0.6	log(x+1)
	Phytoplankton biomass	Phytobio	mg m^{-3}	Spring 1985	50.0	1100.0	150.0	172.0	log(x+1)
	Zooplankton biomass in September	Zoobio	g m^{-2}	1985	5.0	30.0	10.0	8.6	log(x+1)

Table 5.9: Environmental variables used by Mackay *et al.* (2003) as potential explanatory variables for distribution of diatoms in the surface sediments (for original sources see Mackay *et al.* (2003)). New variables created in this study are shown in the shaded area.

5.7 Transfer function development

5.7.1 Species data

Based on the training set of Mackay *et al.* (2003), three training sets have been developed for this study. The first calibration set is the full version used by Mackay *et al.* (2003), the second contains the five most common species corrected for dissolution effects as in Mackay *et al.* (in press). Finally a calibration set has been formulated containing only planktonic species in an attempt to remove the noise created by the presence of a large number of rare benthic taxa. After deletions, remaining taxa were recalculated to sum to 100%. All data sets contain 92 sample sites compared to the 93 of Mackay *et al.* (2003) site B111 was deleted due to the species assemblages being based on a very small number of diatoms counted. Species data were not transformed prior to data analysis, although species data are often square-root transformed to reduce the effect of dominant species. In this case it was decided that transformation would result in an over-truncation of the gradient length of the data set (Ryves pers. comm.).

DCA was used to establish the gradient length, in accordance with Mackay *et al.* (2003) species data was not transformed before analysis, however rare species were downweighted, except in the five species set in which there are no rare species. The results of DCA are shown in table 5.10. Generally, Lepš and Šmilauer (2003) state the longest DCA axis gradient should be larger than 4.0 SD for unimodal methods to be appropriate, while for gradients shorter than 3.0 SD linear methods should be used. Between 3.0 – 4.0 SD both methods may be used. This would imply that linear response model should be used with the data and indeed the species response plots defined by HOF models (section 5.8.2) show predominantly linear responses. However it is always best to use unimodal inference models with percentage data (as is the case here) as linear methods have the tendency to overfit a model to percentage data (Birks, pers. comm.).

	Number of taxa	Number of samples	λ Axis 1	λ Axis 2	Axis 1 length (SD)	Axis 2 length (SD)	Total inertia
Full	86	92	0.402	0.306	3.046	2.922	1.865
5 corrected sp.	5	92	0.515	0.186	2.185	2.004	0.986
Planktonic	30	92	0.406	0.308	2.896	2.914	1.503

Table 5.10: Results of DCA for the floristic data of the three calibration set formulated in this study

5.7.2 Environmental data

Trends in the explanatory environmental data set were explored using PCA (figure 5.8). Axis 1 and 2 eigenvalues are 0.495 and 0.186 respectively which together explain 68.1% of variance in the environmental data. Axis 1 shows a clear gradient between ice types with white ice and snow with negative values, separated from clear ice and areas with higher solar absorption with positive values. Axis 2 mainly shows a gradient related to a mixture of explanatory variables such as depth and water chemistry. To test the significance of these axes it is useful to compare their sizes to those expected under a random model, such as the broken stick model. This model divides the total variance randomly amongst the ordination axes and allows a direct comparison to those results obtained by ordination. The DOS software BSTICK was used to calculate these random axes scores. For the full and planktonic training sets, the first four axes were all significant. However the majority of variance is explained by the first two axes in each case. For the five corrected species training set, only the first axis is significant. Of the new environmental variables created, many appear to be highly related, this is expected as they stem from the same original data set. Environmental vectors in the PCA plot separated by acute angles indicate a very close correlation, while vectors that are polarised show a strong negative correlation. Table 5.11 shows a correlation matrix of all the environmental variables used.

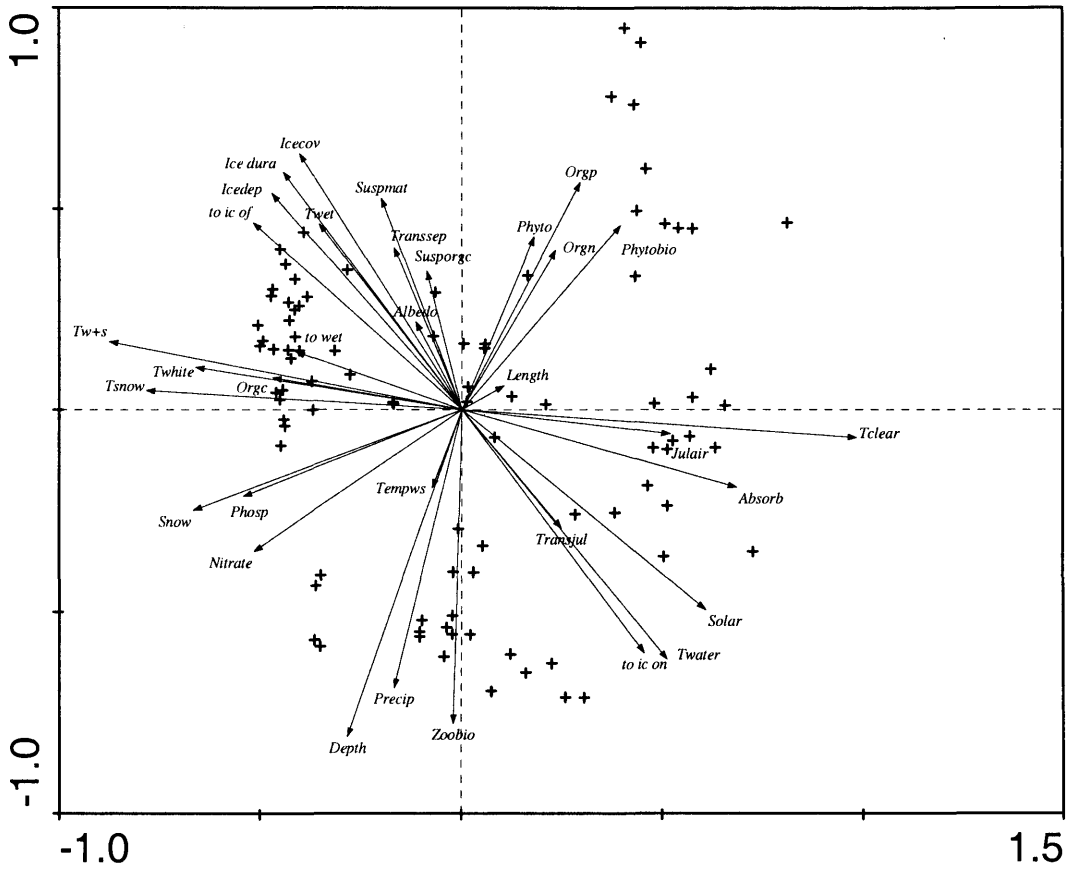

Figure 5.8: PCA biplot of the 33 explanatory variables and 92 sampling locations. See table 5.9 for an explanation of the codes used.

	Depth	Length	Solar	Absorb	Albedo	Tempws	Julair	Precip	Snow	Transjul	Transep	Nitrate	Phosp	Suspmat	Susporgc	Orgc	Orgn	Orgp	Phyto	Phytobi	Zoobio	Icedep	Icecov	Twater	Twhite	Tclear	Tsnow	Twet	Ice dura	to wet	to ic of	to ic on
Depth	1.0000																															
Length	-0.0683	1.0000																														
Solar	0.1204	-0.0276	1.0000																													
Absorb	-0.1125	0.2233	0.7894	1.0000																												
Albedo	-0.1873	-0.2212	-0.0722	-0.2072	1.0000																											
Tempws	0.0022	-0.2087	0.1971	-0.1018	0.2568	1.0000																										
Julair	-0.0669	0.0960	0.4256	0.4280	0.0013	0.2916	1.0000																									
Precip	0.4698	-0.2698	0.3317	-0.0371	0.0936	0.3694	0.0652	1.0000																								
Snow	0.3193	-0.3482	-0.4072	-0.7593	0.2332	0.3436	-0.4553	0.4831	1.0000																							
Transjul	0.0805	0.4648	0.2580	0.4393	-0.6523	-0.2977	-0.0090	-0.0852	-0.3054	1.0000																						
Transsep	-0.2117	0.1913	-0.3719	-0.1271	-0.1190	-0.4064	-0.2256	-0.3809	-0.2258	0.0308	1.0000																					
Nitrate	0.4180	-0.0206	-0.2954	-0.3938	-0.1193	-0.2531	-0.5331	0.3383	0.5352	0.0606	0.1578	1.0000																				
Phosp	0.3637	-0.2584	-0.4285	-0.6300	0.1898	0.1772	-0.4210	0.2200	0.7192	-0.2934	-0.1672	0.4495	1.0000																			
Suspmat	-0.3340	-0.2934	-0.3126	-0.3427	0.4621	-0.0770	-0.1384	-0.1535	0.1637	-0.6197	-0.0593	-0.1140	-0.0076	1.0000																		
Susporgc	-0.2459	-0.3274	-0.1610	-0.2104	0.1602	0.2431	0.0304	-0.0744	0.1171	-0.5099	-0.1753	-0.1166	0.1425	0.4513	1.0000																	
Orgc	0.1216	-0.1742	-0.5261	-0.5819	-0.1062	0.2550	-0.3412	-0.0594	0.5576	-0.1342	0.0769	0.1544	0.5698	0.0353	0.1870	1.0000																
Orgn	-0.1481	-0.0344	-0.0566	-0.0102	0.3254	0.0172	0.3814	-0.2983	-0.2569	-0.4532	-0.0448	-0.4842	-0.2274	0.4568	0.2617	-0.0219	1.0000															
Orgp	-0.4822	0.0548	0.0014	0.0899	0.3477	0.0108	0.3333	-0.4174	-0.3832	-0.3356	-0.0437	-0.6217	-0.2667	0.2822	0.3269	-0.2321	0.6130	1.0000														
Phyto	-0.3204	0.3484	-0.1567	0.0851	-0.0283	-0.2087	0.3504	-0.4104	-0.5172	-0.0051	0.5052	-0.3071	-0.5255	0.0038	-0.1103	-0.3153	0.3382	0.3803	1.0000													
Phytobio	-0.2641	-0.2382	0.0352	0.0897	0.2577	-0.0646	0.2463	-0.2484	-0.2414	-0.4382	-0.0719	-0.4496	-0.1929	0.4409	0.4472	-0.0743	0.6625	0.5553	0.0934	1.0000												
Zoobio	0.4726	-0.0823	0.4967	0.1797	-0.0407	0.3471	0.0345	0.7049	0.3079	0.1561	-0.3751	0.1990	0.1308	-0.3873	-0.1970	-0.1302	-0.3448	-0.3629	-0.3251	-0.3357	1.0000											
Icedep	-0.1292	0.0611	-0.7773	-0.5552	0.1474	-0.2133	-0.4428	-0.4813	0.1947	-0.3225	0.3466	0.1638	0.3612	0.4068	0.2987	0.4491	0.2434	0.1181	0.0992	0.1549	-0.5606	1.0000										
Icecov	-0.2868	0.0900	-0.7702	-0.5744	0.2741	-0.1783	-0.4182	-0.5499	0.1510	-0.3540	0.3786	0.0015	0.2610	0.3898	0.1674	0.3077	0.2872	0.3416	0.2982	0.1082	-0.5160	0.8149	1.0000									
Twater	0.2099	-0.0807	0.7707	0.5906	-0.1675	0.2555	0.4368	0.5395	-0.1592	0.2491	-0.5190	-0.0973	-0.2412	-0.3116	-0.0350	-0.3618	-0.1458	-0.2090	-0.2747	0.0017	0.5561	-0.6987	-0.8330	1.0000								
Twhite	0.0741	-0.0725	-0.3892	-0.4226	0.1002	0.1087	-0.2445	0.1205	0.4101	-0.1707	0.0767	0.1814	0.2718	0.1995	0.0955	0.3712	-0.1358	-0.1326	-0.1150	-0.2427	0.0080	0.2640	0.2179	-0.3983	1.0000							
Tclear	-0.2170	0.1249	0.5944	0.6383	-0.1309	-0.0546	0.4923	-0.1297	-0.6164	0.2652	-0.1735	-0.4622	-0.4780	-0.2428	-0.1321	-0.4419	0.1722	0.2278	0.1741	0.3102	0.0401	-0.4835	-0.3981	0.4935	-0.6169	1.0000						
Tsnow	0.1271	-0.0652	-0.4540	-0.5598	0.1941	0.1996	-0.3894	0.1138	0.4608	-0.3236	0.1456	0.2953	0.4240	0.2380	0.1497	0.2652	-0.2242	-0.1692	0.0079	-0.3433	0.0380	0.3462	0.3830	-0.4274	0.3851	-0.7328	1.0000					
Twet	-0.2005	0.3040	-0.5212	-0.2310	-0.0223	-0.3516	-0.2890	-0.5534	-0.1193	0.0961	0.4799	0.0809	-0.0451	0.0435	-0.1470	0.1494	0.0466	0.1621	0.3482	-0.2169	-0.4811	0.4434	0.5736	-0.7981	0.2940	-0.3477	0.2581	1.0000				
Ice dura	-0.1810	0.1693	-0.7790	-0.5679	0.1079	-0.3334	-0.3834	-0.5736	0.0747	-0.1846	0.5390	0.0975	0.1804	0.2454	-0.0430	0.2907	0.1602	0.2200	0.3743	-0.0195	-0.5610	0.6734	0.8328	-0.9668	0.3226	-0.4114	0.3973	0.8055	1.0000			
to wet	0.1208	-0.3198	-0.4518	-0.5881	0.4672	0.0738	-0.3837	0.0435	0.4939	-0.5366	0.1052	0.1684	0.5442	0.3344	0.0484	0.2469	0.0151	0.0545	-0.1220	0.1441	-0.0906	0.4266	0.5309	-0.5064	0.2100	-0.3661	0.4468	0.0324	0.4568	1.0000		
to ic of	-0.1109	0.0932	-0.6823	-0.5102	0.1753	-0.2673	-0.4451	-0.4805	0.1276	-0.1649	0.5144	0.1460	0.2254	0.1958	-0.0946	0.3020	0.0399	0.1448	0.2500	-0.1424	-0.4800	0.6153	0.7518	-0.9329	0.3691	-0.4899	0.4583	0.8588	0.9189	0.4644	1.0000	
to ic on	0.1834	-0.1233	0.7900	0.6302	-0.0631	0.2253	0.3667	0.4685	-0.2231	0.2486	-0.4313	-0.1427	-0.2595	-0.3039	-0.1631	-0.3805	-0.1820	-0.1375	-0.2742	-0.0970	0.4586	-0.7255	-0.7904	0.8402	-0.3512	0.4270	-0.3325	-0.5255	-0.8343	-0.4448	-0.6527	1.0000
Tw+s	0.0660	-0.0974	-0.5609	-0.6247	0.1868	0.1113	-0.4245	0.1002	0.5397	-0.3061	0.1778	0.2856	0.3827	0.3450	0.1420	0.4061	-0.1699	-0.1600	-0.0576	-0.3075	-0.0191	0.4061	0.4111	-0.5455	0.8469	-0.8322	0.7647	0.3453	0.4782	0.4153	0.5164	-0.4853

Table 5.11: Correlation matrix for the 33 explanatory variables.

5.7.3 Variance partitioning of environmental data

In order to assess the explanatory power of the groups of predictors shown in table 5.9 (climate, limnology, chemistry and biology), it is possible to use a series of constrained ordinations to estimate the amount of variance explained by each group (Lotter *et al.* 1997a). This variance partitioning approach allowed the dataset to be split into fractions signifying the unique contribution of each group to the variance of the species data, and the marginal effects of covariance between groups. Analysis was carried out in CANOCO using redundancy analysis (RDA) due to the short gradient of the data-set. Unique effects for a group of variables were estimated using the group as the sole predictor variables and all others as covariables in the RDA. Marginal effects were estimated by using the group as the sole predictors while excluding all other variables. Total explained variance was given by using all variables as predictors with no covariables. The significance of these groups was assessed using Monte Carlo tests with 499 unrestricted permutations. Results are shown in table 5.12 and show that the climatic variables are the most important in explaining the variance of the surface sediment species data. The unique effect of the climate variables is 7.5%, the other groups being much lower. The covariance of climate is also high at 30.8%. This indicates that of the measured variables, climatic factors are most important in explaining variance of the diatom data.

Variable group	Unique	Marginal
Climate	7.5	30.8
Limnology	3.7	14.9
Chemistry	1.5*	26.6
Biology	2.0	13.2
Total unique effects	14.7	
Total explained variance	73.6	
Sum of covariance terms	58.9	
Unexplained variance	26.4	

Table 5.12: Summary of variance partitioning of the four main groups of environmental variables showing marginal and unique effects as percentage of variance explained. The asterisk indicates results are not statistically significant at a 95% limit.

5.7.4 Explanatory power of environmental variables

The most suitable variables for reconstruction selected by Mackay *et al.* (2003) were chosen by CCA with forward selection, then an assessment of the $\lambda 1/\lambda 2$ value with the variable in question as the sole predictor. In this study, it was decided that a CCA would not be very informative due to the fact that several of the new and existing environmental variables are highly related. When performing CCA, it is necessary to remove variables showing high colinearity in order not to destabilise the dataset. The level of a variable's linear relationship to others is shown by it's variance inflation factors (VIF) being >20 (ter Braak and Šmilauer 1998). In this case, as several variables are highly related (shown by the PCA plot figure 5.8) it is difficult to decide which variables to delete to bring all VIFs below 20. Ultimately, this choice can be subjective in that a variable that is deemed important in spite of a high VIF can remain in the dataset, while others that are related (also with high VIFs) are deleted to bring the VIFs of remaining variables below 20 (Birks pers. comm.).

With the current dataset, a more objective approach to assess the explanatory power of individual environmental variables and to identify which will produce the most robust reconstructions is used. This involves skipping the CCA forward selection stage and using the $\lambda 1/\lambda 2$ value and percentage variance explained alone as given by a DCCA with the environmental variable of interest as the sole predictor. A series of DCCAs were done with each variable in turn as the only constraining variable. This allows the percentage of variance in the biological data explained by individual variables and their gradient lengths, to be calculated (Lotter *et al.* 1997). The significance of this relationship was tested using a Monte Carlo permutation test with 999 unrestricted permutations. The explanatory power of each variable is shown in tables 5.13, 5.14 and 5.15 for the full, five corrected species and planktonic training sets respectively. The suitability of an environmental variable for an inference model can be assessed by calculating the ratio of variance explained by the variable of interest and that of the whole data set (ter Braak 1987, Hall and Smol 1992). This can be achieved by dividing the eigenvalue of axis 1 by that of axis 2. High ratios (>1.0) mean a variable is suitable for an inference model (ter Braak and Prentice 1988), however much lower ratios have been used in the creation of transfer functions. Dixit *et al.* (1991) state the ratio should be >0.50, while Dixit *et al.* (1993) produced a DOC reconstruction with a ratio of 0.21 and Fritz *et al.* (1993) use a ratio of 0.28 for secchi depth reconstruction. Low ratios usually result in larger reconstruction errors. Eigenvalues 1 over 2 values are given in tables 5.13 to 5.15.

Variable	Axis 1 length	λ 1	λ 2	λ1/λ2	% variance	p-value
Snow	1.015	0.208	0.355	0.586	11.2	0.001
Tclear	1.042	0.193	0.358	0.539	10.3	0.001
Twhite	1.649	0.183	0.353	0.518	9.8	0.001
Tw+s	1.437	0.177	0.334	0.530	9.5	0.001
Nitrate	1.274	0.168	0.310	0.542	9.0	0.001
Absorb	0.763	0.166	0.368	0.451	8.9	0.001
Depth	1.488	0.156	0.328	0.476	8.4	0.001
Precip	1.473	0.140	0.343	0.408	7.5	0.001
Solar	1.073	0.136	0.350	0.389	7.3	0.001
Orgc	1.046	0.126	0.362	0.348	6.7	0.001
Twater	1.007	0.124	0.291	0.426	6.6	0.001
Ice dura	0.991	0.124	0.281	0.441	6.6	0.001
Phosp	0.830	0.121	0.328	0.369	6.5	0.001
Zoobio	0.785	0.121	0.378	0.320	6.5	0.001
to ic of	0.947	0.119	0.354	0.336	6.4	0.001
Phyto	1.073	0.117	0.352	0.332	6.3	0.001
Orgp	1.136	0.109	0.342	0.319	5.8	0.001
Tsnow	1.365	0.107	0.323	0.331	5.7	0.001
Julair	0.982	0.102	0.355	0.287	5.5	0.001
Twet	1.209	0.103	0.354	0.291	5.5	0.001
to ic on	0.927	0.092	0.352	0.261	4.9	0.001
Icedep	1.113	0.080	0.357	0.224	4.3	0.001
Icecov	0.893	0.075	0.319	0.235	4.0	0.002
Orgn	0.996	0.073	0.377	0.194	3.9	0.001
Suspmat	1.177	0.070	0.372	0.188	3.8	0.002
Phytobio	0.717	0.070	0.329	0.213	3.7	0.001
Susporgc	0.955	0.067	0.390	0.172	3.6	0.011
Transjul	0.867	0.064	0.370	0.173	3.4	0.009
Transsep	0.962	0.063	0.379	0.166	3.4	0.002
to wet	0.874	0.048	0.376	0.128	2.6	0.033
Length	0.881	0.044	0.319	0.138	2.4	0.026
Tempws	0.822	0.045	0.370	0.122	2.4	0.041
Albedo	0.546	0.035	0.401	0.087	1.9	0.127

Table 5.13: DCCA of full training set with each explanatory variable the sole predictor in turn. Axis 1 and 2 eigenvalues and λ1/λ2 ratio, percentage of total variance explained and p-value from Monte Carlo permutation test (n = 999). Ordered by percentage of variance explained.

	Axis 1 length	λ 1	λ 2	λ1/λ2	% variance	p-value
Snow	1.135	0.287	0.247	1.162	29.8	0.001
Absorb	0.843	0.245	0.374	0.655	25.4	0.001
Phosp	1.022	0.218	0.294	0.741	22.7	0.001
Tclear	1.012	0.207	0.361	0.573	21.6	0.002
Orgc	1.135	0.175	0.344	0.509	18.2	0.001
Nitrate	1.212	0.167	0.308	0.542	17.4	0.001
Solar	1.008	0.158	0.297	0.532	16.4	0.001
Phyto	1.074	0.146	0.281	0.520	15.1	0.001
Tw+s	1.310	0.142	0.359	0.396	14.8	0.001
Depth	1.076	0.133	0.295	0.451	13.9	0.001
Precip	1.250	0.128	0.353	0.363	13.3	0.001
Julair	1.039	0.125	0.409	0.306	13.0	0.001
to ic on	0.956	0.116	0.388	0.299	12.1	0.001
Twater	0.898	0.113	0.279	0.405	11.7	0.001
Ice dura	0.905	0.110	0.295	0.373	11.4	0.002
Tsnow	1.362	0.108	0.338	0.320	11.2	0.001
Zoobio	0.651	0.105	0.493	0.213	11.0	0.001
Icedep	1.204	0.105	0.341	0.308	10.9	0.001
Orgp	0.909	0.095	0.393	0.242	9.8	0.001
to ic of	0.771	0.093	0.400	0.233	9.7	0.002
to wet	1.017	0.092	0.420	0.219	9.6	0.001
Twet	1.012	0.078	0.420	0.186	8.1	0.002
Length	1.018	0.071	0.307	0.231	7.4	0.002
Icecov	0.800	0.071	0.358	0.198	7.4	0.001
Twhite	0.064	0.064	0.422	0.152	6.6	0.002
Transjul	0.703	0.051	0.397	0.128	5.3	0.001
Transsep	0.769	0.042	0.480	0.088	4.4	0.014
Orgn	0.760	0.042	0.494	0.085	4.4	0.011
Suspmat	0.625	0.025	0.482	0.052	2.6	0.069
Phytobio	0.433	0.024	0.424	0.057	2.4	0.082
Albedo	0.351	0.012	0.512	0.023	1.3	0.330
Susporgc	0.390	0.012	0.456	0.026	1.2	0.317
Tempws	0.363	0.008	0.462	0.017	0.8	0.501

Table 5.14: DCCA of 5 corrected species training set with each explanatory variable the sole predictor in turn. Axis 1 and 2 eigenvalues and λ1/λ2 ratio, percentage of total variance explained and p-value from Monte Carlo permutation test (n = 999). Ordered by percentage of variance explained.

Variable	Axis 1 length	λ 1	λ 2	λ1/λ2	% variance	p-value
Snow	1.013	0.213	0.357	0.597	14.2	0.001
Tclear	1.040	0.199	0.357	0.557	13.2	0.001
Twhite	1.620	0.185	0.357	0.518	12.3	0.001
Tw+s	1.430	0.180	0.332	0.542	12.0	0.001
Absorb	0.772	0.172	0.366	0.470	11.4	0.001
Nitrate	1.248	0.169	0.310	0.545	11.3	0.001
Depth	1.323	0.137	0.329	0.416	9.1	0.001
Precip	1.408	0.135	0.347	0.389	9.0	0.001
Solar	1.057	0.134	0.351	0.382	8.9	0.001
Orgc	1.046	0.130	0.364	0.357	8.6	0.001
Phosp	0.836	0.128	0.325	0.394	8.5	0.001
Ice dura	0.947	0.120	0.286	0.420	8.0	0.001
Twater	0.973	0.119	0.295	0.403	7.9	0.001
to ic of	0.909	0.117	0.357	0.328	7.8	0.001
Phyto	1.032	0.115	0.354	0.325	7.7	0.001
Zoobio	0.732	0.111	0.384	0.289	7.4	0.001
Tsnow	1.354	0.110	0.323	0.341	7.3	0.001
Orgp	1.080	0.197	0.345	0.571	7.1	0.001
Twet	1.152	0.100	0.358	0.279	6.7	0.001
Julair	0.961	0.100	0.356	0.281	6.6	0.001
to ic on	0.910	0.088	0.357	0.246	5.8	0.001
Icedep	1.082	0.077	0.358	0.215	5.1	0.002
Orgn	0.926	0.069	0.385	0.179	4.6	0.002
Icecov	0.840	0.069	0.322	0.214	4.6	0.002
Phytobio	0.657	0.065	0.329	0.198	4.4	0.002
Transsep	0.893	0.059	0.382	0.154	3.9	0.003
Transjul	0.778	0.055	0.371	0.148	3.7	0.011
Susporgc	0.751	0.053	0.391	0.136	3.6	0.028
Suspmat	0.951	0.051	0.379	0.135	3.4	0.009
to wet	0.837	0.047	0.375	0.125	3.1	0.019
Tempws	0.766	0.041	0.370	0.111	2.7	0.034
Length	0.787	0.039	0.321	0.121	2.6	0.037
Albedo	0.425	0.025	0.405	0.062	1.7	0.158

Table 5.15: DCCA of planktonic training set with each explanatory variable the sole predictor in turn. Axis 1 and 2 eigenvalues and λ1/λ2 ratio, percentage of total variance explained and p-value from Monte Carlo permutation test (n = 999). Ordered by percentage of variance explained.

Snow depth individually explains the most variance in all training sets: full (11.2%), 5 corrected species (29.8%) and planktonic (14.2%). In all three cases, snow depth has the highest $\lambda 1/\lambda 2$ ratio which means the addition of remotely sensed variables has not improved the data taken from the Atlas Baikala (1993). However, some of the new variables do have high $\lambda 1/\lambda 2$ ratios and quantitative reconstructions may be possible from total days of clear ice (all sets) and total days of white ice/snow coverage (full and planktonic sets). Possible variables for reconstructions are shown in table 5.16, using values of $\lambda 1/\lambda 2 \geq 0.50$ as a cut-off point (*c.f.* Dixit *et al.* 1991, Mackay *et al.* 2003). As light penetration through ice has been shown to be important, this study attempts to reconstruct snow depth, clear ice duration and white ice/snow duration. White ice and snow cover duration has been chosen over white ice duration, as white ice duration alone may underestimate the obstructed/opaque period duration by ignoring snow cover. However, this variable will be very similar to clear ice cover duration as they are dependant on each other, that is with longer white ice/snow cover, clear ice cover duration may also be shorter. However as there are other ice types and different length open water periods recorded at each site (table 5.8), the clear ice duration will not be the residual of white ice/snow duration. Nitrate as an explanatory variable also appears with a $\lambda 1/\lambda 2$ ratio ≥ 0.50 in each of the training sets, however it was decided not to reconstruct this variable as, according to the PCA of environmental variables (figure 5.8), nitrate is correlated to snow depth (a coefficient of 0.5352, table 5.11). Therefore the reconstruction will be very similar to that inferred for snow depth.

Full species set	Five corrected species	Planktonic species
Snow	Snow	Snow
Tclear	Absorb	Tclear
Twhite	Phosp	Twhite
Tw+s	Tclear	Tw+s
Nitrate	Orgc	Nitrate
	Nitrate	
	Solar	
	Phyto	

Table 5.16: Explanatory variables with $\lambda 1/\lambda 2$ ratio ≥ 0.50 in the three training sets (in rank order).

5.7.5 Inference models

5.7.5.1 Statistical methods

As explained in section 5.7.1, unimodal methods (weighted averaging (WA)) of transfer development will be used rather than linear methods, such as partial least squares (PLS). WA methods derive optima for individual species responses to an environmental variable. In theory, for sites with a particular value for the environmental variable, the taxa with optima nearest to this value will be the most abundant taxa present. The optimum for a taxon can be estimated as a simple average of all the values of the environmental variable at sites in which the taxon occurs, weighted relative to its abundance at each site (ter Braak 1987). In addition, a taxon's tolerance can be estimated as the weighted standard deviation of the value of the environmental variable at each site relative to species abundance. A reconstructed estimate of a site's value for an environmental variable of interest is a weighted average of the optima for all the taxa present in the palaeo-record. Simple WA can be enhanced with the inclusion of tolerance down-weighting ($WA_{(tol)}$). This is useful as species with narrow tolerances will be better environmental indicators and hence can be given greater influence in the calibration (Birks *et al.* 1990). However, a problem with these methods is that the average is taken twice: once at the regression stage and a second during calibration. As a result the range of inferred values is reduced. To remove this effect, a 'deshrinking' step is included that adjusts the values by a simple linear regression. This can be done in two ways, firstly by classical regression. Initial inferred values are regressed onto observed values to remove the truncation in these observed values (ter Braak 1988, Birks *et al.* 1990). Secondly, the inverse regression approach regresses the observed values onto the initial inferred values for the environmental variable. The choice of deshrinking methods depends on whether greatest accuracy is required at high or low values of the environmental variable (classical) or if the emphasis is on the mid-range (inverse) (Gasse *et al.* 1995). This gives four versions of simple WA: WA-Inv (with inverse deshrinking), WA-Cla (with classical deshrinking), $WA_{(tol)}$-Inv (tolerance downweighted with inverse deshrinking) and $WA_{(tol)}$-Cla (tolerance downweighted with classical deshrinking).

In addition, a fifth WA method is weighted averaging partial least squares (WA-PLS). This method was developed to take into account residual correlations between environmental variables that are ignored by WA (ter Braak and Juggins 1993). This information in the residuals is used to provide better fit and estimated optima. WA-PLS was developed from the linear technique of PLS and is similar to PCA. However, the addition of the WA component allows for a gaussian species response. The WA-PLS involves a series of regressions and

component extractions from the model. After each extraction, model error becomes less but the model becomes less parsimonious. As in PCA, linear combinations of variables with maximum variance are extracted. In PLS the first component is extracted to maximise the covariance between this extracted linear combination and the environmental variable. Subsequent components are extracted to the same criteria but have to be uncorrelated to earlier components (ter Braak *et al.* 1993). Full formulae for WA-PLS can be found in ter Braak *et al.* (1993) while other WA algorithms can be found in Birks *et al.* (1990).

Estimation of errors in the predictive ability of models was estimated using bootstrapping, a more rigorous test than simple leave-one-out validation methods such as jack-knifing. Bootstrapping involves the creation of an independent test set from the full data set. Samples for model formation are selected at random with replacement, such that samples not selected form a validation set. The model is run on this new test set and errors estimated with comparison to the validation set. This procedure is repeated for a number of cycles, usually 999 or more. Averaging the results of these cycles gives estimates of the r^2 fit of the model and the RMSEP (root mean square error of prediction). The RMSEP is a combination of the error due to variability in estimating species parameters in the training set, and the error (bias) due to variation in species abundance at a given environmental value (RMSEP is the root of: SE of bootstrap estimates plus error between observed values and bootstrap estimates) (Birks *et al.* 1990). The number of WA-PLS components to use in a model is decided by those that give the lowest RMSEP and highest r^2 after bootstrapping. However, to fit with the principle of parsimony, if there is only a slight gain in model performance is gained with the inclusion of another component (i.e. less than a 5% improvement), it is always better not to use an additional component and select the minimum adequate model (Birks 1998). The five weighted averaging methods and bootstrapping were run on the software C2 v1.3 (Juggins 2003). The five WA methods were compared to see which performed best and the method that performed the best was used to develop the inference model. It is good practice to compare several inference models for the same data (Birks 1995).

5.7.5.2 Weighted averaging method selection

The comparative performance (r^2_{boot} and RMSEP) of models reconstructing snow depth, duration of clear ice cover and duration of white ice/snow cover using the full, five corrected species and planktonic training set are given in table 5.17. The method that performed the best was chosen as that which had the highest r^2_{boot} and lowest RMSEP, these are identified in bold type. $WA_{(tol)}$-Inv is used to reconstruct snow depth on ice for all training sets while WA-PLS is used to reconstruct both white ice/snow and clear ice cover duration for all training sets.

	Snow, Full		Snow, 5 species		Snow, Planktonic		Tclear, Full	
	r^2_{boot}	RMSEP	r^2_{boot}	RMSEP	r^2_{boot}	RMSEP	r^2_{boot}	RMSEP
WA-Inv	0.4743	0.1634	0.5386	0.1513	0.4927	0.1604	0.4813	0.5137
WA-Cla	0.4850	0.2043	0.5494	0.2029	0.5039	0.2093	0.4918	0.6253
$WA_{(tol)}$-Inv	**0.4958**	**0.1684**	**0.5517**	**0.1494**	**0.5464**	**0.1523**	0.4575	0.5579
$WA_{(tol)}$-Cla	0.5027	0.1923	0.5628	0.1976	0.5541	0.1851	0.4666	0.6593
WA-PLS	0.4792	0.1708	0.5379	0.1528	0.5492	0.1674	**0.4898**	**0.5225**
(Components)	2		2		3		2	
	Tclear, 5 species		Tclear, Planktonic		Tw+s, Full		Tw+s, Planktonic	
	r^2_{boot}	RMSEP	r^2_{boot}	RMSEP	r^2_{boot}	RMSEP	r^2_{boot}	RMSEP
WA-Inv	0.4144	0.5378	0.4940	0.5066	0.4074	0.1492	0.4026	0.1496
WA-Cla	0.4330	0.8006	0.5057	0.6434	0.4226	0.1829	0.4190	0.1893
$WA_{(tol)}$-Inv	0.4241	0.5334	0.4780	0.5251	0.3058	0.1757	0.3747	0.1543
$WA_{(tol)}$-Cla	0.4427	0.7856	0.4901	0.6595	0.3164	0.2392	0.3882	0.1881
WA-PLS	**0.4650**	**0.5189**	**0.5101**	**0.5074**	**0.4076**	**0.1543**	**0.4112**	**0.1511**
(Components)	3		2		2		2	

Table 5.17: Comparative performance (r^2_{boot} and RMSEP) for the five WA methods for each reconstructed variable (Snow depth: Snow, Clear ice duration: Tclear and white ice/snow duration: Tw+s) for the three training sets: full, planktonic and 5 corrected species. The number of components used in the WA-PLS models are given. The model selected for the development of the final inference model is highlighted in bold type.

5.7.5.3 Outlier detection

Figures 5.9 to 5.11 show graphs of observed values of environmental variables (snow depth, clear ice duration and white ice/snow duration respectively) plotted against bootstrap estimates, and graphs of observed values plotted against residuals (observed minus predicted). A LOWESS smooth line is also applied to residual plots to illustrate under which observed values most bias occurs. A LOWESS curve is a form of regression that fits a model to localised subsets of the data to build up a function that describes the full dataset. For a model with perfect predictive power, observed against predicted values should plot on the line y = x with residual 0 and no RMSEP, such relationships are never observed with ecological data, and r^2 values around 0.65 may be interpreted as robust models (Prairie 1996). Summary statistics of model performance are given in table 5.17. Potential outliers can be identified as those with a bootstrap residual greater than the standard deviation of the environmental parameter of interest (Jones and Juggins 1995). These are identified in the observed versus residual plots (figures 5.9 to 5.11) and named in table 5.18. Outlier deletion does considerably improve the predictive power of the models, but it is not easily justifiable to remove samples on the sole basis of lack of statistical fit rather than on ecological reasoning. Since 38 of the 92 samples appear as outliers in one or more of the models means it is very difficult to find an ecological justification for deletion of all of these species. However, outlier deletion has been

considered necessary in the development of transfer functions, particularly in paleoenvironmental reconstructions, as there will always be sites weakly related to the environmental variable of interest (Birks *et al.* 1990, Jones and Juggins 1995, Bennion *et al.* 1996). Figures 5.12 to 5.14 show the observed against predicted, and observed against residual plots for the three environmental variables of interest after outliers are removed and the models re-run.

5.7.5.4 Final model performance

Of all models run, both r^2_{boot} and RMSEP improved after outlier deletion (table 5.18). As found by Mackay *et al.* (in press), the model created from the five dominant species corrected for dissolution outperformed the full training set; (r^2_{boot} of 0.8178 compared to 0.7796). However the best performance for a model for predicting snow depth was by the planktonic training set under $WA_{(tol)}$-Inv, with an r^2_{boot} of 0.8642 and RMSEP of 0.0942 log cm (1.24 cm). This improved from 0.5464 and 0.1523 log cm (1.42 cm) respectively before outlier deletion. The plots of observed, expected and residual snow depths before outlier deletion (figure 5.9) show most bias at the extremes of the range of observed values, the maximum bias being 0.1801 log cm (1.51 cm) for the full training set. After outlier deletion, bias is high only when predicting at the deeper observed snow depths (figure 5.12). Maximum bias is similar for all snow depth models but highest for the planktonic model at 0.1245 log cm (1.33 cm).

The model performing best in the prediction of clear ice cover duration was WA-PLS using the five corrected species training set. r^2_{boot} is 0.7606 after outlier deletion (0.4650 before outlier removal), while RMSEP is 0.3417 log days (2.2 days), before outlier deletion this was 0.5189 log days (3.3 days). Both the full and planktonic training sets performed in a very similar manner, the full model performing slightly better with an r^2_{boot} of 0.7327 compared to 0.7290 (both after outlier deletion). Before outliers were deleted, figure 5.10 shows that most bias (overestimation) occurred when predicting clear ice cover at locations where no clear ice was actually observed, whilst duration was underestimated at locations with longer duration. After outlier deletion, for the five corrected species training set maximum bias is 0.3260 log days (2.12 days), maximum bias for the other two training sets is slightly lower here. Figure 5.13 shows that for all training sets after outlier deletion, the bias in prediction is relatively standard over the range of observed values.

A model based on white ice and snow duration could not be created for the 5 corrected species training set because of the low $\lambda 1/\lambda 2$ of this variable (table 5.14). For white ice/snow

duration, the best performance by WA-PLS was given by the planktonic training set over the full training set. r^2_{boot} for the planktonic set is 0.6207 and RMSEP is 0.0781 log days (1.20 days) after outliers are removed. This is compared to a r^2_{boot} of 0.5619 and RMSEP of 0.0790 log days (1.21 days). For both training sets, before outlier deletion there was most bias (overestimation) of white ice/snow cover duration at low observed values reaching up to 0.4753 log days (2.99 days) (figure 5.11). After outliers are removed, bias is still high at lower predicted values, but the maximum is much lower at 0.1893 log days (1.55 days) (figure 5.14).

Although statistically the snow cover model performs the best, this result may be spurious due to the categorical nature of the observed snow depth measurements. Results are clustered into six groups, and the regression techniques used in the development of inference models are not particularly robust in this situation. Although the models for clear ice and white ice/snow cover durations do not show such a good statistical fit, these models may be more applicable to palaeoclimatic reconstruction as they are based on a more continuous range of observed values. Possible improvements to the snow depth model are discussed in chapter 9.

In summary the models with the (statistically) best predictive power are: $WA_{(tol)}$-Inv and the planktonic training set for snow depth, WA-PLS and the five corrected species for annual clear ice cover duration and WA-PLS with the planktonic training set for annual white ice/snow cover duration. Although these models performed the best, all models listed in table 5.18 (after outlier deletion) will be used for reconstructions from the Holocene diatom data presented in chapter 6 to allow comparison of the methods used. The second part of this chapter will now summarise all autecological information available concerning the dominant diatoms found during the Holocene in Lake Baikal.

Training set	Model	Variable	Before deletions:		After deletions:		No. of	Comp.	Apparent r^2	RMSE	Bootstrapping validation with 1000 cycles			
			Samples	Taxa	Samples	Taxa	outliers				r^2	RMSEP	Max. bias	Ave. bias
Full	WA-$_{(tol)}$-Inv	Snow	92	86	N/A	N/A	N/A	N/A	0.6479	0.1307	0.4958	0.1684	0.1801	-0.0034
5 species	WA-$_{(tol)}$-Inv	Snow	92	5	N/A	N/A	N/A	N/A	0.5790	0.1429	0.5518	0.1494	0.1639	0.0015
Planktonic	WA-$_{(tol)}$-Inv	Snow	92	30	N/A	N/A	N/A	N/A	0.6344	0.1331	0.5464	0.1523	0.1710	0.0030
Full	WA-PLS	Tclear	92	86	N/A	N/A	N/A	2	0.6113	0.4327	0.4898	0.5225	0.4233	-0.0059
5 species	WA-PLS	Tclear	92	5	N/A	N/A	N/A	3	0.5133	0.4842	0.4650	0.5189	0.5874	-0.0002
Planktonic	WA-PLS	Tclear	92	30	N/A	N/A	N/A	2	0.5838	0.4478	0.5101	0.5074	0.4139	-0.0029
Full	WA-PLS	Tw+s	92	86	N/A	N/A	N/A	2	0.5965	0.1187	0.4076	0.1543	0.4660	0.0004
Planktonic	WA-PLS	Tw+s	92	30	N/A	N/A	N/A	2	0.5492	0.1255	0.4112	0.1511	0.4753	-0.0020
Full	WA-$_{(tol)}$-Inv	Snow	92	86	75	77	17	N/A	0.8532	0.0798	0.7796	0.1369	0.1160	0.0073
5 species	WA-$_{(tol)}$-Inv	Snow	92	5	80	5	12	N/A	0.8361	0.0866	0.8178	0.0935	0.1104	0.0000
Planktonic	WA-$_{(tol)}$-Inv	Snow	92	30	81	28	11	N/A	0.8642	0.0792	0.8642	0.0942	0.1245	0.0015
Full	WA-PLS	Tclear	92	86	77	83	15	2	0.8013	0.3041	0.7327	0.3707	0.1752	0.0013
5 species	WA-PLS	Tclear	92	5	78	5	14	2	0.7858	0.3130	0.7606	0.3417	0.3260	0.0000
Planktonic	WA-PLS	Tclear	92	30	80	30	12	2	0.7804	0.3213	0.7290	0.3730	0.2160	-0.0008
Full	WA-PLS	Tw+s	92	86	78	86	14	2	0.7260	0.0582	0.5619	0.0790	0.1893	0.0017
Planktonic	WA-PLS	Tw+s	92	30	79	30	10	2	0.6929	0.0644	0.6207	0.0781	0.1377	0.0018

Training set	Model	Variable	No. Outliers	Outliers deleted (sample names)
Full	WA-$_{(tol)}$-Inv	Snow	17	B17, B18, B19, B22, B24, B25, B27, B32, B38, B65, B69, B70, B112, B115, B126, B127, B143
5 species	WA-$_{(tol)}$-Inv	Snow	12	B17, B21, B22, B32, B38, B65, B69, B70, B112, B126, B127, B149
Planktonic	WA-$_{(tol)}$-Inv	Snow	11	B17, B24, B25, B32, B38, B65, B69, B70, B112, B126, B127
Full	WA-PLS	Tclear	15	B14, B15, B16, B24, B43, B58, B69, B72, B86, B112, B116, B118, B126, B131, B143
5 species	WA-PLS	Tclear	14	B15, B24, B43, B58, B72, B86, B94, B112, B116, B118, B125, B126, B131, B145
Planktonic	WA-PLS	Tclear	12	B14, B15, B16, B43, B58, B69, B72, B86, B116, B118, B126, B131
Full	WA-PLS	Tw+s	14	B14, B15, B16, B43, B47, B56, B57, B126, B136, B137, B145, B146, B147, B148
Planktonic	WA-PLS	Tw+s	13	B14, B15, B16, B43, B56, B57, B126, B136, B137, B142, B145, B146, B148

Table 5.18: Summary of WA model performance for reconstructed snow depth (snow), clear ice duration (Tclear) and white ice/snow duration (Tw+s) for the full, planktonic and 5 dissolution corrected species training sets. The upper table gives performance before outlier deletion, the middle after outlier deletion and the lower table details the samples selected as outliers in each individual model.

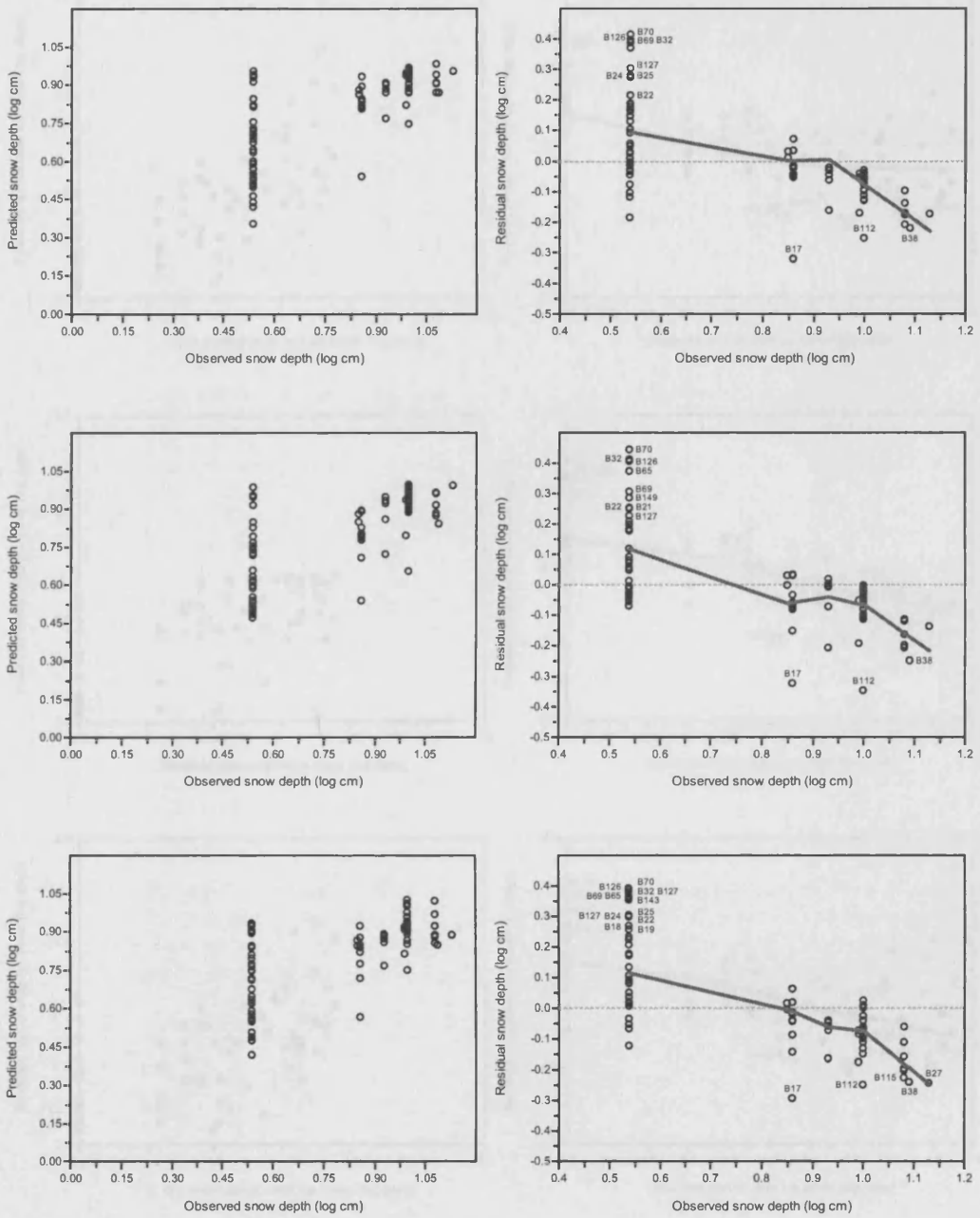

Figure 5.9: Scatterplots of observed snow depth against predicted snow depth (left column), and observed snow depth against residual snow depth with a LOWESS smooth line fitted and outliers identified (right column). All units are log cm. The top set of graphs are for the planktonic training set, middle are for the 5 corrected species training set and the bottom are the full training set.

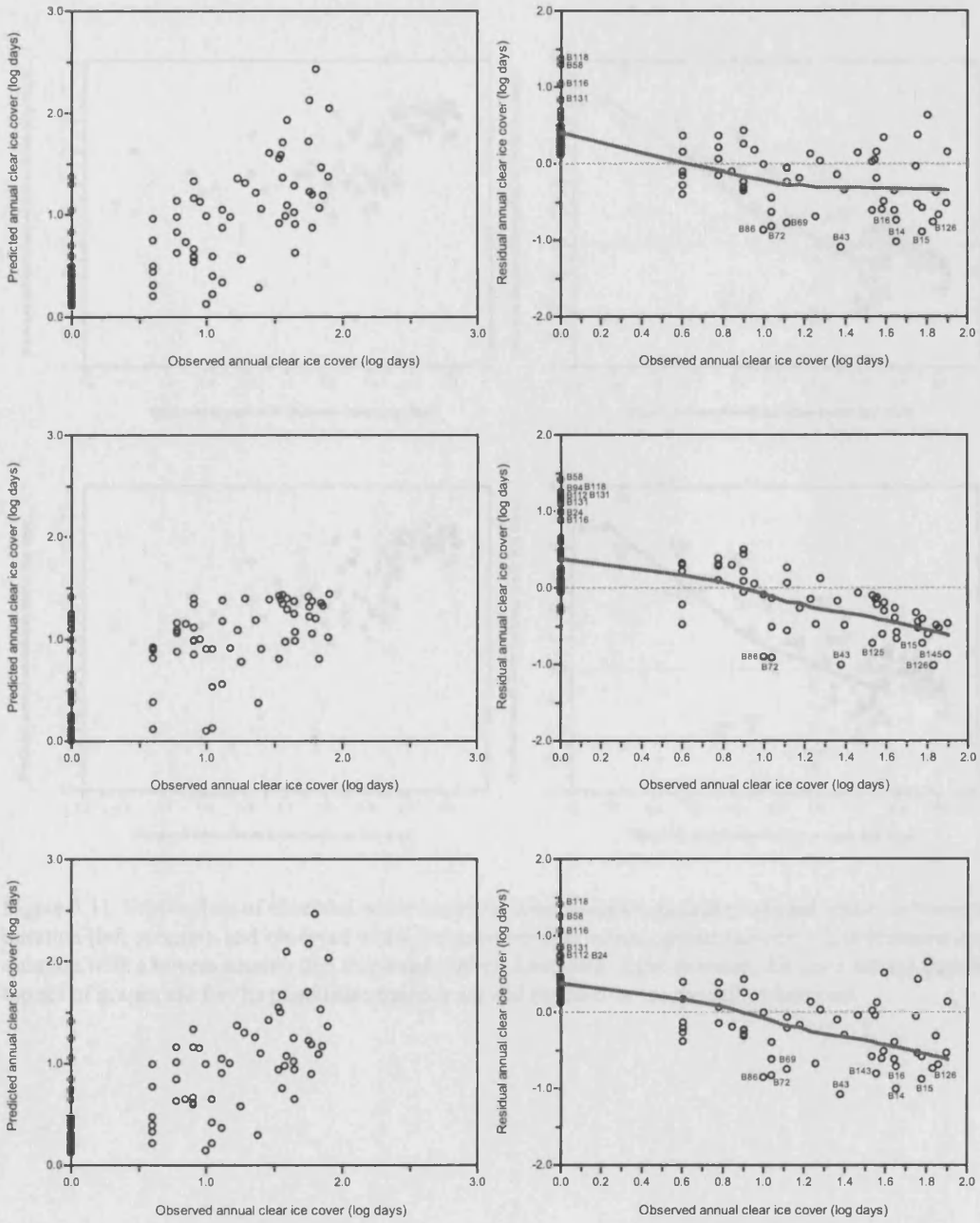

Figure 5.10: Scatterplots of observed clear ice cover duration against predicted clear ice cover duration (left column), and observed clear ice cover duration against residual clear ice cover duration with a LOWESS smooth line fitted and outliers identified (right column). All units are log days.The top set of graphs are for the planktonic training set, middle are for the 5 corrected species training set and the bottom are the full training set.

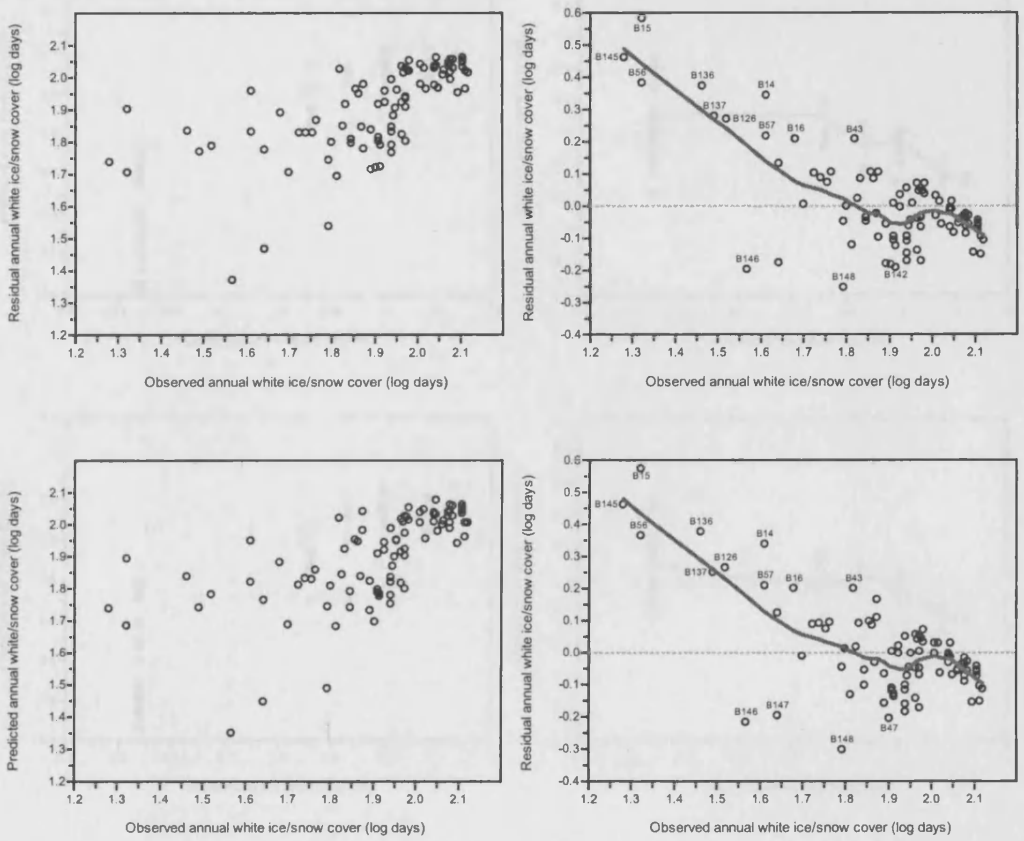

Figure 5.11: Scatterplots of observed white ice/snow cover duration against predicted white ice/snow cover duration (left column), and observed white ice/snow cover duration against residual white ice/snow cover duration with a lowess smooth line fitted and outliers identified (right column). All units are log days.The top set of graphs are for the planktonic training set and the bottom are the full training set.

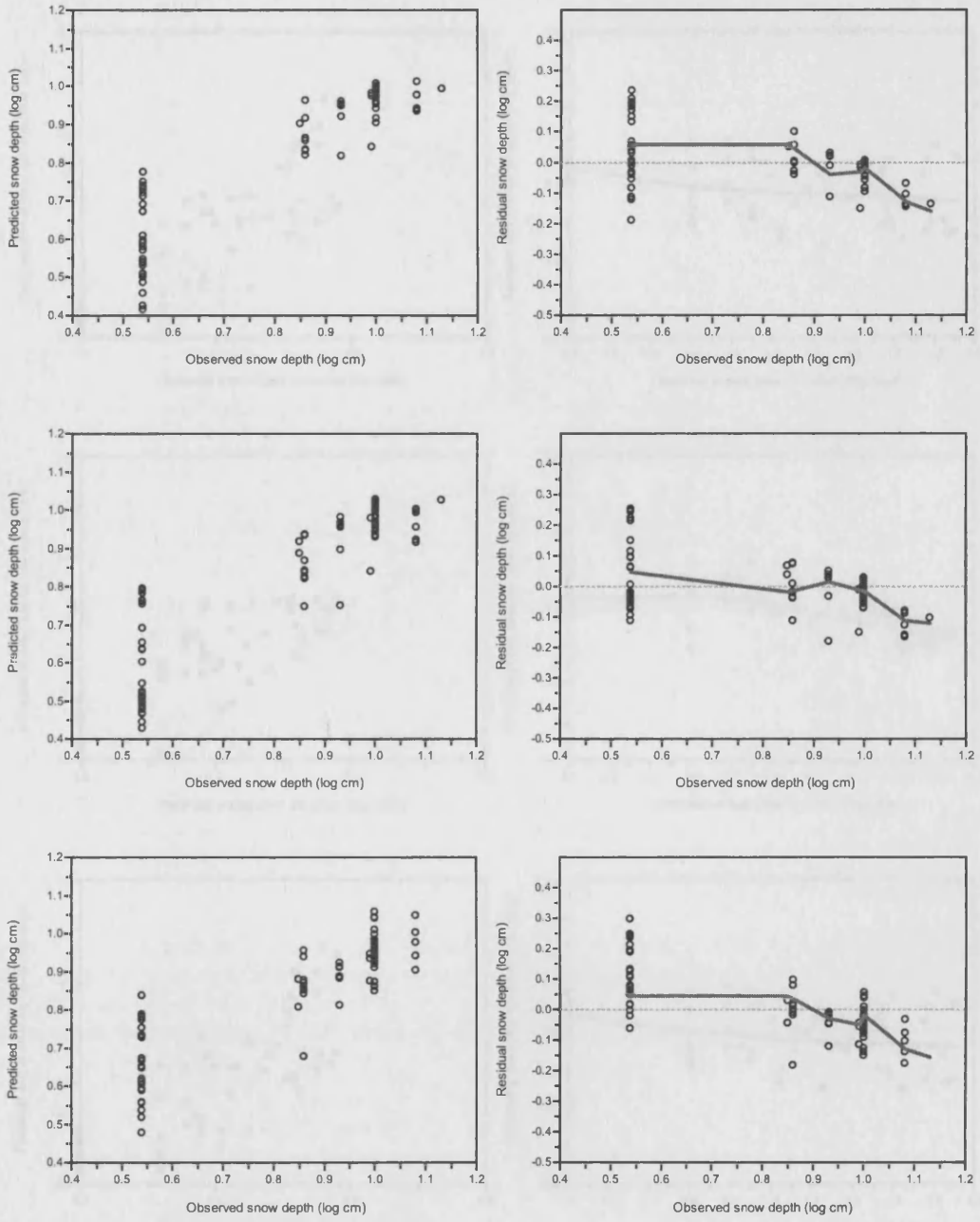

Figure 5.12: Scatterplots of observed snow depth against predicted snow depth (left column) and observed snow depth against residual snow depth with a LOWESS smooth line fitted (right column) after outlier deletion. All units are log cm. The top set of graphs are for the planktonic training set, middle are for the 5 corrected species training set and the bottom are the full training set.

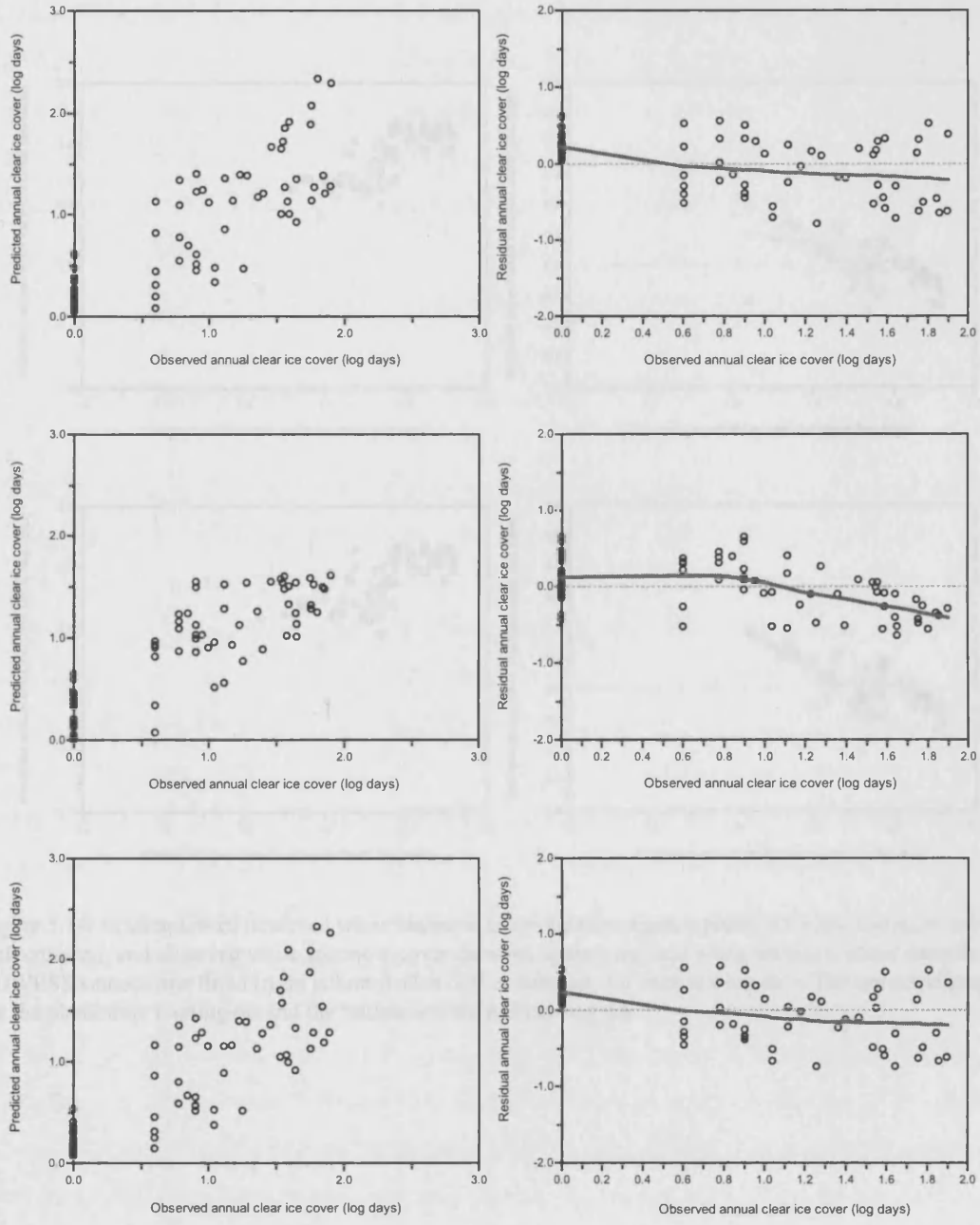

Figure 5.13: Scatterplots of observed clear ice cover duration against predicted clear ice cover duration (left column), and observed clear ice cover duration against residual clear ice cover duration with a LOWESS smooth line fitted (right column) after outlier deletion. All units are log days.The top set of graphs are for the planktonic training set, middle are for the 5 corrected species training set and the bottom are the full training set.

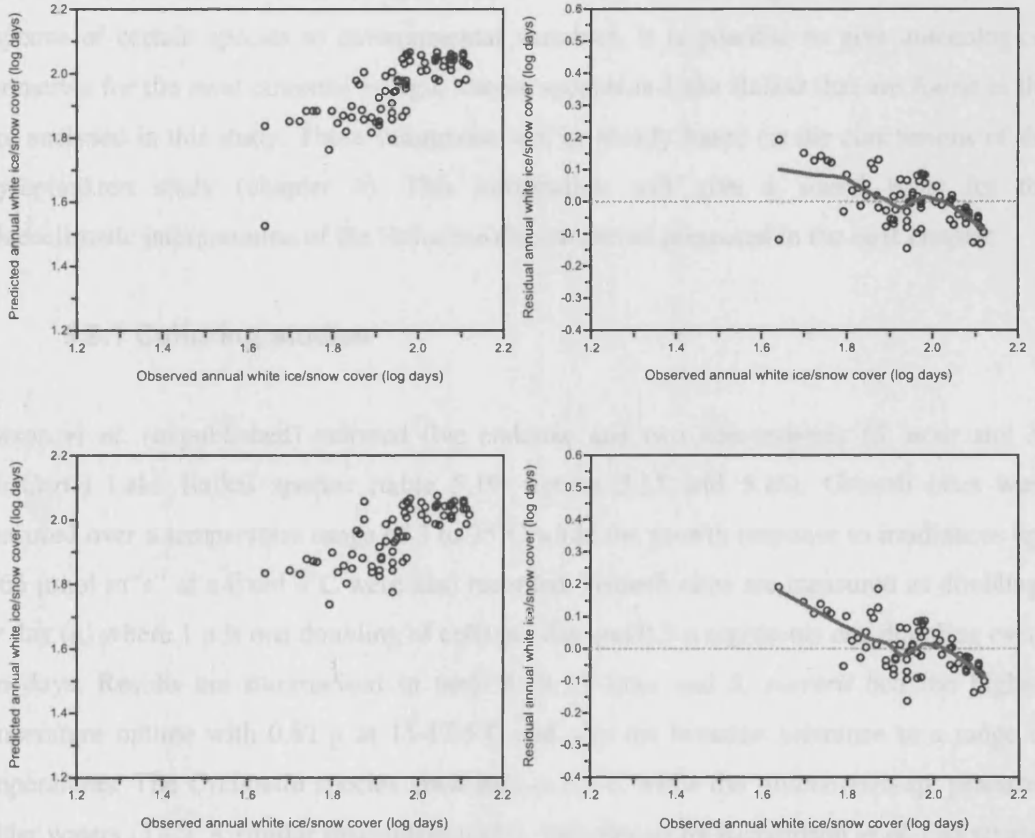

Figure 5.14: Scatterplots of observed white ice/snow cover duration against predicted white ice/snow cover duration (left column), and observed white ice/snow cover duration against residual white ice/snow cover duration with a LOWESS smooth line fitted (right column) after outlier deletion. All units are log days.The top set of graphs are for the planktonic training set and the bottom are the full training set.

5.8 Diatom autecological information

After presenting additional data from culturing studies of Lake Baikal pelagic diatoms, published literature concerning diatom distributions in relation to climatic factors and spatial distributions of diatoms in the surface sediments in the full training set and the individual response of certain species to environmental variables, it is possible to give autecological summaries for the most common pelagic diatom species in Lake Baikal that are found in the core analysed in this study. These summaries will be mostly based on the conclusions of the phytoplankton study (chapter 4). This information will give a sound basis for the palaeoclimatic interpretation of the Holocene diatom record presented in the next chapter.

5.8.1 Culturing studies

Jewson *et al.* (unpublished) cultured five endemic and two non-endemic (*S. acus* and *N. acicularis*) Lake Baikal species (table 5.19, figures 5.15 and 5.16). Growth rates were measured over a temperature range of 3 to 25°C while the growth response to irradiances ups to 65 μmol $m^{-2}s^{-1}$ at a fixed 4°C were also recorded. Growth rates are measured as doublings per day (μ) where 1 μ is one doubling of cells per day and 0.5 μ represents one doubling every two days. Results are summarised in table 5.19. *S. acus* and *S. meyerii* had the highest temperature optima with 0.82 μ at 15-17.5°C and also the broadest tolerance to a range of temperatures. The *Cyclotella* species grew best at 8.5°C while the *Aulacoseira* sp. preferred colder waters (3°C). A similar investigation of *A. baicalensis* by Richardson *et al.* (2000) also came to similar conclusions. The non-endemic taxa also had the highest growth at high irradiances while *A. skvortzowii* had the highest growth of endemic species (0.46 μ at 35 μmol $m^{-2}s^{-1}$). *A. baicalensis* has a lower rate at this irradiance but is totally inhibited by 65 μmol $m^{-2}s^{-1}$. The *Cyclotella* species have their optima at lower light levels, *S. acus, N. acicularis* and *A. skvortzowii* compete best at higher light levels while endemic species appear to be adapted to tolerate low irradiances but are restricted at high irradiance. This allows endemic species to grow under light limitation due to increased vertical mixing and snow cover on ice. There is a caveat with these results in that laboratory conditions differ to the natural environment, which means that optima and tolerances cannot be transferred directly (Jewson *et al.* unpublished).

Diatom species	Temperature optimum	Temperature range
Synedra acus	0.82 μ at 15-17.5°C	Broad – high growth at 25°C
Stephanodiscus meyerii	~0.43 μ at 15-17.5°C	Broad – high growth at 25°C
Cyclotella minuta	0.53 μ at 8.5°C	Mortality rose outside 4-6°C, but doubling occurred at 14.5°C
Cyclotella baicalensis	0.22 μ at 8.5°C	Mortality rose outside 4-6°C
Aulacoseira skvortzowii	0.59 μ at 3°C	Narrow range – 0.55 μ at 6°C
Aulacoseira baicalensis	0.31 μ at 3°C	Narrow range – no growth at 6°C
Nitzschia acicularis	1.02 μ at 4°C	No data

Diatom species	Irradiance optimum	Irradiance range
Synedra acus	0.63 μ at 17 μmol $m^{-2}s^{-1}$	Growth still high at highest irradiance
Stephanodiscus meyerii	0.5 μ at 17 μmol $m^{-2}s^{-1}$	Growth ceased at high irradiance (65 μmol $m^{-2}s^{-1}$)
Cyclotella minuta	0.25-0.30 μ at 17-25 μmol $m^{-2}s^{-1}$ (3°C)	No data
Cyclotella baicalensis	0.18 μ at ~20 μmol $m^{-2}s^{-1}$	Narrow range – similar to *A. baicalensis*
Aulacoseira skvortzowii	0.46 μ at 35 μmol $m^{-2}s^{-1}$	Only partially inhibited at 65 μmol $m^{-2}s^{-1}$
Aulacoseira baicalensis	0.21 μ at 35 μmol $m^{-2}s^{-1}$	Saturated at 17-35 μmol $m^{-2}s^{-1}$, inhibited at 65 μmol $m^{-2}s^{-1}$
Nitzschia acicularis	0.65 μ at 17 μmol $m^{-2}s^{-1}$	Saturated at 17 μmol $m^{-2}s^{-1}$

Table 5.19: Summary of the culturing experiments of Jewson *et al.* (unpublished) showing the optima and range of diatom species growth (μ is doublings per day) to temperature and irradiance.

Figure 5.15: The effect of temperature on the mean (left) and maximum (right) growth rates for Sa (*Synedra acus*), Sm (*Stephanodiscus meyerii*), Cm (*Cyclotella minuta*), Cb (*Cyclotella baicalensis*), Ab (*Aulacoseira baicalensis*) and As (*Aulacoseira skvortzowii*). From Jewson *et al.* (unpublished).

Figure 5.16: The effect of quantum irradiance on the growth rate of Na (*Nitzschia acicularis*), Sa (*Synedra acus*), Sm (*Stephanodiscus meyerii*), Cb (*Cyclotella baicalensis*), Ab (*Aulacoseira baicalensis*) and As (*Aulacoseira skvortzowii*). From Jewson *et al.* (unpublished).

5.8.2 Training set species response to ice cover variables

The response of individual species (in terms of proportions of the complete assemblage) in the full training set to the modelled environmental variables of snow depth on ice, clear ice cover duration and white ice/snow cover duration can be determined by fitting Huisman-Olff-Fresco (HOF) models (Huisman *et al.* 1993) with the software HOF (Oksanen, unpublished). This program fits the simplest response model to species data using maximum likelihood estimation and a Poisson error distribution from the five defined by Huisman *et al.* (1993). These models are a skewed unimodal response (model V), a symmetrical or gaussian model (model IV), a monotonic model with a fixed plateau (model III), a monotonically increasing or decreasing model (model II) and finally the null model which is flat with no significant trend (model I). Initially, the most complex model is fitted (model V), HOF then drops a parameter to fit the next model (model IV) and so on until statistical significance is lost with further model simplification. This method is of particular use when defining the type of species response to an environmental variable, i.e. if there is a linear, unimodal or no response. However, as this is applied to relative rather than absolute abundance data, it is possible that results can be misleading as an individuals response will be influenced by the relative proportions of other species in a sample.

Figures 5.17 to 5.24 show scatterplots of the response of the range of taxa cultured by Jewson *et al.* (unpublished) to snow depth, clear ice cover and white ice/snow cover duration together with the corresponding fitted HOF model. Figure 5.17 shows the response of *C. minuta* to the environmental variables. In all cases this taxon shows a linear response (model II). Percentage abundance increases with snow depth on ice and also with increased white ice/snow cover duration while abundance is highest at sites with low clear ice abundance. The response of *A. baicalensis* is very similar to that of *C. minuta* with model II being the most simple significant HOF model fitted in all cases (figure 5.18). *A. skvortzowii* (figure 5.19) displays a unimodal (model IV) response for all modelled environmental variables meaning the near complete gradient of species response has been captured by the training set. Optimal abundance is found around 6 cm snow depth, 26 days annual clear ice duration and 66 days white ice/snow cover duration. *C. inconspicua* occurs at low abundance (<10%) in the training, the null response is shown for snow depth and white ice/snow duration but a unimodal response to clear ice cover duration of an optimum around 32 days (figure 5.20). As shown below, the distribution of *S. meyerii* is restricted over the lake, however figure 5.21 shows a linear response to snow depths with greatest abundance at low depths. Model III (linear increasing with a fixed plateau) is shown for clear ice cover duration with greatest abundance above 20 days duration, model III is also shown for white ice/snow duration but with a plateau of

maximum abundance below 100 days. Figure 5.22 shows a linear (model II) response under all variables for *S. acus* v. *radians*. This is increasing for clear ice cover but decreasing for snow depth and white ice/snow cover duration. *C. baicalensis* has a very low abundance mostly <2%, as a result no significant response is shown to any of the three variables (figure 5.23). *S. acus* v. *pusilla* shows the null response for snow depth and clear ice cover duration but a unimodal response (model IV) is given for white ice/snow duration with an optimum around 50 days (figure 5.24).

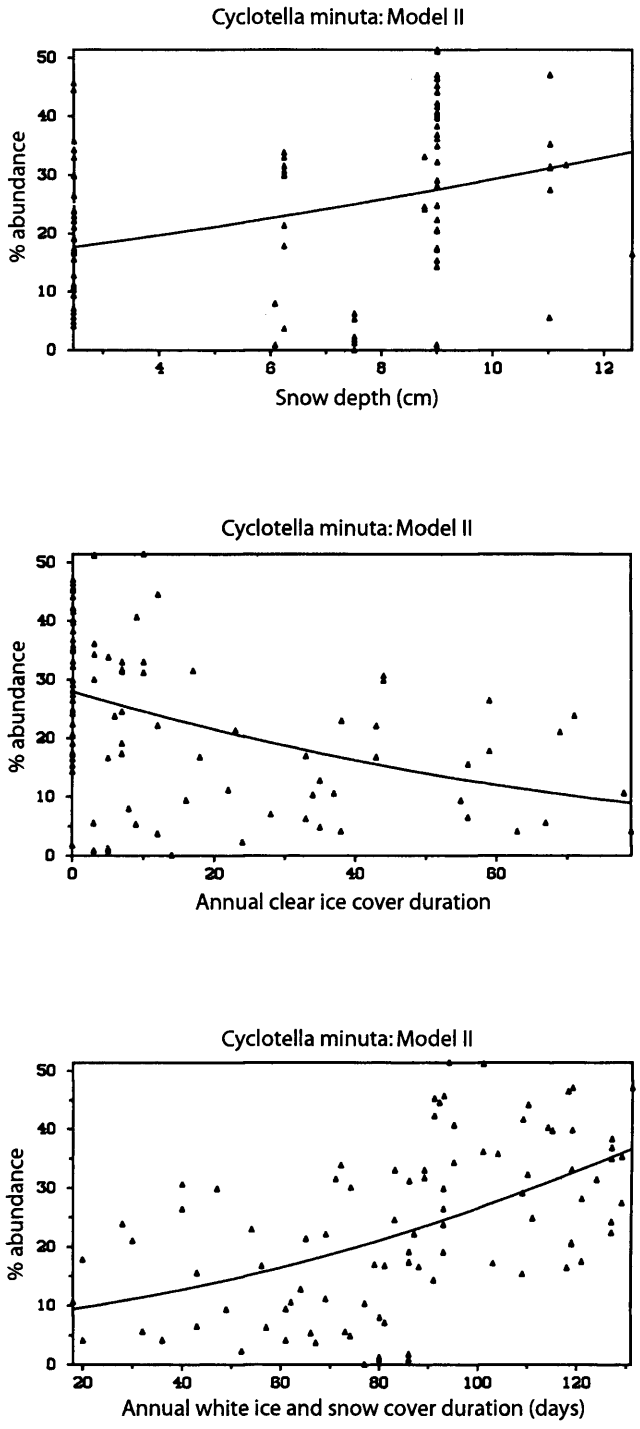

Figure 5.17: Scatterplots of percentage abundance of Cyclotella minuta in the full training set against snow depth on the ice, clear ice cover and white ice/snow cover durations. Fitted HOF response models are also shown.

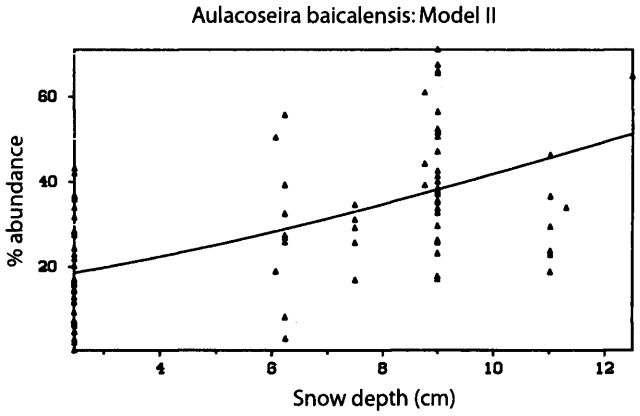

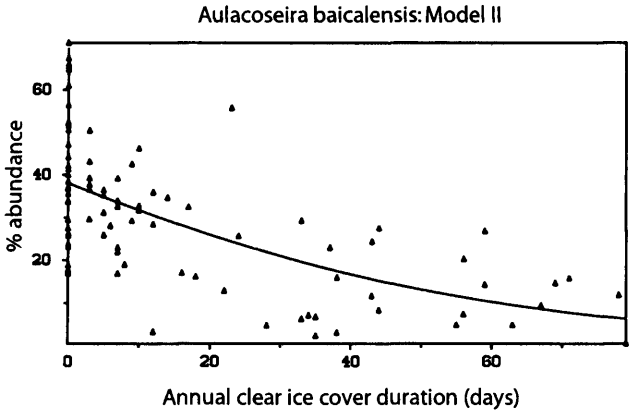

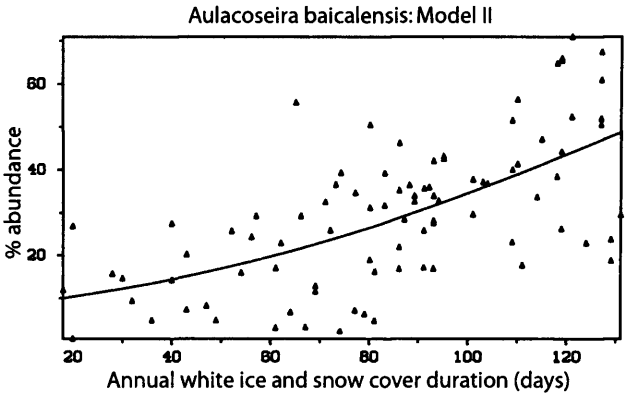

Figure 5.18: Scatterplots of percentage abundance of *Aulacoseira baicalensis* in the full training set against snow depth on the ice, clear ice cover and white ice/snow cover durations. Fitted HOF response models are also shown.

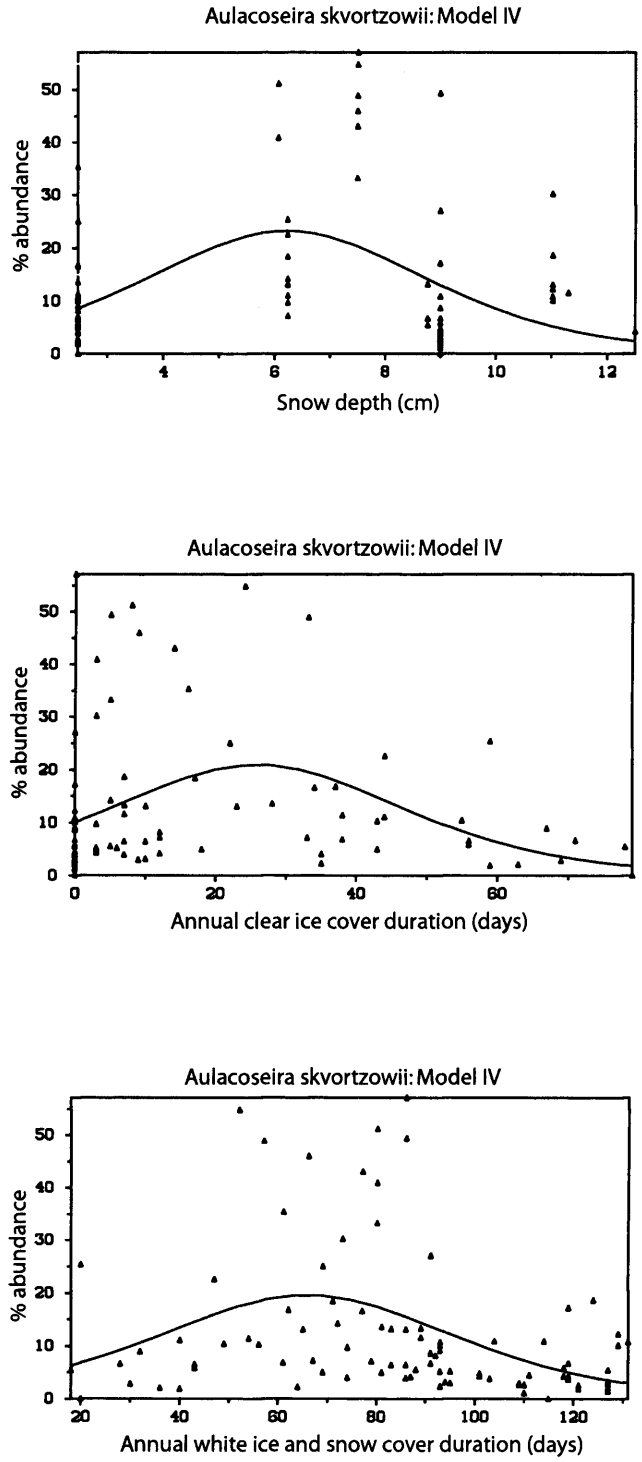

Figure 5.19: Scatterplots of percentage abundance of *Aulacoseira skvortzowii* in the full training set against snowdepth on the ice, clear ice cover and white ice/snow cover durations. Fitted HOF response models are also shown.

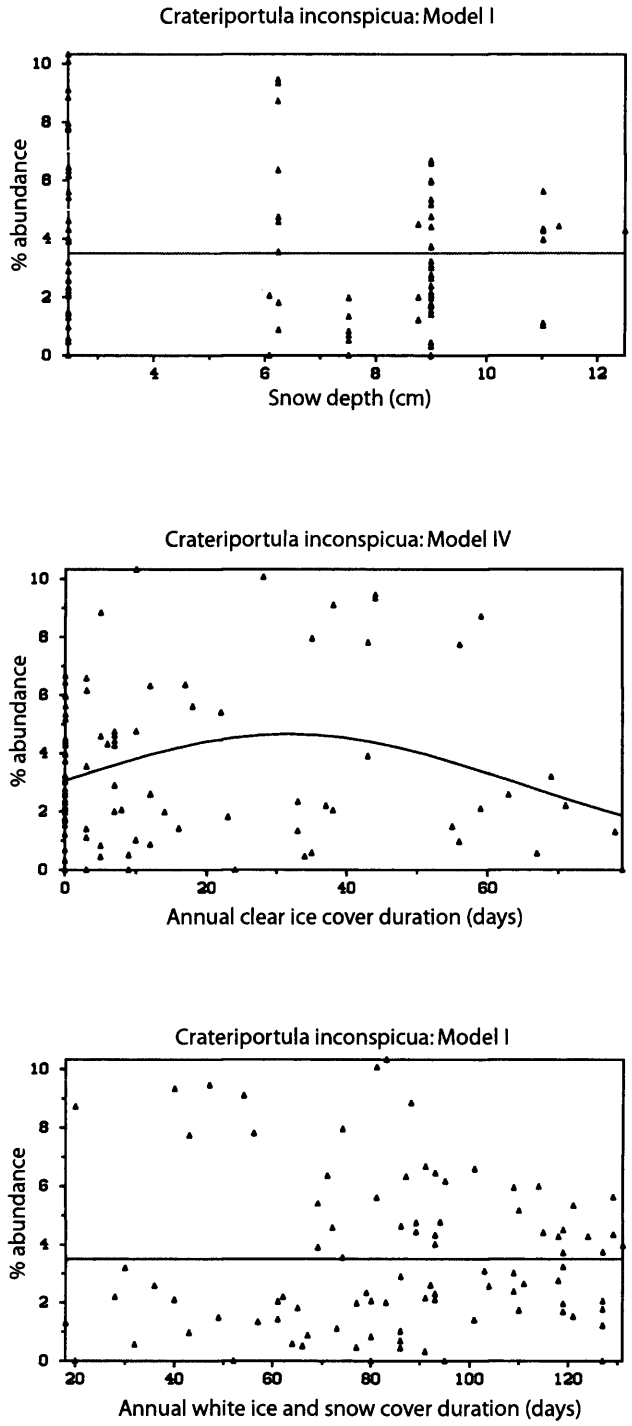

Figure 5.20: Scatterplots of percentage abundance of *Crateriportula inconspcua* in the full training set against snow depth on the ice, clear ice cover and white ice/snow cover durations. Fitted HOF response models are also shown.

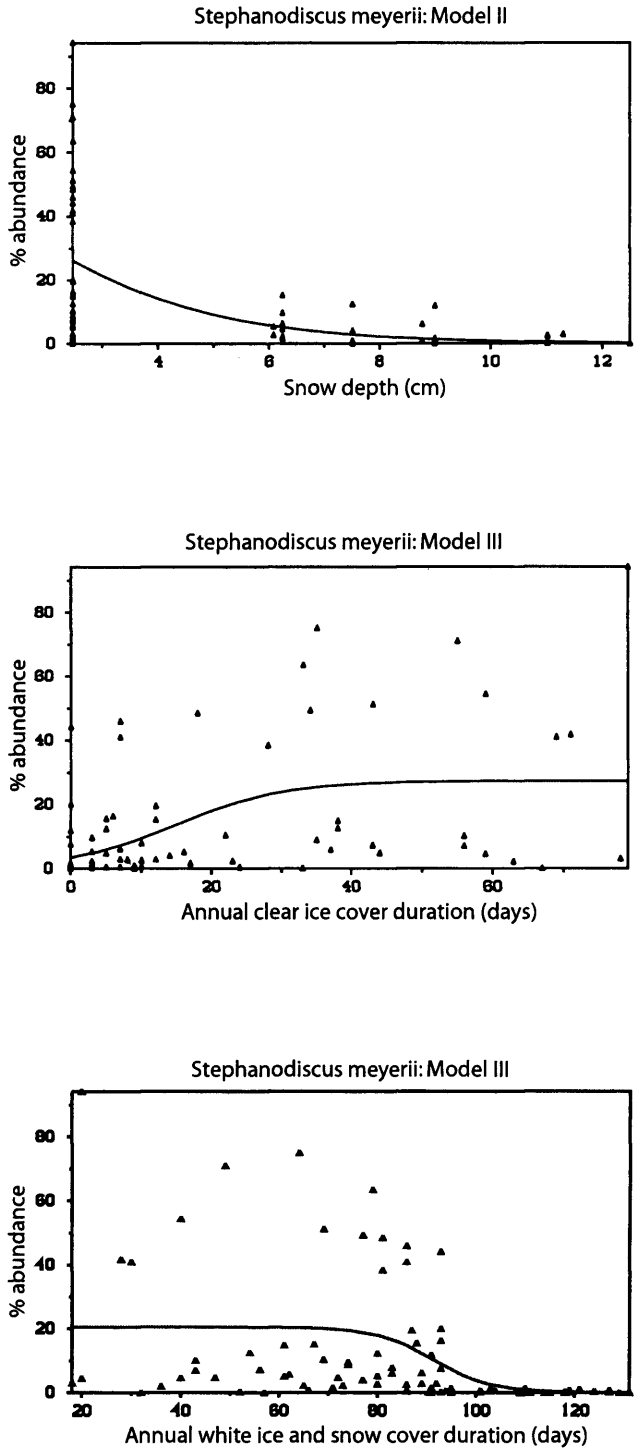

Figure 5.21: Scatterplots of percentage abundance of *Stephanodiscus meyerii* in the full training set against snow depth on the ice, clear ice cover and white ice/snow cover durations. Fitted HOF response models are also shown.

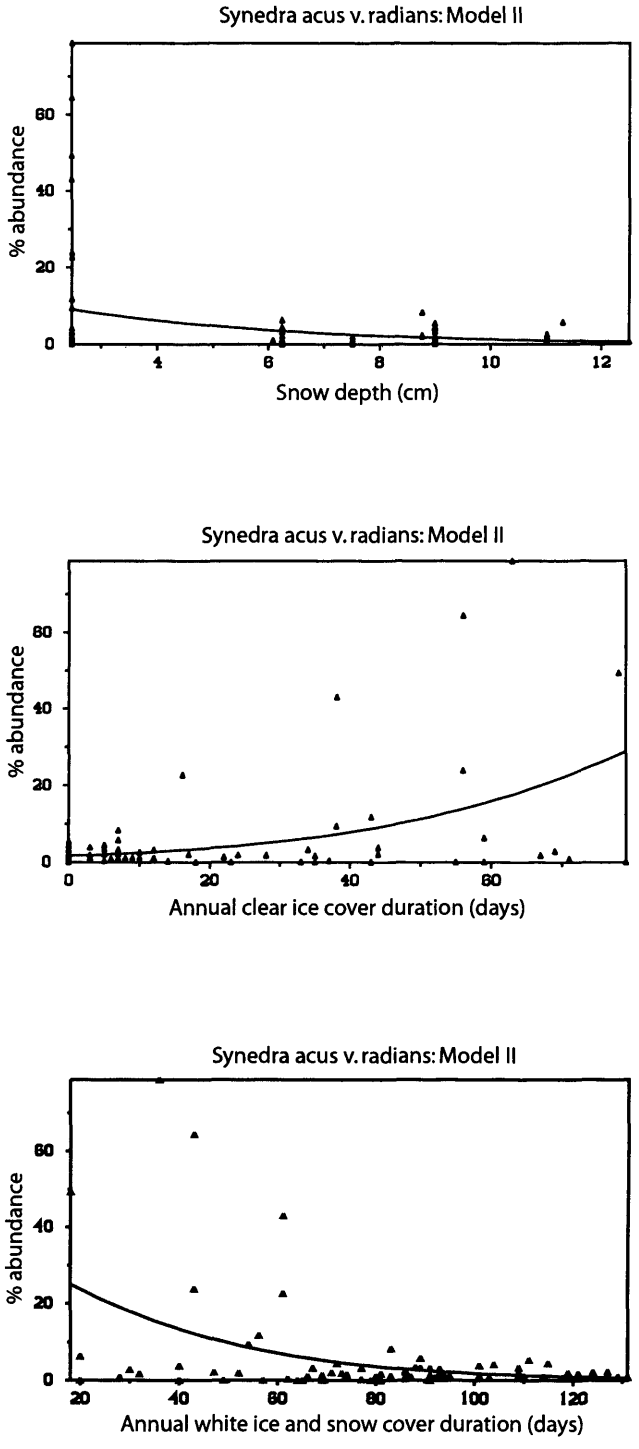

Figure 5.22: Scatterplots of percentage abundance of *Synedra acus* v. *radians* in the full training set against snow depth on the ice, clear ice cover and white ice/snow cover durations. Fitted HOF response models are also shown.

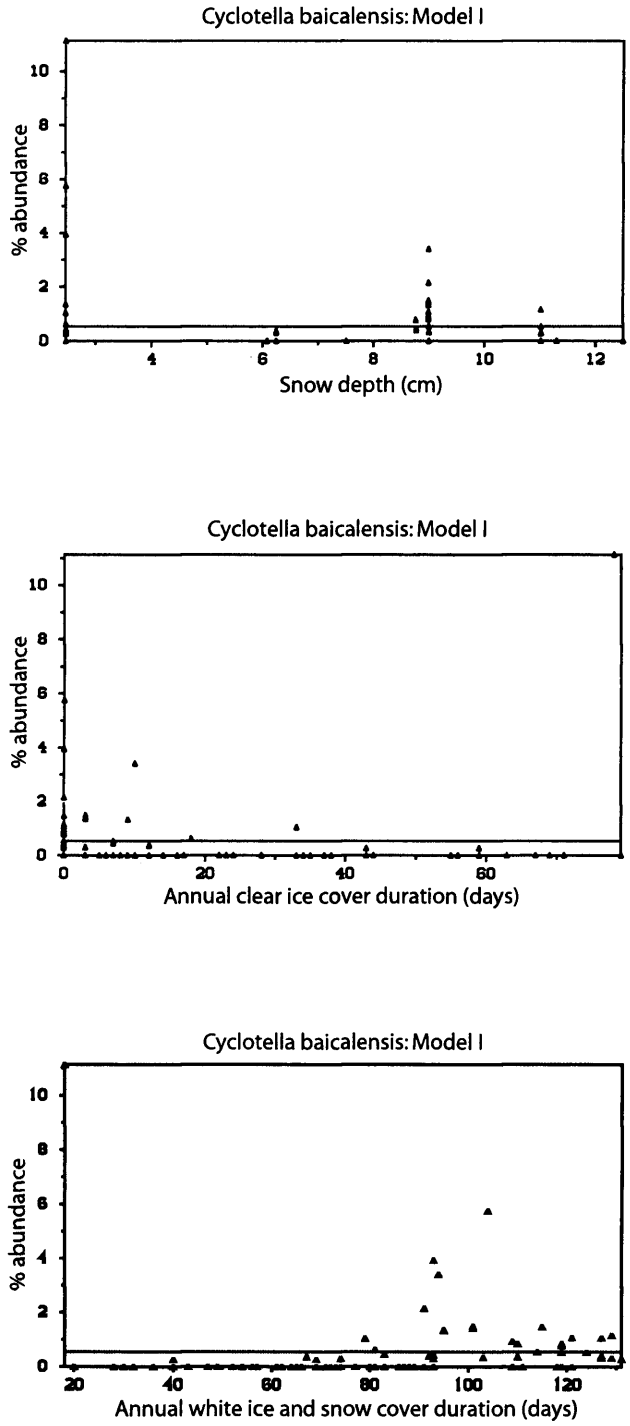

Figure 5.23: Scatterplots of percentage abundance of *Cyclotella baicalensis* in the full training set against snow depth on the ice, clear ice cover and white ice/snow cover durations. Fitted HOF response models are also shown.

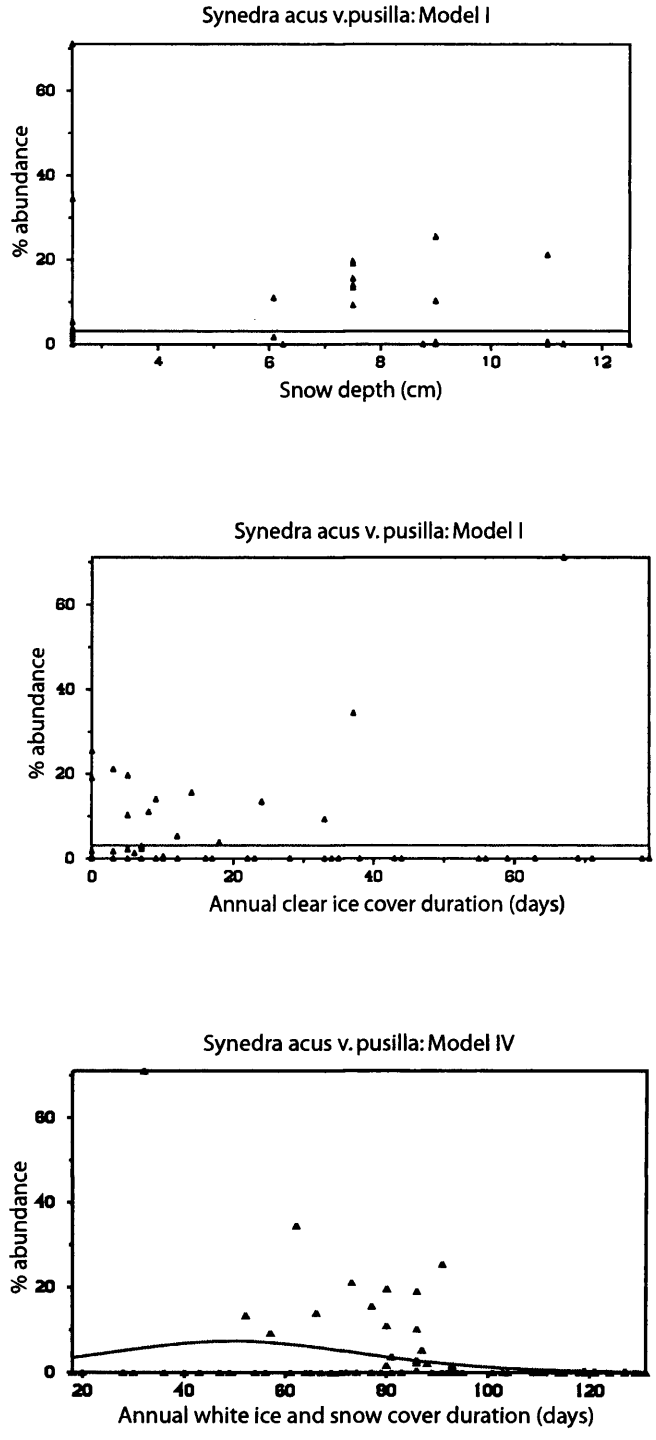

Figure 5.24: Scatterplots of percentage abundance of *Synedra acus* v. *pusilla* in the full training set against snow depth on the ice, clear ice cover and white ice/snow cover durations. Fitted HOF response models are also shown.

5.8.3 Spatial distribution of training set species

The proportional abundance of diatom species in the training set surface sediments have been mapped to get an indication of the spatial distribution of species over the lake (figures 5.25 and 5.26). These species are the same ones as those fitted to HOF models. It will be useful to compare these to the maps of the distribution of phytoplankton in the modern surface waters (section 4.5). The percentage of *A. baicalensis* in the surface sediments (figure 5.25a), is highest in the North Basin with values of around 70%. There is a gradual decline in abundance southwards into the Central Basin which coincides with areas of predominantly clear ice mapped by remote sensing. High values are also recorded in the South Basin, this distribution is similar to the distribution in 2001-2002 surface waters (figure 4.3) but the bloom appears in the North Basin or South Basin at different times. *A. skvortzowii* is only abundant in southern surface sediments and rarely exceeds 10% outside the South Basin (figure 5.25b). This is similar to the distribution as found in the phytoplankton (figure 4.4). Figures 5.25c and 5.25d show the distributions of *C. baicalensis* and *C. inconspicua*, these species appear in low abundance and no real spatial trends are visible. This is also the case for *Cyclostephanos dubius* (Fricke) Round (not shown). As a result it is difficult to get autecological information for these species from this source. *C. minuta* has a similar distribution to *A. baicalensis* being abundant in the North and South Basins but not in the Central Basin (figure 5.26a). However, the surface water plankton shows *C. minuta* over the whole lake in autumn. *S. acus* v. *pusilla* has isolated peaks in the Central Basin surface sediments and a cluster of high abundance in the South Basin reaching a maximum of 25% (figure 5.26b). *S. acus* v. *radians* similarly has low abundance over the whole lake but an area of high abundance in the reaching 80% in the Central Basin (figure 5.26c). Again, this is not in agreement with the phytoplankton data as *S. acus* sp. are found in abundance over most of the South and Central Basins. *S. meyerii* has low percentage abundance in surface sediments over pelagic zones of the lake (especially in the North Basin). It is very abundant in the shallow Maloe More reaching up to 94% of the total assemblage (figure 5.26d). However, *S. meyerii* is very abundant in surface waters of the South Basin (figure 4.9) although no plankton samples were taken in the Maloe More. Dominance of *S. meyerii* in the Maloe More may be due to the presence of phosphorus rich eutrophic waters (Bradbury *et al.* 1994), as supported by high measured values of phosphorus in the Maloe More by Muller *et al.* (in press).

On the whole there is a good accordance between the proportion of species in the surface sediments, and diatom plankton in the surface waters but there are some differences. The causes of discrepancies may be due to variations in interannual species production and the

fact that surface sediments were collected between 1992-1997 and represent more than one year's crop, while water samples were collected in 2001-2002. There are also issues of differential dissolution as species are transferred through the water column into the surface sediments (Ryves *et al.* 2003). This effect will be greatest for *Synedra* species but less for the *Cyclotella* species (Battarbee *et al.* in press, table 5.2). Also, the two types of data are not directly comparable with the surface sediments represented by relative abundance, while phytoplankton cell numbers are absolute values. In addition, the sampling locations of the training set do not match exactly those of the phytoplankton monitoring campaigns. Broad regional comparisons can be drawn, however.

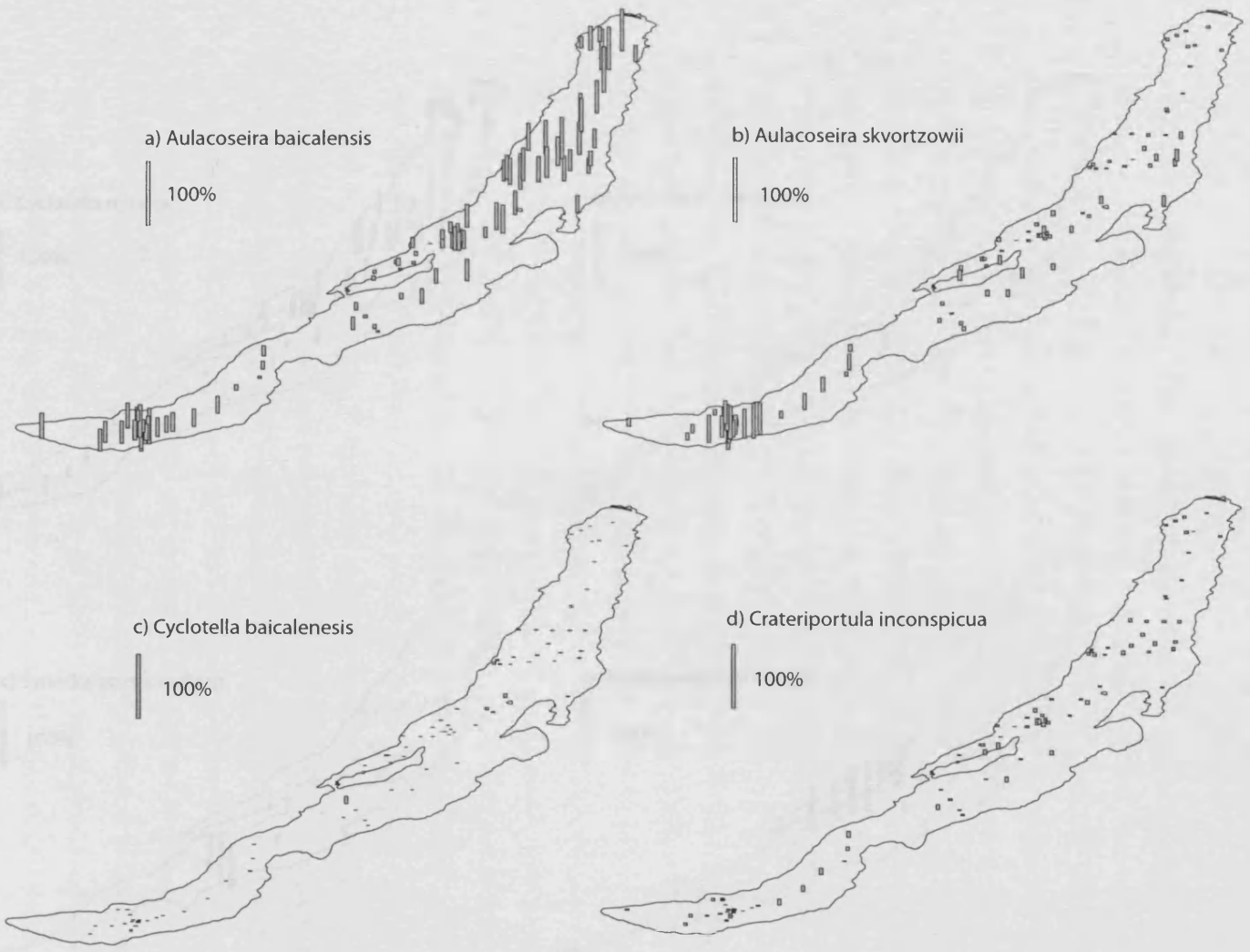

Figure 5.25: Spatial distribution of the percentage abundance of a) *Cyclotella baicalensis,* b) *Crateriportula inconspicua,* c) *Aulacoseira baicalensis* and d) *Aulacoseira skvortzowii* in the full training set.

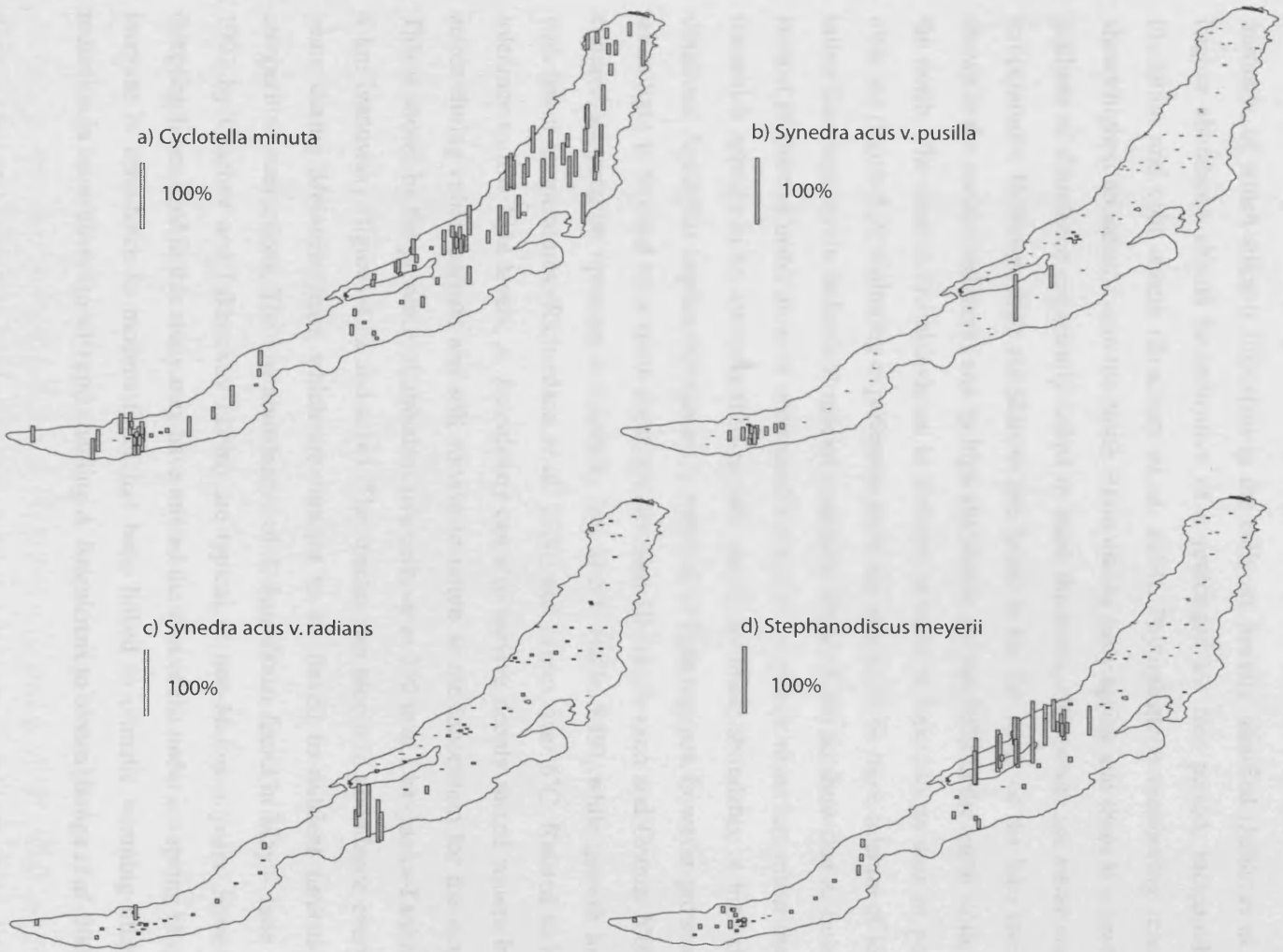

Figure 5.26: Spatial distribution of the percentage abundance of a) *Cyclotella minuta,* b) *Synedra acus* v. *pusilla,* c) *Synedra acus* v. *radians* and d) *Stephanodiscus meyerii* in the full training set.

5.8.4 Diatom species autecological summary

Autecological summaries are given below for the diatom species found in the Vydrino Shoulder core with an abundance of greater than 5% in one or more samples.

Aulacoseira baicalensis: is fully pelagic and blooms under ice in early spring and although tolerant to low light levels requires increasing irradiance, turbulence (Granin *et al.* 2000) and nutrients, of which silica is important as the cells are heavily silicified (Julius *et al.* 1997). Higher abundance should be indicative of a prolonged ice free period, increased spring insolation and cold waters (Bradbury *et al.* 1994). Phytoplankton monitoring (chapter 4) shows highest abundance is in the North Basin during early spring and there is a north-south gradient of abundance empirically linked to snow thickness, clear/white ice cover and water temperatures. However, high abundances are found in the far south of the lake too; this is shown in the surface sediments and by high abundance in June 2002 in the south, compared to the north. The area of low abundance in the central basin is linked to an area of persistent clear ice (figure 5.7). Culturing experiments show the species to be more tolerant of low light rather than high levels. Individual species responses (figure 5.18) do show that *A. baicalensis* is most productive under areas of obstructed ice (snow covered or white ice) rather than clear ice which appears to be detrimental to growth, shown by lower abundance at high clear ice durations. Again this implies this species is sensitive to light regimes, however growth ceases when light is blocked by a snow depth greater than 10 cm (Jewson and Granin 2000). The cultured temperature optimum is relatively low at 3°C (table 5.19), while growth increases with lower temperatures (Richardson *et al.* 2000) and ceases over 6°C. Related to its high tolerance to low light levels, *A. baicalensis* can also survive deeply mixed waters by wind action during colder periods and still survive to return as the innoculum for the next crop. This is shown by the presence of abundant live cells up to 250 m at Listvyanka-Tankhoy and 4 km Ivanowsky (figures 4.12 and 4.14). The species can bloom in abundance every 3 - 4 years during *Melosira* years which are thought to be linked to nutrient limitation and competitive interactions. The low abundances of *A. baicalensis* found in May – June 1991 – 1992 by Grachev and Likhosway (1996) are typical of non-*Melosira* years, however the sampling times used in this study may have missed the start of the under ice spring bloom. An increase in abundance in modern times has been linked to climatic warming allowing a reduction in snow cover (to <10 cm) enabling *A. baicalensis* to bloom (Bangs *et al.* 2000).

Aulacoseira skvortzowii: can also bloom under ice in early spring. It differs from *A. baicalensis* in that it is not fully pelagic but builds up in near shore zones especially behind thermal bars and expands out into pelagic waters in spring (Edlund and Stoermer 2000). This

is due to a different overwintering strategy to *A. baicalensis*. Instead of falling out of the photic zone, the resting stages of *A. skvortzowii* are deposited in surface sediments. In shallower, littoral areas these are resuspended during spring turnover as the innoculum for the new crop which establishes itself initially in littoral areas. The phytoplankton data (both depth and surface profiles) indicate that resting stage production is dominant as the main spring bloom of vegetative cells, which subsequently fall through the water column during summer. According to the HOF responses, *A. skvortzowii* has one of the narrowest tolerances of common diatom species to the modelled environmental variables. It is not tolerant of very deep or shallow snow with an optimum of around 6 cm. A unimodal response is also shown to clear ice and white ice/snow cover durations. These results imply that *A. skvortzowii* cannot tolerate very high and very low light levels under the spring ice. However, the culturing studies show *A. skvortzowii* can tolerate much higher irradiances, and grow more rapidly at lower irradiances, than *A. baicalensis* while Kobanova (2001) also cites higher irradiance as important in promoting growth. As for *A. baicalensis,* the temperature optimum is 3°C, but it is able to grow beyond 6°C unlike *A. baicalensis.* However, Kobanova (2001) found maximum abundance in much colder waters during April 2000 when water temperatures remained around 0.6°C. Currently, abundance is only high in the South Basin as documented by 2001-2002 phytoplankton data (chapter 4) and surface sediments. This is possibly due to earlier ice out time and slightly warmer waters compared to the north of the lake. Bondarenko *et al.* (1996) also found this species in the Central basin during spring 1991 as well as in shallow bays. This is expected as most resting stages will be resuspended here. Overall, this species may indicate warming waters, but a light regime that is increased but not too extreme (either too high or too low).

Cyclotella minuta/ornata/baicalensis: are described here together as they have very similar ecology although the different species do occupy different temporal niches in the lake, the larger types (*C. baicalensis* and *ornata*) being common earlier in the year. All three *Cyclotella* sp. are exclusively pelagic and common in autumn, as summer stratification breaks down and a deeper thermocline develops with increased mixing, turbulence and nutrient regeneration. The innoculum is brought up from deeper pelagic waters by this deeper convection. These *Cyclotella* sp. are also sometimes found in spring during non-*Melosira* years due to increased competitiveness (Edlund and Stoermer 2000). Although *C. baicalensis* shows no relationship to modelled variables (figure 5.23), *C. minuta* in the surface sediments has a very similar response to the snow and ice variables as *A. baicalensis*, shown by the HOF plots (figure 5.17), with increased abundance in areas of deeper snow cover and lower abundance associated with areas of clear ice. This may be because of a low tolerance to high irradiances (Mackay *et al.* 2003). Although no information is available from culturing studies for the

irradiance range of *C. minuta* and *C. ornata*, *C. baicalensis* has a similar tolerance to *A. baicalensis*. As with *A. baicalensis*, this distribution can be related to ice cover and may be due to the presence of persistant clear ice in the Central Basin that allows high irradiance transmission and detrimental conditions for growth. However, as shown by the phytoplankton monitoring (chapter 4), these *Cyclotella* species are dominant in late summer when ice cover is not present. Therefore, the correlation to areas of short clear ice cover duration and deeper snow may be related to dynamics of water column stratification. However, the apparent even distribution of these *Cyclotella* species (lumped together) over the lake's surface in the phytoplankton of 2001 – 2002 may mean abundance is unrelated to ice cover (light transmission) (such a distribution was also found by Grachev and Likhosway (1996)) and the relationship shown in the surface sediments is an artefact due to the percentage abundance data used. Corroborating this, areas with deep snow cover can have higher relative abundance in sediments of *Cyclotella* sp., as increased snow cover limits spring production (of other diatom species) and the sediment record is weighted towards autumn production (Bangs *et al.* 2000). Consequently water temperature may be most important in controlling growth, according to culturing *C. minuta* and *C. baicalensis* are able to tolerate warmer waters with optima at 8.5°C, although mortality for both species rose outside 4-6°C. Karabanov *et al.* (2000) also state *C. minuta* is not as tolerant of very warm waters in which species such as *S. acus* thrive. Overall, high abundance of these species may be related to warming waters and a dominance of autumnal over spring productivity, due to either longer summers (Bradbury *et al.* 1994) or restriction of the size of the spring crop relative to the autumn crop, due to long, cold winters (this is important when interpreting percentage abundance data). The high abundance of dead cells throughout the water column in the depth profiles studied indicates that this species preserves well in the water column (Ryves *et al.* 2003).

***Synedra acus* (v. *radians* and v. *pusilla*):** both develop in nearshore areas and behind thermal bars following ice out, and subsequently expand into pelagic regions during spring and early summer and gradually populate deeper water as summer progresses (shown by the depth profiles, figures 4.12 and 4.14). As these species require high levels of silica they may be indicative of increased river discharges (Bradbury *et al.* 1994). Increases in precipitation due to a warm and wet climate will increase catchment erosion and run-off. Julius *et al.* (1997) also associate these species to increased run-off from glacial meltwater and a warming climate. *S. acus* is common through the year (Edlund and Stoermer 2000) due to its tolerance to a broad range of irradiance levels and temperature and its competitive ability. According to the HOF plots (figures 5.22 and 5.24), *S. acus* v. radians shows linear trends to higher abundance with lower snow depths and shorter white ice/snow cover, but longer annual clear ice duration. *S. acus* v. *pusilla* occurs at low abundance and is unrelated to snow depth and

clear ice cover, but shows a unimodal response to white ice/snow cover duration (optimum 50 days). From these results, it can be inferred that *S. acus* v. *radians* in particular grows best under higher irradiances made possible by lower snow depths and shorter periods of opaque ice. This is supported by the culturing studies, growth is highest at maximum irradiances but is still high at low levels too. Of the species cultured by Jewson *et al.* (unpublished), *S. acus* had the highest temperature optimum at 15 - 17.5°C, but also a broad range high growth at low temperatures as well as up to 25°C. Phytoplankton monitoring (chapter 4) shows *S. acus* sp. are most common in the plankton of the South and Central basins possibly relating to shorter opaque ice cover durations and warmer waters at which these species will be the most competitive, this distribution is also shown (in that the species is rare in the north) by Bondarenko *et al.* (1996). However, the distribution over the South and Central Basins was not consistent while Grachev and Likhosway (1996) also report a 'patchy' distribution for this species. This 'patchy' distribution appears to be present in the surface sediments too, although *S. acus* sp. are highest in abundance in the South and Central Basins. The presence is marked by large isolated peaks, these are possibly related to areas of clear ice or higher nutrient inputs from rivers. As already stated, *S. acus* thrives in areas with increased nutrient loading from rivers. In addition, interpretation of surface sediments may be complicated by the high level of dissolution of this species as shown by Ryves *et al.* (2003). A recent rise of *S. acus* has been assigned to anthropogenic pollution (Julius *et al.* 1997, Bangs *et al.* 2000) but also occurrences over the Holocene have been linked to a warmer climate (Bangs *et al.* 2000, Karabanov *et al.* 2000). Even though there is a broad temperature tolerance, the dominance of these *Synedra* should represent a predominantly warm climate with shorter ice duration as other species are not so tolerant of warmer waters and high irradiances. However, nutrient availability may be a limiting factor as to the distribution of this species in pelagic regions beyond shallower more eutrophic areas.

Stephanodiscus meyerii: like *S. acus, S. meyerii* can build up in shallow waters and develop into pelagic regions in spring. Increased *S. meyerii* abundance may indicate greater nearshore nutrient input due to higher precipitation. Phosphorus levels are probably most important for this species (Bradbury *et al.* 1994). Figure 5.21 shows that *S. meyerii* has a linear response to snow depth over the gradient sampled, with highest abundance at minimum snow depths. Higher abundance is shown with shorter white ice/snow cover and longer clear ice cover. This fits with the assumption of Bradbury *et al.* (1994) that this species is indicative of a dry climate (less snow cover) dominated by water column circulation and nutrient regeneration. Kozhova and Kobanova (2001) also found highest *S. meyerii* abundance in areas that correspond to clear ice cover shown in figure 5.7 (assuming clear ice distribution shows little interannual distribution). Distribution in the surface sediments (figure 5.26d) is mostly

restricted to the shallow, eutrophic waters of the Maloe More, possibly linked to the high phosphorus levels found here (Muller *et al.* in press). However, this area also has shallow snow depths due to high winds (Shimaraev *et al.* 1994), while the region is also relatively dry, receiving less than 200 mm of precipitation annually compared to the 300 - 400 mm falling annually in the South Basin (Atlas Baikala 1993). It is common also in the early summer (2001-2002) plankton in the South and Central Basins and rare in the north (chapter 4). This implies the species favours warmer waters with shorter ice cover duration. This is supported by the culturing experiments with a high optimum temperature of 15 - 17.5°C, with growth still occurring at 25°C (a similar response as *S. acus*, although growth rates are lower). High growth was also recorded at 17 µmol $m^{-2}s^{-1}$ although growth ceased by 65 µmol $m^{-2}s^{-1}$. Abundance in recent sediments has been linked to both climate driven eutophication (Bangs *et al.* 2000) and pollution (Bradbury *et al.* 1994). The fact that this species was extremely abundant in 2002 in the South Basin, but much rarer in 2001, implies a high level of interannual variability possibly linked to nutrient availability and competitive-species interaction factors. Overall, this species is indicative of warm waters and high irradiances linked to a warm and dry climate, however nutrient availability is important, meaning abundances may be highest in shallow eutrophic bays compared to pelagic areas.

Stephanodiscus parvus: is rare in the modern phytoplankton and no significant analogue is given in the training set. However, it is likely that this species has a similar autecology as *S. meyerii.* It is transported from littoral areas where it establishes after ice-out into open waters (Bradbury *et al.* 1994). Nutrients, in particular phosphorus (Kilham *et al.* 1996), are important for growth. This is a non-endemic taxa and has been found in relation to high phosphorus and eutrophication (either anthropogenic or natural), for example in England (Bennion 1994, Sayer 2001).

Stephanodiscus flabellatus and ***Stephanodiscus skabitchevskyii:*** the latter species is apparently extinct in the modern lake, while the former is extremely rare but is found in nearby Lake Hovsgol as well (Edlund *et al.* 2003). *S. flabellatus* is present in the Late Glacial and Early Holocene, while *S. skabitchevskyii* appears abundantly in the Mid Holocene (Bradbury *et al.* 1994). By analogue to similar diatoms elsewhere in the world, these *Stephanodiscus* species should thrive in low light conditions, turbid waters and deep wind driven mixing related to a cold climate (Bradbury *et al.* 1994). These species possibly grew in stable environment between the turbid conditions of the Late Glacial and the more transparent waters of the Holocene. As they are often abundant when *Aulacoseira/Cyclotella* species are not, they may be indicative of a very different lake environment to the modern one (Bradbury *et al.* 1994).

Cyclostephanos dubius: although present in the modern lake, because of a low abundance, little information can be obtained from the phytoplankton analysis or the surface sediments. Bradbury *et al.* (1994) state this species is characteristic of shallow eutrophic waters and develops in late spring to autumn and occasionally appearing in open waters in large numbers. Edlund *et al.*(1995) consider this to be a warm, eutrophic water indicator. This taxon was found in most abundance around the Selenga delta region by Mackay *et al.* (1998) reinforcing the importance of eutrophic and maybe warmer waters for this species. This taxon is non-endemic and its distribution has been described by Krammer and Lange-Bertalot (1986-1991); the most common habitats are in high chloride or brackish waters, again this type of habitat will most likely occur near river mouths, in particular the Selenga delta region. This species is considered an indicator of eutrophic waters, for example in areas such as Denmark (Anderson and Odgaard 1994).

Asterionella formosa: is extremely rare in surface sediments but appears in abundance in the phytoplankton (therefore dissolution of this species is high) in late summer in the South and Central Basins, but is rare in the north, possibly indicating a preference for warmer and eutrophic waters (chapter 4). *A. formosa* was found in abundance in the warm, riverine influenced, relatively eutrophic littoral waters behind the thermal bar during spring in the south of Lake Baikal (Likhosway *et al.* 1996). The species is non-endemic and Krammer and Lange-Bertalot (1986-1991) state this is a cosmopolitan planktonic species in eutrophic waters which can often develop into large blooms. In Lake Baikal, higher abundances can be expected during the summer stratified period (Jewson, pers. comm.). Overall, this species is an indicator of meso- to eutrophic waters (Patrick and Reimer 1966). In the RDAs (figures 4.13 and 4.15), *A. formosa* is correlated with other species proved to be tolerant of warmer waters such as *S. acus*.

Crateriportula inconspicua: again this has a poor analogue in the modern lake, and an apparent low abundance over the lake was observed (not plotted here). The HOF graphs (figure 5.25d) show no response to snow depth or white ice/snow cover but a unimodal response to clear ice duration, although most samples with relatively high abundance are found in areas of short clear ice duration. Edlund *et al.* (1995) consider abundance to be greatest during cold periods such as the LIA, as it is representative of summer production when spring productivity is limited by increased ice and snow cover. Indeed, it may be that *C. inconspicua* is more abundant in the North Basin than estimated in the phytoplankton monitoring of 2001 – 2002 due to problems of identification (Rioual pers. comm.), further supporting the idea of higher abundance with increased (opaque) ice cover. *C. inconspicua*

may also develop in warm, shallow mesotrophic waters (Edlund *et al.* 1995). The species may also be indicative of production in warm waters in early summer after the main spring bloom of other species (Jewson, pers. comm.). Overall, *C. inconspicua* may represent productivity in warmer summer waters after a spring with longer opaque ice cover.

Cyclotella ocellata (Pantocsek): has not been found in any published Holocene records but is present during the colder periods especially during the Eemian (Rioual pers. comm.).

Benthic diatoms: (species with abundance >5% in any one sample are; ***Amphora pediculus* (Kutz.) Grun., *Staurosirella pinnata* (Ehrenb.) Williams and Round, *Achnanthidium minutissimum* v. *minutissima* Kutz.**). Increased abundance of benthic diatoms may be due to increases in river discharge bringing in river diatoms, or greater within lake mixing causing greater entrainment of littoral species. Littoral production may also become dominant as ice cover restricts pelagic diatom production *c.f.* Smol (1988). This moat hypothesis is fully described in section 2.6. Increased relative abundance should therefore indicate a decline of phytoplankton productivity due to a longer ice covered period (Edlund *et al.*1995).

Chapter Six

Diatom based palaeoclimatic reconstruction

6.1 Diatom records from Lake Baikal

As Lake Baikal can be regarded as a stable, ancient, well-buffered lake it will record the low frequency changes of many glacial/interglacial cycles over millions of years (Bradbury 2000). This rationale has been applied by the Baikal Drilling Project (BDP) (Williams *et al.* 2001). The BDP began in 1989 with the primary objective of reconstructing the long-term climatic response of a continental interior location and to compare with results from the Ocean Drilling Project (ODP) and link to the PAGES-PEPII transect (Williams *et al.* 2001). The principal proxy used has been biogenic silica (BioSi) abundance (a measure of productivity of siliceous flora), and its content is thought to be directly linked to insolation forcing (Qui *et al.* 1993, Colman *et al.* 1995, BDP-Members 1997a, b, Williams *et al.* 1997, Kashiwaya *et al.* 1999, Karabanov *et al.* 2000, Antipin *et al.* 2001, Khursevich *et al.* 2001, Prokopenko *et al.* 2001a, Kashiwaya *et al.* 2001a, b). BioSi is also closely correlated to absolute diatom abundance (Prokopenko *et al.* 2001a, Antipin *et al.* 2001), although dissolution processes may severely bias the signal (e.g. Ryves *et al.* 2001, Battarbee *et al.* in press).

BioSi records over 250 ka (Colman *et al.* 1995) and 5 Ma (Williams *et al.* 1997) show BioSi is responding to Milankovitch orbital parameters, as spectral analysis of the records reveal precession, obliquity and eccentricity components. Although the BioSi record is 'clipped' by zero values in glacial periods (Colman *et al.* 1999), the record matches the marine $\delta^{18}O$ profile suggesting continental regions are responding in the same way as oceanic regions. The correlation of recent glacial cycles to marine $\delta^{18}O$ records has been supported in a higher resolution study by Colman *et al.* (1999). However, the chronology often used is the tuning of the BioSi records to the SPECMAP chronology (Martinson *et al.* 1987, Kashiwaya *et al.* 1998). This is assuming a climatic response of BioSi and is a circular argument (Oberhänsli 2000).

BioSi has been used to reconstruct the last interglacial (Eemian, MIS 5e) as an analogue to the Holocene. There has been debate as to whether this period was stable as in Europe (Woillard 1978, Björk *et al.* 2000, Rioual *et al.* 2001) or unstable as in Greenland (Dansgaard *et al.* 1993) although the new NGRIP Greenland core may now show that the Eemian in Greenland

was stable with temperatures 5°C above present (NGRIP Members 2004). The same type of question is also being asked about the stability of the Holocene (O'Brien *et al.* 1995). Lake Baikal Eemian BioSi records show a mid-Eemian cooling corresponding to a similar event in the North Atlantic suggesting a teleconnection (Karabanov *et al.* 2000). Linked to this, Karabanov *et al.* (1998) find evidence of an extreme Siberian glaciation during MIS 5d corresponding to Milankovitch cooling and increased moisture transport from the North Atlantic. This glaciation is most intense in Siberia, prompting Karabanov *et al.* (1998) to propose that glaciations may begin in Siberia and develop through positive feedback of albedo changes linked to ice/snow cover. However, results based on Lake Baikal diatom assemblage change by Rioual and Mackay *et al.* (in press) support the view of teleconnections between Europe, China and Siberia. For the last glacial, Prokopenko *et al.* (2001a) also show Heinrich Events, Dansgaard-Oeschger Events and Bond Cycles are recorded in Baikal as they are in the North Atlantic.

Studies utilizing diatom assemblages, although very informative are less common. Grachev *et al.* (1998) found changes in diatom communities over 2.5 Ma and 19 glacial periods. A few taxa dominated each interval, and rapid extinction and speciation occurred. Investigation of the succession of individual diatom species over the last 800 ka has been carried out by Khursevich *et al.* (2001). Here, extinction events were related to transitions to glacial periods while interglacials saw rapid speciation. Diatom species changes over the last few interglacial and glacial periods has been investigated by Julius *et al.* (1997). However, this study was at very coarse resolution and the Holocene was only represented by two samples. A study by Edlund *et al.* (1995) assessed possible climatic significance of individual diatom species. The period investigated was the past 200 ka but at low resolution again. It was stated that only very little was known about the autecologies of the endemic diatoms species.

Most Holocene records of climate change based on Lake Baikal sediments have used percentage biogenic silica as an indicator of warmer or colder periods, in the same way it has been applied to the study of glacial cycles (e.g. Qiu *et al.* 1993). Holocene diatom records have been presented by Chenyeva (1970) and Chebykin *et al.* (2002) while Bradbury *et al.* (1994) published a summary paper of records from Lake Baikal. Six sites over the whole lake were studied at low resolution (often the Holocene was only represented by 30 levels). A good correlation was noted between sites but differences were put down to changes in diatom production, differences in sedimentation and preservation. One core (305-a5, near the Selenga Delta) provided a full Late Glacial-Holocene record. Between 15-14 ^{14}C kaBP diatom abundance increased with *Cyclotella* sp. and *S. flabellatus* most common. *S. flabellatus* with *A. baicalensis* were most common between 14-11.5 ^{14}C kaBP. A period of low concentration

occurred between 11-9 ^{14}C kaBP possibly relating to the Younger Dryas (GS-1). The start of the Holocene (8.5-6 ^{14}C kaBP) saw increased diatom abundance with *Aulacoseira* and *Cyclotella* sp. and *C. dubius*. Finally, the Late Holocene period of 5-3.5 ^{14}C kaBP was marked by a reduction in *Aulacoseira* sp. but increased *Cyclotella* sp. and small *Stephanodiscus* sp. Climatic variation altering the physical limnology of the lake was linked to the succession of diatom species. Chebykin *et al.* (2002) also claimed Holocene species succession is a response to climate driven gradual eutrophication. Bradbury *et al.* (1994), Karabanov *et al.* (2003) and Chebykin *et al.* (2002) all identify Bølling-Allerød and Younger Dryas periods that are synchronous with the North Atlantic. Prokopenko *et al.* (1999) claim the Lake Baikal record lags GISP2 by 1 ka but this may be due to the difficulties of dating Lake Baikal sediments and may not be a true climatic lag (Grachev 2000, Prokopenko 2000). A study of nearby (200 km) Lake Khubsugul indicates a Late Glacial climatic oscillation apparently synchronous with Greenland ice records (Karabanov *et al.* 2004).

Diatom histories of recent sediments have investigated the role of pollution versus climate in controlling microfossil succession. Edlund *et al.* (1995) suggest anthropogenic pollution is affecting species composition, while Flower *et al.* (1995), Mackay *et al.* (1998) and Bangs *et al.* (2000) identify climatic cycles as the main control on diatom flora. In particular, a current trend of increasing *A. baicalensis* (and also a decline of endemic taxa and a rise in dominance of cosmopolitan *N. acicularis* and *S. acus*) is linked to a warming climate while a dominance of *C. minuta* occurs during the LIA. This is preceded by a zone of greater *S. acus* v. *radians* abundance possibly linked to the MWP. The dominance of *C. minuta* during the LIA is thought to be increased anticyclonic activity causing longer winters and greater snow accumulation, thus suppressing spring *A. baicalensis* growth and promoting dominance of autumn diatom production, although diatom productivity is also much lower during this period (Mackay *et al.* in press).

There is still the need for a high-resolution study of Holocene diatom assemblage shifts in Lake Baikal as this will contain much more information than simple percentage biogenic silica abundance profiles. However, a range of problems need to be addressed before this can be achieved (Flower *et al.* (1998), Flower *et al.* (1999), Mackay *et al.* (2000) and Bangs *et al.* (2000)). These include the need to understand sedimentary processes and turbitide formation which has been tackled with the use of seismic surveys and careful selection of coring locations (Charlet *et al.* in press, section 2.3.1). Problems of reliable dating are also raised which can be resolved with the AMS dating of pollen extracts rather than bulk TOC (Piotrowska *et al.* 2004, section 2.4). The differential dissolution of diatom species has been quantified by monitoring the modern water column with sediment trap arrays and comparing

to surface sediments (Ryves *et al.* 2003), and correction factors for some species have been calculated (Battarbee *et al.* in press, section 5.4). One of the most important obstacles in interpreting diatom records from Lake Baikal is the lack of autecological knowledge of the diatom species. This has been addressed by the derivation of a transfer function (Mackay *et al.* 2003, chapter 5), phytoplankton monitoring (chapter 4) and also with culturing studies (Richardson *et al.* 2000, Jewson *et al.* unpublished.).

6.2 Methodology

6.2.1 Diatom slide preparation and counting

Standard diatom slide preparation methods using oxidising chemicals (*c.f.* Battarbee *et al.* 2001) are not necessary for Lake Baikal sediments as they are of low organic content and chemical treatments can have an adverse effect on the preservation of species with lightly silicified frustules (Flower 1993). As a result, a known weight between 0.1 – 0.2 g of wet sediment was placed in centrifuge tube and a known weight of microspheres added to allow determination of diatom concentrations (Battarbee and Kneen 1982). The sample was then shaken and a fraction of the sediment (now homogenised with the microspheres) was diluted with distilled water and pipetted onto glass coverslips (diameter 19 mm) and allowed to dry. A concentrated and dilute coverslip was prepared for each sample. Coverslips were mounted on slides with Naphrax (refractive index 1.7) and fixed by heating on a hotplate at 130°C for at least 15 minutes.

Diatoms were counted at 0.5 cm intervals for the whole Vydrino shoulder Holocene profile (trigger/piston/gravity cores) using a light microscope (Leitz Laborlux S) with phase contrast and x1250 magnification. At least 300 valves were counted per level and a total of 534 levels make up the Holocene profile. Chrysophyte cysts were also enumerated but not identified. Diatom valves were further assigned a dissolution stage 1, 2 or 3, (1 being pristine and 3 being badly dissolved) which allows the creation of a diatom dissolution index. This is the *F*-Index and consists of the sum of pristine valves divided by the sum of non-pristine valves counted per level (Ryves *et al.* 2003) (equation 6.1), where n_{ij} is the number of pristine valves of species j (of m) counted in a sample i, compared to N_{ij}, the total number of classifiable valves of species j. F varies between 0, all values visibly dissolved and 1, all valves perfectly preserved. Examples of dissolution stages 1 to 3 are shown in figure 6.1 for *A. baicalensis* and *C. minuta.*

Aulacoseira baicalensis

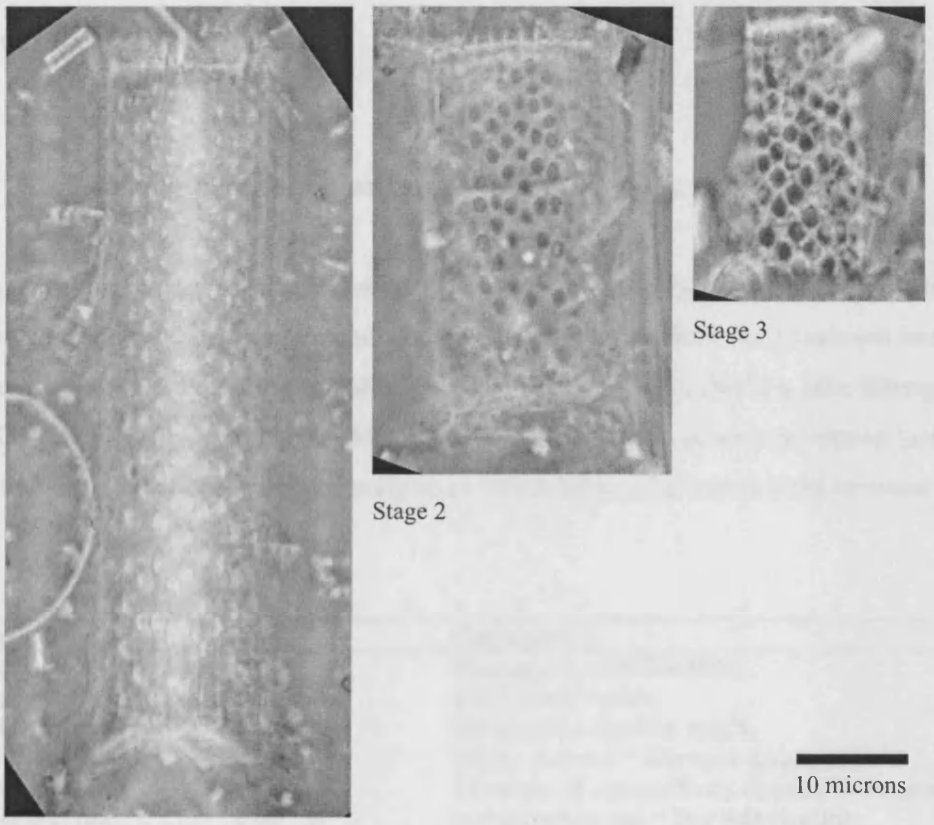

Cyclotella minuta

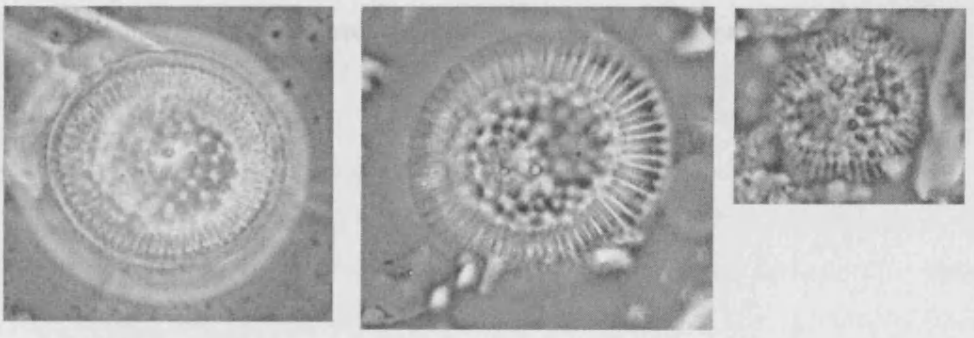

Figure 6.1: Examples of dissolution stages 1 to 3 for *Aulacoseira baicalensis* and *Cyclotella minuta*.

$$F_i = \frac{\Sigma_j^m nij}{\Sigma_j^m Nij}$$

Equation 6.1.

6.2.2 Calculation of diatom concentration, flux and biovolume

The equations were used to calculate diatom concentrations and fluxes are shown in table 6.1. Data for percentage water content and wet bulk density come from the Continent and were measured at the GFZ, Potsdam soon after the cores were opened in 2001 by Jens Klump using a GeoTek multi-sensor core logger (MSCL). These data are at a coarser resolution (intervals of 1.5 to 2 cm) to that of the diatom analysis so values have to be interpolated between points (figure 6.2).

Variable	Unit	Calculation
% water content	%	Measured by GeoTek MSCL
% dry material	%	100-%water content
Wet bulk density	g cm^{-3}	Measured by GeoTek MSCL
Dry bulk density	g cm^{-3}	(% dry material * Wet bulk density)/100
Accumulation rate	cm yr^{-1}	Thickness of sample/Years covered by sample
Dry mass acc. rate	g cm^{-2} yr^{-1}	Accumulation rate * Dry bulk density
Microspheres (MS) added	number	MS conc.*MS weight added
Diatom conc. (wet weight)	10^6 valves g^{-1}	(MSadded*Diatoms counted/MScounted)/sed. weight
Diatom conc. (dry weight)	10^6 valves g^{-1}	(Diatom conc. (wet weight)*100)/%dry material
Diatom species flux	Valves cm^{-2} yr^{-1}	Diatom conc. (dry weight)*diatom %* Dry mass acc. rate

Table 6.1: Calculation of diatom fluxes and concentrations (* means multiply and / divide).

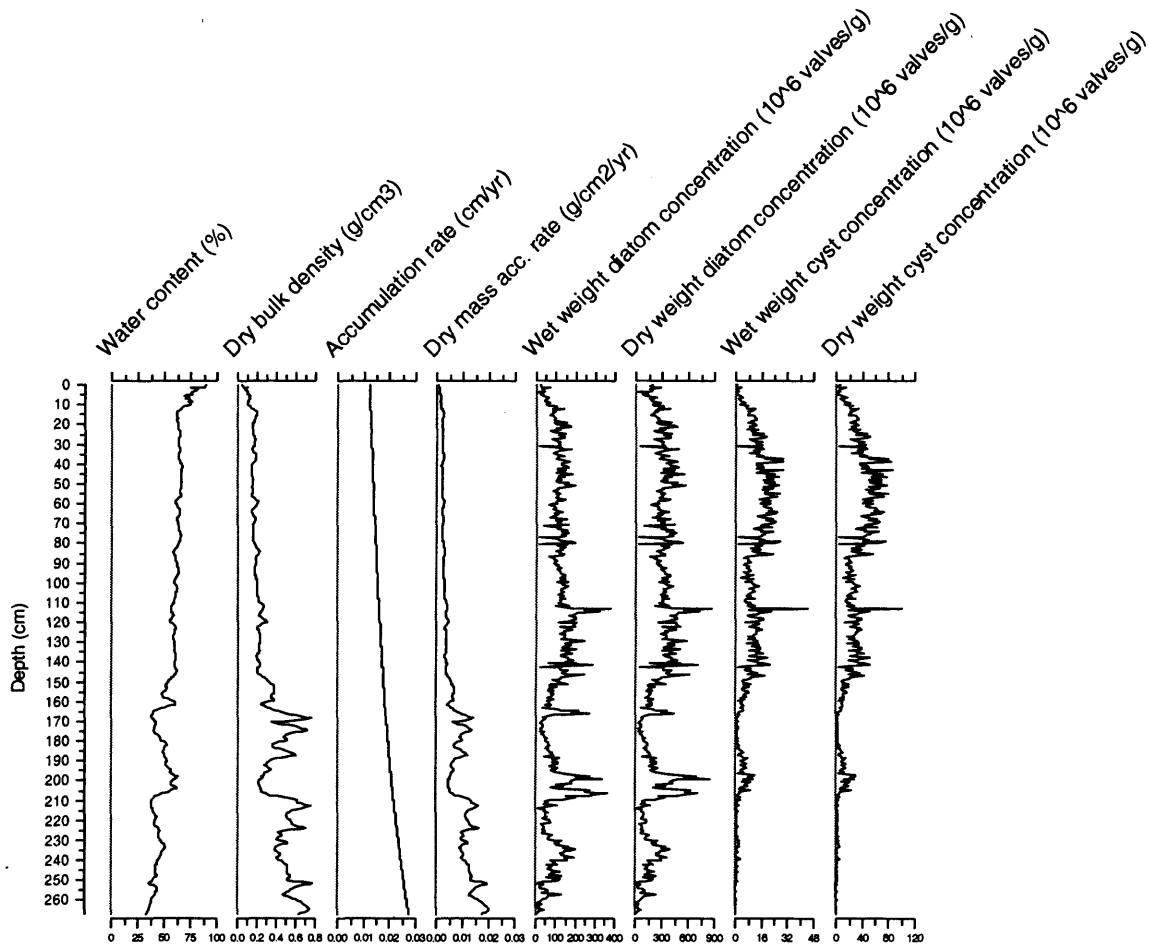

Figure 6.2: Water content, dry bulk density, accumulation rates and diatom and chrysophyte cyst calculations per gram wet weight and per gram dry weight for the Vydrino Shoulder Holocene profile. Equations for calculation given in table 6.1.

For the calculation of biovolumes (μm^3), the estimates from Rioual and Mackay (in press.) for some species were used (table 6.2). For those not estimated in this study, at least 30 valves were measured using a micrometer eyepiece. Although the study of Rioual and Mackay (in press) is based on Eemian diatoms, a comparison to Holocene diatoms confirmed all species of interest have not varied in size. For centric taxa, cell depths were taken as half of the diameter unless measured (Bailey-Watts *et al.* 1989). Mean biovolumes were then calculated for the major planktonic species and multiplied by the diatom cell concentration (valve concentration doubled) to get the biovolume of each species present in a sample. These are expressed as volume divided by one million per gram dry weight ($\mu m^3 \times 10^6 g^{-1}$). Due to the fragmentation of *A. formosa*, the biovolume for this species had to be taken as an average of biovolumes measured by Anderson (1994) in Sweden. It would be too difficult to estimate biovolume for all species due to the large range of benthic species in the record.

Species	Cell biovolume μm^3	Source
Aulacoseira baicalensis	2220	Rioual and Mackay (in press)
Aulacoseira skvortzowii	2570	Rioual and Mackay (in press)
Aulacoseira skvortzowii (spore)	2420	Rioual and Mackay (in press)
Cyclotella minuta	4920	Rioual and Mackay (in press)
Cyclotella ornata	47740	Rioual and Mackay (in press)
Stephanodiscus flabellatus	2350	Rioual and Mackay (in press)
Synedra acus v. radians	1440	Rioual and Mackay (in press)
Stephanodiscus formosus v. minor	185	Rioual and Mackay (in press)
Cyclotella sp #1	208	This study
Cyclotella baicalensis	81502	This study
Cyclotella ocellata	232	This study
Synedra acus v. pusilla	566	This study
Crateriportula inconspicua	602	This study
Hannaea arcus	3853	This study
Cylostephanos dubius	1008	This study
Stephanodiscus skabitchevskyiii	1461	This study
Stephanodiscus parvus	247	This study
Stephanodiscus meyerii	947	This study
Asterionella formosa	650	Anderson (1994)

Table 6.2: Estimated biovolumes of the common diatom taxa in Lake Baikal.

6.2.3 Numerical and graphical methods

Raw diatom counts were stored and converted to percentage abundances in Microsoft Excel 97. For graphical representation and ordinations, only taxa that occurred in any one sample with abundance >5% were included. Diatom diagrams were plotted against both depth and age and were drawn using the stratigraphic plotting software TILIA and TILIA.GRAPH v.2 (Grimm 1991), and in the case of the diatom flux data, the software C2 v.1.3 (Juggins 2003). Excel files were converted into a format acceptable for TILIA and also for CANOCO v.4.5 using WinTran v.1.5 (Juggins 2002).

Diatom diagrams were zoned using constrained incremental sums of squares cluster analysis with the software CONISS (Grimm 1991), with a square root transformation of the percentage data. Clusters were calculated with Edwards Cavalli-Sforza's chord distance. The resultant dendrogram can be plotted with the stratigraphic data in TILIA.GRAPH. Other clustering methods are available but software packages such as Zone v.1.2 (Juggins 1991) that offers a range of clustering methods were unable to process the large dataset used here.

6.2.4 Diatom taxonomy

Figure 6.3 shows light photomicrographs of the most common taxa present in this study, while figure 6.4 shows SEM photomicrographs of selected taxa. The taxonomy of non-endemic diatoms mainly followed the floras of Krammer and Lange-Bertalot (1986-1991)

with the new genus names defined by Round *et al.* (1990). As the diatom flora of Lake Baikal consists predominantly of endemic species (Kozhov 1963), taxonomy and standardisation between studies can be problematic (Flower 1994, Flower *et al.* 1998). Identification was aided by the taxonomic works of Meyer (1930), Skvortzow (1937), Skabitchevskyii (1960), Gleser *et al.* (1988), Khursevich (1989), Genkal and Popovskaya (1990), Foged (1993), Genkal (1993), Nikiteeva and Likhoshway (1994), Kociolek *et al.* (2000) and Reid and Williams (2001) amongst others. The taxonomy of the main planktonic species followed the guidelines of the Lake Baikal diatom taxonomy workshop (Ryves and Flower 1998). The *Cyclotella* species (*minuta/ornata/baicalensis*) were split as follows, according to Flower (1993), although there is still doubt whether these are individual species or morpho-types of the same species. Also, due to dissolution it is sometimes difficult to distinguish between these types. *C. ornata* (figure 6.3a) range from 30 – 80 μm in diameter, the valve is characterised by fine marginal radiating striae occupying one third of the valve face. The central area is undulate and colliculate with a number of clearly visible processes and the rimoportula located near the inner edge. *C. minuta* (figures 6.3b, 6.3c, 6.4a) often appear slightly oval with short marginal striation and a diameter between 11 - 42 μm. The undulating central area has <6 centrally located puncta and a rimoportula located at the inner edge. *C. baicalensis* (figure 6.3d) ranges from 80 - 150 μm in diameter, and have many processes over a slightly undulating face. Again the rimoportula is located at the inner edge of the striated zone.

Characteristics of *Aulacoseira baicalensis* (figures 6.3e, 6.4b) have been given by Babanazrova *et al.* (1996) and are outlined in Ryves and Flower (1998). Cell diameters range from 6 - 37 μm with length 10 - 72 μm and 6.5 – 11 rows of areolae in 10 μm with 3 - 13 areolae per 10 μm. The structure of the velum and girdle bands has been investigated by SEM (Likhoshway *et al.* 1992). *Aulacoseira skvortzowii* (figures 6.3f, 6.4c) has been described by Edlund *et al.* (1996). Vegetative valves are 4.3 – 18.4 μm in diameter with mantles 15.4 – 26.0 μm high and 13.3 – 18.3 striae in 10 μm. This species also forms a bullet shaped resting spore (figures 6.3g, 6.4d), 5.2 – 18.7 μm in diameter and 12.9 – 24.2 μm long. Aerolae on the mantle are distributed with 11.8 – 16.5 striae in 10 μm. *A. baicalensis* can be further split into a square punctae form (figure 6.3h) and also resting stages (figure 6.3i) which are heavily silicified and of length 30 - 40 μm, width 5 μm. The areolar density and the form of linking spines have been shown to be highly variable in *A. baicalensis* and *A. skvortzowii* even within cells of the same filament, while these two species can be morphologically similar in early spring during auxospore production (Babanazarova *et al.* 1996).

Stephanodidcus meyerii (figure 6.3j), was described by Genkal and Popovskaya (1987) with diameter 7.7 – 12.3 μm, 12 – 14 spines/10 μm and 27 - 35 μm areolae/10 μm. This species is synonomous with *Stephanodiscus binderanus* v. *baicalensis* Genkal and Popovskaya used in older publications. One central fultoportula is present with two satellite pores. This species is probably closely related to *Stephanodiscus parvus* (figures 6.3k, 6.3l) (Ryves and Flower 1998). *S. parvus* measures 5 - 11 μm in diameter with 25 – 30 areolae/10 μm and the flat valve face is divided with 13 – 15 costae/10 μm. There is one central fultoportula and one rimoportula with marginal fultoportulae under spines. *Stephanodiscus formosa* v. *minor* Khursevich and Loginova (figure 6.3m, 6.4e) has a diameter of 9 - 16 μm and a structureless central area with only a few processes (Ryves and Flower 1998). *Stephanodiscus flabellatus* (figure 6.3n, 6.4f) was described by Loginova and Khursevich (1986) with a diameter of 22 – 55 μm. Uniseriate striae become multiseriate in the sub-marginal zone. No central processes are observed. A similar species *Stephanodiscus skabitchevskyii* (figure 6.3o) defined by Popovskaya (1966) is often 10 - 20 μm in diameter with a highly undulate valve face. *Crateriportula inconspicua* (figure 6.3p) is closely related to the *Stephanodiscus* genus and was defined by Flower and Håkansson (1994) having a circular slightly concentrically waved surface with a diameter of 6 - 10 μm. The marginal area has short striae and interstriae with 15 – 16 in 10 μm. At the end of each interstria a short spine is present and beneath some a mantle fultoportula occurs.

The species *Synedra acus* was further split in this study into *S. acus* v. *radians* (figure 6.3q), *S. acus* v. *pusilla* (figure 6.3r) and *S. acus* v. *acus* (figure 6.3s) mainly on the basis of size (Ryves and Flower 1998). *S. acus* v. *radians* has length 140 – 290 μm, width 2 –4 μm with 12 – 16 striae in 10 μm. *S. acus* v. *pusilla* has length 140 – 290 μm, width 2 – 2.5 μm and 18 - 22 μm in 10 μm. *S. acus* v. *acus* has a length 90 - 250 μm, width 5 μm and 10 – 22 striae in 10 μm.

Two species that occurred at >5% abundance in at least one sample could not be identified beyond genus level. Firstly *Cyclotella* sp. #1 (figures 6.3t, 6.3u) has a diameter of 5 - 9 μm, a colliculate central area and coarse marginal striae. Further description is complicated by high levels of dissolution. This species may be related to *Cyclotella comensis* Grunow (P. Rioual, pers. comm.). Secondly, *Pennate* sp. #1 (figure 6.3v, 6.3w, 6.3x) is a small (length 5 - 8 μm, width 2 - 3 μm) taxon with coarse striae ~12/10 μm, again identification is complicated by high levels of dissolution. This species appears *Navicula*-like but sometimes appears asymmetric similar to *Gomphonema* species. It was attempted to identify both of these species using SEM but unfortunately suitable examples were unable to be located.

Of the most common cosmopolitan taxa, *Hannaea arcus* (figure 6.3y) is described by Krammer and Lange-Bertalot (1986-1991) as banana shaped of length 15 – 150 μm and breadth 4 - 8 μm with 13 – 16 straiae in 10 μm. *Cyclostephanos dubius* (figure 6.3z) has a broad range in diameter of 4.5 - 35 μm (Krammer and Lange-Bertalot 1986-1991).

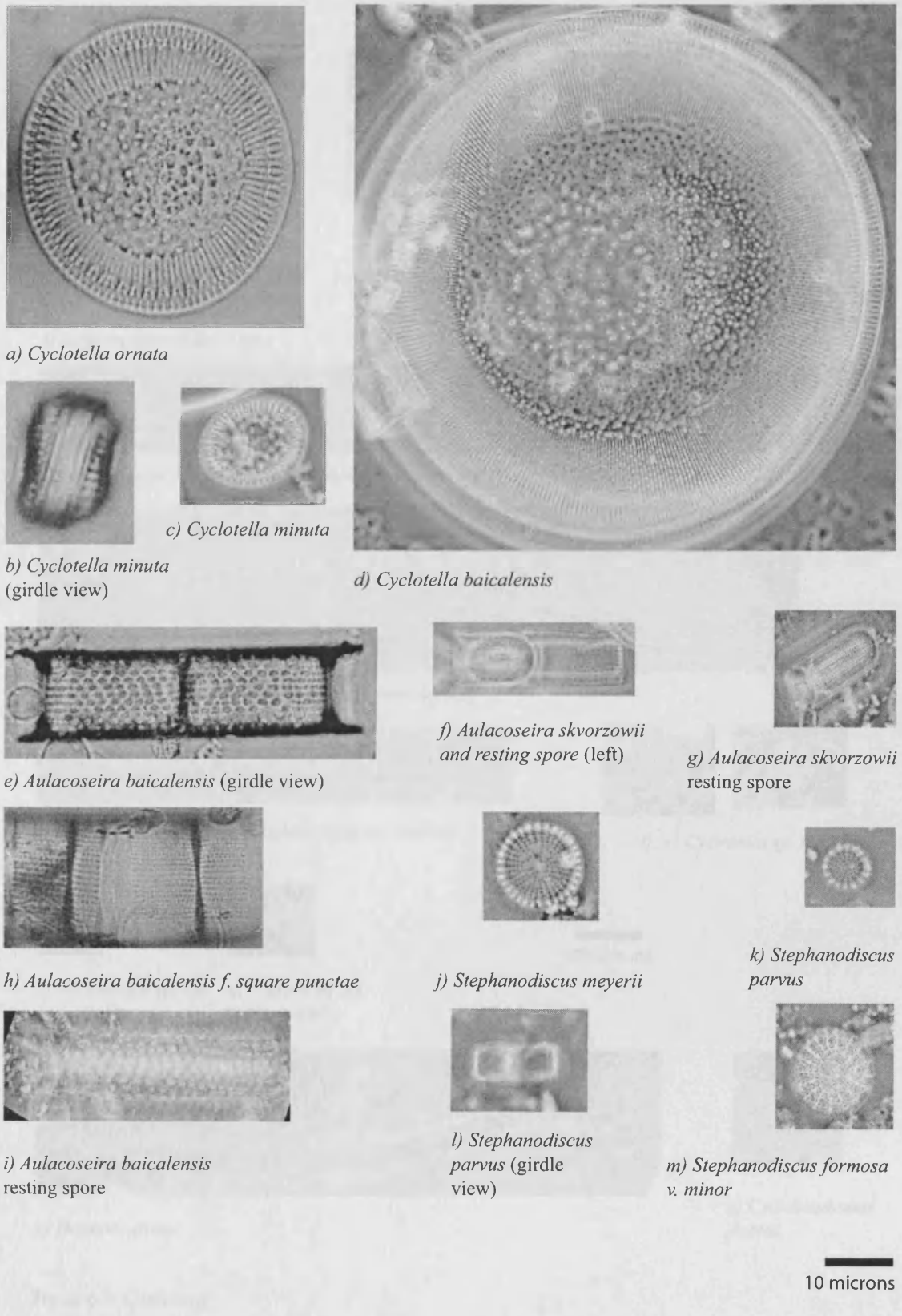

Figure 6.3: LM Photographs of common diatom species found at the Vydrino Shoulder, Lake Baikal

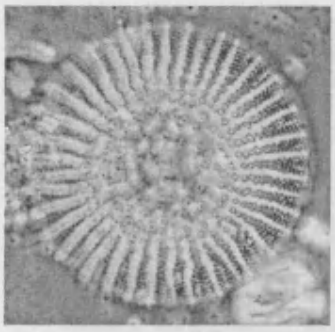

n) Stephanodiscus flabellatus

o) Stephanodiscus skabitchevskyii

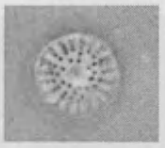

p) Crateriportula inconspicua

q) Synedra acus v. radians (complete valve not shown)

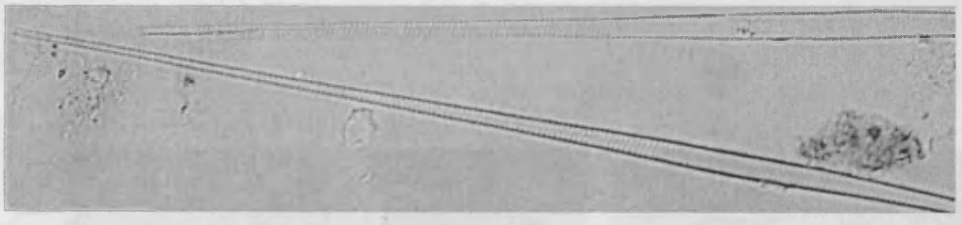

r) Synedra acus v. pusilla (complete valve not shown)

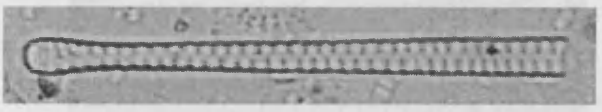

s) Synedra acus v. acus (complete valve not shown)

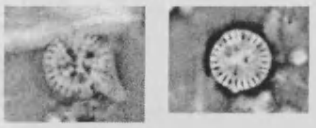

t), u) Cyclotella sp. #1

v), w) Pennate sp. #1

x) Pennate sp. #1 (girdle view)

10 microns

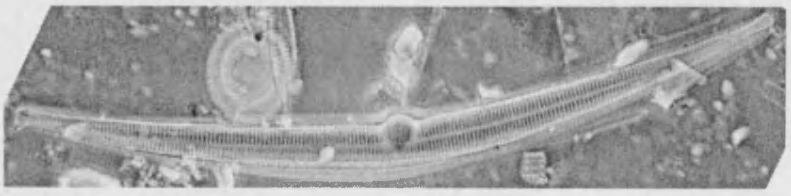

y) Hannaea arcus

z) Cyclostephanos dubius

Figure 6.3: Continued

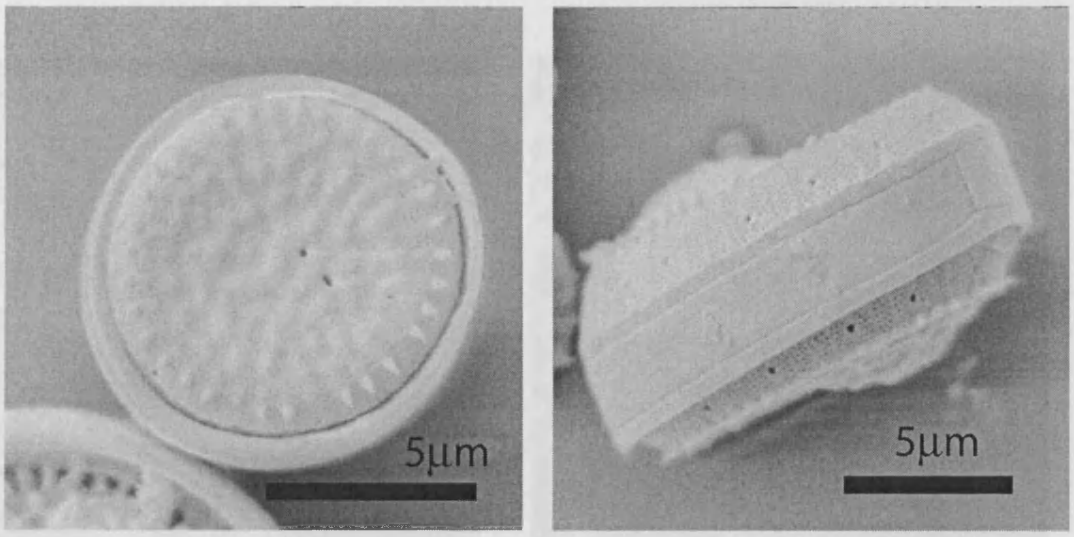

a) *Cyclotella minuta* (valve view) and girdle view (right)

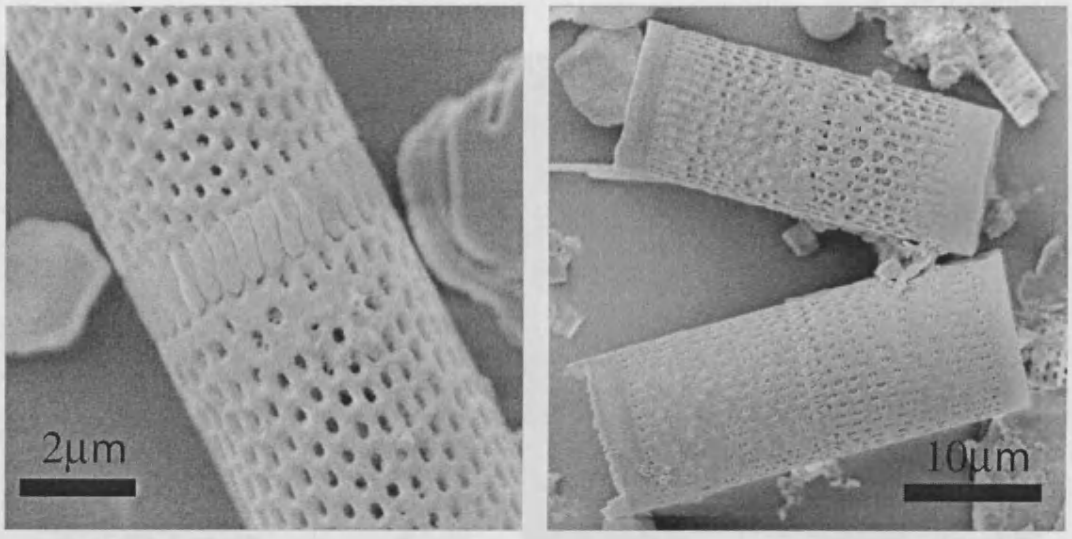

b) *Aulacoseira baicalensis*

Figure 6.4: SEM photographs of some common diatom species found in Lake Baikal.

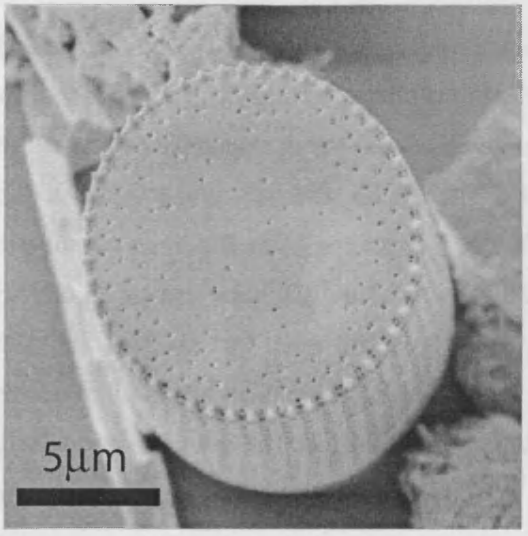

c) *Aulacoseira skvortzowii* (valve view)

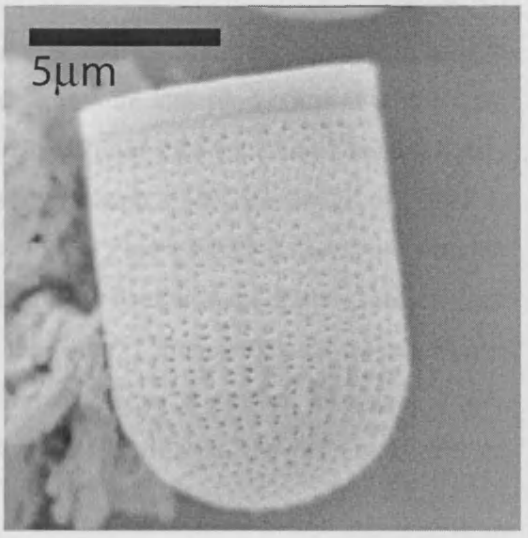

d) *Aulacoseira skvortzowii* resting spore

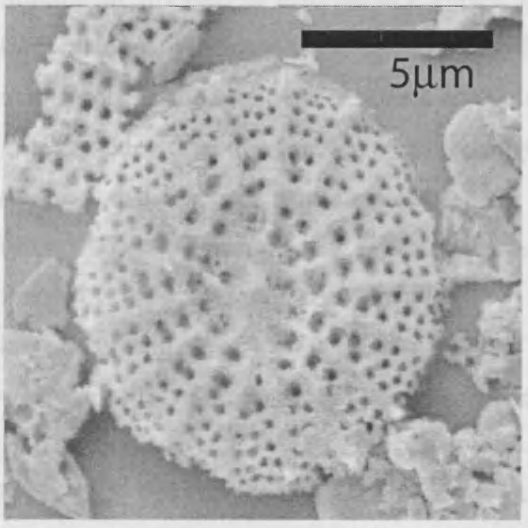

e) *Stephanodiscus formosus* v. *minor*

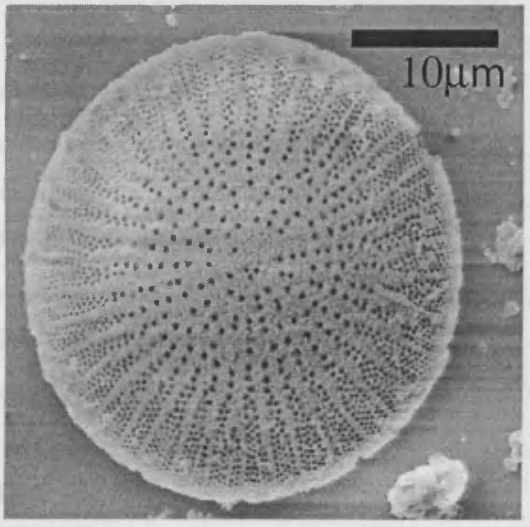

f) *Stephanodiscus flabellatus*

Figure 6.4: Continued

6.3 Results

6.3.1 Diatom percentage abundance, fluxes and biovolumes

Figure 6.5 shows the percentage diatom abundance for species occurring in any one sample with abundance >5% against depth. In total 456 species were identified, most of which were benthic. Also shown on figure 6.5 are diatom and chrysophyte cyst concentrations, PCA axis one and two scores, the ratio of planktonic to benthic diatoms, the percentage of valves at dissolution stage 1, 2 and 3 and the F-index of dissolution. Figure 6.6 is the same diagram but plotted on an age scale. Figure 6.7 shows the diatom flux for the main diatom species (note that this diagram has three different scales for the x-axes). Figure 6.8 shows biovolume estimations for the main species, again there are three different scales for the x-axes. Zones displayed on figures 6.7 and 6.8 are those defined by CONISS on the percentage diatom abundance data.

VYD-D18: 267.0 – 259.0 cm (15700 – 15450 aBP)

Significant amounts of diatoms first appear in this zone, however concentration is relatively low. Planktonic diatoms make up only 50 – 80% of the total assemblage. This assemblage is unique to this zone with species such as *C. ocellata* and *Cyclotella* sp. #1 that do not appear in later zones. The dominant species are *S. flabellatus* reaching a maximum of 27% and *A. formosa* also reaching a maximum of 27%. Other common species include *A. skvortzowii* resting spore, *C. minuta* and *C. inconspicua.* Due to low diatom concentration the actual fluxes of diatoms in this zone are very low. Biovolumes are also low for most species, the largest contributor is *S. flabellatus* supplying 13000 $\mu m^3 x10^6 g^{-1}$. Diatom dissolution is high with over 40% of diatoms classed as poorly preserved (stage 3).

VYD-D17: 259.0 – 250.0 cm (15450 – 15110 aBP)

Diatom concentrations peak slightly in this zone meaning an increase in diatom flux rates, however these are still very low. Throughout this zone, the proportion of *A. skvortzowii* (mostly resting spores) rises to 85%, this is interrupted by an incursion of benthic diatoms at 253 cm. *A. skvortzowii* provides most of the biovolume in this zone with values up to 75000 $\mu m^3 x10^6 g^{-1}$ while *S. flabellatus* also has a high value of 32000 $\mu m^3 x10^6 g^{-1}$, despite making up only around 11% of the total assemblage.

VYD-D16: 250.0 – 229.0 cm (15110 – 14245 aBP)

This zone, marked by a small peak in diatom concentrations reaching 210 $x10^6$ valves g^{-1}, is dominated by *A. skvortzowii* resting spores at a constant proportion of around 80%. The remainder of the assemblage is predominantly made up of benthic diatoms. The flux and biovolume data show this peak to be real and not an artefact of low diatom concentrations. Biovolume production of *A. skvortzowii* spores reaches high values of 40300 μm^3 $x10^6$ g^{-1} while fluxes are also very high at around 2.2 valves $x10^6$ cm^2 yr^{-1}. Dissolution in this zone is lower with more fewer diatoms classed as highly dissolved (stage 3).

VYD-D15: 229.0 – 209.0 cm (14245 – 13355 aBP)

In relative terms, the peak in *A. skvortzowii* declines gradually over zone VYD-D15 to an abundance of around 50%. However, as diatom concentration declines rapidly over the zone boundary, fluxes are relatively low for the whole zone at around 0.5 valves $x10^6$ cm^2 yr^{-1} and correspondingly biovolume also falls in a similar manner. Diatom productivity is low over this period and as the importance of *A. skvortzowii* becomes less, the proportion of benthic diatoms increases.

VYD-D14: 209.0 – 204.5 cm (13355 – 13145 aBP)

This short zone is marked by a peak in diatom concentration to 710 $x10^6$ valves g^{-1} and an increase in planktonic diatoms to around 85% of the total. Proportions of *A. skvortzowii* decline to less than 5% and *S. flabellatus* disappears from the record while the assemblage is now dominated by the first occurrence of *S. acus* v. *radians* at 40%. *C. inconspicua* is also present at around 20% with a large peak in flux, while isolated peaks of Pennate sp. #1, *S. acus* v. *pusilla* and *S. acus* v. *acus* occur. At the end of the zone, a peak in *A. formosa* to 24% is present. Diatom flux is high in this zone while the greatest amount of biovolume is supplied by *S. acus* v. *radians* at 206000 μm^3 $x10^6$ g^{-1}. Chrysophyte cyst concentrations begin to rise in this zone for the first time.

VYD-D13: 204.5 – 199.0 cm (13145 – 12885 aBP)

A sharp decline in diatom concentrations (to 230 $x10^6$ valves g^{-1}) and a return to an assemblage similar to that of zone VYD-D15 characterises this short zone. The dominant species again is *A. skvortzowii* spores with a peak relative abundance of 34%, while *C.*

inconspicua remains abundant at around 20%. Biovolume levels in this zone are very low. Towards the end of the zone diatom, concentrations begin to increase along with levels of *S. acus* v. *radians*.

VYD-D12: 199.0 – 194 .0cm (12885 – 12640 aBP)

With a similar duration as VYD-D13 and D14, this zone marks a return to very high diatom concentrations (860 x10^6 valves g^{-1}). *A. skvortzowii* all but disappears from the record and is replaced by *S. acus* v. *radians* reaching peak abundance at 70%, *A. baicalensis* also becomes co-dominant near the end of the zone rising to 41% from a baseline level of 5 – 15% over the whole record. Diatom flux through this period is high, deposition of *S. acus* v. *radians* reaches 3.0 valves x10^6 cm^2 yr^{-1} while biovolume is also very high with a maximum of 430000 μm^3 x10^6 g^{-1} contributed by *S. acus* v. *radians* and 208000 μm^3 x10^6 g^{-1} by *A. baicalensis*. Towards the end of the zone, diatom concentration declines to levels similar to those of the preceding zone.

VYD-D11: 194.0 – 184.0 cm (12640 – 12150 aBP)

Low diatom concentrations (90 - 240 x10^6 valves g^{-1}) and a sharp increase in *A. skvortzowii* to around 35% with a corresponding decline of *S. acus* v. *radians* and *A. baicalensis*, define this zone. Both biovolume and fluxes are low, while there is an increase in benthic diatom abundance from around 20% to 30% of the total assemblage. The benthic diatom *H. arcus* also occurs with abundances of approximately 5% throughout the zone.

VYD-D10: 184.0 – 166.0 cm (12150 – 11210 aBP)

Similar conditions to those in VYD-D15 are present in this zone. Fluxes and diatom concentrations reach very low values (34 x10^6 valves g^{-1}). *S. flabellatus* returns to the assemblage, albeit at less than 5%, while proportions of *S. acus* v. *radians* and *C. inconspicua* decline to under 5% and 10% respectively. The dominant species is *A. skvortzowii* spore with proportions in the early part of the zone around 70%, declining to below 50% by the end of the zone. In absolute terms however, this peak is small, with relatively low maximum flux at 0.6 valves x10^6 cm^2 yr^{-1}. Diatom dissolution increases in this zone with up to 81% classed as badly preserved (stage 3). An increase in benthic diatoms (41%) also coincides with the period of lowest total diatom concentrations.

VYD-D9: 166.0 – 161.0 cm (11210 – 10940 aBP)

This zone defines a short-lived peak in diatom concentration to 448 $x10^6$ valves g^{-1} and an associated peak in *A. formosa* (26%). The first part of this zone has a peak in relative abundance of *S. acus* v. *radians* to 33%, it is replaced by a peak of *A. skvortzowii* (45%) which is subsequently replaced by another similar peak of *S. acus* v. *radians* (35%). *C. inconspicua* rises from below 5% to around 20%. In terms of flux data, only the peak *A. formosa* and the first peak of *S. acus* v. *radians* seem to be significantly large, due to low diatom concentrations in the later part of the zone. Biovolumes are low for this zone for most species, the greatest contribution being from the first peak of *S. acus* v. *radians, C. inconspicua* and *A. formosa.*

VYD-D8: 161.0 – 147.0 cm (10940 – 10165 aBP)

Throughout this zone, both diatom and chrysophyte cyst concentration consistently rise, while the proportion of *A. skvortzowii* declines from 40% to around 10% by the end of the zone. Although highly variable, the relative abundance of *C. inconspicua* is high at approximately 20%. There is also the first significant appearance and gradual rise of the planktonic species *C. dubius* (maximum of 27%), *S. skabitchevskyii* (<9%) and *C. minuta* (maximum of 19%). High proportions of the benthic *H. arcus* are also present with a peak (35%) in the early stage of the zone. Diatom fluxes are highest towards the end of the zone while biovolumes remain relatively constant with the exception of a peak marked by *H. arcus* (144000 $\mu m^3 x10^6 g^{-1}$).

VYD-D7: 147.0 – 117.0 cm (10165 – 8390 aBP)

Higher diatom concentrations and fluxes occur throughout this zone. The decline of *A. skvortzowii* spores continues and levels are now below 10%, although according to flux data the amounts are similar to those of the previous zone. Several species are co-dominant including *C. inconspicua, A. baicalensis, S. acus* v. *radians* and *C. minuta* all with abundances at approximately 20%, while *H. arcus, C. dubius* and *S. skabitchevskyii* are still present, the latter peaking at the end of the zone at 23%. Biovolume levels are higher in this zone than in previous zones with *A. baicalenisis* and *S. acus* v. *radians* providing the greatest amounts. Total biovolume of measured species reaches 800000 $\mu m^3 x10^6 g^{-1}$ by the end of the zone.

VYD-D6: 117.0 – 86.5 cm (8390 – 6425 aBP)

At the beginning of this zone a large peak in diatom concentration occurs to 860 $x10^6$ valves g^{-1}. Subsequently, fluxes are high in the early part of the zone, especially for *C. inconspicua* which rises from 0.2 to 1.0 valves $x10^6$ cm^2 yr^{-1} while flux declines towards the end of the zone. Total biovolume also decreases towards the end of the zone. The most noticeable assemblage shift is the almost total disappearance of *S. acus* v. *radians* and *S. skabitchevskyii* with an increase in proportion of *A. skvortzowii* spore to around 20% and *C. inconspicua,* of which abundance is highly variable. As in the preceding zone, *C. minuta* seems to show lower abundance towards the start and end of the period, and peaks around 20%. Preservation also begins to rise near the end of the zone with around 33% of diatoms classed as stage 3 rather than 60% at the start.

VYD-D5: 86.5 – 68.5 cm (6425 – 5190 aBP)

Biovolume values are high in zone VYD-D5 reaching upwards of 900000 μm^3 $x10^6$ g^{-1}, although this is highly variable. This variation is caused by a couple of large shifts in diatom concentration from values as low as 31 $x10^6$ valves g^{-1}, up to 470 $x10^6$ valves g^{-1}. *C. minuta* shows a marked increase in relative abundance through this zone from 10% up to 35%. *S. acus* v. *radians* returns to the assemblage from 0% up to 25% and *S. skabitchevskyii* also returns with abundances not exceeding 13%. *C. inconspicua* shows a marked decline from 30%, to a baseline of around 5%. *A. skvortzowii* also declines to below 10%. Preservation begins to improve with an increase in pristine valves from 0 to 10%.

VYD-D4: 68.5 – 35.5 cm (5190 – 2790 aBP)

Diatom concentrations and fluxes remain relatively high, while an increase in total measured biovolume towards the end of the zone to around 10000000 μm^3 $x10^6$ g^{-1} occurs. This is mainly due to the increasing abundance of the large *C. minuta, C. ornata* and *C. baicalensis.* The dominant species at the start and end of the zone is *C. minuta,* reaching 51% but declining to 13% near the zone middle. At this point, *S. acus* v. *radians* becomes dominant with an abundance of 45%. This alternation in species is also apparent in the flux data. *S. parvus* makes its first appearance in the record with some scattered peaks not exceeding 15%, while both *A. skvortzowii* and *C. dubius* decline to near zero values. Chrysophyte cyst concentration reaches a maximum for the record at 86 $x10^6$ cysts g^{-1}.

VYD-D3: 35.5 – 24.5 cm (2790 – 1950 aBP)

Overall diatom concentration begins to fall, but biovolume production remains high due to the abundance of *C. minuta* and *C. ornata,* with maximum abundance of 64% and 7% respectively. Biovolume production of *C. minuta* alone, exceeds 600000 $\mu m^3 x10^6 g^{-1}$. *S. acus* v. *radians* continues its decline and is not present at the zone end. *S. parvus* is the only other significant planktonic diatom, peaking from 5% to 43% with maximum flux of 0.13 $x10^6$ valves $x10^6 cm^2 yr^{-1}$. However maximum flux of this diatom occurred in zone VYD-D4 (0.20 valves $x10^6 cm^2 yr^{-1}$) where proportional abundance was lower. Diatom preservation increases markedly from around 10% to around 45% of diatoms being classed as pristine.

VYD-D2: 24.5 – 10.0 cm (1950 – 810 aBP)

This zone sees the dominance of *C. minuta* with abundances in excess of 70% and also *C. ornata* at a maximum of 15%. As a result total biovolume reaches its highest levels of 20000000 $\mu m^3 x10^6 g^{-1}$ with *C. minuta* and *C. ornata* contributing the most to total biovolume at this point. *C. baicalensis* also contributes greatly to this despite its low relative abundance. Total diatom concentrations and flux of diatoms are in decline throughout this zone. There is an almost total disappearance of other planktonic species such as *A. skvortzowii, A. baicalensis, S. acus* v. *radians* and *S. parvus.*

VYD-D1: 10.0 – 0.0 cm (810 – -50 aBP)

Diatom concentration continues to decline up to the modern surface sediments to 189 $x10^6$ valves g^{-1}, while biovolumes also decline to values below 5000000 $\mu m^3 x10^6 g^{-1}$. The abundance of *C. minuta* falls to between 20 – 30%, while there is a noticeable rise in *A. baicalensis* from near zero values to around 30%, *A. skvortzowii* also returns with an abundance of 10 – 15% and *S. acus* v. *pusilla* returns at low abundance. *Stephanodiscus meyerii* appears for the first time in the record peaking with 21% but declining to 3% at the surface. The assemblage is over 90% planktonic with over 40% of valves classed as pristine. Due to low diatom concentration and the decline of the large *Cyclotella* sp. both fluxes and biovolumes are lower.

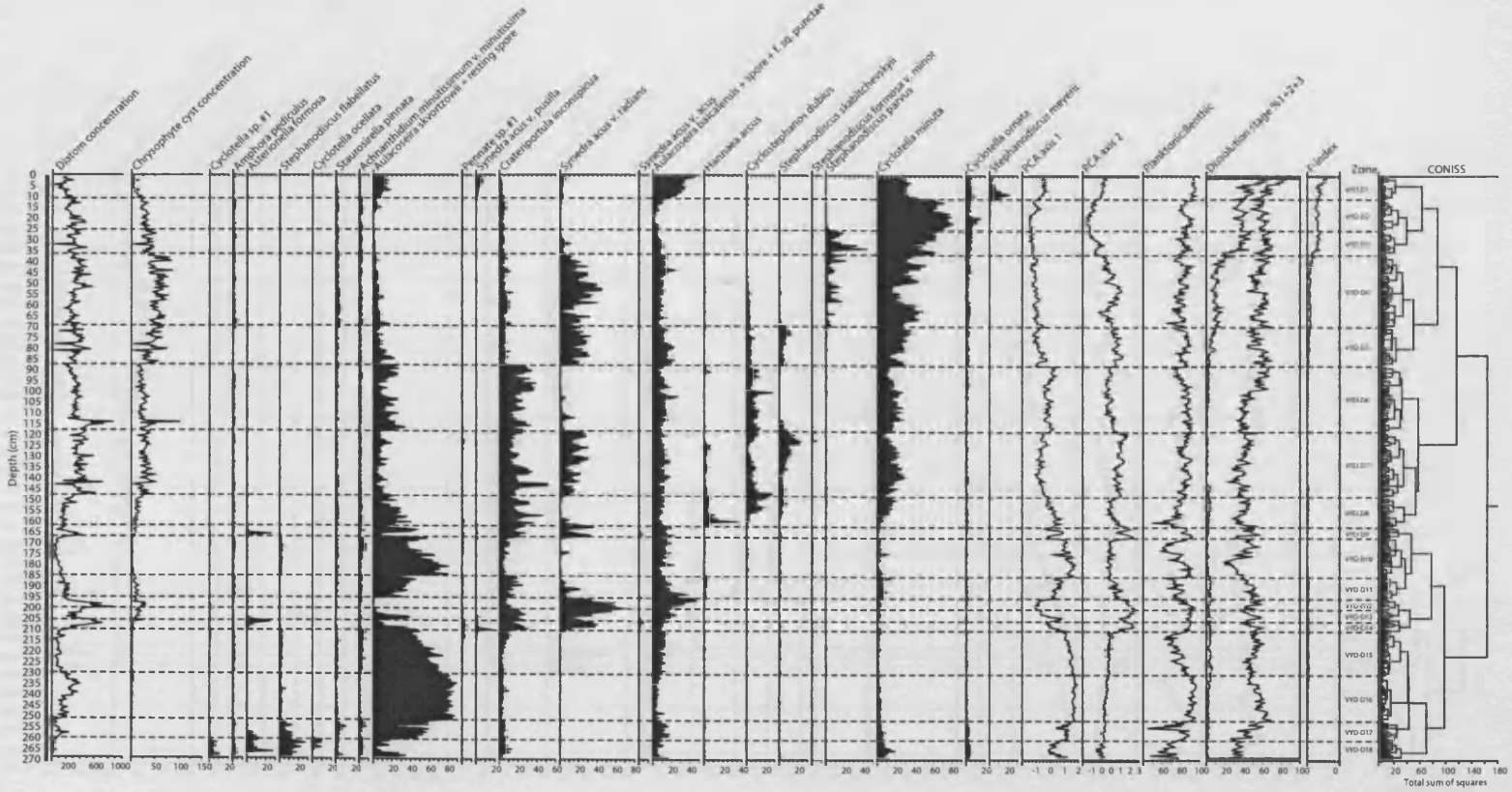

Figure 6.5: Percentage diatom abundance (Vydrino Shoulder, Lake Baikal) plotted against depth (cm) and zoned according to CONISS. Also shown are diatom and chrysophyte cyst concentrations ($x10^6$), PCA axis 1 and 2 scores (SD units), planktonic:benthic ratio, percentage dissolution stage and F-index.

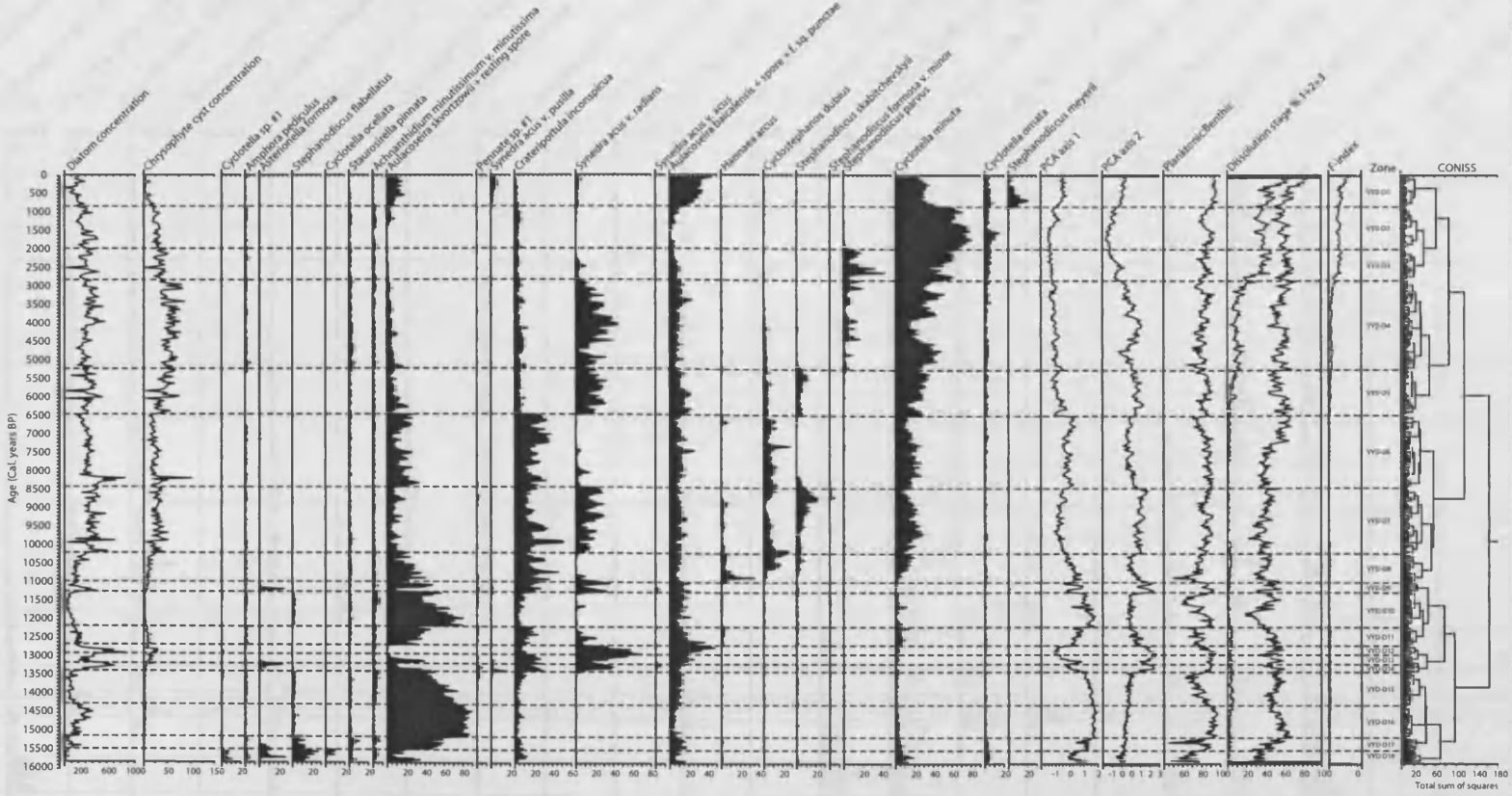

Figure 6.6: Percentage diatom abundance (Vydrino Shoulder, Lake Baikal) plotted against age (cal. aBP) and zoned according to CONISS. Also shown are diatom and chrysophyte cyst concentrations (x10^6), PCA axis 1 and 2 scores (SD units), planktonic:benthic ratio, percentage dissolution stage and F-index.

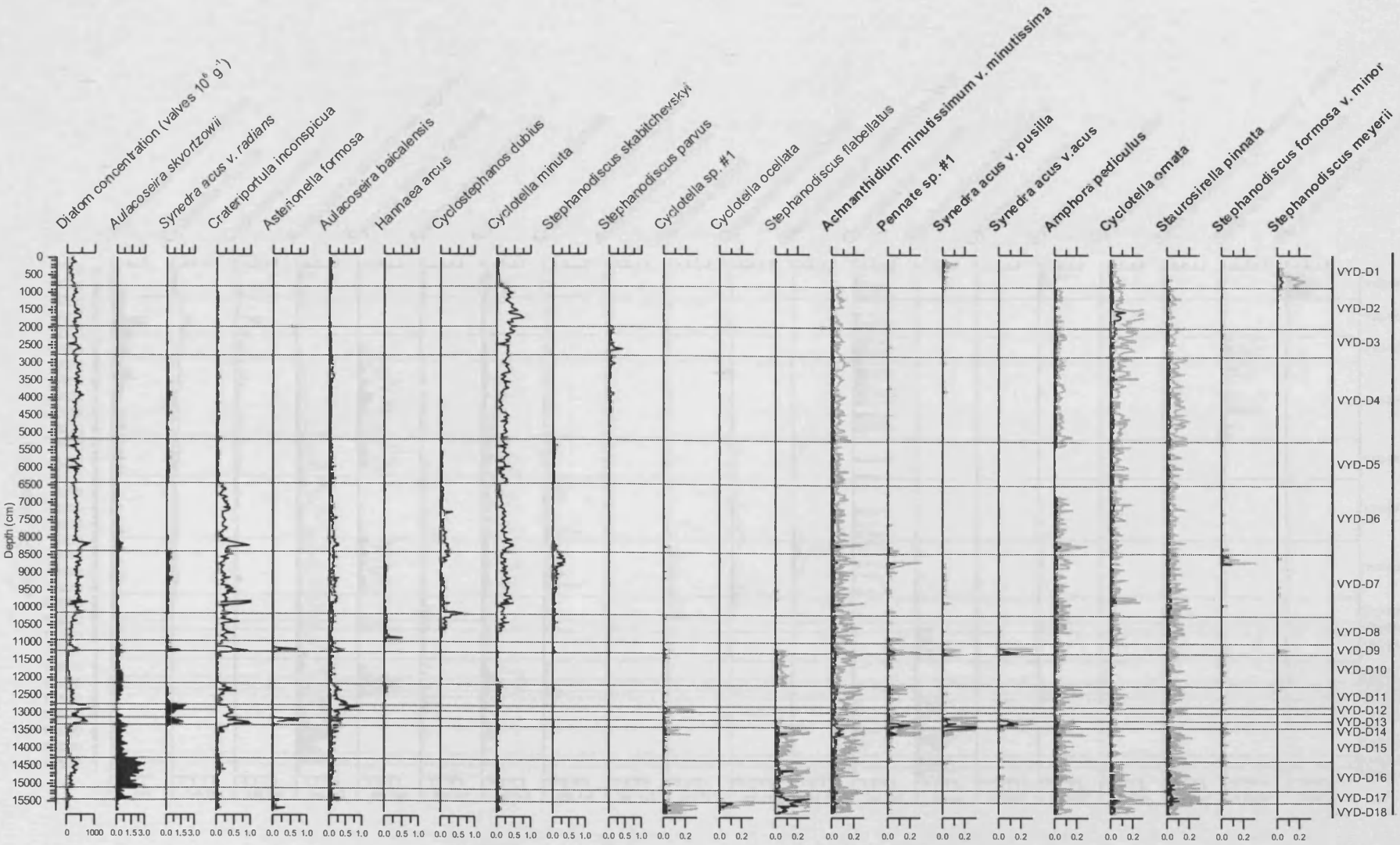

Figure 6.7: Flux of diatom species (x10^6 Valves cm^2 yr^{-1}) for species occuring with abundance >5% in any one sample plotted against age (cal. aBP). Note that the axes are on different scales. Graphs with a black fill have an upper limit of 3 x10^6 Valves cm^2 yr^{-1}, graphs with no fill have an upper limit of 1 x10^6 Valves cm^2 yr^{-1} and graphs with a gray fill have an upper limit of 0.3 x10^6 Valves cm^2 yr^{-1}. An exageration line (five times) is also shown.

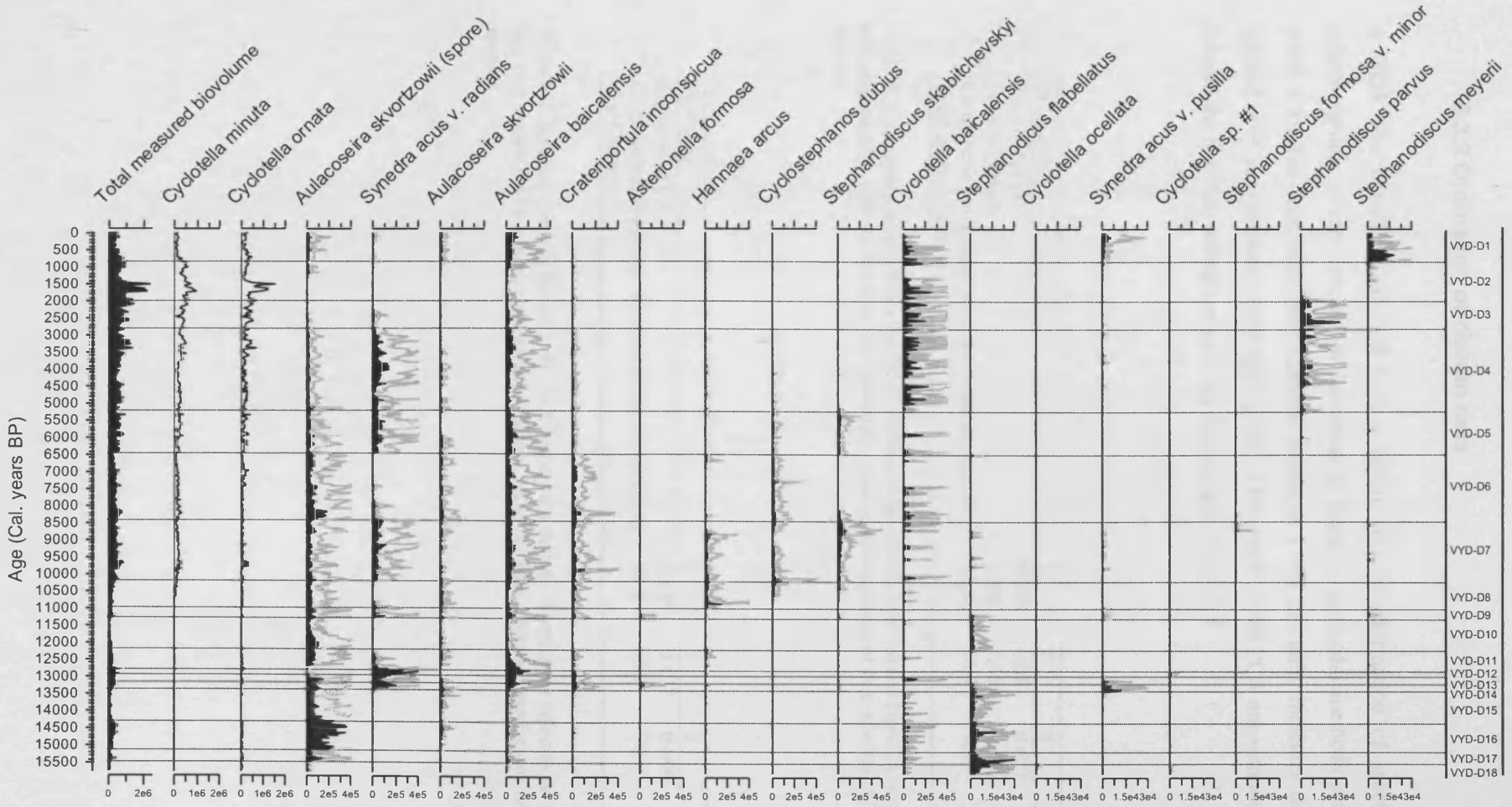

Figure 6.8: Estimated biovolume per sample in μm^3 for the main species occuring in the profile plotted against age (cal. aBP). Note that the axes are on diferent scales. Graphs with no fill have an upper limit of 2×10^6 μm^3, graphs with a black fill have an upper limit of 4×10^5 μm^3 while graphs with a gray fill have a limit to 3×10^4 μm^3. An exageration line (five times) is also shown.

6.3.2 Ordination of diatom data

A DCA was initially conducted with a square root transformation of species data and downweighting of rare species, to determine if linear or unimodal methods should be used (table 6.3). The relatively short gradient length of 1.999 SD units indicates that the linear method of PCA is probably most appropriate. The results of the PCA are summarised in table 6.4 and the first two ordination axes are displayed in figure 6.9.

DCA axis	1	2	3	4
Eigenvalue (λ)	0.213	0.087	0.077	0.052
Gradient length	1.999	1.452	1.692	1.511
Cumulative percentage variance of the species data	25.8	36.4	45.7	51.9
Total inertia, 0.826				

Table 6.3: Summary results from the DCA of percentage diatom abundances (species occurring >5% in any one sample) with square root transformation and downweighting of rare species. 534 samples, 23 species.

PCA axis	1	2	3	4
Eigenvalue (λ)	0.425	0.177	0.099	0.058
Cumulative percentage variance of the species data	42.5	60.2	70.1	75.9
Total inertia, 1				

Table 6.4: Summary results from the PCA of percentage diatom abundances (species occurring >5% in any one sample) with square root transformation, focus on inter-species correlations and centring by species.

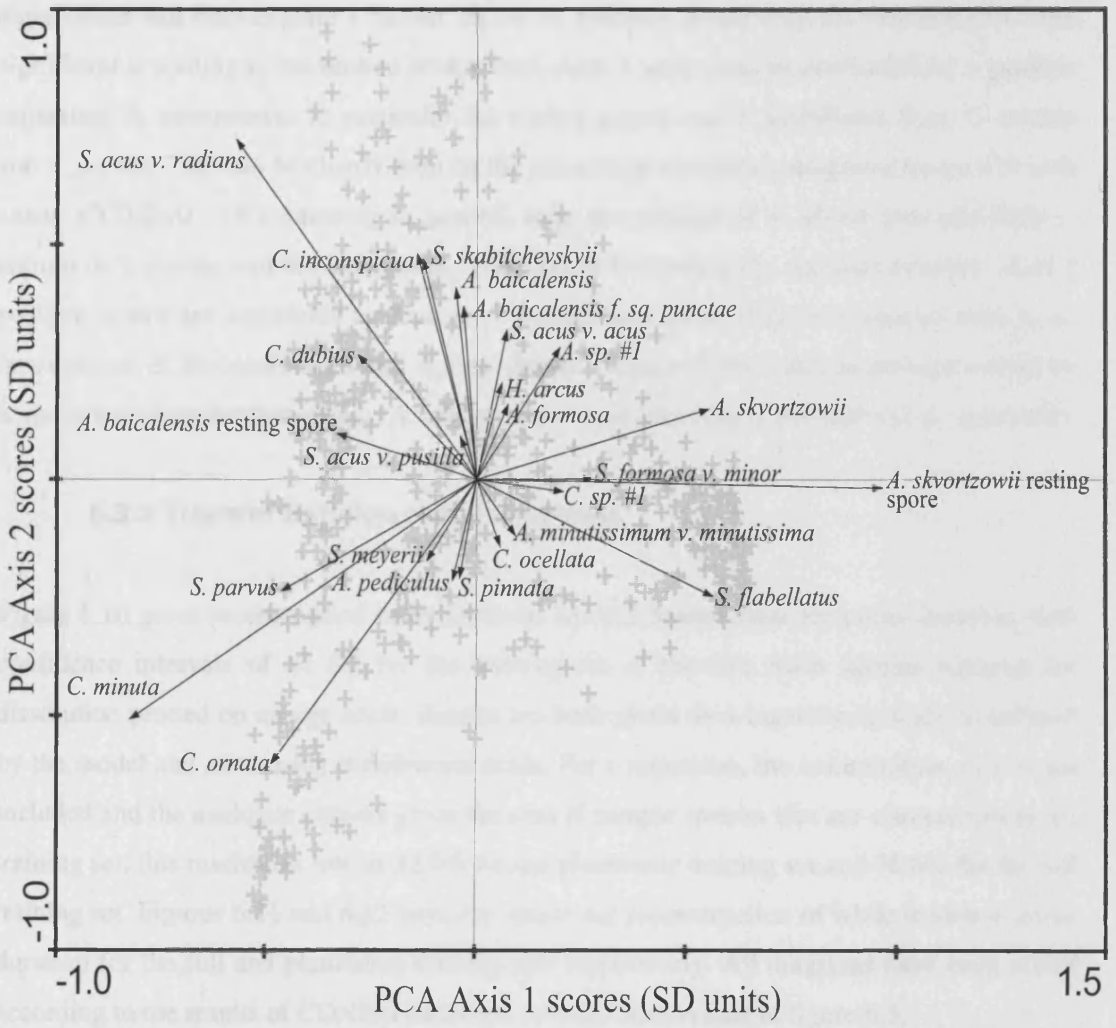

Figure 6.9: PCA biplot of the axis 1 vs. axis 2 scores for the 534 samples and 23 diatom species appearing >5% in any one sample. Points and arrows represent samples and species respectively. Species data was square root transformed with focus on inter-species distances and the graph is centred by species.

PCA axis 1 captures 42.5% of the species variation in the data, while axis 2 captures 17.7%, in total axis 1 and 2 represent 60.2% of total variation. Axes 3 and 4 have relatively small eigenvalues and only explain a further 15.7% of variance, while only the first three axes are significant according to the broken stick model. Axis 1 appears to be dominated by a gradient separating *A. skvortzowii,* in particular the resting spores and *S. flabellatus* from *C. minuta* and *S. parvus*. This can be clearly seen on the percentage abundance diagram (figure 6.6) with zones VYD-D10 - 18 containing in general, large proportions of *A. skvortzowii* and little *C. minuta* or *S. parvus* and the later zones, VYD-D1 to D4 having the opposite situation. Axis 2 positive scores are associated to *S. acus* v. *radians* and other planktonic species such as *C. inconspicua, S. skabitchevskyii* and *A. baicalensis*. Negative axis 2 scores are represented by *S. meyerii* and the benthic species *A. minutissium* v. *minutissima, S. pinnata* and *A. pediculus*.

6.3.3 Transfer function reconstructions

Figure 6.10 gives reconstructed snow depth on ice and annual clear ice cover duration, with confidence intervals of ±1 SE for the training set of the five main species adjusted for dissolution plotted on an age scale. Results are both given on a logarithmic scale as inferred by the model and an anti-log transformed scale. For comparison, the main diatom species are included and the analogue column gives the sum of sample species that are also present in the training set, this reaches as low as 32.0% for the planktonic training set and 36.6% for the full training set. Figures 6.11 and 6.12 have the additional reconstruction of white ice/snow cover duration for the full and planktonic training sets respectively. All diagrams have been zoned according to the results of CONISS on the percentage diatom data in figure 6.5.

Results for the reconstructions based on the training set of the five main dissolution corrected species may only give reliable inferences in the Late Holocene zones VYD-D1 to D3 (Mackay *et al.* in press). In these zones the main species in the training set are also present in the core, in older sections these species become less important (in particular the disappearance of *S. meyerii*) and other species (either not in the training set or rare) actually become dominant. For example, *S. flabellatus* and *S. skabitchevskyii* are not present in the training set while *C. dubius* and *C. inconspicua* are rare. For this reason it is an oversimplification just to rely on five diatom species. As a result, inferences from the full and planktonic models that include much more of the species variability will be more suitable for longer term reconstructions. Even though transfer functions give quantitative results, the large errors and uncertainties involved in such an approach makes a qualitative interpretation more

appropriate. For example, an assessment of increasing or decreasing snow depths rather than an absolute change in snow depth.

The full and planktonic models give very similar results and will be discussed together. The main difference is a higher low amplitude variability over the general trend in the full training set, due to the greater number of species used. Inferences in the earliest zones (VYD-D18 and D17) are complicated by the presence of species that have no analogue in the modern environment (*C. ocellata, C.* sp. #1 and *S. flabellatus*). Through zones VYD-D16 and D15, relatively deep snow cover is predicted but also the highest values of clear ice, cover duration and low duration of white ice/snow cover. The duration of clear ice cover declines through zone VYD-D15. Overall, the reconstructed clear ice duration displays a marked similarity to the abundance of *A. skvortzowii,* mainly due to this species being almost exclusively present in this section of the core. The series of short zones VYD-D14 to D11 show oscillations in the reconstructed variables. Beginning in VYD-D14 there is a much reduced snow depth and white ice/snow duration, while clear ice cover duration increases. VYD-D13 sees a return to deeper snow and shorter clear ice cover, while VYD-D12 has conditions similar to those of VYD-D14. Zones VYD-D11 to D10 record a gradual deepening of the lake's snow cover, while the duration of white ice/snow cover also returns to higher values, however the period of clear ice cover also rises to a longer duration. The Early to Mid Holocene is represented by zones VYD-D9 to D6, the predominant change is a shift to inferred lower snow depths but also to very low durations of clear ice cover, while white ice/snow cover duration remain relatively constant. Possible limitations with these results are again the lack of analogues. Although, *S. skabitchevskyii* is the main species totally absent from the training sets, abundant species such as *C. dubius* and *C. inconspicua* have very low abundance in the training set (figure 6.6) or in the case of *S. acus* v. *radians,* have a very poor distribution over the environmental gradients (figure 5.22). Zones VYD-D5 and D4 display an increased snow depth with a further decrease in clear ice duration, while the duration of white ice/snow cover becomes highly variable, this variability appears to be driven by the abundance of. *S. acus* v. *radians.* The disappearance of *A. skvortzowii* from the record also sees an inferred duration of clear ice cover to zero days in VYD-D3, while white ice/snow cover increases to its highest values. VYD-D2 has a slightly deeper snow depth and longer white ice/snow duration than VYD-D1. Results from the five corrected species training set infers low clear ice cover during VYD-D2 increasing into VYD-D1, coinciding with an initial reduction in snow depth that rises again towards the end of the record.

In summary, the high species variability of the record and either no-analogue situations or poor analogue situations in sections of the profile, make reconstruction of climatic variables

problematic. Although this method gives an interesting summary of the data it may be more appropriate to interpret the record on the basis of the autecological information summarised in chapter 5.

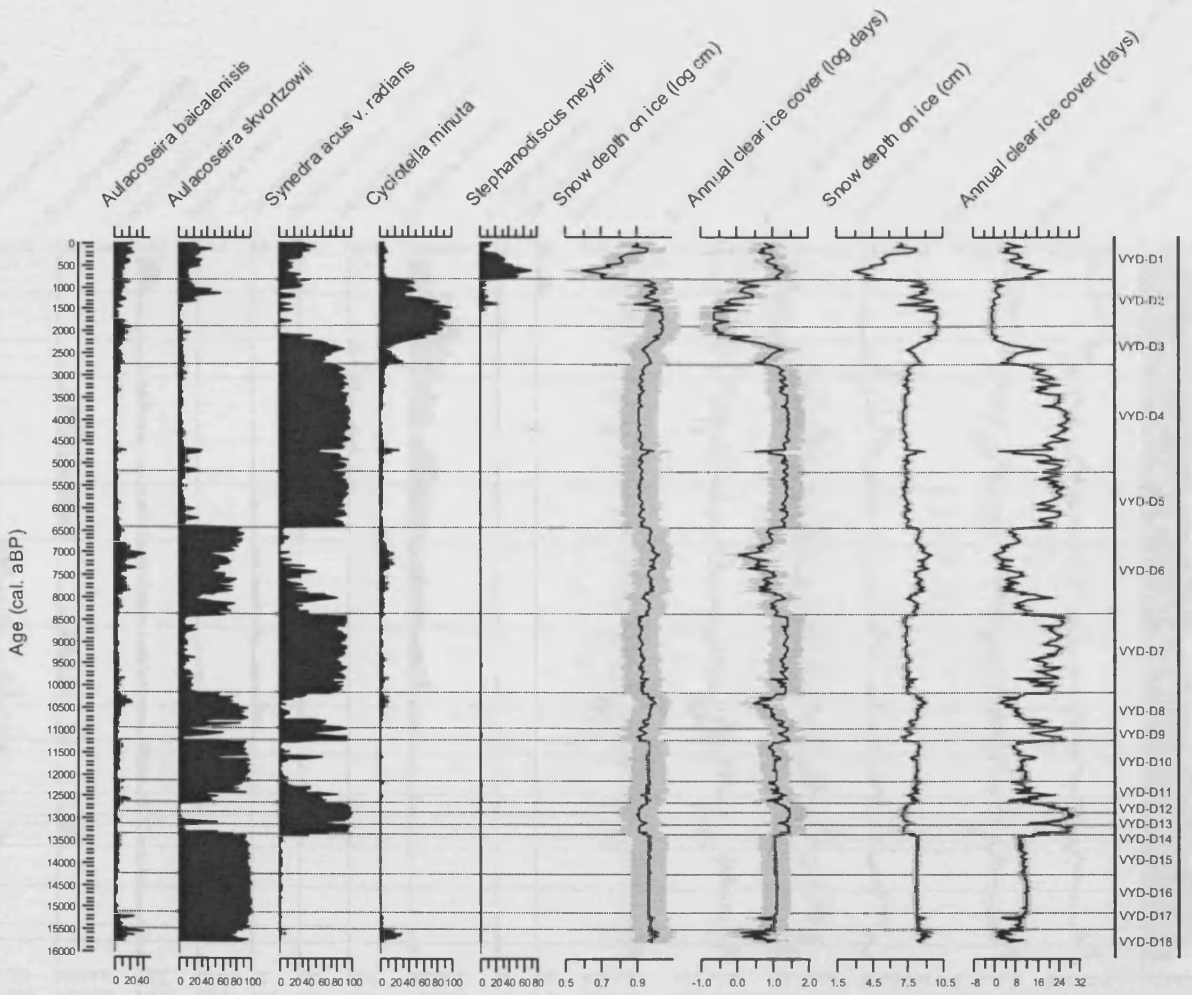

Figure 6.10: Reconstructed snow depth on ice and annual clear ice cover and error +/- 1 SD against age (cal. aBP) for the training set of the five main species adjusted for dissolution. Results are given as log transformed and anti-logged.

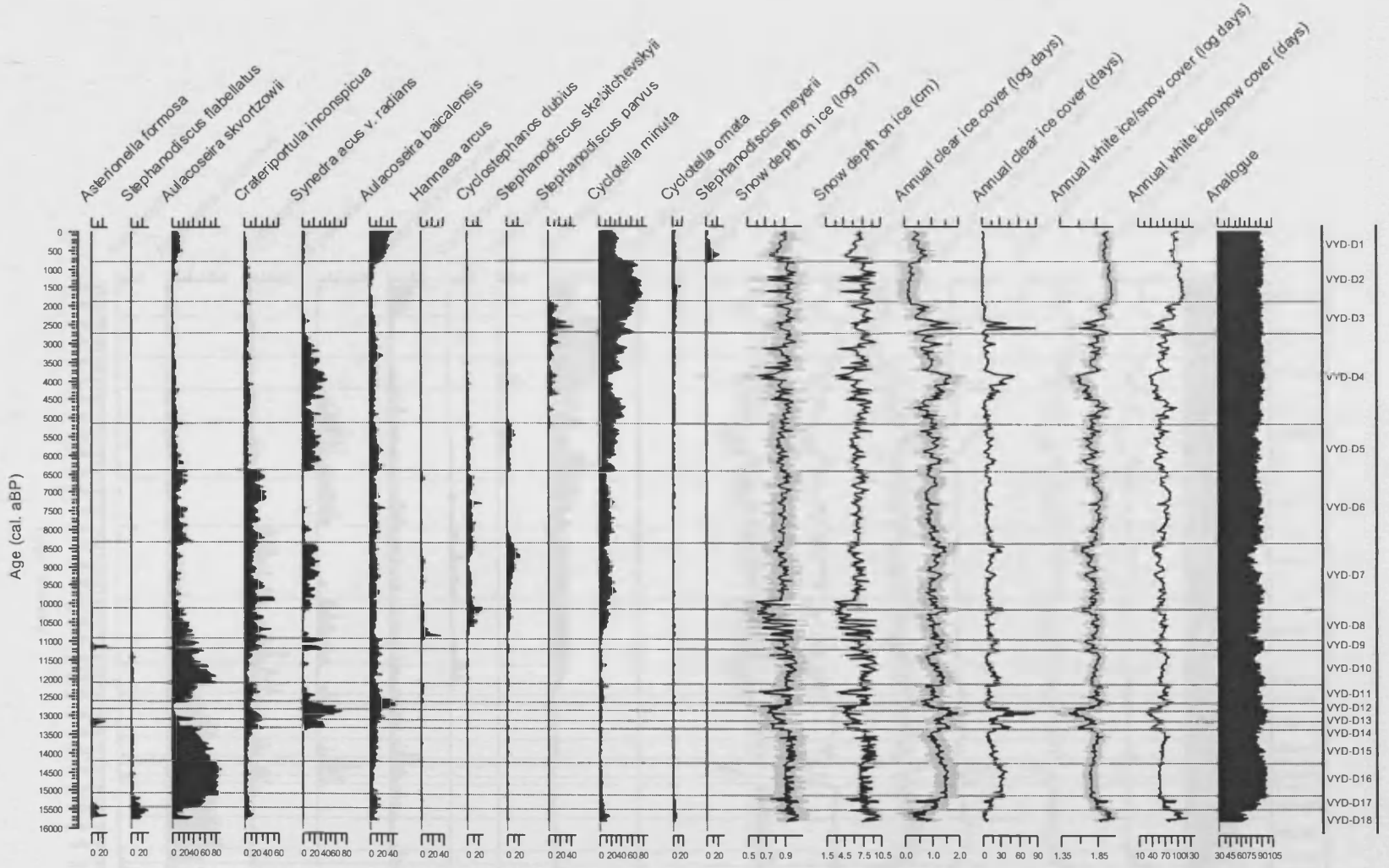

Figure 6.11: Reconstructed snow depth on ice, annual clear ice and white ice/snow cover and error +/- 1 SD against age (cal. aBP) for the full training set of all species. Results are given as log transformed and anti-logged. The main diatom species are shown.

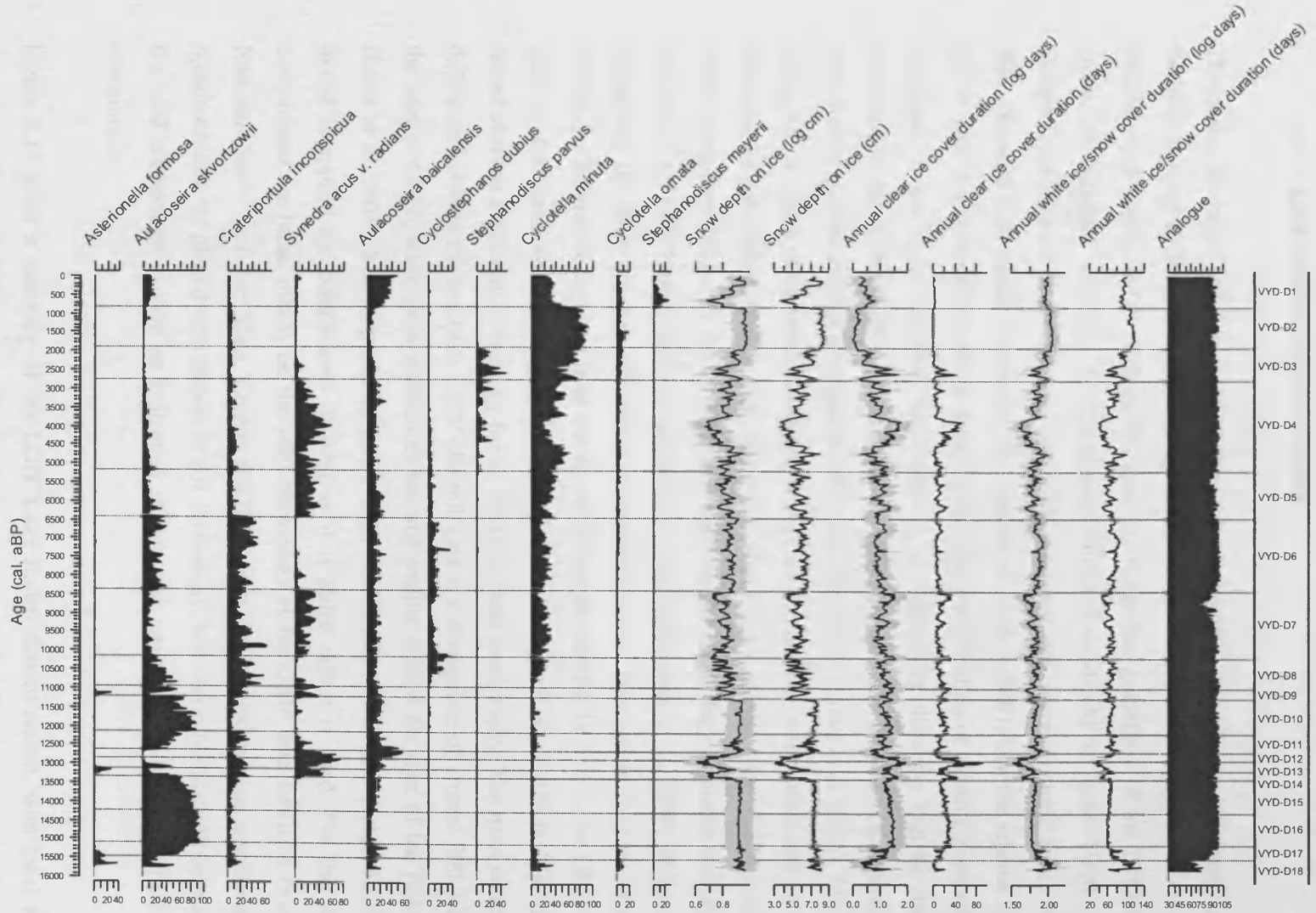

Figure 6.12: Reconstructed snow depth on ice, annual clear ice and white ice/snow cover and error +/- 1 SD against age (cal. aBP) for the training set of planktonic species. Results are given as log transformed and anti-logged. The main diatom species are shown.

6.4 Discussion

6.4.1 Late Glacial climatic events

The global stratotype and nomenclature for the last Glacial – Interglacial transition (LGIT) has been defined by the INTIMATE group based on the GRIP ice core (Björck *et al.* 1998, Walker *et al.* 1999), and is outlined in table 1.1. Under the guidelines of the INTIMATE group, an inductive approach to stratigraphic correlations should be used. Firstly local climatic zones should be located and independently dated, and secondly these zones can be then compared to the GRIP stratotype. It is stressed by Walker (2001) that the scheme should not be used in a chronostratigraphic sense and it is the identification of climatic events that is important. It has to be assumed that events in geographically disparate regions may be diachronous and different in magnitude and duration. Overall, the INTIMATE scheme is a basis for comparison and not a replacement for local stratotypes (Lowe *et al.* 2001). The main reason for this type of approach is the problem of dating, as both radiocarbon and ice layer chronologies have limitations. Several chronologies exist for Greenland ice core records: the ss08c chronology is used by the INTIMATE group but the chronology available with the on-line archive of GRIP data is the ss09 chronology (von Grafenstein *et al.* 1999) while a new chronology for GRIP known as NGRIP is forthcoming. All of these age models are based on counting of annual ice layers at least during the Holocene. Beyond 14.5 ka in the GRIP core, ages are estimated with the help of ice-flow models (Dansgaard *et al.* 1993). The GISP2 record also has a different chronology for an identical event stratigraphy. The most noticeable difference between the available GRIP chronologies is a divergence of around 200 years at the start of GI-1e, while these differences become smaller toward the start of the Holocene (Lowe *et al.* 2001). It is proposed by Lowe *et al.* (2001) that it does not matter which age model is applied for comparisons as long as it is stated which is used. For this study, comparisons are based mostly on the ss09 chronology as the GRIP data available from the National Snow and Ice Data Centre (NSIDC: http://nsidc.org/data/gisp_grip/document /gispisot.html), are plotted with respect to this chronology, however reference will be made to the ss08 chronology to give an indication of how the results differ based on these two chronologies.

Figure 6.13 gives a summary of the LGIT Lake Baikal diatom record, with local zones according to CONISS and GRIP $\delta^{18}O$ plotted against the ss09 chronology. The Lake Baikal Vydrino Shoulder diatom record shows considerable variability over the LGIT, possibly

equivalent to the North Atlantic event stratigraphy. Using the autecological summary it is possible to make inferences about water temperature, tolerances to different snow depths on ice also gives an idea of winter precipitation, as well as temperature in terms of ice/snow cover annual duration. The beginning of the diatom record (VYD-D18 and D17) is marked by low diatom concentrations and planktonic biovolume production, and indicates a cold, unproductive time for diatoms of possible glacial climate. A high abundance of benthic diatoms indicate an undeveloped planktonic community and longer ice cover duration with benthic productivity in littoral open 'moat' areas during summer while pelagic areas remain ice covered for long periods (*c.f.* Smol 1988). Indeed, the transfer function results point to a shorter duration of clear ice cover and also deeper snow cover. High relative abundance of *S. flabellatus* possibly signifies low light conditions, turbid waters and deep wind mixing. Warming after the LGM has begun, as diatoms are present, whereas below these zones only glacial clays are present. This absence of diatoms here need not imply that there is no diatom growth (*sensu* Karabanov *et al.* 2004), but is partly due to very low productivity and also poor preservation in the sediments due to dissolution.

The start of zone VYD-D16 at 15100 aBP sees a switch to a predominantly planktonic diatom assemblage, a greater biovolume and flux of species driven almost exclusively by *A. skvortzowii* resting spores. The dominance of resting spores may be due to harsh environmental conditions but also because the vegetative cell preserves poorly. *A. skvortzowii* indicates the presence of cold waters according to culturing experiments, although these waters will be warmer than those of the LGM. Their dominance at this time of climatic amelioration may be because the cells are light and easy to suspend in waters of low heat driven turbulence (Julius *et al.* 1997). Populations build up at near-shore areas (e.g. Vydrino Shoulder) and then expand into pelagic zones. This is a different strategy to *A. baicalensis*, a cold-tolerant diatom not present in abundance as it is heavily silicified, and which blooms predominantly in pelagic areas which would still be extremely harsh and unconducive to diatom growth. The dominance of *A. skvortzowii* during relatively cooler intervals of the Late Glacial may also be a function of increased water column convection linked to hydrodynamic factors and higher winds. This dominance is strengthened by the fact that this species is present despite a high relative level of dissolution (table 5.2). During colder intervals, the depth of the mixed layer may have reached 500 m during a glacial maximum and be only 200 – 250 m during a warm interglacial (Shimaraev *et al.* 1992). The strengthening of winds during colder intervals (due to increased temperature gradients) and in turn deeper mixing, can lead to increased entrainment of *A. skvortzowii* resting spores from a deeper littoral zones and a subsequent greater innoculum. Overall, the higher diatom abundance indicates a warming climate from the cold LGM, perhaps synonymous with the GI-1e event (Bølling in

older terminology) at 14700 aBP, according to the ss08c chronology (Björck *et al.* 1998) but around 200 years later according to the ss09 chronology (figure 6.13). Having identified common events in both records, that is the first major post LGM warming, it is difficult to assess if the onsets are synchronous, especially as the errors in radiocarbon dating at this point are ±800 years. However, there is an apparent lead of 400 years for the Lake Baikal event.

The GRIP record shows a short-lived cooling of 150 years at 14050 (ss08c) and 150 years earlier according to (ss09). This is termed the GI-1d and is similar to what was previously known as the Older Dryas. A decrease in diatom concentration and biovolume in zone VYD-D15, while relative abundance of *A. skvortzowii* remains high, indicates a cooling. Transfer function results indicate snow depths remain high and clear ice durations low. The duration of this event before the next warm phase is 890 years, which is much longer than the GI-1d event. This discrepancy could be due to suppression of diatom productivity by a factor independent of a direct climatic influence, such as nutrient limitation and the dominance of other algal groups. After greater productivity in the preceding warm phase, nutrient levels may be depleted for example, as the lake is not being sufficiently replenished by either inwash from a catchment with poorly developed tundra soils (Demske *et al.* in press), or by limited water column circulation linked to longer ice cover. In addition any water overturn occurring would be very deep (*c.f.* Shimaraev *et al.* 1992) meaning diatoms would be light-limited as they would be periodically removed from the photic zone for long intervals. When Lake Baikal is limited by nitrogen, for example, algal productivity is dominated by picoplankton rather than diatoms (Popovskaya 2000), this is also the case in summer when the upper waters become depleted in nutrients (Nagata *et al.* 1994). Supporting this, it will be shown in chapter 8 that the presence of higher $\delta^{13}C$ values during colder intervals of the Late Glacial may be linked to a dominance of cyanobacteria and low diatom productivity.

The presence of *S. acus* v. *radians* in zone VYD-D14 indicates the warmest conditions of the record so far, as this species has high temperature and irradiance optima, and a preferred distribution relating to reduced ice cover and on ice snow depth (less winter precipitation). An increase in both biovolume and flux is due to both climatic warming but may also be due to increased glacial melt, river discharge, catchment soil development or nutrient supply to the lake. Waters may become warmer (>6°C) reaching the restrictive temperatures for the growth of *A. skvortzowii.* This warm period in the Lake Baikal record is similar in the event stratigraphy to the GI-1c event (Allerød) at 13900 aBP (ss08c) and 13750 aBP (ss09) but appears to start several hundred years later. This close correlation between Lake Baikal and GRIP is within the errors of radiocarbon dating at 300 – 900 years meaning the events may be synchronous, but it may be that the equivalent of the GI-1c event in Lake Baikal is delayed in

comparison to the GRIP record. The transfer function reconstructions indicate decreased snow depth with increased clear ice and lower white ice/snow duration. Other diatom species indicating a warmer climate are *S. acus* v. *pusilla* and a spike of *A. formosa,* possibly indicating a pulse of nutrients or more eutrophic waters linked to river discharge (chapter 4). Such short-lived spikes in abundance of *A. formosa* are not reported elsewhere in the lake. It may be that the marginal location of the Vydrino Shoulder experienced greater nutrient input from rivers than cores studied from more pelagic areas. As *A. formosa* thrives in the summer period, it may indicate greater summer productivity and with a large bloom preservation will increase as sedimentation will occur with groups of *A. formosa* clumped together and sinking through the water column (Jewson, pers. comm., Boës *et al.* in press). Lower abundances of *A. formosa* are therefore probably not preserved in the sediments. The GI-1c in Greenland lasts 750 years compared to just 210 years in Lake Baikal.

A notable colder excursion in Greenland is the GI-1b event (Gerzensee Oscillation, IACP) at 13150 aBP in the ss08c chronology, this lasted 250 years before returning to warmer conditions. In Lake Baikal this possibly equates to VYD-D13, beginning also at 13150 aBP and lasting 260 years, although the errors in the dates at the point are in the region of ±300 – 550 years. A drop in diatom concentrations and the return of *A. skvortzowii,* at the expense of *S. acus* v. *radians,* indicates colder waters. As explained above, this return of *A. skvortzowii* may be caused by increased wind driven mixing and entrainment of resting spores into the water column. Transfer function results also estimate shorter clear ice duration and increasing winter precipitation shown by snow depths. This is an important finding as although the GI-1b event is thought to have at least a hemispheric signature (Anderson *et al.* 2000), it is not usually observed outside North Atlantic regions.

The return to warm conditions (GI-1a) at 12900 aBP (Greenland chronologies become divergent at this point) is also synchronous in Lake Baikal with zone VYD-D12 at 12900 aBP. The zone begins with rising flux of the warm indicator *S. acus* v. *radians* and towards the end of the zone diatom concentrations fall and the abundance of *A. baicalensis* increases. This may be due to a cooling trend indicated by rising snow depths on ice and longer ice duration. By 12640 aBP and the start of zone VYD-D11 this cooling is complete. The decline of *A. baicalensis,* indicating snow depths beyond the threshold for growth, the return of *A. skvortzowii* and *S. flabellatus* with the absence of *S. acus* v. *radians* and the increased proportion of benthic diatoms indicate longer ice duration and colder waters and reduced pelagic productivity. This cool period marked is equivalent to the GS-1 period (Younger Dryas) beginning around 12650 aBP (ss08c) in the GRIP ice core. The GS-1 lasts 1150 years in Greenland and the corresponding zones of low diatom abundance (VYD-D11 and D10)

span 1430 years, again radiocarbon errors may be in the range of ±300 – 550 years. A warming marked by a sharp peak of *A. formosa* in VYD-D9 at 11210 is the beginning of the Holocene. The Holocene starts at around 11500 aBP in Greenland, apparently synchronous to Lake Baikal. Diatom concentrations rise slowly into zone VYD-D8 with variable *S. acus* v. *radians* and *A. skvortzowii* possibly displaying the pre-Boreal oscillation, or as a response to turbid conditions caused by increased input of glacial meltwater (Karabanov *et al.* 2003). The gradual increase of *C. dubius*, *C. minuta* and *C. inconspicua* indicate warmer, more eutrophic waters. Transfer function estimates also show a declining snow depth on ice. However, the simulations of Bush *et al.* (2004) indicate that the climate becomes more humid in the Early Holocene compared to the Late Holocene, and winter snow fall actually increases into the Holocene. However, despite this apparent contradiction, the annual ice covered period will be declining with Holocene warming (Shimareaev *et al.* 1992) and the winter period of snow covered ice will be much shorter even though more snow may have fallen.

Overall, the Lake Baikal diatom LGIT record and the GRIP ice core share a similar event stratigraphy but with some apparent differences in the timing and duration of some events. It is not possible to determine leads/lags accurately between the regions, due to the limitations of the dating methods used. The events are synchronous within the errors of the radiocarbon dates, however. In particular the GI-1a, b and GS-1 events appear to have similar timing, duration and magnitude in both regions. There is less accord with later events in the stratigraphy, the GI-1c event has a delayed start and shorter duration while the GI-1d event is several hundred years longer in Lake Baikal. The first warming in Lake Baikal (VYD-D16) may be synchronous to the warming phase GI-1e in Greenland, as dates are within radiocarbon confidence intervals but the Lake Baikal warming appears to be smaller in magnitude to that of Greenland. The later zones in Lake Baikal corresponding to GI-1a and c are possibly warmer than the equivalent of GI-1e. Conversely, the earlier warming in Greenland (GI-1e) is the warmest of the whole GI-1 event. The reasons for discrepancies between the two records may be due to local climatic variability which is investigated in the next section, with reference to other Central Asian palaeoclimatic records. For this reason, an exact correlation to the GRIP record should rarely be expected (Walker *et al.* 1999). Also, during the development of the lake ecosystem from the LGM there may have been occasions where diatom productivity was limited by factors only indirectly influenced by climate. For example, lower productivity and the apparent longer GI-1d event may have been caused by nutrient limitation and/or turbid waters caused by input of glacial meltwater and glacially eroded materials.

In general, the results presented here concur with other records in that the LGIT in Central Asia was structured in a similar way to the North Atlantic records. In terms of other Lake Baikal records, Prokopenko *et al.* (1999) initially found no evidence for the Bølling (GI-1d) but identified a possible Allerød period (GI-1a to c) and a well defined Younger Dryas period. However with an alternate interpretation of the age model, it may be that what was interpreted as the Allerød is synonymous to the whole Bølling-Allerød (GI-1) period which occurs at a similar time in the GRIP (Grachev 2000, Prokopenko 2000). Other Lake Baikal studies, in particular Chebykin *et al.* (2002) claim the Bølling-Allerød timing is similar to that in Europe, suggesting an identical causal mechanism, while Karabanov *et al.* (2003) also find a Bølling-Allerød period synchronous to the North Atlantic, but an attenuated Younger Dryas apportioned to an Early Holocene productivity suppression by the input of glacial nutrient poor meltwater.

Owing to the similarity of records from Lake Baikal and Greenland, a common causal climatic mechanism could be expected. This is commonly considered to be Westerly transport from the Atlantic (Kutzbach *et al.* 1993). However it has been postulated that Westerly transport in the Late Glacial was restricted by a high pressure cell persisting above the remnants of the Fennoscandian ice sheet effectively blocking the Westerlies (Khotinsky 1984, Velichko 1995, Bush *et al.* 2004). Westerly transport can also be reduced in cooler intervals to a decrease in the north-south temperature gradient that drives air movement as a result of incoming solar radiation. Velichko *et al.* (1997) consider this lack of Westerly transport to be the reason that an attenuated GS-1 in Siberian pollen records occurs, as climate will be driven by local air mass changes and not direct North Atlantic teleconnections. This possible restriction of Westerly transport may be responsible for the variations seen in the Late Glacial record presented here. The greatest variability between warm and cold events occurred in Europe at the boundaries of the Fennoscandian Ice Sheet meaning variability will be less pronounced in continental areas (Velichko *et al.* 2002). Linked to this, Nakagawa *et al.* (2003) show that a varved record in Japan lags the Greenland record by 250 – 400 years and postulate this may be due to an unknown slow teleconnection across Eurasia or that continental areas responded faster to local changes in insolation than oceanic regions. However, there is ample of evidence for semi-synchronous events over Eurasia during the Late Glacial implying the presence of a common hemispheric or global teleconnection mechanism. Despite the possible restrictions to Westerly transport described above they remain the most likely mechanism to transfer either cold air during North Atlantic ice discharge events, to strengthen the Siberian High and increase Eurasian snow extent, and increase albedo related cooling feedbacks, or to advect warmer air masses eastwards during times of higher SST and THC.

To investigate this further, it is important to consider regions of Eurasia influenced predominantly by the Monsoons and only indirectly by the Westerlies. Lake Baikal is outside the direct influence of the East Asian Monsoon and is influenced directly by the Westerlies (section 1.5.3.1). Bush *et al.* (2004) found the East Asian Monsoon variability to be broadly synchronous with Greenland records albeit with some variability related to local climatic and hydrological factors, while a teleconnection via the Westerlies has been outlined by Porter and An (1995) that drives Winter Monsoon strengths. Ice discharge events in the North Atlantic allow cold air to be carried across Eurasia strengthening the Siberian High. The Summer Monsoon can also be strengthened during warming in the North Atlantic with warm air masses effecting snow cover and albedo over Eurasia and increasing the land – sea (Pacific) temperature gradient that drives the Summer Monsoon. This process is confirmed by the speleotherm record of Zhao *et al.* (2001) and the loess records of Zhou *et al.* (1996, 1999), both showing event synchronicity to the North Atlantic.

In summary, the apparent synchronicity of Late Glacial events between the North Atlantic and Central Asia (Lake Baikal) is due to a teleconnection mechanism of Westerly air flow, transferring climate changes manifest in the North Atlantic THC and ice sheet feedbacks, possibly driven by insolation changes. Variation between records may be due to the influence of local atmospheric circulation changes or differing responses of proxies to climate change. However, it is still not known how viable this mechanism is for the lower amplitude Central Asian changes seen over the Holocene (Zhou *et al.* 1999).

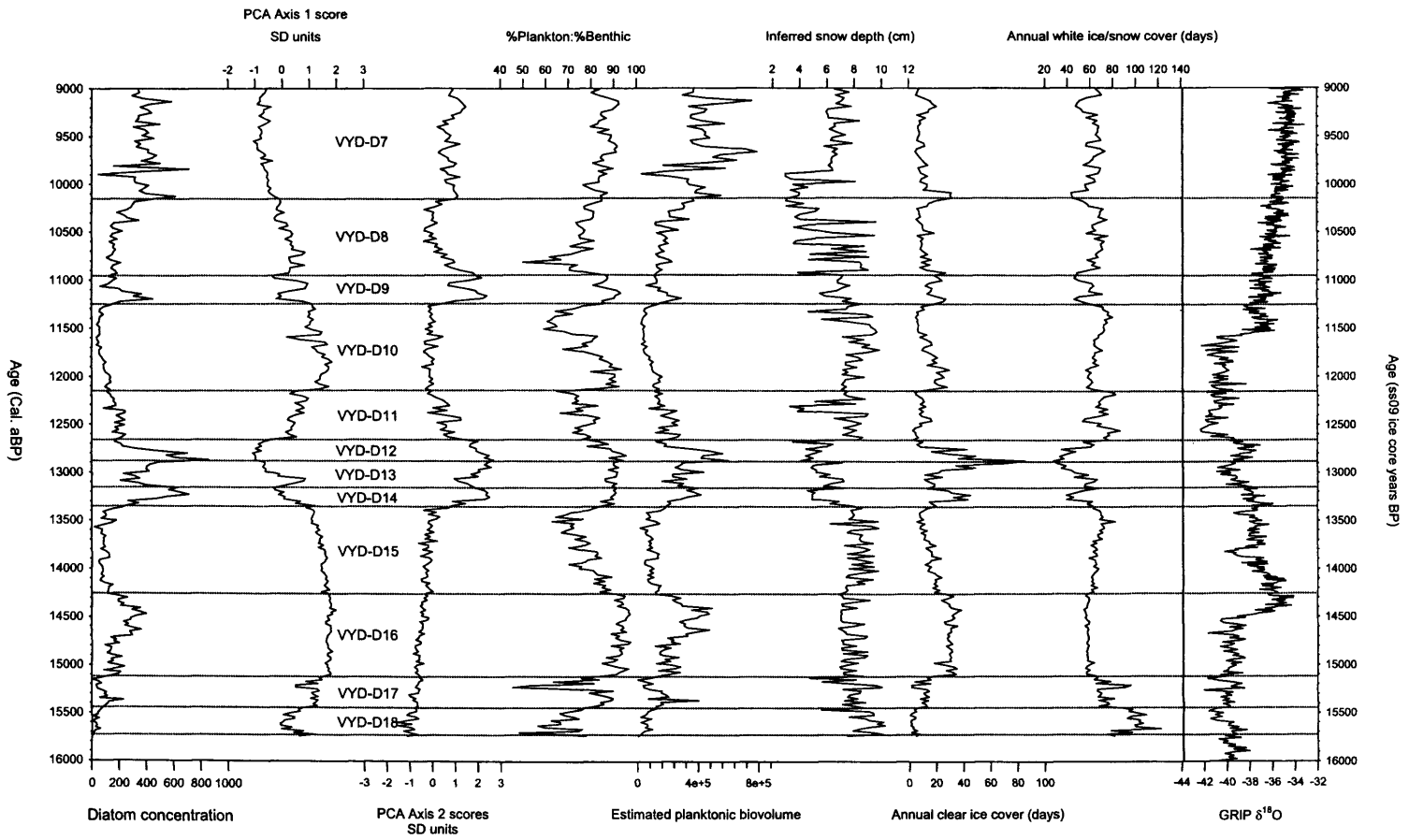

Figure 6.13: Summary diagram for the Late Glacial period (VYD-D18 to VYD-D7) for the diatom record from the Vydrino Shoulder. The oxygen isotope curve from GRIP on the ss09 timescale is shown for comparison.

6.4.2 Holocene climatic events

Although the Blytt-Sernander generalisation of Holocene climate (Sernander 1908) is considered a poor tool for regional palaeoclimatic comparisons, due to the failure to incorporate local variability (Smith 1981, Bradbury *et al.* 1994), it has been used extensively in studies of Lake Baikal and Central Asia to compartmentalise periods of differing climate, in particular the Holocene climatic optimum. Here it will be used only to define similar time periods between records where the scheme has been used. The boundaries of the scheme are summarised in table 6.5.

Period	^{14}C aBP boundaries	Cal. aBP boundaries	Climatic conditions
Sub-Atlantic	0 – 2500	0 – 2570	Wet/cool
Sub-Boreal	2500 – 5000	2570 – 5730	Dry/Warm
Atlantic	5000 – 8000	5730 – 8810	Wet/Warmest
Boreal	8000 – 10000	8810 – 11350	Dry/warm

Table 6.5: The boundaries of the Blytt-Sernander division of the Holocene and generalised climatic conditions for Europe (Sernander 1908) given in radiocarbon years and calibrated dates from OxCal v. 3.8.

The beginning of the Holocene is zone VYD-D8 as described above, and contains warmer water and lower snow depth on ice indicator species, but also a peak of *H. arcus* with a gradual decline over the next 2000 years. No records of such an abundance of *H. arcus* can be found in previous studies of Lake Baikal. *H. arcus* is a benthic diatom that can tolerate fast flowing alpine river waters (Krammer and Lange-Bertalot 1986-1991), so its presence in the Early Holocene may be due to deglaciation in the Khamar-Daban mountains (figure 2.1) as the Vydrino Shoulder is close to the inlets of many small rivers sourced in the mountains. The influx of *H. arcus* therefore, may have been due to increased discharge and also greater production of *H. arcus* in these rivers that lasted to around 9 kaBP. The following period of very high diatom concentrations (*c.* 380 x10^6 valves g^{-1}) in VYD-D7 marks an Early Holocene warm period (10170 – 8390 aBP) although biovolume levels are still relatively low. Warmer waters are indicated by the decline of *A. skvortzowii* and possibly by *C. inconspicua* representing greater summer productivity. Increased *S. acus* v. *radians* implies both warmer waters and more clear ice cover (reduced winter precipitation) which is also indicated in the

transfer function reconstructions. Although *S. acus* v. *radians* is an opportunistic species and predominantly a warm indicator, it is important to note that it also has a broad temperature tolerance and can also dominate at cooler temperatures, but here it is associated with other warm indicators. This warming is coincident with the Early Holocene insolation maximum (Berger and Loutre 1991) and is expected by the modelling studies of Bush (in press) and has been reported over the whole of Central Asia (Starkel 1998). It is also manifest in treeline fluctuations in Northern Eurasia (MacDonald *et al.* 2000) and forest development in Mongolia (Tarasov *et al.* 2000). The pollen records of Berkozova *et al.* (1992) and Demske *et al.* (in press) both show this time to be a period of the establishment of forests in the Lake Baikal catchment. This amelioration is also noted in Europe with rapid warming of 3-4°C every 500 years from the start of the Holocene inferred from French pollen data (Guiot *et al.* 1987). Temperatures were possibly comparable to or warmer than those of today (Atkinson *et al.* 1987).

The boundary of zones VYD-D7 and D6 at 8390 aBP may be considered similar to the Boreal-Atlantic boundary in that a climatic shift occurs. Karabanov *et al.* (2000) assume the Atlantic period to be the climatic optimum for the whole of Europe but not for Lake Baikal. Indeed, this period is commonly considered as the European temperature optimum, while optimum temperature conditions over Russia were achieved several millennia later (Bell and Walker 1992). The Vydrino Shoulder record here indicates a possible cooling at the start of the Atlantic period and not a climatic optimum with a decrease of diatom concentration, although biovolume values remain stable. However, this only implies a shift from fewer small taxa to more large taxa, and maybe does not indicate a significant climatic shift. The disappearance of *S. acus* v. *radians* and the re-establishment of *A. skvortzowii* can imply cooler conditions and increased winter precipitation, although *S. acus* v. *radians* can still thrive in cooler waters. The presence of *C. inconspicua* and *C. dubius* also imply that the climate was still relatively warm but perhaps, as indicated by diatom concentrations, not as warm as the preceding zone. Conditions may have been windier too as the increase of *A. skvortzowii* can also be explained by increased mixing entraining resting spores from littoral sediments. Therefore this is in agreement with Karabanov *et al.* (2000) in that the so-called Atlantic period in Lake Baikal, although warm, was not the climatic optimum as in the Blytt-Sernander scheme, and optimal conditions occurred later. However, since the climatic optimum is very variable over Europe too (Smith 1981), highlights the difficulty of making such comparisons over an even wider area. In addition to this, comparisons are also hindered by poorly developed age models in some studies. There is however, evidence of a cooler interval corresponding to the Atlantic period in other Asian records, such as lake levels in Mongolia (Peck *et al.* 2002), while Bush *et al.* (2004) simulate a peak in snow accumulation

over Asia at 8.0 –7.5 kaBP. On the other hand, Khotinsky (1984) states the Atlantic time period contained the climate optimum for much of Eurasia but also acknowledged that huge spatial variability occurred. However, the lack of *S. acus* v. *radians* may also just indicate an increase in winter precipitation under a warmer climate. The presence of cold water *A. skvortzowii* does imply a coincident temperature decrease though.

Within this slightly cooler period, the fall of diatom concentration to *c.* 300 x10^6 valves g^{-1} is predated by a sharp increase at *c.* 8.2 kaBP for around 200 years, with no major change in diatom species assemblage. Due to the limitations of dating, it is impossible to tell if this peak is related to the cooling event in North Atlantic records at 8.2 kaBP (Alley *et al.* 1997, section 1.3.3) or if it occurs before or after the cooling. It may be that the cold event led to increased precipitation and/or erosion, and nutrient input.

The Sub-Boreal period defined as the Lake Baikal climatic optimum by Karabanov *et al.* (2000) corresponds to zones VYD-D4 and D5 which also represent a warm period and possibly the Holocene climatic optimum of this record. However, there is a more detailed structure to the climatic event over this period. A distinct species shift occurs at the boundary of zones VYD-D5 and D6 (6425 aBP) with a replacement of *C. inconspicua* with *S. acus* v. *radians* but there is also less *A. skvortzowii* together with rising diatom and chrysophyte cyst concentrations. The sudden switch between *C. inconspicua* to *S. acus* v. *radians* may also be due to a warming as *C. inconspicua* is found in the colder North Basin in the modern environment (chapter 4). This possible warming event coincides with a 'late Atlantic warming' at 6000 – 5000 ^{14}C aBP (6840 - 5730 aBP) in a synthesis of Central Asian pollen records shown by the expansion of Eurasian forests at this time (Khotinsky 1984), while Horiuchi *et al.* (2000) show a pollen defined climatic optimum at 6000 ^{14}C aBP (6840 aBP) that is claimed to be synchronous to the European climatic optimum. A late Atlantic warming (6500 – 6000 aBP) is also expected in the modelling work of Bush (in press). This coincides with high abundance of *S. acus* v. *radians* over VYD-D5 and also indicates less winter precipitation. A decline of *S. acus* v. *radians* at 4750 – 4250 ±115 - 140 aBP, may show a cooling, increased snow depth limiting spring production and a dominance of autumn production shown by rising *C. minuta.* Again this is modelled by Bush (in press) who predicts increased snow accumulation at 4500 aBP. Following this, a warm period is simulated (3500 – 2600 aBP). This is coincident with the later part of VYD-D4 which sees a return of *S. acus* v. *radians,* but also high proportions of *C. minuta.* Again, this is indicative of increased winter precipitation creating deep spring snow cover. Diatom concentrations are also higher over this part of the zone. This is in accord with Karabanov *et al.* (2000) who state the climatic optimum in Lake Baikal is represented by the dominance of *S. acus.* This series of events of

the Sub-Boreal time period is also seen throughout Eurasia (Khotinsky 1984, Peck *et al.* 2002) and a marked cooling is seen in the North Atlantic regions also at around 4200 aBP, that may be part of the millennial scale periodicity (O'Brien *et al.* 1995, Bond *et al.* 1997).

In the Blytt-Sernander scheme the Sub-Boreal gives way to the Sub-Atlantic cooler period. A possible global cooling event is evident at 2785 aBP thought to be caused by reduced solar output (van Geel *et al.* 1996, 2000). This may also be manifest in Lake Baikal with a disappearance of *S. acus* v. *radians* and gradually rising *C. minuta,* indicating increased snow depth on ice (increased proportion of autumnal blooming species). The transition to zone VYD-D3 at 2790 ±70 – 115 aBP shows apparent synchronicity to this possible global event.

The following period to the present day has been termed the neoglaciation with reduced temperatures on a global scale after the warmer climatic optimum (Porter and Denton 1967). This is seen in the Vydrino record with steadily declining diatom concentrations, however biovolume peaks in VYD-D2 due to the dominance of the large *Cyclotella* species. These species are indicative of increased winter precipitation with longer and deeper snow cover, an autumn production dominance and high levels of wind driven convection, enabling the large cells to be suspended. The temperature tolerances of these species are lower (8.5°C) than the optimum of *S. acus* v. *radians* that was dominant during the climatic optimum. The neoglaciation period is possibly linked to declining insolation and is manifest over Northern Eurasia with retreating treelines (MacDonald *et al.* 2000), and over the Tibetan Plateau with lower lake levels (Lehmkuhl and Haselein 2000).

The final zone VYD-D1 begins at 810 aBP with a rise in proportions of *A. baicalensis, S. acus* v. *radians, S. meyerii* and *S. acus* v. *pusilla,* while *C. minuta* declines indicating a gradual warming. The presence of low values of *C. minuta,* high *A. baicalensis* and *S. acus* v. *radians* in zones equivalent to VYD-D3 and D1 with *C. minuta* dominance in VYD-D2, has previously been linked to the MWP, LIA and modern warming, and this diatom succession is found lake-wide (Mackay *et al.* 1998, Bangs *et al.* 2000, Mackay *et al.* in press). These studies were based on ^{210}Pb chronologies, the radiocarbon chronology used in this study puts these species shifts beyond the possible range of documented dates for the MWP and LIA. Even taking into account the errors of radiocarbon dating does not reconcile this, for example, the upper boundary for the onset of the LIA accounting for radiocarbon error is still at 1860 aBP, over 1000 years before the well documented beginning of this event. If the radiocarbon dates here are in error, the events still occur over 36 cm of sediment which, in the context of the whole Holocene – Late Glacial record of 267 cm implies an unrealistically fast accumulation rate for these events. This study sees no evidence of a LIA or MWP, possibly

due to these events being relatively short and of low magnitude compared to much larger shifts (for example the Late Glacial oscillations) and not resolved in the record (*c.f.* Morrill *et al.* 2003), although there is evidence of a MWP-LIA over the whole Northern Hemisphere. Only when constrained by ^{210}Pb chronologies do the species shifts defined above (those also observed lake-wide) correspond to a MWP-LIA oscillation, when using a radiocarbon chronology these shifts occur over several thousand years. Therefore, there is a challenge here to somehow account for the differences between chronologies used, clearly one (or both) are erroneous. It has already been shown radiocarbon dating is difficult in Lake Baikal (Colman *et al.* 1995) although this has partly been solved by the analysis of isolated pollen. Also, in the context of a complete Holocene – Late Glacial record, the older ages given by radiocarbon dating seem to fit the profile, assuming a complete Holocene record is present. Possible errors with the ^{210}Pb used may also be due to extrapolation of a ^{210}Pb age model to depths beyond those dated, for example, by Bangs *et al.* (2000).

Overall, high amplitude climate changes over the Holocene recorded in Europe and the North Atlantic, appear to be semi-synchronous over Central Asia according to the diatom record presented here and other palaeoclimatic records over the region. This implies that a similar teleconnection mechanism is operating over the Holocene as was during the Late Glacial. However, although similar, records over Asia are highly variable, in particular the timing of the climatic optimum, due to significant local climatic variations (Starkel 1998, Morrill *et al.* 2003, He *et al.* 2004). Possible reasons for this include the influence of local air masses and atmospheric circulation change, and changes to local albedo and hydrological cycle. The level of continentality is also important, with the areas most isolated experiencing a buffered influence from the oceans (Velichko *et al.* 1997, 2002) and also the varying responses of proxies used in climatic reconstructions.

6.4.3 Taphonomic considerations and core representivity

An investigation into the benthic flora at several sites in Lake Baikal by Martin *et al.* (in press) shows that the top 15 cm of sediment contain live benthic animals capable of disturbing the sediment by bioturbation. Species found include Oligochaeta, Nematoda, Ostracoda, Copepoda, Gammaridae, Amphipoda, Chironomidae and Hydrachnidia. Bioturbation has been mostly neglected as a possible factor altering core representivity and the accuracy of palaeoenvironmental reconstructions. However, the overall effect in Lake Baikal is considered limited in abyssal regions (deeper than 250 m) (Martin *et al.* in press), this means bioturbation should be limited at the Vydrino Shoulder with a water depth of 675 m. Also according to the visual interpretation of the Vydrino core stratigraphy, shown in figure 2.14,

no visible bioturbation is present. In addition, the fact that upper sediments contain traces of ^{137}Cs and ^{241}Am from atomic weapons testing (Appleby *et al.* 1998), and a peak in spheroidal carbonaceous particles linked to recent industrialisation (Rose *et al.* 1998), further confirms sediments are not bioturbated.

It has already been stated that differential diatom dissolution is a problem in Lake Baikal, with only 0.1% to 9% of produced valves preserved in the sediment, dependent on the species (Ryves *et al.* 2003). Therefore, dissolution can affect the ability to make reliable palaeoclimatic inferences (Ryves 1994). Dissolution correction factors for five of the main species have been formulated (table 5.2, Battarbee *et al.* in press). A diatom stratigraphy for these five species corrected for dissolution is shown in figure 6.10. It is difficult to make palaeoclimatic inferences from this as the assemblage is limited to five species rescaled to represent 100%, this is misleading as other species (uncorrected) are also present but not shown. However, by a simple comparison of this stratigraphy to the uncorrected assemblage (figure 6.6), it is clear that during the Holocene *C. minuta* has been overrepresented due to its resistance to dissolution. Abundances through zones VYD-D7 to D4, range from 20 – 40%, while according to the corrected assemblage, abundances are low at around 10%. However, this species is still dominant in zones VYD-D3 and D2. Overall, the corrected assemblage is dominated by *A. skvortzowii* and *S. acus* v. *radians*. This highlights the significance of even low abundances of these species in the uncorrected record, whilst *C. minuta* and *A. baicalensis* should be given less weight in interpretations. Obviously, a much more accurate palaeoclimatic interpretation of the Vydrino Shoulder could be given if dissolution correction factors existed for all extant species present and this should perhaps be the focus of future studies.

The palaeoclimatic records from Lake Baikal presented here are being used to draw comparisons with the North Atlantic. Such broad connections are viable from studies of Lake Baikal due to its size. Williams *et al.* (2001) state that as Lake Baikal is so large it records climate changes over a large region (as is the case with marine records) and therefore can be used for inter-regional climatic event comparisons. Palaeoclimatic interpretations in this study are based on one site in the south of Lake Baikal, it is hoped that this is representative of the lake as a whole. To investigate this, the Vydrino Shoulder record can be compared to the synthesis of Holocene diatom records of Bradbury *et al.* (1994) and to the two other profiles analysed as part of the CONTINENT project from the Continent Ridge and Posolsky Bank (figure 2.1) (Rioual, unpublished). These two sites have a much slower accumulation rate than Vydrino, with the Holocene represented by 86 cm (although there may be a hiatus in this record (Rioual pers. comm.)) at Posolsky, 110 cm at Continent, but 165 cm at Vydrino.

Diatom assemblage changes are broadly similar but not identical, due to the latitudinal environmental gradients that exist over the lake. Local factors are also important, for example, the influence of river inputs on a peak of *H. arcus* at Vydrino (discussed above), and tectonic activity affecting water depth and benthic diatom productivity near the Continent Ridge (Rioual, pers. comm.). High abundance of *A. skvortzowii,* as seen at Vydrino during the Late Glacial, is also present at both Continent and Posolsky and the sites studied by Bradbury *et al.* (1994). Also observable in all records is an Early Holocene extinction of *S. flabellatus*, increasing *C. minuta* through the Holocene, but highly variable *S. acus* v. *radians* abundance. This may be due to localised factors, such as variable ice and snow cover dynamics, gyre circulations, river inputs and grazing by zooplankton and dissolution. A 'patchy' distribution for this species is expected with reference to its distribution in the modern phytoplankton (Grachev and Likhoshway 1996). The distribution of *S. skabitchevskyii, C. dubius* and *S. parvus* is broadly similar at each of these sites, but there are some differences in timing of onsets and peaks relative to other species, again this is possible due to local variation, dating errors, but also the latitudinal climatic gradient over the lake. Lake-wide in the upper sediments, *A. baicalensis* and *S. meyerii* are abundant while *C. minuta* is dominant in sediments below this (Mackay *et al.* 1998), this is also comparable to the Vydrino record.

Therefore, diatom assemblage changes at Vydrino are broadly representative of the Lake as a whole, but differences in timing of the appearance of some species and differences in abundances, are a result of differing responses of diatom species related to the north – south climatic gradient in the lake linked predominantly to snow cover depth and ice cover duration. The Vydrino Shoulder site also appears to have a faster accumulation rate, possibly related to a longer growing season (due to a shorter ice covered period) but maybe also to river inputs, as the site is located near to many small rivers draining the Khamar-Daban mountains (figure 2.1). As a result, the Vydrino Shoulder gives a higher resolution record than sites such as the Continent Ridge and Posolsky Bank, and combined with high resolution analysis, it makes it possible to resolve a highly detailed climatic record. It was also important to have a coring location on an isolated topographic high as cores from the abyssal zones of the lake are often effected by turbidites (Mackay *et al.* 1998).

6.5 Conclusion

The diatom record for the Late Glacial and Holocene from the Vydrino Shoulder, Lake Baikal shows a remarkable similarity to records from the North Atlantic. In particular the Late Glacial climate oscillations recorded in the GISP2 ice core appear to be semi-synchronous to

similar events recorded in at the Vydrino Shoulder. Specifically, the glacial to Holocene transition and the GS-1, GI-1a, GI-1b and GI-1c events appear to match best in terms of timing. During the Holocene, the shifts in diatom species interpreted as representing climate changes also match some of the larger climatic shifts in the North Atlantic region, implying a teleconnection between Central Asia and the North Atlantic over the Late Glacial and Holocene. There is still a great amount of variability in the timing of events due to local climatic influences, this asynchroneity is noted between most Holocene records, especially in the Central Asian region (He *et al.* 2004), and is entirely expected. However, broadly similar patterns of Holocene change are observed in other records from Central Asia in particular the Chinese Loess Plateau. The most likely teleconnection mechanism is Westerly transport from the North Atlantic (Kutzbach *et al.*1993, Porter and An 1995, Overpeck *et al.* 1996). As explained in section 1.5.3.1, colder intervals and reduced NADW production in the North Atlantic can lead to increased westerly flow of cold air which in turn strengthens the Siberian High causing cold, arid and prolonged winters. It will also be true that the climatic signal will be influenced by the NAO/AO systems (Todd and Mackay 2003) and changes in albedo (Eurasian snow cover extent) (Lui and Xanai 2002), this will be further explored in the next chapter with reference to the record of $\delta^{18}O$ from diatom silica.

Chapter seven

Biogenic silica oxygen isotope climate reconstruction

7.1 Oxygen isotope records from Lake Baikal

Currently no palaeoclimate records of $\delta^{18}O$ exist for Lake Baikal mainly due to the lack of carbonate material. This is due to the dilute, oligotrophic status of Lake Baikal's waters, meaning dissolution of carbonates is very high. However, it has been shown carbonates are present in Lake Baikal (Qiu 1992, Prokopenko *et al.* 1999) and so an attempt was made to analyse carbonates from the a core taken near the Vydrino Shoulder, but the replicability of the results was poor due to low carbonate content of samples. The analysis of diatom silica provides an alternative medium to carbonates, but a method to obtain clean samples for the technique needs to be developed. The reconstruction of $\delta^{18}O$ changes from Lake Baikal is important as this will provide a complementary but independent proxy to biological indicators (diatoms), and as shown in chapter 3, results may be interpreted climatically as variations in relative inputs from Lake Baikal's tributaries related to precipitation changes. Details of modern isotope dynamics and the modern climate are given in sections 3.1 and 2.2.3 respectively.

7.2 Applications to palaeoclimatic research

$\delta^{18}O$ from diatoms has been applied to marine and lacustrine palaeoclimatic reconstructions. The temperature dependence of $\delta^{18}O$ fractionation has been calculated by Juillet-Leclerc and Labeyrie (1987) based on surface sediment material from the Pacific Ocean (equation 7.1).

$$t = 17.2 - 2.4(\delta^{18}O_{DIAT} - \delta^{18}O_W - 40) - 0.2(\delta^{18}O_{DIAT} - \delta^{18}O_W - 40)^2$$

Equation 7.1.

where: t is temperature of formation (°C)
$\delta^{18}O_{DIAT}$ is value of silica (‰) to SMOW
$\delta^{18}O_W$ is value of formation water (‰) to SMOW

This can be applied to the estimation of SST, for example by Shemesh *et al.* (1992). In this study, planktonic diatom silica $\delta^{18}O$, thought to record SST was combined with $\delta^{18}O$ records of benthic foraminifera to allow the solution of the unknowns $\delta^{18}O_w$ and formation temperature, as the benthic water temperature was considered to be constant. However, this approach has been critised by Clayton (1992) as only part of Leclerc and Labeyrie's (1987) calibration was used, meaning the sensitivity of SST estimates may have been overestimated by a factor of six. Also, if the conclusions of Schmidt *et al.* (1997, 2001) are correct then diatoms may not record SST as the $\delta^{18}O$ value would be acquired in the surface sediment.

Other quantitative studies using the above calibration include a 430 ka reconstruction in the Southern Ocean (Shemesh *et al.* 1995) and the Allerød – Younger Dryas transition from a lake in north-eastern USA. Rietti-Shati *et al.* (1998) reconstructed a temperature record on Mt. Kenya but recognised that input of depleted glacial meltwater to the lake could distort the temperature signal. However, Barker *et al.* (2001) considered changes in lake water balance rather than temperature to be dominant. Shifting air masses were found to be important in influencing the temperature signal by Shemesh *et al.* (2001a). A 9500 year record from Swedish Lapland followed the GISP2 core and a 3.5 – 4.0°C shift was interpreted as the movement of the Arctic Polar Continental air mass.

Quantitative reconstructions may be doubtful, as shown above by the role of the water balance and atmospheric circulation in possibly influencing the values of both water and silica $\delta^{18}O$. Therefore, in some cases a more qualitative approach is needed. Local water balance rather than temperature is considered in studies of Ribains Maar, France by Shemesh *et al.* (2001b) and Rioual *et al.* (2001), and in Lake Pinarbasi, Turkey where Leng *et al.* (2001) identify the importance of isotopically depleted meltwater input. Rosqvist *et al.* (1999) attempt to reconstruct Late Glacial temperatures from the Southern Ocean but recognise again that meltwater input and atmospheric circulation are important influences.

As diatoms bloom in a well defined seasonal cycle, the $\delta^{18}O$ value of silica should be weighted towards the $\delta^{18}O$ of water and temperature during the months of diatom growth. This information can be complementary to other records such as carbonates (Leng *et al.* 2001). This seasonal weighting was also expected by Raubitschek *et al.* (1999) from experiments with sediment traps and by Shemesh *et al.* (2001a).

7.3 Methodology

7.3.1 Development of the $\delta^{18}O_{DIAT}$ technique

Mopper and Garlick (1971) first analysed oxygen isotopes from radiolaria but their analysis suffered from poor reproducibility due to a loosely bonded outer hydrous layer present in the material (Si-OH). This layer freely exchanges oxygen with the atmosphere and water used during sample preparation. Subsequent procedures attempt to remove this layer and analyse the strongly bonded inner silica layer (Si-O-Si). Labeyrie (1974) removed the hydroxyl layer by sintering at 1000°C under a vacuum. This vacuum heating (VH) method was used by Mikkelsen *et al.* (1978), Knauth and Epstein (1982), Labeyrie and Juillet (1982) and Wang and Yeh (1985). There were still problems of isotopic exchange after dehydration. To partition the effect of the hydroxyl layer, Labeyrie and Leclerc (1982) and Juillet-Leclerc and Labeyrie (1987) developed the controlled isotope exchange (CIE) technique. This involved labelling the hydroxyl layer with water of known $\delta^{18}O$, thereby allowing this signal to be removed, leaving the value of $\delta^{18}O$ of non-exchangeable silica oxygen.

Another approach was taken by Haimson and Knauth (1983), and Matheney and Knauth (1989). Stepwise fluorination (SWF) recovers oxygen from a sample in separate stages by increasing the amount of reagent (ClF_3 of BrF_5) during fluorination. Early reactions remove the hydroxyl layer, leaving the innermost silica to be reacted in an excess of reagent, the gas from which is collected for analysis. The first $\delta^{18}O$ values recorded are generally depleted, when values stabilize, the $\delta^{18}O$ of silica is being recorded. This plateau is reached after about 25% of the silica has been fluorinated. In some cases depleted values are recorded after this plateau, thought to be due to metal oxide impurities reacting last (Haimson and Knauth 1983). Tests have shown CIE and SWF give comparable results although it is necessary to calibrate CIE using SWF (Schmidt *et al.* 1997).

7.3.2 Method used at NERC Isotope Geosciences Laboratory (NIGL)

The following method described is the standard method for extracting oxygen (Leng *et al.* 1998) from diatom silica prior to mass spectrometry used at the NIGL. Firstly, the hydrous layer is stripped by out gassing in nickel reaction tubes, followed by a prefluorination clean-up step involving a stoichiometric deficiency of the reagent, chlorine trifluoride (ClF_3), heated at 250°C for several minutes (to be determined for each 'type' of sample), before full reaction at 450°C for 14 hours with an excess of ClF_3. The length of time the diatom silica is subjected

to a prefluorination is based on finding the plateau $\delta^{18}O$ value, beyond which the $\delta^{18}O$ value of the diatomite is stable. $\delta^{18}O$ values of samples which are not subjected to prefluorination, or when an insufficient prefluorination time is used, yield $\delta^{18}O$ values which are a mixture of oxygen derived from the hydrous layer and diatom oxygen. (In these cases the oxygen isotope ratios are generally lower, as would be expected if the hydrous layer exchanges with available H_2O and OH). The oxygen liberated is then converted to CO_2, according to the procedure outlined by Clayton and Mayeda (1963) and oxygen yields monitored by comparison with the calculated theoretical yield. The diatomite is analysed alongside a standard laboratory quartz and a diatomite control sample. $^{18}O/^{16}O$ ratios are measured on a dual inlet mass spectrometer. $\delta^{18}O$ values are normalised through standards and corrected according to Craig (1957) and Deines (1970). Reproducibility of the standard and samples is generally 0.2 – 0.3‰.

7.3.3 Possible limitations of the technique

Several fractionation factors have been published for diatom silica. As for carbonates, the coefficient is negative, which reduces the bandwidth of the signal (Schleser *et al.* 1999). Rising temperature would normally result in the enrichment of lake water, that is if the lake is evaporating and precipitation amount does not alter greatly. However, the $\delta^{18}O$ value of precipitating silica will shift to lighter values. Published estimates of temperature fractionation in ocean water range from ~0.2 to 0.5‰$°C^{-1}$ although the lower end of the range is more likely for lake water (Brandriss *et al.* 1998). Examples of these studies include: Clayton *et al.* (1972), Shiro and Sakai (1972), Labeyrie (1974), Knauth and Epstein (1976), Kita *et al.* (1985), Juillet-Leclerc and Labeyrie (1987), Matheney and Knauth (1989), Shemesh *et al.* (1992) and Brandriss *et al.* (1998). These equations are mainly based on coupling measurements of diatom silica $\delta^{18}O$, values of water $\delta^{18}O$ and temperature during formation. A huge range is shown by these relationships and the error involved means that precise quantitative palaeoclimatic work is problematic. The reasons for the divergence of these calibrations may be due to the uncertainty of silica-oxygen fractionation. Other problems include differences in the type of material analysed (fresh or fossil), variation may also be due to varying sample preparation and inherent problems of analytical techniques, or to the lack of a broad-scale systematic study.

Schmidt *et al.* (1997) analysed fresh marine diatoms from water of known temperature and $\delta^{18}O$. The $\delta^{18}O$ values of the living diatoms was 3‰ to 10‰ lower than that predicted by the silica-water fractionation curve of Juillet-Leclerc and Labeyrie (1987), which was based on fossil material. This resulted in Schmidt *et al.* (1997) concluding that fractionation during

sedimentation controls the $\delta^{18}O$ value of fossil diatoms. Brandriss *et al.* (1998) also analysed fresh diatoms cultured under known water $\delta^{18}O$ and temperature. Again, the fractionation was 3 to 8‰ lower than predicted by the curve of Juillet-Leclerc and Labeyrie (1987). However, Brandriss *et al.* (1998) considered the discrepancy to be due to the different isotopic characteristics of fresh and fossil diatoms. The unstable hydroxyl layer of fresh diatoms may be causing the difference as it is isotopically lower, while the strongly bonded inner silica layer contains an unchangeable record of $\delta^{18}O$. Juillet (1980) found the removal of the outer layer in acid caused the $\delta^{18}O$ value of fresh diatoms to increase but the value was constant for older material. Schmidt *et al.* (2001) question this assumption by stating the dissolution of the surficial silica may involve both silica dissolution and reprecipitation processes that would imply secondary exchange during settling. Spectroscopic analysis of strongly bonded Si-O-Si and weakly bonded Si-OH showed that the Si-OH groups were not preferentially dissolved and that diatom silica is isotopically homogenous. In apparent agreement to this is the fact Shemesh *et al.* (1995) found no relationship between fossil valve dissolution state and $\delta^{18}O$ value. The 3‰ to 10‰ difference in fossil diatoms is put down to secondary complex silica condensation and exchange with surface sediment pore waters. As a result $\delta^{18}O$ of diatoms may not be representative of surface temperatures (Schmidt *et al.* 2001). Despite the uncertainty concerning the fractionation of diatom silica and oxygen, it is thought that once buried, the fossil material will retain its isotopic signal (Shemesh *et al.* 1995)

Other factors thought to alter the $\delta^{18}O$ value of diatom silica, include the growth rate causing non-equilibrium fractionation. This may be an issue for some Lake Baikal diatoms as species such as *S. acus* can grow much faster than *A. baicalensis* and *C. minuta.* The culture experiments of Schmidt *et al.* (2001) show that faster growing diatoms fractionate relatively less than slower growing diatoms. Also, it has been suggested by Brandriss *et al.* (1998) that fractionations may be species dependent, although both Juillet-Leclerc and Labeyrie (1987) and Shemesh *et al.* (1995) analysed two different size fractions of their diatom assemblages and found that no vital effects were exhibited. However, Brandriss *et al.* (1998) states the difference of 0.2‰ dismissed as insignificant by Juillet-Leclerc and Labeyrie (1987) appears to be real and replicable, however there is still analytical error to consider here as the results may be due to a lack of measuring accuracy. Shemesh *et al.* (1995) found differences ranging from 0.03‰ to 0.45‰, and again considered these differences insignificant.

While the fluorination technique removes oxygen from the diatom silica for analysis, it will also remove any oxygen from impurities in the sample, such as organic matter, carbonates, clay and silt which all contain oxygen that can alter the $\delta^{18}O$ value. Applications of the

technique may be most restricted by the need for a sample free of contaminates. The presence of clay and silt may resulted in the $\delta^{18}O$ silica profile for the Eemian in Baikal to mirror the amount of biogenic silica present (figure 7.1). This has also been shown in other sites, for example Lochnagar (Scotland) where $\delta^{18}O$ values follow indicators of the level of catchment inwash (Jones *et al.*, unpublished). As a result, a very pure diatom sample is required. In some cases the contribution from impurities can be the overriding signal (figure 7.1). Therefore, a technique has to be developed to give pure samples and a meaningful climatic signal.

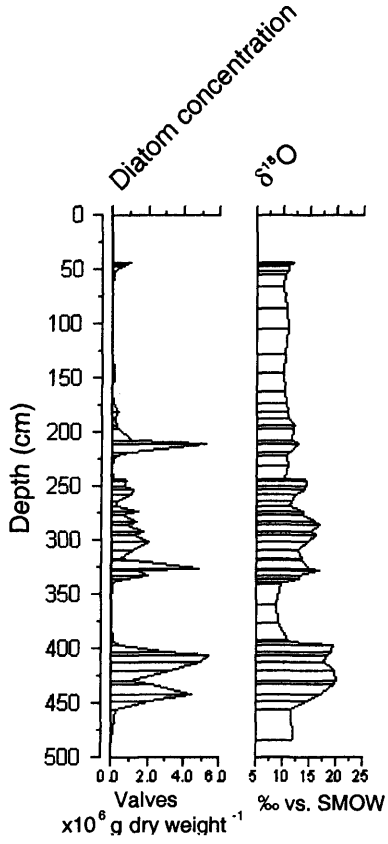

Figure 7.1: Diatom concentration and bulk $\delta^{18}O$ for a core representing the Eemian to Early Holocene from the Academician Ridge, Lake Baikal. Clay and silt with $\delta^{18}O \sim +10‰$ provide a signal in the parts of the core where diatoms are essentially absent and must influence the $\delta^{18}O$ from other parts where diatom concentrations can be variable (Morley *et al.* 2004).

7.3.4 Summary of published cleaning techniques

Previously published cleaning methods are similar in that they are based on several stages that attempt to remove organic matter, carbonate, fine clay and silt, and larger clastic material. The effectiveness of these methods has been assessed using visual inspection under SEM and LM, as well as X-ray diffraction to assess clay content. The first stage of the method published by Juillet-Leclerc (1986), used chemical attacks to destroy organic matter. She states oxidising agents such as chlorox and hydrogen peroxide are not strong enough and recommends a 50/50 mix of potassium permanganate and nitric acid. This will also dissolve the surficial layer of silica removing any clay stuck to the frustules as described by van Bennekom and van der Gaast (1976). The second stage involves the removal of clay and fine material by sieving at 5 or 10 μm. Thirdly, remaining heavy contaminants are removed by five successive settlings of decreasing duration (5, 3, 2, 2 and 1 minutes). After each interval the upper part of the solution is removed with a syringe and settled again while the bottom is discarded. This method was applied by Juillet-Leclerc and Labeyrie (1987) with the slight modification of using sieve sizes of 20-160 μm or 10-160 μm.

The method of Shemesh *et al.* (1995) is based on the three stages above, albeit with some modification and the addition of a fourth stage to further remove heavy contaminates. Firstly, the sample is disaggregated with a sonication probe and the heavy contaminates removed by a series of rapid settling (15-30 s). The sample is then sieved for the fraction between 20-63 μm. Further settling removes more heavy material but sodium polytungstate solution is used as an additional method to remove heavy material. The chemical cleaning method follows that of Juillet-Leclerc (1986) but with the addition of an initial treatment in 1% hydroxyl amine/acetic acid at 60°C.

An additional method to separate particles of differing densities is to use a heavy liquid such as sodium polytungstate (SPT) ($3Na_2WO_49WO_3.H_2O$). The density of SPT can be varied by dilution with distilled water and concentration by evaporation (Munsterman and Kerstholt 1996). It is commonly used to separate materials of different densities where the density of the SPT can be set to an intermediary value (*c.f.* Turney 1998). It is expensive, but can be recycled by filtering three times through a 0.45 μm filter paper. The SPT density or specific gravity (sg) is achieved by diluting or concentrating the solution. SPT has been used to remove heavy material (silt, larger organic matter) from pollen samples (Munstermann and Kerstholt 1996), diatom samples Gaiser *et al.* (2001), Battarbee *et al.* (2001) and to isolate tephra (Turney 1998). SPT is added to a sample and centrifuged at high speed (1500 to 3100

rpm), as a result three distinctive layers are visible allowing easy separation of fractions. At the top, any material with a density less than that of the SPT, in the middle a layer of SPT and at the base all the heavy material denser than the SPT. Shemesh *et al.* (1995) suggest a specific gravity of 2.1 for the separation of diatoms, but gravities ranging of 2.0-2.5 are also used (Gaiser *et al.* 2001).

An alternative technique to differential settling is to use a SPLITT fractionation cell (Rings *et al.* 2004). The cell is 371 μm high and 20 cm long and particles of differing size, shape or density are gradually separated in a laminar flow. Sediment is introduced through an upper inlet while deionised water is fed through a lower inlet. Inside the cell the two flows merge into a laminar current and particles separate in accordance to their density size and shape, to one of two outlets. Different particles separations are achieved by varying the flow rates and the inclination of the cell. The SPLITT cell has the main advantage of being able to work with small samples, and it may also be possible to separate a specific species on the basis of size and density. However, the main disadvantage of the SPLITT is the initial purchasing cost.

7.4 Cleaning experiment design

7.4.1 Introduction

To assess the impact of varying sample cleanliness on the $\delta^{18}O$ silica signal, it was necessary to develop a cleaning method consisting of several stages based on the above published techniques, and to measure the $\delta^{18}O$ value at different stages in the cleaning process. At each stage the percentage of diatoms and impurities was estimated using LM at x1000 magnification. A 10x10 graticule was used to 'throw' random quadrats and quantify the area covered by diatoms, silt, chrysophyte cysts, sponges, pollen and other unidentified impurities. The final percentages for each sample are an average of 10 quadrat counts with each component as a proportion of non-empty squares counted. Also, to assess the effect of the various cleaning techniques on diatom assemblages, 400 valves were counted from each stage of the cleaning process for the Lake Baikal Holocene samples. Even though this technique will only be applied to a core from Lake Baikal in this study, results of cleaning trials from Lochnagar are also presented here, as they are important in terms of the development of the technique which should be applicable to studies on sites other than Lake Baikal (Morley *et al.* 2004).

7.4.2 Site selection

Cleaning techniques will vary for specific sites depending on the type of diatoms and impurities present. In addition to Baikal Holocene sediments, Baikal Eemian sediments and sediments from Lochnagar (a small (0.1 km^2) upland lake in Scotland) were subjected to varying cleaning techniques. Lochnagar was chosen as this site has been studied previously for $\delta^{18}O$ of silica, and the sediment contains a large size range of clays and silts as well as varying amounts of organic matter (Yang 2000). A summary of the samples taken for cleaning is shown in table 7.1. These were chosen to try and give clean samples from periods of low and high diatom concentration, varying diatom assemblages and, for Lochnagar, high and low organic content as shown by loss on ignition curve.

Sample no.	Site	Age	Organic content	% Diatoms : Clastic grains	Mean silt size (μm)	Dominant diatom species and average sizes (μm)
1	Lochnagar	Recent	~35% LOI	High - 22:78	>75	*Achnanthes marginulata*: ~ 6 x 20, *A. helvetica* ~6 x 15, *Eunotia incisa* - ~ 6 x 40
2	Lochnagar	Recent	~5% LOI	High - 21:79	>75	*Achnanthes marginulata*: ~ 6 x 20, *A. helvetica* ~6 x 15, *Eunotia incisa* - ~ 6 x 40
3	Lake Baikal	Late Holocene	~3% TOC	High - 14:86	<20	*Cyclotella minuta* ~ Ø10-40, *Aulacoseira baicalensis* ~ Ø9-35x10-40
4	Lake Baikal	Early Holocene	~3%TOC	Moderate - 7:93	<20	*Aulacoseira skvortzowii* ~ Ø8x15
5	Lake Baikal	Mid Holocene	~3%TOC	Low - 6:94	<20	*Aulacoseira skvortzowii* ~ Ø8x15
6	Lake Baikal	Eemian	~<2%TOC	High - 19:81	<30	*Stephanodiscus grandis* ~ Ø80-100
7	Lake Baikal	Eemian	~<2%TOC	Very low - 1:99	<50	*Aulacoseira baicalensis* ~ Ø9-35x10-40, *Stephanodiscus grandis* ~ Ø80-100

Table 7.1: Site and age, organic content, diatom to detrital ratio, typical silt size and common diatom species and sizes (diameter Ø or width and length) of Samples 1-7 used in cleaning experiment. (% LOI for Lochnagar from Yang (2000)).

7.4.3 Development of a cleaning method

In order to develop a final protocol for sample cleaning, previously published methods were tested on the samples shown in table 7.1. Firstly, to remove organic material, samples were boiled for two hours in 50 ml of 30% H_2O_2 or until any reaction had stopped (Battarbee *et al.* 2003). To remove carbonates the samples were left in 50 ml of 5% HCl for 12 hours. To remove fine silt and clay, the next step was the sieve the samples. For each sample fraction between 5, 10, 20, 38, 45, 50, 75 and 150 μm were obtained using an electrically powered sieve shaker and at least 1 litre of water for 30 minutes. Although it was found that for the Baikal Holocene and Lochnagar samples the 38-50 μm sample contained the most diatoms to silt, it was decided to use the 10-75 μm fraction to maximise the size of the sample and to not bias the assemblage in favour of the larger diatoms. For the Baikal Eemian samples, a fraction of greater than 10 μm was sufficient because of the dominance of large *Stephanodiscus* species. To further remove silt, a settling stage was attempted as in Juillet-Leclerc (1986). The sieved sample was centrifuged for 4 minutes at 1500 rpm. The top of the spun down pellet was removed with a disposable pipette. The supernatant was left in the centrifuge tube and often a clear boundary formed between the settled out diatoms at the top of the pellet and more brown/grey/buff coloured silt beneath. The pipette was used to skim off this top layer of diatoms and transfer it to another centrifuge tube. As a final stage, the settled samples were floated in SPT (Shemesh *et al.* 1995). Initially SPT at 2.1, 2.3, 2.45, 2.55, 2.6, 2.75 and 2.85 sg was used on sieved fractions with varying success as the SPT simply floated out diatoms and silt of similar specific gravities, however the best performance was with 2.1 sg. Shemesh *et al.* (1995) used SPT at 2.1 sg to float out diatoms from any remaining heavier contaminates. Inspection of the material floated off in the SPT and the remaining residue by LM, shows that SPT at 2.1 sg is a good method to remove final contaminates. The SPT method shown below is based on Turney (1998).

7.4.4 Protocol for obtaining clean diatom samples

The experiments briefly described above led to a final method detailed below but also published in Morley *et al.* (2004) (figure 7.2).

Stage 1: Organic and carbonate removal. Standard methods are used to remove organic and carbonate material (Battarbee *et al.* 2001). A few grams of sediment are heated at 90°C in 30% H_2O_2 for two hours (or until any reaction has ended). After centrifuge washing each

sample three times in distilled water, carbonate is then removed using 5% HCl for 12 hours. The sample is centrifuge washed three times in distilled water.

Stage 2: Sieving. The samples are sieved between 10 μm and 75 μm using sieve cloth and a sieve shaker for 15 minutes with 1 litre of distilled water to remove clay and the larger detrital grains. At this stage any diatoms of <10 μm will also be removed. There is a possibility that this may bias the sample, especially where there are a large quantity of diatom material in the <10 μm range (Shemesh *et al.* 1995, Brandriss *et al.* 1998). However, this is an important step since it removes a large proportion of the clay sized material. The >75 μm portion should contain mainly detrital mineral grains since most species of diatoms are generally smaller than this (although there are exceptions). However, to maximise mineral grain and clay loss without overly biasing the species assemblage of the sample, specific mesh sizes should be chosen for each type of sediment by comparing the size of diatoms present with that of detrital material. For the samples chosen here the 10-75 μm sieves were optimal, although Samples 6 and 7 (Table 7.1) were only sieved at 10 μm in order to retain the large *Stephanodiscus grandis* Khursevich and Logina, which has a diameter >75 mm.

Stage 3: Differential settling. The 10-75 μm sieved fraction is placed in a centrifuge tube, topped up with distilled water and centrifuged (*c.* 4 minutes at 1500 rpm). Stratification occurs and the coarser, faster settling silt underlies the slower settling diatoms. The diatom layer is carefully removed using a pipette, and the remainder of the sample is remixed using a vortex mixer and repeatedly centrifuged until the majority of the diatoms are removed. Excess water is decanted away but the samples are kept wet.

Stage 4: Samples from Stage 3 were added to 3-5 ml of 2.1 sg SPT in centrifuge tubes and mixed using a vortex mixer. Separation occurs during continuous centrifuging at 2500 rpm for 20 minutes. (The brake should not be applied while centrifuging as it causes remixing of separated material). The material which floats to the top of the liquid (called the float) is predominantly diatoms (<2.1 sg), and is decanted into a second centrifuge tube leaving the heavier detrital grain residue (>2.1 sg) at the bottom of the tube. The SPT is best removed from the diatom sample by rinsing over a 10 μm sieve, because it is difficult to remove the SPT by centrifuge washing alone, as the sediment pellet tends to retain a proportion of the relatively heavy SPT. When testing the method using standard laboratory diatomite, the standard material yielded a $\delta^{18}O$ value 6.5‰ lower than expected without this final sieve stage, which is attributed to insufficient removal of the SPT. When the standard was washed over a 10 μm mesh with distilled water, the diatomite yielded the expected $\delta^{18}O$ value.

Finally, the purified diatom samples are dried at 40°C for 24 hours. For the purpose of this study, subsamples of the concentrated diatom from each of the stages described above, as well as the residue from the differential settling stage, were collected for visual inspection and $\delta^{18}O$ analysis.

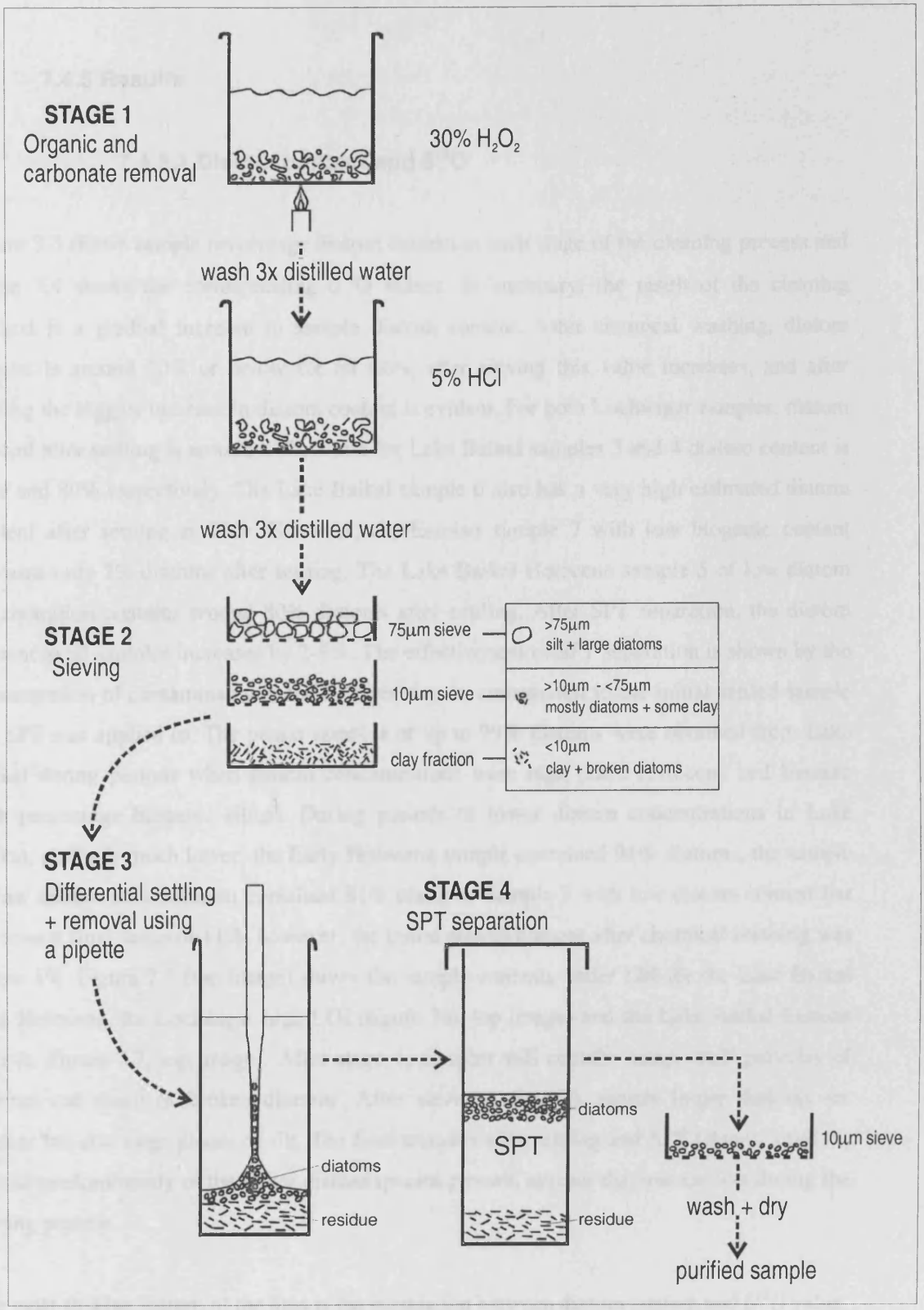

Figure 7.2: Flow diagram showing the four stage cleaning method for concentrating diatom for oxygen isotope analysis from lake sediments (Morley *et al.* 2004).

7.4.5 Results

7.4.5.1 Diatom content and $\delta^{18}O$

Figure 7.3 shows sample percentage diatom content at each stage of the cleaning process and figure 7.4 shows the corresponding $\delta^{18}O$ values. In summary, the result of the cleaning method is a gradual increase in sample diatom content. After chemical washing, diatom content is around 20% or below for all sites, after sieving this value increases, and after settling the biggest increase in diatom content is evident. For both Lochnagar samples, diatom content after settling is around 87%, while for Lake Baikal samples 3 and 4 diatom content is 95% and 89% respectively. The Lake Baikal sample 6 also has a very high estimated diatom content after settling at 96%. However, the Eemian sample 7 with low biogenic content contains only 7% diatoms after settling. The Lake Baikal Holocene sample 5 of low diatom concentration contains around 80% diatoms after settling. After SPT separation, the diatom content in all samples increases by 2-5%. The effectiveness of SPT separation is shown by the concentration of contaminants in the SPT residue, in comparison to the initial settled sample the SPT was applied to. The purest samples of up to 99% diatoms were obtained from Lake Baikal during periods when diatom concentrations were high (Late Holocene and Eemian high percentage biogenic silica). During periods of lower diatom concentrations in Lake Baikal, purity is much lower; the Early Holocene sample contained 91% diatoms, the sample of low diatom concentration contained 81% diatoms. Sample 7 with low diatom content has the lowest final value of 11%, however, the initial diatom content after chemical washing was below 1%. Figure 7.5 (top image) shows the sample contents under LM for the Lake Baikal Late Holocene, for Lochnagar high LOI (figure 7.6, top image) and the Lake Baikal Eemian sample (figure 7.7, top image). After stage 1, samples still contain many small particles of detritus and small or broken diatoms. After sieving (stage 2), mostly larger diatoms are present but also large pieces of silt. The final samples after settling and SPT (stages 3 and 4), consist predominantly of the larger diatom species present, smaller diatoms are lost during the sieving process.

The most striking feature of the data is the correlation between diatom content and $\delta^{18}O$ value. In each case, a higher content of diatom silica in a sample provides a higher $\delta^{18}O$ value. This is generally true for all sites, although there are some inconsistencies such as the Lake Baikal Eemian low percentage biogenic silica sample settled fraction, having a similar value to that of the fraction after acid washing. This is probably due to the low diatom content of the sample as a whole. The lowest $\delta^{18}O$ is almost always found in samples with the highest

amount of contamination, this is clearly shown by the settled residue of both Lochnagar samples. Figures 7.5, 7.6 and 7.7 are LM photographs showing the state of the samples from the Lake Baikal Holocene, Lochnagar high LOI and Lake Baikal Eemian high biogenic silica respectively. Initially samples have a high content of fine (<10 μm) material which is removed after the sieving stage. However, it can be seen that large clastic material is still present although this is removed after the settling and SPT treatment.

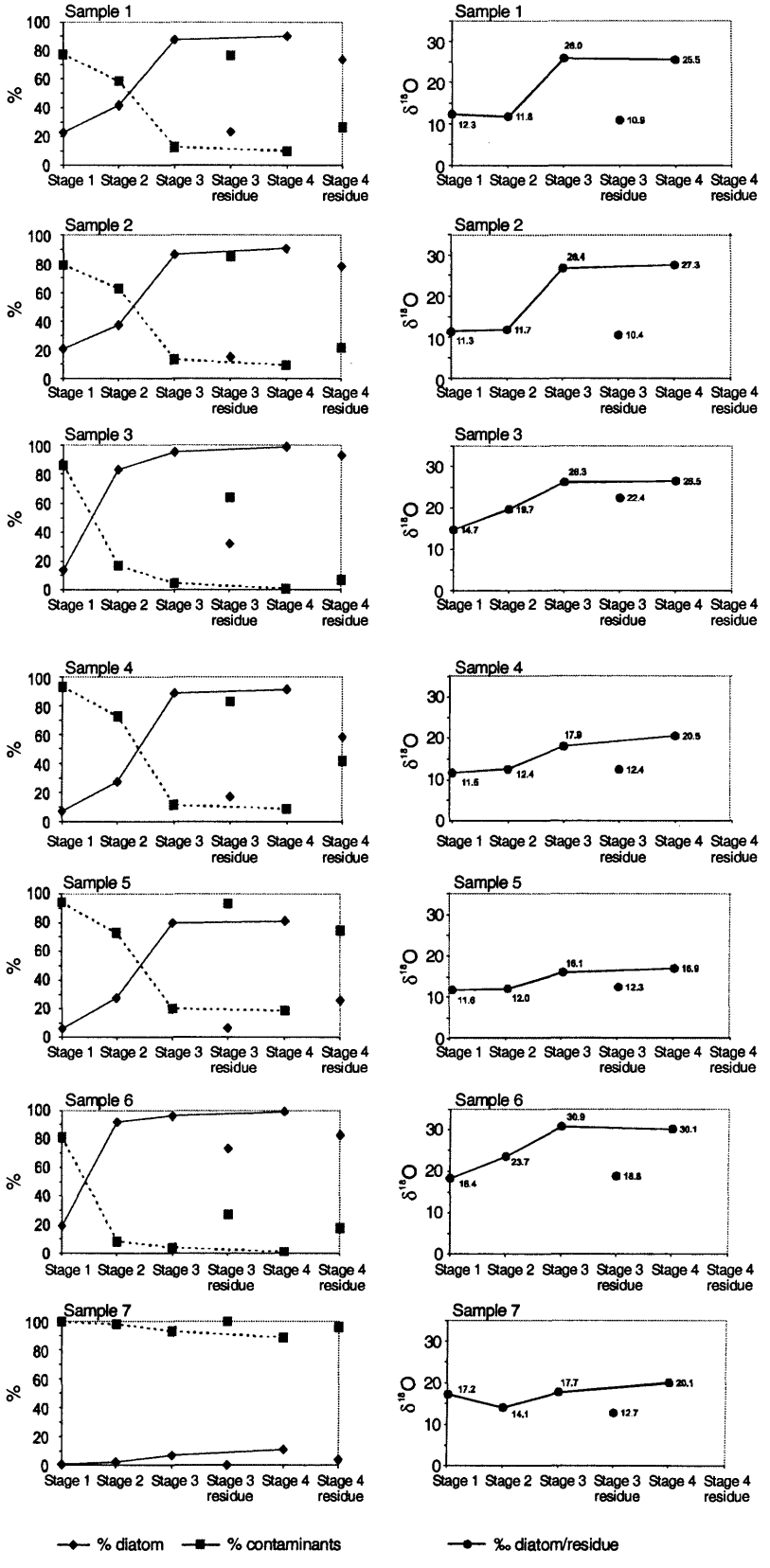

Figure 7.3: (left column) Samples 1-7 showing percentage diatom and contaminant content.

Figure 7.4: (right column) $\delta^{18}O_{DIAT}$ for Samples 1-7 after the four cleaning stages and the residue left after Stages 3 (no residue after stage 4 measured). $\delta^{18}O_{DIAT}$ values are given next corresponding points.

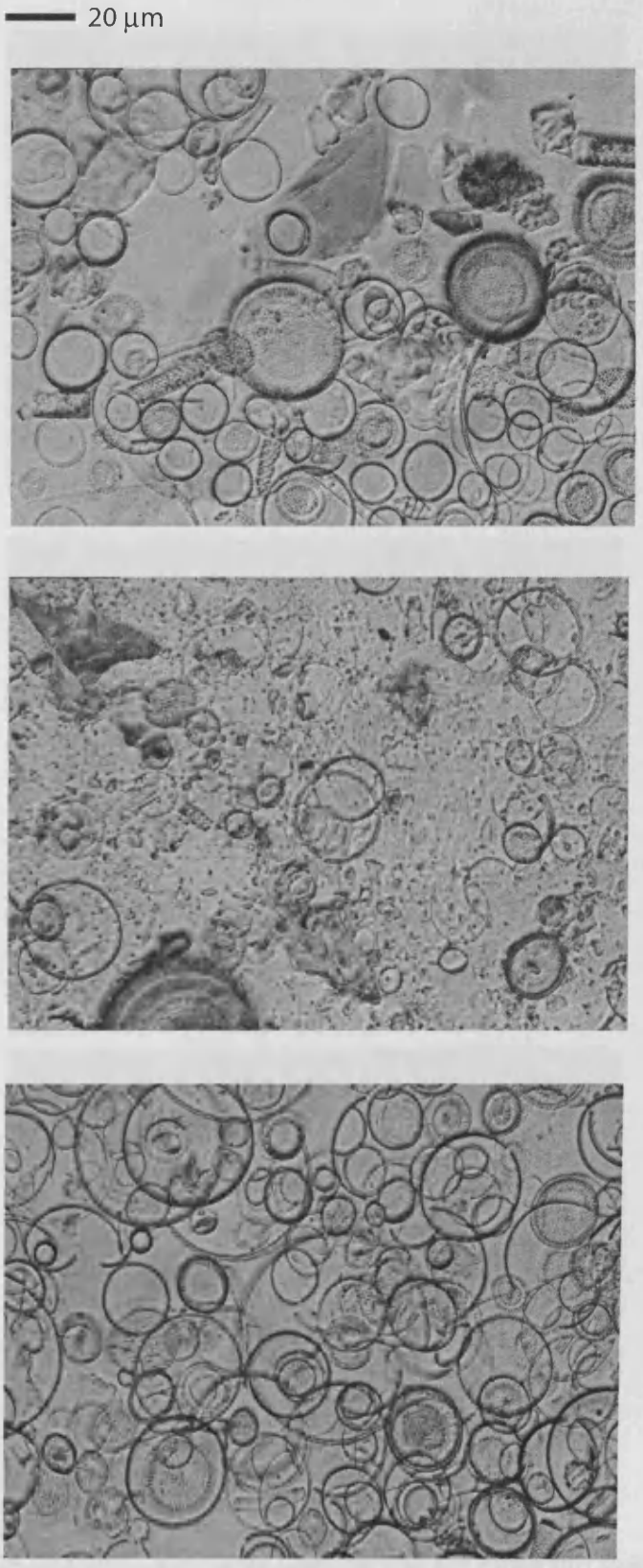

Figure 7.5: LM photographs showing the Lake Biakal Late Holocene sample after stage 1 of the cleaning protocol (top), after stage 2 (middle) and the final clean sample (bottom).

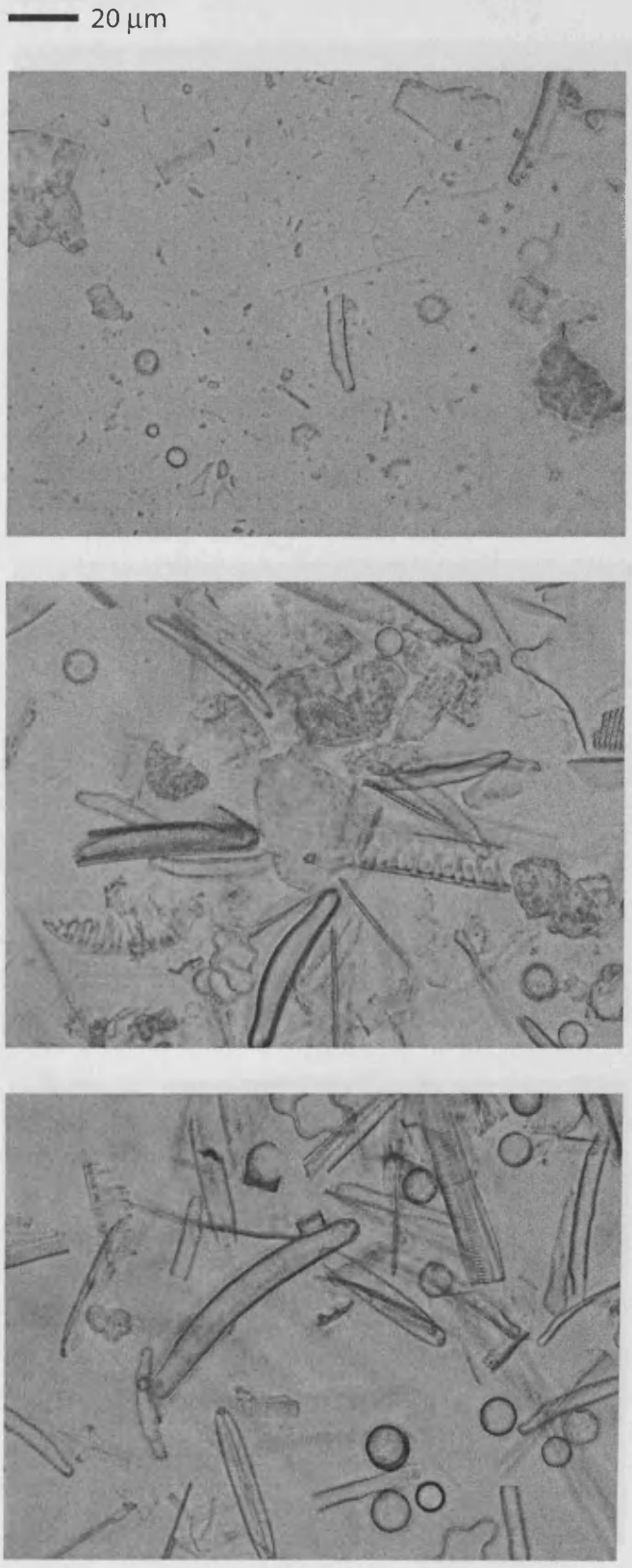

Figure 7.6: LM photographs showing the Lochnagar high LOI sample after stage 1 of the cleaning protocol (top), after stage 2 (middle) and the final clean sample (bottom).

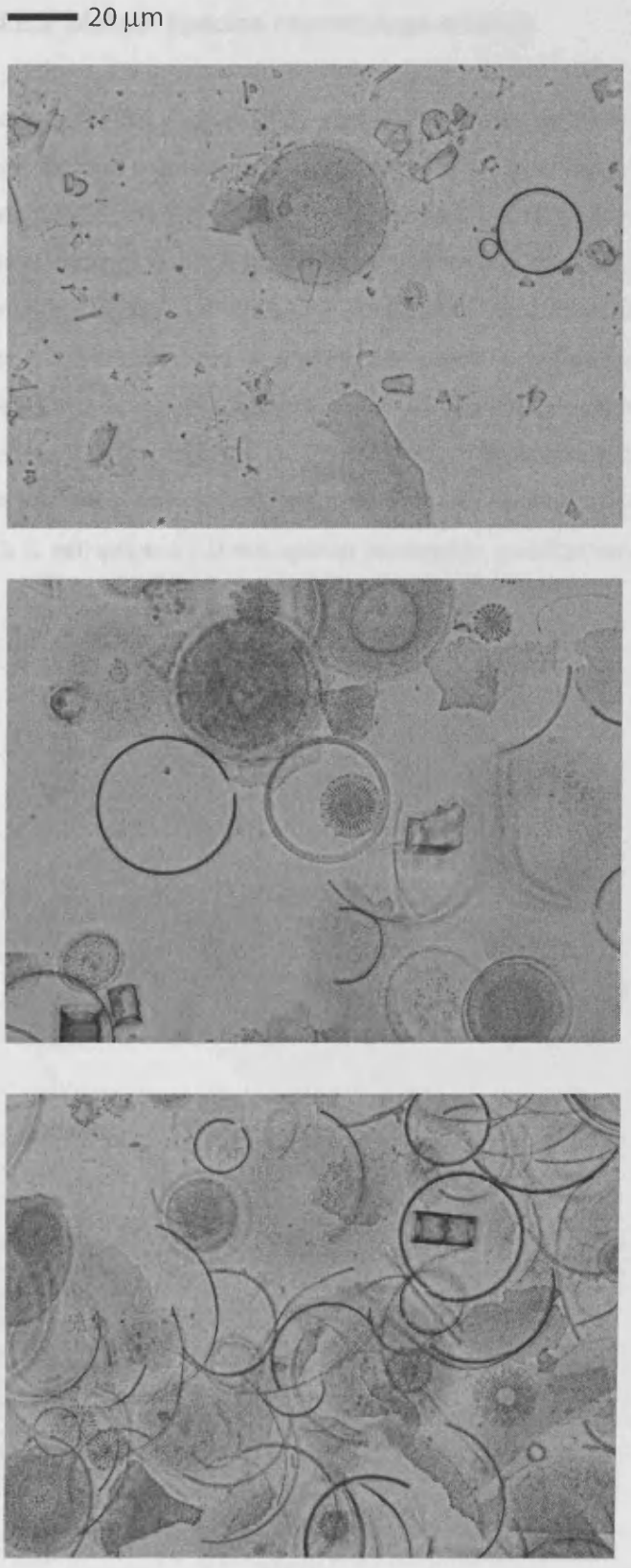

Figure 7.7: LM photographs showing the Lake Biakal Eemian high biogenic silica sample after stage 1 of the cleaning protocol (top), after stage 2 (middle) and the final clean sample (bottom).

7.4.5.2 Diatom species assemblage change

Because the cleaning stages for diatom silica may alter the species composition and cause biasing of the sample, diatoms were counted at each stage of the cleaning process for the Lake Baikal Holocene samples. Figure 7.8, 7.9 and 7.10 show how Baikal Holocene diatom species percentage abundance, changes through the cleaning process. For the Late Holocene (sample 3), the species assemblage remains on the whole unchanged, being dominated by *C. minuta.* However, the 'other' category declines in importance, which is probably due to the loss of small benthic diatoms during sieving. Sample 4 and 5, initially contain more abundant smaller diatom species such as *C. inconspicua, A. skvortzowii* resting spores and small benthic diatoms. As a result of sieving and settling, larger diatoms such as *H. arcus* and *A. baicalensis* become dominant. It is still unknown if this species biasing has an effect on $\delta^{18}O$ values.

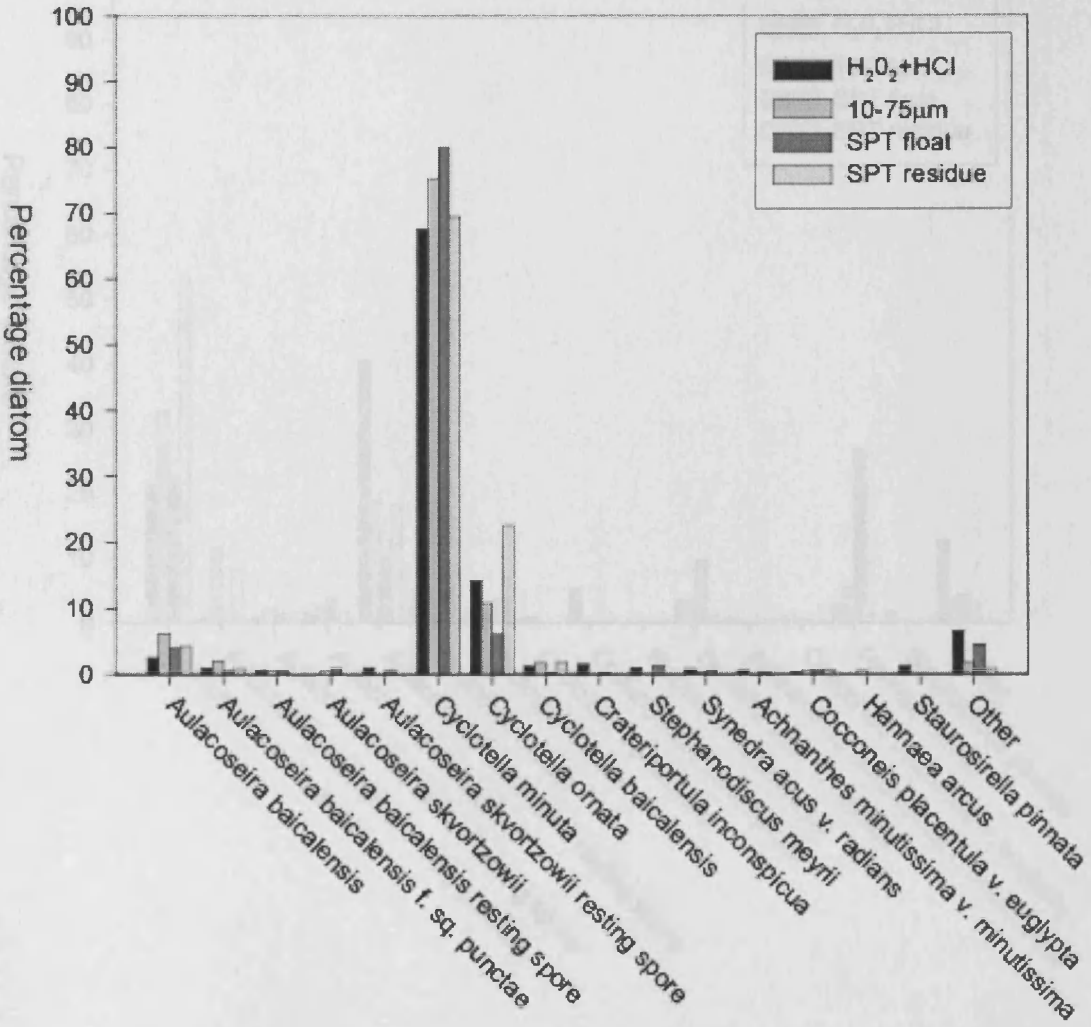

Figure 7.8: Changing species assemblages through the cleaning process, after stage 1, stage 2, the residue left after stage 3 and after stage 4 for the Lake Baikal Late Holocene samples (Sample 3).

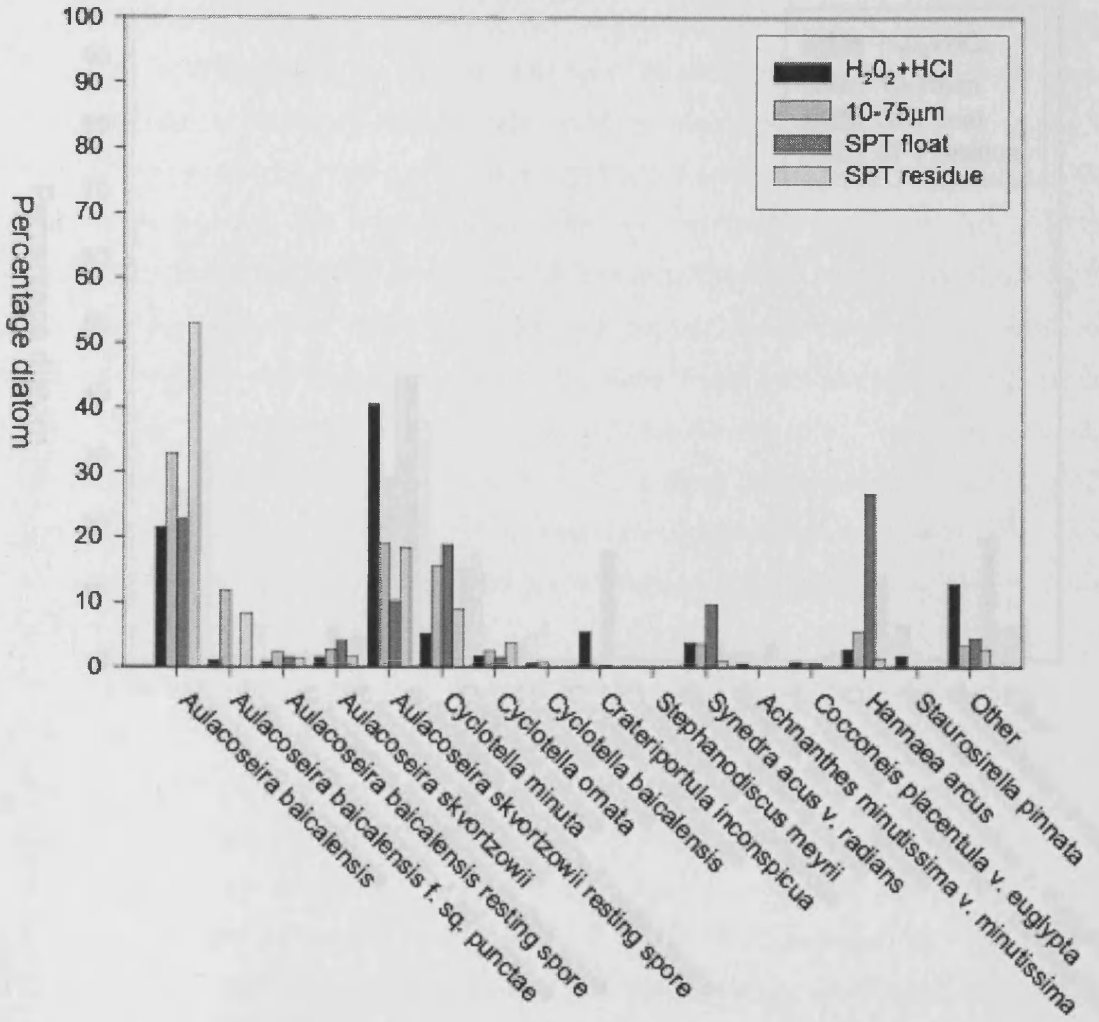

Figure 7.9: Changing species assemblages through the cleaning process, after stage 1, stage 2, the residue left after stage 3 and after stage 4 for the Lake Baikal Mid Holocene sample (Samples 5).

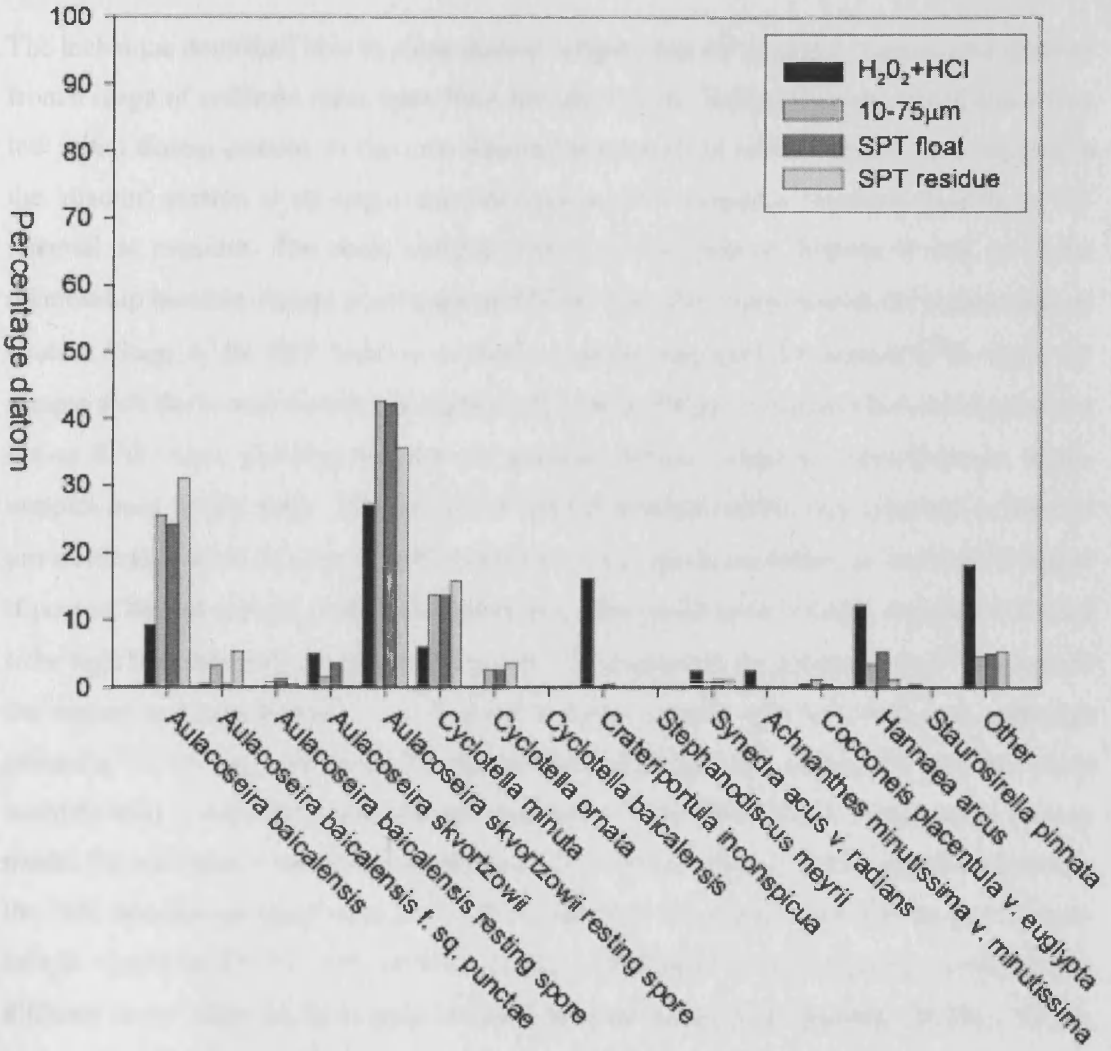

Figure 7.10: Changing species assemblages through the cleaning process, after stage 1, stage 2, the residue left after stage 3 and after stage 4 for the Lake Baikal Early Holocene sample (Sample 4).

7.4.6 Discussion

The technique described here to clean diatom samples has successfully concentrated diatoms from a range of sediment types apart from Sample 7 (Lake Baikal, Eemian) which had a very low initial diatom content. In this case significant amounts of mineral grains were retained in the 'diatom' portion at all stages and this suggests that continual rigorous checking of the material is required. The most striking feature of the data in Figures 4 and 5, is the relationship between diatom percentage and $\delta^{18}O$ value. The fraction with the highest diatom content (Stage 4, the SPT float) is in most cases the one with the highest $\delta^{18}O$, while the sample with the lowest diatom and highest silt content (Stage 3 residue after settling) has the lowest $\delta^{18}O$ value, showing that the end member isotope values are very disparate in the samples used in this study. The amount of detrital material (either clay removed in the <10 μm sieve stage or 10-75 μm silt) will therefore have a significant influence on the $\delta^{18}O$ signal if poor or limited sample clean up is undertaken. The purity of the sample required will need to be high but ultimately the percentage purity will depend on the comparative $\delta^{18}O$ values of the diatom and contaminant. It is doubtful that any sample will be 100% pure, although assuming the residue from Stage 3 represents the mean detrital contaminant, then this value could be used to calculate out the detrital component in the final sample using a linear mixing model. For example, if the residue in Sample 1 has a mean value of 10.9‰ and this represents the 10% non-diatom material in the final sample, then the actual value for the pure diatom sample would be 27.1‰ (10% of $\delta^{18}O$ 10.9‰ + 90% of $\delta^{18}O$ pure diatom) - substantially different to the value of the sample obtained after the 4 stages of cleaning (25.5‰). To put these shifts in $\delta^{18}O$ associated with changing sample diatom content in a palaeoclimatic context, it is interesting to compare them to published shifts of $\delta^{18}O$ that have been interpreted as climatically driven. For example, Leng *et al.* (2001) interpret swings of 16-32‰ as the influence of spring snow melt supplying isotopically depleted water to a small lake in Turkey, Shemesh *et al.* (2001a) related a 3.5‰ depletion to a 2.5-4.0°C cooling in Lapland since the early Holocene, while Shemesh and Peteet (1998) measured a shift of 4‰ associated with the transition between the Allerød and Younger Dryas in north-eastern USA. The magnitude of published $\delta^{18}O$ shifts is generally less than or comparable to the shifts of >10‰ found here as a result of different levels of contaminant removal. This highlights the importance of sample purity when undertaking analysis of $\delta^{18}O$ from diatom silica, as even small increases in contaminants will have a marked influence on the $\delta^{18}O$ value and may lead to possible misinterpretation of a palaeoclimatic signal. For example, wetter or colder conditions would result in a lowering of $\delta^{18}O$ but an inwash of a larger proportion of detrital material would result in the same effect on the $\delta^{18}O$ value if the extra detrital component were not removed. It

is always important that palaeoclimatic interpretations from $\delta^{18}O$ diatom are supported by other proxy data.

7.4.7 Conclusions

It has been shown that the amount of detrital grain contamination in a diatom sample can considerably influence the $\delta^{18}O_{DIAT}$ signal. In order to obtain a climatic signal, pure samples must be used. This can be achieved via a series of cleaning stages including chemical attack, sieving, differential settling and heavy liquid separation. A problem with this method is that it removes the smallest and possibly the largest diatoms at Stage 2, hence biasing the species composition. It is hoped that such biasing will only have a minor influence on the $\delta^{18}O$ signal. The method described here works best for sediments of initial moderate to high diatom concentration (>20%) and it may be impossible to clean samples of very low diatom concentration. However, even after 4 stages of purification, many of the 'pure' samples include some detrital grains, but in some cases the samples are probably clean enough to give a meaningful $\delta^{18}O$ (e.g. 99% diatoms in Samples 3 and 6). However other samples may produce meaningful data only if the detrital component is partitioned from the final data (i.e. using a linear mixing model to unravel the diatom $\delta^{18}O$ signal from that of silt, e.g. Samples 1, 2 and 3 which have a final diatom content of *c.* 90%). Samples with low initial diatom concentration (e.g. Samples 5 and 7) may not yield any reliable climatic information, simply because there were insufficient diatoms in the sediments to produce a clean enough sample by this method because the large sample size (10's of grams) probably needed to produce enough diatoms for analysis are seldom available from lake and marine sediment cores.

7.5 Application of $\delta^{18}O_{DIAT}$ analysis to Lake Baikal sediments

7.5.1 Methodology

The piston/trigger core (CON01-605-3/3a) was analysed for $\delta^{18}O_{DIAT}$ at contiguous 2 cm intervals using the preparation protocol described above. The percentage of diatoms and silt contamination in each sample was also analysed in the same way as in the above experiments using a 10x10 grid graticule to assess LM slides at x1000 magnification. $\delta^{18}O$ analysis was carried out at NIGL, Keyworth using the methodology outlined in section 7.3.2.The results presented here are also detailed in Morley *et al.* (in press).

7.5.2 Results

Figure 7.11a and 7.11b show bulk $\delta^{18}O_{DIAT}$ and percentage diatom content respectively. For comparison, the concentration of diatoms calculated in chapter 6 is also shown. Analysis was carried out at 0.5 cm intervals but the results presented in figure 7.11 have been smoothed by a five point moving average. Diatom contents even after applying the above cleaning method range from 33% to 99% and isotope values between 14.4‰ and 34.3‰. By carefully checking each sample after purification, it appears that it is virtually impossible to get 100% pure diatom samples when starting with a few grams of sediment. Even with minor amounts of silt present it is evident that silt content has a major influence on $\delta^{18}O$, since samples containing most silt have correspondingly lower $\delta^{18}O$ values. To overcome this contamination problem, all samples of less than 90% diatom content were omitted, and using a mass balance calculation, the effect of the silt contamination was removed. The bulk $\delta^{18}O$ value was taken as a linear mixture of oxygen from silt and diatoms, taking the $\delta^{18}O$ value of silt as 12.3±1.8‰ (2 sd, n = 6). This value was calculated as an average of rock fragments and silt (measured after a treatment with sodium hydroxide to dissolve out diatoms) found in the Vydrino core. A value for pure diatoms is estimated using the percentage content of diatoms and silt. Silt contamination is not a problem exclusive to Lake Baikal although most studies dealing with $\delta^{18}O_{DIAT}$ do not give this adequate consideration (Morley *et al.* 2004). This investigation is the first of its type to actively consider the role silt has on the $\delta^{18}O_{DIAT}$ of individual samples.

The $\delta^{18}O_{DIAT}$ composition of the purified samples with a mass balance correction (figure 7.11c), displays a trend of gradually lowering values throughout the Late Glacial from 27.0‰ to 20.6‰. During the latter part of the GS-1 and Early Holocene (VYD-D10 to D8), pure samples could not be obtained due to low diatom abundance and the presence of small or fragmented diatoms. The mid-Holocene (VYD-D5) drop in sample cleanliness at 5.5-7 kaBP is not concordant with a similar drop in sediment diatom concentration (fig. 7.11d). The dominant diatom present at this point are *S. acus* v. *radians* and this species fragments very easily due to its needle like form. Therefore the resultant drop in $\delta^{18}O_{DIAT}$ is due to a higher sample silt content as the cleaning method would have removed many of these smaller diatom fragments. During the earlier stages of the Holocene (VYD-D7 and onwards), $\delta^{18}O$ gradually switches to higher values and remains relatively stable throughout this period varying between 24.7‰ and 30.0‰, apart from a large excursion of one sample at *c.*8.0 kaBP to 32.0‰ that also coincides with a peak in diatom concentration.

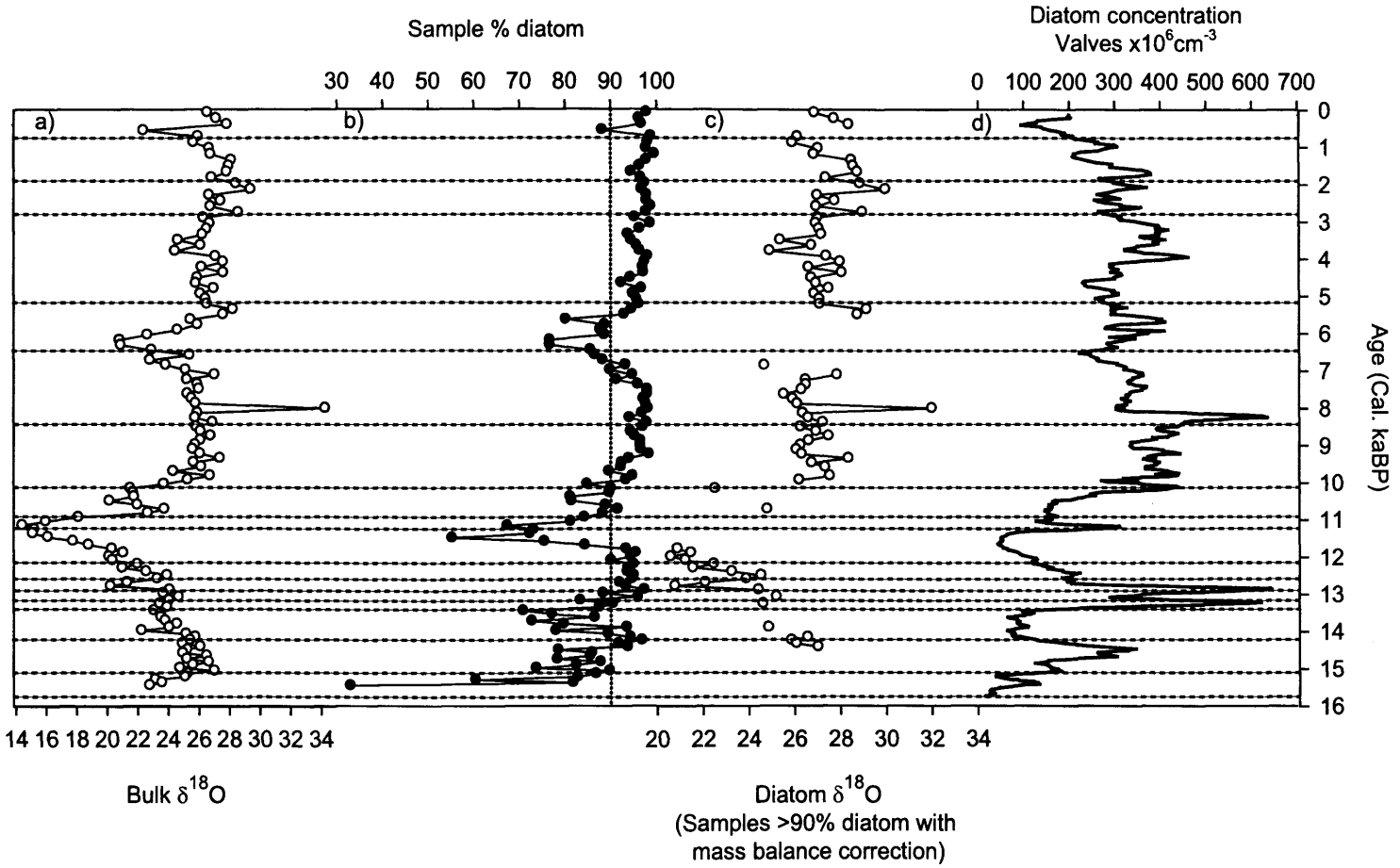

Figure 7.11: a) Bulk $\delta^{18}O$ for a core taken from the Vydrino Shoulder, Lake Baikal b) Estimated sample percentage diatom content with limit of 90% purity marked. c) Mass balanced $\delta^{18}O$ ($\delta^{18}O_{DIAT}$) calculated using samples >90% purity and a mass balance correction to remove the effects of small amounts of silt still present after cleaning. d) Diatom concentration of sediments before cleaning. The diagram is zoned according to diatom assembalge zones defined by CONISS Plotted against Cal. aBP.

7.5.3 Discussion

Possible controls on $\delta^{18}O$ of Lake Baikal's water include evaporative enrichment, input of depleted meltwater from glacier retreat, changing $\delta^{18}O$ of precipitation due to temperature, and changes in seasonal precipitation amounts linked to atmospheric circulation changes. As the $\delta^{18}O$ of lake water remains constant throughout the year (table 3.1), there is no seasonal weighting of the $\delta^{18}O_{DIAT}$ signal associated with lake water isotopic signature at the time of the diatom bloom (*c.f.* Leng *et al.* 2001, Jones *et al.* 2004). Evaporation has little impact on Lake Baikal as outflow dominates over evaporation and the lake water conforms to the GMWL (figure 3.1).

Assuming that the temperature and isotopic composition of the source of precipitation was constant, then if the variations through the core were based on temperature alone, the temperature change required to account for the variation of 6.4‰ seen over the Late Glacial can be calculated. By combining the rainfall water-temperature fractionation of $+0.36‰^{\circ}C^{-1}$ (the Dansgaard temperature dependence in precipitation at Irkutsk, (Seal and Shanks (1998)) and a mineral-temperature fractionation of -0.5 to $-0.2‰^{\circ}C^{-1}$ (Shemesh *et al.*, 1992; Brandriss *et al.*, 1998) we would get a temperature change that is unacceptably large for summer lake-water temperature variation, assuming that these relationships hold for the Late Glacial. Estimates of temperature deviations from present day values during the GS-1 are around -11°C in winter and -5°C in summer (Velichko *et al.* 2002). Even just taking this extreme winter temperature difference to the present day, an 11°C variation alone accounts for only a 4‰ shift in $\delta^{18}O$ using the modern Dansgaard relationship. If considering the average annual temperature shift over this period, the amount of $\delta^{18}O$ variation explained by temperature will be even less.

Meltwater input can have a significant role in determining lake water $\delta^{18}O$ (Leng *et al.* 2001). Wastage of glaciers in Lake Baikal's catchment may have been an important source of isotopically depleted water. Melting events should follow a climatic warming, and increases in the sediment diatom concentration curve (fig. 7.11d) give a basic indication of warmer periods. Several warming events are evident over the Late Glacial comparable to the GI-1 events (chapter 6). A sudden drop in $\delta^{18}O$ at *c.*12.8 kaBP (VYD-D12) may represent a meltwater pulse response to a warmer period, possibly the GI-1a found in GISP2. However, isotopic lowering continues into the GS-1(VYD-D11 and D10) when glaciers would be advancing, and possible lag effects due to water residence time are too short to explain this continuing depletion. A considerable amount of glacial wastage would also be expected at the

termination of the glacial period and the start of the Holocene. Despite few data points at this interval (VYD-D9 and D8), $\delta^{18}O$ values appear to be becoming higher and therefore not conforming to the idea of increased meltwater input. Possible explanations for this may be due to the fact that the region was very arid during glacial times, limiting the growth of mountain glaciers. Wolfe *et al.* (2000) show that the Eurasian continental interior was much drier than areas with an oceanic influence. This is mainly due to the presence of the Fennoscandian Ice Sheet causing the development of anticyclonic conditions directly above itself, thus limiting the penetration of moist westerlies from the North Atlantic (Khotinsky 1984). Also, the resultant buffering effect of the lake's size and long residence time may have dampened any meltwater signals.

The most likely explanation for the majority of $\delta^{18}O_{DIAT}$ variation shown in figure 7.11c is the changing importance of input from northern rivers compared to southern rivers (chapter 3, figure 3.5). This can be linked to changes in atmospheric circulation altering seasonal patterns of precipitation. The reason for the north-south isotopic gradient in river inputs is due to varying proportions of isotopically low winter precipitation (snowmelt runoff) versus isotopically higher summer precipitation from cyclonic activity. Indeed diatom based reconstructions of snow depth on ice (chapter 6) reveal deeper snow cover during colder periods of the Late Glacial than during the Holocene. However, these reconstructions are presently only available for the South Basin. As shown in figure 3.1, Irkutsk summer precipitation has considerably higher $\delta^{18}O$ than winter snowfall. In the modern lake, the Upper Angara (North Basin) is sourced 32% from snowmelt and 20% from summer precipitation, while the Selenga (South Basin) contains much less snow input (15%) and more summer precipitation (37%) (Afanasjev 1976). Both rivers have similar inputs from groundwater (Afanasjev 1976). Hence dominance of snowmelt input in the north and summer precipitation in the south drives the modern isotopic north-south gradient of river waters. In order to explain variations in the $\delta^{18}O_{DIAT}$ record by changing river inputs, a change in seasonal precipitation distribution and/or amount is needed over the catchment. Using the data of Seal and Shanks (1998) it is possible to calculate a first order estimate that the 6.4‰ shift over the GS-1 would have needed an increase of over 60% in discharge from North Basin rivers if all flows remained constant. If there was a total cessation of the Selenga's flow (while all other river discharge remained at present values), this would only result in a $\delta^{18}O$ lowering to approximately –19‰. As both of these situations appear extreme, it is most likely that $\delta^{18}O$ variations are caused by a coupling of flow variations in northern and southern rivers. In other words, a $\delta^{18}O$ lowering of lake water can be forced by a simultaneous relative increase in northern river discharge and a relative decrease in the south, in particular from the

Selenga River. Mechanisms to explain this may be linked to alterations in atmospheric circulation related to changing boundary conditions.

Such a change in atmospheric circulation that may cause an increase in North Basin river discharge linked to increased winter precipitation and snowmelt while also causing a summer drying over the south of the catchment, is due to a feedback stemming from Eurasian spring snow cover extent (ESSC). Using instrumental and remotely sensed data, Liu and Yanai (2002) noted a negative correlation between ESSC and the following Asian summer rainfall amount over the last century. This decline in summer precipitation related to high ESSC during the preceding winter, was most pronounced to the south of Lake Baikal over the Selenga River catchment. Cooler climates and a longer winter can lead to increased ESSC, this in turn creates cyclonic circulation in the lower troposphere over northern Eurasia due to the cooling effect of the snow cover. This cooling delays and weakens the East Asian summer monsoon and also results in anticyclonic activity and aridity over the southern areas of Lake Baikal's catchment. As a result, high $\delta^{18}O$ summer inflow will be reduced while increased winter precipitation and snow cover will allow low $\delta^{18}O$ water to enter the Lake. During warmer years with reduced ESSC, the opposite situation occurs with cyclonic activity and increased summer precipitation in the south. Increased ESSC should also result in an increase in discharge through all Lake Baikal tributaries, although snow cover (winter precipitation) is highest in the north (Mackay *et al.* 2003), while the summer anticyclonic conditions should only affect flow in the south. Zhang and Crowley (1989) note a reduction in precipitation documented by instrumental records over North China in cold periods such as the Little Ice Age linked to this phenomenon. GCM experiments have also modelled the development of summer anticyclonic conditions to the south of Lake Baikal, in summers following a winter of extensive Eurasian snow cover (Bartlett *et al.* 1988). Combined with this, the winter Siberian High pressure system can persist longer over the year during cold periods, as it is strengthened by inflow of cold Arctic air (Ding *et al.* 1995), hence prolonging winter conditions and delaying the development of summer cyclonic conditions.

The results of pollen analysis by Demske *et al.* (in review) generally confirm that the south of Baikal was drier than the north during colder periods. Three sites were analysed in Lake Baikal, the Vydrino Shoulder in the south, Posolsky Bank in the Central Basin and the Continent Ridge in the north (figure 2.1). Aridity in the south is indicated at the start of the $\delta^{18}O$ record by higher non-arboreal pollen than at the other sites, due to the presence of steppe vegetation while *Picea* forests began to develop in the moister north. Higher levels of *Alnus fruiticosa* pollen in the north during the Younger Dryas indicate that this period was cold and

moist while in the south, persistence of steppe communities indicate a cold but drier climate. The beginning of the Holocene is marked by lower moisture availability over the whole region as shown by a decline in *Alnus fruiticosa* pollen, while the south was still much drier than the north, suggested by the lack of *Betula/Pinus* forests. This may explain why Early Holocene $\delta^{18}O$ is lower than later Holocene values with the lack of summer input from the Selenga and a dominance of snow melt (as well as possible inputs from glacier wastage) in the moister northern regions. Progressive warming into the Holocene and a decrease in summer anticyclonic activity allowed increased moisture in the south, shown by the development of dense dark taiga forests during the Early to Mid-Holocene. This moisture increase coincides with enriched $\delta^{18}O$, related to greater summer precipitation and lower snowmelt input.

Warmer periods during the Late Glacial as shown by increased diatom concentration have $\delta^{18}O$ values similar to those of the Holocene. These findings confirm the theory that a warmer climate generally results in enriched $\delta^{18}O_{DIAT}$ from less winter precipitation and strengthened summer cyclonic activity, while cooler periods should cause depleted $\delta^{18}O_{DIAT}$. Cooler periods could not be fully investigated for comparison however, due to the lack of diatoms present at these times. The large spike to 32.0‰ (this value was replicated after re-running the sample several times) at *c.*8 kaBP coincides with a peak in sediment diatom concentration. Although Morrill *et al.* (2003) find little evidence for an 8.2 kaBP event in a synthesis of Asian Monsoon palaeoclimatic data, this peak may be related (see section 1.3.3). Due to the precision of the dating here, it is not possible to determine whether this peak in both $\delta^{18}O_{DIAT}$ and diatom concentration occurs before or after 8.2 kaBP. The corresponding peaks in these two curves do not coincide exactly due to the coarser sampling resolution used in $\delta^{18}O_{DIAT}$ analysis. While it is not clear what caused this excursion shown in figure 7.11c, it is possible that this peak marks either a change in lake hydrology associated with a change in the catchment, or an abrupt climatic event.

Several assumptions concerning the relationship of $\delta^{18}O_{DIAT}$ to climatic forcing have had to be made when interpreting this record. It is assumed that the modern relationship of $\delta^{18}O$ in precipitation and temperature, holds for the entire period studied. However, studies in other regions have shown that variations in the amount of precipitation can also affect $\delta^{18}O$. Johnson and Ingram (2004) describe how variations in monsoon intensity can not only lead to significant spatial variability in the $\delta^{18}O$-precipitation relationship over China, but also temporal variability. Similarly, Hammarlund *et al.* (2002) noted deviations from the modern Dansgaard relationship (of about 2‰) before 6000 aBP in Sweden, by comparing the isotope

record to pollen inferred temperatures. This deviation was attributed to shifts in atmospheric circulation. Deviations from modern Dansgaard relationships have also been acknowledged in Canada by Edwards *et al.* (1996), and in Europe by von Grafenstein *et al.* (1999) and Teranes and McKenzie (2001). It may be therefore, that fluctuations in atmospheric circulation patterns and the strength of Westerlies reaching Lake Baikal may alter the slope of the Dansgaard relationship. However, as this study has not attempted to make quantitative temperature inferences, it is hoped the broad scale $\delta^{18}O_{DIAT}$ shifts faithfully record relative seasonal precipitation and river discharge changes.

It has also been assumed that changes in the hydrology of the lake and catchment conditions over the period of study are small (the lake was a similar size during the Last Glacial Maximum with a water level only 2 m lower than at present (Colman 1998)), and changes do not have a significant influence on isotopic values. The spatial variation of succession between steppe vegetation and taiga forest over the catchment (Demske *et al.* in review) may have had some influence in altering catchment hydrology and river flows. However, this effect may be small, due to the large volumes of water involved, i.e. the modern combined annual river input stands at 61.1 km^3 (Gronskaya and Litova 1991). Finally, the effect of species dependant fractionation has been considered to be minimal. In other mediums such as ostracods, such vital effects are known to occur (Leng and Marshall 2004), however it is not known if this is the case for diatom silica (section 7.3.3).

7.5.4 Conclusions

The analysis of $\delta^{18}O$ from diatom silica is a useful technique to provide complementary data to the biological proxy used in this study. However, it is important to note that clean samples must be obtained before $\delta^{18}O$ is measured. This can be seen here by the relationship between the bulk $\delta^{18}O$ curve (Fig. 7.11a) and the sample percentage diatom content (Fig. 7.11b). Such problems can be overcome by checking the purity of each sample and excluding those with high contaminant content. In some parts of the core it was impossible to provide pure diatom samples. However, by carefully cleaning the lake sediments and by undertaking mass balance calculations it is hoped that the effects of <10% silt have been removed, and that variations in $\delta^{18}O$ recorded by diatom silica in Lake Baikal's sediments over the Late Glacial – Holocene are controlled by atmospheric circulation changes altering the seasonal balance of precipitation to the lake's tributaries. During colder periods such as the GS-1 (VYD-D11 and D10), depletion in $\delta^{18}O$ of lake water and subsequently $\delta^{18}O_{DIAT}$, may be caused by a simultaneous increase in discharge northern tributaries to Lake Baikal and a decrease in flow

of southern rivers. Increased winter snowfall can provide increased depleted meltwater run-off, particularly to the North Basin where snowfall is highest. A subsequent feedback through the climate system related to this higher snow cover, can cause anticyclonic conditions over the catchments of southern rivers and a reduction in enriched summer precipitation and river discharge. This changing catchment moisture gradient with climate is confirmed independently through pollen data. However, it has to be assumed that the modern spatial trends in $\delta^{18}O$ shown in figure 3.1 can be extrapolated to past climatic regimes, and it may be that there is a lag of lake water response to climate change due to the lake's long residence time. Other factors may have a role in altering $\delta^{18}O_{DIAT}$, such as evaporation, changes in the Dansgaard relationship and input of depleted glacial meltwater. However, it is likely these factors have a secondary role and cause only minor variation.

Chapter eight

Palaeoclimatic reconstruction from organic material

8.1 Previous work on the possible controls on $\delta^{13}C_{ORG}$ and C/N in Lake Baikal

The general controls of $\delta^{13}C$ and C/N in organic matter have been discussed in section 2.7.1, while the sources of organic matter in the modern Lake Baikal environment have been explored in section 3.2. The controls on $\delta^{13}C_{ORG}$ and C/N are often a mixture of several factors making interpretation difficult. As a result the possible controls on the Holocene – Late Glacial variability in Lake Baikal will be reviewed here with reference to previously published studies, and assessed as to their importance in influencing the record.

There are several published Late Glacial – Holocene $\delta^{13}C_{ORG}$ and C/N records from Lake Baikal, although most are of low resolution, and as with other previously published Lake Baikal diatom records, interpretations are hampered by inadequate chronological control. $\delta^{13}C_{ORG}$ and C/N records for the Late Glacial – Holocene period in Lake Baikal all show the same general trend of a shift in $\delta^{13}C_{ORG}$ from higher values in the Late Glacial to lower values in the Holocene, while C/N is generally lower in the Late Glacial than in the Holocene, this general trend is shown in figure 8.1. These trends were first seen in a study by Ishiwatari *et al.* (1992) although there was no real investigation as to the causes of these shifts because the core analysed was not dated. However, due to the depth of the core it is likely that it covers the Holocene to Late Glacial. Several mechanisms have been put forward to explain these shifts, including catchment vegetation change, algal species composition, palaeo-pCO_2 level and gas hydrate release. These are critically reviewed below.

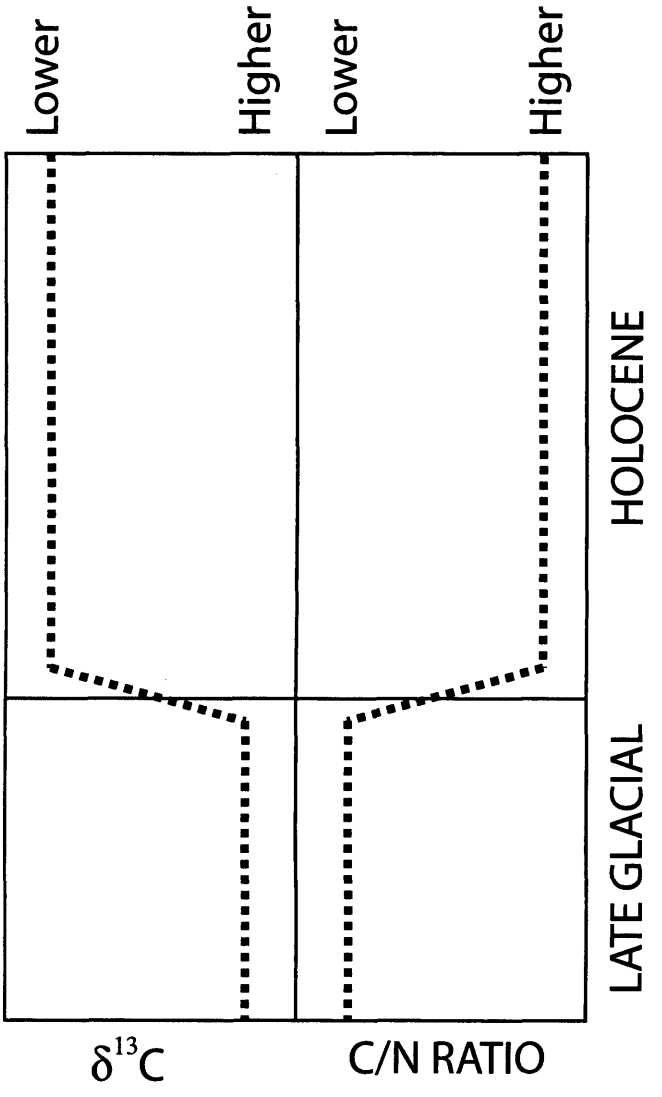

Figure 8.1: Schematic diagram showing the generalised changes in $\delta^{13}C$ and C/N ratio over the Late Glacial and Holocene as found in previous studies of Lake Baikal (Ishiwateri *et al.* 1992, Horiuchi *et al.* 2001).

8.1.1 Catchment vegetation changes

Horiuchi *et al.* (2000) suggest that the higher Late Glacial values of $\delta^{13}C_{ORG}$ demonstrate that diatoms were not the primary producer in the lake during this period as prevailing cold oligotrophic conditions in the lake are likely to have led to diatoms with lower $\delta^{13}C$. This is because during periods of high diatom productivity more ^{13}C is utilised, as the ^{12}C pool is depleted leading to higher $\delta^{13}C_{ORG}$. Diatoms also generally have low $\delta^{13}C$ values (~-28‰, Meyers and Lallier-Vergès 1999) (figure 3.9). Their low abundance as indicated by low biogenic silica abundance implies the dominant source of organic material has higher $\delta^{13}C$. Therefore, Horiuchi *et al.* (2000) suggest that the lower $\delta^{13}C_{ORG}$ values in the Holocene represents a response to a change over the LGIT in catchment vegetation from C_4 grasses to C_3 trees. However, increased diatom abundance in the Holocene will also result in lower $\delta^{13}C_{ORG}$. It has to be assumed that a portion of the organic material is allochtonous, as argued by Ishiwatari *et al.* (1992) who state high C/N ratios demonstrate a dominance of allochtonous organic matter in the Holocene. Horiuchi *et al.* (2000) also suggest that this interpretation is supported by pollen evidence for vegetation changes. Qiu *et al.* (1993) have a similar interpretation for their $\delta^{13}C_{ORG}$ record but find higher C/N values in the Late Glacial. However, this record has since proved to be erroneous due to inadequate sample preparation techniques (Prokopenko *et al.* 1999).

All previous studies of Lake Baikal interpret the C/N ratio in the same way: higher C/N ratios indicate increased catchment inwash of carbon during warmer periods of soil development. Under colder climates, when soil formation is limited, inputs of terrestrial carbon are lower, and C/N ratios become lower as sedimentary material has greater relative amounts of nitrogen due to dominant algal productivity. During warmer periods there is greater soil development and inwash of organic material with higher C/N ratio. Levels of both carbon and nitrogen can rise in this situation and the relative changes between the two are shown by the C/N ratio.

The role of a shift in C_4 to C_3 catchment plants in the observed lowering in $\delta^{13}C_{ORG}$ over the Late Glacial – Holocene has been questioned using compound specific $\delta^{13}C$ analysis of long-chain *n*-alkanes in Lake Baikal sediments. Brincat *et al.* (2000) studied the same material as Ishiwatari *et al.* (1992) and found a switch over the LGIT, from predominantly C_{31} *n*-alkanes to C_{27} *n*-alkanes. Although pollen evidence shows a shift in catchment vegetation from C_4 grasses to C_3 trees over this period (Bezrukova *et al.* 1992), the $\delta^{13}C$ of all the main *n*-alkanes through the core ranges from –31.0 to –33.5 ‰ which is in the range of leaf wax for C_3 plants indicating the prevalence of C_3 vegetation in Lake Baikal's catchment, not only over the

Holocene, but also during the Late Glacial. This compound specific work does however indicate a change in the type of C_3 vegetation over the LGIT but shows that the input of C_4 plant material cannot be invoked to explain relatively higher $\delta^{13}C_{ORG}$ during the Late Glacial. However fragments of C_4 plants have been found in the surface sediments of littoral areas and shallow bays of Lake Baikal, suggesting that at times there may have been some C_4 influence on $\delta^{13}C$ values (Horiuchi *et al.* 2000). There are, however, no data on how this observed C_4 material preserves in the sediments, or if it is present in deeper water sites.

8.1.2 Algal species composition and productivity

An alternative explanation for the higher $\delta^{13}C_{ORG}$ during the Late Glacial could be the increased productivity of cyanobacteria and reduced diatom productivity. As cyanobacteria discriminate very little against ^{13}C in comparison to diatoms and higher plants, their dominance in glacial periods would explain higher $\delta^{13}C_{ORG}$ values (Watanabe *et al.* 2004). With warming and increased diatom productivity, as shown by biogenic silica levels and increased influx of catchment material shown by rising C/N values, $\delta^{13}C_{ORG}$ became lower in the Holocene. This interpretation suggests that $\delta^{13}C_{ORG}$ responds to a switch between authigenic cyanobacteria dominance in cold periods and allogenic catchment inwash, but also diatom productivity (low $\delta^{13}C$) in warm intervals. However, there is a lead in observed $\delta^{13}C_{ORG}$ shifts over the last 130 ka in Lake Baikal compared with increasing diatom abundance (Prokopenko and Williams 2004). For example, during interstadial MIS 5e, $\delta^{13}C_{ORG}$ values are higher even though the amount of biogenic silica does not change from the preceding stadial stage, this is possibly due to this proxy not being sensitive enough to record the climate shift as it is tempered by silica dissolution. The type of phytoplankton clearly does not explain all $\delta^{13}C_{ORG}$ variation in Lake Baikal. However, proxies of diatom abundance, such as biogenic silica amounts, show that diatom productivity increases in warmer periods. Since diatoms have $\delta^{13}C_{ORG}$ values in the range similar to C_3 land plants, the observed isotopic lowering in the Holocene may be due to increased diatom productivity rather than increased inwash of C_3 land plant material. This is supported by the relatively low C/N values of Lake Baikal sediments, commonly less than 11 (Horiuchi *et al.* 2000), while lakes with high terrestrial plant input can have C/N values >20 (Lamb *et al.* 2004).

The level of aquatic productivity can alter the value of $\delta^{13}C_{ORG}$. During periods of high productivity, the preferential utilisation of ^{12}C can cause a high $\delta^{13}C$ in the remaining carbon pool. Consequently during periods of low productivity, the $\delta^{13}C$ pool stays lower. However the observed shifts to isotopically lower $\delta^{13}C_{ORG}$ occur during climatic warming and increased productivity (as shown by productivity indicators such as total carbon, total nitrogen and

diatom abundance). Therefore, the opposite situation occurs than that expected if productivity level is the main driving mechanism on $\delta^{13}C_{ORG}$. It is most likely that this mechanism is superimposed on the main trends as minor variability. For example, Prokopenko *et al.* (1999) consider an observed +2‰ shift during the mid-Holocene to be due to increased productivity.

8.1.3 Palaeo-*p*-CO_2 levels

An alternative interpretation of the shift to lower $\delta^{13}C_{ORG}$ over the LGIT has been given by Prokopenko *et al.* (1999) linked to palaeo-pCO_2 levels. They note a –3.5‰ shift in $\delta^{13}C_{ORG}$ over the LGIT. As explained above, this cannot be due to productivity changes. Instead, they suggest that the observed lowering of $\delta^{13}C_{ORG}$ is due to increases in global palaeo-pCO_2 at the LGIT and subsequent increases in the levels of dissolved CO_2 in lake water. This was supported by a correlation of the Lake Baikal record to the Greenland ice core records of pCO_2. With increased CO_2 availability there is more discrimination against ^{13}C by algae, and deposited organic matter will have lower $\delta^{13}C$ values. During periods of lower lake-pCO_2 levels, phytoplankton may switch to use HCO_{3-} as a carbon source. In this scenario, $\delta^{13}C_{ORG}$ becomes higher, as the $\delta^{13}C$ of HCO_{3-} is 1‰ compared to -7‰ for CO_2 (general values from Meyers and Teranes 2001).

However, the interpretation of the observed lowering of $\delta^{13}C_{ORG}$ into the Holocene as a response to global palaeo-pCO_2 levels, has been reassessed after a longer record showed little correlation to the Greenland pCO_2 record, this is shown in figure 8.2 (Prokopenko and Williams 2004), although this does not mean that palaeo-*p*-CO_2 levels will have no influence on $\delta^{13}C_{ORG}$, The Lake Baikal $\delta^{13}C_{ORG}$ curve presented by Prokopenko and Williams (2004) does follow broad general scale changes in global palaeo-pCO_2 level, although records of methane levels show a much better correlation (figure 8.2), possible reasons for which are given below.

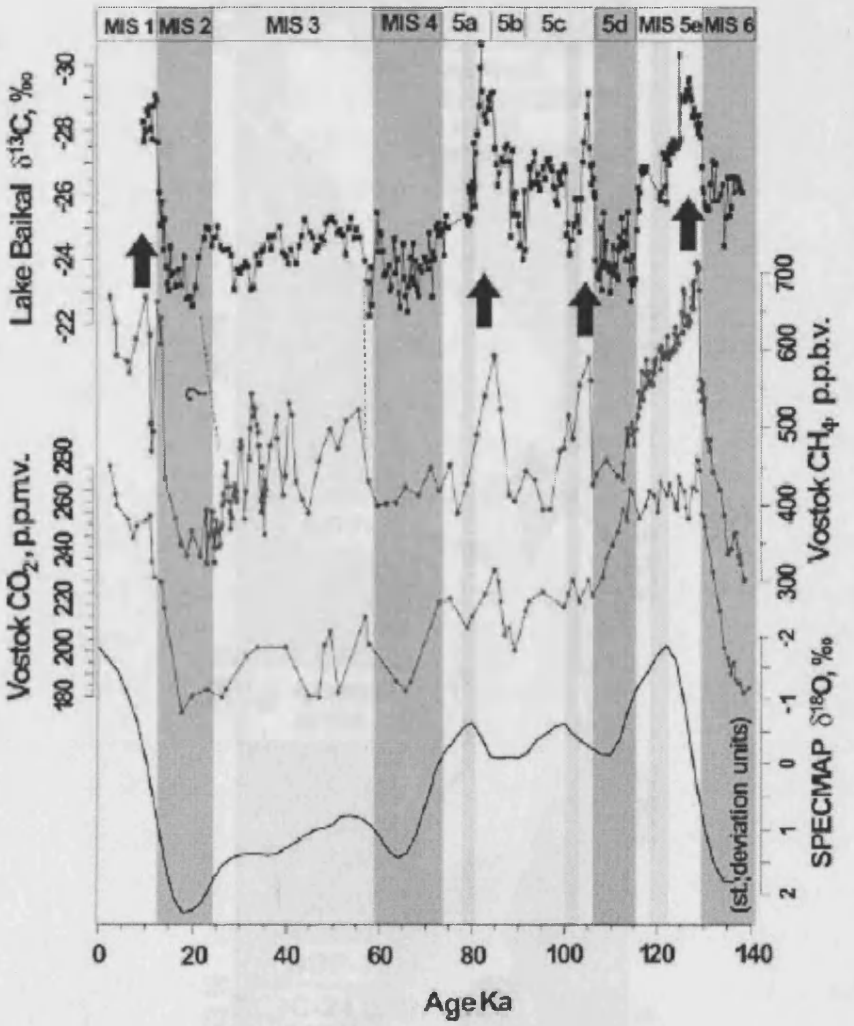

Figure 8.2: The correlation of the Lake Baikal $\delta^{13}C_{ORG}$ record of Prokopenko and Williams (2004) with the SPECMAP template, Vostock ice core methane and carbon dioxide content. Note the better correlation of $\delta^{13}C_{ORG}$ to methane rather than carbon dioxide (from Prokopenko and Williams 2004).

8.1.4 Gas hydrate release

Gas hydrates are an important global reservoir of methane most commonly found in marine sediments and permafrost regions of high latitudes (Klerkx *et al.* 2003), but have been detected in Lake Baikal by Golmshtok *et al.* (1997) through the observation of a bottom-simulating reflection (BSR) during seismic profiling. The extent of gas hydrate layers are thought to be limited to the South and Central Basins to an area either side of the Selenga Delta covering over 4000 km^2 and are between 34 m to 450 m deep (Figure 8.3) (Golmshtok *et al.* 1997, Kuzmin *et al.* 1998, 2000).

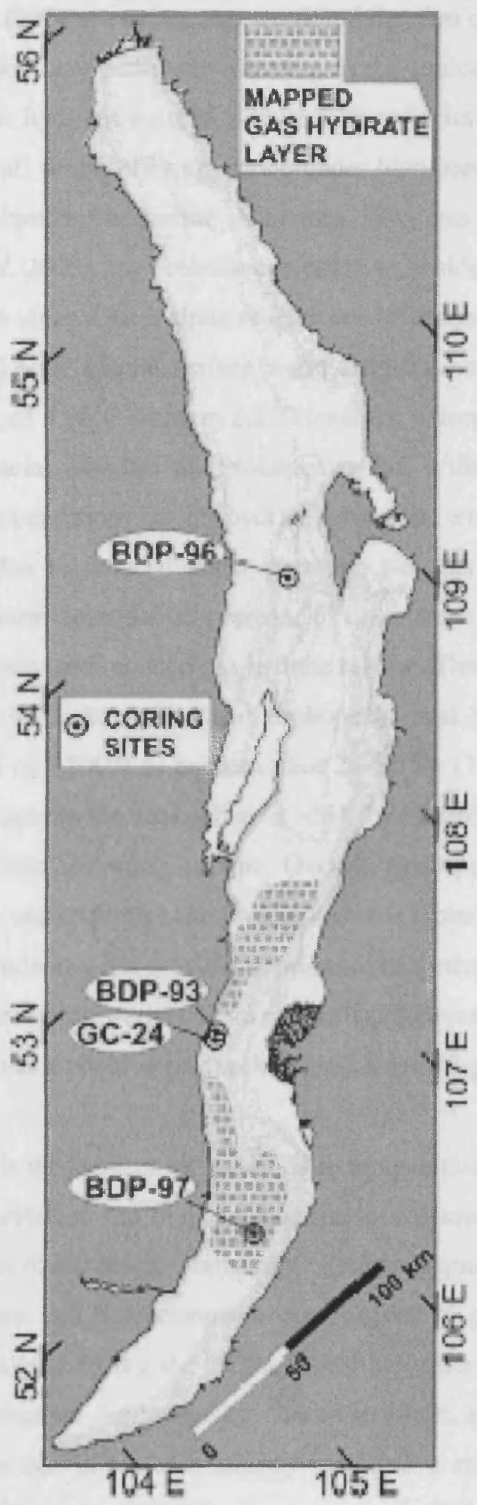

Figure 8.3: Locations of mapped areas of gas hydrate layers after Kuzmin *et al.* (2000) and the locations of the cores studied by Prokopenko and Williams (2004). From Prokopenko and Williams (2004).

Prokopenko and Williams (2004) postulate that the destabilisation of methane gas hydrates in the sediments of Lake Baikal due to climatic warming, is the source of depleted carbon to the lake TDIC pool. These gas hydrates exist in a crystalline solid form and consist of methane (CH_4) of biogenic (bacterial) origin, they are stable under high pressure and low temperature conditions and are most abundant in marine sediments. Since gas hydrates have a very low $\delta^{13}C$ of -60‰ (Klerkx *et al.* 2003), their release can cause a considerable isotopic lowering of the TDIC pool available to algae. Gas hydrate release can be caused by destabilisation due to warming of lake waters. Lower glacial surface water temperatures, estimated to be around 2.2°C, were not at the T_{md} of 3.96°C (section 2.2.2) meaning a deeper free convection to 500 m rather than the interglacial 250-300 m (Prokopenko and Williams 2004). These colder deeper waters create stable conditions for gas hydrate formation, with warming these formerly stable zones destabilise due to reduced water pressure, and gas hydrates are released. It follows then that over warm interglacial periods, $\delta^{13}C_{ORG}$ tends to higher values due to increased aquatic productivity and reduced gas hydrate release. There is a shift in $\delta^{13}C_{ORG}$ of -4‰ to -5‰ at the LGIT in Lake Baikal and Prokopenko and Williams (2004) used the calculations of Kennett *et al.* (2000) to estimate that 26-33 Tg (1 Tg is 1 million tons, the current annual flux of methane to the atmosphere is ~510 Tg (Khalil and Rasmussen 1995)) of methane was be released into the water column. Overall, Prokopenko and Williams (2004) claim their 130 ka $\delta^{13}C_{ORG}$ record from Lake Baikal, matches global methane levels shown by the Vostok ice core. This indicates the possible importance of methane release from sediments (although mostly marine and from wetlands and permafrost sources with Lake Baikal being a extremely minor reservoir) as a positive feedback in global warming.

Possible problems with this mechanism are mainly due to uncertainties with the extent of the gas hydrate reservoirs themselves and their mechanisms of release, concerning whether they are related to either climate or tectonics. Granin and Granina (unpublished) review previously published Russian literature and note extensive observations of gas hydrate release in the form of gas bubbles in the lake during the 1930s, linked to earlier occurrence of ice off and increased episodes of widespread fish mortality. Since the 1930s, such events are much rarer and this is linked to a decline in tectonic activity in the area rather than climate change. Linked to this, studies by Batist *et al.* (2002), Vanneste *et al.* (2003) and Van Rensbergen *et al.* (2003) find evidence through seismic profiling, that gas hydrate release is caused by an upward flow of warm hydrothermal fluids into the zone of stable gas hydrate and such thermal pulses are released as a result of tectonic activity. As a result, under current conditions Lake Baikal gas hydrate release can be seen to be of tectonic origin, rather than a climatically induced alteration of water density and mixing regimes as assumed by Prokopenko and Williams (2004).

The actual extent of the gas hydrate reservoir in Lake Baikal is not fully known, as no estimates of the volume stored in the sediments exist. Therefore, there may not be enough gas hydrates stored to account for such large shifts in $\delta^{13}C_{ORG}$, at least over the last 130 ka. Carbon from gas hydrates are transferred into the TDIC pool by diffusion into the water column, although transfer is not complete as some escapes into the atmosphere (Kennett *et al.* 2000). As a result the estimates of methane release that is sufficient to create a shift of around -4‰ will only be the absolute minimum amount. To date, gas hydrates are only known to occur in the abyssal areas near the Selenga Delta (figure 8.3) and although the lake is well mixed (as shown in chapter 3), it may be that their effects can only be noted in regions containing gas hydrate layers. However, at least for the Holocene, similar $\delta^{13}C_{ORG}$ trends occur lakewide, for example the core analysed by Ishiwateri *et al.* (1992) was taken in the far north of the lake where gas hydrates have not been detected, while cores taken by Prokopenko *et al.* (1993) and Prokopenko and Williams (2004), were taken in the South and Central Basins. All these records show temporally similar $\delta^{13}C_{ORG}$ records. If gas hydrates (transported to the North Basin by lake mixing) cannot be invoked to explain the similar shifts in the north, an alternate mechanism is needed.

8.1.5 Summary of previous work

In summary, C/N ratios in Lake Baikal are thought to indicate the amount of allogenic material derived from catchment inwash (high C/N) versus the amount of autogenic algal production (low C/N). This is partly confirmed by remote sensing analysis of the modern lake which shows high terrigenous input after storms in the catchment, providing allogenic carbon to Lake Baikal's sediment (Heim *et al.* in press). Therefore, consistently higher rainfall and river discharges may be shown by high C/N. The interpretation of $\delta^{13}C_{ORG}$ is more challenging. A lowering of $\delta^{13}C_{ORG}$ over the LGIT by a switch from C_4 to C_3 catchment plants, has been shown to be flawed by compound specific $\delta^{13}C$ analysis (Brincat *et al.* 2000). Changes in palaeo-pCO_2 levels also cannot solely explain lowerings at all glacial/interglacial transitions, as the $\delta^{13}C_{ORG}$ record does not correspond to the global pCO_2 record (figure 8.2). An important cause of the shift to lower $\delta^{13}C_{ORG}$ with warming is possibly the addition of vast amounts of isotopically lower carbon in methane to the lake TDIC pool. Low $\delta^{13}C_{ORG}$ values are maintained over the Holocene with increased inwash from catchment C_3 shown by higher C/N values. However, it may be that a shift in dominance of picoplankton to diatom productivity may be responsible for isotopic lowering. This is very likely as diatoms account for the majority of aquatic productivity in the Holocene.

Although past studies have favoured a single mechanism and found reasons to disregard all others, the $\delta^{13}C_{ORG}$ signal will be a mixture of several mechanisms including gas hydrate release, palaeo-pCO_2 levels, aquatic productivity levels, the type of algae dominant in the lake, the type of vegetation in the catchment, and the amount of inwash of this material into the lake. The effects of these individual processes on $\delta^{13}C_{ORG}$, total organic carbon, total organic nitrogen and C/N are given in table 8.1 assuming all other factors remain constant. There is a need for a high resolution and well dated Late Glacial – Holocene $\delta^{13}C_{ORG}$ and C/N record from Lake Baikal that can be interpreted as a climatic record. In particular, Prokopenko and Williams (2004) stated that a higher resolution study may resolve shifts in $\delta^{13}C_{ORG}$ related to Late Glacial climate oscillations and gas hydrate release.

Process	TOC	TN	C/N	$\delta^{13}C_{ORG}$
Increased C_3 terrestrial input	Increase	Increase	Increase	Decrease
Increased C_4 terrestrial input	Increase	Increase	Increase	Increase
Increased diatom abundance	Increase	Increase	Decrease	Decrease
Increased picoplankton abundance	Increase	Increase	Decrease	Increase
Increased aquatic productivity	Increase	Increase	Decrease	Increase
Increased gas hydrate release	No change	No change	No change	Decrease
Increased atmospheric p-CO_2	No change	No change	No change	Decrease
Plant CO_2 to HCO_3^- usage	No change	No change	No change	Increase
Increased lakewater p-CO_2	No change	No change	No change	Decrease

Table 8.1: Process and their effects on Total organic carbon (TOC), nitrogen (TN), C/N and $\delta^{13}C_{ORG}$ in Lake Baikal sediments (assuming only one process varies at a time).

8.2 Methodology

The combined box/piston core profile was analysed for $\delta^{13}C_{ORG}$ and C/N at a continuous 0.5 cm resolution giving a total of 550 samples. Samples were placed in approximately 100 ml of 5% HCl in glass beakers for 12 hours to remove any carbonate material. It is generally regarded that acid treatment of organic material will remove some of the more liable compounds, although in this case it was thought necessary due to the sporadic occurrence of carbonates in the core (*c.f.* Prokopenko *et al.* 1999). After acid treatment, samples were then washed three times over Whatman 41 filter papers with deionised water and dried at 40°C in a drying cabinet. When dry, samples were ground to a fine powder and stored in glass vials. Carbon isotopes ($\delta^{13}C$), percentage carbon and percentage nitrogen (used to calculate C/N) were analysed during combustion in a Carlo Erba 1500 on-line to a VG Triple Trap and dual-inlet mass spectrometer. $\delta^{13}C$ values were converted to the V-PDB scale using a within-run laboratory standard calibrated against NBS-19 and NBS-22, with C/N ratios calibrated against

an Acetanilide standard. Replicate analysis of sample material indicated a precision of ±0.1‰ for $\delta^{13}C$ and ±0.1 for C/N.

8.3 Results

Figure 8.4 shows $\delta^{13}C_{ORG}$, C/N, percentage carbon and nitrogen for the box/piston core profile plotted against age and zoned according to diatom assemblage zones defined by CONISS on percentage diatom abundance (chapter 6). Figure 8.5 shows a biplot of C/N vs. $\delta^{13}C_{ORG}$, all samples are in the range of algae, or fall on a mixing line heading towards terrestrial C_3 plants with $\delta^{13}C_{ORG}$ ranging from –22.4‰ to –32.7‰, C/N values range from 4.1 to 14.9. Some of the core samples have similar C/N and $\delta^{13}C_{ORG}$ values as the core tops measured by Prokopenko *et al.* (1993) and to the tributary material measured in this study. There are a small number of outlying core samples with high $\delta^{13}C_{ORG}$ and low C/N corresponding to colder periods of the Late Glacial, while other samples with higher C/N (>13) tend towards C_3 trees and $\delta^{13}C_{ORG}$ are the lowest in the record.

Sample percentage carbon is very low (< 0.5%) in the earliest part of the record and into zone VYD-D18, values of nitrogen are even lower (<0.05%) resulting in a high C/N ratio. There was not enough carbon (<0.1%) in the samples to analyse $\delta^{13}C_{ORG}$ over much of this period, although values recorded in VYD-D18 are the highest of the whole record at around –22.4‰. In zone VYD-D18, C/N values fall from around 14.0 to 9.5, $\delta^{13}C_{ORG}$ also shows a decline from high values to –30.0‰. In zone VYD-D17 there is an increase in percentage carbon to 1.4% and percentage nitrogen to 0.09% giving a subsequent increase in C/N to around 15. $\delta^{13}C_{ORG}$ also peaks in this zone at –27.0‰. A gradual fall in C/N occurs over zone VYD-D16 to 10.0 while $\delta^{13}C_{ORG}$ falls to –32.7‰ mid-zone before recovering to –27.2‰ by zone VYD-D15. This rise in $\delta^{13}C_{ORG}$ continues into VYD-D15, reaching a plateau of around –25.0‰, C/N values continue to fall to 10 but recover to 13 by the zone end. Throughout the short zones VYD-D14, D13 and D12, $\delta^{13}C_{ORG}$ falls back rapidly to around –30.0‰, although C/N remains relatively stable, both percentage carbon and nitrogen increase sharply to 2% and 0.2% respectively. $\delta^{13}C_{ORG}$ begins to increase again in zone VYD-D11 and all other values remain stable. VYD-D10 is marked by a continued increase in $\delta^{13}C_{ORG}$ but a sharp decline in percentage carbon to 0.7% and in percentage nitrogen to 0.07%, C/N also falls to 9 in the first half of the zone then declines further to 4. These values return back to around 9 into zone VYD-D9 to levels as seen in VYD-11, while $\delta^{13}C_{ORG}$ decline sharply to –30.0‰. Values of $\delta^{13}C_{ORG}$ remain relatively low from this point onwards for the rest of the record. From VYD-

D8 onwards, percentages of carbon and nitrogen both start to rise. Both rise gradually and do not fall below 1.2% or 0.12% respectively, C/N also rises slowly.

During VYD-D7, C/N reaches very high values of 13.5, these values fall back again into VYD-D6 to a low of around 10. An inverse of this trend is seen in $\delta^{13}C_{ORG}$, with lower values in VYD-D7 increasing slightly into VYD-D6. Percentage of total carbon and nitrogen reach peak values across zones VYD-D5 and D4 with maxima at 2.7% and 0.23% respectively. Both $\delta^{13}C_{ORG}$ and C/N are stable in VYD-D5 at around –29.5‰ and 11 respectively. Percentage carbon and nitrogen both decline in zone VYD-D4, while C/N remains high over the first part of the zone but declines sharply at *c.* 3900 aBP to 10. $\delta^{13}C_{ORG}$ also increases rapidly at this point to –27.0‰. Levels of both $\delta^{13}C_{ORG}$ and C/N are variable to the end of the zone.

Over zones VYD-D3 and D4, $\delta^{13}C_{ORG}$ fluctuates around –28.5‰ while C/N declines gradually from 12 to 10. However percentages of nitrogen and carbon are both rising. The upper zone, VYD-D1 was not recovered by the box core so no results are present for this section.

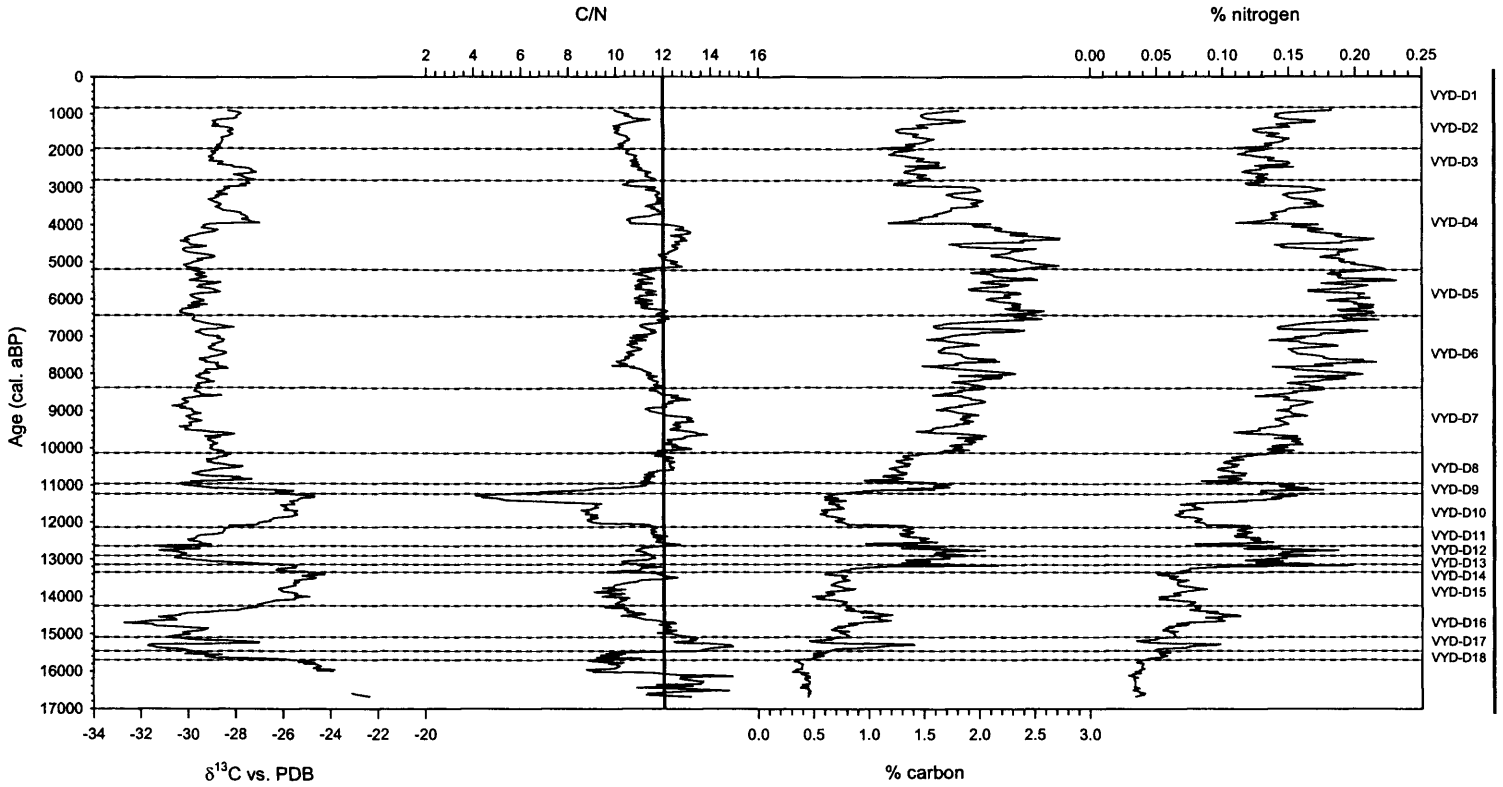

Figure 8.4: $\delta^{13}C$ vs. PDB, C/N ratio (and line C/N = 12), percentage carbon and percentage nitrogen plotted against age (cal. aBP) for the box/piston profile from the Vydrino Shoulder, Lake Baikal. Zoned according to those defined by diatom analysis.

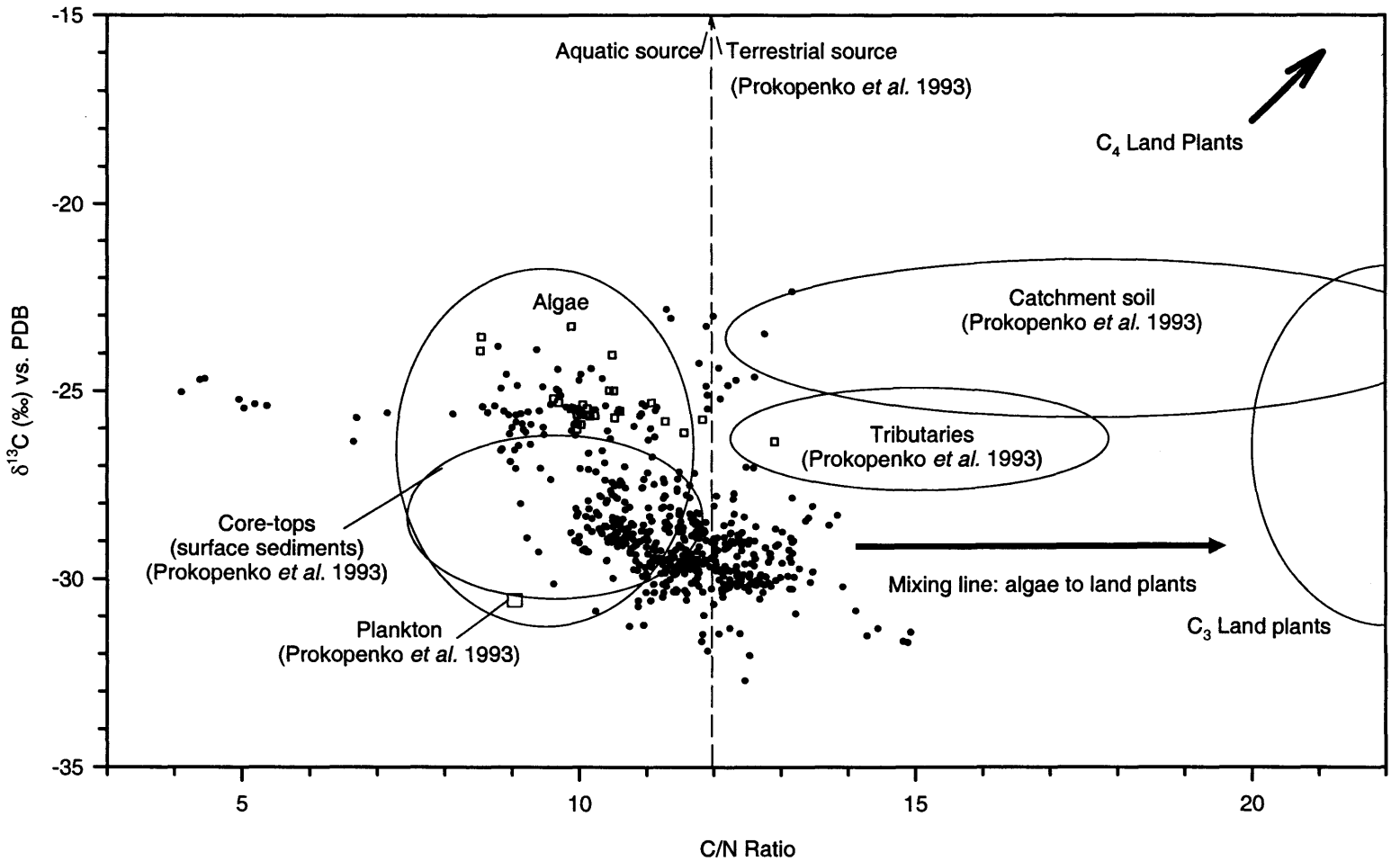

Figure 8.5: Plot of C/N ratio vs. $\delta^{13}C$ for the Vydrino Shoulder core (·), Selenga River catchment and tributaries measured in this study (▫), generalised values of C_3 and C_4 from Meyers and Lallier-Verges (1999), and catchment soils, core-top material (surface sediments) tributary material and plankton measured (□) by Prokopenko *et al.* (1993) as shown in figure 3.9.

8.4 Discussion

As climatic boundaries have been defined by diatoms in chapter six and discussed in terms of Central Asian – North Atlantic teleconnections, the interpretation of $\delta^{13}C_{ORG}$ and C/N will be based on assessment of how these results compare to the diatom data. $\delta^{13}C_{ORG}$ and C/N will be a complex response to biological, climatic and geological factors and may show leads or lags in response to climatic events in comparison to diatoms. Overall, this proxy is complementary to the diatom reconstructions and pollen analysis carried out in the CONTINENT project (Demske *et al.* in press). The results shown in figure 8.4 generally follow those previously published with high $\delta^{13}C_{ORG}$ in the Late Glacial, however there are also intervals of much lower $\delta^{13}C_{ORG}$ that have not been reported in previous studies. $\delta^{13}C_{ORG}$ values in the Holocene do follow previously published trends with lower values. C/N ratios are variable throughout the record and do not show the trend expected in figure 8.4 very clearly, with values being highly variable over the Late Glacial and Holocene. This possibly means the controls on C/N at this site are different to those at previously studied, perhaps due to the littoral location of the Vydrino Shoulder and the continued influence of river input (shown by the presence of *H. arcus*, even during the Late Glacial. As shown above in the discussion of possible controls in $\delta^{13}C_{ORG}$ and C/N records from Lake Baikal, there are several possible mechanisms which are not mutually exclusive that can explain the trends shown in figure 8.4. The discussion below will focus on each of these in turn.

8.4.1 Catchment vegetation changes

The biplot (figure 8.5) shows that core results may be interpreted as contributions from both authigenic algal production but also inwash (higher C/N), caused by greater soil development and higher rainfall. Few samples are similar to bulk organic matter tributaries measured by Prokopenko *et al.* (1993) although several correspond to the tributary material measured in this study. These core samples are from colder periods during the Late Glacial (before VYD-D18, VYD-D15 and VYD-D10), during these colder intervals it is possible that organic material from tributaries was the dominant supply of material to the coring location. However, as Prokopenko *et al.* (1993) note, higher isotopic values in lake sediments are expected compared to measured tributary material due to diagenesis, meaning tributary material is not directly comparable to core material due to diagenesis (see section 3.2).

At the base of the core at 16700 aBP, the $\delta^{13}C_{ORG}$ has the highest value at ~-22‰. Interpretation of this solely in terms of vegetation changes, would imply a dominance of C_4 grasses and herbs in the catchment that are able to tolerate glacial environments with low

temperatures and atmospheric CO_2 levels. This is supported by the pollen analysis of Demske *et al.* (in press) who analysed the same material that the current organic record is based on. An abundance of *Poaceae* (40%) and a lack of tree and shrub pollen (<20%) is found in material deeper than VYD-D18 covering the end of the LGM. High C/N over this period shows a predominance of catchment inwash but TOC and TN are low, indicating an overall low level of productivity. Zones VYD-D18 to D16 are marked by rapidly declining $\delta^{13}C_{ORG}$. According to the diatom zonation, this corresponds to the GI-1e warm interval. This would imply increased development of C_3 woodlands and a decline of C_4 plants. From the pollen data of Demske *et al.* (in press) this is again shown to be the case with gradually declining *Poaceae* pollen and an increase in shrub pollen to around 60% from around 20%, *Salix* and *Betula* being the dominant species. C/N falls throughout this period possibly implying declining catchment input and increased algal productivity, however both TOC and TN rise gradually. The colder GI-1d interval (VYD-D15) has relatively higher $\delta^{13}C_{ORG}$ values, a return to catchment C_4 vegetation would be expected. However, pollen data shows there is no change in the relative proportions of trees and grasses. The only discernable shift is a decline of *Salix* and an increase in *Alnus fruticosa* pollen, a species indicative of colder conditions (Demske *et al.* in press). As C/N values are low (around 10), it may mean that a factor other than catchment vegetation change is controlling $\delta^{13}C_{ORG}$. Diatom assemblage zones VYD-D14 and D12 represent warmer conditions corresponding to the GI-1c and GI-1a events separated by the short GI-1b cooling (VYD-D13). This short event is not resolved in the organic record possibly due to the relatively slow response of vegetation to climate change. This overall period of warming is marked by lower $\delta^{13}C_{ORG}$ and again the pollen record shows no change in the proportion of trees to grasses and herbs. However the abundance of *Filicales* increases relative to tree pollen, this will still provide a C_3 signal. The GS-1 cold period (VYD-D11 and D10) sees gradually rising $\delta^{13}C_{ORG}$ combined with lowered C/N. Lower C/N implies much less catchment inwash, while higher $\delta^{13}C_{ORG}$ cannot be explained by the pollen data as there is no change in the proportions of trees, shrubs and herbs over this boundary. Low terrestrial input can be inferred from $\delta^{18}O_{DIAT}$ (chapter 7) which shows river discharge to be low during the GS-1 especially in the South Basin. As a result less terrigenous carbon will be supplied to the lake. The beginning of the Holocene (VYD-D9) is marked by a lowering of $\delta^{13}C_{ORG}$ (-30‰ to -28‰) and a concurrent rise in C/N to around 10 to 11. At this point, the proportion of trees compared to shrubs and herbs rises to 90% with *Pinus* becoming the dominant species. Pollen concentrations rise considerably meaning catchment forests became much more extensive, the higher C/N and lower $\delta^{13}C_{ORG}$ may be explained by rapidly expanding *Pinus* forest. As shown in chapter 7 by $\delta^{18}O_{DIAT}$, increased discharge of South Basin rivers is expected at the start of the Holocene. Such an increase in discharge will result in a greater inwash of allogenic material (Heim *et al.* in press). This theory is supported by higher (>12)

C/N values in this part of the record. However, C/N does not remain high for the entire Holocene, even though pollen data shows the catchment to be heavily forested for the whole period indicating a dominance of algal productivity. $\delta^{13}C_{ORG}$ and C/N values stay relatively stable for the remainder of the Holocene, a similar stability is shown in the pollen records with 85% to 95% tree pollen. A mid-Holocene (4 to 6 kaBP) increase in pollen concentration does correspond to increases in both TOC and TN implying greater productivity, this is also marked as a generally warmer period in the diatom record with high abundance of *S. acus* v. *radians*. As accumulation rates throughout the Holocene appear to be relatively stable, according to previously published age models (Colman *et al.* 1995) and also the current age models (figure 2.16 and 2.17) with non-linear relationships possibly only the result of compaction of deeper sediments, the values of TOC and TN should not be biased by changing degradation caused by varying sediment accumulation rates.

It appears that broad changes, such as the start of deglaciation and the commencement of the Holocene, can be mirrored by larger shifts in pollen assemblages. However smaller scale changes such as the oscillations of the GI-1 event cannot be matched by variations in C_3 and C_4 pollen, although they are shown in the pollen record by changes in the dominant tree species and the presence of *Filicales* species. Although Brincat *et al.* (2000) find no presence of C_4 plants in a core from a pelagic area, C_4 plant fragments have been noted in more littoral areas. Russell and Rosell-Melé (in press) also claim terrestrial input to be highest in littoral zones. This shows C_4 input may have an influence on organic records, especially from littoral areas (such as Vydrino).

Other studies in Asia have invoked the alternation of C_4 grasses with C_3 plants to explain $\delta^{13}C_{ORG}$ changes recorded in Pakistan palaeosols as a result of climate changes over the last 17 Ma, linked to the development and intensification of the Asian Monsoon (Quade and Cerling 1995). However the authors also note that if changes synchronous to their record are found to be universal on a global scale, an alternate mechanism such as palaeo-p-CO_2 is more likely to be the driving mechanism. Similar conclusions of a possible joint role for C_4 and C_3 plant switches, and changes in atmospheric CO_2 are drawn from a study of carbonate material covering the last 7 Ma on the Chinese Loess Plateau (Ding and Yang 2000).

8.4.2 Algal species composition and productivity

If the conclusions of Brincat *et al.* (2000) are adopted, and it is accepted that C_4 plant input to Lake Baikal sediments has been negligible, another explanation is needed to account for the higher values of $\delta^{13}C_{ORG}$ (and usually lower C/N) during colder periods and the converse

situation during warmer intervals. However, this conclusion has been reached in only one study of Lake Baikal and may need further confirmation. The diatom concentration curve (figure 6.6) does show that diatoms are of low abundance during cold periods, such as the end of the LGM (VYD-D18 and D17), GI-1d (VYD-D15) and GS-1 (VYD-D11 and D10). These periods generally have higher $\delta^{13}C_{ORG}$ while warmer periods (with higher diatom abundance) have lower $\delta^{13}C_{ORG}$. It can be seen that diatoms have a low $\delta^{13}C_{ORG}$ value (figure 3.9) so their presence during warm periods can be invoked to explain low $\delta^{13}C_{ORG}$ during warm intervals. However, as shown above, C_3 plant inwash may be also be influencing the observed trends, so the signal is more likely to be a mixture of the two sources. C/N values partly help to solve this problem with lower C/N indicating a dominance of algal productivity over inwash, and *vice versa.* For example, during VYD-D17 and D16 high C/N may indicate greater catchment inwash than diatom productivity. During colder periods, higher $\delta^{13}C_{ORG}$ can be explained by the lack of diatoms and the dominance of cyanobacteria that discriminate very little against ^{13}C (Watanabe *et al.* 2004). This is supported by low C/N values during such periods, in particular VYD-D10 (GS-1). Although shifts to higher $\delta^{13}C_{ORG}$ can be expected with increasing productivity, during the LGIT climate changes $\delta^{13}C_{ORG}$ actually becomes lower with increased diatom abundance, meaning this mechanism cannot explain the observed changes alone.

The $\delta^{13}C$ of phytoplankton will also be controlled by the availability of dissolved CO_2 in the photic zone. Low river discharges during cooler, arid periods may reduce the input of CO_2 into the lake, therefore high $\delta^{13}C_{ORG}$ may also be caused by a switch of the plants to use the HCO^{3-} pool. However, as productivity is low, and solubility of CO_2 is high during cold periods, this effect should be minimal in Lake Baikal (Watanabe *et al.* 2004). Although variation in $\delta^{13}C_{ORG}$ and C/N is relatively low over the Holocene, shifts to higher $\delta^{13}C_{ORG}$ that are also linked to increases in diatom concentration may be caused by a raising of $\delta^{13}C_{TDIC}$ by increased productivity. Such intervals include the start of VYD-D7 and also the second part of VYD-D4.

8.4.3 Palaeo-*p*-CO_2 levels

A negative shift in $\delta^{13}C_{ORG}$ is observed in both marine and terrestrial sites over the LGIT (Rau *et al.* 1991, Meyers and Horie 1993) coinciding with an increase in palaeo-*p*-CO_2. Such an increase would influence all marine and terrestrial records in the same way, thereby explaining the universal LGIT $\delta^{13}C_{ORG}$ lowering. Other mechanisms such as catchment changes will be site specific. In a study of the LGIT, the $\delta^{13}C_{ORG}$ of Lake Baikal was shown to match palaeo-*p*-CO_2 changes documented in the GISP2 core (figure 8.6) (Prokopenko *et al.*

1999), however at least over the last 130 ka the two records do not correspond, causing Prokopenko and Williams (2004) to disregard palaeo-p-CO_2 levels as the major cause of $\delta^{13}C_{ORG}$ variation in Lake Baikal.

In comparison to the GISP2 palaeo-p-CO_2 record, the $\delta^{13}C_{ORG}$ record from the Vydrino Shoulder shows only broad correlations, further supporting the conclusions of Prokopenko and Williams (2004). However, GISP2 palaeo-p-CO_2 was low during the last glacial, being generally less than 220 ppmv, increasing to around 260 ppmv during the GI-1d event, and the subsequent decline in $\delta^{13}C_{ORG}$ may be a result of this. This correlation is not apparent for the rest of the GI-1 event with slowly increasing palaeo-p-CO_2, but large oscillations in $\delta^{13}C_{ORG}$ suggesting atmospheric CO_2 change cannot explain the variability in the palaeo record at least for this period. $\delta^{13}C_{ORG}$ also rises gradually during the GS-1, while GISP2 palaeo-p-CO_2 falls by about 90 ppmv midway through this cold event. Such a pattern is not exactly mirrored in the $\delta^{13}C_{ORG}$ record although $\delta^{13}C_{ORG}$ values become higher which would be expected under lowered palaeo-p-CO_2. The transition into the Holocene sees palaeo-p-CO_2 rise to 300 ppmv, $\delta^{13}C_{ORG}$ responds instantaneously to this with lower values that remain relatively stable over the whole Holocene possible a result of greater availability of CO_2. Overall, palaeo-p-CO_2 changes over the LGIT do correspond to some changes in $\delta^{13}C_{ORG}$, although oscillations relating to the series of stadials and interstadials during the GS-1 cannot be explained by this mechanism alone. Previous studies in north-eastern Asia over long timescales have linked $\delta^{13}C_{ORG}$ changes predominantly to palaeo-p-CO_2 change, albeit with a superimposed signal from terrestrial carbon input (Hasegawa 2003). The influence of atmospheric CO_2 is also shown in Lake Biwa by Meyers and Horie (1993). A shift to lower $\delta^{13}C_{ORG}$ values over the LGIT is also noted in tropical lakes (Street-Perrott *et al.* 1998, 2004) which has been attributed to increased palaeo-p-CO_2. However, it has also been stated that this shift is so large contributions from other mechanisms in addition to palaeo-p-CO_2 increase have to be included (Talbot and Johannessen 1992).

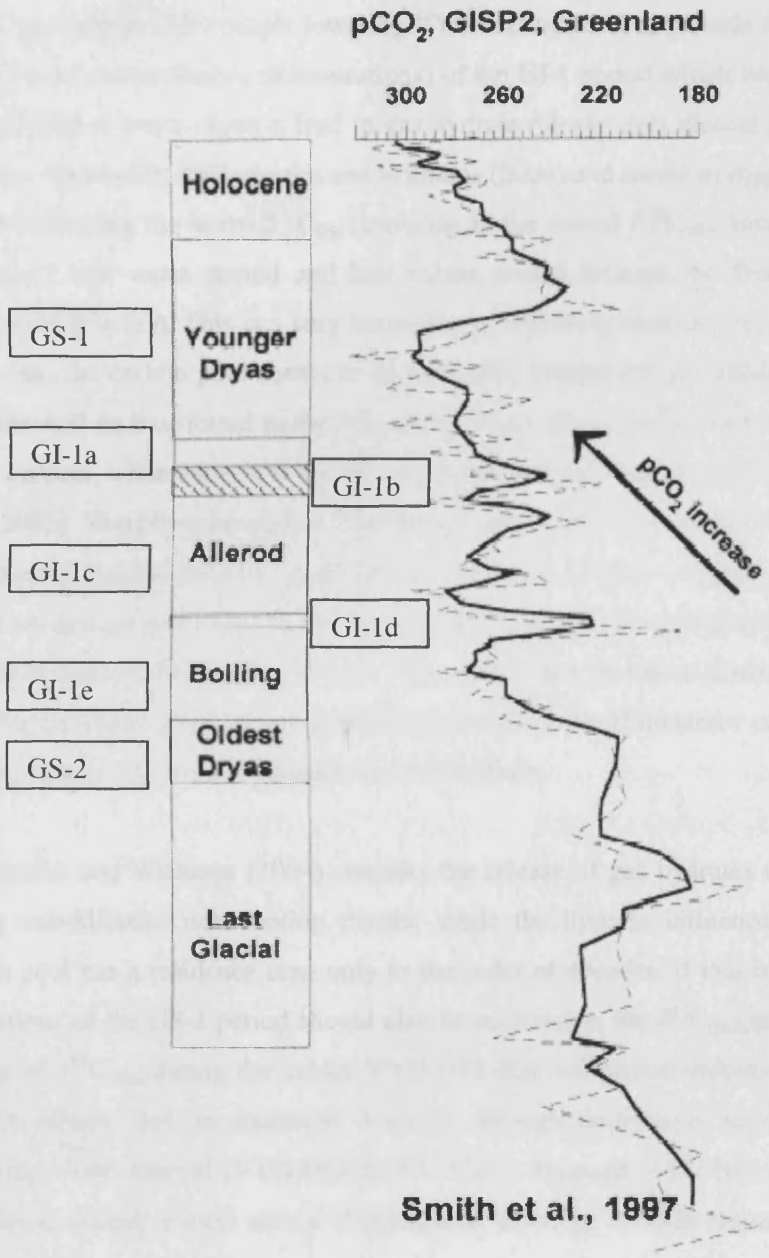

Figure 8.6: The palaeo-p-CO_2 LGIT record from GISP2 after Smith *et al.* (1997) modified from Prokopenko *et al.* (1999), units are parts per million by volume (ppmv) the dashed line is the raw data while the solid line indicates a three point moving average.

8.4.4 Gas hydrate release

The destabilisation of extremely low $\delta^{13}C$ gas hydrates due to warming of the water column and the subsequent incorporation of this into the lake TDIC pool, can have a significant effect on $\delta^{13}C_{ORG}$ values. The isotopic lowering VYD-D18 appears to precede the main warming (as shown by increased diatom concentrations) of the GI-1 period which begins in VYD-D17 by several hundred years. Such a lead in gas hydrate release over diatom productivity increase was also expected by Prokopenko and Williams (2004) and seems to support this mechanisms role in explaining the initial $\delta^{13}C_{ORG}$ lowering in the record. $\delta^{13}C_{ORG}$ values fall by over 10‰ throughout this warm period and low values persist through the following warm period (VYD-D16 (GI-1e)). This is a very large change and the release of very low $\delta^{13}C$ methane (-60‰) into the carbon pool seems to be a credible mechanism in explaining this large shift. Methane will be transferred to the lake carbon reservoir by diffusion as it passes through the water column, while some will not be exchanged and will escape to the atmosphere (Kennett *et al.* 2003). Therefore the carbon used during aquatic productivity in the photic zone should be modified immediately by escaping gas hydrates, however in regions where gas hydrate layers are not present (such as the North Basin), water with isotopically lower $\delta^{13}C$ would have to be transported to these regions. Since the water residence times are 500, 250 and 90 years for the North, Central and South Basins respectively (Shimaraev *et al.* 1994), there may be a lag in response to gas hydrate in the North Basin.

Prokopenko and Williams (2004) consider the release of gas hydrates to be greatly reduced during sub-Milankovitch cooling events, while the hydrate influenced isotopically lower carbon pool has a residence time only in the order of decades. If this is correct, the climatic oscillations of the GS-1 period should also be mirrored in the $\delta^{13}C_{ORG}$ profile. Indeed a rapid raising of $\delta^{13}C_{ORG}$ during the colder VYD-D15 (GS-1d) period indicates a reduction in gas hydrate release due to increased stability through decreasing water temperature. The following warm interval (VYD-D14 to VYD-D12, although VYD-D13 can be regarded as a short-lived cooling event) sees a simultaneous lowering of both diatom concentration and $\delta^{13}C_{ORG}$ by as much as 7‰, such a large increase may be due to the renewal of gas hydrate release. However, there is no lead in $\delta^{13}C_{ORG}$ over diatom concentration increases, according to Prokopenko and Williams (2004), such a lead would be expected. The gradual raising of $\delta^{13}C_{ORG}$ over the GS-1 (VYD-D10 and D11) could be caused by a decreasing gas hydrate release, while the lowering of $\delta^{13}C_{ORG}$ into the Holocene could be explained by further release. However, problems with this hypotheses include the fact if gas hydrates are invoked as the only explanation causing lower $\delta^{13}C_{ORG}$, a constant release would be needed over the Holocene, as modern observations do not support this (Granin and Granina, unpublished,

Batist *et al.* 2002). An alternative explanation for the shift to lower $\delta^{13}C_{ORG}$ is likely to be more viable. As stated above, gas hydrate release in Lake Baikal may have a tectonic cause which is generally independent of climate changes. Also the extent of the methane reservoir in Lake Baikal is not accurately known. In addition, the presence of gas hydrates layers have not been detected in the North Basin but the northern $\delta^{13}C_{ORG}$ record of Ishiwateri *et al.* (1992) showed broadly similar trends to the Central and South Basins.

Studies in the marine environment have shown massive gas hydrate releases may be the indirect result of climate changes through slope failures linked to destabilisation caused by increased water temperature (Kennett *et al.* 2003), but also greater sediment loading on slopes due to increased river discharges with climatic warming (Maslin *et al.* 1998) and isostatic rebound causing shallower water in some areas, along with increased seismic activity. Although periodic gas hydrate releases have been linked to Dansgaard-Oeschger millennial scale events, Maslin *et al.* (2004) state as slope failures also occur during stadials this cannot be the case. However, the mechanism described by Kennett *et al.* (2003) can be invoked during glacial-interglacial transitions to account for gas hydrate release.

The effect of gas hydrate release on $\delta^{13}C_{ORG}$ has been demonstrated in the marine environment with an estimated deglacial annual flux of methane over 6.4 Tg yr^{-1} (~1.3% of modern annual flux) causing an ~-5‰ $\delta^{13}C_{ORG}$ shift in the Santa Barbara Basin (Pacific Ocean) (Kennett *et al.* 2003). An investigation by X.C. Wang *et al.* (2001) estimated that gas hydrate seeps contributed 40% – 60% to the $\delta^{13}C$ value of sedimented organic matter at a site in the Gulf of Mexico, while $\delta^{13}C_{TDIC}$ as low -48‰ are attributed to gas hydrate release in the same area (Torres *et al.* 2003). This means that the observed large (~10‰) $\delta^{13}C_{ORG}$ shifts in Lake Baikal are generally greater than those from marine environments implying either an extremely large gas hydrate release in Lake Baikal, or more likely, a contribution for one or more of the mechanisms outlined above.

In order to clarify the gas hydrate mechanism on $\delta^{13}C_{ORG}$, Prokopenko and Williams (2004) suggest that the study of biomarkers indicative of methanotrophy preserved in the record to demonstrate the influence of methane hydrates on organic matter, ought to be carried out on Lake Baikal. Such a study has been successfully applied to organic matter in marine sediments (Hinrichs *et al.* 2003).

8.5 Conclusion

The new record of $\delta^{13}C_{ORG}$ and C/N mirrors the climatic changes shown by the diatom palaeoclimatic reconstructions. As teleconnections between Lake Baikal and the North Atlantic have been demonstrated (section 6.4), this complementary proxy further supports the notion of simultaneous climatic events in the two regions. There appears to be no one predominant forcing that can explain the observed changes in the $\delta^{13}C_{ORG}$ and C/N record although all possibilities have direct or indirect climatic causes. Catchment vegetation change, algal species composition and productivity, palaeo-*p*-CO_2 levels and gas hydrate may all be important. It is almost certain that the signal is a mixture of these process that cannot be easily be interpreted as the result of a single mechanism. Past studies of $\delta^{13}C_{ORG}$ and C/N in Lake Baikal have attempted to explain a general trend of lower $\delta^{13}C_{ORG}$ and higher C/N with the transition to the Holocene using only one process. However, this is almost certainly too simplified and it seems more viable to consider the role of several mechanisms.

The large oscillation in $\delta^{13}C_{ORG}$ and C/N over the Late Glacial period can be interpreted as either a shift from C_4 to C_3 plant or diatom dominance, changes in the dominant algal species between diatoms and picoplankton, increased palaeo-*p*-CO_2 or periodic release of methane gas hydrates. However, in spite of the multiple hypotheses for variations in the record of organic material, the climatic interpretation is the similar in all cases. In general, higher $\delta^{13}C_{ORG}$ is indicative of colder climates and is forced by either greater C_4 plant input, picoplankton abundance, lower palaeo-*p*-CO_2 and reduced gas hydrate release. However, this is tempered by increased aquatic productivity during warm intervals also tending to result in higher values of $\delta^{13}C_{ORG}$.

Mechanisms such as palaeo-*p*-CO_2 and C_4 to C_3 plant changes are shown only to correlate to $\delta^{13}C_{ORG}$ changes at larger scale, such as the start of the GI-1 and Holocene, while the Late Glacial oscillations cannot be explained by these two mechanisms after comparison to GISP2 palaeo-*p*-CO_2 and pollen records respectively, which show palaeo-*p*-CO_2 and vegetation change do not correspond to $\delta^{13}C_{ORG}$ variation. As a result, where these supposed mechanisms do correlate to $\delta^{13}C_{ORG}$, the relationship may be coincidental rather than causal. However, this does not mean no influence on the organic record is assumed, rather that they have just a secondary influence.

Changes in algal species linked to climate change is a robust explanation for the observed changes as this can be supported by the curve of diatom abundance (figure 6.6). Periods of higher diatom abundance are marked by lower $\delta^{13}C_{ORG}$ values, while higher values are shown

where picoplankton is assumed to be dominant (Nagata *et al.* 1999, Watanabe *et al.* 2004). Superimposed on this will be the influence of C_3 organic material from the catchment during warmer intervals. This can be partly distinguished from aquatic productivity as C/N values should rise with greater terrestrial inwash.

Although much more work is needed in defining the extent and mechanisms of release, linked to climate change of isotopically low methane gas hydrates in Lake Baikal, the periodic release of methane gas during warmer intervals does match the $\delta^{13}C_{ORG}$ record. If this mechanism is the dominant force on altering $\delta^{13}C_{ORG}$, the sub-Milankovitch scale LGIT climate oscillations can be seen to have caused release of methane during warm periods but a slowing or ceasing of venting with the return of colder periods, as speculated by Prokopenko and Williams (2004). Due to the extremely low $\delta^{13}C$ of gas hydrates, they are capable of explaining the large shifts in $\delta^{13}C_{ORG}$ of up to 10‰.

Overall, the $\delta^{13}C_{ORG}$ signal must be seen as a mixture of several processes, although C/N values are useful in distinguishing between relative levels of aquatic productivity and terrestrial inwash. The unravelling of the $\delta^{13}C_{ORG}$ signal will be aided by compound specific and biomarker analysis, to identify the actual source of carbon and type of plant material present in the palaeo record (Russell and Rosell-Melé in press), and also by a full assessment of the interchanging role of cyanobacteria and diatoms, by analysis of fossil pigments (Fietz *et al.* in press).

Chapter Nine

Summary, conclusions and future research

9.1 Introduction

The primary goal of this research was to reconstruct high resolution records of climatic variability over the Late Glacial and Holocene from the sediments of Lake Baikal. The methodology used was a combination of diatom and stable isotope analyses, coupled with an investigation of the dynamics of these proxies in the modern environment to aid interpretation of the palaeo record. In addition, inference models were also developed to infer snow depth on lake ice, and durations of annual clear ice and white ice/snow cover. Another aim of this work was to compare this Central Asian site to documented climate change from the North Atlantic region to assess teleconnections processes. Firstly, the main inferred palaeoclimatic changes are synthesised below (reconstructions are summarised in figure 9.1), and secondly the similarities of these changes with North Atlantic palaeoclimate records are examined. An assessment of possible teleconnections between Lake Baikal and the North Atlantic is given. This chapter will conclude with ideas for future research and a brief introduction to work currently underway to identify periodicities in the diatom species data.

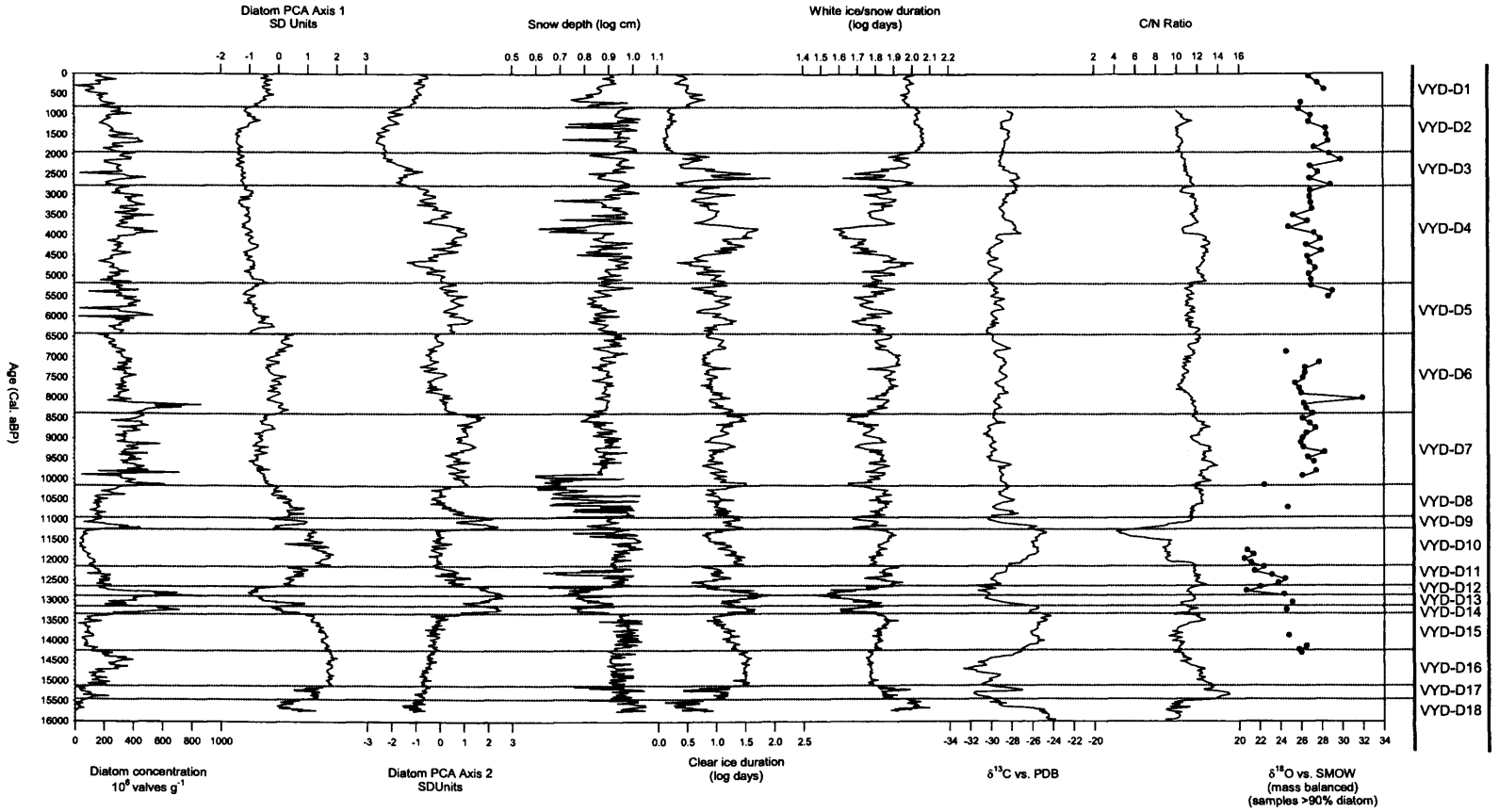

Figure 9.1: Summary diagram of selected palaeoclimatic reconstructions from the Vydrino Shoulder, Lake Baikal. Zoned according to diatom assemblage zones.

9.2 Late Glacial climate change

The INTIMATE event stratigraphy for the LGIT (Björck *et al.* 1998) has been used to compare the local Lake Baikal LGIT events to those of the North Atlantic (i.e. recorded in the GRIP ice core). The initial onset of warming (GS-1e) at 14500 ss09aBP, compares to zone VYD-D16 at 15700 aBP in Lake Baikal. This event lasts about 700 years in Greenland and is of similar duration in Lake Baikal, defined mostly by an increase in diatom concentration, but also lower $\delta^{13}C_{ORG}$ possibly due to gas hydrate release, increased diatom productivity and/or increased inwash of catchment C_3 vegetation under a warmer climate. The succeeding cold event (GI-1d) at 14200 ss09aBP in GRIP lasts for 150 years. In Lake Baikal this is much longer at ~890 years but with an almost synchronous onset at 14245 years. These earlier events of the Late Glacial may not correlate exactly with GRIP in terms of duration and onset, due to poor chronological control in this part of the record, but also diatom production may be being limited by nutrient availability as well. Later events in the GS-1 interval show better correlation within dating uncertainties. The warmer interval VYD-D14 equates to the GI-1c (onset 13750 ss09aBP in GRIP and 13355 aBP in Lake Baikal), marked by increased *S. acus* v. *radians* flux and the beginning of a lowering in $\delta^{13}C_{ORG}$. Transfer function results also indicate shallower snow cover on ice and longer clear ice duration. This event is followed by a short-lived cold event (~150 years) in both records (VYD-D13, GS-1b which is synonymous to the IACP). This event is not resolved in the stable isotope proxies. The following GI-1a warm event is synchronous with the VYD-D12 event in Lake Baikal, shown by increasing *S. acus* v. *radians* and lowering $\delta^{13}C_{ORG}$ with high C/N. Values of $\delta^{18}O_{DIAT}$ are relatively high, indicating a weak Siberian High, less Eurasian snow cover extent and enhanced summer cyclonic activity, leading to a dominance of water supplied to the South Basin of Lake Baikal.

The GS-1 (Younger Dryas) occurs at around 12650 aBP in GRIP and at 12640 aBP (VYD-D11) in Lake Baikal which is an extremely good correlation in terms of timing for this global event. This cooling is shown in all proxies investigated; with low diatom concentration, rising $\delta^{13}C_{ORG}$ and low C/N, deeper inferred snow depths and lowering $\delta^{18}O_{DIAT}$, indicating a stronger Siberian High and increased Eurasian snow cover extent and enhanced anticyclonic activity over the southern catchment of Lake Baikal in summer, thereby reducing input from southern rivers with respect to northern tributaries.

9.3 Holocene climate changes

The comparison of reconstructed Holocene climate changes to the North Atlantic are problematic due to the huge observed variability between different regions (*c.f.* Smith 1981, He *et al.* 2004). However, some broad comparisons can be made. The Early Holocene (10940 to 8390 aBP) warm interval in Lake Baikal is defined by a shift to higher $\delta^{18}O_{DIAT}$ values, indicating a weaker Siberian High and increased summer precipitation. $\delta^{13}C_{ORG}$ also shifts to lower values indicating warmer conditions (both $\delta^{13}C_{ORG}$ and $\delta^{18}O_{DIAT}$ remain relatively stable for the remainder of the Holocene). Increases in *S. acus* v. *radians* and diatom concentration with a fall in *A. skvortzowii* also show this period to be warm. Similar warm intervals are also seen in other Central Asian and Lake Baikal records (section 6.4.2). An extreme, short-lived climatic cooling is recorded in the GRIP record at 8.2 kaBP, in Lake Baikal this may correspond to a sharp peak in diatom concentration and $\delta^{18}O_{DIAT}$, although reasons why a cooling event should cause a massive increase in diatom concentration are not clear. Following this, a cooler interval occurs between 8390 to 6425 aBP, coincident with the commonly reported period of optimal climatic conditions over Europe. This cooling is marked with increased inferred snow depth and less clear ice cover duration. The subsequent warmer zone (6425 to 2790 aBP) may be synonymous with the Late Atlantic warming and Sub-Boreal period shown in pollen records (section 6.4.2). Evident within this warm period is a 'Sub-Boreal cooling' centred around 4.6 kaBP with reduced *S. acus* v. *radians*, deeper inferred snow cover and increases in autumnal blooming diatom species. Such a cooling can be seen in Asian, but also in North Atlantic records (O'Brien *et al.* 1995, Bond *et al.* 1997). Another cooling at 2790 aBP in Lake Baikal (the boundary of VYD-D4 and D3) may mark the beginning of the neoglaciation period. A global event at this exact date has been described by van Geel *et al.* (1996, 2000) and may be due to reduced solar output. Neoglaciation is shown by dominant autumnal production with increased *C. minuta* and inferred longer white ice/snow cover duration, as well as snow depths limiting spring diatom productivity.

There is no evidence for well defined MWP or LIA intervals in this record, which may be due to the relatively low amplitude of these events. Morrill *et al.* (2003) also found limited evidence for these events in records from the Chinese Loess Plateau. Since 810 aBP, abundance of *A. baicalensis* and *S. meyerii* has increased, which may imply a warming climate. However such assemblage shifts pre-date industrial development in the area and cannot be attributed to pollution (*c.f.* Mackay *et al.* 1998).

It is evident that some larger magnitude Holocene climatic events appear to be semi-synchronous between the North Atlantic and Lake Baikal. It was stated in section 1.3.3, that

Holocene climate change in the North Atlantic region appears to be proceeding on a millennial periodicity. If these periodicities can be shown in the Lake Baikal record, it will further strengthen the conclusion that climate changes between Central and the North Atlantic are at least semi-synchronous. An initial investigation into the presence of a 1470 year cycle in the flux records of three Lake Baikal diatom species is presented below.

9.4 Teleconnection mechanisms

From the results presented above, it is clear that a teleconnection exists between Lake Baikal and the North Atlantic over the Late Glacial and Holocene. Within the limits of the dating methods applied, there are no significant leads or lags in climate changes between the two regions. In particular, this is demonstrated by the good correlation of Late Glacial climatic events (GS-1 and GI-1).

Teleconnection mechanisms have been described in sections 1.5.3.1 and 6.4.2. In short, Central Asia and the North Atlantic are linked by an atmospheric teleconnection controlled by the strength of the Westerlies (Kutzbach *et al.* 1993, Porter and An 1995, An and Porter 1997). Increased North Atlantic iceberg discharge and declining NADW production leads to colder SSTs and enhanced cold airflow to Central Asia, strengthening the Siberian High and cold, arid, prolonged winters. This will also subsequently increase the strength of the East Asian Winter Monsoon and reduce the power of the Summer Monsoon. During periods of reduced iceberg discharge in the North Atlantic and enhanced NADW production, the Siberian High weakens under reduced cold Westerlies with a subsequent increase in strength of the East Asian Summer Monsoon.

Other teleconnection mechanisms are also evident, in particular the NAO/AO (Livingstone 1999, Todd and Mackay 2003), while the extent of Eurasian snow cover is also important in controlling anticyclonic activity over Lake Baikal's catchment (Clark *et al.* 1999, Ye *et al.* 2001a, b). This is demonstrated by variations in $\delta^{18}O_{DIAT}$ indicating links to the changing relative importance of Lake Baikal's tributaries. Overall, the apparent high level of association between palaeoclimatic records from the North Atlantic and Central Asia implies that Late Glacial and Holocene climate changes are related and synchronous, and not independent of each other as speculated in previous studies such as Velichko *et al.* (1997).

9.5 Future work

There are several possible options for future work that can further develop the conclusions of this study. Initial work has already been carried out with an investigation of periodicities present in the diatom flux data. This is in collaboration with Annette Witt of the University of Potsdam. It has already been shown that there is evidence for a pervasive 1470±500 year periodicity in North Atlantic sediments, this signal can also be observed in the Greenland ice core glaciochemical series (Mayewski *et al.* 1997, Witt and Schuman, in prep.). Investigation of the flux data of *A. baicalensis, A. skvortzowii* and *C. inconspicua,* using wavelet analysis (Torrence and Compo 1998), has revealed a strong 1470 periodicity in these data. Investigation of the phase differences between these cycles in Lake Baikal and the North Atlantic have shown that, although the records are out of phase, they are consistently so. This means such differences may be due to the optimum responses of individual diatom species non necessarily responding to optimum temperature conditions as defined by the 1470 cycle in the North Atlantic.

These results indicate the importance of the Holocene 1470 periodicity outside the North Atlantic region. Future work to further verify these initial conclusions will involve a thorough investigation of the flux of other diatom species in Lake Baikal with wavelet analysis and comparison to other North Atlantic records, in particular, other components of the GISP2 glaciochemical series. Wavelet analysis is also being applied to the $\delta^{14}C$ record of Stuiver and Braziunas (1993) to allow comparison to the Lake Baikal data. Spectral analysis by Stuiver and Braziunas (1993) indicated amongst others, the presence of 1470, 2200 and 500 year periodicities in this data. Therefore, the isolation of other cycles in the Lake Baikal diatom data may yield periodicities in the range of known solar cycles. Indeed, initial wavelet analysis of the plankton to benthic diatom ratio and diatom concentrations, show strong periodicities in the range of 2.2 to 2.6 ka, which may be linked to solar cycles and the quasi-2.6 ka cycle found in the North Atlantic by O'Brien *et al.* (1995), and in Holocene glacial advances by Denton and Karlen (1973). Finally, the Lake Baikal data will be compared to other reported Holocene periodicities in the North Atlantic region, for example, the 550 and 1000 year cycles linked to NADW production (Chapman and Shackleton 2000, Hughes *et al.* 2000) and the 900 year cycle identified by Schulz and Paul (2002).

In terms of the remote sensing work carried out in chapter 5, an assessment of snow and ice cover from 2001-2002 may provide a much clearer interpretation of the surface water phytoplankton data from these years. Linked to this, as snow depth on ice was found to be the

most important variable in controlling diatom assemblages in the training sets, a study using radar data to estimate actual snow depths, combined with a ground-truthing surveys to calibrate these data, would be very useful.

It was stated in chapter 4, that an integration of the phytoplankton results from 2001-2002 would give much sounder autecological information for the endemic diatom species. This work is currently being co-ordinated by David Jewson. In addition, future investigations of the dynamics of Lake Baikal phytoplankton will be based on both diatom algae and the other types of plankton that were enumerated but not presented in this thesis. These data will be linked to the measured limnological and chemical data using multivariate statistics.

In terms of the isotopic studies, it was shown in chapter 8, that there is a discrepancy between modern samples measured for d13C in this study compared to those measured by Prokopenko *et al.* (1993). An inter-laboratory comparison would help to elucidate these differences.

Finally, the conclusions that a teleconnection exists between Lake Baikal and the North Atlantic can be further developed by investigating other sites nearby, but unlike Lake Baikal, with a direct influence from the Asian Monsoons. Potential sites include crater lakes in north east China which are known to have a record extending back to the Late Glacial (Mingram *et al.* 2004). It has been noted that climate changes are asynchronous across China (He *et al.* 2004), high resolution palaeoclimatic reconstruction investigations of north-south and east-west transects over this region would further clarify if climate changes are lagged over spatial gradients or if they are synchronous.

References

Aaby B. (1976) Cyclic climatic variations in climate over the past 5500 years reflected in raised bogs. *Nature* 263, 281-284.

Abell P.I. and Hoelzmann P. (2000) Holocene palaeoclimates in northwestern Sudan: stable isotope studies on molluscs. *Global and Planetary Change* 26,1-12.

Acker F. (2002) NAWQA Program phytoplankton samples. Protocol P-13-52. In: Charles D.F., Knowles C. and Davis R.S. (eds.). Protocols for the analysis of algal samples collected as part of the U.S. Geological Survey National Water-Quality Assessment Program. Report No. 02-06, Patrick Center for Environmental Research, Philadelphia. 87-96.

Adams J., Maslin M. and Thomas E. (1999) Sudden climate transitions during the Quaternary. *Progress in Physical Geography* 23,1-36.

Afanasjev A.N. (1976) Vodnye resursy i vodnyi balans rek basseina Baikala. (The Water Resources and Water Balance of the Lake Baikal Basin). Nauka, Novosibirsk. [in Russian].

Aizen E.M., Aizen V.B., Melack J.M., Nakamura T. and Ohta T. (2001) Precipitation and atmospheric circulation patterns at mid-latitudes of Asia. *International Journal of Climatology* 21, 535-556.

Albrecht M.L. (1964) Die Lichtdurchlässigkeit von Eis und Schnee und ihre Bedeutung für die Sauerstoffproduktion im Wasser. *Deutsche Fischerei-Zeitung* 11, 371-376. [in German].

Alley R.B. (2000) The Younger Dryas cold interval as viewed from central Greenland. *Quaternary Science Reviews* 19, 213-226.

Alley R.B. and Clark P.U. (1999) The deglaciation of the northern hemisphere: A global perspective. *Annual Review of Earth and Planetary Sciences* 27, 149-182.

Alley R.B., Mayewski P.A., Sowers T., Stuiver M., Taylor K.C. and Clark P.U. (1997) Holocene climatic instability: a prominent, widespread event 8200 yr ago. *Geology* 25, 483-486.

Amundson R., Chadwick O., Kendall C., Wang Y. and de Niro M. (1996) Isotopic evidence for shifts in atmospheric circulation patterns during the late Quaternary in mid-North America. *Geology* 24, 23-26.

An Z. (2000) The history and variability of the East Asian paleomonsoon climate. *Quaternary Science Reviews* 19, 171-187.

An Z.S., Porter S.C., Zhou W.J., Lu Y.C., Donahue D.J., Head M.J., Wu X.H., Ren J.Z. and Zheng H.B. (1993) Episode of strengthened summer monsoon climate of Younger Dryas age on the loess plateau of Central China. *Quaternary Research* 39, 45-54.

An Z. and Porter S.C (1997) Millennial-scale climatic oscillations during the last interglaciation in central China. *Geology* 25, 603-606.

Anderson D.M., Overpeck J.T. and Gupta A.K. (2002) Increase in the Asian southwest monsoon during the past four centuries. *Science* 297, 596-599.

Anderson L., Abbott M. B. and Finney B. P. (2001) Holocene climate inferred from oxygen isotope ratios in lake sediments, Central Brooks Range, Alaska. *Quaternary Research* 55, 313-321.

Anderson N.J. (1994) Comparative planktonic diatom biomass responses to lake and catchment disturbance. *Journal of Plankton Research* 16, 133-150.

Anderson N.J. (1995) Temporal scale, phytoplankton ecology and paleolimnology. *Freshwater Biology* 34, 367-78.

Anderson N.J. (2000) Diatoms, temperature and climatic change. *European Journal of Phycology* 35, 307-314.

Anderson N.J. and Odgaard B.V. (1994) Recent paleolimnology of 3 shallow Danish lakes. *Hydrobiologia* 276, 411-422.

Anderson N.J., Blomqvist P. and Renberg I. (1997) An experimental and palaeoecological study of algal responses to lake acidification and liming in three central Swedish lakes. *European Journal of Phycology* 32, 35-48.

Andres M.S., Bernasconi S.M., McKenzie J.A. and Rohl U. (2003) Southern Ocean deglacial record supports global Younger Dryas. *Earth and Planetary Science Letters* 216, 515-524.

Andresen C.S., Björck S., Bennike O., Heinemeier J. and Kromer B. (2000) What do Delta $\delta^{14}C$ changes across the Gerzensee oscillation/GI-1b event imply for deglacial oscillations? *Journal of Quaternary Science* 15, 203-214.

Anneville O., Ginot V., Druart J.C. and Angeli N. (2002) Long-term study (1974-1998) of seasonal changes in the phytoplankton in Lake Geneva: a multi-table approach. *Journal of Plankton Research* 24, 993-1007.

Antipin V., Afonina T., Badalov O., Bezrukova E., Bukharov A., Bychinsky V., Dmitriev A. A., Dorofeeva R., Duchkov A., Esipko O., Fileva T., Gelety V., Golubev V., Goreglyad A., Gorokhov I., Gvozdkov A., Hase Y., Ioshida N., Ivanov E., Kalashnikova I., Kalmychkov G., Karabanov E., Kashik S., Kawai T., Kerber E., Khakhaev B., Khlystov O., Khursevich G., Khuzin M., King J., Konstantinov K., Kochukov V., Krainov M., Kravchinsky V., Kudryashov N., Kukhar L., Kuzmin M., Nakamura K., Nomura S., Oksenoid E., Peck J., Pevzner L., Prokopenko A., Romashov V., Sakai H., Sandimirov I., Sapozhnikov A. , Seminsky K., Soshina N., Tanaka A., Tkachenko L., Ushakovskaya M. and Williams D. (2001) The new BDP-98 600-m drill core from Lake Baikal: a key Late Cenozoic sedimentary section in continental Asia. *Quaternary International* 80-1, 19-36.

Appleby P.G., Flower R.J., Mackay A.W. and Rose N.L. (1998) Paleolimnological assessment of recent environmental change in Lake Baikal: sediment chronology. *Journal of Paleolimnology* 20, 119-133.

Atkinson T.C., Briffa K.R. and Coope G.R. (1987) Seasonal temperatures in Britain during th last 22,000 years, reconstructed using beetle remains. *Nature* 325, 587-589.

Atlas Baikalia (1993) Baikal Atlas. Federal Service of Surveying and Cartography, Moscow [in Russian].

Bailey-Watts A. E., Smith I. R. and Kirika A. (1989) The dynamics of silica in a shallow loch II: The influence of diatoms on an annual budget. *Diatom Research* 4, 191–205.

Babanazrova O.V. Likhoshway Y.V and Sherbakov D.Y. (1996) On the morphological variability of *Aulacoseira baicalensis* (Bacillariophyta) of Lake Baikal, Russia. *Phycologia* 35, 113-123.

Bangs M., Battarbee R.W., Flower R.J., Jewson D., Lees J.A., Sturm M., Vologina E.G. and Mackay A.W. (2000) Climate change in Lake Baikal: diatom evidence in an area of continous sedimentation. *International Journal of Earth Sciences* 89, 251-259.

Barber D.C., Dyke A., Hillaire-Marcel C., Jennings A.E. , Andrews J.T., Kerwin M.W., Bilodeau G., McNeely R., Southon J., Morehead M.D. and Gagnon J.M. (1999) Forcing of the cold event of 8,200 years ago by catastrophic drainage of Laurentide lakes. *Nature* 400, 344-348.

Barker P. (1992) Differential diatom dissolution in Late Quaternary sediments from Lake Manyara, Tanzania: An experimental approach. *Journal of Paleolimnology* 7, 235-251.

Barker P., Gasse F., Roberts N. and Taieb M. (1990) Taphonomy and diagenesis in diatom assemblages: a Late Pleistocene palaeoecological study from Lake Magadi, Kenya. *Hydrobiologia* 214, 267-272.

Barker P.A., Roberts N., Lamb H.F., van der Kaars S. and Benkaddour A. (1994a) Interpretation of Holocene lake-level change from diatom assemblages in Lake Sidi Ali, Middle Atlas, Morocco. *Journal of Paleolimnology* 12:223-234.

Barker P., Fontes J.C., Gasse F. and Druart J.C. (1994b) Experimental dissolution of diatom silica in concentrated salt- solutions and implications for paleoenvironmental reconstruction. *Limnology and Oceanography* 39, 99-110.

Barker P.A., Street-Perrott F.A., Leng M.J., Greenwood P.B., Swain D.L., Perrott R.A., Telford R.J. and Ficken K.J. (2001) A 14,000-year oxygen isotope record from diatom silica in two alpine lakes on Mt. Kenya. *Science* 292, 2307-2310.

Bartlett T.P., Dümenil L., Schlese U. and Roeckner, E. (1988) The effect of Eurasian snow cover on regional and global climate. *Science* 239, 504-507.

Bartlett T.P., Dümenil L., Schlese U., Roeckner, E. and Latif M. (1989) The effect of Eurasian snow cover on regional and global climate variations. *Journal of Atmosphere Science* 46, 661-685.

Barry R.G. and Chorley R.J (2003) Atmosphere, weather and Climate: Eighth edition. Routledge, London.

Battarbee R.W. (1986) Diatoms. In: Berglund B. E. (ed.). Handbook of Holocene Palaeoecology and Palaeohydrology. Wiley, Chichester. 527-570.

Battarbee R.W. (2000) Palaeolimnological approaches to climate change, with special regard to the biological record. *Quaternary Science Reviews* 19, 107-24.

Battarbee R.W. and Kneen M. (1982) The use of electronically counted microspheres in absolute diatom analysis. *Limnology and Oceanography* 27, 184-188.

Battarbee R.W., Jones V.J., Flower R.J., Cameron N.G., Bennion H., Carvalho L. and Juggins S. (2001) Diatoms In: Smol J.P., Birks H.J.B. and Last W.M. (eds.). Tracking Environmental Change Using Lake Sediments: Terrestrial, Algal, and Siliceous Indicators. Kluwer Academic Publishers, Dortrecht. 1-48.

Battarbee R.W., Mackay A.W., Jewson D.H., Ryves D.B., Sturm M. and Granin N.G. (in press) Differential dissolution of Lake Baikal diatoms: correction factors and implications for palaeoclimatic reconstruction. *Global and Planetary Change.*

BDP-96 Members (1997a) Continuous paleoclimate record recovered for last 5 million years. *EOS Transactions of the American Geophysical Union* 78, 597-604.

BDP-96 Members (1997b) Preliminary results of the first scientific drilling on Lake Baikal, Buguldeika site, southeastern Siberia. *Quaternary International* 37, 3-17.

Belcher H. and Swale E. (1976) A beginner's guide to freshwater algae. NERC, London.

Bell M. and Walker M.J.C. (1992) Late Quaternary Environmental Change. Longman, Harlow.

Bennion H. (1994) A Diatom-phosphorus transfer-function for shallow, eutrophic ponds in Southeast England. *Hydrobiologia* 276, 391-410.

Bennion H, Juggins S. and Anderson N.J. (1996) Predicting epilimnetic phosphorus concentrations using an improved diatom-based transfer function and its application to lake eutrophication management. *Environmental Science & Technology* 30, 2004-2007.

Benson L.V. (1994) Stable isotopes of oxygen and hydrogen in the Truckee River Pyramid Lake surface-water system .1. data-analysis and extraction of paleoclimatic information. *Limnology and Oceanography* 39, 344-355.

Berger A. and Loutre M.F. (1991) Insolation values for the climate of the last 10 million years. *Quaternary Science Reviews* 10, 291-317.

Berger W.H. (1990) The Younger Dryas cold spell - a quest for causes. *Palaeogeography Palaeoclimatology Palaeoecology* 89, 219-237.

Berkozova E., Letunova P. and Karabanov E. (1992) Palynological investigations of Holocene deposits in Lake Baikal. *IPPCCE Newsletter* 6, 59-67.

Birks H.J.B. (1995) Quantitative Palaeoenvironmental Reconstructions. In: Maddy D, Brew J.S. (eds.). Quaternary Research Association, Cambridge, 161-251.

Birks H.J.B. (1998) D.G. Frey & E.S. Deevey review #1 - Numerical tools in palaeolimnology - progress, potentialities, and problems. *Journal of Paleolimnology* 20, 307-332.

Birks H.J.B., Line J.M., Juggins S., Stevenson A.C. and ter Braak C.J.F. (1990) Diatoms and pH reconstruction. *Philosophical Transactions of the Royal Society of London Series B-Biological Sciences* 327, 263-78.

Bitner D., Carroll T., Cline D. and Romanov P. (2002) An assessment of the differences between three satellite snow cover mapping techniques. *Hydrological Processes* 16, 3723-3733.

Björck S., Walker M.J.C., Cwynar L.C., Johnsen S., Knudsen K.L., Lowe J.J. and Wohlfarth B. (1998) An event stratigraphy for the Last Termination in the north Atlantic region based on the Greenland ice-core record: a proposal by the INTIMATE group. *Journal of Quaternary Science* 13, 283-92.

Björck S., Noe-Nygaard N., Wolin J., Houmark-Nielsen M., Hansen H.J. and Snowball I. (2000) Eemian Lake development, hydrology and climate: a multi- stratigraphic study of the Hollerup site in Denmark. *Quaternary Science Reviews* 19, 509-36.

Black D.E. (2002) The rains may be a-comin'. *Science* 297, 528-529.

Boës X., Piotrovska N. and Fagel N. (in press) Annual climate reconstruction of Termination I in Lake Baikal sediments inferred from Grey Density Scale. *Global and Planetary Change.*

Bloemendal J., Liu X. M., And Rolph T. C. (1995) Correlation of the magnetic-susceptibility stratigraphy of Chinese loess and the marine oxygen-isotope record - chronological and paleoclimatic implications. *Earth and Planetary Science Letters* 131, 371-380.

Bolgrien D.W., Granin N.G and Levin L. (1995) Surface temperature dynamics of Lake Baikal observed from AVHRR images. *Photogrammetric Engineering and Remote Sensing* 61, 211-216.

Bolsenga S.J., Herdendorf C.E. and Norton D.C. (1991) Spectral transmittance of lake ice from 400 – 850 nm. *Hydrobiologia* 218, 15-25.

Bond G., Broecker W., Johnsen S., McManus Labeyrie L., Jouzel J. and Bonanl G. (1993) Correlations between climate records from the North Atlantic sediments and Greenland Ice. *Nature* 365, 143-146.

Bond G.C. and Lotti R. (1995) Iceberg discharges into the North-Atlantic on millennial time scales during the last glaciation. *Science* 267, 1005-1010.

Bond G., Showers W., Cheseby M., Lotti R., Almasi P., de Menocal P., Priore P., Cullen H., Hajdas I. and Bonani G. (1997) A pervasive millennial-scale cycle in North Atlantic Holocene and glacial climates. *Science* 278, 1257-1266.

Bond G., Kromer B., Beer J., Muscheler R., Evans M.N., Showers W,. Hoffmann S., Lotti-Bond R., Hajdas I. and Bonani G (2001) Persistent solar influence on north Atlantic climate during the Holocene. *Science* 294, 2130-2136.

Bonderenko N.A. (1999) Floral shift in the phytoplankton of Lake Baikal, Siberia: recent dominance of *Nitzschia acicularis*. *Plankton Biology and Ecology* 46, 18-23.

Bondarenko N.A., Guselnikova N.E., Logacheva N.F. and Pomazkina G.V. (1996) Spatial distribution of phytoplankton in Lake Baikal, spring 1991. *Freshwater Biology* 35, 517-23.

Botte V. and Kay A. (2000) A numerical study of plankton population dynamics in a deep lake during the passage of the spring thermal bar. *Journal of Marine Systems* 26, 367-286.

Bradbury J.P. (1999) Continental diatoms as indicators of long-term environmental change. In: The diatoms. In: Stoermer E.F. and Smol J.P. (eds.). The Diatoms: Applications for the Environmental and Earth Sciences. Cambridge University Press, Cambridge. 169-182.

Bradbury J.P. and Dietrich-Rurup K.V. (1993) Holocene diatom paleolimnology of Elk Lake, Minnesota. *Geological Society of America Special Paper* 276, 215-237.

Bradbury J.P., Bezrukova E.V., Chernyaeva G., Colman S., Khursevich G.K., King J. and Likhoshway Y.V. (1994) A synthesis of post-glacial diatom records from Lake Baikal. *Journal of Paleolimnology* 10, 213-252.

Bradbury P., Cumming B. and Laird K. (2002) A 1500-year record of climatic and environmental change in Elk Lake, Minnesota - III: measures of past primary productivity. *Journal of Paleolimnology* 27, 321-40.

Bradley R.S. (2003) Climate forcing during the Holocene. In: Mackay A., Battarbee R., Birks J. and Oldfield F. (eds.). Global Change in the Holocene. Arnold, London. 10-19.

Bradshaw E.G. and Anderson N.J. (2003) Environmental factors that control the abundance of *Cyclostephanos dubius* (Bacillariophyceae) in Danish lakes, from seasonal to century scale. *European Journal of Phycology* 38, 265-276.

Brandriss M.E., O'Neil J.R., Edlund M.B. and Stoermer E.F. (1998) Oxygen isotope fractionation between diatomaceous silica and water. *Geochimica et Cosmochimica Acta* 62, 1119-1125.

Brincat D., Yamada K., Ishiwatari R., Uemura H. and Naraoka H. (2000) Molecular-isotopic stratigraphy of long-chain n-alkanes in Lake Baikal Holocene and glacial age sediments. *Organic Geochemistry* 31, 287-294.

Broecker W.S. (1994) Massive iceberg discharges as triggers for global climate- change. *Nature* 372, 421-4.

Broecker W.S. (1998) Paleocean circulation during the last deglaciation: A bipolar seesaw? *Paleoceanography* 13, 119-121 .

Broecker W.S., Kennett J.P., Flower B.P., Teller J.T., Trumbore S., Bonani G., Wolfli W. (1989) Routing of meltwater from the Laurentide Ice-Sheet during the Younger Dryas cold episode *Nature* 341, 318-321.

Broecker W.S. And Denton G.H. (1990) What drives glacial cycles. *Scientific American* 262, 48-56.

Bronk-Ramsey C. (2001) Development of the Radiocarbon Program OxCal. *Radiocarbon* 43, 355-363.

Brovkin V., Hofmann M., Bendtsen J. and Ganopolski A. (2002) Ocean biology could control atmospheric $\delta^{13}C$ during glacial-interglacial cycle. *Geochemistry Geophysics Geosystems* 3, arcticle number 1027.

Brown T.A, Nelson D.E., Mathewes R.W., Vogel J.S. and Southon J.R. (1989) Radiocarbon dating of pollen by accelerator mass-spectrometry. *Quaternary Research* 32, 205-212.

Brown T.A., Farwell G.W., Grootes P.M., and Schmidt F.H. (1992) Radiocarbon AMS dating of pollen extracted from peat samples. *Radiocarbon* 34, 550-556.

Brugam R.B., McKeever K. and Kolesa L. (1998) A diatom-inferred water depth reconstruction for an Upper Peninsula, Michigan, lake. *Journal of Paleolimnology* 20, 267-276.

Bush A.B.G. (in press) CO_2/H_2O and orbitally-driven climate variability over Central Asia through the Holocene. *Quaternary International.*

Bush A.B.G., Little E.C., Rokosh D., White D. and Rutter N.W. (2004) Investigation of the spatio-temporal variability in Eurasian Late Quaternary loess-paleosol sequences using a coupled atmosphere-ocean general circulation model. *Quaternary Science Reviews* 23, 481-498.

Cameron N.G. (1995) The representation of diatom communities by fossil assemblages in a small acid lake. *Journal of Paleolimnology* 14, 185-223.

Campbell J.B. (1996) Introduction to Remote Sensing: Second Edition. Taylor and Francis, London.

Canter-Lund H. and Lund J.W.G. (1995) Freshwater Algae: Their Microscopic World Explored. Biopress, Bristol.

Chambers F. M., Ogle M. I. and Blackford J. J. (1999) Palaeoenvironmental evidence for solar forcing of Holocene climate: linkages to solar science. *Progress in Physical Geography* 23, 181-204.

Chapman M.R. and Shackleton N.J. (2000) Evidence of 550-year and 1000-year cyclicities in North Atlantic circulation patterns during the Holocene. *The Holocene* 10, 287-291.

Charlet F., Fagel N., De Batist M., Hauregard F., Minnebo B., Meischner D. and the SONIC Team (in press) Study of the sedimentary dynamics on elevated plateaus in Lake Baikal (Russia) based on sediment cores and high-resolution geophysical data. *Global and Planetary Change.*

Chebykin E.P., Edgington D.N., Grachev M.A., Zheleznyakova T.O,. Vorobyova S.S., Kulikova N.S., Azarova I.N., Khlystov O.M. and Goldberg E.L. (2002) Abrupt increase in precipitation and weathering of soils in East Siberia coincident with the end of the last glaciation (15 cal kyr BP) *Earth and Planetary Science Letters* 200, 167-175.

Chen C.T. and Millero F.J. (1986) Precise thermodynamic properties for natural waters covering the limnological range. *Limnology and Oceanography* 31, 657-662.

Chen C.T., Lan H.C., Lou J.Y. and Chen Y.C. (2003) The Dry Holocene Megathermal in Inner Mongolia. *Palaeogeography, Palaeoclimatology, Palaeoecology* 193, 181-200.

Chen F.H., Bloemendal J., Wang J.M., Li J.J. and Oldfield F. (1997) High-resolution multi-proxy climate records from Chinese loess, evidence for rapid climatic changes over the last 75 kyr. *Palaeogeography, Palaeoclimatology, Palaeoecology* 130, 323-335.

Chenyeva G.E. (1970) Diatoms in the bottom sediments of northern Lake Baikal. In: Bottom deposits of Lake Baikal. Acadamy of Sciences, Moscow. 144-160.

Chlachula J. (2003) The Siberian loess record and its significance for reconstruction of Pleistocene climate change in north-central Asia. *Quaternary Science Reviews* 22, 1879-1906.

Christensen T.R., Johansson T.R., Akerman H.J., Mastepanov M., Malmer N., Friborg T., Crill P. and Svensson B.H. (2004) Thawing sub-arctic permafrost: Effects on vegetation and methane emissions. *Geophysical Research Letters* 31, art. no. L04501

Clark I. and Fritz I. (1997) Environmental Isotopes in Hydrogeology. Boca Ranton, Lewis.

Clark M.P., Serreze M.C. and Robinson D.A. (1999) Atmospheric controls on Eurasian snow extent. *International Journal of Climatology* 19, 27-40.

Clayton R.N. and Mayeda T.K. (1963) The use of bromine pentaflouride in the extraction of oxygen from oxide and silicates for isotope analysis. *Geochimica et Cosmochima Acta* 27, 43-52.

Clayton R.N., O'Neil J.R. and Mayeda T.K. (1972) Oxygen isotope exchange between quartz and water. *Journal of Geophysical Research* 77, 3057-67.

Colman S.M. (1998) Water-level changes in Lake Baikal, Siberia: Tectonism versus climate. *Geology* 26, 531-4.

Colman S. M., Peck J. A., Karabanov E. B., Carter S. J., Bradbury J. P., King J. W. and Williams D. F. (1995) Continental climate response to orbital forcing from biogenic silica records in Lake Baikal. *Nature* 378, 769-771.

Colman S.M., Jones G.A., Rubin M., King J.W., Peck J.A. and Orem W.H. (1996) AMS radiocarbon analyses from Lake Baikal, Siberia: challenges of dating sediments from a large, oligotrophic lake. *Quaternary Science Reviews* 15, 669-684.

Colman S.M., Peck J.A., Hatton J., Karabanov E.B. and King J.W. (1998) Biogenic silica records from the BDP93 drill site and adjacent areas of the Selenga Delta, Lake Baikal, Siberia. *Journal of Paleolimnology* 21, 9-17.

CONTINENT: The CONTINENT project (High-resolution CONTINENTal paleoclimate record in Lake Baikal). Contract no. EVK2-2000-00057. http://continent.gfz-potsdam.de/

Cox E.J. (1996) Identification of Freshwater Diatoms from Live Material. Chapman and Hall, London.

Craig H. (1957) Isotopic standards for carbon and oxygen and correction factors for mass-spectrometric analysis of carbon dioxide. *Geochimica et Cosmochimica Acta* 12, 133-149.

Craig H. (1961) Isotopic variation in meteoric waters. *Science* 133, 1702-1703.

Craig H., Gordon L. I. and Horibe Y. (1963) Isotopic exchange effects in the evaporation of water. *Journal of Geophysical Research* 68, 5079-5087.

Cumming B.F., Wilson S.E., Hall R.I. and Smol J.P. (1995) Diatoms from British Columbia (Canada) lakes and their relationship to salinity, nutrients and other limnological variables. In: Bibliotheca Diatomologica 31. J. Cramer, Stuttgart.

Czernik J. and Goslar T. (2001) Preparation of graphite targets in the Gliwice Radiocarbon Laboratory for AMS ^{14}C dating. *Radiocarbon* 43, 283–91.

Dansgaard W. (1964) Stable isotopes in precipitation. *Tellus* 16, 436-468.

Dansgaard W., Johnsen S.J., Clausen H.B., Dahljensen D., Gundestrup N.S., Hammer C.U., Hvidberg C.S., Steffensen J.P., Sveinbjornsdottir A.E., Jouzel J. and Bond G. (1993) Evidence for general instability of past climate from a 250-kyr ice-core record. *Nature* 364, 218-20.

de Batist M, Klerkx J., van Rensbergen P., Vanneste M., Poort J., Golmshtok A.Y., Kremlev A.A., Khlystov O.M. and Krinitsky P. (2002) Active hydrate destabilization in Lake Baikal, Siberia? *Terra Nova* 14, 436-442.

de Menocal P. (2001) Cultural response to climate change during the Holocene. *Science* 292, 667-673.

Dean W., Anderson R., Bradbury J.P. and Anderson D. (2002) A 1500-year record of climatic and environmental change in Elk Lake, Minnesota - I: Varve thickness and gray-scale density. *Journal of Paleolimnology* 27, 287-99.

Deerskin C. and Redrew E. (2000) Variability and change in terrestrial snow cover: data acquisition and links to the atmosphere. *Progress in Physical Geography* 24, 469-498.

Deines P. (1970) Mass spectometer correction factors for the detection of small isotopic variation of carbon and oxygen. *International Journal of Mass Spectromometry and Ion Physics* 4: 283-295.

Delaygue G., Jouzel J., Masson V., Koster R. D. and Bard E. (2000) Validity of the isotopic thermometer in Central Antarctica: limited impact of glacial precipitation seasonality and moisture origin. *Geophysical Research Letters* 27, 2677-2680.

Demske D., Heumann G., Granoszewski W., Nita M., Mamakowa K., Tarasov P.E. and Oberhänsli H. (in press) Late glacial and Holocene vegetation and regional climate variability evidenced in high-resolution pollen records from Lake Baikal. *Global and Planetary Change.*

Denton G.H. and Karlen W. (1973) Holocene climatic variations – their pattern and possible cause. *Quaternary Research* 3, 155-205.

Ding Z., Liu T., Rutter N.W., Yu Z., Guo Z. and Zhu R. (1995) Ice-volume forcing of East Asian Winter Monsoon variations in the Past 800,000 years. *Quaternary Research* 44, 149-159.

Ding Z.L. and Yang S.L. (2000) C3/C4 vegetation evolution over the last 7.0 Myr in the Chinese Loess Plateau: evidence from pedogenic carbonate $\delta^{13}C$. *Palaeogeography, Palaeoclimatology, Palaeoecology* 160, 291-299.

Dixit S.S., Dixit A.S. and Smol J.P. (1991) Multivariable environmental inferences based on diatom assemblages from Sudbury (Canada) lakes. *Freshwater Biology* 26, 251-66.

Dodson, J. and Lui, T. (1995) PEPII: The Austral-Asian Transect. In: Paleoclimates of the Northern and Southern Hemispheres. PAGES, Bern. 43-64.

Douglas M.S.V. and Smol J.P. (1999) Freshwater diatoms as indicators of environmental change the High Arctic. In: Stoermer E.F. and Smol J.P. (eds.) The Diatoms: Applications for the Environmental and Earth Sciences. Cambridge University Press, Cambridge. 227-244.

Driscoll N.W. and Haug G.H. (1998) A short circuit in thermohaline circulation: A cause for northern hemisphere glaciation? *Science* 282, 436-8.

Drummond C.N., Patterson W.P. and Walker J.C.G. (1995) Climate forcing of carbon-oxygen isotopic covariance in temperate-region marl lakes. *Geology* 23, 1031-1034.

Edlund M.B., Stoermer E.F., and Pilskaln C.H. (1995) Siliceous microfossil succession in the recent history of 2 basins in Lake Baikal, Siberia. *Journal of Paleolimnology* 14, 165-184.

Edlund M.B. and Stoermer E.F. (2000) A 200,000-year, high-resolution record of diatom productivity and community makeup from Lake Baikal shows high correspondence to the marine oxygen-isotope record of climate change. *Limnology and Oceanography* 45, 948-962.

Edlund M.B., Williams R.M. and Soninkhishig N. (2003) The planktonic diatom diversity of ancient Lake Hovsgol, Mongolia. *Phycologia* 42, 232-260.

Edwards T. W. D., Wolfe B. B., and MacDonald G. M. (1996) Influence of changing atmospheric circulation on precipitation $\delta^{13}C$-temperature relations in Canada during the Holocene. *Quaternary Research* 46, 211-218.

Eicher U. and Siegenthaler U. (1976) Palynological and oxygen isotope investigations on Late-Glacial sediment cores from Swiss lakes. *Boreas* 5, 109-117.

Eklund H. (1965) Stability of lakes near the temperature maximum density. *Science* 149, 632-633.

Epstein S. and Mayeda T. (1953) Variation of O^{18} content of water from natural sources. *Geochimica et Cosmochimica Acta* 4, 213-224.

Esper J., Cook E.R. and Schweingruber F.H. (2002) Low-frequency signals in long tree-ring chronologies for reconstructing past temperature variability. *Science* 295, 2250-2253.

Eugster W., Rouse W.R., Pielke RA, McFadden J.P., Baldocchi D.D., Kittel T.G.F, Chapin F.S., Liston G.E., Vidale P.L., Vaganov E. and Chambers S, (2000) Land-atmosphere energy exchange in Arctic tundra and boreal forest: available data and feedbacks to climate. *Global Change Biology* 6, 84-115.

Evans M.E., Rutter N.W., Catto N., Chlachula J. and Nyvlt D. (2003) Magnetoclimatology: Teleconnection between the Siberian loess record and North Atlantic Heinrich events. *Geology* 31, 537-540.

Evstaf'ev V.K. and Bondarenko N.A. (2002) The "standing waves" model of Baikalian phytoplankton interannual dynamics. *Biofizika* 45, 1089-1095.

Falkner K.K, Measures C.I, Herbelin S.E., Edmond J.M. and Weiss R.F. (1991) The Major And Minor Element Geochemistry Of Lake Baikal. *Limnology and Oceanography* 36, 413-23.

Falkner K.K., Church M., Measures C.I., LeBaron G., Thouron D., Jeandel C., Stordal M.C., Gill G.A., Mortlock R., Froelich P. and Chan L.H. (1997) Minor and trace element chemistry of Lake Baikal, its tributaries, and surrounding hot springs. *Limnology and Oceanography* 42, 329-345.

Fietz S. and Nicklisch A. (2004) An HPLC analysis of the summer phytoplankton assemblage in Lake Baikal. *Freshwater Biology* 49, 332-345.

Fietz S., Kobanova G., Izmest'eva L. and Nicklisch A. (in prep.) Recent regional, vertical and seasonal distribution of phytoplankton and photosynthetic pigments in Lake Baikal

Fietz S., Sturm M. and Nicklisch A. (in press) Flux of lipophilic photosynthetic pigments to the surface sediments of Lake Baikal. *Global and Planetary Change.*

Flachseen-Forschung in Deutschland (2003) Water quality – Guidance standard for the routine analysis of phytoplankton abundance and composition using inverted microscopy (Utermöhl technique).

Flower R.J. (1993a) A taxonomic re-evaluation of endemic *Cyclotella* taxa in Lake Baikal, Siberia. *Nova Hedwigia Beiheft* 106, 203-220.

Flower R.J. (1993b) Diatom preservation: experiments and observations on dissolution and breakage in modern and fossil material. *Hydrobiologia* 269/270, 473-484.

Flower R.J. (1994) A review of current biological and environmental research on Lake Baikal from a British perspective. *Freshwater Forum* 4, 8-22.

Flower R.J. and Håkansson H. (1994) *Crateriportula* gen. nov., a new genus with close affinities to the genus *Stephanodiscus*. *Diatom Research* **9**, 259-264.

Flower R.J., Mackay A.W., Rose N.L., Boyle J.L., Dearing J.A., Appleby P.G., Kuzmina A.E., and Granina L.Z. (1995) Sedimentary records of recent environmental-change in Lake Baikal, Siberia. *The Holocene* 5, 323-327.

Flower R.J., Battarbee R.W., Lees J.A., Levina O., Jewson D., Mackay A.W., Ryves D., Sturm M., and Vologina E.G. (1998) A GEOPASS-NERC project on diatom deposition and sediment accumulation in Lake Baikal, Siberia. *Freshwater Forum* 11, 16-29.

Flower R.J., Ryves D., Battarbee R.W., Mueller J. and Sturm M. (1999) Lake Baikal: some topical aspects of current research. *Journal of Paleolimnology* 22, 223-4.

Flower R.J., Pomazkina G., Rodionova E. and Williams D.M. (2004) Local and meso-scale diversity patterns of benthic diatoms in Lake Baikal. In: Poulin M. (ed.). 17th International Diatom Symposium 2002. Biopress, Bristol. 69-92.

Foged N. (1964) Freshwater diatoms from Spitzbergen. In: Tromsö Museums Skrifter no. 11. Universitetsforlaget, Oslo.

Foged N. (1993) Some diatoms from Siberia especially from Lake Baikal. *Diatom Research* 8, 231-279.

Foley J.A., Kutzbach J.E., Coe M.T. and Levis S. (1994) Feedbacks between climate and boreal forests during the Holocene epoch. *Nature* 371, 52-53.

Fricke H.C. and O'Neil J.R. (1999) The correlation between O^{18}/O^{16} ratios of meteoric water and surface temperature: its use in investigating terrestrial climate change over geologic time. *Earth and Planetary Science Letters* 170, 181-196.

Friis-Christensen E. and Lassen K. (1991) Length of the solar-cycle - an indicator of solar-activity closely associated with climate. *Science* 254, 698-700.

Fritsen C.H. and Priscu J.C. (1999) Seasonal change in the optical properties of the permanent ice cover on Lake Bonney, Antarctica: Consequences for lake productivity and phytoplankton dynamics. *Limnology and Oceanography* 44, 447-454.

Fritz P., Anderson T. W. and Lewis C. F. M. (1975) Late-Quaternary climatic trends and history of Lake Erie from stable isotope studies. *Science* 190, 267-269.

Fritz S.C., Juggins S. and Battarbee R.W. (1993) Diatom assemblages and ionic characterization of freshwater and saline lakes of the Northern Great Plains, North America: a tool for reconstructing past salinity and climate fluctuations. *Canadian Journal of Fisheries and Aquatic Sciences* 50, 706-708.

Fritz S. C., Juggins S., Battarbee R. W., and Engstrom D. R. (1991) Reconstruction of past changes in salinity and climate using a diatom-based transfer-function. *Nature* 352, 706-708.

Fritz S.C., Cumming B.F., Gasse F. and Laird K. (1999) Diatoms as indicators of hyrologic and climatic change in saline lakes. In: Stoermer E.F. and Smol J.P. (eds.). The Diatoms: Applications for the Environmental and Earth Sciences. Cambridge University Press, Cambridge. 41-72.

Gaiser E.E., Taylor B.E. and Brooks M.J. (2001) Establishment of wetlands on the southeastern Atlantic Coastal Plain: Paleolimnological evidence of a mid-Holocene hydrologic threshold from a South Carolina pond. *Journal of Paleolimnology* 26, 373-91.

Ganopolski A., Kubatzki C., Claussen M., Brovkin V. and Petoukhov V. (1998) The influence of vegetation-atmosphere-ocean interaction on climate during the mid-Holocene. *Science* 280, 1916-1919.

Gasse F., Ledee V., Massault M., And Fontes J. C. (1989) Water-level fluctuations of lake Tanganyika in phase with oceanic changes during the last glaciation and deglaciation. *Nature* 342, 57-59.

Gasse F., Arnold M., Fontes J.C., Fort M., Gibert E., Huc A., Li B.Y, Li Y.F., Lju Q., Melieres F., Vancampo E., Wang F.B. and Zhang Q.S. (1991) A 13,000-year climate record from Western Tibet. *Nature* 353, 742-5.

Gasse F., Juggins S. and Khelifa L.B. (1995) Diatom-based transfer-functions for inferring past hydrochemical characteristics of African lakes. *Palaeogeography Palaeoclimatology Palaeoecology* 117, 31-54.

Gat J.R. (1971) Comments on stable isotope method in regional groundwater investigations. *Water Resources Research* 7, 980-993.

Gat J.R., Bowser C.J. and Kendall C. (1994) The contribution of evaporation from the Great-Lakes to the continental atmosphere - estimate based on stable-isotope data. *Geophysical Research Letters* 21, 557-60.

Genkai-Kato M., Sekino T., Yoshida T., Miyasaka H., Khodzher T.V., Belykh O.A., Melnik N.G., Kawabata Z., Higashi M. and Nakanishi M. (2002) Nutritional diagnosis of phytoplankton in Lake Baikal. *Ecological Research* 17, 135-142.

Genkal S.I. (1993) Large celled, undulate species of the genus *Stephanodiscus* Ehr. in USSR reservoirs: morphology, ecology and distribution. *Diatom Research* 8, 45-64.

Genkal S.I. and Popovskaya G.I. (1987) New data on the flora of Centricea Diatomea of Lake Baikal. *Information Bulletin for Biology of Inland Waters* 73, 8-13.

Genkal S.I. and Popovskaya G.I. (1990) Peculiarities of spore and auxospore morphology and biology of *Aulacoseira islandica* (Bacillariophyta). *Information Bulletin for Biology of Inland Waters* 89, 3-6. [in Russian].

Genkal S.I. and Popovskaya G.I. (1991) New data on the frustule morphology of *Aulacosira islandica* (Bacillariophyta). *Diatom Research* 6, 255-66.

Gibson C.E., Anderson N.J. and Haworth E.Y. (2003) *Aulacoseira suharctica*: taxonomy, physiology, ecology and palaeoecology. *European Journal of Phycology* 38, 83-101.

Gleser S.I., Makarova I.V., Moisseeva A.I. and Nikolaev V.A. (eds.) (1988) The diatoms of the USSR, fossil and recent, volume 2. Nauka, St. Petersberg.

Goldberg E.L., Grachev M.A., Phedorin M.A., Kalugin I.A., Khlystov O.M., Mezentsev S.N., Azarova I.N., Vorobyeva S.S., Zheleznyakova T.O., Kulipanov G.N., Kondratyev V.I., Miginsky E.G., Tsukanov V.M., Zolotarev K.V., Trunova V.A., Kolmogorov Y.P. and Bobrov V.A. (2001) Application of synchrotron X-ray fluorescent analysis to studies of the records of paleoclimates of Eurasia stored in the sediments of Lake Baikal and Lake Teletskoye. *Nuclear Instruments and Methods in Physics Research Section A-Accelerators Spectrometers Detectors and Associated Equipment* 470, 388-395

Goldman C.R., Elser J.J., Richards R.C., Reuter J.E., Priscu J.C. and Levin A.L. (1996) Thermal stratification, nutrient dynamics, and phytoplankton productivity during the onset of spring phytoplankton growth in Lake Baikal, Russia. *Hydrobiologia* 331, 9-24.

Goldman J.C. (1977) Temperature effects on phytoplankton growth in continuous culture. *Limnology and Oceanography* 22, 932-6.

Goldman J.C. and Carpenter E.J. (1974) A kinetic approach to the effect of temperature on algal growth. *Limnology and Oceanography* 19, 756-66.

Golmshtok A.Y., Duchkov A.D., Hutchinson D.R., Khanukaev S.B. and Elnikov A.I. (1997) Estimation of heat flow on Baikal from seismic data on the lower boundary of the gas hydrate layer. *Russian Geology and Geophysics* 38, 1714-1727.

Goslar T. and Czernik J. (2000) Sample preparation in the Gliwice Radiocarbon Laboratory for AMS ^{14}C dating. *Journal of Methods and Applications of Absolute Chronology* 18, 1-8.

Grachev M.A. (2000) Comment on 'Response of Lake Baikal ecosystem to climate forcing and pCO_2 change over the Last Glacial/Interglacial transition' A.A. Prokopenko, D.F. Williams, E.B. Karabanov, G.K. Khursevich, Earth Planet. Sci. Lett, 172 (1999) 239-253 *Earth and Planetary Science Letters* 181, 265-266.

Grachev M.A. and Likhosway Y.V. (1996) Phytoplankton of Lake Baikal: changes over different time intervals and suggestions on monitoring. Limnological Institute, Irkutsk.

Grachev M.A., Vorobyova S.S., Likhoshway Y.V., Goldberg E.L., Ziborova G.A., Levina O.V., Khlystov O.M. (1998) A high-resolution diatom record of the palaeoclimates of East Siberia for the last 2.5 My from Lake Baikal. *Quaternary Science Reviews* 17, 1101-6

Granin N.G. and Granina L.Z. (unpublished) Gas hydrates and escapes of gases in Lake Baikal (a review).

Granin N.G., Jewson D.H., Gnatovsky R.Y., Levin L.A., Zhdanov A.A., Gorbunova L.A., Tsekhanovsky V.V., Doroschenko L.M. and Mogilev N.Y. (2000) Turbulent mixing under ice and the growth of diatoms in Lake Baikal. *Verhandlungen International Vereinigung Limnologie* 27, 2812-2814.

Griffiths S.J, Street-Perrott F.A., Holmes J.A., Leng M.J. and Tzedakis C. (2001) Chemical and isotopic composition of modern water bodies in the Lake Kopais Basin, central Greece: analogues for the interpretation of the lacustrine sedimentary sequence. *Sedimentary Geology* 148, 79-103.

Grimm, E.C (1991) TILIA and TILIAGRAPH. Illinois State Museum, Springfield.

Gronskaya T.P. and Litova T.E. (1991) Kratkaya harakteristika vodnogo balansa ozera Baikal za period 1962-1988. (Short characteristics of the water balance of Lake Baikal during 1962-1988). In: Izrael, Y.A. and Anokhin, Y.A. (eds.). Monitoring okruzhayuschei sredy osera Baikal. (Monitoring of Lake Baikal Environment). Gidrometeoizdsat, Leningrad. 153-158. [in Russian].

Guiot J. (1987) Late quaternary climatic change in France estimated from multivariate pollen time series. *Quaternary Research* 28, 100-118.

Haimson M. And Knauth L. P. (1983) Stepwise fluorination - a useful approach for the isotopic analysis of hydrous minerals. *Geochimica et Cosmochimica Acta* 47, 1589-1595.

Hammarlund D., Barnekow L., Birks H.J.B. Buchardt B. and Edwards, T.W.D. (2002) Holocene changes in atmospheric circulation recorded in the oxygen-isotope stratigraphy of lacustrine carbonates from northern Sweden. *The Holocene* 12, 355-367.

Hasegawa T. (2003) Cretaceous terrestrial paleoenvironments of northeastern Asia suggested from carbon isotope stratigraphy: Increased atmospheric *p*CO2-induced climate. *Journal of Asian Earth Science* 21, 847–857.

Hasle G.R. (1976) The biogeography of some marine planktonic diatoms. *Deep-Sea Research* 23, 319-338.

Haworth E.Y. (1980) Comparison of continuous phytoplankton records with the diatom stratigraphy in the recent sediments of Blelham Tarn. *Limnology and Oceanography* 25, 1093-1103.

Hays J.D., Imbrie J., and Shackleton N.J. (1976) Variations in the Earth's orbit: pacemaker of the Ice Ages. *Science* 194, 1121-1132.

He Y., Theakstone W.H., Zhang Z.L., Zhang D.A., Yao T.D., Chen T., Shen Y.P. and Pang H.X. (2004) Asynchronous Holocene climatic change across China. *Quaternary Research* 61, 52-63.

Heim B., Oberhaensli H. and Kaufmann H. (in press) Estimation of climate proxies in Lake Baikal using ocean colour data. *Global and Planetary Change.*

Hill M.O. and Gauch H.G. Jr (1980) Detrended correspondence analysis: an improved ordination technique. *Vegetatio* 42, 47-58.

Hinrichs K.U., Hmelo L.R. and Sylva S.P. (2003) Molecular fossil record of elevated methane levels in late pleistocene coastal waters. *Science* 299, 1214-1217

Hostetler S.W. and Benson L.V. (1994) Stable isotopes of oxygen and hydrogen in the Truckee River Pyramid Lake surface-water system .2. A predictive model of $\delta^{18}O$ and δD in pyramid lake. *Limnology and Oceanography* 39, 356-64.

Hohmann R., Kipfer R., Peeters F., Piepke G., Imboden D.M. and Shimaraev M.N. (1997) Deep-water renewal in Lake Baikal *Limnology and Oceanography* 42, 841-855

Holmes J.A. (1996) Trace-element and stable-isotope geochemistry of non-marine ostracod shells in quaternary palaeoenvironmental reconstruction. *Journal of Paleolimnology* 15, 223-235.

Hondzo M. and Stefan H.G. (1993) Regional water temperature characteristics of lakes subjected to climate-change. *Climatic Change* 24, 187-211.

Hong Y.T., Jiang H.B., Liu T.S., Zhou L.P., Beer J., Li H.D., Leng X.T., Hong B. and Qin X.G. (2000) Response of climate to solar forcing recorded in a 6000-year delta O-18 time-series of Chinese peat cellulose. *The Holocene* 10, 1-7.

Horiuchi K., Minoura K., Hoshino K., Oda T., Nakamura T. and Kawai T. (2000) Palaeoenvironmental history of Lake Baikal during the last 23000 years. *Palaeogeography Palaeoclimatology Palaeoecology* 157, 95-108.

Hughes P.D.M., Mauquoy D., Barber K.E. and Langdon P.G. (2000) Mire-development pathways and palaeoclimatic records from a full Holocene peat archive at Walton Moss, Cumbria, England. *The Holocene* 10, 465-479.

Huisman J., Olff H. and Fresco L.F.M. (1993) A hierarchical set of models for species response analysis. *Journal of Vegetation Science* 4, 37-46.

Hurrell J.W. (1995) Decadal trends in the North-Atlantic oscillation - regional temperatures and precipitation. *Science* 269, 676-9.

Hurrell J.W. (1996) Influence of variations in extratropical wintertime teleconnections on Northern Hemisphere temperature. *Geophysical Research Letters* 23, 665-668.

Hustedt F. (1956) Kieselalgen (Diatomeen). Kosmos-Verlag Franckh, Stuttgart.

Hutchinson, G.E. (1961) The paradox of the plankton. *American Nature* 95, 137-145.
Hutson 1977

IAEA. Isotope Hydrology Information System. The ISOHIS Database. Accessible at: http://isohis.iaea.org

Imbrie J. and Kipp N.G. (1971) A new micropaleonological mrthod for quantitative paleoclimatology: application to a late Pleistocene Caribbean core. In: Turekian K.K. (ed.). The Late Cenozoic Glacial Ages. Yale University Press, New Haven. 77-181.

Imbrie J, Boyle E.A., Clemens S.C., Duffy A., Howard W.R, Kukla G., Kutzbach J., Martinson D.G., Mcintyre A., Mix A.C., Molfino B., Morley J.J., Peterson L.C., Pisias N.G., Prell W.L., Raymo M.E., Shackleton N.J. and Toggweiler J.R. (1992) On the structure and origin of the major glaciation cycles. 1. Linear responses to Milankovitch forcing. *Paleoceanography* 7, 701-38.

Ishiwatari R., Uzaki M., Yamada K., and Ogura K. (1992) organic matter records of environmental changes in lake baikal sediments. 1: carbon isotopes, organic carbon and nitrogen. *IPPCCE Newsletter* 6, 80-88.

Jewson D.H. (1992) Size-reduction, reproductive strategy and the life-cycle of a centric diatom. *Philosophical Transactions of the Royal Society of London Series B-Biological Sciences* 336, 191-213.

Jewson D.H., Granin N.G. and Yakuskin, A. (unpublished) Affects of temperature and light on the growth of endemic planktonic diatoms from Lake Baikal.

Jewson D. and Granin N.G. (2000) How can present day studies of diatoms help in understanding past climatic change in baikal? *Terra Nostra* 9, 29-33.

John D.M., Whitton B.A. and Brook A.J. (eds.) (2003) The Freshwater Algal Flora of the British Isles: An Identification Guide to Freshwater and Terrestrial Algae. Cambridge University Press, Cambridge.

Johnson K.R. and Ingram B.L. (2004) Spatial and temporal variability in the stable isotope systematics of modern precipitation in China: implications for paleoclimatic reconstructions. *Earth and Planetary Science Letters* 220, 365-377.

Johnson S., Clausen H.B., Dansgaard W., Gundestrup N., Hansson M., Jonsson P., Steffensen J.P. and Sveinbjornsdottir A.E. (1992) A 'deep' ice core from East Greenland. *Meddeleser om Gronland, Geoscience* 29, 1-22.

Jones V.J. and Juggins S. (1995) The construction of a diatom-based nutrient transfer function and its application at three lakes on Signy Island (maritime Antarctic) subject to differing degrees of nutrient enrichment. *Freshwater Biology* 34, 433-445.

Jones V.J., Leng M.J., Solovieva N., Sloane H.J. and Tarasov P. (2004) Holocene climate on the Kola Peninsula; evidence from the oxygen isotope record of diatom silica. *Quaternary Science Reviews* 23, 833-839.

Jouzel J., Hoffmann G., Koster R.D. and Masson V. (2000) Water isotopes in precipitation: data/model comparison for present-day and past climates. *Quaternary Science Reviews* 19, 363-379.

Juggins S. (1991) ZONE version 1.2, unpublished computer software.

Juggins S. (2002) WinTran version 1.5, unpublished computer software.

Juggins S. (2003) C2 version 1.3, unpublished computer software.

Juillet A. (1980) Structure de la silice biogénic: nouvelles données apportées par l' analyse isotopique de l'oxygène. *C.R. Acad. Sc. Paris* 290D, 1237-1239.

Juillet-Leclerc A. (1986) Cleaning process for diatomaceous samples. In: Ricard M. (ed.). 8th Diatom Symposium. Koeltz Scientific Books, Koenigstein.733-736.

Juillet-Leclerc A. J. And Labeyrie L. (1987) Temperature-dependence of the oxygen isotopic fractionation between diatom silica and water. *Earth and Planetary Science Letters* 84, 69-74.

Julius M.L., Stoermer E.F., Colman S.M. and Moore T.C. (1997) A preliminary investigation of siliceous microfossil succession in late quaternary sediments from Lake Baikal, Siberia. *Journal of Paleolimnology* 18, 187-204.

Karabanov E.B., Prokopenko A.A., Williams D.F. and Colman S.M. (1998) Evidence from Lake Baikal for Siberian glaciation during oxygen-isotope substage 5d. *Quaternary Research* 50, 46-55.

Karabanov E.B., Prokopenko A.A., Williams D.F. and Khursevich G.K. (2000) A new record of holocene climate change from the bottom sediments of Lake Baikal. *Palaeogeography Palaeoclimatology Palaeoecology* 156, 211-224.

Karabanov E., Williams D., Khursevich G., Bezrukova E., Kuzmin M., Prokopenko A., Fedenia S., Gvozdkov S. and Krapivina S. (2003) The LGM-Holocene high-resolution record from Lake Baikal (Siberia): evidence for glacial ecological collapse and Holocene recovery of lake's ecosystem.

http://www.pages.unibe.ch/shighlight/archive03/karabanov.html

Karabanov E., Williams D., Kuzmin M., Sideleva V., Khursevich G., Prokopenko A., Solotchina E., Tkachenko L., Fedenya S., Kerber E., Gvozdkov A., Khlustov O., Bezrukova E., Letunova P. and Krapivina S. (2004) Ecological collapse of Lake Baikal and Lake Hovsgol ecosystems during the Last Glacial and consequences for aquatic species diversity *Palaeogeography Palaeoclimatology Palaeoecology* 209, 227-243.

Kashiwaya K., Ryugo M., Sakai H. and Kawai T (1998) Long-term climato-limnological oscillation during the past 2.5 million years printed in Lake Baikal sediments. *Geophysical Research Letters* 25, 659-62.

Kashiwaya K., Ryugo M., Horii M., Sakai H., Nakamura T. and Kawai T (1999) Climato-limnological signals during the past 260 000 years in physical properties of bottom sediments from Lake Baikal. *Journal of Paleolimnology* 21, 143-50.

Kashiwaya K., Sakai H., Ryugo M., Horii M. and Kawai T. (2001a) Long-term climato-limnological cycles found in a 3.5-million- year continental record. *Journal of Paleolimnology* 25, 271-8.

Kashiwaya K., Ochiai S., Sakai H. and Kawai T. (2001b) Orbit-related long-term climate cycles revealed in a 12-Myr continental record from Lake Baikal. *Nature* 410, 71-4.

Keeling C.D. and Whorf T.P. (1997) Possible forcing of global temperature by the oceanic tides. *Proceedings of The National Academy of Sciences of the United States of America.* 94, 8321-8328.

Keeling C.D. and Whorf T.P. (2000) The 1,800-year oceanic tidal cycle: A possible cause of rapid climate change. *Proceedings of The National Academy of Sciences of the United States of America* 97, 3814-3819.

Kelley D.E. (1997) Convection in ice-covered lakes. Effects on algal suspension. *Journal of Plankton Research* 19, 1859-1880.

Kellogg W.W. (1987) Mankinds impact on climate - the evolution of an awareness. *Climate Change* 10, 113-136.

Kennett J.P., Cannariato K.G., Hendy I.L. and Behl R.J. (2000) Carbon isotopic evidence for methane hydrate instability during Quaternary interstadials. *Science* 288, 128-133.

Kennett J.P., Cannariato K.G., Hendy I.L. and Behl R.J. (2003) Methane hydrates in Quaternary climate change: The clathrate gun hypothesis. American Geophysical Union, Washington D.C.

Kent M. and Coker P. (1992) Vegetation description and analysis. John Wiley and Sons, Chichester.

Khalil M.A.K. and Rasmussen R.A. (1995) In: Singh H.B. (ed.). Composition, Chemistry, and Climate of the Atmosphere. Van Nostrand Reinhold, New York. 58-87.

Khilyuk L.F. and Chilingar G.V. (2003) Global warming: Are we confusing cause and effect? *Energy Sources* 25, 357-370.

Khotinsky N.A. (1984) Holocene Climatic Changes. In: Wright Jr H.E. and Barnosky C.W. (eds.). Late Quaternary Environments of the Soviet Union. University of Minnesota Press, Minneapolis. 305-309.

Khursevich G.K. (1989) Atlas of *Stephanodiscus* and *Cyclostephanos,* Bacillariophyta, from the Upper Cenozoic deposits of the USSR. In: Velichkevich F.Y. (ed.). Nauka and Teknika, Russia. [in Russian].

Khursevich G.K., Karabanov E.B., Prokopenko A.A., Williams D.F., Kuzmin M.I., Fedenya S.A. and Gvozdkov A.A. (2001) Insolation regime in siberia as a major factor controlling diatom production in Lake Baikal during the past 800,000 years. *Quaternary International* 80-1, 47-58.

Kilham P. and Kilham S.S. (1980) The evolutionary ecology of phytoplankton. In: Morris I. (ed.). The Physiological Ecology of Phytoplankton. University of California Press, Berkeley. 571-597.

Kilham S.S., Theriot E.C. and Fritz S.C. (1996) Linking planktonic diatoms and climate change in the large lakes of the Yellowstone ecosystem using resource theory. *Limnology and Oceanography* 41, 1052-1062.

Kita I., Taguchi S. and Matsubaya O. (1985) Oxygen isotope fractionation between amorphous silica and water at 34-93°C. *Nature* 314, 83-84.

Klerkx J, Zemskaya T.I., Matveeva T.V., Khlystov O.M., Namsaraev B.B., Dagurova O.P., Golobokova L.P., Vorob'eva S.S., Pogodaeva T.P., Granin N.G., Kalmychkov G.V., Ponomarchuk V.A., Shoji H., Mazurenko L.L., Kaulio V.V., Solov'ev V.A. and Grachev MA (2003) Methane hydrates in deep bottom sediments of Lake Baikal. *Doklady Earth Sciences* 393A, 1342-1346.

Klitgaard-Kristensen D., Sejrup H.P., Haflidason H., Johnsen S. and Spurk M. (1998) A regional 8200 cal. yr bp cooling event in northwest europe, induced by final stages of the Laurentide Ice-Sheet deglaciation? *Journal of Quaternary Science* 13, 165-169.

Knauth L.P., and Epstein S. (1976) Hydrogen and oxygen isotope ratios in nodular and bedded cherts. *Geochimica et Cosmoschima Acta* 40, 1095-1108.

Knauth L.P and Epstein S. (1984) The nature of water in hydrous silica *American Mineralogist* 67, 510-520.

Kobanova G.I. (2001) Some peculiarities of the life cycle of *Aulacoseira Skvortzowii* in Lake Baikal. In: Economou-Amilli A. (ed.). Proceedings of the 16th International Diatom Symposium. University of Athens, Greece. 205-212.

Kociolek J.P., Flower R. and Reid G. (2000) Valve ultrastructure of *Didymosphenia dentata* (Bacillariophyta): an endemic diatom species from Lake Baikal. *Nova Hedwigia* 71, 113-120.

Koinig K.A., Schmidt R., Sommaruga-Wograth S., Tessadri R. and Psenner R. (1998) Climate change as the primary cause for pH shifts in a high alpine lake. *Water Air and Soil Pollution* 104, 167-180.

Kolokoltseva E.M. (1968) Morfometricheskie harakteristiki ozera Baikal (Morphometric characteristics of Lake Baikal). In: Zhuze A.P. and Florensov N.A. (eds.). Mezoziskie I kainozoiskie ozera Sibiri (Mesozoic and Cenozoic lakes of Siberia). Nauka, Moscow. 183-8. [in Russian].

Kovach W.L. (1995) Multivariate data analysis. In: Maddy D. and Brew J.S. (eds.). Statistical Modelling of Quaternary Science Data,. Quaternary Research Association Technical Guide No. 5. Quaternary Research Association, Cambridge. 1-36.

Kozhov M. (1963) Lake Baikal and its Life. W. Junk, The Hague.

Kozhova O.M. and Izmest'eva L.R. (eds.) (1998) Lake Baikal, Evolution and Diversity. Backhuys, Leiden.

Kozhova O.M. and Kobanov G.I. (2001) Ecological peculiarities of diatoms in Lake Baikal. In: Economou-Amilli A. (ed.). Proceedings of the 16th International Diatom Symposium. University of Athens, Greece. 279-290.

Krammer K. and Lange-Bertalot H. (1986-1991) Süßwasserflora von Mitteleuropa, Volumes 2/1, 2/2, 2/3, 2/4. Gustav Fischer Verlag, Stuttgart.[in German].

Kutzbach J.E., Guetter P.J., Behling P.J. and Selin R. (1993) Simulated climatic changes: Results of the COHMAP climate-model experiments. In: Wright Jr H.E., Kutzbach J.E., Webb III T., Ruddiman W.F., Street-Perrott F.A. and Bartlein P.J. (eds.). Glabal Climates Since the Last Glacial Maximum. University of Minnesota Press, Minneapolis. 24-93.

Kuzmin, M.I., Kalmychkov G.V., Geletii R.F., Gnilusha V.A., Goreglyad A.V., Khakhaev B.N., Pevzner L.A., Kawai T., Yoshida N., Duchkov A.D., Ponomarchuk V.A., Kontorovich A.E., Abazhin N.M., Makhov G.A., Dyadin Yu. A., Kuznetsov F.A., Larionov E.G., Manakov A.Yu., Smolyakov B.S., Mandel'baum M.M., and Zheleznyakov N.K. (1998) The first find of gas-hydrates in the sedimentary rocks of Lake Baikal. *Doklady Earth Sciences* 362, 1029-1031.

Kuzmin M.I., Geletij V.F., Kalmychkov G.V., Kuznetsov F.A., Larionov E.G., Manakov A.Y., Mironov Y.I., Smolyakov B.S., Dyadin Y.A., Duchov A.D., Bazin N.M. and Mahov G.A. (2000) The discovery of the first gas hydrates in the sediments of Lake Baikal. In: Holder G.D. and Bishnoi P.R. (eds.). Gas Hydrates. Challenges for the Future. *Annals of the New York Academy of Science* 912, 112-115.

Labeyrie L. (1974) New approach to surface seawater palaeotemperatures using $^{18}O/^{16}O$ ratios in silica diatom frustules. *Nature* 248, 40-43.

Labeyrie L.D. and Juillet A. (1982) Oxygen isotope exchangeability of diatom valve silica; interpretation and consequences for paleoclimatic studies. *Geochimica et Cosmochimica Acta* 46, 967-975.

Laing T.E., Ruhland K.M. and Smol J.P. (1999) Past environmental and climatic changes related to tree-line shifts inferred from fossil diatoms from a lake near the Lena River Delta, Siberia. *Holocene* 9,547-57.

Laird K.R., Fritz S.C., Maasch K.A. and Cumming B.F. (1996a) Greater drought intensity and frequency before AD 1200 in the Northern Great Plains, USA. *Nature* 384:552-4

Laird K.R., Fritz S.C., Grimm E.C. and Mueller P.G. (1996b) Century-scale paleoclimatic reconstruction from Moon Lake, a closed-basin lake in the northern Great Plains. *Limnology and Oceanography* 41, 890-902.

Lamb A.L., Leng M.J., Lamb H.F. and Mohammed M.U. (2000) A 9000-year oxygen and carbon isotope record of hydrological change in a small Ethiopian crater lake. *The Holocene* 10, 167-77.

Lamb A.L., Leng M.J., Mohammed M.U. and Lamb H.F. (2004) Holocene climate and vegetation change in the Main Ethiopian Rift Valley, inferred from the composition (C/N and delta C-13) of lacustrine organic matter. *Quaternary Science Reviews* 23, 881-891.

Lamb H., Roberts N., Leng M., Barker P., Benkaddour A. and van der Kaars S. (1999) Lake evolution in a semi-arid montane environment: response to catchment change and hydroclimatic variation. *Journal of Paleolimnology* 21, 325-343.

Laws E.A, Popp B.N., Bidigare R.R., Kennicutt M.C, Macko S.A. (1995) Dependence of phytoplankton carbon isotopic composition on growth-rate and CO_2(aq) - theoretical considerations and experimental results. *Geochimica et Cosmochimica Acta* 59, 1131-1138.

Le Core H.L. (1998) Use of numerical models and satellite data to study physical processes in Lake Baikal. Unpublished Ph.D. Thesis, University of Leicester.

Lehmkuhl F. and Haselein F. (2000) Quaternary paleoenvironmental change on the Tibetan Plateau and adjacent areas (Western China and Western Mongolia) *Quaternary International* 65-6, 121-145.

Leibovich-Granina L.Z. (1987) Iron and manganese cycle in Lake Baikal. *Vodnye Resursy* 15, 67-72.

Leng M.J. (2003) Stable-isotopes in lakes and lake sediment archives. In: Mackay A.W., Battarbee R.W., Birks H.J.B. and Oldfield F. (eds.) Global Change in the Holocene: approaches to reconstructing fine-resolution climate change. Arnold, London. 124-139.

Leng M.J., Greenwood P.B. and Sloane H.J. (1998) Oxygen isotopes in diatomite from Lake Pinarbasi, Turkey. *NIGL Report no. 131.*

Leng M.J., Heaton T.H.E., Lamb H.F. and Naggs F. (1998) Carbon and oxygen isotope variations within the shell of an African land snail (limicolaria kambeul chudeaui germanin): a high-resolution record of climate seasonality? *The Holocene* 8, 407-412.

Leng M.J., Roberts N., Reed J.M., and Sloane H.J. (1999) Late Quaternary palaeohydrology of the Konya Basin, Turkey, based on isotope studies of modern hydrology and lacustrine carbonates. *Journal of Paleolimnology* 22, 187-20.

Leng M., Barker P., Greenwood P., Roberts N., and Reed J. (2001) oxygen isotope analysis of diatom silica and authigenic calcite from Lake Pinarbasi, Turkey. *Journal of Paleolimnology* 25, 343-349.

Leng M.J. and Marshall J.D. (2004) Palaeoclimate interpretation of stable isotope data from lake sediment archives *Quaternary Science Reviews* 23, 811-831.

Lepš J. and Šmilauer P. (2003) Multivariate Analysis of Ecological Data using CANOCO. Cambridge University Press, Cambridge.

Leuschner D.C. and Sirocko F. (2000) The low-latitude monsoon climate during Dansgaard-Oeschger cycles and Heinrich Events. *Quaternary Science Reviews* 19, 243-254.

Li H.C. and Ku T.L. (1997) $\delta^{13}C$-$\delta^{18}O$ covariance as a paleohydrological indicator for closed-basin lakes. *Palaeogeography Palaeoclimatology Palaeoecology* 133, 69-80.

Likhoshway Y.V., Yakuskin A.O. and Bondarenko N.A. (1992) Fine structure of the velum and girdle bands in *Aulacoseira baicalensis*. *Diatom Research* 7,87-94

Likhoshway Y.V., Kuzmina A.Y., Potyemkina T.G., Potyemkin V.L. and Shimaraev M.N. (1996) The distribution of diatoms near a thermal bar in Lake Baikal. *Journal of Great Lakes Research* 22, 5-14.

Lui X. and Yanai M. (2002) Influence of Eurasian spring snow cover on Asian summer rainfall. *International Journal of Climatolology* 22, 1075-1089.

Livingstone D.M. (1997) Break-up dates of Alpine lakes as proxy data for local and regional mean surface air temperatures. *Climatic Change* 37, 407-439.

Livingstone D.M. (1999) Ice break-up on southern Lake Baikal and its relationship to local and regional air temperatures in Siberia and to the North Atlantic oscillation. *Limnology and Oceanography* 44, 1486-1497.

Loginova L.P. and Khursevich G.K. (1986) New and rare diatom species of the genera *Cyclotella* and *Stephanodiscus* from the deposits of Lake Baikal. In: Goretsky G.I. (ed.). New and rare diatom species of the fossil animals and plants of Byelorussia. Nauka, Minsk. 142-148. [in Russian].

Lotter A.F., Birks H.J.B. and Zolitschka B. (1995) Late-Glacial pollen and diatom changes in response to 2 different environmental perturbations - volcanic-eruption and Younger Dryas cooling. *Journal of Paleolimnology* 14, 23-47.

Lotter A.F., Birks H.J.B., Hofmann W., And Marchetto A. (1997) Modern diatom, cladocera, chironomid, and chrysophyte cyst assemblages as quantitative indicators for the reconstruction of past environmental conditions in the Alps .1. Climate. *Journal of Paleolimnology* 18, 395-420.

Lotter A.F., Birks H.J.B., Hofmann W. and Marchetto A. (1998) Modern diatom, cladocera, chironomid, and chrysophyte cyst assemblages as quantitative indicators for the reconstruction of past environmental conditions in the Alps. II. Nutrients. *Journal of Paleolimnology* 19, 443-63.

Lotter A.F., Birks H.J.B., Eicher U., Hofmann W., Schwander J., Wick L. (2000) Younger Dryas and Allerød summer temperatures at Gerzensee (Switzerland) inferred from fossil pollen and cladoceran assemblages. *Palaeogeography Palaeoclimatology Palaeoecology* 159, 349-361.

Lowe J.J. (2001) Climatic oscillations during the last Glacial cycle – nature, causes and the case for synchronous effects. *Biology and Environment: Proceedings of the Royal Irish Academy* 101B, 19-33.

Lowe J.J., Hoek W.Z. and the INTIMATE group (2001) Inter-regional correlation of palaeoclimatic records of the last Glacial - Interglacial Transition: a protocol for improved precision recommended by the INTIMATE project group. *Quaternary Science Reviews* 20, 1175-1187.

Lund J.W.G. (1949) Studies on *Asterionella.* The origin and nature of the cells producing seasonal maxima. *Journal of Ecology* 37, 389-419.

Lund J.W.G. (1950) Studies on *Asterionella formosa* Hass. II. Nutrient depletion and the spring maximum (parts I and II). *Journal of Ecology* 38, 1-35.

Lund J.W.G. (1954) The seasonal cycle of the plankton diatom, *Melosira italica* (Ehr.). Kutz. subsp. *subarctica* O. Müll, *Journal of Ecology* 42, 151-179.

Lund J.W.G., Mackereth F.J.H. and Mortimer C.H. (1963) Changes in depth and time of certain physical conditions and of the standing crop of *Asterionella formosa* Hass. in the north basin of Windermere in 1947. *Philosophical Transactions of the Royal Society* 246B, 255-290.

Lydolph P. E. (1977) *Geography of the USSR.* Elsevier, The Hague.

Lythe M., Hauser A. and Wendler G. (1999) Classification of sea ice types in the Ross Sea, Antarctica from SAR and AVHRR imagery. *International Journal of Remote Sensing* 20, 3073-3085.

MacAyeal D.R. (1993) Binge/purge oscillations of the Laurentide ice-sheet as a cause of the North-Atlantic's Heinrich events. *Paleoceanography* 8, 775-784.

MacDonald G.M., Velichko A.A., Kremenetski C.V., Borisova O.K., Goleva A.A., Andreev A.A., Cwynar L.C., Riding R.T., Forman S.L., Edwards T.W.D., Aravena R., Hammarlund D., Szeicz J.M. and Gattaulin V.N. (2000) Holocene treeline history and climate change across northern Eurasia. *Quaternary Research* 53, 302-11.

Machavaram M.V. And Krishnamurthy R.V. (1995) Earth surface evaporative process - a case-study from the Great-Lakes region of the United-States based on deuterium excess in precipitation. *Geochimica et Cosmochimica Acta* 59, 4279-4283.

Mackay A.W., Flower R.J., Kuzmina A.E., Granina L.Z., Rose N.L., Appleby P.G., Boyle J.F., And Battarbee R.W. (1998) Diatom succession trends in recent sediments from Lake Baikal and their relation to atmospheric pollution and to climate change. *Philosophical Transactions of the Royal Society of London Series B-Biological Sciences* 353, 1011-1055.

Mackay A.W., Battarbee R.W., Flower R.J., Jewson D., Lees J.A., Ryves D.B., Sturm M. (2000) The deposition and accumulation of endemic planktonic diatoms in the sediments of Lake Baikal and an evaluation of their potential role in climate reconstruction during the Holocene. *Terra Nostra* 9:34-48.

Mackay A.W. Flower R. and Granina L. (2002) Lake Baikal. In: Shahgedanova M. (ed.). The Physical Geography of Northern Eurasia. Oxford University Press, Oxford. 403-421.

Mackay A.W., Battarbee, R.W., Flower, R.J., Granin, N.G., Jewson, D.H., Ryves, D.B. and Sturm, M. (2003) Assessing the potential for developing internal diatom-based transfer functions for Lake Baikal. *Limnology and Oceanography* 48, 1183-1192.

Mackay A.W., Ryves D.B., Battarbee R.W., Flower R.J., Granin N., Jewson D., Rioual P.M.J. and Sturm, M. (in press) 1000 years of climate variability in central Asia: assessing the evidence using Lake Baikal diatom assemblages and the application of a diatom-inferred model of snow thickness. *Global and Planetary Change.*

McKenzie J.A. (1985) Carbon isotopes and productivity in the lacustrine and marine environment. In Stumm W. (ed). Chemical Processes in Lakes. Wiley, New York.

Magnuson J.J., Robertson D.M., Benson B.J., Wynne R.H., Livingstone D.M., Arai T., Assel R.A., Barry R.G., Card V., Kuusisto E., Granin N.G., Prowse T.D., Stewart K.M., Vuglinski V.S. (2000) Historical trends in lake and river ice cover in the Northern Hemisphere. *Science* 289, 1743-1746.

Mangerud J., Andersen S.T., Berglund B.E. and Donner J.J. (1974) Quaternary stratigraphy of Norden: a proposal for terminology and classification. *Boreas* 3, 109-127.

Martin P., Goddeeris B. and Martens K (1993) Oxygen concentration profiles in soft-sediment of Lake Baikal (Russia) near the Selenga-Delta. *Freshwater Biology* 29, 343-9.

Martin P. and Goddeeris B. (in press) A qualitative assessment of the importance of bioturbation in subrecent sediments of Lake Baikal. *Global and Planetary Change.*

Martinson D.G., Pisias N.G., Hays J.D., Imbrie J., Moore T.C. and Shackleton N.J. (1987) Age dating and the orbital theory of the ice ages - development of a high-resolution-0 to 300,000-year chronostratigraphy. *Quaternary Research* 27, 1-29.

Maslin M.A., Adams J., Thomas E., Faure H., and Haines-Young R. (1995) Estimating the carbon transfer between the oceans, atmosphere and the terrestrial biosphere since the last glacial maximum. *Terra Nova* 7, 358-366.

Maslin M.A., Mikkelsen N., Vilela C. and Haq B. (1998) Sea-level- and Gas-hydrate-controlled catastrophic sediment failures of the Amazon Fan. *Geology* 26, 1107-1110.

Maslin M.A. and Thomas E. (2003) Balancing the deglacial global carbon budget: the hydrate factor. *Quaternaty Science Reviews* 22, 1729-1736.

Maslin M., Pike J., Stickley C. and Ettwein V. (2003) Evidence of Holocene climate variability in marine sediments. In: Mackay A.W., Battarbee R.W., Birks H.J.B. and Oldfield F. (eds.). Global Change in the Holocene: approaches to reconstructing fine-resolution climate change. Arnold, London. 185-209.

Maslin M.A., Owen M., Day S. and Long D. (2004) Linking continental slope failure to climate change: Testing the Clathrate Gun Hypothesis. *Geology* 32, 53-56.

Matheney R.K. And Knauth L.P. (1989) Oxygen-isotope fractionation between marine biogenic silica and seawater. *Geochimica et Cosmochimica Acta* 53, 3207-3214.

Mayewski P.A., Meeker L.D., Twickler M.S., Whitlow S., Yang Q.Z., Lyons W.B., Prentice M. (1997) Major features and forcing of high-latitude northern hemisphere atmospheric circulation using a 110,000-year-long glaciochemical series *Journal of Geophysical Research-Oceans* 102 (C12), 26345-26366.

Mazepova G.F. (1998) The role of copepods in the Baikal ecosystem. *Journal of Marine Systems* 15, 113-120.

Merlivat L. and Jouzel J. (1979) Global climatic interpretation of the deuterium-oxygen 18 relationship for precipitation. *Journal of Geophysical Research* 84, 5029-5033.

Meyer K.I. (1930) Introduction into the algae flora of Lake Baikal. *Bulletin of the Moscow Society of Nature* 39, 179-396. [in Russian].

Meyers P.A. (1994) Preservation of elemental and isotopic source identification of sedimentary organic-matter. *Chemical Geology* 114, 289-302.

Meyers P.A and Horie S. (1993) An organic carbon isotope record of glacial-postglacial change in atmospheric *p*CO2 in the sediments of Lake Biwa, Japan. *Palaeogeography, Palaeoclimatology, Palaeoecology* 105, 171-178.

Meyers P.A. and Lallier-Verges E. (1999) Lacustrine sedimentary organic matter records of Late Quaternary paleoclimates. *Journal of Paleolimnology* 21, 345-372.

Meyers P.A. and Teranes J.L. (2001) Sediment organic matter. In: Last W.M. and Smol J.P. (eds.). Tracking Environmental Change Using Lake Sediments. Volume 2, Physical and Geochemical Methods. Kluwer, Dortrecht. 239-269.

Meyers P.A. and Ishiwatari R. (1993) Lacustrine organic geochemistry - an overview of indicators of organic-matter sources and diagenesis in lake-sediments. *Organic Geochemistry* 20, 867-900.

Mikkelsen N., Labeyrie L. and Berger W. H. (1978) Silica oxygen isotopes in diatoms: a 20,000 yr record in deep-sea sediments. *Nature* 271, 536-538.

Mingram J., Allen J.R.M., Bruchmann C., Liu J., Luo X., Negendank J.F.W., Nowaczyk N. and Schettler G. (2004) Maar and crater lakes of the Long Gang Volcanic Field (NE China) - overview, laminated sediments, and vegetation history of the last 900 years. *Quaternary International* 123-25, 135-147.

Mopper K. and Garlick G. D. (1971) Oxygen isotope fractionation between biogenic silica and ocean water. *Geochimica et Cosmochimica Acta* 35, 1185-1187.

Morley D.W., Leng M.J., Mackay A.W., Sloane H.J., Rioual P. and Battarbee R.W. (2004) Cleaning of lake sediment samples for diatom oxygen isotope analysis. *Journal of Paleolimnology* 31, 391-401.

Morley D.W., Leng M.J., Mackay A.W. and Sloane H.J. (in press) Late Glacial and Holocene environmental change in the Lake Baikal region documented by oxygen isotopes from diatom silica. *Global and Planetary Change.*

Morrill C., Overpeck J.T. and Cole J.E. (2003) A synthesis of abrupt changes in the Asian summer monsoon since the last deglaciation. *The Holocene* 13, 465-476.

Müller B., Maerki M., Schmid M., Vologina E.G., Wehrli B., Wüest A. and Sturm M. (in press) Internal carbon and nutrient cycling in Lake Baikal: Sedimentation, upwelling and early diagenesis *Global and Plantary Change.*

Munk W., Dzieciuch M. and Jayne S. (2002) Millennial climate variability: Is there a tidal connection? *Journal of Climate* 15, 370-385.

Munstermann D. and Kerstholt S. (1996) Sodium polytungstate, a new non-toxic alternative to bromoform in heavy liquid seperation. *Review of Palaeobotany and Palynology* 91, 417-422.

Nagata T., Takai K., Kawanobe K., Kim D.S., Nakazato R., Guselnikova N., Bondarenko N., Mologawaya O., Kostrnova T., Drucker V., Satoh Y., Watanabe Y. (1994) Autotrophic Picoplankton in Southern Lake Baikal - abundance, growth and grazing mortality during summer. *Journal of Plankton Research* 16, 945-59.

Nakagawa T., Kitagawa H., Yasuda Y., Tarasov P.E., Nishida K., Gotanda K. and Sawai Y. (2002) Asynchronous climate changes in the North Atlantic and Japan during the last termination. *Science* 299, 688-691.

NGRIP Members (2004) High-resolution record of Northern Hemisphere climate extending into the last integlacial period. *Nature* 431, 147-151.

Nikiteeva T.A. and Likhoshway Y.V. (1994) *Cyclotella gracilis* sp. nov. from Pleistocene material of Lake Baikal, Russia. *Diatom Research* 9, 349-353.

O'Brien S. R., Mayewski P. A., Meeker L. D., Meese D. A., Twickler M. S. and Whitlow S. I. (1995) Complexity of Holocene climate as reconstructed from a Greenland ice core. *Science* 270, 1962-1964.

O'Leary M.H. (1988) Carbon isotopes in photosynthesis. *Bioscience* 38, 328-336.

Oberhänsli H. (2000) Searching for climate proxies stored in Lake Baikal sediments: A few comments. *Terra Nostra* 9, 140-7.

Overpeck J., Anderson D., Trumbore S. and Prell W. (1996) The southwest Indian Monsoon over the last 18000 years. *Climate Dynamics* 12, 213-225.

Padisak J., Krienitz L., Scheffler W., Koschel R., Kristiansen J. and Grigorszky I. (1998) Phytoplankton succession in the oligotrophic Lake Stechlin (Germany) in 1994 and 1995 *Hydrobiologia* 370, 179-197.

Patrick R. (1971) Ecology of freshwater diatoms and diatom communities. In: Werner D. (ed.). The biology of the diatoms. Blackwell Scientific, London. 284-332.

Patrick R. (1974) The effects of increasing light and temperature on the structure of diatom communities. *Limnology and Oceanography* 16, 405-21.

Patrick R. and Reimer C.W. (1966) The diatoms of the United States I. Monographs of Natural the Academy of Natural Sciences of Philadelphia 13. Academy of Natural Sciences of Philadelphia, Philadelphia.

Patrick R., Crum B. and Coles J. (1969) Temperature and manganese as determining factors in the presence of diatom or blue-green algal floras in streams. *Proceedings of the Natural Academy of Science USA* 64, 472,478.

Peck J.A., Khosbayar P., Fowell S.J., Pearce R.B., Ariunbileg S., Hansen B.C.S., Soninkhishig N. (2002) Mid to Late Holocene climate change in north central Mongolia as recorded in the sediments of Lake Telmen. *Palaeogeography Palaeoclimatology Palaeoecology* 183, 135-153.

Peteet D. (1995) Global Younger Dryas. *Quaternary International* 28, 93-104.

Pichon J.J., Labeyrie L.D., Bareille M., Labracherie J., Duprat J. and Jouzel J. (1992) Surface water temperature changes in the high latitudes of the southern hemisphere over the last glacial-interglacial cycle. *Paleoceanography* 7, 289-318.

Pienitz R., Smol J.P. and Birks H.J.B. (1995) Assessment of fresh-water diatoms as quantitative indicators of past climatic-change in the Yukon and Northwest-territories, Canada. *Journal of Paleolimnology* 13, 21-49.

Piotrowska N., Bluszcz A., Demske D., Granoszewski W. and Heumann G. (2004) Extraction and AMS Radiocarbon Dating of Pollen from Lake Baikal Sediments, *Radiocarbon* 46, 181-187.

Plummer L.N. (1993) Stable-isotope enrichment in paleowaters of the Southeast Atlantic Coastal-Plain, United-States. *Science* 262, 2016-20.

Popovskaya G.I. (1966) Species nova generis Stephanodiscus Ehr. Novitates. *Systematicae Plantarum non Vascularum* 39-42. [in Russian].

Popovskaya G.I. (2000) Ecological monitoring of phytoplankton in Lake Baikal. *Aquatic Ecosystem Health and Management* 3 215-225.

Porter S.C. (2001) Chinese loess record of monsoon climate during the last glacial-interglacial cycle. *Earth-Science Reviews* 54, 115-128.

Porter S.C. and An Z.S. (1995) Correlation between climate events in the North-Atlantic and China during last Glaciation. *Nature* 375, 305-308.

Porter S. C. and Denton G. H. (1967). Chronology of Neoglaciation in the North American Cordillera. *American Journal of Science* 265, 177-210.

Prairie Y.T. (1996) Evaluating the predictive power of regression models. *Canadian Journal of Fisheries and Aquatic Sciences* 53, 490-492.

Prokopenko A.A. (2000) Challenges in constructing the age model for the Lake Baikal cores during the last glacial/interglacial transition: the response to M.A. Grachev. *Earth and Planetary Science Letters* 181, 267-70.

Prokopenko A., Williams D. F., Koval P. and Karabanov E. (1993) The organic indexes in the surface sediments of Lake Baikal water system and the processes controlling their variation. *IPPCCE Newsletter* 7, 49-55.

Prokopenko A.A., Williams D.F., Karabanov E.B. and Khursevich G.K. (1999) Response of Lake Baikal ecosystem to climate forcing and pCO_2 change over the last Glacial/Interglacial transition. *Earth and Planetary Science Letters* 172, 239-253.

Prokopenko A. A., Karabanov E. B., Williams D. F., Kuzmin M. I., Shackleton N. J., Crowhurst S. J., Peck J. A., Gvozdkov A. N. and King J. W. (2001a) Biogenic silica record of the Lake Baikal response to climatic forcing during the Brunhes. *Quaternary Research* 55, 123-132.

Prokopenko A.A., Karabanov E.B., Williams D.F., Kuzmin M.I., Khursevich G.K. and Gvozdkov A.A. (2001b) The detailed record of climatic events during the past 75,000 yrs BP from the Lake Baikal drill core BDP-93-2. *Quaternary International* 80-1, 59-68.

Prokopenko A.A. and Williams D.F. (2004) Deglacial methane emission signals in the carbon isotopic record of Lake Baikal. *Earth and Planetary Science Letters* 218, 135-147.

Psenner R. and Schmidt R. (1992) Climate-driven pH control of remote alpine lakes and effects of acid deposition. *Nature* 356, 781-783.

Quade J. and Cerling T.E. (1995) Expansion of C_4 grasses in the Late Miocene of Northern Pakistan - evidence from stable isotopes in paleosols. *Palaeogeography Palaeoclimatology Palaeoecology* 115, 91-116.

Qui L. (1992) Geochemical indicators of productivity and climate in recent and Holocene sediments of Lake Baikal, Russia. Unpublished Ph.D Thesis, University of South Carolina.

Qiu L. Q., Williams D. F., Gvorzdkov A., Karabanov E. and Shimaraeva M. (1993) Biogenic silica accumulation and paleoproductivity in the northern basin of Lake Baikal during the Holocene. *Geology* 21, 25-28.

Rahmstorf S. (1994) Rapid climate transition in a coupled ocean atmosphere model. *Nature* 372 , 82-85.

Rahmstorf S. (1995) Bifurcations of the Atlantic thermohaline circulation in response to changes in the hydrological cycle. *Nature* 378, 145-149.

Ramrath A., Sadori L. and Negendank J. F. W. (2000) Sediments from Lago di Mezzano, Central Italy: a record of Lateglacial/Holocene climatic variations and anthropogenic impact. *The Holocene* 10, 87-95.

Ranzi R., Grossi G. and Bacchi B. (1999) Ten years of monitoring areal snowpack in the Southern Alps using NOAA-AVHRR imagery, ground measurements and hydrological data. *Hydrological Processes* 13, 2079-95.

Rau G.H., Takahashi T, Desmarais D.J. and Sullivan C.W. (1991)Particulate organic-matter delta-c-13 variations across the Drake Passage. *Journal of Geophysical Research-Oceans* 96 C8, 15131-15135.

Raubitschek S., Lucke A. and Schleser G.H. (1999) Sedimentation patterns of diatoms in Lake Holzmaar, Germany - (on the transfer of climate signals to biogenic silica oxygen isotope proxies). *Journal of Paleolimnology* 21, 437-48.

Ravens T.M., Kocsis O., Wuest A. and Granin N. (2000) Small-scale turbulence and vertical mixing in Lake Baikal. *Limnology and Oceanography* 45, 159-173.

Raynaud D., Jouzel J., Barnola J.M., Chappellaz J., Delmas R.J. and Lorius C. (1993) The ice record of greenhouse gases. *Science* 259, 926-934.

Reed J.M. (1994) The potential of diatom, ostracod and mineralogical analyses in Spanish saline lakes as indicators of climate change. Unpublished Ph.D thesis, University College London.

Reed J.M. (1998) A diatom-conductivity transfer function for Spanish salt lakes. *Journal of Paleolimnology* 19,399-416.

Reid G. and Williams D.M. (2000) On *Eunotia clevei* var. hispida Skvortzov from Lake Baikal. In: Economou-Amilli A (ed) University of Athens, Athens, pp 89-106

Renssen H. and Lautenschlager M. (2000) The effect of vegetation in a climate model simulation on the Younger Dryas. *Global and Planetary Change* 26, 423-443.

Renssen H., Van Geel B., Van Der Plicht J. and Magny M. (2000) Reduced solar activity as a trigger for the start of the Younger Dryas? *Quaternary International* 68, 373-383.

Renssen H., Isarin R.F.B. and Vandenberghe J. (2001) Rapid climatic warming at the end of the last glacial: new perspectives. *Global and Planetary Change* 30, 155-165.

Reynolds C.S. (1990) Temporal scales of variability in pelagic environments and the response of phytoplankton. *Freshwater Biology* 23, 25-53.

Reynolds C.S. (1973) Growth and buoyancy of *Microcystis aeruginosa* Kütz. emend. Elenkin in a shallow eutrophic lake. *Proceedings of the Royal Society of London B* 184, 29-50.

Reynolds C.S. (1984) The ecology of freshwater phytoplankton. Cambridge University Press, Cambridge.

Reynolds C.S. (1997) Vegetation processes in the pelagic: a model for ecosystem theory. Ecology Institute, Oldendorf.

Richardson F. and Hall V.A. (1994) Pollen concentrate preparation from highly organic Holocene peat and lake deposits for AMS dating. *Radiocarbon* 36, 407-412.

Richardson T.L., Gibson C.E. and Heaney S.I. (2000) Temperature, growth and seasonal succession of phytoplankton in Lake Baikal, Siberia. *Freshwater Biology* 44, 431-440.

Rietti-Shati M., Shemesh A. and Karlen W. (1998) A 3000-year climatic record from biogenic silica oxygen isotopes in an equatorial high-altitude lake. *Science* 281, 980-982.

Riggs G., Hall D. and Salomonson V. (1994) A snow index for the Landsat Thematic Mapper and MODIS. In: Proceedings of IGARSS '94 - International Geoscience and Remote Sensing Seminar. ESA Publications, Noordwijk. 1-10.

Rings A., Lucke A. and Schleser G.H. (2004) A new method for the quantitative separation of diatom frustules from lake sediments. *Limnology and Oceanography: Methods* 2, 25-34.

Rioual P., Andrieu-Ponel V., Rietti-Shati M., Battarbee R.W., de Beaulieu J.L., Cheddadi R., Reille M., Svobodova H. and Shemesh A. (2001) High-resolution record of climate stability in France during the last interglacial period. *Nature* 413, 293-6.

Rioual P. and Mackay A.W. (in press) High-resolution diatom record of the Kazantsevo Interglacial stage in Lake Baikal (Siberia). *Global and Planetary Change.*

Rodhe W. (1948) Environmental requirements of freshwater plankton algae. Experimemtal studies in the ecology of phytoplankton. *Symbol. Bot. Upsalien* 10, 149-155.

Rose N.L., Appleby P.G., Boyle J.F., Mackay A.W. and Flower R.J. (1998) The spatial and temporal distribution of fossil-fuel derived pollutants in the sediment record of Lake Baikal, eastern Siberia. *Journal of Paleolimnology* 20, 151-162.

Rosén P., Hall R., Korsman T. and Renberg I. (2000) Diatom transfer-functions for quantifying past air temperature, pH and total organic carbon concentration from lakes in Northern Sweden. *Journal of Paleolimnology* 24, 109-123.

Rosqvist G. C., Rietti-Shati M. and Shemesh A. (1999) Late Glacial to middle Holocene climatic record of lacustrine biogenic silica oxygen isotopes from a southern ocean island. *Geology* 27, 967-970.

Rosell-Melé A. (2003) Biomarkers as proxies of climate change. In: Mackay A.W., Battarbee R.W., Birks H.J.B. and Oldfield F. (eds.). Global Change in the Holocene: approaches to reconstructing fine-resolution climate change. Arnold, London. 358-371.

Rozanski K., Araguasaraguas L. and Gonfiantini R. (1992) Relation between long-term trends of O-18 isotope composition of precipitation and climate. *Science* 258, 981-985.

Ruddiman W.F. (2003a) The anthropogenic greenhouse era began thousands of years ago. *Climatic Change* 61, 261-293.

Ruddiman W.F. (2003b) Orbital insolation, ice volume, and greenhouse gases. *Quaternary Science Reviews* 22, 1597-1629.

Rundgren M., Loader N.J. and Hammarlund D. (2003) Stable carbon isotope composition of terrestrial leaves: inter- and intraspecies variability, cellulose and whole-leaf tissue difference, and potential for climate reconstruction. *Journal of Quaternary Science* 18, 583-590.

Russell M. and Rossell-Melé A. (in press) Major lipid biomarker classes in the water column and sediments of Lake Baikal. *Global and Planetary Change.*

Rychkov I.L., Kuzevanova E.N. and Pomazkova G.I. (1989) Long-term natural changes in plankton of the southern Baikal. In: Salánki J, Herodek S (eds.). Akadémiai Kiadó, Budapest, 361-6.

Ryves D.B. (1994) Diatom dissolution in saline lake sediments: an experimental study in the Great Plains of North America. Unpublished Ph.D thesis, University College London.

Ryves D. and Flower R. J. (1998) Lake Baikal international diatom taxonomy workshop: taxonomic agreements of principal species. ECRC Research Report 53.

Ryves D.B., Juggins S., Fritz S.C. and Battarbee R.W. (2001) Experimental diatom dissolution and the quantification of microfossil preservation in sediments *Palaeogeography Palaeoclimatology Palaeoecology* 172, 99-113.

Ryves, D., Jewson, D.H., Sturm, M.J., Battarbee, R.W., Flower, R.J., Mackay, A.W. and Granin, N.G. (2003) Quantitative and qualitative relationships between planktonic diatom communities and diatom assemblages in sedimenting material and surface sediments in Lake Baikal, Siberia. *Limnology and Oceanography* 48, 1643-1661.

Sayer C.D. (2001) Problems with the application of diatom-total phosphorus transfer functions: examples from a shallow English lake *Freshwater Biology* 46, 743-757.

Schleser G. H., Helle G., Lucke A. and Vos H. (1999) Isotope signals as climate proxies: the role of transfer functions in the study of terrestrial archives. *Quaternary Science Reviews* 18, 927-943.

Schelske C.L. and Hodell D.A. (1991) Recent changes in productivity and climate of Lake-Ontario detected by isotopic analysis of sediments. *Limnology and Oceanography* 36, 961-975.

Schelske C.L. and Hodell D.A. (1995) Using carbon isotopes of bulk sedimentary organic-matter to reconstruct the history of nutrient loading and eutrophication in Lake Erie. *Limnology and Oceanography* 40, 918-929.

Schmidt M., Botz R., Stoffers P., Anders T., and Bohrmann G. (1997) oxygen isotopes in marine diatoms: a comparative study of analytical techniques and new results on the isotope composition of recent marine diatoms. *Geochimica et Cosmochimica Acta* 61, 2275-2280.

Schmidt M., Botz R., Rickert D., Bohrmann G., Hall S.R. and Mann S. (2001) Oxygen isotopes of marine diatoms and relations to opal-A maturation. *Geochimica et Cosmochimica Acta* 65, 201-11.

Schulz M. (2002a) The tempo of climate change during Dansgaard-Oeschger interstadials and its potential to affect the manifestation of the 1470-year climate cycle *Geophysical Research Letters* 29, article no. 1002.

Schulz M. (2002b) On the 1470-year pacing of Dansgaard-Oeschger warm events. *Paleoceanography* 17, article no. 1014.

Schulz M. and Paul A. (2002) Holocene climate variability on centennial-to-millennial time scales: 1. Climate records from the North-Atlantic realm. In: Wefer G., Berger W. H., Behre K.E. and Jansen E. (eds.). Climate development and history of the North Atlantic Realm. Springer Verlag, Berlin. 41-54.

Schwalb A., Locke S. M. and Dean W. E. (1995) Ostracode $\delta^{18}O$ and $\delta^{13}C$ evidence of Holocene environmental-changes in the sediments of 2 Minnesota lakes. *Journal of Paleolimnology* 14, 281-296.

Schwander J., Eicher U. and Ammann B. (2000) Oxygen isotopes of lake marl at Gerzensee and Leysin (Switzerland), covering the Younger Dryas and two minor oscillations, and their correlation to the GRIP ice core. *Palaeogeography Palaeoclimatology Palaeoecology* 159, 203-214.

Seal R. R. and Shanks W. C. (1998) Oxygen and hydrogen isotope systematics of Lake Baikal, Siberia: implications for paleoclimate studies. *Limnology and Oceanography* 43, 1251-1261.

Semovski S.V., Mogilev N.Y. and Sherstyankin P.P. (2000) Lake Baikal ice: analysis of AVHRR imagery and simulation of under-ice phytoplankton bloom. *Journal of Marine Systems* 27, 117-30.

Semovski S.V. and Mogilev N.Y. (2003) The use of satellite imagery in investigating the dynamics of the ice and snow cover Lake Baikal. *Nordic Hydrology* 34, 33-50.

Sernander R. (1908) On the evidence of posrglacial changes of climate furnished by the peat-mosses of northern Europe. *Geol. Fören. Förh.* 30, 465-478.

Severinghaus J. P., and Brook E. J. (1999) Abrupt climate change at the end of the last glacial period inferred from trapped air in polar ice. *Science* 286, 930-934.

Shahgedova M. (2002) Climate at present and in the historical past. *In:* Shahgedanova M. (ed.). The Physical Geography of Northern Eurasia. Oxford University Press, Oxford. 70-102.

Shemesh A., Charles C. D. and Fairbanks R. G. (1992) Oxygen isotopes in biogenic silica - global changes in ocean temperature and isotopic composition. *Science* 256, 1434-1436.

Shemesh A., Burkle L. H. and Hays J. D. (1995) Late Pleistocene oxygen-isotope records of biogenic silica from the Atlantic sector of the southern-ocean. *Paleoceanography* 10, 179-196.

Shemesh A. and Peteet D. (1998) Oxygen isotopes in fresh water biogenic opal - Northeastern US Allerod-Younger Dryas temperature shift. *Geophysical Research Letters* 25, 1935-1938.

Shemesh A., Rosqvist G., Rietti-Shati M., Rubensdotter L., Bigler C., Yam R., and Karlen W. (2001a) Holocene climatic change in Swedish Lapland inferred from an oxygen-isotope record of lacustrine biogenic silica. *Holocene* 11, 447-454.

Shemesh A., Rietti-Shati M., Rioual P., Battarbee R., de Beaulieu J.L., Reille M., Andrieu V., Svobodova H. (2001b) An Oxygen isotope record of lacustrine opal from a European Maar indicates climatic stability during the last interglacial. *Geophysical Research Letters* 28, 2305-8.

Shi Y. F., Yu G., Liu X. D., LI B. Y. and Yao T. D. (2001) Reconstruction of the 30-40 ka BP enhanced Indian monsoon climate based on geological records from the Tibetan Plateau. *Palaeogeography Palaeoclimatology Palaeoecology* 169, 69-83.

Shimaraev M.N. (1977) Elements of heat regime of Lake Baikal. Nauka, Novosibirsk. [in Russian].

Shimaraev M.N. and Granin N.G. (1991) Temperature stratification and the mechanisms of convection in Lake Baikal. *Doklady Akademii Nauk* 321, 831-835. [in Russian]

Shimaraev M.N., Granin N.G. and Kuimova L.N. (1992) Possible changes of hydrophysical conditions in Lake Baikal during the Late Pleistocene. *IPCCEE Newsletter* 6, 47-52.

Shimaraev M.N, Granin N.G. and Zhdanov A.A (1993) Deep ventilation of Lake Baikal waters due to spring thermal bars. *Limnology and Oceanography* 38, 1068-72.

Shimaraev, M.N. Verbolov V.I., Granin. N.G. and Sherstyankin P.P. (1994) Physical Limnology of Lake Baikal: a review. BICER, Irkutsk.

Shindell D.T., Schmidt G.A., Mann M.E., Rind D. and Waple A. (2001) Solar forcing of regional climate change during the maunder minimum. *Science* 294, 2149-2152.

Shiro Y. and Sakai, H. (1972). Calculation of the reduced partition function ratios of α-, ß-quartz and calcite. *Bulletin of the Chemical Society of Japan* 45, 2355–2359.

Siegenthaler U. and Oeschger H. (1980) Correlation of ^{18}O in precipitation with temperature and altitude. *Nature* 285, 314-317.

Siegenthaler U., Eicher U., Oeschger H. and Dansgaard W. (1984) Lake-sediments as continental $\delta^{18}O$ records from the glacial post-glacial transition. *Annals of Glaciology* 5, 149-52.

Siegenthaler U. and Eicher U. (1986) Stable oxygen and carbon isotope analyses. In: Berglund B.E. (ed.). Handbook of Holocene Palaeoecology and Palaeohydrology. Wiley, Chichester. 407-422.

Sirocko F., GarbeSchonberg D., McIntyre A. and Molfino B. (1996) Teleconnections between the subtropical monsoons and high-latitude climates during the last deglaciation *Science* 272, 526-529.

Skabitchevskyii A.P. (1960) Planktonic diatoms of the freshwaters of the USSR: Systematics, ecology and distribution. Moscow State University, Moscow. [in Russian].

Skabitchevskyii A.P. (1977) Importance of size, and of cell and colony shapes of some species of *Melosira* for the planktonic form of life. *Hydrobiological Journal* 13, 1-14.

Skvortzow B.W. (1937) Bottom diatoms from Olhon Gate of Baikal Lake, Siberia. *Philippine Journal of Science* 62, 293-377.

Šmilauer P. (2002) CanoDraw for Windows 4.0. www.canodraw.com

Smith A.G. (1981) The Neolithic. In: Simmons I.G. and Tooley M.J. (eds.). The Environment in British Prehistory. Duckworth, London 125-209.

Smith H.J., Wahlen M., Mastroianni D. and Taylor K.C. (1997) The CO_2 concentration of air trapped in GISP2 ice from the last glacial maximum-Holocene transition *Geophysical Research Letters* 24, 1-4.

Smith M.A. and Hollander D.J. (1999) Historical linkage between atmospheric circulation patterns and oxygen isotopic record of sedimentary carbonates from Lake Mendota, Wisconsin, USA. *Geology* 27, 589–592.

Smol J.P. (1983) Paleophycology of a High Arctic lake near Cape Herschel, Ellesmere-Island. *Canadian Journal of Botany-Revue Canadienne de Botanique* 61, 2195-2204

Smol J.P. (1988) Paleoclimate proxy data from freshwater arctic diatoms. *Verhandlungen der Internationale Vereinigung für Limnologie* 23, 837-844.

Smol J.P. (1991) Are we building enough bridges between paleolimnology and aquatic ecology? *Hydrobiologia* 214, 201-206.

Sokol J., Pultz T.J. and Walker A.E. (2003) Passive and active airborne microwave remote sensing of snow cover. *International Journal of Remote Sensing* 24, 5327-5344.

Sommaruga-Wögrath S., Koinig K.A., Schmidt R., Sommaruga R., Tessadri R. and Psenner R. (1997) Temperature effects on the acidity of remote alpine lakes. *Nature* 387 64-67.

Sommer U. (1994) The impact of light intensity and daylength on silicate and nitrate competition among marine phytoplankton. *Limnology and Oceanography* 39, 1680-1688.

Sonntag V. C., Klitzsch E., El Shazly E. M., Kalinke C. and Münnich K. O. (1978) Paläoklimatische Information im Isotopengehalt ^{14}C-datierter Saharawässer: Kontinentaleffeckt in D und ^{18}O. *Geologische Rundschau* 67, 413-423. [in German].

Srivastan K.S. and Singh R.P. (1991) Microwave radiometry of snow-covered terrains. *International Journal of Remote Sensing* 12, 2117-2131.

Stager J.C. and Mayewski P.A. (1997) Abrupt early to mid-Holocene climatic transition registered at the equator and the poles. *Science* 276, 1834-6.

Stager J.C., Cumming B. and Meeker L. (1997) A high-resolution 11,400-yr diatom record from Lake Victoria, East Africa. *Quaternary Research* 47, 81-89.

Starkel L. (1998) Geomorphic response to climatic and environmental changes along a Central Asian transect during the Holocene. *Geomorphology* 23, 293-305.

Steig E.J. (1999) Paleoclimate - Mid-Holocene climate change *Science* 286, 1485-1487.

Stoermer E.F., Edlund M.B., Pilskaln C.H. and Schelske C.L. (1995) Siliceous microfossil distribution in the surficial sediments of Lake Baikal. *Journal of Paleolimnology* 14, 69-82.

Straskrabova V., Izmest'yeva L.R., Maksimova E.A., Fietz S., Nedoma J., Borovec J., Kobanova G.I., Shchetinina E.V. and Pislegina E.V. (in press) Primary production and microbial activity in the euphotic zone of Lake Baikal (Southern Basin) during late winter. *Global and Planetary Change.*

Street-Perrott F.A., Huang Y., Perrott A. and Eglinton G. (1998) Carbon isotopes in lake sediments and peats of the last glacial age: implications for the global carbon cycle. In: Griffiths H. (ed.). Stable isotopes and integration of biological, ecological and geochemical process, Bios Scientific Publisher, Oxford. 381-396.

Street-Perrott F.A., Ficken K.J., Huang Y.S. and Eglinton G. (2004) Late quaternary changes in carbon cycling on Mt. Kenya, East Africa: an overview of the $\delta^{13}C$ record in lacustrine organic matter. *Quaternary Science Reviews* 23, 861-879.

Stuiver M. (1970) Oxygen and carbon isotope ratios of fresh-water carbonates as climatic indicators. *Journal of Geophysical Research* 75, 5247-5257.

Stuiver M., and T. F. Braziunas (1993) Sun, ocean, climate and atmospheric $^{14}CO_2$: An evaluation of causal and spectral relationships. *The Holocene* 3, 189–305.

Stuiver M., Grootes P.M. and Braziunas T.F. (1995) The GISP2 ^{18}O climate record of the past 16,500 years and the role of the sun, ocean and volcanoes. *Quaternary Research* 44, 341-354.

Stuiver M., Braziunas T. F., Grootes P. M. and Zielinski G. A. (1997) Is there evidence for solar forcing of climate in the GISP2 oxygen isotope record? *Quaternary Research* 48, 259-266.

Swann G.E.A., Mackay A.W., Leng M.J. and Demory F. (in press) Climatic change in Central Asia during MIS 3: a case study using biological responses from Lake Baikal. *Global and Planetary Change.*

Talbot M. R. (1990) A review of the paleohydrological interpretation of carbon and oxygen isotopic-ratios in primary lacustrine carbonates. *Chemical Geology* 80, 261-279.

Talbot M.R. and Johannessen T. (1992) A high resolution palaeoclimatic record for the last 27500 years in tropical West Africa from the carbon and nitrogen isotopic composition of lacustrine organic matter. *Earth and Planetary Science Letters* 110, 23–37.

Tarasov P., Dorofeyuk N. and Metel'tseva E. (2000) Holocene vegetation and climate changes in Hoton-Nur basin, northwest Mongolia. *Boreas* 29, 117-126.

Taylor K.C., Lamorey G.W., Doyle G.A., Alley R.B., Grootes P.M., Mayewski P.A., White J.W.C. and Barlow L.K. (1993) The flickering switch of late Pleistocene climate change. *Nature* 361, 432-436.

ter Braak C.J.F. (1988) Partial canonical correspondence analysis. In: Bock H.H. (ed.). Classification and related methods of data analysis. North Holland, Amsterdam. 551-558.

ter Braak C.J.F. (1995) Ordination. In: Jongman R.H.G., ter Braak C.J.F. and van Tongeren O.F.R. (eds.). Data Analysis in Landscape and Community Ecology (eds). Cambridge University Press, Cambridge. 91-174.

ter Braak C.J.F. and Prentice I.A. (1989) A theory of gradient analysis. *Advances In Ecological Research* 18, 271-317.

ter Braak C.J.F. and Juggins S. (1993) Weighted averaging partial least-squares regression (WA-PLS) - an improved method for reconstructing environmental variables from species assemblages. *Hydrobiologia* 269, 485-502.

ter Braak C.J.F., Juggins S., Birks H.J.B. and van der Voet H. (1993) Weighted-averaging-partial least square regression (WA-PLS): Definition and comparison with other methods for species-environmental calibration. In: Patil G. P. and Rao C.R. (eds.). Multivariate Environmental Statistics. Elsevier Science Publishers, Amsterdam. 525-560.

ter Braak C.J.F. and Šmilauer P. (2002) Canoco for Windows 4.5. Biometrics, The Netherlands.

Teranes J. L. and McKenzie J. A. (2001) Lacustrine oxygen isotope record of 20th-century climate change in Central Europe: evaluation of climatic controls on oxygen isotopes in precipitation. *Journal of Paleolimnology* 26, 131-146.

Tilman D. and Kilham S.S. (1976) Phosphate and silicate growth and uptake kinetics of the diatoms *Asterionella formosa* and *Cyclotella meneghiniana* in batch and semicontinuous culture. *Journal of Phycology* 12, 375-383.

Timmermann A., Gildor H., Schulz M. and Tziperman E. (2003) Coherent resonant millennial-scale climate oscillations triggered by massive meltwater pulses. *Journal of Climate* 16, 2569-2585.

Timoshkin O.A. (1995) Guide and key to pelagic animals of Baikal. Nauka, Novosibirsk. [in Russian].

Todd M.C. and Mackay A.W. (2003) Large-scale climatic controls on Lake Baikal ice cover. *Journal of Climate* 16, 3186-3199.

Torrence C. and Compo G.P. (1998) A Practical Guide to Wavelet Analysis. *Bulletin of the American Meteorological Society* 79, 61–78.

Torres M.E., Mix A.C., Kinports K., Haley B., Klinkhammer G.P., McManus J. and de Angelis M.A. (2003) Is methane venting at the seafloor recorded by $\delta^{13}C$ of benthic foraminifera shells? *Paleoceanography* 18, art. no. 1062.

Turney C.S.M., (1998) Isotope stratigraphy and tephrochronolgy of the last glacial – interglacial transition (14-9ka ^{14}C BP) in the British Isles. Unpublished PhD Thesis, University of London.

Tziperman E. (1997) Inherently unstable climate behaviour due to weak thermohaline ocean circulation. *Nature* 386, 592-595.

Utermöhl H. (1958) Toward the improvement of the quantitative phytoplankton method. *Mitteilungen-Internationale Vereiningung fur Limnologie.* 9, 1-38. [In German].

van Bennekom A. J. and Van der Gaast S. J. (1976) Possible clay structures in frustules of living diatoms. *Geochimica et Cosmochimica Acta* 40, 1-6.

van Geel B., Buurman J. and Waterbolk H.T. (1996) Archaeological and palaeoecological indications of an abrupt climate change in The Netherlands, and evidence for climatological teleconnections around 2650 BP. *Journal of Quaternary Science* 11, 451-60.

van Geel B., Raspopov O. M., Renssen H., van der Plicht J. , Dergachev V. A. and Meijer H. A. J. (1999) The role of solar forcing upon climate change. *Quaternary Science Reviews* 18, 331-338.

van Geel B., Heusser C. J., Renssen H., and Schuurmans C. J. E. (2000) Climatic change in Chile at around 2700 BP and global evidence for solar forcing: a hypothesis. *The Holocene* 10, 659-664.

van Rensbergen P., de Batist M., Criel W., Klerkx J., Granin N., Gnatovsky R. and Krinitsky P. (2003) An inventory of hydrate-related gas seeps in Lake Baikal. *Geophysical Research Abstracts* 5,

Vanneste M., Poort J., De Batist M. and Klerkx J. (2003) Atypical heat-flow near gas hydrate irregularities and cold seeps in the Baikal Rift Zone. *Marine and Petroleum Geology* 19, 1257-1274.

Velichko A.A. (1995) The pleistocene termination in northern Eurasia. *Quaternary International* 28, 105-111.

Velichko A.A., Andreev A.A. and Klimanov V.A. (1997) Climate and vegetation dynamics in the tundra and forest zone during the Late Glacial and Holocene. *Quaternary International* 41-2, 71-96.

Velichko A.A. Catto N., Drenova A.N., Klimanov V.A., Kremenetski K.V. and Nechaev V.P. (2002) Climate changes in East Europe and Siberia at the Late Glacial-Holocene transition. *Quaternary International* 91, 75-99.

Verbolov V.I., Sokol'nikov V.N. and Shimaraev M.N. (1965) Hydrometeorlogical conditions and heat balance of Lake Baikal. Nauka, Moscow. [in Russian].

Verkhozina V.A., Kozhova O.M. and Kusner Y.S. (2000a) Hydrodynamics as a limiting factor in the Lake Baikal ecosystem. *Aquatic Ecosystem Health and Management* 3, 203-210.

Verkhozina V.A., Kusner Y.S., Pavlova T.V. and Potemkin V.L. (2000b) Manifestation of climatic changes in the plankton productivity periodicity in Lake Baikal. *Doklady Earth Sciences* 374, 1158-1160.

Viau A.E, Gajewski K., Fines P., Atkinson D.E. and Sawada M.C. (2002) Widespread evidence of 1500 yr climate variability in North America during the past 14 000 yr. *Geology* 30, 455–458.

von Grafenstein U., Erlenkeuser H., Kleinmann H., Müller J. and Trimborn P. (1994) High-frequency climate oscillations during the last deglaciation as revealed by oxygen-isotope records of benthic organisms (Ammersee, Southern Germany). *Journal of Paleolimnology* 11, 349-357.

von Grafenstein U., Erlenkeuser H., Muller J., Trimborn P., and Alefs J. (1996) A 200 year mid-European air temperature record preserved in lake sediments: an extension of the $\delta^{18}O$ (p)-air temperature relation into the past. *Geochimica et Cosmochimica Acta* 60, 4025-4036.

von Grafenstein U., Erlenkeuser H., Muller J., Jouzel J. and Johnsen S. (1998) The cold event 8200 years ago documented in oxygen isotope records of precipitation in Europe and Greenland. *Climate Dynamics* 14, 73-81.

von Grafenstein U., Erlenkeuser H., Brauer A., Jouzel J., Johnsen S.J. (1999) A mid-European decadal isotope-climate record from 15,500 to 5000 years BP. *Science* 284, 1654-1657.

von Grafenstein U., Eicher U., Erlenkeuser H., Ruch P., Schwander J. and Ammann B. (2000) Isotope signature of the Younger Dryas and two minor oscillations at Gerzensee (Switzerland): palaeoclimatic and palaeolimnologic interpretation based on bulk and biogenic carbonates. *Palaeogeography Palaeoclimatology Palaeoecology* 159, 215-229.

Votintsev K.K., Meshcheryakova A.I. and Popovskaya G.I. (1975) Cycle of organic substance in Lake Baikal. Nauka, Novosibirsk.

Vyverman W. and Sabbe K. (1995) Diatom-temperature transfer-functions based on the altitudinal zonation of diatom assemblages in Papua-New-Guinea - a possible tool in the reconstruction of regional paleoclimatic changes. *Journal of Paleolimnology* 13, 65-77.

Walker M.J.C. (2001) Rapid climate change during the last glacial-interglacial transition; implications for stratigraphic subdivision, correlation and dating. *Global and Planetary Change* 30, 59-72.

Walker M.J.C., Bjorck S. and Lowe J.J. (1999) Integration of ice core, marine and terrestrial records (INTIMATE) from around the North Atlantic region: an introduction *Quaternary Science Reviews* 20, 1169-1174.

Wang C.H. and Yeh H.W. (1985) Oxygen isotopic compositions of DSDP site-480 diatoms - implications and applications. *Geochimica et Cosmochimica Acta* 49, 1469-1478.

Wang X.C., Chen R.F., Whelan J. and Eglinton L. (2001) Contribution of "old" carbon from natural marine hydrocarbon seeps to sedimentary and dissolved organic carbon pools in the Gulf of Mexico. *Geophysical Research Letters* 28, 3313-3316.

Wang Y.J., Cheng H., Edwards R.L., An Z.S., Wu J.Y., Shen C.C. and Dorale J.A. (2001) A high-resolution absolute-dated Late Pleistocene monsoon record from Hulu Cave, China. *Science* 294, 2345-2348.

Wanner H., Brönnimann S., Casty C., Gyalistras, D., Luterbacher J., Schmutz C., Stephenson D.B. and Xoplaki E. (2001) North Atlantic Oscillation - Concepts and Studies. *Surveys in Geophysics* 22, 321-381.

Watanabe T., Naraoka H., Nishimura M. and Kawai T. (2004) Biological and environmental changes in Lake Baikal during the late Quaternary inferred from carbon, nitrogen and sulfur isotopes. *Earth and Planetary Science Letters* 222, 285-299.

Weckström J., Korhola A. and Blom T. (1997a) The relationship between diatoms and water temperature in thirty subarctic Fennoscandian lakes. *Arctic and Alpine Research* 29, 75-92.

Weckström J., Korhola A. and Blom T. (1997b) Diatoms as quantitative indicators of pH and water temperature in subarctic Fennoscandian lakes. *Hydrobiologia* 347, 171-184.

Weiss R.F., Carmack E.C. and Koropalov V.M. (1991) Deep-water renewal and biological production in Lake Baikal. *Nature* 349, 665-669.

Wetzel R.G. (2001) Limnology: Lake and River Ecosystems, third edition. Academic Press, San Diego.

Whittington G., Fallick A.E. and Edwards K.J. (1996) Stable oxygen isotope and pollen records from eastern Scotland and a consideration of late-glacial and early Holocene climate change for Europe. *Journal of Quaternary Science* 11, 327-40.

Williams D. F., Peck J., Karabanov E. B., Prokopenko A. A., Kravchinsky V., King J. and Kuzmin M. I. (1997) Lake Baikal record of continental climate response to orbital insolation during the past 5 million years. *Science* 278, 1114-1117.

Williams D.F., Kuzmin M.I., Prokopenko A.A., Karabanov E.B., Khursevich G.K., Bezrukova E.V. (2001) The Lake Baikal drilling projects in the context of a global lake drilling initiative. *Quaternary International* 80-1, 3-18.

Witt A. and Schuman A.Y (in prep.) Holocene climate variability on millennial scales recorded in Greenland ice cores. *Nonlinear Processes in Geophysics.*

Woillard G.M. (1978) Grand Pile Peat Bog: a continuous pollen record for the last 140,000 years. *Quaternary Research* 9, 1-21.

Wolfe A.P. (1994) Late Wisconsinan and Holocene diatom stratigraphy from Amarok Lake, Baffin Island, N.W.T., Canada. *Journal of Paleolimnology* 10, 129-39.

Wolfe B.B., Edwards T.W.D., Aravena R., Forman S.L., Warner B.G., Velichko A.A. and MacDonald G.M. (2000) Holocene paleohydrology and paleoclimate at treeline, north-central Russia, inferred from oxygen isotope records in lake sediment cellulose. *Quaternary Research* 53, 319-29.

Wolfe B.B., Edwards T.W.D. Aravena R. and MacDonald G.M. (1996) Rapid Holocene hydrologic change along boreal treeline revealed by delta C-13 and delta O-18 in organic lake sediments, Northwest territories, Canada. *Journal of Paleolimnology* 15, 171-181.

Wolfe B.B., Edwards T.W.D. and Aravena R. (1999) Changes in carbon and nitrogen cycling during tree-line retreat recorded in the isotopic content of lacustrine organic matter, Western Taimyr Peninsula, Russia. *The Holocene* 9, 215-222.

Xia J., Haskell B.J., Engstrom D.R. and Ito E. (1997a) Holocene climate reconstructions from tandem trace-element and stable-isotope composition of ostracodes from coldwater lake, North Dakota, USA. *Journal of Paleolimnology* 17, 85-100.

Xia J., Ito E. and Engstrom D. R. (1997b) Geochemistry of ostracode calcite .1. An experimental determination of oxygen isotope fractionation. *Geochimica et Cosmochimica Acta* 61, 377-382.

Xia J., Engstrom D. R. and Ito E. (1997c) Geochemistry of ostracode calcite .2. The effects of water chemistry and seasonal temperature variation on *Candona rawsoni*. *Geochimica et Cosmochimica Acta* 61 , 383-391.

Xiao J., Porter S.C., An Z.S., Kumai H. and Yoshikawa S. (1995) Grain-size of quartz as an indicator of winter monsoon strength on the Loess Plateau of central China during the last 130,000-yr. *Quaternary Research* 43, 22-29.

Xu H., Bailey J.O., Barrett E.C. and Kelly R.E.J. (1993) Monitoring snow area and depth with integration of remote sensing and GIS. *International Journal of Remote Sensing* 14, 3259-3268.

Yakushev V.S. and Chuvilin E.M. (2000) Natural gas and gas hydrate accumulations within permafrost in Russia. *Cold Regions Science and Technology* 31, 189-197.

Yan G., Wang F. B., Shi G. R. and Li S. F. (1999) Palynological and stable isotopic study of palaeoenvironmental changes on the Northeastern Tibetan Plateau in the last 30,000 years. *Palaeogeography Palaeoclimatology Palaeoecology* 153, 147-159.

Yang, H. (2000). Trace metals and lake sediments. Unpublished Ph.D Thesis, University College London.

Ye, H. (2001a) Quasi-Biennial and Quasi-Decadal Variations in Snow Accumulation over Northern Eurasia and Their Connections to the Atlantic and Pacific Oceans. *Journal of Climate* 14, 4573-4584.

Ye, H. (2001b) Characteristics of Winter Precipitation Variation over Northern Central Eurasia and Their connections to Sea Surface Temperatures over the Atlantic and Pacific Oceans. *Journal of Climate* 14, 3140-3155.

Ye, H. and Bao, Z. (2001) Lagged teleconnections between snow depth in Northern Eurasia, rainfall in Southeast Asia and sea-surface temperatures over the tropical pacific ocean. *International Journal of Climatology* 21, 1607-1621.

Yu Z. C. and Eicher U. (1998) Abrupt climate oscillations during the last deglaciation in central North America. *Science* 282, 2235-2238.

Yu Z.C., McAndrews J.H. and Eicher U. (1997) Middle Holocene dry climate caused by change in atmospheric circulation patterns: Evidence from lake levels and stable isotopes. *Geology* 25, 251-4.

Zhang, J. and Crowley, T.J. (1989) Historical climate records in China and reconstruction of past climates. *Journal of Climate* 2, 833-849.

Zhao J.X., Wang Y.J., Collerson K.D. and Gagan M.K. (2003) Speleothem U-series dating of semi-synchronous climate oscillations during the last deglaciation. *Earth and Planetary Science Letters* 216, 155-161.

Zhou W.J., Donahue D.J., Porter S.C., Jull T.A., Li X.Q., Stuiver M., An Z.S., Matsumoto E. and Dong G.G. (1996) Variability of monsoon climate in East Asia at the end of the last glaciation. *Quaternary Research* 46, 219-29.

Zhou W.J., Donahue D. and Jull A.J.T. (1997) Radiocarbon AMS dating of pollen concentrated from eolian sediments: implications for monson climate change since the late Quaternary. *Radiocarbon* 39, 19-26.

Zhou W.J., Head M.J., Lu X.F., An Z.S., Jull A.J.T. and Donahue D. (1999) Teleconnection of climatic events between East Asia and polar, high latitude areas during the last deglaciation. *Palaeogeography Palaeoclimatology Palaeoecology* 152, 163-172.

Zielinski G.A., Mayewski P.A., Meeker L.D., Whitlow S., Twickler M.S., Morrison M., Meese D.A., Gow A.J. and Alley R.B. (1994) Record of volcanism since 7000-BC from the GISP2 Greenland ice core and implications for the volcano-climate system. *Science* 264, 948-952.